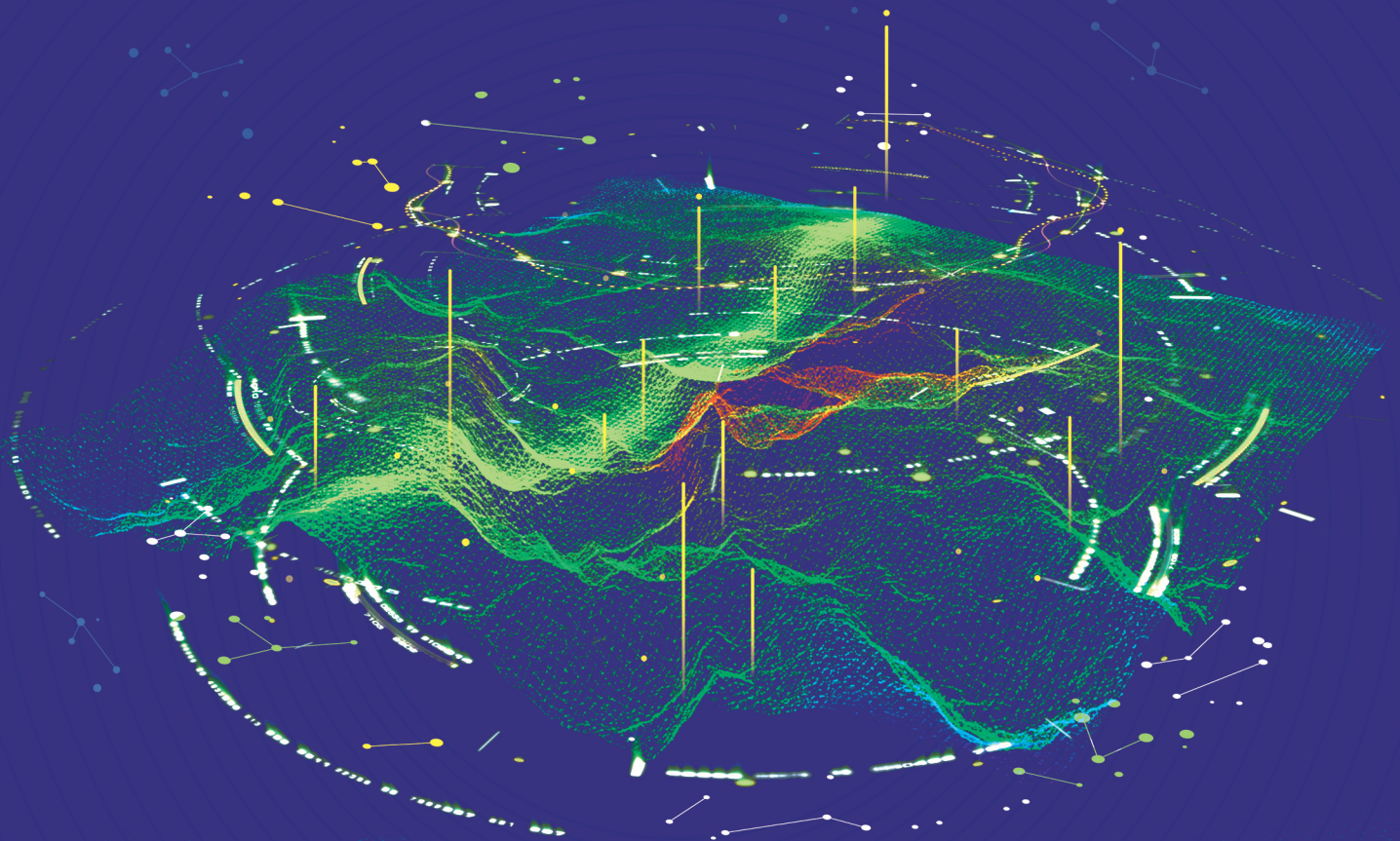


IAG 2021  Beijing
June 28–July 2
2021

Geodesy for a Sustainable Earth
Scientific Assembly of
the International Association
of Geodesy

ABSTRACT BOOK



Beijing • June 28–July 2, 2021



Content

Symposium 1: Reference Frames

S1.1: International Terrestrial Reference Frame: strengths, weaknesses and strategies for future improvements

S1-001	Combined IVS contribution to the ITRF2020 <i>Hendrik Hellmers, Daniela Thaller, Mathis Bloßfeld, Manuela Seitz, John Gipson, Sadegh Modiri</i>	2
S1-002	Assessing daily and sub-daily ocean tidal loading displacements using GPS, Galileo, and GLONASS observations <i>Hanane Ait-Lakbir, Alvaro Santamaria, Félix Perosanz</i>	3
S1-003	The International Laser Ranging Service (ILRS) Contribution to the Development of the ITRF2020 <i>Erricos Pavlis, Cinzia Luceri, Antonio Basoni, David Sarrocco, Magda Kuzmicz-Cieslak, Keith Evans, Giuseppe Bianco</i>	4
S1-004	Quality Evaluation of the Continental Water Storage models for correcting the Crustal Movement Observation Network of China height time series <i>Zhao Li, Weiping Jiang, Liansheng Deng, Tonie van Dam</i>	5
S1-005	Evaluation of the IGS contribution to ITRF2020 <i>Paul Rebischung</i>	6
S1-006	Status of ITRF2020 analysis and early results <i>Zuheir Altamimi, Paul Rebischung, Laurent Métivier, Xavier Collilieux, Kristel Chanard</i>	7
S1-007	Shimosato co-location of the SLR and GNSS stations <i>Yuto Nakamura, Shun-ichi Watanabe, Yusuke Yokota, Akira Suzuki, Haruka Ueshiba, Noritsune Seo</i>	8
S1-008	Geodetic VLBI data processing of the specific experiments <i>Anastasiia Girdiuk, Gerald Engelhardt, Dieter Ullrich, Hendrik Hellmers, Daniela Thaller</i>	9
S1-009	Local Ties at SLR station Riga <i>Kalvis Salmins, Viesturs Sproģis, Imants Bijņskis, Jorge del Pino</i>	10
S1-010	The 2021 Local Ties Campaign at GRAZ <i>Helmut Titz, Jürgen Fredriksson</i>	11
S1-011	The impact of the EOT20 global ocean tide model on space geodetic measurements, satellite orbits and derived geodetic parameters <i>Mathis Blossfeld, Mike Hart-Davis, Matthias Glomsda, Denise Dettmering</i>	12
S1-012	Densification of the VLBI network in the Southern hemisphere: advanced simulation for a VLBI antenna on Tahiti <i>Vladimir Schott Guilmault, David Coulot, Sébastien Lambert, Arnaud Pollet, Jean-Yves Richard, Christian Bizouard, Richard Biancale</i>	13
S1-013	New Developments on the IDS Contribution to the ITRF2020 <i>Guilhem Moreaux, Frank Lemoine, Hugues Capdeville, Petr Štěpánek, Michiel Otten, Jérôme Saunier, Pascale Ferrage</i>	14
S1.2: Advancements and open problems in global reference frame theory and methodology		
S1-014	Modelling and prediction of GPS time series with machine learning approaches <i>Wenzong Gao, Yanming Feng</i>	16

S1-015	Denoising method of elevation time series based on CEEMD algorithm and time-lapse multi-scale permutation entropy	<i>Peixian Wang, Haoran Li</i>	17
S1-016	The cross-correlations of the Helmert transformation parameters as an additional diagnostic tool for Terrestrial Reference Frames assessment	<i>Dimitrios Ampatzidis, Daniela Thaller, Lin Wang</i>	18
S1-017	Observation density method for selecting independent baselines in GNSS network	<i>Tong Liu, Guochang Xu, Zhiping Lv, Yujun Du, Jian Liu</i>	19
S1-018	Handling of tropospheric and range biases in Satellite Laser Ranging	<i>Mateusz Drożdżewski, Krzysztof Sośnica, Dariusz Strugarek</i>	21
S1-019	A Refined Global GNSS Velocity Field Modeling Station Seismic Deformation based on Constrained Nonlinear Optimization	<i>Yingying Ren, Hu Wang, Jiexian Wang, Yangfei Hou, Pengyuan Li</i>	22
S1-020	Periods Extraction of GNSS Coordinate Time Series Based on Significance Level	<i>Yanfeng JIA, Xinhui ZHU, Fuping SUN</i>	23
S1-021	Characteristics and Predictability of Postseismic Deformation in Reference Frame Models	<i>Jeff Freymueller</i>	24

S1.3: Terrestrial and space geodetic ties for multi-technique combinations

S1-022	Dilution of Precision (DOP) factors for evaluating observations to Galileo satellites with VLBI	<i>Helene Wolf, Johannes Böhm, Matthias Schartner, Urs Hugentobler</i>	26
S1-023	Reference frame realization using co-location in space onboard Galileo satellites	<i>Grzegorz Bury, Krzysztof Sośnica, Radosław Zajdel, Dariusz Strugarek, Urs Hugentobler</i>	27
S1-024	Large-scale dimensional metrology for geodesy - first results from the European GeoMetre Project	<i>Florian Pollinger, Clément Courde, Cornelia Eschelbach, Luis Garcia-Asenjo, Joffray Guillory, Per Olof Hedekvist, Ulla Kallio, Thomas Klügel, Pavel Neyezhnikov, Damien Pesce, Marco Pisani, Jeremias Seppä, Robin Underwood, Kinga Wezka, Mariusz Wiśniewski, for the GeoMetre Consortium</i>	28
S1-025	Determination of Galileo and GLONASS orbits based on combined SLR and GNSS data	<i>Grzegorz Bury, Krzysztof Sośnica, Radosław Zajdel, Dariusz Strugarek, Urs Hugentobler</i>	30
S1-026	Radar Corner Reflector installation at the OCA geodetic Observatory (France)	<i>Xavier Collilieux, Clément Courde, Bénédicte Fruneau, Mourad Aimar, Guillaume Schmidt, Isabelle Delprat, Damien Pesce, Guy Wöppelmann</i>	31
S1-027	Datum problem in terrestrial local ties	<i>Ulla Kallio, Thomas Klügel, Simo Marila, Svetlana Mähler, Markku Poutanen, Torben Schüler, Heli Suurmäki</i>	33
S1-028	Multi-technique combinations using a closure in time	<i>Jan Kodet, Ulrich Schreiber, Thomas Klügel</i>	34
S1-029	Close Range Photogrammetry for High Precise Reference Point Determination – A proof of concept at Satellite Observing System Wettzell	<i>Michael Lösler, Cornelia Eschelbach, Thomas Klügel</i>	35

S1-030	Combination of SLR observations to LEO, LAGEOS, LARES, and GNSS satellites	<i>Dariusz Strugarek, Krzysztof Sośnica, Daniel Arnold, Adrian Jäggi, Grzegorz Bury, Radosław Zajdel</i>	36
S1-031	On DORIS and SLR simulation studies to single-satellite space-ties to achieve the Global Geodetic Observing System goals	<i>Patrick Schreiner, Nicat Mammadaliyev, Susanne Glaser, Rolf Koenig, Karl Hans Neumayer, Harald Schuh</i>	37
S1-032	Differences in geocenter coordinate estimates delivered from GPS, GLONASS, and Galileo	<i>Radosław Zajdel, Krzysztof Sośnica, Grzegorz Bury, Dariusz Strugarek, Mateusz Drożdżewski</i>	38
S1-033	Towards tropospheric ties in the computation of terrestrial reference frames	<i>Changyong He, Arnaud Pollet, David Coulot</i>	39
S1-034	Intra- and Inter-Technique Atmospheric Ties: Derivation, Implementation, and Results	<i>Kyriakos Balidakis, Daniela Thaller, Mateusz Drożdżewski, Claudia Flohrer, Changyong He, Robert Heinkelmann, Chaiyaporn Kitpracha, Frank Lemoine, Lisa Lengert, Tobias Nilsson, Arnaud Pollet, Víctor Puente, Marcelo Santos, Benedikt Soja, Krzysztof Sośnica, Jungang Wang, Xiaoya Wang, Dudy Wijaya, Florian Zus, David Coulot</i>	40
S1-035	A Study on Differencing Approaches for SLR Observations	<i>Iván Herrera Pinzón, Markus Rothacher</i>	41
S1-036	SLR station range bias and coordinate determination using independent multi-LEO DORIS- and GNSS-based precise orbits	<i>Heike Peter, Daniel Arnold, Alexandre Couhert, Eléonore Saquet, Flavien Mercier, Oliver Montenbruck</i>	42
S1-037	Assessment of Local VLBI Baselines: The Wettzell Case	<i>Iván Herrera Pinzón, Markus Rothacher</i>	43
S1-038	Demonstration of 1 mm Precision for Kilometer Co-location Ties at McDonald Geodetic Observatory	<i>Jullian Rivera, Srinivas Bettadpur, John Griffin</i>	44

S1.4: Regional reference frames and networks

S1-039	GEODETIC DATUME TRANSFORMATION WITH THE MINIMUM CURVATURE SURFACE INTERPOLATION APPROACH in IRAQ	<i>Yasir Ammar Abed Al-husseinawi, mzahim Abdul Al-Kareem, Ghydaa Abdul-Rehman</i>	46
S1-040	Recent achievements and current challenges in the maintenance of the geodetic reference frame of the Americas	<i>José Antonio Tarrío, Laura Sánchez, Sonia Alves, Alberto Silva, Jesarella Inzunza, Gustavo Caubarrere, Alejandro Martínez, Óscar Rodríguez, Emilio Aleuy, Hernán Guagni, Guido González</i>	47
S1-041	Crustal block modelling using a combination of Euler pole and cluster analysis of GNSS velocities in Greece	<i>Stylianos Bitharis, Christos Pikridas, Aristeidis Fotiou, Dimitrios Rossikopoulos</i>	49
S1-042	BEV DC 2.0	<i>David Mayer, Philipp Mitterschiffthaler</i>	50
S1-043	Approaches to time-dependent transformations between reference frames in deforming regions	<i>Richard Stanaway</i>	51
S1-044	The North American Terrestrial Reference Frame of 2022: Its Definition and Plans for Adoption	<i>Dru Smith, Mike Craymer, Daniel Roman</i>	52

S1-045	On the impact of individual PCC errors on regional networks using different processing strategies.....	<i>Tobias Kersten, Grzegorz Krzan, Karol Dawidowicz, Steffen Schön</i>	53
S1-046	ADELA : Analysis of DEformation beyond Los Andes(2009-2021). The urgency to change from static to kinematic in any geodetic reference frame for Chile.....	<i>José Antonio Tarrío Mosquera, Jesarella Inzunza, Fernando Isla, Marcelo Caverlotti, Catalina Cáceres, Cristian Mardones</i>	54
S1-047	Extraction of common mode error of GNSS coordinate time series in Xinjiang with independent component analysis	<i>Chuanjin Lei, Guanjun Wei, Maoning Gao, Pei Zhang</i>	55
S1-048	ITRF densification in Cyprus	<i>Chris Danezis, Miltiadis Chatzinikos, Christopher Kotsakis</i>	56
S1-049	A three-dimensional crustal velocity field in mainland China from denser permanent GPS networks	<i>Zhikai Li, Kaihua Ding, Peng Zhang</i>	57
S1-050	GIANT-REGAIN: A comprehensive analysis of geodetic GNSS recordings in Antarctica for geodetic and geodynamic applications	<i>Eric Buchta, Mirko Scheinert, Peter Busch, Matt A. King, Terry Wilson, Christoph Knöfel, Eric Kendrick, Demián Gómez, Michael Bevis, Martin Horwath</i>	58
S1-051	Towards an European Deformation Model	<i>Elmar Brockmann, Simon Lutz</i>	59
S1-052	Research on the realization of the regional reference frame	<i>Fan Wang, Danan Dong</i>	60
S1-053	Frame accuracy of daily/weekly combined EPN solutions	<i>Miltiadis Chatzinikos, Christopher Kotsakis</i>	61
S1-054	Scientific goals and strategic actions of EUREF in a changing landscape.....	<i>Martin Lidberg, Carine Bruyninx, Elmar Brockmann, Rolf Dach, Ambrus Kenyeres, Karin Kollo, Juliette Legrand, Tomas Liwosz, Rosa Pacione, Martina Sacher, Wolfgang Söhne, Christof Völksen, Zuheir Altamimi, Alessandro Caporali, Markku Poutanen</i>	62

S1.5: Comparison and combination of space geodesy techniques for improving consistency between TRF, CRF and EOPs

S1-055	Astronomy VLBA campaign MOJAVE used in geodesy	<i>Hana Krasna, Leonid Petrov</i>	65
S1-056	Estimation of Earth rotation parameter UT from Lunar Laser Ranging observations.....	<i>Liliane Biskupek, Vishwa Vijay Singh, Juergen Mueller, Mingyue Zhang</i>	66
S1-057	Multi-technique Integrated Processing on the Observation Level for Consistent Determination of TRF, CRF and EOPs.....	<i>Jungang Wang, Maorong Ge, Susanne Glaser, Robert Heinkelmann, Harald Schuh</i>	67
S1-058	Automatic detection of offsets in GNSS station position time-series using DIA and multivariate analysis algorithm.....	<i>Jin Zhang, Lizhen Lian, Chengli Huang</i>	68
S1-059	The NTSC geodetic VLBI system and its application of UT1 measurements	<i>Yuanwei WU</i>	69
S1-060	Identify the Multi-technology systematic errors: the relations among reference point determination, telescope pointing calibration and VLBI observing	<i>Zhibin Zhang, Xiaohui Ma, Zhongmiao Sun, Ali Zhang, Ye Yuan, Zhengxiong Sun</i>	70
S1-061	Combination of GNSS and VLBI data for consistent estimation of Earth Orientation Parameters	<i>Lisa Lengert, Daniela Thaller, Claudia Flohrer, Hendrik Hellmers, Anastasiia Girdiuk</i>	71
S1-062	Earth rotation parameters estimation using satellite laser ranging measurements to multiple LEO satellites	<i>Hongmin Zhang, Yongqiang Yuan, Qian Zhang, Jiaqi Wu, Wei Zhang, Yujie Qin, Xingxing Li</i>	72

S1-063	Combination of the VLBI, GNSS and LLR station coordinates using SINCOM software..... <i>Svetlana Mironova, Sergei Kurdubov, Iskander Gayazov</i>	73
S1-064	Inter- and intra-technique evaluation of UT1-UTC estimates using Legacy S/X VLBI, VGOS and their combination with co-located GNSS. A case study comparing INT1 to VGOS-B sessions... <i>Periklis-Konstantinos Diamantidis, Rüdiger Haas, Eskil Varenius, Matthias Schartner, Saho Matsumoto</i>	74
S1-065	Weekly Terrestrial Reference Frame realization from a combination of GNSS/SLR/VLBI/DORIS at the parameter level..... <i>Lizhen LIAN, Chengli HUANG, Jin ZHANG</i>	75
S1-066	Geodetic VLBI observations in single-frequency mode with 30-meter Warkworth radio telescope <i>Oleg Titov, Alexei Melnikov, Sergey Gulyaev, Stuart Weston Weston, Tim Natusch, Fengchun Shu, Bo Xia, Mikhail Kharinov</i>	76

S1.6: Vertical Reference Systems: methodologies, realization, and new technologies

S1-067	Geodetic SAR for Height System Unification and Sea Level Research - Observation Concept and Results in the Baltic Sea <i>Thomas Gruber, Jonas Ågren, Detlef Angermann, Artu Ellmann, Christoph Gisinger, Jolanta Nastula, Markku Poutanen, Marius Schlaak, Faramarz Nilfouroushan, Sander Varbla, Ryszard Zdunek, Simo Marila, Andreas Engfeldt, Timo Saari, Anna Świątek⁶, Xanthi Oikonomidou</i>	78
S1-068	Estimation of vertical datum parameters of Hong Kong using the GBVP approach based on combined global geopotential models <i>Panpan Zhang, Lifeng Bao, Lin Wu, Qianqian Li, Hui Liu</i>	79
S1-069	Chronometric Height: a genuine general relativistic definition of height measures <i>Dennis Philipp, Hu Wu, Eva Hackmann, Claus Laemmerzahl, Juergen Mueller</i>	80
S1-070	Using kriging interpolation for local geoid construction: accuracy evaluation in dependence of point density <i>Emanuele Alcaras, Pier Paolo Amoroso, Ugo Falchi, Claudio Parente</i>	81

Symposium 2a: Earth's Static Gravity Field

S2a.1: Terrestrial, Marine and Airborne Gravimetry

S2a-001	Determination Of The Vertical Gravity Gradient At A Few Sites Of The Absolute Gravity Network Of Algeria <i>Rabah HAMIDI, Mohamed HAMOUDI</i>	83
S2a-002	Current status and future improvements of digital zenith camera VESTA..... <i>Inese Varna, Ansis Zarins, Augusts Rubans</i>	84
S2a-003	Preliminary Results of a Gravity Observing experiment at 848m under the earth surface <i>Xiaodong Chen, Miaomiao Zhang, Heping Sun, Jianqiao Xu, Jiangcun Zhou, Xiaoming Cui</i>	85
S2a-004	Extracting Long - Period Surface Waves Using Ambient Noise Data Recorded by Superconducting Gravimeters..... <i>Hang Li, Xiaodong Chen, Jianqiao Xu, Heping Sun, Jiangcun Zhou, Qingchao Liu, Miaomiao Zhang, Lingyun Zhang</i>	86
S2a-005	Recent Airborne Gravity Surveys in Denmark with Strapdown Technology..... <i>Tim Jensen, René Forsberg</i>	87

S2a-006	The Airborne Gravity Measurement for Development of a New Precise Gravimetric Geoid Model in Japan	MASAHIRO NAKASHIMA, Kento Iio, Yasuhiro Iitsuka, Shinobu Kurihara, Kumikazu Ochi, Shuichi Omori, Tokuro Kodama, Masato Kuroyanagi, Masami Handa, Hiroaki Yamamoto, Takashi Toyofuku, Chiaki Kato, Koji Matsuo	88
S2a-007	Results from a car-based 3D-strapdown gravimetry campaign in the Bavarian Estergebirge	Peter Schack, Roland Pail, Thomas Gruber	89
S2a-008	A Magnetic Field Calibration Approach to Mitigate Accelerometer Errors in Strapdown Gravimetry	Felix Johann, David Becker, Matthias Becker, Matthias Hoss, Alexander Löwer, Christoph Förste	90
S2a-009	An approach to airborne vector gravimetry based on spherical scaling functions	Vadim Vyazmin	91
S2a-010	Recent results of strapdown dynamic gravimeter on different platforms	KAIDONG ZHANG	92
S2a-011	Gravity anomalies of large lakes from ICESAT-2 laser altimetry.	Ole Baltazar Andersen, Nielsen Karina, Forsberg Rene	93
S2a-012	Strapdown airborne gravimetry: postprocessing algorithms and some results	Vadim Vyazmin, Andrey Golovan, Yuri Bolotin	94
S2a-013	The convergence of gravity change rates from repeated absolute gravity measurements	Mirjam Bilker-Koivula, Jaakko Mäkinen, Hannu Ruotsalainen, Jyri Näränen, Timo Saari	95
S2a-014	Moving base gravimetry on a land vehicle: The first results from a short traverse drive in central Turkey.....	İlyas AKPINAR, Mehmet SİMAV, Kamil TEKE, Yunus Aytaç AKDOĞAN, Hasan YILDIZ, Murat DURMAZ	96
S2a-015	Validation of the Hellenic gravity network in the frame of the ModernGravNet project.....	Vassilios Grigoriadis, Vassilios Andritsanos, Dimitrios Natsiopoulos	97
S2a-016	Evaluation of the Muquans Absolute Quantum Gravimeter AQG-A02 against a precise gravity reference	Julian Glässel, Hartmut Wziontek, Axel Rülke	98

S2a.2: Vertical Reference Systems: methodologies, realization, and new technologies

S2a-017	Realization of the International Height Reference System in the region of Mount Qomolangma (Everest).....	Tao Jiang, Yamin Dang, Chunxi Guo, Chuanyin Zhang	100
S2a-018	First attempt to establish connection between the Russian height system and the International Height Reference System (IHRS)	Ilya Oshchepkov, Maria Gridchina	101
S2a-019	Can the Earth Gravitational Model augmented by the Topographic Gravity Field Model realize the International Height Reference System accurately?	Jianliang Huang, Marc Véronneau, John W. Crowley, Bianca D'Aoust, Goran Pavlic	102
S2a-020	An overview of SIRGAS activities towards the IHRF	Gabriel do Nascimento Guimarães, Ana Cristina Oliveira Cancoro de Matos, Ayelen Pereira, Ezequiel Darío Antokoletz, José Luis Carrión Sánchez, Laura Sánchez, SIRGAS WG III Team	103
S2a-021	GEOPOTENTIAL NUMBER FOR THE IHRF ESTABLISHMENT IN BRAZIL	Valeria Silva, Gabriel do Nascimento Guimarães, Denizar Blitzkow, Ana Cristina Oliveira Cancoro de Matos, Iuri Bjorkstrom	105
S2a-022	An Investigation on the Geoid-Quasigeoid Separation with the Case Study in Colorado, U.S.	Mustafa Serkan Işık, Bihter Erol, Muhammed Raşit Çevikalp, Serdar Erol	106

S2a-023	Status of the International Height Reference Frame (IHRF)	107
 <i>Laura Sanchez, on behalf of the IHRF Computation Team</i>	

S2a.3: Local and Regional Geoid and Gravity Modelling

S2a-024	Examining the optimal depth of the condensed topographic masses for precise geoid determination based on the Stokes-Helmert scheme – A case study in Colorado ...	109
 <i>Koji Matsuo</i>	
S2a-025	Local gravity field modelling in spatial domain using the FEM approach on the discretized Earth's surface: case study in Slovakia	110
 <i>Robert Cunderlik, Marek Macák, Zuzana Minarechová, Karol Mikula</i>	
S2a-026	Iterative refinement of regional marine geoid models by using sea surface height and dynamic topography datasets	111
 <i>Sander Varbla, Artu Ellmann</i>	
S2a-027	Gravimetric Geoid Modeling by Stokes and Second Helmert's Condensation Method in Yogyakarta, Indonesia	112
 <i>Brian Bramanto, Kosasih Prijatna, Muhammad Syahrullah Fathulhuda, Arisauna Maulidyan Pahlevi</i>	
S2a-028	On the Optimum DHM Resolution for the Window Remove-Restore Technique: Case Study for Africa	113
 <i>Hussein Abd-Elmotaal, Norbert Kührtreiber</i>	
S2a-029	Preliminary results of the spatial distribution of tidal factors measured by recent continuous gravity stations	114
 <i>Jin Wei, Chongyang Shen, Mingzhang Hu, Ying Jiang, Ziwei Liu</i>	
S2a-030	Improved geoid models in Taiwan and its offshore islands	115
 <i>Huang Wenhsuan, Hwang Cheinway</i>	
S2a-031	Integrating NGS GRAV-D gravity observations into high-resolution global models	116
 <i>Philipp Zingerle, Xiaopeng Li, Martin Willberg, Roland Pail, Daniel R. Roman</i>	
S2a-032	Gravimetric quasigeoid modelling by the GGI method in the Colorado mountains area	117
 <i>Marek Trojanowicz, Magdalena Owczarek-Wesołowska, Yan Ming Wang, Olgierd Jamroz</i>	
S2a-033	Regularization parameter determination in case of combining different types of gravity data for regional gravity field refinement	118
 <i>Qing Liu, Michael Schmidt</i>	
S2a-034	Application of 3-dimensional least-squares collocation for free-air vertical gravity gradient modelling	119
 <i>Yunus Aytaç Akdoğan, Gonca Okay Ahi, Hasan Yildiz</i>	
S2a-035	On the computation of the complete geoid-quasigeoid separation term for the experiential geoid 2020	120
 <i>Yanming Wang, Marc Veronneau, Jianliang Huang, Kevin Ahlgren, Xiaopeng Li, Jordan Krcmaric, Ryan Hardy, David Avalos</i>	
S2a-036	Modernization of the Danish Gravity Network in Preparation of the New 5 mm Danish Geoid ...	121
 <i>Hergeir Teitsson, René Forsberg, Gabriel Strykowski, Tim Enzlberger Jensen, Adolffientje Kasenda Olesen, Kristian Keller</i>	
S2a-037	A new model of the quasigeoid for the Baltic Sea area	122
 <i>Adam Łyszkowicz, Adam Łyszkowicz, Janusz Zieliński, Monika Biryło</i>	
S2a-038	Seamless Processing for Shipborne Gravity Data	123
 <i>Baogui Ke, Jinzhong Mi, Chuanyin Zhang, Yamin Dang, Hanjiang Wen</i>	
S2a-039	A 3-Dimensional Realization of Molodensky Heights	124
 <i>Robert Kingdon, Ismael Foroughi, Marcelo Santos</i>	
S2a-040	The improvement of global earth's gravity field model with airborne gravity data: case study in Maowusu	125
 <i>Wei Liang, Xinyu Xu, Jiancheng Li</i>	

S2a-041	Assessments on Terrestrial Gravity Data Grid Densification and Its Effects on Local Geoid Modeling Accuracy	<i>Muhammed Raşit Çevikalp, Serdar Erol, Bihter Erol</i>	126
S2a-042	Gravimetric Geoid Modelling Using the Least Squares Modification of Hotine Integral in Turkey ·	<i>Mustafa Serkan Işık, Bihter Erol, Fatıma Feyza Sakil, Muhammed Raşit Çevikalp, Serdar Erol</i>	127
S2a-043	An improved regional gravity field solution for Antarctica for geodetic and geophysical applications	<i>Mirko Scheinert, Philipp Zingerle, Theresa Schaller, Roland Pail, Martin Willberg</i>	128
S2a-044	Indian gravimetric geoid model: IndGG-CUT2021	<i>Ropesh Goyal, Will Featherstone, Sten Claessens, Onkar Dikshit, Nagarajan Balasubramanian</i>	129
S2a-045	Filtering and downward continuation of GOCE SGG data for regional geoid improvement	<i>Dimitrios Natsiopoulos, Elisavet Mamagiannou, Eleftherios Pitenis, Georgios Vergos, Ilias Tziavos</i>	130
S2a-046	An oral rebuttal to “the shape of the quasigeoid”	<i>Marcelo Santos, Robert Kingdon, Petr Vaníček, Zdeněk Martinec, Ismael Foroughi</i>	131

S2a.4: Global Gravity Field Modelling

S2a-047	Reconstruction of mathematical foundations for satellite gravimetry from tracking: solutions to problems incorrectly solved for 100 years	<i>Peiliang Xu</i>	133
S2a-048	XGM202x: The impact of extending the dense modelling to d/o 1440	<i>Philipp Zingerle, Roland Pail, Thomas Gruber</i>	135
S2a-049	Analysis of the potential contribution of the Tianwen-1 extended mission to the solution of Mars' low-order gravity field	<i>Shanhong LIU, Jianguo YAN</i>	136
S2a-050	DTU21 Global high resolution gravity field - first evaluation	<i>Ole Baltazar Andersen, Adil Abulaitjiang, Shengjuin Zhang</i>	137
S2a-051	Numerical Algorithm and Realization of Ellipsoidal Harmonic Expansion of the Earth Gravity Field	<i>Cong Liu, Zhengtao Wang, Yang Xiao, Yonggang Zhang</i>	138
S2a-052	Joint modelling of the lithospheric and deep Earth gravity field to study the density structure of the lithosphere	<i>Bart Root, Javier Fulla, Zdenek Martinec, Jörg Ebbing, Sergei Lebedev</i>	139
S2a-053	On the Fast Computation of Model Gravity Gradient Tensor	<i>Zhibin Xing, Shanshan Li, Yao Meng, Na Yang, Qian Li, Jianchen Shan</i>	140
S2a-054	Establishment of the global geoid model 2021 (GGM2021)	<i>Wenbin Shen, Youchao Xie, Jiancheng Han, Jiancheng Li</i>	141

S2a.5: Satellite Altimetry and Oceanography

S2a-055	Performance of Five Satellite Altimetry Observations in Marine Gravity Inversion over the Gulf of Guinea	<i>Richard Annan, Xiaoyun Wan</i>	143
S2a-056	Altimeter-derived marine gravity variations reveal the magma mass motions within the subaqueous volcano	<i>Qianqian Li, Lifeng Bao, Lin Wu, Panpan Zhang, Hui Liu</i>	144
S2a-057	Optimal gravity anomaly and vertical gravity gradient in the South China Sea from multi-altimeter data	<i>Daocheng Yu, Cheinway Hwang</i>	145
S2a-058	Estimating Snow Depth in Arctic Using the Sea Ice Surface Height from Heterologous Altimeter Satellites	<i>Wenxuan Liu, Taoyong Jin, Hailan Huang</i>	146
S2a-059	DTU21 Mean Sea Surface for Vertical Offshore Reference Frame	<i>Ole Baltazar Andersen, Adil Abulaitjiang, Shengjuin Zhang, Stine Kildegaard Rose</i>	147

S2a-060	The mean dynamic topography and geostrophic current estimation based on a Least-square method.....	<i>Hongkai Shi, Yihao Wu, Ole Andersen, Xiufeng He</i>	148
S2a-061	Inversion of gravity anomalies in the South China Sea and Hawaii area derived from ICESat-2 ocean products	<i>Hang Li, Shengjun Zhang</i>	149
S2a-062	Radar Altimeter-Based Water Level and Wind Speed Monitoring Over the Laurentian Great Lakes	<i>Yuanyuan Jia, Philip Chu, C.K. Shum</i>	150

S2a.6: Gravity Inversion for Solid Earth

S2a-063	Correlation between gravitational and magnetic anomalies and crustal susceptibility in the Three Gorges area, China	<i>Yi Zhang, Yunlong Wu, Chao Chen, Kai Sun, Jiawei Wang</i>	152
S2a-064	Possible Deep Structure and Composition of Venus with Respect to the Current Knowledge from Geodetic Data	<i>Chi Xiao, Fei Li, Jianguo Yan, Michel Gregoire, Weifeng Hao, Harada Yuji, Mao Ye, Jean-Pierre Barriot</i>	153
S2a-065	Research on the basement depth of Sichuan basin with real gravity data	<i>Menglong Xu, Yabin Yang, Chengye Sun, Liang Chen, Gengen Qiu</i>	154
S2a-066	Crustal geological provinces seen by gravity field data: an automatic Bayesian approach applied to the Central Eastern Mediterranean area	<i>Martina Capponi, Daniele Sampietro</i>	156
S2a-067	The contribution of gravity to crust and upper mantle structure modeling – an example in Tibet Plateau.....	<i>Jiakuan Wan, Zhicai Luo</i>	157
S2a-068	Mapping the upper mantle thermochemical heterogeneity from coupled geophysical-petrological inversion of seismic waveforms, heat flow, surface elevation and gravity satellite data	<i>Javier Fullea, Sergei Lebedev, Zdenek Martinec, Nicolas Celli</i>	158
S2a-069	A Method of Determining Moho Topography from On-orbit GOCE Gravity Gradients: A Case Study in Tibetan Plateau	<i>Chuang Xu</i>	159
S2a-070	Improving the GEMMA inversion algorithm towards a new release of the GOCE-based crustal model.....	<i>Lorenzo Rossi, Mirko Reguzzoni, Biao Lu, Islam Fadel, Daniele Sampietro, Mark van der Meijde</i>	160
S2a-071	Crustal configuration of the West and Central African Rift System from gravity and seismic data analysis	<i>Franck Eitel Kemgang Ghoms, Robert Tenzer, Rebekka Steffen, Emmanuel Njinju</i>	161

S2a.7: Topography and Bathymetry Gravity Modelling

S2a-072	Marine Gravimetry, Ship Sounding and Ocean Bottom Topography Estimation in the South-western Coastal Area of the Baltic Sea	<i>Biao Lu, Chuang Xu, Jinbo Li, Bo Zhong, Mark van der Meijde</i>	163
S2a-073	The omission error modelling of global gravity field models using different digital terrain models	<i>Martin Pitonak, Matej Varga, Michal Sprlak</i>	164
S2a-074	Topographic gravity field modelling for improving high resolution global gravity field models.....	<i>E. Sinem Ince, Christoph Foerste, Oleh Abrykosov, Frank Flechtner</i>	165
S2a-075	Bathymetry of northeast Greenland revealed by Oceans Melting Greenland (OMG) airborne gravity	<i>Junjun Yang, Zhicai Luo, Liangcheng Tu</i>	166
S2a-076	Harmonic Correction for Residual Terrain Modelling (RTM) Technique in Physical Geodesy Applications	<i>Meng Yang, Xiao-Le Deng, Wei Feng, Chang-Qing Wang, Min Zhong</i>	167

Symposium 2b: Earth's Time-variable Gravity Field

S2b.1: Analysis Techniques

S2b-001	Monthly low-degree gravity field models from Swarm GPS data for the last 7 years····· ····· <i>Joao Encarnacao, Daniel Arnold, Ales Bezdek, Christoph Dahle, Junyi Guo, Jose van den IJssel, Adrian Jaeggi, Jaroslav Klokocnik, Sandro Krauss, Torsten Mayer-Guerr, Ulrich Meyer, Josef Sebera, CK Shum, Pieter Visser, Yu Zhang</i>	169
S2b-002	Status of temporal gravity field modeling at HUST····· ····· <i>Hao Zhou, Zhicai Luo, Lijun Zheng, Yaozong Li, Kang Wang</i>	170
S2b-003	Angular velocity recovery method based on satellite gravity gradient measurement based on quaternion joint of astrometry····· <i>Yunlong Wu</i>	171
S2b-004	Time-variable Gravity Signals in Reprocessed GOCE Gradient Data····· ····· <i>Betty Heller, Frank Siegismund, Roland Pail, Thomas Gruber, Roger Haagmans</i>	172
S2b-005	HUST-ERA5: A new 1-hourly atmosphere de-aliasing product for satellite gravity mission····· ····· <i>Fan Yang, Zhicai Luo</i>	173
S2b-006	Treatment of ocean tide background model errors in GRACE/GRACE-FO data processing ···· ····· <i>Petro Abrykosov, Roman Sulzbach, Roland Pail</i>	174
S2b-007	Combination Service for Time-variable Gravity fields (COST-G): operations and new developments ······ <i>Ulrich Meyer, Martin Lasser, Adrian Jäggi, Frank Flechtner, Christoph Dahle, Eva Boergens, Christoph Förste, Torsten Mayer-Gürr, Andreas Kvas, Saniya Behzadpour, Jean-Michel Lemoine, Stephane Bourgogne, Igor Koch, Jakob Flury, Andreas Groh, Annette Eicker, Benoît Meyssignac, Ingo Sasgen, João de Teixeira da Encarnação, Heike Peter, Hao Zhou, Zhengwen Yan, Qiujie Chen, Xiang Guo, Wei Feng, Changqing Wang</i>	175
S2b-008	On the combination of gravity field time series derived from kinematic positions of Low Earth Orbiting satellites····· ····· <i>Thomas Grombein, Martin Lasser, Daniel Arnold, Ulrich Meyer, Adrian Jäggi</i>	176
S2b-009	Combined gravity solution from SLR and GRACE/GRACE-FO····· ····· <i>Zhigui Kang, John Ries, Srinivas Bettadpur, Himanshu Save</i>	177
S2b-010	Determination of Terrestrial Water Storage without Stripes using Grace-Like Geopotential Models····· <i>Hussein Abd-Elmotaal, Ayman Hassan, Mostafa Abd-Elbaky</i>	178
S2b-011	Data-Driven Self-De-Aliasing approach for monthly GRACE and GRACE-FO gravity retrieval ·· ····· <i>Michael Murböck, Petro Abrykosov, Christoph Dahle, Frank Flechtner, Roland Pail</i>	179
S2b-012	LOW-DEGREE GRAVITY FIELD ESTIMATION FROM THE SLR DATA PROCESSING OF SPHERICAL SATELLITES ······ ····· <i>Linda Geisser, Ulrich Meyer, Thomas Grombein, Daniel Arnold, Adrian Jäggi</i>	180
S2b-013	On Validating the Swarm Data to Fill-in the GRACE/GRACE-FO Gap Employing Artificial Neural Networks Applied to Africa ······ ····· <i>Hussein Mohasseb, WenBin Shen, Mostafa Ashry, Hussein Abd-Elmotaal</i>	181
S2b-014	High-precision Light Time Correction Model in GRACE and GRACE Follow-On Mission ····· <i>Yihao Yan, Vitali Müller, Changqing Wang, Min Zhong, Wei Feng, Lei Liang</i>	182
S2b-015	Evaluating the regional reanalysis COSMO REA6 vs ERA Interim for dealiasing analysis of the GRACE/GRACE-FO Datasets····· <i>Shashi Dixit, Petra Freidrichs, Andreas Hense</i>	183

S2b.2: Spaceborne and terrestrial gravimetry for hydrology

S2b-016	Sub-regional groundwater storage recovery in North China Plain after the South-to-North water diversion project	<i>Chong Zhang, Qingyun Duan, Pat J.-F. Yeh, Yun Pan</i>	185
S2b-017	Gravity response to a monsoonal rain event in the Pingtung Plain, southern Taiwan	<i>KUAN-HUNG CHEN, Cheinway Hwang</i>	186
S2b-018	Retrieving daily terrestrial water storage changes based on an independent component analysis-based inversion method	<i>Zhongshan Jiang, Dingfa Huang</i>	187
S2b-019	Quantifying water storage change over Lake Baikal using GRACE and GRACE Follow-On	<i>Min Wei, Hao Zhou, Zhicai Luo, Min Dai, Siyou Xu</i>	188
S2b-020	Reconstructing Climate-driven Water Storage Anomalies using GRACE Satellite Data	<i>Bingshi Liu, Xiancai Zou, Shuang Yi, Nico Sneeuw, Jianqing Cai, Jiancheng Li</i>	189
S2b-021	Reconstruction of Water Storage Change and Drought Monitoring in the Yangtze River Basin Combining Satellite Gravity and Hydrological Data	<i>Xiaolong Li, Taoyong Jin</i>	190
S2b-022	Inversion of Regional Surface Mass Anomalies using GRACE Geopotential Differences Based on Slepian Basis Functions	<i>Jiangtao Tan, Bo Zhong, Xianpao Li, Tao Liu</i>	191
S2b-023	Drought Events over the Amazon River Basin (1993-2019) as Detected by the Climate-driven Total Water Storage Change	<i>Kunjun Tian, Zhengtao Wang, Fupeng Li, Yu Gao, Yang Xiao, Cong Liu</i>	192
S2b-024	Using Swarm to Detect Total Water Storage Changes in 26 Global Basins (Taking the Amazon Basin, Volga Basin and Zambezi Basin as Examples)	<i>Zhengtao Wang, Kunjun Tian, Fupeng Li, Si Xiong, Yu Gao, Lingxuan Wang, Bingbing Zhang</i>	193
S2b-025	Method for GRACE/GRACE-FO data de-stripe based on image processing perspective	<i>Peng-Hui Wang, Hao Zhou, Zhi-Cai Luo, Lu Tang</i>	194
S2b-026	Detect Songhua River Basin Groundwater Spatiotemporal Variation Characteristics by GRACE and Multi-source Hydrological Data	<i>Zhiming XU, Zhengtao WANG</i>	195
S2b-027	Hydrological Load Effect in the Tibetan Plateau: from GRACE or Hydrological data?	<i>Weilong Rao, Wenke Sun</i>	196
S2b-028	Monitoring groundwater storage change in China by satellite gravimetry	<i>Xiaotao Chang, Guang Zhu, Wei Liu, Miao Zhou, Haozhe Zhang, Qingliang Que</i>	197
S2b-029	Recent Changes in Surface and Groundwater in Large Arctic River Basins	<i>Hong Lin, Xiao Cheng, Lei Zheng</i>	198
S2b-030	Machine Learning approach to study groundwater depletion in Central Valley, California using GRACE and other hydrological data	<i>VIBHOR AGARWAL, Orhan Akyilmaz, CK Shum, Wei Feng, Ehsan Forootan, Umesh Haritashya, Tajdarul Syed</i>	199
S2b-031	Monitoring fast water storage variations in Karst through gravimetry: a study case from the Classical Karst	<i>Tommaso Pivetta, Carla Braitenberg, Franci Gabrovšek, Bruno Meurers, Gerald Gabriel</i>	201
S2b-032	Bridging the gap between GRACE and GRACE-FO by simulating GRACE-like terrestrial water storage anomalies using deep machine learning tools	<i>Merve Keleş, Tuğçe Ay, Bihter Tandoğdu, Metehan Uz, Yu Zhang, Orhan Akyilmaz, C.K. Shum, Kazım Gökhan Atman</i>	203
S2b-033	Regional inversion of GRACE/-FO KBRR/-LRI observations to estimate high resolution total water storage changes	<i>Metehan Uz, Yu Zhang, Orhan Akyilmaz, Junyi Guo, C.K. Shum</i>	205

S2b-034	Inter-annual terrestrial water storage changes over the Lake Victoria region from GRACE/GFO and satellite altimetry observations	<i>Jin Li, Song-Yun Wang, Jianli Chen, Xiaogong Hu</i>	206
S2b-035	Flood monitoring over the Yangtze River basin using GLDAS daily data products based on GRACE data assimilation	<i>Xiao Yan, Bao Zhang, Yibin Yao</i>	207
S2b-036	Satellite Gravimetry-based Monitoring System for Natural Hazards and Water Resources Management	<i>C K Shum, Yu Zhang, Orhan Akyilmaz, Ehsan Forootan, Wei Feng, Metehan Uz</i>	208

S2b.3: Cryospheric changes from gravity data

S2b-037	Advanced estimation of regional ice mass losses in Greenland from GRACE data	<i>Linyang XIN, Jiangjun RAN</i>	210
S2b-038	Performance of Tongji-RegGrace2019 Solution over Major Mountain Glaciers	<i>Wei Wang, Yunzhong Shen, Qiujie Chen</i>	211
S2b-039	New Constrains on Glacier Mass Balance on High Mountain Asia	<i>Qiuyu Wang, Shuang Yi, Wenke Sun</i>	212
S2b-040	An Investigation on the Ice Mass Loss in Antarctica Using Different Geosensors Data	<i>Bilal Mutlu, Serdar Erol, Bihter Erol</i>	213
S2b-041	Inter-annual variability in the Antarctic ice sheets using multi-technique geodesy and modeling	<i>Athul Kaitheri, Anthony Mémin, Frédérique Rémy</i>	214
S2b-042	Antarctica Ice-Mass Variations on Intraseasonal-Interannual Timescale: East-West Coastal Dipole and Eastward Circumpolar Wave	<i>Zhen Li, Benjamin Fong Chao, Hansheng Wang</i>	215
S2b-043	Two decades of Antarctic surface elevation changes from multi-mission satellite altimetry and gravimetry	<i>Lianzhe Yue, Nengfang Chao, Shuai Wang, Ying Hu, Yanze Zhang</i>	216
S2b-044	Mass Variations of the Greenland Ice Sheet based on GRACE/GARCE Follow-On Satellite Gravimetry and Mass Budget Method	<i>Peisi Shang, Xiaoli Su, Zhicai Luo</i>	217
S2b-045	Low Degree Spherical Harmonic Influences on Polar Ice Sheet Mass Change Derived from GRACE/GRACE-FO Gravimetry	<i>Xiaoli Su, Junyi Guo, C.K. Shum, Zhicai Luo, Lin Liu</i>	218
S2b-046	Bridging the data gap between GRACE and GRACE-FO using artificial neural network in Greenland	<i>Bao Zhang, Yulin He, Yibin Yao</i>	219
S2b-047	Filling the data gaps within GRACE missions using Singular Spectrum Analysis	<i>Shuang Yi, Nico Sneeuw</i>	220
S2b-048	Extraction of GRACE/GRACE-FO Observed Mass Change Patterns across Antarctica via Independent Component Analysis (ICA)	<i>Tianyan Shi, Yoichi Fukuda, Koichiro Doi, Jun'ichi Okuno</i>	221

S2b.4: Satellite Altimetry and Oceanography

S2b-049	Quantitative Analysis of Global Sea-Level Budget Based on GRACE, Satellite Altimetry and Argo Observations	<i>Fengwei Wang, Yunzhong Shen, Qiujie Chen</i>	223
S2b-050	The ways to improve the accuracy of determining the height of the geoid using GNSS signals reflected from the ocean surface	<i>Vladislav Lopatin, Vyacheslav Fateev</i>	224
S2b-051	Leading Edge Identification with Prior Information (LEIPI): a new approach to retracking inland altimetry waveforms	<i>Nico Sneeuw, Sajedah Behnia, Mohammad Tourian</i>	225

S2b-052	Data quality analysis of Argo float observations from 2016 to 2020	227
 <i>Lu Tang, Jin Li, Hao Zhou, Zhicai Luo, Penghui Wang</i>	
S2b-053	Quantifying the precision of retracked Jason-2 sea level data in the 0-5 km Australian coastal zone	228
 <i>Fukai Peng, Xiaoli Deng, Xiao Cheng</i>	
S2b-054	Global Ocean Mass Change Estimates in 1993~2004 from LEO Gravity Field Models Determined at Tongji University	229
 <i>Qiuji Chen, Xingfu Zhang, Fengwei Wang, Yunzhong Shen</i>	
S2b-055	Spatial-temporal prediction of regional sea level changes from the ocean Climate Data Records	230
 <i>Ruiyang Cai, Jian Zhao</i>	
S2b-056	Mechanism of Interannual Variability of Ocean Bottom Pressure in the South Indian Ocean	231
 <i>Yuting Niu, Jianhuang Qin, Xuhua Cheng</i>	
S2b-057	High-resolution water level changes in coastal and estuarine regions in North Sea and Baltic ..	
 <i>Luciana Fenoglio, Joanna Staneva, Salvatore Dinardo, Jürgen Kusche, Jerome Benveniste, Matthias Gärtner, Bernd Uebbing</i>	232
S2b-058	Detecting regional deep ocean warming below 2000m based on altimetry, GRACE, Argo, and CTD data	233
 <i>Yuanyuan Yang, Min Zhong, Wei Feng, Dapeng MU</i>	
S2b-059	Retracking of radar altimetry waveforms over inland water bodies	
 <i>Xiaoli Deng, Andrew Marshall, Fukai Peng</i>	234
S2b-060	Impact of hydrological loading signals on the tide gauge observations of sea level	
 <i>Balaji Devaraju, Milaa Murshan</i>	235
S2b-061	Spatio-temporal variations of the steric sea level in the seas around India during the GRACE era	
 <i>Balaji Devaraju, Gaurav Jiwan, Shivam Chaudhary, Yasir Malik</i>	236

S2b.5: Gravity Inversion for Solid Earth

S2b-062	Vertical Deformation Analysis with GNSS and GRACE Data in North China Using Independent Component Analysis	238
 <i>Tengfei Feng, Yunzhong Shen, Qiuji Chen</i>	
S2b-063	Comparison of GRACE and GNSS seasonal load displacements considering regional averages and discrete points	239
 <i>Lan Zhang, He Tang, Wenke Sun</i>	
S2b-064	Data-driven separation of past and present-day surface loading from GRACE and GNSS observations	
 <i>Yann Ziegler, Bramha Dutt Vishwakarma, Aoibheann Brady, Stephen Chuter, Sam Royston, Jonathan Rougier, Richard Westaway, Jonathan Bamber</i>	240
S2b-065	Coseismic gravity changes of the Wenchuan earthquake observed by surface gravimetry	
 <i>Hongtao Hao, Minzhang Hu</i>	241
S2b-066	Horizontal deformation of GNSS on the improvement of mass load inversion	
 <i>Song-Yun Wang, Jin Li, Jianli Chen, Pengfei Wang</i>	242
S2b-067	Time-Space Characteristics of Viscoelastic Post-Seismic Deformations Corresponding to Different Rheology Models	
 <i>He Tang, Wenke Sun</i>	243

S2b.6: Future Gravity Mission Concepts

S2b-068	The expected performance of the inclined satellite formation mission for temporal gravity field determination	245
 <i>Hao Zhou, Zhicai Luo</i>	

S2b-069	Simulation studies for a Mass change And Geosciences International Constellation (MAGIC) – An ESA/NASA joint mission concept in preparation	<i>Roland Pail, Frank Flechtner, Sean Bruinsma, Pieter Visser, Andreas Güntner, The MAGIC Science Team</i>	246
S2b-070	Laser space gravity gradiometer with free test mass	<i>Ruslan Davlatov, Vyacheslav Fateev</i>	247
S2b-071	Multi-satellite formations and constellations of CubeSats and their potential in NGGMs	<i>Nikolas Pfaffenzeller, Roland Pail</i>	248
S2b-072	GRACE-I mission for gapless observation of mass transport and biodiversity	<i>Frank Flechtner, Christoph Dahle, Markus Hauk, Josefine Wilms, Michael Murböck</i>	249
S2b-073	Mass change And Geosciences International Constellation (MAGIC) – An ESA/NASA joint mission in preparation	<i>Ilias Daras, Lucia Tsaoussi, Charley Dunn, Roger Haagmans, Günther March, Luca Massotti, Bernardo Carnicero, Charles Webb, Pierluigi Silvestrin</i>	251
S2b-074	Climatological, tectonic and volcanic gravity signals compared to the sensitivity of the proposed MOCAS+ gravity mission	<i>Carla Braitenberg, Alberto Pastorutti, Tommaso Pivetta</i>	253
S2b-075	Simulations of the Next Generation Gravity Field Missions Based on Multi-Pair Constellations and Status of Chinese TianQin Mission	<i>Wei Feng, Changqing Wang, Yihao Yan, Min Zhong, Hou-Tse Hsu, Meng Yang, Hsien-Chi Yeh</i>	255
S2b-076	Simulations on gravity field recovery from potential differences and gravity gradients for the MOCAS+ quantum mission proposal	<i>Öykü Koç, Khulan Batsukh, Lorenzo Rossi, Mirko Reguzzoni, Federica Migliaccio</i>	256

Symposium 3: Earth Rotation and Geodynamics

S3.1: Earth rotation, low-degree gravitational change and mass transport in geophysical fluids

S3-001	Influence of core-mantle topographic coupling on the frequency of the free core nutation	<i>Huifeng Zhang, Wenbin Shen</i>	258
S3-002	Why the Earth accelerates its rotation since 2016?	<i>Leonid Zotov, Olesya Marchukova, Christian Bizouard, Nikolay Sidorenkov</i>	259
S3-003	Preparations for a Second Earth Orientation Parameters Prediction Comparison Campaign	<i>Jolanta Nastula, Henryk Dobslaw, Justyna Śliwińska, Tomasz Kur, Małgorzata Wińska, Aleksander Partyka</i>	260
S3-004	Oceanic mass-related excitation of polar motion: an assessment based on GRACE and multi-mission satellite altimetry	<i>Franziska Göttl, Dharani Jyothi Nandagopalakrishnan, Sam Royston, Michael Schmidt, Christian Schwatke, Florian Seitz</i>	261
S3-005	Characterization of a noise level of hydrological and cryospheric angular momentum determined from GRACE and GRACE Follow-On data	<i>Justyna Śliwińska, Małgorzata Wińska, Jolanta Nastula, Aleksander Partyka, Tomasz Kur</i>	262
S3-006	Long-Range Predictability of the Length of Day and Extratropical Climate.	<i>Adam Scaife</i>	263
S3-007	The Earth and Mars' Variable Rotations Excited by Surficial Fluids	<i>Yonghong Zhou, Xueqing Xu, Cancan Xu, Zhaoyang Kong, Xianran An, Xinhao Liao, Jianli Chen, David Salstein</i>	264

S3-008	On improved precession-nutation models	265
 <i>Jose M. Ferrandiz, Miguel A. Juárez, Santiago Belda, Tomás Baenas, Sadegh Modiri, Robert Heinkelmann, Alberto Escapa, Harald Schuh</i>	
S3-009	Effects of the observed Earth's oblateness variation on precession-nutation: A first assessment	266
 <i>Jose M. Ferrandiz, Alberto Escapa, Tomás Baenas, Ahmed Z. Zerifi, Isabel Vigo</i>	
S3-010	Chandler wobble excitation by external geophysical fluids estimated from GRACE gravity data	267
 <i>Aleksander Brzezinski, Justyna Sliwiska</i>	
S3-011	Internal co-seismic displacement and strain changes inside a homogeneous spherical Earth	268
 <i>Jie Dong, Pengfei Cheng, Hanjiang Wen, Wenke Sun</i>	

S3.2: Observations and modeling of deformation related to changing ice loads

S3-012	Spatiotemporal glacial isostatic model resolution testing for small ice loads: Input parameter recommendations and examples for mountain glaciers in southcentral and southeast Alaska	270
 <i>Kimberly DeGrandpre, Jeffrey Freymueller</i>	
S3-013	GNSS observations and GIA modelling of vertical crustal motion in the Lützow-Holm Bay region, East Antarctica	271
 <i>Junichi Okuno, Akihisa Hattori, Takeshige Ishiwa, Yoshiya Irie, Yuichi Aoyama, Koichiro Doi, Yoichi Fukuda</i>	
S3-014	Dependence of upper mantle viscosity profile on GIA-induced gravity change in Antarctica	272
 <i>Yoshiya Irie, Jun'ichi Okuno, Takeshige Ishiwa, Koichiro Doi, Yoichi Fukuda</i>	
S3-015	The mid-Holocene sea-level highstand and Glacial Isostatic Adjustment modelling	273
 <i>Tanghua Li, Hansheng Wang, Stephen Chua, Nicole Khan, Patrick Wu, Benjamin Horton</i>	
S3-016	Vertical Land Motion From Present - Day Deglaciation in the Wider Arctic	274
 <i>Carsten Bjerre Ludwigsen, Ole Baltazar Andersen</i>	
S3-017	Bedrock uplift in response to recent ice-mass variability on northern Marguerite Bay, Antarctic Peninsula	275
 <i>Nahidul Hoque Samrat, Matt King, Christopher Watson, Andrea Hay, Valentina Barletta, Andrea Bordonni</i>	
S3-018	A study of sea level change around Greenland based on multi-source data	276
 <i>Jiachun An, Baojun Zhang, Zemin Wang, Songtao Ai, Yu Feng, Hong Geng</i>	
S3-019	Quantitative Analysis of Arctic Ice Flow Acceleration with Increasing Temperature	277
 <i>Zemin Wang, Boya Yan, Songtao Ai, Kim Holmén, Jiachun An, Hongmei Ma</i>	
S3-020	Surface mass balance loading displacement as a dominant source of error in GPS estimates of Antarctic glacial isostatic adjustment and its relevance to a critical sector of East Antarctica	278
 <i>Matt King, Christopher Watson</i>	
S3-021	Monitoring glacier mass balance of the West Kunlun Mountains over the past 20 years by ICESat-2 altimetry and bistatic InSAR	279
 <i>Tao Li, Liming Jiang</i>	
S3-022	Spatio-temporal evolution of the Greenland ice sheet and associated deformation of the Earth: a multi-technique geodetic approach	280
 <i>Ana Sanchez, Laurent Métivier, Luce Fleitout, Marianne Greff, Kristel Chanard, Romain Hugonnet, Etienne Berthier</i>	
S3-023	Glacier velocity monitoring and the potential points of geological hazards monitoring in A'nyemaqen Glacier	282
 <i>Zhaoxia Miao, Lin Bai, Zhenhong Li, Longyan Wang, Chenglong Zhang</i>	

S3.3: Geodetic observations in volcanic and tectonically active areas

S3-024	Horizontal and vertical deformation rates linked to the Magallanes-Fagnano Fault System, Tierra del Fuego: interpretation of the geodetic observations in the context of geological evidence and the current seismic cycle	<i>Luciano Pedro Oscar Mendoza, Andreas Richter, Eric Rodolfo Marderwald, José Luis Hormaechea, Gerardo Connon, Mirko Scheinert, Reinhard Dietrich, Raúl Anibal Perdomo</i>	284
S3-025	Crustal rheology and heterogeneity impact on tectonic stress characteristics of North China revealed by GNSS observations ..	<i>Yuan Gao, Wei Qu, Qin Zhang, Hailu Chen, Shichuan Liang</i>	285
S3-026	Spatiotemporal functional modeling of postseismic deformation after the 2011 Tohoku-Oki earthquake	<i>Satoshi Fujiwara, Mikio Tobita, Shinzaburo Ozawa</i>	286
S3-027	On the detection of structural breaks in GNSS station coordinate time series caused by earthquakes using machine learning	<i>Laura Crocetti, Matthias Schartner, Benedikt Soja</i>	287
S3-028	Grey Wolf Optimal Combination Algorithm for Inversion of Seismic Source Parameters: A Case Study of the Bodrum-Kos earthquake in 2017	<i>Longxiang Sun, Leyang Wang</i>	288
S3-029	Retrieving 3D coseismic deformation of the 2016 Mw 7.8 Kaikoura earthquake using different combinations of SAR and optical data	<i>Ajian Zou, Leyang Wang</i>	289
S3-030	Coeruptive and posteruptive crustal deformation associated with the 2018 Kusatsu-Shirane phreatic eruption based on PALSAR-2 time series analysis	<i>Yuji Himematsu, Taku Ozawa, Yosuke Aoki</i>	290
S3-031	Measuring the Recent Status of Land Subsidence in Bandung Basin, Indonesia, by InSAR and GPS methods	<i>Irwan Gumilar, Teguh Purnama Sidiq, Gigih Pambudi, Brian Bramanto, Hasanuddin Zainal Abidin</i>	291
S3-032	Earthquake Risk Analysis of Anqiu-Juxian Section of Yishu Fault Zone	<i>Cunpeng Du, Haitao Yin</i>	292
S3-033	Research on Integrating Multi-track InSAR Deformation Maps	<i>Jun Hua, Xinjian Shan, Wenyu Gong, Zhenjie Wang, Lingyun Ji, Chuanjin Liu, Yongsheng Li, Dezheng Zhao</i>	293
S3-034	InSAR observation and inversion of the seismogenic fault for The 2009 Yao'an Ms6.0 earthquake in China	<i>Bing Zhang, Yongchao Ma, Guochang Xu, Zhiping Lv</i>	294
S3-035	Complementary afterslip process following the 2016 Mw 7.8 Kaikoura earthquake from ~4 years GPS observations and its implication for seismic hazard	<i>Lupeng Zhang, Dingfa Huang, CK Shum</i>	295
S3-036	Preliminary forecast model of crustal earthquakes in southwest Japan based on GNSS data ..	<i>Takuya Nishimura</i>	296
S3-037	InSAR-derived earthquake catalog: Source locations and focal mechanisms of 30+ earthquakes (Mw4.1-6.6) in west China from time-series Sentinel-1 SAR images	<i>Teng Wang, Heng Luo, Shengji Wei, Mingsheng Liao</i>	297
S3-038	Monitoring The Activity of Changbaishan Tianchi Volcano with Time Series InSAR and Geophysical Modeling	<i>Jiaqi Zhang, Lianhuan Wei, Guoming Liu, Cristiano Tolomei, Guido Ventura, Elisa Trasatti, Christian Bignami, Stefano Salvi, Tiejun Gao, Francesca Romana Cinti</i>	298
S3-039	Estimation and correction of error sources in MTInSAR	<i>Hongyu LIANG, Lei ZHANG</i>	299
S3-040	Detecting transient signals in GPS time series using machine learning	<i>Xueming Xue</i>	300

S3-041	Causative fault geometries of two blinded dip-slip earthquakes in the interior of Asia Continent revealed by InSAR	<i>Yuqing He, Teng Wang, Lihua Fang, Li Zhao</i>	301
S3-042	COSEISMIC DEFORMATION DUE TO THE EARTHQUAKE IN SAN JUAN (ARGENTINA) OF JANUARY 18, 2021 (MW 6.4) AS MEASURED BY CONTINUOUS GNSS DISPLACEMENTS ·	<i>Juan Navarro, Silvia Miranda, Alfredo Herrada</i>	303
S3-043	Time-dependent Modeling of the Long-lasting Afterslip due to the 2016 Moderate Earthquakes along Chaman Fault using InSAR Time Series	<i>Masato Furuya, Matsumoto Fumiko</i>	304
S3-044	Mapping vertical crustal deformation over Weihe Basin, China using Sentinel-1 and ALOS-2 ScanSAR imagery	<i>Yufen Niu, Feifei Qu, Wu Zhu, Qin Zhang, Chaoying Zhao, Wei Qu, Yuxuan Hu</i>	305
S3-045	Earthquake triggering by tidal stresses at global scale	<i>Laurent Métivier, Marianne Greff-Lefftz, Gwendoline Pajot-Métivier, Kristel Chanard</i>	306
S3-046	Extraction of crustal deformation by using InSAR and GPS at the eastern margin of Tibet Plateau	<i>Weiwei Bian, Jicang Wu</i>	307
S3-047	The GNSS observed modulated seasonal signals in Yunnan, southwest China	<i>Weijie Tan, Junping Chen</i>	308
S3-048	Modeling of the volcano-tectonic activity of Deception Island (Antarctica) from 30 years of GPS observations (1991-2021)	<i>Belén Rosado, Manuel Berrocoso, Javier Antonio Ramírez-Zelaya, Alberto Fernández-Ros, Jorge Gárate, Gonçalo Prates, Amós de Gil</i>	309
S3-049	GNSS-GPS Time Series Analysis: Application to the southern region of the Iberian Peninsula and North Africa.	<i>Javier Antonio Ramírez Zelaya, Manuel Berrocoso Domínguez, Belén Rosado Moscoso, Alejandro Pérez Peña, Jorge Gárate Pasquín, Amos de Gil, Alberto Fernández-Ros, Gonzalo Prates, Paola Barba, Sonia Pérez-Plaza, Fernando Fernández-Palacín</i>	310

Symposium 4: Positioning and applications

S4.1: Geodetic Remote Sensing

S4-001	Estimation of 4D Atmospheric Water Vapor from GNSS and Infrared Sensor Data: A Combined Tomography Approach	<i>Wenyuan Zhang, Nanshan Zheng, Gregor Moeller, Nan Ding, Shubi Zhang</i>	312
S4-002	Evaluation of shipborne GNSS precipitable water vapor from six cruises based on multiple datasets	<i>Zhilu Wu, Cuixian Lu, Yuxin Zheng, Yang Liu, Yanxiong Liu, Qihua Tang</i>	313
S4-003	Soil moisture retrieved using multi-constellation and multi-frequency GNSS signals	<i>Nikolaos Antonoglou, Jens Wickert, Bodo Bookhagen</i>	314
S4-004	Remote Sensing of Soil Moisture using Spaceborne GNSS Relectometry Measurements	<i>Mina Rahmani, Jamal Asgari, Milad Asgarimehr</i>	315
S4-005	Alternative ionospheric correction algorithm for Galileo single frequency users	<i>M Mainul Hoque, Juan Andrés Cahuasquí</i>	316
S4-006	Application of the Total Variation Method in near real-time GNSS Tropospheric Tomography	<i>Zohreh Adavi, Robert Weber</i>	317

S4-007	Extracting ionospheric phase scintillation index from 1 Hz GNSS observations·····	
	····· <i>Dongsheng Zhao, Wang Li, Kefei Zhang</i>	318
S4-008	An operational GNSS processing system for near-real-time tropospheric ZTD and IWW monitoring in South America: breaking the 2-hour lateness barrier! ·····	
	····· <i>Juan Manuel Aragón Paz, Luciano Pedro Oscar Mendoza, Laura Isabel Fernández</i>	319
S4-009	Using the spaceborne GNSS-R coherent signals to detect the flood of South Asia ·····	
	····· <i>Qi Liu, Shuangcheng Zhang</i>	320
S4-010	IAG JWG 4.3.1 Real-time Ionosphere Monitoring and Modeling: Status during 2019-2021 ·····	
	<i>Ningbo Wang, Zishen Li, Yunbin Yuan, Manuel Hernández-Pajares, Alexis Blot, Andrzej Krankowski, Andre Hauschild, Alberto Garcia-Rigo, Andreas Goss, Attila Komjathy, Cheng Wang, Eren Erdogan, German Olivares, Kenji Nakayama, Libo Liu, Nicolas Bergeot, Qile Zhao, Raul Orús, Reza Ghoddousi-Fard, Wookyoung Lee, Xingliang Huo, Xiaodong Ren, Zhizhao Liu</i>	321
S4-011	Fast Snow Water Equivalent estimation with GPS interferometric reflectometry (GPS-IR) snow Depth·····	
	····· <i>Jiatong Wang, Yufeng Hu, Zhenhong Li, Chenglong Zhang, Miaomiao Zhang, Jing Yang, Wandong Jiang</i>	323
S4-012	From spaceborne to ground-based polarimetric observations: Is precipitation detectable in GNSS reflected signals? ·····	
	····· <i>Milad Asgarimehr, Mostafa Hoseini, Maximilian Semmling, Markus Ramatschi, Adriano Camps, Hossein Nahavandchi, Rüdiger Haas, Jens Wickert</i>	325
S4-013	Multi-GNSS Meteorology: Computation of tropospheric delays and gradients at GFZ Potsdam ·····	
	····· <i>Karina Wilgan, Galina Dick, Florian Zus, Jens Wickert</i>	327
S4-014	Bounding the Residual Tropospheric Error by Interval Analysis ·····	<i>Jingyao Su, Steffen Schön</i> 328
S4-015	Tomographic fusion strategies for the reconstruction of atmospheric water vapor·····	
	<i>Gregor Moeller, Chi Ao, Zohreh Adavi, Riccardo Biondi, Hugues Brenot, André Sá, George Hajj, Natalia Hanna, Chaiyaporn Kitpracha, Eric Pottiaux, Witold Rohm, Endrit Shehaj, Estera Trzcina, Kuo-Nung Wang, Karina Wilgan, Wen Yuan Zhang, Kefei Zhang</i>	329
S4-016	A New Method of Predicting the Global Ionospheric Map ·····	
	····· <i>Yan ZHANG, Ningbo WANG, Zishen LI</i>	330
S4-017	Near Real-Time Global Ionospheric Modeling Based on Multi-GNSS and Virtual Observation Stations ·····	
	····· <i>Xulei Jin, Shuli Song</i>	331
S4-018	ASHAK: Adjusted Spherical Harmonic and Kriging method for Regional Ionospheric TEC Modeling ·····	
	····· <i>Ang Liu, Zishen Li, Ningbo Wang, Yan Zhang, Hong Yuan</i>	332
S4-019	BDS/GNSS Atmospheric Monitoring And Retrieval Terminal (BDSMART): Progress and Experiment ·····	
	····· <i>Zishen Li, Ningbo Wang, Liang Wang, Kai Zhou, Hong Yuan</i>	333
S4-020	An enhanced atmospheric model of integrating GNSS CORS network and ERA5 for augmenting PPP-RTK ·····	
	····· <i>Yaxin Zhong, Cuixian Lv, Xingxing Li, Zhilu Wu, Yuxin Zheng, Bo Wang</i>	334
S4-021	Analysis of tropospheric estimates from multi-frequency low-cost GNSS receivers·····	
	····· <i>Katarzyna Stępniaak, Jacek Paziewski, Radosław Baryła</i>	335
S4-022	Based on InSAR Monitoring and Discrete Element Numerical Simulation Research on the Damage Trend Mountain Deformation in Jinsha River Basin ·····	
	····· <i>Xiong Guohua, Yang Chengsheng, Lv Sen, Dong Jihong, He Guoqiang</i>	336

S4-023	Near Real-time Regional Ionospheric Modeling and Navigation Enhancing..... <i>Chunyuan Zhou, Ling Yang, Bofeng Li, Xiaoning Su</i>	337
S4-024	Sensitivity of ship-borne GNSS troposphere retrieval to processing parameters <i>Aurélie Panetier, Pierre Bosser, Ali Khenchaf</i>	338
S4-025	Development of the next-generation GNSS-Meteo stations <i>Matthias Aichinger-Rosenberger, Alexander Wolf, Philippe Limpach, Gregor Moeller</i>	339
S4-026	Spatial-Temporal Characteristics of the Tropopause Height over Global Tropical and Subtropical Regions Using COSMIC-2 Radio Occultation Data <i>Jiaqi Shi, Kefei Zhang</i>	340
S4-027	GNSS-R coastal sea level altimetry with an open-source low-cost sensor: initial evaluation of high elevation angle satellites <i>Manuella Fagundes, Felipe Geremia-Nievinski</i>	341
S4-028	Comparison of the Effective Isotropic Radiate Power parameter in CYGNSS v2.1 and v3.0 level 1 data and its impact on soil moisture estimation <i>Paulo de Tarso SETTI JUNIOR, Tonie VAN DAM</i>	342
S4-029	Sea-ice signatures in coherently reflected GNSS signals: Findings from the MOSAiC expedition <i>Maximilian Semmling, Jens Wickert, Frederik Kreß, Mainul Hoque, Dmitry Divine, Sebastian Gerland</i>	343
S4-030	Detection of earthquake and tsunami signatures in the ionosphere from the combination of different observation techniques <i>Michael Schmidt, Andreas Goss, Eren Erdogan, Wojciech Jarmołowski, Pawel Wielgosz, Anna Krypiak-Gregorczyk, Beata Milanowska, Manuel Hernández Pajares, Alberto García-Rigo, Enric Monte-Moreno, Victoria Graffigna, Heng Yang, Anna Belehaki, Ioanna Tsagouri, Evangelos Paouris, Roger Haagmans</i>	344
S4-031	High-precision SLR tropospheric zenith delay prediction <i>Haoyue Zhang</i>	346
S4-032	Improving the global estimation of zenith wet delay and weighted mean temperature with machine/deep learning methods <i>Zhangyu Sun, Bao Zhang, Yibin Yao</i>	347
S4-033	A global latitude zone weighted mean temperature (T _m) augment method for empirical T _m model <i>Fei Yang, Di Zhang, Ming Chen, Jiming Guo, Xiaolin Meng</i>	348
S4-034	Sea level estimation using signal strength indicator data based on GNSS multipath reflectometry <i>Nazi Wang, Tianhe Xu, Fan Gao</i>	349
S4-035	Determination of water vapor content using low-cost dual-frequency GNSS receivers..... <i>Tomasz Hadas, Grzegorz Marut, Jan Kaplon, Witold Rohm</i>	350
S4-036	An improved method for real-time tropospheric delay modeling with a regional GNSS network · <i>Hongxing Zhang, Yunbin Yuan</i>	351
S4-037	Cross-polarization Correction for Soil Moisture Retrieval Using GNSS SNR data <i>Mutian Han, Dongkai Yang, Bo Zhang, Xuebao Hong</i>	352
S4-038	Further evaluation of a GNSS-R synthetic vertical array for high-rate water level altimetry <i>Mauricio Yamawaki, Felipe Geremia-Nievinski</i>	353
S4-039	Mitigating Long Wavelength Ocean Tide Loading Effects on InSAR Observations Over Wide Regions <i>Chen Yu, Nigel Penna, Zhenhong Li</i>	354
S4-040	An empirical zenith wet delay model using piecewise height functions based on a sliding window algorithm for China <i>Ge Zhu, Liangke Huang, Lilong Liu, Si Xiong, Junyu Li, Chao Ren</i>	355
S4-041	Satellite-based GNSS-R: A New Tool for Flood Monitoring — Flood monitoring of the Yangtze River Basin in 2020 using CYGNSS data <i>Wenxiao Ma, Xuerui Wu</i>	356

S4-042	An alternative MTInSAR framework for deformation retrieval over areas with heavy decorrelation	<i>Lei Zhang, Hongyu Liang</i>	357
S4-043	Spatial-temporal evolutionary behaviors of global ionospheric response to severe storms on 7-8 September 2017 using the GNSS, SWARM, COSMIC and TIE-GCM techniques	<i>Wang Li, Dongsheng Zhao, Kefei Zhang</i>	358
S4-044	The Study of the Coupling relationship between Land subsidence and Resources and Environmental carrying capacity in Plain area of Beijing	<i>Rui Liu</i>	359
S4-045	InSAR modeling and deformation estimation for drilling soluble rock salt mine based on CT-PIM function	<i>Xuemin Xing, Xiangbin Liu, Tengfei Zhang, Yikai Zhu, Wei Peng</i>	360
S4-046	Detection of snow depth on the Tibetan Plateau by satellite-based GNSS-R	<i>Wenxiao Ma, Xuerui Wu</i>	361
S4-047	The gridded tide corrections of the long-strip differential InSAR measurements estimated using the GPS network and tide models	<i>Wei Peng</i>	362
S4-048	Based on Sentinel-1A images revealing the co-seismic and post-seismic deformation mechanism of the Ms6.4 Jiashi earthquake in Xinjiang in 2020	<i>Ting Wang, Chengsheng Yang</i>	363
S4-049	The inversion, characterization and assessment of 3-D water vapor using tomography during typhoon weather over Hong Kong	<i>Laga Tong, Kefei Zhang</i>	364
S4-050	Recent activities of the JWG 4.3.4 - Validation of VTEC models for high-precision and high resolution applications	<i>Anna Krypiak-Gregorczyk, Attila Komjathy, Beata Milanowska, Wojciech Jarmołowski, Paweł Wielgosz, Qi Liu, Haixia Lyu, Manuel Hernández-Pajares, Andreas Goss, Eren Erdogan, Michael Schmidt, Mainul Hoque, Gu Shengfeng, Reza Ghoddousi-Fard, Raul Orus-Perez, Bruno Nava, Dieter Bilitza, Tam Dao, Shuanggen Jin, Yunbin Yuan, Heather Nicholson</i>	365
S4-051	TropNet: A deep spatio-temporal model for tropospheric parameters forecasting	<i>Yuxin Zheng, Cuixian Lu, Zhilu Wu</i>	366
S4-052	Current status of the IAG working group 4.3.7 on geodetic GNSS-R	<i>Sajad Tabibi, Felipe Geremia-Nievinski, Nikolaos Antonoglou, Karen Boniface, Estel Cardellach, Clara Chew, Rüdiger Haas, Thomas Hobiger, Chung-Yen Kuo, Kristine Larson, Wei Liu, Manuel Martín-Neira, Jihye Park, Dave Purnell, Joerg Reinking, Ole Roggenbuck, Maximilian Semmling, Rashmi Shah, Kegen Yu, Jens Wickert, Simon Williams</i>	367
S4-053	Multi-mode multi-frequency GNSS-IR combination method for water level retrieval	<i>Xiaolei Wang, Xiufeng He</i>	369
S4-054	Land subsidence monitoring in Tongzhou and Three Northern Counties of Langfang based on time series InSAR Technology	<i>Sun GuangTong</i>	370
S4-055	Research on segmented fitting ranging model based on multiple filter	<i>Wang Minmin, Deng Yang, Jian Wang</i>	371
S4-056	Analysis of the BDGIM Performance in BDS Single Point Positioning	<i>Guangxing Wang, Zhihao Yin, Zhigang Hu, Yadong Bo</i>	372
S4-057	Landslide Detection and Segmentation Using Mask R-CNN with Simulated Hard Samples	<i>Wandong Jiang, Jiangbo Xi, Xinyu Dou, Ligong Yang</i>	373

S4-058	Feasibility of GNSS-R Altimetry Using CyGNSS 8-Satellite Constellation Mission Data	
	<i>C K Shum, Yuchan Yi, Weiqiang Li, Yihang Ding, Haibo Ge, Maorong Ge, Yu Zhang, Chungyen Kuo, Chi-Ming Lee, Estel Cardellach, Yuanyuan Jia, Yixin Xiao, Xiaochun Wang</i>	374
S4-059	GNSS-R monitoring of St. John river water levels: implementation and first results	
 <i>Alexandrer Turner, Marcelo Santos, Thalia Nikolaidou, Felipe Nievinski</i>	375

S4.2: Next Generation Positioning

S4-060	Kinematic determination of state-space representation corrections for unified RTK and PPP-RTK solutions	<i>Yanming Feng, Wenzong Gao</i>	377
S4-061	Multipath Characterization using Ray-Tracing in Urban Trenches	<i>Lucy Icking, Fabian Ruwisch, Steffen Schön</i>	378
S4-062	VISION BASED NAVIGATION IN INDOOR ENVIRONMENT: EVALUATION OF PERFORMANCE USING SMARTPHONE SENSOR	<i>Fickrie Muhammad, Reiner Jäger</i>	379
S4-063	Analysis of BDS Two-way Time Synchronization	<i>Bin Wang, Jie Cui, Junping Chen, Binghao Wang</i>	380
S4-064	Investigation of the informativeness of the gravity field for indoor navigation	<i>Dmitry Bobrov</i>	382
S4-065	Fusion of GNSS/INS and Maps for lane-level vehicle navigation	<i>Emerson Cavalheri, Marcelo Santos</i>	383
S4-066	Robust constrained Kalman filter with GNSS/INS vehicle tightly coupled navigation application	<i>Meng Zhang, Cheng Yang, Yan Liu, Xingyu Long</i>	384
S4-067	GNSS positioning accuracy of smartphones and sports watches	<i>Piotr Patynowski, Marcin Mikoś, Krzysztof Sośnica, Kamil Kaźmierski</i>	385
S4-068	Facial Feature Recognition Based on Deep Neural Network	<i>Yihan Yang, Wei Sun</i>	386
S4-069	A cloud platform and hybrid positioning method for Indoor location service	<i>Jinzhong Bei, Dehai Li</i>	387
S4-070	Geomatics and Soft Computing techniques for road infrastructure monitoring: a case study	<i>Antonino Fotia, Vincenzo Barrile</i>	388
S4-071	A 3D map based place recognition solution for underground positioning using laser scanning ..	<i>Liu Jingbin, Dong Xu, Yifan Liang, Hongyu Qiu</i>	389
S4-072	A State-Domain Robust Fault Detection Algorithm for GNSS/INS Integration Positioning	<i>Zhangjun Yu, Qiuzhao Zhang, Nanshan Zheng</i>	390
S4-073	Towards collaborative positioning of pedestrian and UAS platforms by integrating vision, UWB, and IMU data	<i>Andrea Masiero, Paolo Dabove, Vincenzo Di Pietra, Antonio Vettore, Charles Toth, Vassilis Gikas, Harris Perakis, Jelena Gabela, Laura Ruotsalainen</i>	391
S4-074	Decentralized information filter with delayed states for cooperative location of UUVs	<i>Zhenqiang Du, Hongzhou Chai, Xiao Yin, Minzhi Xiang, Fan Zhang</i>	392

S4.3: Techniques and Applications in High Precision GNSS

S4-075	Network RTK performance analysis on moving vehicle in challenging environments	<i>Ali Karimidoona, Steffen Schön</i>	394
--------	--	---------------------------------------	-----

S4-076	Virtual Reference Station Technology in Geological Hazard Monitoring·····	395
	····· <i>Qinglan Zhang, Ming Chen, Junli Wu, Chaoqian Xu, Fan Wang</i>	
S4-077	Adaptive Stochastic Model Based on LS-VCE for GNSS Kinematic Precise Point Positioning ···	396
	····· <i>Qieqie Zhang, Long Zhao, Bin Wang</i>	
S4-078	Integer-estimable FDMA model as an enabler of GLONASS PPP-RTK·····	397
	····· <i>Baocheng Zhang</i>	
S4-079	Accuracy analysis of GNSS multi-system single point positioning algorithm with different cut-off altitude angles ·····	399
	····· <i>Guanpeng Yin, Meng Gao</i>	
S4-080	BDSBAS-B1C Service Performance Evaluation Model and Experimental Analysis ·····	400
	····· <i>Xiancai Tian, Longping Zhang, Haichun Wang, Shiming Gu, Dezhi Zhang</i>	
S4-081	Quality control of outlier detection, identification and adaptation in GNSS positioning ·····	401
	····· <i>Ling Yang, Yunzhong Shen, Bofeng Li</i>	
S4-082	Ambiguity-fixed relative positioning with GNSS dual-frequency observations of Huawei Mate20 smartphones·····	403
	····· <i>Weikai Miao</i>	
S4-083	ADDTID: An Efficient Tool for Characterizing Travelling Ionospheric Disturbances·····	404
	····· <i>Heng Yang, Enrique Monte-Moreno, Manuel Hernández-Pajares</i>	
S4-084	A new ambiguity resolution method for single-receiver LEO precise orbit determination ·····	405
	····· <i>Xingyu Zhou, Hua Chen, Weiping Jiang, Yan Chen, Tianjun Liu, Mingyuan Zhang</i>	
S4-085	A New Underwater Positioning Model Based on Average Sound Speed·····	406
	····· <i>Yixu Liu, Shengli Wang, shuqiang Xue, Xiushan Lu</i>	
S4-086	The evaluation of position and attitude accuracy for MS GNSS receiver with SD algorithm ·····	407
	····· <i>Chenglong Zhang, Wen Chen, Danan Dong</i>	
S4-087	Establishing a new method for heavy precipitation detection using optimal anomaly-based thresholds of predictors derived from GNSS-PWV·····	408
	····· <i>Haobo Li, Xiaoming Wang, Kefei Zhang, Suqin Wu, Jinglei Zhang, Cong Qiu</i>	
S4-088	BDS-3 SISRE assessment as well as comparison between D1 and B-CNAV (B-CNAV1, B-CNAV2 and B-CNAV3) navigation messages ·····	410
	····· <i>Zhenghua Dong, Songlin Zhang</i>	
S4-089	The estimation of inter-receiver pseudorange biases and its impact on the BDS-2 GEO satellite precise orbit determination ·····	411
	····· <i>Ran Li, Ningbo Wang, Jiatong Wu, Zishen Li, Kai Li, Yang Li</i>	
S4-090	Assessments on multi-GNSS real-time precise point positioning ·····	412
	····· <i>Ruohua Lan, Jie Lv, Junyao Kan, Zhouzheng Gao</i>	
S4-091	On the Limits of State-of-the-art GNSS Receivers in Frequency Transfer ·····	413
	····· <i>Thomas Krawinkel, Steffen Schön</i>	
S4-092	A modified global tropospheric delay model considering diurnal variation ·····	414
	····· <i>Guolin Liu, Lei Li, Xin Chen, Ying Xu</i>	
S4-093	Precise orbit determination for FY3D satellite using onboard BDS and GPS observation data and orbit forecast accuracy analysis·····	415
	····· <i>Mingming Liu, Yunbin Yuan</i>	
S4-094	Estimation and Validation of Codephase Center Correction using the Empirical Mode Decomposition·····	416
	····· <i>Yannick Breva, Johannes Kröger, Tobias Kersten, Steffen Schön</i>	
S4-095	Optimal kernel functions of Gaussian process regression for TEC prediction on the Ring of Fire Region ·····	417
	····· <i>Nhung Le Thi, Benjamin Männel, Pierre Sakic, Thai Chinh Nguyen, Hoa Thi Pham, Harald Schuh</i>	

S4-096	Disturbance analysis of underwater locating sound line and design of piecewise exponential weight function·····	<i>Xinpu WANG, Shuqiang XUE, Guoqing QU, Yixu LIU, Wenlong YANG</i>	418
S4-097	Integrity monitoring of precise satellite orbit and clock products for real-time precise point positioning ·····	<i>Jiaojiao Zhao, Zishen Li, Ningbo Wang</i>	419
S4-098	A Modified Interpolation Method for Regional Tropospheric Delay Modeling in Network RTK····	<i>Yakun Pu, Yunbin Yuan, Min Song</i>	420
S4-099	Characteristics of BDS-3 multipath effect and its mitigation methods in precise point positioning ·····	<i>Ran Lu, Wen Chen, Danan Dong, Lei Li, Luyao Huang</i>	421
S4-100	Measurement of Dynamic Structural Parameters of Super High-rise Buildings Based on Beidou-3 System ·····	<i>Xuece Miao, Keliang Ding, Qijie Luo, Tianzong Xue</i>	422
S4-101	INS/Visual Odometry aided GNSS data gap repairmen in urban environment ·····	<i>Tianxia Liu, Bofeng Li, Ling Yang</i>	423
S4-102	PPP with raw GNSS observation data of smartphones ·····	<i>Marcus Franz Glaner, Klaus Gutleiderer, Robert Weber</i>	424
S4-103	On the Potential of Image Similarity Metrics for Comparing Phase Center Corrections ·····	<i>Johannes Kröger, Tobias Kersten, Yannick Breva, Steffen Schön</i>	425
S4-104	A de-noising method of landslide deformation monitoring data based on CEEMDAN and enhanced multi-scale permutation entropy ·····	<i>Hao Xu, Li Wang, Bao Shu, Chen Yi, Yunqing Tian</i>	426
S4-105	Methods and assessments on the integration of inter-satellite differential BDS PPP and INS····	<i>Yu Min, Jie Lv, Qiaozhuang Xu, Zhouzheng Gao</i>	427
S4-106	A DIA Method based on Maximum A Posteriori Estimate for Multiple Outliers ·····	<i>Yangkang Yu, Yang Ling, Yunzhong Shen</i>	428
S4-107	Antarctic GNSS station of the National Geographic Institute of Spain. Geodetic purposes ·····	<i>Esther Azcue, Unai Quintana, Sergio Calvo, Victor Puente</i>	429
S4-108	A new strategy of tropospheric gradient estimation and its application in GNSS PPP····	<i>Di Zhang, Fei Yang, Lv Zhou, Jiming Guo</i>	430
S4-109	Research on LEO constellations enhancing GNSS orbit determination and precise point positioning ·····	<i>Junjun Yuan, Shanshi Zhou, Xiaogong Hu, Kai Li, Min Liao</i>	431
S4-110	The mean dynamic topography model MDTVN2020 on Vietnam sea surface····	<i>Thanh Thach Luong, An Dinh Nguyen, Van Hai Tran, Dinh Thanh Nguyen, Nhung Le Thi</i>	432
S4-111	An improved tropospheric mapping function modeling method for space geodetic techniques ···	<i>Yaozong Zhou, Yidong Lou, Weixing Zhang, Jingna Bai, Zhenyi Zhang</i>	433
S4-112	Multi-GNSS code biases: from the perspectives of DCB and OSB ·····	<i>Fei Guo, Yuanfan Deng, Xiaohong Zhang</i>	434
S4-113	Precise Orbit Determination of Low, Middle and High Satellite Network Based on Regional Ground Stations ·····	<i>Xuewen Gong, Jizhang Sang, Fuhong Wang, Xingxing Li</i>	435
S4-114	A method to compensate for the missing of real time phase biase products from CNES ·····	<i>Shi Du, Guanwen Huang, Yulong Ge, Bao Shu</i>	436
S4-115	Triple-frequency ambiguity resolution of BDS/Galileo precise point position with raw GNSS data ·····	<i>Jin Wang, Shengli Wang</i>	437
S4-116	Improvement of ISLs on BDS-3 Orbit Dtermination and Time Sychronization ·····	<i>Xia Ren, yufei Yang</i>	439

S4-117	Precise Orbit Determination of CubeSats Using a Proposed Observations Weighting Model	<i>Amir Allahverdizadeh, Ahmed El-Mowafy</i>	440
S4-118	Robust RTK method for short baselines with high sample rate	<i>Zhiteng Zhang, Bofeng Li</i>	441
S4-119	Comprehensive assessment Precise position and velocity determination for airborne gravimetry over long baselines	<i>Min Li, Tianhe Xu</i>	442
S4-120	Recognition of periodic signals in coordinate time series from GPS, GLONASS, and Galileo Precise Point Positioning	<i>Radosław Zajdel, Kamil Kaźmierski, Krzysztof Sośnica</i>	443
S4-121	An ADOP-based integrating multi-GNSS algorithm for fast and high-precision positioning	<i>Xin Liu, Shubi Zhang, Qiuzhao Zhang</i>	444
S4-122	Performance Analysis of Multi-GNSS Real-Time Kinematic Timing	<i>Baoqi Sun, Jiawei Liu, Xiaosong Dong, Zhe Zhang, Haiyan Yang, Xuhai Yang</i>	445
S4-123	A simplified reduced dynamic orbit determination for LEOs with orbit variation constraints	<i>Shoujian Zhang, Jiancheng Li, Geng Gao, Kemin Zhu, Hui Wei</i>	446
S4-124	GNSS real-time troposphere monitoring	<i>Jan Douša, Pavel Václavovic</i>	447
S4-125	Comparison of the RAIM availability performance of the maximum value method and the matrix maximum eigenvalue method under the condition of double-satellite faults	<i>Xiaping Ma, Qinzhen Li, Ershen Wang, Xiaoxing He</i>	448
S4-126	LEO's Contribution on Ambiguity and Positioning Convergence in Urban Canyons	<i>Yanning Zheng, Bofeng Li, Haibo Ge</i>	449
S4-127	BDS2 / BDS3 / GPS Multi-Frequency and Multi-System Fusion Long-Baseline Relative Positioning Analysis	<i>Xiaoting Lei, Huizhong Zhu, Jingfa Zhang</i>	450
S4-128	A deformation monitoring system based on BDS-2/BDS-3 PPP with optimal stochastic model	<i>Chenhao Ouyang, Junbo Shi, Jiming Guo</i>	451
S4-129	Characteristics analysis of raw multi-GNSS measurement from Huawei P30 and positioning performance	<i>Chen Yi, Li Wang, Bao Shu, Hao Xu, Yunqing Tian</i>	452
S4-130	High-precision deeply-coupled GNSS/INS positioning technology and its application for survey vehicle	<i>Baoguo Yu, Cailun Wu, Teng Long, Song Xie, Yixiong Sun</i>	453
S4-131	Positioning performance with low-cost GNSS receivers	<i>Kamil Kazmierski, Kamil Dominiak, Krzysztof Sośnica, Tomasz Hadas</i>	454
S4-132	Precise positioning using low-cost dual-frequency GNSS receivers	<i>Tomasz Hadas, Natalia Wielgocka, Adrian Kaczmarek, Grzegorz Marut</i>	455
S4-133	Multi-GNSS satellite inter-frequency clock bias estimation based on IGS clock datum in the multi-frequency context	<i>Lei Fan, Chuang Shi</i>	456
S4-134	Multi-level augmentation and highly reliable BeiDou/GNSS precise cloud positioning and space atmospheric effect control	<i>Yunbin Yuan</i>	457
S4-135	BDS-3 multi-frequency PPP-RTK for vehicle navigation in urban environments	<i>Bo Wang, Xin Li, Jiaxin Huang, Hongbo Lv, Guolong Feng, Xingxing Li</i>	458
S4-136	High-rate hourly ultra-rapid multi-GNSS precise clock estimation	<i>Guoqiang JIAO, Shuli SONG, Qinming CHEN</i>	459
S4-137	A Real-time Ionospheric Estimation Method Based on Undifferenced and Uncombined Precise Point Positioning	<i>Changxin Chen, Xu Lin, Wei Li, Lin Cheng, Hongyue Wang, Qingqing Zhang</i>	460

S4-138	Optimization of GNSS PDOP assessment and monitoring algorithm based on equal-area grid models	<i>Zhitao Wang, Shuli Song</i>	461
S4-139	How much does the price matter? Real-time geohazard monitoring with low-cost GNSS	<i>Roland Hohensinn, Raphael Stauffer, Reto Spannagel, Yara Rossi, Iván Dario Herrera Pinzón, Gregor Moeller, Markus Rothacher</i>	462
S4-140	Assessment of the Galileo System Contribution on RT-PPP Using Different Real-Time Correction Services in the Antarctic Region	<i>Serdar Erol, Bilal Mutlu, Bihter Erol</i>	463
S4-141	Continuous multipath and partial obstruction monitoring in high-precision GNSS base stations	<i>Marco Mendonca, Marcelo C. Santos</i>	464
S4-142	Performance Analysis of a Low-cost MARG Sensor/Single-antenna GNSS System for Land Vehicle Attitude Estimation	<i>Wei Ding, Yang Gao</i>	465
S4-143	Study on crustal movement characteristics before Yutian MS6.4 earthquake in 2020 based on GNSS	<i>Zhiguo Zhu</i>	466
S4-144	Validation and Evaluation of BDS-3 PPP-B2b service	<i>Haibo Ge, Bofeng Li, Yuhang Bu, Yanning Zheng</i>	467
S4-145	High order ionospheric delay characteristics and its influence on uncombined PPP	<i>Xiangyu Tian, Hongzhou Chai, Xiao Yin</i>	468
S4-146	Refinement of BeiDou Satellite Antenna Phase Center Correction Model and Its Impact on Precision Orbit Determination and Positioning	<i>Xingyuan Yan, Qin Zhang, Guanwen Huang, Shichao Xie, Yu Cao</i>	469
S4-147	CAS Real-time SSR Corrections in support of High Accuracy GNSS Applications	<i>Yunbin Yuan, Zishen Li, Wenwu Ding, Ningbo Wang, Bingfeng Tan</i>	470
S4-148	Rupture process variations analysis of the 2020 Mw7.4 La Crucecita, Oaxaca, Mexico Earthquake using high-rate GPS, InSAR and Teleseismic data	<i>Guisen Wen, Xingxing Li, Yingwen Zhao, Guangyu Xu</i>	471
S4-149	A Comparative Study of BDS Triple-frequency Ambiguity Fixation Algorithm for RTK Positioning	<i>Yangyang Lu, Huizhong Zhu</i>	472
S4-150	The RINEX Ina-CORS Data Download System Enhancement for One Map Policy Implementation Convenient in Indonesia	<i>Isnaini Annuriah Mundakir, Ossy Maulita Budiawati, Wilma Fitri, Akhmad Yulianto Basuki</i>	473
S4-151	Smart-PPP: Towards Real-Time GNSS Precise Point Positioning for Low-cost Smart Devices	<i>Liang Wang, Zishen Li, Ningbo Wang, Zhiyu Wang</i>	474
S4-152	Characteristic analysis of the GNSS satellite clock error	<i>Haojun Li, Jinxing Xiao</i>	475
S4-153	An enhanced foot-mounted PDR method with adaptive ZUPT and multi-sensors fusion for seamless pedestrian navigation	<i>Xianlu Tao, Xianlu Tao, Feng Zhu, Xiaohong Zhang</i>	476
S4-154	Stochastic Model Real-Time Adjustment of Ionospheric Delay in Long-Range RTK Positioning	<i>Jun Li, Huizhong Zhu, Yangyang Lu</i>	477
S4-155	An evaluation of solar radiation pressure models during eclipse seasons for GPS satellite	<i>Longjiang Tang, Aigong Xu, Huizhong Zhu, Maorong Ge</i>	478
S4-156	An experimental combination of IGS repro3 campaign's orbit and clock products using a variance component estimation strategy	<i>Pierre Sakic, Benjamin Männel, Gustavo Mansur, Andreas Brack, Harald Schuh</i>	479

S4-157	Rapid earthquake rupture process inversion with real-time high-rate GPS displacements	<i>Jianfei Zang, Caijun Xu</i>	480
S4-158	An analysis of inter-system biases in BDS/GPS combination kinematic precise point positioning	<i>Nannan Yang, Zongqiu Xu, Yantian Xu, Longjiang Tang, Aigong Xu, Bo Cheng</i>	481
S4-159	Estimation of the ionospheric VTEC and satellite DCB from BDS single-frequency PPP with multi-layer mapping function	<i>Ke Su, Shuanggen Jin</i>	482
S4-160	A combined GNSS and UWB locationing algorithm for indoor and outdoor mixed scenario ..	<i>Siyuan Wang</i>	483
S4-161	Performance Analysis of GNSS Augmented by LEO Constellation	<i>Xing Su, Hanlin Chen, Qiang Li, Zhimin Liu</i>	484
S4-162	Study on the stability of GNSS ISB	<i>Shuli Song, Hanyu Wang, Weili Zhou, Guoqiang Jiao, Zhitao Wang</i>	485
S4-163	Non-isotropy of the troposphere and its effect on the long-rang RTK	<i>Lei Li, Ying Xu, Xin Chen, Guolin Liu</i>	486
S4-164	Kinematic positioning through multi-GNSS android pseudoranges: Preliminary tests and results	<i>Amarildo Haxhi, Harris Perakis, Vangelis Zacharis, George Piniotis, Vassilis Gikas</i>	487

Symposium 5: Global Geodetic Observing System (GGOS): the metrological basis for the monitoring of the System Earth

S5.1: Geodetic infrastructure for Earth System Monitoring

S5-001	New Daily Coordinates of GNSS CORS in Japan Based on the GEONET 5th Analysis Strategy	<i>Naofumi Takamatsu, Hiroki Muramatsu, Naohiro Tada, Keitaro Ohno, Satoshi Abe, Satoshi Kawamoto</i>	489
S5-002	Accuracy evaluation of gravity continuous observation at key comparison site of absolute gravimeter	<i>Lishuang Mou, Jinyang Feng, Shuqing Wu</i>	491
S5-003	Coordinating global geodesy in Japan: GGOS Japan	<i>Toshimichi Otsubo, Basara Miyahara, Shinobu Kurihara, Yusuke Yokota, Yu Takagi, Shun-ichi Watanabe, Hiroshi Takiguchi, Yuichi Aoyama, Koji Matsuo</i>	492
S5-004	Four Achievable Control Schemes for Inertial Reference System in Space	<i>Chunyu Xiao, Yun Ma, Hongyin Li, Zebing Zhou</i>	493
S5-005	GGOS Bureau of Networks and Observations: Network Status and Related Activities	<i>Michael Pearlman, Dirk Behrend, Allison Craddock, Erricos Pavlis, Jérôme Saunier, Elizabeth Bradshaw, Riccardo Barzaghi, Daniela Thaller, Benjamin Maennel, Ryan Hippenstiel, Roland Pail, C.K. Shum, Nicholas Brown, Claudia Carabajal</i>	494
S5-006	VLBI-GNSS co-location at the Ishioka Geodetic Observing Station	<i>Saho Matsumoto, Haruka Ueshiba, Tomokazu Nakakuki, Yu Takagi, Kyonosuke Hayashi, Katsuhiko Mori, Toru Yutsudo, Tomokazu Kobayashi, Yudai Sato</i>	496
S5-007	The SUT Method for Precision Estimation of Mixed Additive and Multiplicative Random Error Model in Geodetic Measurement	<i>Chen Tao, Wang Leyang</i>	497
S5-008	RAEGE: a Spanish-Portuguese infrastructure of geodetic stations	<i>Jose A. Lopez-Perez</i>	498
S5-009	Absolute Positioning of Active Radar Transponders from Sentinel-1 Observations — Experiences and Results	<i>Marius Schlaak, Christoph Gisinger, Thomas Gruber</i>	499

S5-010	Probing a southern hemisphere VLBI intensive baseline configuration for dUT1 determination · <i>Sigrid Böhm, Jakob Gruber, Lisa Kern, Jamie McCallum, Lucia McCallum, Jonathan Quick, Matthias Schartner</i>	500
S5-011	Determination of the Earth's mantle structure based on a joint analysis of gravimetric and seismometric earthquake recordings at the Borowa Gora Geodetic-Geophysical Observatory · <i>Kamila Karkowska, Monika Wilde-Piórko, Przemysław Dykowski, Tomasz Olszak, Marcin Sękowski, Marcin Polkowski</i>	501
S5-012	ILRS: Recent Progress and Plans ·········· <i>Ulrich Schreiber, Michael Pearlman, Erricos Pavlis, Claudia Carabaial, Jean-Marie Torre, Toshimichi Obsubo, Michael Steindorfer</i>	503
S5-013	Systematic errors in SLR observation residuals to Swarm satellites ·········· <i>Dariusz Strugarek, Krzysztof Sośnica, Daniel Arnold, Adrian Jäggi, Mateusz Drożdżewski, Grzegorz Bury, Radosław Zajdel</i>	504
S5-014	Status of the future GGOS core site Metsähovi, Finland ·········· <i>Jyri Näränen, Hannu Koivula, Markku Poutanen, Arttu Raja-Halli, Joonas Eskelinen, Mirjam Bilker-Koivula, Nataliya Zubko, Ulla Kallio</i>	505
S5-015	Interoperability of the GGOS-PL infrastructure in the framework of EPOS-PL+ ·········· <i>Krzysztof Sośnica, Jerzy Nawrocki, Jolanta Nastula, Mateusz Drożdżewski, Radosław Zajdel, Jan Kapłon, Dariusz Strugarek, Kamil Kaźmierski, Piotr Patynowski, Marcin Mikoś, Przemysław Dykowski, Jan Kryński, Witold Rohm, Dorota Olszewska, Grzegorz Mutke, Adam Lurka</i>	506
S5-016	Optimizing GNSS RTK Infrastructure from the perspective of tropospheric effects ·········· <i>Zhenhong Li, Chen Yu, Nigel Penna</i>	508
S5-017	Development of Wideband Receiver for Novel Ground-based Microwave Radiometer -field experiments of the new 20-60 GHz wide-band receiver and its implications to new development of the wide-band VLBI receiver-········· <i>Ryuichi ICHIKAWA, Hideki UJIHARA, Shinsuke SATOH, Yusaku OHTA, Basara MIYAHARA, Hiroshi MUNEKANE, Tomokazu KOBAYASHI, Takeshi NAGASAKI, Osamu TAJIMA, Kentaro ARAKI, Takuya TAJIRI, Takeshi MATSUSHIMA, Hiroshi TAKIGUCHI, Nobuo MATSUSHIMA, Tatsuya MOMOTANI, Kenji UTSUNOMIYA, Mamoru SEKIDO, Takaaki JIKE, Tomoaki OYAMA, Hiroshi TAKEUCHI, Hiroshi IMAI</i>	510
S5-018	The importance of geodetic infrastructure and its connection to the UN 2030 Agenda ·········· <i>Martin Lidberg, Rudiger Haas</i>	512
S5-019	Two-dimensional mining surface deformation monitoring and accuracy analysis of ascending and descending SBAS and MSBAS InSAR ·········· <i>Yu Han, Qiuxiang Tao, Guolin Liu, Anye Hou, Zaijie Guo, Fengyun Wang</i>	513
S5-020	The development of spaceborne interferometric synthetic aperture radar missions in China ······ <i>Junli Chen, Yanyang Liu</i>	514

S5.2: Gravity observations and networks in the framework of GGOS

S5-021	Summary of the Absolute Gravity Measurements using FG5-210 at Antarctic Research Stations in Antarctica during 2017-2020 Austral Summer Season	<i>Yoichi Fukuda, Yuichi Aoyama, Jun'ichi Okuno, Akihisa Hattori, Koichiro Doi, Jun Nishijima, Takahito Kazama</i>	516
S5-022	Evaluation of the gravity reference function at the Borowa Gora Observatory	<i>Przemyslaw Dykowski, Jan Krynski, Marcin Sekowski, Monika Wilde-Piorko, Tomasz Olszak</i>	518
S5-023	Investigation of systematic effects of FG5/FG5X gravimeters	<i>Vojtech Pálinkáš, Petr Křen, Pavel Mašika, Miloš Vaľko</i>	519
S5-024	Progress of International Gravity Reference System and Frame	<i>Hartmut Wziontek, Sylvain Bonvalot, Reinhard Falk, Germinal Gabalda, Jaakko Mäkinen, Vojtech Pálinkáš, Axel Rülke, Leonid Vitushkin</i>	520
S5-025	GGOS Focus Area Unified Height System: achievements and open challenges	<i>Laura Sanchez, Jianliang Huang, Riccardo Barzaghi, Georgios S. Vergos</i>	522
S5-026	The pole tide in terrestrial gravimetry	<i>Jaakko Mäkinen</i>	523

S5.3: Standardized geodetic products for a reliable System Earth observation

S5-027	Geodetic Analyses at the National Geographic Institute of Spain. Current and future projects and prospects	<i>José Carlos Rodríguez, Esther Azcue, Víctor Puente, José Antonio López Fernández, José Antonio López-Pérez, José Antonio Sánchez Sobrino, Marcelino Valdés Pérez, Beatriz Vaquero, Pablo De Vicente</i>	525
S5-028	New GGOS Website – An Extensive Information Platform about Geodetic Products, Observations and Services	<i>Martin Sehnal, Detlef Angermann, Laura Sánchez, Kosuke Heki</i>	527
S5-029	Understanding the causes of coastal sea level change from geodetic measurements	<i>Dapeng Mu</i>	528
S5-030	Machine learning prediction for filling the interruptions of tide gauge data using a least square estimation method from nearest stations	<i>Vahidreza Jahanmard, Nicole Delpeche-Ellmann, Artu Ellmann</i>	529
S5-031	The role and activities of the GGOS Bureau of Products and Standards	<i>Detlef Angermann, Thomas Gruber, Michael Gerstl, Robert Heinkelmann, Urs Hugentobler, Laura Sanchez, Peter Steigenberger</i>	530
S5-032	Evaluating of sea surface heights from multi-mission satellite altimetry by utilizing hydrodynamic and geoid models	<i>Majid Mostafavi, Nicole Delpeche-Ellmann, Artu Ellmann</i>	531
S5-033	Defining Essential Geodetic Variables	<i>Richard Gross</i>	532
S5-034	ICGEM's Current Activities and Future Plans	<i>E. Sinem Ince, Sven Reissland</i>	533
S5-035	Metrological support of astronomical-geodesic and gyroscopic azimuth measuring instruments	<i>Maksim Khanzadian, Andrey Mazurkevich</i>	534
S5-036	Using WGM2012 to Compute Gravity Anomaly Correction of Leveled Height Differences	<i>Yanhui CAI, Li Zhang, Xu Ma</i>	535
S5-037	On the Earth dynamical ellipticity	<i>Alberto Escapa, Tomas Baenas, Jose Manuel Ferrandiz</i>	536
S5-038	Assigning Digital Object Identifiers to Geoid Models in the ISG Repository	<i>Mirko Reguzzoni, Kirsten Elger, Lorenzo Rossi, Daniela Carrion</i>	537

S5.4: Geodetic space weather research

S5-039	Ionospheric TEC analysis and modeling using Empirical Mode Decomposition (EMD)	539
 <i>Hamid Moghadaspour, Siavash Iran Pour, Alireza Amiri-Simkooei, Nico Sneeuw, Saniya Behzadpour, Torsten Mayer-Gürr</i>	
S5-040	Use of Empirical Mode Decomposition (EMD) method to investigate the solar storms impact on GRACE range-rate residuals	540
 <i>Hamid Moghadaspour, Siavash Iran Pour, Saniya Behzadpour, Torsten Mayer-Gürr, Nico Sneeuw, Alireza Amiri-Simkooei</i>	
S5-041	3D model to explore the ionosphere and plasmasphere exclusively using satellite-based GNSS Data	541
 <i>Fabricio Prol, Mainul Hoque</i>	
S5-042	An enhanced mapping function for spaceborne TEC conversion based on the plasmaspheric scale height	542
 <i>Mengjie Wu, Peng Guo, Xiaogong Hu</i>	
S5-043	Ensemble Machine Learning for Geodetic Space Weather Forecasting	543
 <i>Randa Natras, Michael Schmidt</i>	
S5-044	Impact of 09-15 November 2012 magnetic cloud storm on vTEC along west Euro-African GPS Chain	544
 <i>Amira Shimeis</i>	
S5-045	Ground and spaced based GNSS for Space Weather Monitoring at GFZ: Overview and Recent Results	545
 <i>Jens Wickert, Christina Arras, Andreas Brack, Galina Dick, Ankur Kepkar, Benjamin Männel, Chinh Nguyen Thai, Temitope Oluwadare, Torsten Schmidt, Florian Zus, Harald Schuh</i>	
S5-046	SWEETS – forecast of satellite orbit decay using L1 interplanetary magnetic field measurements and thermospheric density estimates.	546
 <i>Sandro Krauss, Sofia Kroisz, Lukas Drescher, Manuela Temmer, Barbara Suesser Rechberger, Saniya Behzadpour, Torsten Mayer-Guerr</i>	
S5-047	Forecasting Global Thermospheric Neutral Density through Calibration and Data Assimilation of GRACE Measurements into the NRLMSISE-00 model	547
 <i>Mona Kosary, Ehsan Forootan, Saeed Farzaneh, Kristin Vielberg, Timothy Kodikara, Maike Schumacher</i>	
S5-048	A latitude-dependent ionospheric variogram model	549
 <i>Tong Liu, Yiping Jiang, Li Liu, Mengfei Sun, Guochang Xu, Zhibin Yu</i>	
S5-049	Deep Learning for Global Ionospheric TEC Forecasting: Different Approaches and Validation ..	550
 <i>Xiaodong Ren, Pengxin Yang, Jun Chen, Xiaohong Zhang</i>	
S5-050	Detection of ionospheric disturbances by modelling the electron density as three-dimensional B-spline expansions: a simulation study	551
 <i>Andreas Goss, Michael Schmidt, Eren Erdogan, Denise Dettmering, Florian Seitz, Jennifer Müller, Ernst Lexen, Barbara Görres, Wilhelm F. Kersten</i>	
S5-051	Towards a better understanding of space weather events and their impact on geodetic Measurements	552
 <i>Alberto Garcia-Rigo, Benedikt S. Soja, Anna Belehaki, Jens Berdermann, Consuelo Cid, Denise Dettmering, Jinsil Lee, Anthony J. Mannucci, Enric Monte-Moreno, Xiaoqing Pi, Rami Qahwaji, Pietro Zucca</i>	

S5.5: Assimilation of geodetic observations in the modelling of the Atmosphere, Cryosphere and Hydrosphere

S5-052	Crustal response to heavy rains in Japan 2017-2020 ...	555
 <i>Kosuke Heki, Wei Zhan, Syachrul Arief</i>	

S5-053	Development of synergized method to determine accurate sea level using satellite altimetry and high-resolution geoid model ···· <i>Vahidreza Jahanmard, Nicole Delpeche-Ellmann, Artu Ellmann</i>	556
S5-054	Long-period Accuracy Evaluation and Spatial-temporal characterization Analysis of Global GNSS-derived Precipitable Water Vapor····· <i>Junsheng Ding, Junping Chen</i>	557
S5-055	Temporal error covariances of satellite gravimetry-derived ice mass change products····· ····· <i>Andreas Groh, Eric Buchta, Martin Horwath, Matthias O. Willen, Thorben Döhne, Benjamin D. Gutknecht, Maria T. Kappelsberger</i>	558
S5-056	Investigation of the influence factors on ionospheric scintillation monitoring with conventional geodetic receiver and performance evaluation····· <i>Wei Li, Shuli Song</i>	559
S5-057	A Tropospheric Delay Model of Multi-source Data Considering System Deviation Correction··· ····· <i>Yongchao Ma, Bing Zhang, Guochang Xu, Zhiping LV</i>	560
S5-058	Evaluation of Precipitable Water Vapor from COSMIC-2 Radio Occultation using Radiosonde and GNSS Data ······ <i>Shuaimin Wang, Tianhe Xu</i>	561
S5-059	Penetration Depth Inversion in Hyper-Arid Desert from L-band InSAR Data Based on a Coherence Scattering Model ······ ····· <i>Guanxin Liu, Haiqiang Fu, Jianjun Zhu, Changcheng Wang, Qinghua Xie</i>	563
S5-060	On the assessment of ERA5 and GPS-based WRFDA for InSAR Atmospheric Correction ····· ····· <i>Zhenyi Zhang, Weixing Zhang, Yidong Lou, Hua Wang, Yaozong Zhou, Jingna Bai</i>	564
S5-061	A Metrological Assessment of the Zenith Total Delays from GPS Data Processing in Tropical Areas: The Tahiti ······ <i>Fangzhao Zhang, Jean-Pierre Barriot, Peng Feng, Guochang Xu</i>	565

S5.6: Geodesy contributions to address societal challenges

S5-062	The Global Geodetic Observing System (GGOS) - fundamental infrastructure for science and society -····· <i>Basara Miyahara, Laura Sánchez, Martin Sehnal, Allison Craddock</i>	567
S5-063	The status and development of the Asia Pacific Reference Frame (APREF) and its applications ······ <i>Guorong Hu, John Dawson, Ryan Ruddick, Minghai Jia, Simon McClusky</i>	568
S5-064	The UN Global Geodetic Centre of Excellence (GGCE)····· <i>Johannes Bouman</i>	569
S5-065	GGOS D-A-CH – A new regional affiliate of the Global Geodetic Observing System ······ ····· <i>Hansjoerg Kutterer, Johannes Boehm, Johannes Bouman, Roland Pail, Markus Rothacher, Harald Schuh</i>	570
S5-066	Investigation of a method for reducing the measurement error of time delays between optical signals in phase rangefinders····· <i>Anna Deikun</i>	571
S5-067	Status and Future Development of GNSS enhancement of Tsunami Early Warning Systems (GTEWS)····· <i>John LaBrecque, Allison Allison Craddock, Brendan Crowell, John Rundle</i>	572
S5-068	Identifying tools to connect Global Geodetic Reference Frame (GGRF) Capacity Development within the United Nations GGIM Integrated Geospatial Information Framework (IGIF)····· ····· <i>Allison Craddock, Graeme Blick, Ryan Keenan, Mikael Lilje, Rob Sarib</i>	573
S5-069	Embracing challenges through national, regional & international partnership in the Pacific ······ ····· <i>Andrick Lal</i>	575
S5-070	Absolute 3D positioning of corner reflectors with Sentinel-1 SAR images for deformation monitoring of Shanghai Yangtze River Bridge····· ····· <i>Ruiqing Song, Jicang Wu, Xinyou Song, Yuting Li, Guowei Tan</i>	577

S5-071	Coseismic and early postseismic deformations due to the 2019 earthquake sequence in Ridgecrest, California	<i>Kefeng He, Caijun Xu, Yangmao Wen</i>	578
S5-072	GGOS Service and Application Under the PNT Mode	<i>Yamin Dang, Shuqiang Xue, Tao Jiang, Qiang Yang, Wei Wang</i>	579
S5-073	News from the GGOS DOI Working Group	<i>Kirsten Elger, GGOS DOI Working Group</i>	580
S5-074	Thinking for the Integration of Satellite Communication, Navigation and Remote-sensing based on the network information SoS	<i>Zuoya Zheng</i>	581
S5-075	SIRGAS and GRFA WG UN-GGIM: Americas interactions for sustainable geodesy	<i>Sonia Costa, Diego Piñón, José Antonio Tarrío Mosquera, Demián Gomez, Gabriel Guimarães</i>	582
S5-076	Group on Earth Observations (GEO) Disaster Risk Reduction (DRR) WG	<i>David Borges</i>	584
S5-077	Towards Indian Forest Sustainability: Satellite-Based Ecological and Nature Hazards Monitoring	<i>C K Shum, Soumitri Das, Junyi Guo, Yuanyuan Jia, Samuel Malloy, John Horack, Vibhor Agarwal, Orhan Akyilmaz, Xiaobin Cai, Tom Darrah, Ehsan Forootan, Steve Lee, Peter Luk, Joseph Mascaro, Rongjun Qin, Hassan Syed, Metehan Uz, Yu Zhang</i>	585

S5.7: Advances in Geodesy for Geohazard Monitoring and Disaster Risk Reduction

S5-078	Time series InSAR for stability analysis of Ankang airport with expansive soil before operation	<i>Jinzhao SI, Shuangcheng ZHANG, Yufen NIU</i>	588
S5-079	Improved multi-baseline maximum likelihood estimation algorithm for InSAR phase unwrapping	<i>Shenke Xiao</i>	589
S5-080	An Improved Adaptive Method on Mitigating Differential Tropospheric Delays in Time-series InSAR	<i>Mengyao Shi, Junhuan Peng, Honglei Yang, Yuhan Su</i>	590
S5-081	Real-time multi-GNSS solutions for earthquake monitoring in Spain	<i>Victor Puente</i>	591
S5-082	Adjustment of Measurements With Multiplicative Random Errors and Trends	<i>Yun Shi, Peliang Xu</i>	592
S5-083	Lessons Learned from the 2020 Uzbekistan Sardoba Dam Failure: An Imaging Geodesy Perspective	<i>Ruya Xiao, Mi Jiang, Zhenhong Li, Xiufeng He</i>	593
S5-084	Metrological support of laser coordinate measuring systems	<i>ANDREY MAZURKEVICH</i>	594
S5-085	Spatio-temporal variations of afterslip and viscoelastic relaxation following the Mw 7.8 Gorkha (Nepal) earthquake	<i>Zhen Tian, Jeffrey Freymueller, Zhiqiang Yang</i>	595
S5-086	The landslide susceptibility mapping based on machine learning methods and InSAR-derived deformation: a case study on the upper reaches of the Jinsha River	<i>Zhuo Jiang, Chaoying Zhao, Xiaojie Liu</i>	596
S5-087	An approach based on coherence matrix decomposition to improve small baseline processing for land subsidence monitoring	<i>Qian He</i>	598
S5-088	Different gradient deformation monitoring of the landslide based on Intermittent SBAS (ISBAS) InSAR and SAR offset-tracking methods	<i>Liquan Chen, Chaoying Zhao, Ya Kang, Xiaojie Liu</i>	599
S5-089	Landslide detection, monitoring and failure mechanism research in Guizhou Province, China with multi-sensor SAR datasets	<i>Chaoying Zhao, Liquan Chen, Hengyi Chen</i>	601
S5-090	A Strain-Model Based InSAR Time Series Method for Geohazards Deformation Monitoring	<i>Jihong Liu, Jun Hu, Roland Burgmann, Zhiwei Li, Qian Sun, Zhangfeng Ma</i>	603

S5-091	Retrieving complete 3-D ice velocities from multi-baseline and multi-aperture InSAR measurements	<i>Wanji Zheng, Jun Hu</i>	604
S5-092	Quantifying glacier displacement and glacial lake outburst floods with SAR and optical images: A case study in Jinweng Co Lake, Tibet, China	<i>Liye Yang, Zhong Lu, Chaoying Zhao, Chengsheng Yang</i>	605
S5-093	Monitoring and analysis of geological hazards based on loading impact change	<i>Wei Wang, Yamin Dang, Chuanyin Zhang, Qiang Yang</i>	606
S5-094	Differential Interferometric Synthetic Aperture Radar data for more accurate earthquake catalogs	<i>Chuanhua Zhu, Chisheng Wang, Bochen Zhang, Xiaoqiong Qin, Xinjian Shan</i>	607
S5-095	Multi-scale Crustal Deformation around the Southeastern Margin of the Tibetan Plateau from GNSS Observations	<i>Keke Xu</i>	609
S5-096	An Improved Two-tier Network for Robust PSI Parameter Estimation and Its Application on Deformation Monitoring of Urban Area	<i>Wenqing Wu, Jun Hu</i>	610
S5-097	Structural dynamic displacements detecting through robust integrated model using GNSS and accelerometers	<i>Xu Liu, Jian Wang, Houzeng Han</i>	611
S5-098	Monitoring phosphate mining induced landslides in karst mountainous area using multi-temporal InSAR	<i>Hengyi Chen, Chaoying Zhao, Baohang Wang, Liquan Chen</i>	612
S5-099	Attention guided U-Net model for landslide detection	<i>Xuerong Chen, Chaoying Zhao, Zhong Lu</i>	613
S5-100	Evaluating the performance of global atmospheric models in correcting InSAR tropospheric delay over the Kanto Plain using statistical metrics	<i>Guangqi Jiao, Yu Sun</i>	614
S5-101	Landslide susceptibility assessment using Conv-LSTM model along the Sichuan-Tibet railway ·	<i>Wubiao Huang, Mingtao Ding, Zhenhong Li, Jianqi Zhuang</i>	616
S5-102	Active geohazards along the Jinsha River Corridor revealed by Sentinel-1 SAR pixel offsets and InSAR observations	<i>Chenglong Zhang, Zhenhong Li, Bo Chen, Jing Yang, Zhenjiang Liu</i>	617
S5-103	Scientific infrastructure for monitoring of safety pillars in underground coal mines - Polish study case within EPOS-PL+ project	<i>Jan Kapłan, Maya Ilieva, Krzysztof Sośnica, Grzegorz Józków, Kamila Pawłuszek-Filipiak, Kamil Kaźmierski, Przemysław Tymków, Paweł Bogusławski, Jan Sierny, Adrian Kaczmarek, Natalia Wielgocka, Krzysztof Stasch, Grzegorz Marut, Marcin Mikoś, Piotr Pałynowski, Adam Pałęcki, Mateusz Drożdżewski</i>	618
S5-104	The new pilot system for Earthquake and Tsunami Risk Estimation by ionospheric sounding (ETREbis) at the IGP Caribbean observatories	<i>Michela Ravanelli, Fabio Manta, Giovanni Occhipinti, Mattia Crespi</i>	619
S5-105	Analysis of the crustal deformation characteristics of Mount Everest and Tibetan region in the past 20 years	<i>Yamin Dang, Chuanlu Cheng, Guangwei Jiang, Qiang Yang, Yangyang Sun</i>	621
S5-106	CyCLOPS: A National Integrated GNSS/InSAR Strategic Research Infrastructure for Monitoring Geohazards and Forming the Next Generation Datum of the Republic of Cyprus	<i>Chris Danezis, Dimitris Kakoullis, Kyriaki Fotiou, Marina Pekri, Miltiadis Chatzinikos, Christopher Kotsakis, Ramon Brcic, Michael Eineder, George Melillos, Marios Nikolaidis, Georgios Ioannou, Andreas Christofe, Nicholas Kyriakides, Marios Tzouvaras, Sylvana Pilidou, Kyriacos Themistocleous, Diofantos Hadjimitsis</i>	622

S5-107	Identification of Potential Landslide in Ya'an-Linzhi Section of Sichuan-Tibet Railway Based on InSAR Technology	<i>Jinmin Zhang, Wu Zhu</i>	624
S5-108	Monitoring Ground Deformation of Subway Area Using PS-InSAR in Suzhou	<i>Lina Zhang, Jicang Wu, Ruiqing Song, Ming Yuan, Jinwei Qiu</i>	626
S5-109	Numerical Simulation of Storm Surge in the Sea Near Long Island, New York Based on MIKE21	<i>Chengcai Ren, Fanlin Yang, Zejie Tu, Ruijie Shen, Dianpeng Su</i>	627
S5-110	Multi-sensor geodetic approach to deformation monitoring	<i>Ashutosh Tiwari, Avadh Bihari Narayan, Onkar Dikshit</i>	628
S5-111	Estimating 3D Mining Displacements from Multi-Track InSAR by Incorporating with a Prior Deformation Model	<i>Zefa Yang, Jianjun Zhu, Zhiwei Li, Lixin Wu</i>	629
S5-112	Comparing Natural Hazards Assessment using Satellite Imagery Data and Geodetic Earth Observation Data	<i>Thomas Chen</i>	630

Symposium 6: ICC symposium

S6.1: ICCT Geodetic Theory

S6-001	A CFD-based gravitational field modeling method and its potential applications in deep space exploration	<i>Zhi Yin, Nico Sneeuw</i>	632
S6-002	The general rule of potential field parameters especially for Laplace's equation	<i>Xiao-Le Deng, Wen-Bin Shen, Meng Yang, Jiangjun Ran</i>	633
S6-003	An quality assessment of the official GOCE Level 2 GRD SPW 2 products over Norway, Czechia, and Slovakia	<i>Martin Pitonak, Michal Sprlak, Vegard Ophaug, Ove C. D. Omang, Pavel Novak</i>	634
S6-004	Inclusion of data uncertainty in machine learning and its application in geodetic data science ..	<i>Mostafa Kiani Shahvandi, Benedikt Soja</i>	636
S6-005	Adaptive Quasi-Monte Carlo Algorithm for Covariance Propagation of GNSS Baseline Vector ..	<i>Xinlei Luo, Leyang Wang</i>	637
S6-006	Crustal density and forward global gravitational field model on the Moon determined from GRAIL and LOLA satellite data	<i>Michal Šprlák, Shin-Chan Han, Will Featherstone</i>	638
S6-007	A new robust estimation algorithm for the superstrong breakdown point based on Quasi-Accurate Detection	<i>Hailu Chen, Wei Qu, Qin Zhang, Yuan Gao, Shichuan Liang</i>	639
S6-008	On determination of the geoid from measured gradients of the Earth's gravity field potential ..	<i>Pavel Novak, Michal Šprlák, Martin Pitoňák</i>	640
S6-009	Tensor calculus and functional analysis in the iteration solution of the geodetic boundary value Problema	<i>Petr Holota, Otakar Nesvadba</i>	641
S6-010	Bayesian modelling of discontinuities and piecewise trends (trend changes) improves coastal vertical land motion estimates	<i>Julius Oelsmann, Marcello Passaro, Laura Sanchez, Denise Dettmering, Christian Schwatke, Florian Seitz</i>	642
S6-011	Sensitivity of GNSS orbits to General Relativistic effects	<i>Krzysztof Sośnica, Grzegorz Bury, Radosław Zajdel, Javier Ventura-Traveset, Luis Mendes</i>	643
S6-012	Impact of accelerometers calibration and empirical forces modelling on GRACE precise orbit determination	<i>Thomas Papanikolaou, Dimitrios Tsoulis</i>	644

S6.2: ICCG Geodesy for Climate Research

S6-013	Determination of the velocity field of the African plate from GNSS.....	
	<i>Saturday Ehisemhen Usifoh, Benjamin Männel, Pierre Sakic, Joseph Dodo, Harald Schuh</i>	646
S6-014	Recovering Climate-Related Mass Transport Signals by current and next-generation gravity missions	
	<i>Marius Schlaak, Roland Pail, Henryk Dobsław, Annette Eicker, Laura Jensen</i>	647
S6-015	The initial process of post-fire ground deformation in Northeastern Siberian permafrost areas detected by L-band and C-band InSAR	
	<i>Kazuki Yanagiya, Masato Furuya, Go Iwahana, Petr Danilov</i>	648
S6-016	Quantifying barostatic sea-level change from satellite altimetry, GRACE and Argo observations	
	<i>Hadi Amin, Mohammad Bagherbandi, Lars Sjöberg</i>	649
S6-017	Assessments of integrated water vapor from atmospheric reanalyses against ground-based GPS Over Europe	
	<i>Peng Yuan, Roeland Van Malderen, Xungang Yin, Hannes Vogelmann, Joseph Awange, Hansjörg Kutterer</i>	650
S6-018	Preliminary results of the third IGS TIGA Reprocessing at GFZ	
	<i>Benjamin Männel, Tilo Schöne, Markus Bradke, Harald Schuh</i>	651
S6-019	Evaluating hydrological angular momentum determined from CMIP6 historical simulations	
	<i>Jolanta Nastula, Justyna Śliwińska, Małgorzata Wińska, Tomasz Kur, Aleksander Partyka</i>	652
S6-020	Innovative methodology for downscaling GRACE observations for the purpose of groundwater storage determination.....	
	<i>Monika Birylo, Zofia Rzepecka, Justyna Śliwińska, Jolanta Nastula</i>	653
S6-021	GNSS for the Global Climate Observing System: Precipitable Water Vapor Processing Centre at GFZ	
	<i>Galina Dick, Florian Zus, Jens Wickert, Benjamin Männel, Markus Bradke, Markus Ramatschi, Kyriakos Balidakis, Karina Wilgan, Harald Schuh</i>	654
S6-022	What can long-term trend estimates from satellite gravimetry contribute to climate research?...	
	<i>Andreas Kvas, Eva Boergens, Henryk Dobsław, Andreas Guentner</i>	655
S6-023	Investigating the relationship between Length of Day and El-Nino using wavelet coherence Method.....	
	<i>Shrishail Raut, Sadegh Modiri, Robert Heinkelmann, Kyriakos Balidakis, Santiago Belda, Chaiyaporn Kitpracha, Harald Schuh</i>	656
S6-024	Meteorological and Tidal Effects on GNSS Reflected Signal in Mediterranean Coasts of Turkey	
	<i>Cansu Beşel, Emine Tanır Kayıkçı</i>	657
S6-025	Spatial-temporal variations in ice velocity of the Northeast Greenland Ice Stream and their control factors related with climate warming	
	<i>Xi Lu</i>	658
S6-026	Contribution of glacier mass loss to river runoff in the source region of the Yangtze River during 2000-2018.....	
	<i>Lin Liu, Liming Jiang, Hansheng Wang</i>	659
S6-027	Land Water Storage Variabilities in GRACE and Climate Models – How do they compare and which future changes can we expect? ...	
	<i>Laura Jensen, Annette Eicker, Henryk Dobsław, Roland Pail</i>	660
S6-028	Using satellite geodesy for carbon cycle research	
	<i>Alexandra Klemme, Thorsten Warneke, Heinrich Bovensmann, Matthias Weigelt, Jürgen Müller, Justus Notholt, Claus Lämmerzahl</i>	661
S6-029	River discharge estimation from high-resolution altimetry	
	<i>Luciana Fenoglio, Elena Zakharova, Quang Duong, Salvatore Dinardo, Jürgen Kusche, Matthias Gärtner, Hakan Ahmet, Jerome Benveniste, Bahtiyor Zohidov</i>	662

S6-030	Closure of global sea-level and ocean-mass budgets: progress and prospects with a focus on uncertainty characterization	<i>Martin Horwath, Benjamin D. Gutknecht, Anny Cazenave, Hindumathi Kulaiappan Palanisamy, Florence Marti, Ben Marzeion, Frank Paul, Raymond Le Bris, Anna E. Hogg, Inès Ootosaka, Andrew Shepherd, Petra Döll, Denise Cáceres, Hannes Müller Schmied, Johnny A. Johannessen, Jan Even Øie Nilsen, Roshin P. Raj, René Forsberg, Louise Sandberg Sørensen, Valentina R. Barletta, Sebastian B. Simonsen, Per Knudsen, Ole Baltazar Andersen, Heidi Randall, Stine K. Rose, Christopher J. Merchant, Claire R. Macintosh, Karina von Schuckmann, Kristin Novotny, Andreas Groh, Marco Restano, Jérôme Benveniste</i>	663
S6-031	Solid Earth Deformation Sensing Using Multi-Decadal Satellite Altimetry	<i>C K Shum, Ting-Yi Yang, Chungyen Kuo, Vibhor Agarwal, Orhan Akyilmaz, Lifeng Bao, Chunxi Guo, Yuanyuan Jia, Jianliang Nie, Metehan Uz, Xuechen Yang, Yuchan Yi</i>	665

S6.3: ICCM Seafloor geodesy, marine positioning and undersea navigation

S6-032	Geoscientific contributions of the GNSS-A Seafloor Geodetic Observation array (SGO-A) in the subduction zones around Japan, operated by the Japan Coast Guard	<i>Yusuke Yokota, Tadashi Ishikawa, Shun-ichi Watanabe, Yuto Nakamura</i>	668
S6-033	Overview of the GNSS-A Seafloor Geodetic Observation Array (SGO-A) in the subduction zones around Japan, operated by the Japan Coast Guard	<i>Shun-ichi Watanabe, Tadashi Ishikawa, Yuto Nakamura, Yusuke Yokota</i>	669
S6-034	Robust adaptive Kalman filter for underwater acoustic navigation with systematic error model correction	<i>Junting Wang, Tianhe Xu, Yangfan Liu, Dapeng Mu</i>	670
S6-035	Multi-beam underwater topography distortion correction based on SVP inversion	<i>Yangfan Liu, Tianhe Xu, Junting Wang, Dapeng Mu</i>	671
S6-036	High Precision Positioning in Coastal Areas via GNSS/INS Equipped Buoys: A Case Study from the Bass Strait Altimeter Validation Site	<i>Boye Zhou, Christopher Watson, Matt King, Jack Beardsley, Benoit Legresy</i>	672
S6-037	A Nonlinear Gauss-Helmert Model and Its Robust Solution for Seafloor Control Point Positioning	<i>Yingcai Kuang, Zhiping Lu, Fangchao Wang</i>	673
S6-038	BATHYMETRIC DATA FITTING BASED ON LINEAR-COMPLEMENTARY FOURIER SERIES OF B-SPLINE FUNCTION	<i>Ruichen Zhang, Shaofeng Bian, Bing Ji</i>	674
S6-039	Further evaluation of the impact of Earth's curvature on coastal sea level altimetry with ground-based GNSS Reflectometry	<i>Vitor Hugo Almeida Junior, Felipe Geremia-Nievinski</i>	676
S6-040	Outlier Detection Based on Epoch-differential for Seafloor Geodetic Positioning	<i>Shuqiang XUE</i>	677
S6-041	Comparative analysis of construction methods of regional marine three-dimensional sound velocity field	<i>Chaoyi Wu, Fanlin Yang, Mingzhen Xin, Jinjin Wei, Xiaofei Zhang</i>	678
S6-042	Analysis of Interactive Multiple Model Kalman Filter Algorithm for Ultra Short Baseline Tracking Autonomous Underwater Vehicle	<i>Xiaofei Zhang, Mingzhen Xin, Fanlin Yang, Jinjin Wei, Chaoyi Wu</i>	679
S6-043	Research on the Method of Establishing Calibration System for Marine Sonar Equipment Based on Prototype Tank	<i>Yunyue Chen, Anmin Zhang, Yufen Cao, Yicheng Liu, Minming Zhang</i>	680

- S6-044 Seafloor single point positioning using GNSS-Acoustic technique with horizontal sound speed gradient estimation *Yang Liu, Yanxiong Liu, Guanxu Chen, Menghao Li* 681

S6.4: QuGe Novel Sensors and Quantum Technology for Geodesy

- S6-045 Improved evaluation of the transportable strontium lattice clock at PTB for chronometric leveling *Ingo Nosske, Chetan Vishwakarma, Sofia Herbers, Roman Schwarz, Sören Dörscher, Christian Lisdat* 683
- S6-046 Characteristics of Novel Differential Lunar Laser Ranging Compared to Classical Lunar Laser Ranging *Mingyue Zhang, Jürgen Müller, Liliane Biskupek, Vishwa Vijay Singh* 684
- S6-047 Towards high-precision International Height Reference System Using Two-Way Space Laser Time Transfer Link *Abdelrahim Ruby, Wen-Bin Shen, Ahmed Shaker, Ziyu Shen, Pengfei Zhang, Chenghui Cai, Wei Xu, Mostafa Ashry, An Ning, Lei Wang, Lihong Li* 685
- S6-048 The Benefit of Accelerometers based on Cold Atom Interferometry for Future Satellite Gravity Missions *Anniko Knabe, Manuel Schilling, Hu Wu, Alireza HosseiniArani, Jürgen Müller, Franck Pereira dos Santos, Quentin Beauflis* 687
- S6-049 A geodetic determination of the gravitational potential difference toward a 100-km-scale clock frequency comparison in a plate subduction zone *Yoshiyuki Tanaka, Yosuke Aoki* 689
- S6-050 Towards a transportable aluminum ion quantum logic optical clock for relativistic geodesy *Stephan Hannig, Benjamin Kraus, Constantin Nauk, Johannes Kramer, Fabian Dawel, Lennart Pelzer, Nicolas Spethmann, Piet Schmidt* 690
- S6-051 A Simplified Comparison Between Two Proposed Designs for a Future Earth Gravity Mission With and Without Strongly Reduced Non-Gravitational Acceleration Noise Level Requirements *Peter Bender* 691
- S6-052 ESA Activities and Perspectives on Quantum Space Gravimetry *Olivier Carraz, Luca Massotti, Ilias Daras, Roger Haagmans, Pierluigi Silvestrin* 692
- S6-053 The Application Sagnac Interferometry in the Geosciences *Ulrich Schreiber, Jan Kodet, Alexander Velikoseltsev, Thomas Kluegel* 693
- S6-054 Kalman-filter Based Hybridization of Classic and Cold Atom Interferometry Accelerometers for Future Satellite Gravity Missions *Alireza HosseiniArani, Benjamin Tennstedt, Manuel Schilling, Anniko Knabe, Hu Wu, Jürgen Müller, Steffen Schön* 694
- S6-055 Geopotential difference determination by TWSTFT *Peng Cheng, Wenbin Shen* 696
- S6-056 Unifying the world height system based on gravity frequency shift equation via optic fibers *Anh The Hoang, Wen-Bin Shen* 697
- S6-057 The MOCAS+ study: proposal of a quantum gravimetry mission integrating atomic clocks and cold atom gradiometers *Federica Migliaccio, Carla Braitenberg, Sergio Mottini, Gabriele Rosi, Mirko Reguzzoni, Fiodor Sorrentino, Guglielmo Maria Tino, Khulan Batsukh, Öykü Koç, Alberto Pastorutti, Tommaso Pivetta, Lorenzo Rossi* 698
- S6-058 Determination of the geopotential difference and orthometric height difference based on the two-way satellite time transfer observations *An Ning, Wen-Bin Shen, Ziyu Shen, Chenghui Cai, Wei Xu, Lihong Li* 700

S6-059	Status of gravimetric measurements and modelling along a 10m atom interferometer..... <i>Manuel Schilling, Étienne Wodey, Ludger Timmen, Dorothee Tell, Klaus H. Zipfel, Dennis Schlippert, Christian Schubert, Ernst M. Rasel, Jürgen Müller</i>	701
S6-060	High-Performance Clock Networks and Their Application in Geodesy..... <i>Hu Wu, Dennis Philipp, Eva Hackmann, Jürgen Müller, Claus Lämmerzahl</i>	702
S6-061	Gravimetry by nanoscale parametric amplifiers driven by radiation-induced dispersion force modulation..... <i>Fabrizio Pinto</i>	704
S6-062	Defining a unified height system for Egypt using the ACES microwave links..... <i>Mostafa Ashry, WenBin Shen, Abdelreheem Ruby, Hussein Abd-Elmotaal</i>	705
S6-063	Higher order ionospheric effects on microwave frequency transfer between spacecraft and ground station..... <i>Pengfei Zhang, Wen-Bin Shen, Chenxiang Wang, Ziyu Shen, Rui Xu, Chenghui Cai, Wei Xu, Abdelrahim Ruby, Mostafa Ashry</i>	706
S6-064	Novel Sensors and Quantum Technology for Geodesy (QuGe)..... <i>Jürgen Müller, Marcelo Santos</i>	708
S6-065	Gravity data acquisition with the transportable absolute Quantum Gravimeter QG-1..... <i>Nina Heine, Marat Musakaev, Sven Abend, Ludger Timmen, Waldemar Herr, Jürgen Müller, Ernst M. Rasel</i>	709

Symposium 1: Reference Frames

S1.1: International Terrestrial Reference Frame: strengths, weaknesses and strategies for future improvements

Category: Symposium 1: Reference Frames =» 1.1: International Terrestrial Reference Frame: strengths, weaknesses and strategies for future improvements

122

S1-001

Combined IVS contribution to the ITRF2020

Hendrik Hellmers¹、Daniela Thaller¹、Mathis Bloßfeld²、Manuela Seitz²、John Gipson³、Sadegh Modiri¹

1. Federal Agency for Cartography and Geodesy (BKG)
2. Deutsches Geodätisches Forschungsinstitut at TU München
3. Goddard Space Flight Center - NASA

As the successor of the currently used frame ITRF2014, the ITRF2020 describes the next official solution of the International Terrestrial Reference Frame. The global ITRF2020 solution is based on an inter-technique combination of the four space geodetic techniques VLBI, GNSS, SLR and DORIS. In this context, the Combination Centre of the IVS (International VLBI Service for Geodesy and Astrometry) operated by the Federal Agency for Cartography and Geodesy (BKG, Germany) in close cooperation with the Deutsches Geodätisches Forschungsinstitut at TUM (DGFI-TUM, Germany) generates the final VLBI contribution of the IVS. Thereby, an intra-technique combination utilizing the individual contributions of multiple Analysis Centres (AC) is applied.

For the upcoming ITRF2020 solution, sessions containing 24h VLBI observations from 1979 until the end of 2020 were (re-)processed by 11 different ACs and submitted to the IVS Combination Centre. Datum-free normal equations containing station coordinates and source positions as well as full sets of Earth Orientation Parameters (EOP) are delivered. For ensuring consistency of the combined solution, time series of EOPs, source positions and station coordinates as well as a VLBI-only Terrestrial Reference Frame (VTRF) and a Celestial Reference Frame (CRF) were generated and further investigated. Finally, the IVS contribution to the ITRF2020 solution consists of normal equations including EOPs and station coordinates via SINEX format.

To assess the quality of the data, internal as well as external comparisons of the estimated EOP are carried out. Thereby, the determined combined solution as well as external time series (e.g. Bulletin A) serve as a reference.

Additionally, the scale of the IVS contribution is investigated as VLBI is one of the space geodetic techniques realizing the scale of the ITRF2020. The evaluation of the contributions by the ACs, the combination procedure and the results of the combined solution for station coordinates, source positions and EOPs will be presented.

Key words ITRF2020, IVS Combination Centre, VLBI

Category: Symposium 1: Reference Frames => 1.1: International Terrestrial Reference Frame: strengths, weaknesses and strategies for future improvements

125

S1-002

Assessing daily and sub-daily ocean tidal loading displacements using GPS, Galileo, and GLONASS observations

Hanane Ait-Lakbir¹, Alvaro Santamaria¹, Félix Perosanz^{2,1}

1. CNRS

2. CNES, Toulouse, France

In today's GNSS precise positioning, station positions are assumed constant over a period of time, commonly a solar day. Terrestrial reference frames and precise GNSS orbits/clocks products are built upon this assumption. For that reason, all the tidal deformations of the crust near or below the daily period are removed using conventional model predictions. Among all the tidal phenomena, the ocean tidal loading (OTL) is probably the one prone to the largest prediction errors. OTL errors at the diurnal and sub-diurnal ranges can affect not only short-term station coordinates, and therefore the estimation of precise GNSS products, but show also long-term effects, which can both perturb the realization and the stability of the reference frame.

To assess the uncertainties of OTL models and even provide constraints to improve them, precise point positioning (PPP) is used to estimate the amplitudes of the residual tidal displacements relatively to an a priori model. This approach has been widely implemented based on GPS observations. The estimation for the K1/S1 and K2/S2 tidal constituents, which are close to the GPS orbital and constellation repetition period, is limited by GPS-related errors. These could be reduced by using PPP with integer ambiguity, even if not totally removed. Recently, the combination with GLONASS, which provides a different constellation configuration, has been considered to mitigate such GPS-specific errors. Since late 2018, the Galileo constellation provides PPP performances on the same level as GPS, in addition to the possibility of integer-ambiguity fixing, and similarly to GLONASS, a constellation configuration different from GPS. Here, we propose to analyze how Galileo can contribute to the estimation of the uncertainties in OTL model predictions. The results show that the inconsistency between observed and predicted displacements at solar-driven tidal frequencies is reduced while using Galileo-only or GPS+Galileo PPP solutions.

Key words Ocean tidal loading, GALILEO, GPS, GLONASS, PPP

Category: Symposium 1: Reference Frames =» 1.1: International Terrestrial Reference Frame: strengths, weaknesses and strategies for future improvements

134

S1-003

The International Laser Ranging Service (ILRS) Contribution to the Development of the ITRF2020

Erricos Pavlis¹、Cinzia Luceri²、Antonio Basoni²、David Sarrocco²、Magda Kuzmicz-Cieslak³、Keith Evans³、Giuseppe Bianco⁴

1. JCET, University of Maryland Baltimore County, USA

2. e-GEOS SpA, ASI/CGS-Matera, Italy

3. University of Maryland Baltimore County

4. Agenzia Spaziale Italiana (ASI), CGS-Matera, Italy

The ILRS contribution to ITRF2020 was submitted in April after a complete re-analysis of the 1993 to 2020 data. Based on improved modeling of the data and a novel approach that ensures the results are free of systematic errors in the underlying data, this contribution resulted in minimizing the difference in the scale between SLR and VLBI at below 2 mm (in ITRF2014 ~9 mm). This reanalysis incorporates an improved “target signature” model (CoM) that allows better separation of true systematic error of each tracking system from the errors in the model describing the target’s signature. The ILRS Analysis Standing Committee (ASC) devoted all its efforts on developing the new analysis approach over the past 5 years. The robust estimation of persistent systematic errors at the millimeter level, while still considering information provided by the stations, permitted the adoption of a consistent set of series of long-term mean corrections for each station’s data set that are now applied a priori. The reanalysis used these corrections, leading to improved results for the TRF attributes, reflected in the new time series of the TRF origin and especially in its scale. Seven official ILRS Analysis Centers contributed time series of weekly solutions, computed according to the guidelines defined by the ILRS ASC. These series were combined by the ILRS Combination Center to obtain the official ILRS product contribution to ITRF2020. In a second step, the ILRS ASC analyzed the data spanning the time period 1983 to 1992 to generate an extension of the SLR contribution to ITRF2020 spanning now 38 years.

The presentation will provide an overview of the analysis procedures and models, and it will demonstrate the level of improvement with respect to the previous ILRS product series; the stability and consistency of the solution are discussed for the individual AC contributions and the combined SLR time series.

Key words Reference frames, laser ranging, SLR, ILRS, ITRF

Category: Symposium 1: Reference Frames => 1.1: International Terrestrial Reference Frame: strengths, weaknesses and strategies for future improvements

155

S1-004

Quality Evaluation of the Continental Water Storage models for correcting the Crustal Movement Observation Network of China height time series

Zhao Li¹, Weiping Jiang¹, Liansheng Deng², Tonie van Dam³

1. Wuhan University

2. Hubei Polytechnic University

3. The University of Utah

The Crustal Movement Observation Network of China (CMONOC) is an important part of China's infrastructure with Global Navigation Satellite System (GNSS) as its main technological element, aiming at monitoring the crustal movement of the Chinese mainland and providing basic data for studying the three-dimensional (3-D) characteristics of structural deformation. Previous researches have already confirmed the strong correlation between continental water storage (CWS) and CMONOC GPS height time series. This environmentally driven displacement adds noise to the GPS data being used for investigating related geodynamic processes, for example, the plate tectonics. To remove this environmental signal from the GPS data, the CWS mass models are required to predict the surface displacements. However, these CWS model induced vertical surface displacement are often not consistent with each another and with seasonal variations of the GPS reference stations, thus it is of great necessity to evaluate the quality of different CWS models and their impacts on correcting the CMONOC height.

Under this background, eight different CWS models, including MERRA-Land, MERRA-2, NCEP-R-1, NCEP-R-2, ERA-Interim, together with another three GLDAS models with different versions and spatial resolutions, are used to estimate the surface displacements for the 28 CMONOC fiducial reference stations. Then we reprocess the GPS observations of these 28 stations spanning years of 2000~2016 based on state-of-the-art models so as to eliminate or reduce GPS-related systematic error. Through inter-comparison between different CWS models, outer-comparison between CWS and the obtained GPS height time series, we confirm that big discrepancy exists among CWS-derived CMONOC displacement. Among the 8 models, MERRA-Land performs the best in correcting CMONOC height (92.6%), which outperforms the latest MERRA-2 products by about 18.5%, thus we conclude that a new land-only "MERRA-2-Land" product would be possibly needed in the future.

Key words CMONOC, GPS height, Continental Water Storage, MERRA-Land, MERRA-2, NCEP, ERA-Interim, GLDAS

Category: Symposium 1: Reference Frames =» 1.1: International Terrestrial Reference Frame: strengths, weaknesses and strategies for future improvements

168

S1-005

Evaluation of the IGS contribution to ITRF2020

Paul Rebischung

IGN / IPGP

The International GNSS Service (IGS) recently finalized its third reprocessing campaign (repro3). Ten Analysis Centers (ACs) reanalyzed the history of GPS, GLONASS and Galileo data collected by a global tracking network over the period 1994-2020. Combinations of the daily repro3 AC terrestrial frame solutions constitute the IGS contribution to the next release of the International Terrestrial Reference Frame, ITRF2020. Compared to the previous IGS reprocessing campaign, a number of new models and strategies have been implemented in repro3, including the new IERS linear pole model, the new IERS-recommended sub-daily EOP tide model, and rotations of phase center corrections for tracking antennas not oriented North. Besides, a new set of satellite antenna phase center offsets was adopted in repro3, based on the published pre-flight calibrations of the Galileo satellite antennas. As a consequence, the IGS contribution to ITRF2020 provides for the first time an independent Galileo-based realization of the terrestrial scale, instead of being conventionally aligned in scale to the previous ITRF. In this presentation, results from the daily repro3 terrestrial frame combinations will be reviewed, impacts of the newly adopted models will be discussed, and IGS repro3 station position time series will finally be confronted to other products.

Key words IGS; GNSS; reprocessing; ITRF

Category: Symposium 1: Reference Frames =» 1.1: International Terrestrial Reference Frame: strengths, weaknesses and strategies for future improvements

182

S1-006

Status of ITRF2020 analysis and early results

Zuheir Altamimi¹, Paul Rebischung¹, Laurent Métivier¹, Xavier Collilieux^{1,2}, Kristel Chanard¹

1. IGN-IPGP France

2. ENSG - Chaps sur Marne, France

The ITRF2020 will be the occasion to enhance the modelling of the nonlinear station motions, including post-seismic deformation (PSD) models for stations subject to major earthquakes, and periodic signals embedded in the station position time series. In addition to the classical annual and semi-annual signals, we foresee to simultaneously adjust some satellite draconitic harmonics and evaluate their impact on the estimated frame parameters. The ITRF2020 is expected to be provided in the form of an augmented reference frame so that in addition to station positions and velocities, parametric models for both PSD and periodic signals (expressed in the CM frame of satellite laser ranging) will also be delivered to the users. We expect to show and discuss some early results, including the frame parameters (origin, scale and orientation), the level of agreement of periodic signals between techniques at collocation sites and give some indications regarding the specifications of the final ITRF2020 solution.

Key words Reference Frame, ITRF, ITRF2020

Category: Symposium 1: Reference Frames => 1.1: International Terrestrial Reference Frame: strengths, weaknesses and strategies for future improvements

325

S1-007

Shimosato co-location of the SLR and GNSS stations

Yuto Nakamura¹、Shun-ichi Watanabe¹、Yusuke Yokota²、Akira Suzuki³、Haruka Ueshiba³、Noritsune Seo⁴

1. Japan Coast Guard

2. Institute of Industrial Science, University of Tokyo

3. Geospatial Information Authority of Japan

4. Shimosato Hydrographic Observatory, Japan Coast Guard

The Japan Coast Guard (JCG) has been operating Satellite Laser Ranging (SLR) since 1982 at the Shimosato Hydrographic Observatory (SHO) to link the origin of the nautical charts to the global geodetic reference frame. The SLR observation results are submitted to the International Laser Ranging Service (ILRS), contributing to the development of the International Terrestrial Reference Frame (ITRF). Along with the SLR, SHO also operates a GNSS station that is registered to the International GNSS Service (IGS). The SHO, operating both SLR and GNSS, is a co-location site where these space geodetic techniques can be linked together by precisely measuring the local tie. In November 2020, JCG collaborated with the Geospatial Information Authority of Japan (GSI) and performed a local tie survey to precisely determine the local tie between the IGS stone marker and the Azimuth-Elevation (AZ-EL) intersect of the SLR telescope. In our survey, we conducted triangulation and levelling between the temporary sites set in the observatory and the antenna reference point of the IGS station. The AZ-EL intersect of the SLR telescope was determined by observing the targets mounted on the telescope from the temporary sites. During the target observation, the SLR telescope was rotated around the AZ and EL axes; thus, the observed target positions form arcs around the axes. The AZ-EL intersect was calculated by determining the AZ and EL axes from these target arcs. For the calculation of the local tie vector, we used the software pyaxis, released by Land Information New Zealand. The calculated local tie SINEX file was submitted to the IERS, to contribute to the development of the upcoming ITRF2020.

Key words satellite laser ranging, GNSS, co-location, local tie survey, ITRF

Category: Symposium 1: Reference Frames =» 1.1: International Terrestrial Reference Frame: strengths, weaknesses and strategies for future improvements

385

S1-008

Geodetic VLBI data processing of the specific experiments

Anastasiia Girdiuk, Gerald Engelhardt, Dieter Ullrich, Hendrik Hellmers, Daniela Thaller

Federal Agency for Cartography and Geodesy BKG

The VLBI observations are conducted as sessions of the defined length, 24-h and 1-h duration, in the specific days. The VLBI experiments are also characterized by the available stations, which detect group delays of the mutually visible sources. According to these determinants the VLBI experiments can be divided into the specific programs to improve or monitor the Earth Orientation Parameters (EOPs), station or source positions. For instance, R1 and R4 sessions are designed for EOPs monitoring, T2 and EURO sessions for the station position enhancement and CRF sessions for the celestial reference system realization. Since VLBI observations are irregular, especially in 80e and 90e, and include numerous campaigns, the most recent International VLBI Service for Astronomy and Geodesy (IVS) contribution to the last International Terrestrial Reference Frame ITRF2020 incorporates almost all available VLBI sessions. We have participated in this activity and built the new BKG2020a solution according with ITRF2020 requirements on the applied models and parameterization. A broad variety of the regular and specific VLBI experiments in our contribution are revised in order to evaluate an impact of the most recent specific experiments, namely 24-h VGOS broadband observations, mixed mode sessions and Onsala local sessions. The majority of the new VGOS stations participate only in the VGOS broadband observations, so that the data processing is focused on their station position determination. Additionally, the station positions of the new Onsala twin stations can be improved by the analysis of the recently released local campaign.

Key words VLBI, data analysis, ITRF2020, station positions, VGOS stations

Category: Symposium 1: Reference Frames =» 1.1: International Terrestrial Reference Frame: strengths, weaknesses and strategies for future improvements

653

S1-009

Local Ties at SLR station Riga

Kalvis Salmins¹、Viesturs Sproģis²、Imants Bijņskis²、Jorge del Pino¹

1. University of Latvia

2. Latvian Geospatial Information Agency

The station Riga operates a satellite laser ranging system since 1989 and collocated GPS system is operational since 1995. In 1991 the SLR system was collocated with the mobile laser ranging system MTLRS. The first local ties realization, connecting the ITRF points 12302S002 Riga (SLR Riga 1884) and 12302M001 (MTLRS geodetic mark), was done in 1992. The collocated permanent GNSS station started operation in December 1995 (ITRF 12302M002). The local ties were determined in 1995 using a six hour GPS session. Later two auxiliary geodetic points were added. This local network configuration remained unchanged for 25 years. During this period several surveys were done, the results were used only for monitoring purposes. The transit instrument dome was removed in 2013 establishing direct line of sight between 12302M002 and 12302M001. In 2018 Latvian Geospatial Information Agency (LGIA) installed three additional geodetic pillars to improve the local network. In January, 2021 a survey using tachymetry and GNSS was done by LGIA and the new local ties vectors were obtained and submitted to ITRF. It is planned to repeat last measurements of local ties in order to control their accuracy. In future we plan to do these measurements more regularly.

Key words Local ties, SLR, GNSS

Category: Symposium 1: Reference Frames =» 1.1: International Terrestrial Reference Frame: strengths, weaknesses and strategies for future improvements

772

S1-010

The 2021 Local Ties Campaign at GRAZ

Helmut Titz, Jürgen Fredriksson
Federal Office of Metrology and Surveying (BEV)

GRAZ has a very long tradition and is contributing to the ITRF continuously since the beginning. The SLR station has been build up in 1982 and GNSS has been operational since 1992. GRAZ contributes to the ILRS and the IGS as well as the EPN and is one of their oldest pillars. Absolute gravity measurements and nivellement connections have been done on regular intervals since 1998 too and the station has been integrated in the ECGN and will also be part of the upcoming IHRS. In 2018 an additional second laser telescope has been installed which is mainly used for quantum optics projects like transfers of kryptografic quantum keys via satellites over optical links and space debris studies. The new telescope may also be used for routine SLR measurements and may be a candidate site for future ITRF realisations too. At the moment the new telescope is not used in the production process but only used for tests. To include the new telescope into the local coordinate system and to check and update the old local ties which are from 2005 the BEV remeasured the local system this year on March 24, 2021. A new developed measurement strategy and refined calculation methods brought some differences in the connecting vector between SLR and GNSS monuments to daylight. Using the newly improved local ties in ITRF calculations may therefore be a next step for improving the quality of the ITRF. The poster illustrates the results of the 2021 local tie campaign.

Key words GRAZ SLR SDGS GNSS IGS EPN ECGN IHRS ISR/AAS BEV GGOS

Category: Symposium 1: Reference Frames => 1.1: International Terrestrial Reference Frame: strengths, weaknesses and strategies for future improvements

799

S1-011

The impact of the EOT20 global ocean tide model on space geodetic measurements, satellite orbits and derived geodetic parameters

Mathis Blossfeld, Mike Hart-Davis, Matthias Glomsda, Denise Dettmering
DGFI-TUM

The modelling of geophysical effects plays a crucial role when analyzing space geodetic observations. Among them, the accurate modelling of ocean tides is important for (i) the accurate computation of gravitational forces acting on near-Earth satellites and (ii) to reliably account for site displacements at the Earth's crust. At DGFI-TUM, the latest version of an empirical ocean tide model, EOT20, has been developed based on the residual tidal analysis of multi-mission satellite altimetry observations. EOT20 takes advantage of recent developments made in coastal altimetry, particularly in the use of the ALES retracker, to produce global atlas' of ocean and load tides for 17 tidal constituents. EOT20 shows significant improvements in the estimation of ocean tides compared to the previous iteration of the global model, EOT11a, particularly in the coastal and shelf regions.

In this presentation, the new EOT20 model is briefly introduced. Afterwards, we evaluate EOT20 by comparison to other state-of-the-art ocean tide models and to tide gauge records. In addition, the impact of the new ocean tide corrections on space geodetic measurements such as Satellite Laser Ranging (SLR) or Very Long Baseline Interferometry (VLBI) is quantified. Namely, we analyze estimated geodetic parameters like station coordinates (TRF parameters) and Earth Orientation Parameters (EOP) together with orbits of near-Earth satellites in order to judge the quality of the new empirical model for ocean tides for geodetic applications.

Key words EOT20, ocean tide model, SLR, VLBI, TRF, EOP, geodetic parameter

Category: Symposium 1: Reference Frames =» 1.1: International Terrestrial Reference Frame: strengths, weaknesses and strategies for future improvements

814

S1-012

Densification of the VLBI network in the Southern hemisphere: advanced simulation for a VLBI antenna on Tahiti

Vladimir Schott Guilmault¹、 David Coulot^{1,4}、 Sébastien Lambert²、 Arnaud Pollet¹、
Jean-Yves Richard²、 Christian Bizouard²、 Richard Biancale³

1. IPGP, IGN, Université Paris Diderot, Sorbonne Paris Cité, UMR 7154 CNRS, Paris, France

2. SYRTE, Observatoire de Paris, Université PSL, CNRS, Sorbonne Universités, UPMC Univ. Paris 06, LNE, Paris, France

3. GFZ, Potsdam, Germany

4. ENSG, Champs-sur-Marne

The current distribution of the VLBI network across the globe is unbalanced. Most of the antennas are located in the Northern hemisphere, and, consequently, a majority of VLBI observations is made on radio-sources in the Northern hemisphere. This situation has an effect on the determination of the positions of quasars in the Southern hemisphere, which is generally less accurate than in the Northern one. Furthermore, it impacts the realization of TRF: any effect on the propagation delay that is not modeled with enough precision can shift vertical positions of stations, and the more important weight of the northern stations can impact the scale factor.

Taking advantage of the project to create a geodetic observatory on Tahiti island (in the South Pacific), which plan to install a VLBI antenna, we decided to assess the effect on the TRF and EOP determination when we add Tahiti to the existing VLBI network. We recreated the observation schedules on the 2012.0-2017.0 period including Tahiti, and attempted to simulate uncertainties for all phenomenon affecting VLBI.

Final analysis shows that adding Tahiti to this VLBI network clearly improves the distribution of observations between quasars in the Northern and Southern hemispheres, reducing more the residuals on quasars' positions in the south, and significantly improving the determination of the TRF scale factor.

Key words VLBI ; simulations ; TRF ; network

Category: Symposium 1: Reference Frames => 1.1: International Terrestrial Reference Frame: strengths, weaknesses and strategies for future improvements

856

S1-013

New Developments on the IDS Contribution to the ITRF2020

Guilhem Moreaux¹、 Frank Lemoine²、 Hugues Capdeville¹、 Petr Štěpánek³、
Michiel Otten⁴、 Jérôme Saunier⁵、 Pascale Ferrage⁶

1. Collecte Localisation Satellites

2. NASA, Goddard Space Flight Center

3. Research Institute of Geodesy, Topography and Cartography

4. ESA, European Space Operations Centre

5. IGN

6. CNES

In the context of the realization of the new International Terrestrial Reference Frame (ITRF2020), the International DORIS Service (IDS) delivered to the IERS a first version of its contribution (series IDS 15) by April 10th. This solution is a set of 1456 weekly SINEX files containing DORIS stations positions and Earth orientation parameters from January 1993 to December 2020 (series IDS 15).

Even if that new IDS combined solution shows better performances in terms of both stability of the origin and station positioning when compared to the IDS contribution to the ITRF2014, the IDS Analysis Centers reviewed their contributions in order to improve the scale stability between the arrival of Jason-2 (2008.5 - with onboard first DORIS receiver capable to track up to seven beacons simultaneously) and of HY-2A (2011.8), leading to a newest IDS combined solution (series IDS 16)

The primary objective of this study is present the major evolutions between the two latest IDS combined series and the impact on origin, scale, station positioning and EOPs.

The second purpose is to evaluate the benefits of including the estimation of annual, semi-annual and first Jason draconitic signals while stacking the IDS weekly combined solution from 1993.0 to 2021.0 to get mean positions and velocities of the 200 stations at the 86 DORIS sites.

Key words ITRF, DORIS

Symposium 1: Reference Frames

S1.2: Advancements and open problems in global reference frame theory and methodology

Category: Symposium 1: Reference Frames => 1.2: Advancements and open problems in global reference frame theory and methodology

74

S1-014

Modelling and prediction of GPS time series with machine learning approaches

Wenzong Gao, Yanming Feng
Queensland University of Technology

Causes for GPS site vertical motions include the redistribution of environmental surface masses, such as continental water variations, atmospheric pressure changes, tidal and non-tidal ocean fluctuations, redistribution of ice and snow. The coordinate time series of each GNSS site has been conventionally modeled by least-squares fitting with harmonic functions. The daily repeatability in vertical components after least-squares fitting is normally in the order of 4 to 6 millimeters. The current modeling basically involves two variables: time and location, despite various underlying physical mechanisms responsible for the site motion. This work seeks to use a Machine Learning (ML) approach to reflect the relationships between site motions and physical factors, including polar motion parameters, the Sun and the Moon ephemerides, the temperature parameter, the atmospheric pressure parameter, and the hydrological parameters. These parameters are constructed as the input vector of each ML training sample, while the height of the GPS sites is regarded as the output. In the study, the artificial neural networks algorithm is introduced as the primary ML method for the GPS time series modeling and predicting process. To verify this method, we analyzed the time series datasets collected from 6 GPS sites, namely MOBS, SYDN, PERT, DARW, KARR, KAT1, respectively over the period of 11 years. The results indicate that the ML modeling repeatability values from 3 sites are under 4 mm and these from other 3 sites are under 5 mm. Overall, the precision of the ML-derived vertical GPS site motion model is improved by 15-20% with respect to the repeatability results from the traditional least square fitting method. We also analysed the GNSS time series prediction results for the future 3 months. The results show that the ML prediction precision is slightly lower than the ML fitting precision, but still within the range of 4-7mm for the tested stations.

Key words GPS; Time series; Modelling; Prediction; Machine learning; Artificial neural networks

Category: Symposium 1: Reference Frames =» 1.2: Advancements and open problems in global reference frame theory and methodology

161

S1-015

Denoising method of elevation time series based on CEEMD algorithm and time-lapse multi-scale permutation entropy

Peixian Wang、 Haoran Li
Liaoning University of technology

The elevation time series of satellite navigation and positioning reference station is difficult to extract useful signals due to various kinds of noises. In allusion to this problem, this paper proposes a denoising method based on CEEMD algorithm and time-lapse multi-scale permutation entropy (TSMPE). In this method, the noise IMF, signal IMF and mixed IMF were demodulated by using the difference of time-lapse multi-scale permutation entropy values of noise and signal components. Secondly, the soft threshold method was used to denoise the mixed IMF. Finally, the denoised mixed IMF and signal IMF were reconstructed to obtain the final denoising result. Besides, the elevation time series of BJFS station and JOEN station from 2000 to 2020 was taken as the experimental data. As shown by experimental results, the proposed method can effectively determine the signal-noise boundary point and complete noise reduction. Compared with EMD and EEMD denoising methods, the denoising method in this paper improves the signal-to-noise ratio of elevation time series by more than 14% and reduces the root mean square error by more than 13%, which can not only better realize the denoising of elevation time series but also provide more real and reliable data support for further research.

Key words CEEMD; elevation time series; time-lapse multi-scale permutation entropy; threshold denoising; signal-to-noise ratio

Category: Symposium 1: Reference Frames => 1.2: Advancements and open problems in global reference frame theory and methodology

287

S1-016

The cross-correlations of the Helmert transformation parameters as an additional diagnostic tool for Terrestrial Reference Frames assessment

Dimitrios Ampatzidis, Daniela Thaller, Lin Wang
Federal Agency for Cartography and Geodesy

The accuracy and the consistency of the Terrestrial Reference Frames (TRFs) are mainly assessed through the well-known Helmert transformation parameters. The magnitude of the estimated Helmert parameters which connect e.g. a technique-only and a combined solution of a global TRF, respectively, can identify possible inconsistencies or/and deficiencies. Another tool with respect to the assessment of the TRFs are the cross-correlations of the different Helmert transformation parameters. Initially, one can observe the dependency among the Helmert transformation parameters and therefore revealing some deficiencies of a particular technique. Additionally, the cross-correlations comparison between a technique-only and a combined solution of global TRF, respectively, could crystalize the impact of combined TRF versus a single technique one for some significant static and dynamical features, like the origin and the scale (and their associate rates). We compare the a. Helmert parameters correlations of the SLR-only and VLBI-only and the fully-combined DTRF2014 TRFs and b. the cumulative International DORIS Service (IDS) TRF and the official ITRF2014, respectively. The results reveal some interesting facts regarding the merit of the cross-correlations of the 14 Helmert transformation parameters as an additional diagnostic tool for the TRF assessment.

Key words cross-correlations, Helmert parameters, SINEX, TRF assessment, datum effect

Category: Symposium 1: Reference Frames => 1.2: Advancements and open problems in global reference frame theory and methodology

492

S1-017

Observation density method for selecting independent baselines in GNSS network

Tong Liu¹、Guochang Xu¹、Zhiping Lv^{1,3}、Yujun Du²、Jian Liu¹

1. Harbin Institute of Technology at Shenzhen

2. The University of New South Wales

3. Information Engineering University

The maintenance of the geodetic coordinate system requires the networked calculation of large GNSS observation data. The generation of independent baselines is a necessary part of data processing for large GNSS observation networks.

In a network of n stations, $n-1$ independent baselines need to be selected. Different independent baseline selection methods can affect the final accuracy of GNSS networks. The default operation utilizes the maximum common observation (OBS-MAX) or the shortest total distance (SHORTEST). OBS-MAX makes use of maximal number of observations to participate in the adjustment to improve the final solution accuracy. The advantage of SHORTEST is that, it uses baselines with the shortest possible total distance to minimize the effect of ionospheric and tropospheric errors while ensuring an adequate number of observations. Recent studies have shown that a weighted treatment normalizing these two methods (WEIGHT), i.e., when considering both the maximum observation and the shortest path, yields better accuracy. However, this weighting model is empirically based. When treating these two methods with equal weights, it only guarantees better accuracy of the network solution for about 1/3 of the days in the annual statistical results. When the posterior accuracy of each net solution is used as the weight, although the proportion of high-precision net solution days can be improved, this will greatly increase the computational burden.

With the above discussion, a baseline selection method without a posteriori or empirical statistics are proposed here. The criterion it uses to select the independent baseline is the observation density (OBS-DEN). This criterion is the ratio of the number of common observations to the distance between every two stations. Its physical meaning is the consequent change in the number of common satellite observations for every 1 km increase in the distance between the two stations. If the distance between these two stations is short enough while the number of common observations is high enough, then this baseline will be preferred. We conducted experiments using the globally distributed stations on January 3, 2012. The results show that the errors in XYZ direction of

OBS-DEN are 4.63mm, 4.77mm and 5.49mm, and the 3D error is 8.62mm, while in WEIGHT, it is 4.67mm, 5.24mm, 5.28mm, and the 3D error is 8.78mm. This demonstrates that OBS-DEN can obtain higher accuracy of the network solution. This method extends the advantages of maximum observation and shortest path and avoids the shortcomings of WEIGHT which requires empirical and a posteriori accuracy. OBS-DEN can be used as a better solution in network solution.

Key words GNSS network; independent baseline; observation-max; shortest

Category: Symposium 1: Reference Frames => 1.2: Advancements and open problems in global reference frame theory and methodology

518

S1-018

Handling of tropospheric and range biases in Satellite Laser Ranging

Mateusz Drożdżewski, Krzysztof Sośnica, Dariusz Strugarek
Wrocław University of Environmental and Life Sciences

Satellite laser ranging (SLR) is the only space geodetic technique that provides the most reliable information about geocenter motion, as well as low-degree spherical harmonics of the Earth's gravity field. SLR is the only technique in which in-situ meteorological observations are used to determine the zenith total delays (ZTD) at the epochs of observations with no estimated corrections. The tropospheric parameters are not estimated in SLR because of the low number of observations, low sensitivity of laser measurements to the wet part of the tropospheric delays, which changes in time and space rapidly, and the high precision of meteorological data collected together with SLR measurements. Currently, all errors occurring at SLR stations are typically accumulated in additional estimated parameters: range biases; however, the source of biases is typically unknown. Some SLR stations, such as Graz and Wettzell, recently discovered biases of the barometer readings, which may introduce a systematic error to the SLR measurements. In this contribution, we introduce an approach based on the separation of systematic errors in SLR into two groups. One error type depends on the elevation angle and is handled by adding a troposphere bias parameter proportional to the SLR tropospheric delay. The second group includes errors that are the same for all elevation angles: range biases.

We analyze the contribution of the troposphere bias to the total amount of systematic errors at SLR stations, as well as the impact on the other geodetic parameters, such as station coordinates, geocenter coordinates, and the global scale. We check the correlations between range biases, tropospheric biases, and the height components of SLR station coordinates, as well as the repeatability of SLR station coordinates. Finally, we conduct an additional solution with artificial pressure biases of 5 hPa that correspond to an overestimation of ZTD at the level of 11.4 mm in the zenith direction.

Key words SLR, troposphere biases, range biases

Category: Symposium 1: Reference Frames => 1.2: Advancements and open problems in global reference frame theory and methodology

630

S1-019

A Refined Global GNSS Velocity Field Modeling Station Seismic Deformation based on Constrained Nonlinear Optimization

Yingying Ren¹、Hu Wang²、Jiexian Wang¹、Yangfei Hou¹、Pengyuan Li¹

1. tongji university

2. Chinese Academy of Surveying and Mapping

With the rapid development of Global Navigation Satellite System (GNSS) technology, the long-term accumulated GNSS observations of global reference stations provide valuable research materials for geodesy and geodynamics studies since the 1990s. In GNSS time series analysis, we usually need to model the offset, velocity, and period terms finely. However, the nearby major seismic activities will seriously damage the station's typical motion trajectory. By analyzing the calculated GNSS coordinate time series with high precision, the single site's motion trajectory can be accurately modeled for describing the kinematic features of the local or global reference frame. Therefore, our research is motivated to refine a new global GNSS velocity field modeling nonlinear station motions from the nearly long-term GNSS station observations. Firstly, we improve the GNSS data processing strategies to obtain GNSS coordinate time series with mm precision, which provides the necessary input data for time series analysis. Secondly, an Integrated Time Series Model (ITSM) adding seismic deformation is proposed to describe the station's nonlinear motion trajectory accurately. The ITSM directly calculates seismic relaxation time by using Constrained Nonlinear Optimization (CNO), which can overcome the problem of separating relaxation time from other time series parameters in the existing research, to improve the accuracy and reliability of velocity parameters significantly. Furthermore, some case results verify the accuracy and reliability of the model, which shows that the fitting accuracy of GNSS displacement in the horizontal direction is better than 5 mm and that in the vertical direction is better than 1 cm. Finally, the global GNSS station velocity field is refined using long-term GNSS observations, which helps explain global plate tectonic motion and establish a Dynamic Terrestrial Reference Frame (DTRF) for better studying geodynamic processes. The velocity results further verify the accuracy of the global GNSS velocity, which shows that the accuracy of global velocity is better than 1 mm/a, and the averages of velocity Root Mean Square Error (RMSE) are 0.19 mm/a, 0.19 mm/a, and 0.33 mm/a in the 3D direction. Compared with ITRF2014, there is a difference of about 1 mm/a between them due to data duration, processing model, and geodetic technology.

Key words GNSS; time series analysis; motion trajectory; velocity field; crustal movement

Category: Symposium 1: Reference Frames => 1.2: Advancements and open problems in global reference frame theory and methodology

706

S1-020

Periods Extraction of GNSS Coordinate Time Series Based on Significance Level

Yanfeng JIA¹、Xinhui ZHU²、Fuping SUN²

1. Information Engineering University

2.

At present, the method for periodic detection and identification in coordinate time series is easily affected by noise and sidelobes, and is not conducive to large-scale data processing. In order to solve this problem, a method based on significance level is proposed. The method could automatically detect and identify the periods in GNSS coordinate time series. After the performance is verified by simulation data, this method is used to extract the periods in the coordinate time series of 1082 stations distributed globally. The result shows that the method can realize the automatic detection and extraction of potential periods under the influence of noise and sidelobes, and has good performance. In the simulation experiment, it still has an accuracy of 70% when the SNR is -10dB. And by extracting the periods of the measured data in the three directions of N, E and U, it is found that in addition to the annual and semi-annual period, there are periods with spans of about 120d, 88d, 71d, 59d, 50d and 14d around the world. It is consistent with the research results of related scholars, which proves the feasibility of this method in practical application.

Key words coordinate time series; non-linear variations; periods extraction; Lomb–Scargle periodogram; significance level

Category: Symposium 1: Reference Frames => 1.2: Advancements and open problems in global reference frame theory and methodology

870

S1-021

Characteristics and Predictability of Postseismic Deformation in Reference Frame Models

Jeff Freymueller
Michigan State University

Postseismic deformation is commonly observed after large earthquakes, in the form of transient non-linear station motions. Afterslip and viscoelastic relaxation are two of the known physical causes for postseismic deformation are afterslip. Afterslip is continued fault creep on the fault plane, often occurring deeper or shallower than the earthquake rupture area itself. Viscoelastic relaxation occurs within a viscoelastic medium near or surrounding the fault, and commonly occurs at greater depth than the earthquake, within the Earth's mantle. Physical models can be developed for these processes, but these always contain some adjustable parameters that describe the fault zone's frictional properties or mantle viscosity. Empirical time series models for deformation can be estimated as well, but again with adjustable parameters that describe the non-linear relaxation process. Because both processes are often active at the same time, estimating the adjustable parameters is prone to problems caused by parameter tradeoffs.

For use in a reference frame model, it is important to be able to predict postseismic deformation forward in time, and to predict the uncertainty as a function of time. Because of the parameter tradeoffs, the predictive power of postseismic models often has been poor. In particular, in a time series model, it is critical that the relaxation times of the non-linear functions be known well; if those are not known accurately, the models will rapidly diverge from the true values. However, suites of trial forward models can be used to assess the likely uncertainty range as a function of time. While determining the "best" postseismic model parameters can be challenging, a relatively small number of observations (in time) can be used to weight individual models within a suite of trial models to make reasonably accurate future predictions. The ensemble of potentially valid predictions can then give not just an estimate but a measure of prediction uncertainty.

Key words postseismic, model, uncertainty, deformation

Symposium 1: Reference Frames

S1.3: Terrestrial and space geodetic ties for multi-technique combinations

Category: Symposium 1: Reference Frames => 1.3: Terrestrial and space geodetic ties for multi-technique combinations

123

S1-022

Dilution of Precision (DOP) factors for evaluating observations to Galileo satellites with VLBI

Helene Wolf¹, Johannes Böhm¹, Matthias Schartner², Urs Hugentobler³

1. TU Wien

2. ETH Zürich, Department of Civil, Environmental and Geomatic Engineering,
Space Geodesy, Zürich, Switzerland

3. TU München, Institute for Astronomical and Physical Geodesy, München,
Germany

Observing satellites besides natural extra-galactic radio sources (quasars) with Very Long Baseline Interferometry (VLBI) telescopes permits the extension of the current research of this interferometric technique. These observations offer a variety of new applications such as the direct determination of the absolute orientation of the satellite constellation with respect to the International Celestial Reference Frame (ICRF). In addition, observing satellites with VLBI telescopes enables high precision tying of space geodetic techniques and therefore results in improvement of long-term reference frames. In order to observe quasars and geodetic satellites with the same instruments it is necessary that satellites transmit signals that can be observed by VLBI telescopes. Therefore, ideas of installing a dedicated VLBI transmitter on board of future Galileo satellites have been proposed over the last years.

The following contribution provides an evaluation study of observations to Galileo satellites with VLBI telescopes. Recently, the scheduling software VieSched++ was equipped with a newly developed satellite scheduling module, which is used for the determination of possible observation periods to Galileo satellites from a selected VLBI network. These possible observations are evaluated through their sensitivity towards changes of the satellite position concerning the radial, along-track and cross-track component. The sensitivities of an observation towards changes in the respective components are indicated by different Dilution of Precision (DOP) factors, which are the radial DOP, the along-track DOP and the cross-track DOP. The lower the value of the respective DOP the more sensitive the observation is towards the corresponding component.

Key words VLBI, Galileo, VieSched++

Category: Symposium 1: Reference Frames => 1.3: Terrestrial and space geodetic ties for multi-technique combinations

124

S1-023

Reference frame realization using co-location in space onboard Galileo satellites

Grzegorz Bury¹, Krzysztof Sośnica¹, Radosław Zajdel¹, Dariusz Strugarek¹, Urs Hugentobler²

1. Wrocław University of Environmental and Life Science

2. Institute for Astronomical and Physical Geodesy, Technical University of Munich

Terrestrial reference frames (TRF) constitute the time-space reference for all phenomena observed in the Earth system. Current TRFs are solved using observations provided by space geodetic techniques, i.e., Global Navigation Satellite System (GNSS), Satellite Laser Ranging (SLR), Very Long Baseline Interferometry (VLBI), and Doppler Orbitography and Radiopositioning Integrated by Satellite (DORIS). The integration of all the space techniques is solved by the so-called local ties which comprise the local ground measurements at the co-located stations. Therefore, the space technique integration plays a crucial role in the realization of TRF. Currently, GNSS satellites of Galileo and GLONASS are equipped with laser retroreflector arrays for SLR providing a possibility for co-location of GNSS and SLR techniques in space onboard navigation satellites.

In this study, we elaborated the methodology of a realization of TRF using GNSS-SLR co-location onboard Galileo and GLONASS satellites. We established that the best way to realize common GNSS and SLR networks is by imposing the no-net-translation and no-net-rotation minimum constraints to GNSS and SLR core stations. Based on the estimated GNSS and SLR station coordinates we estimated a linkage between co-located stations which constitutes an equivalent of the ground measured local tie. Moreover, we revised the methodology of the SLR range biases calculation. Now, the calculated range biases consider the impact of the SLR observations to geodetic satellites, not only to the GNSS spacecraft. Such a treatment improved the estimated value of the local tie from 4.4 mm to 2.4 mm for the co-located station in Wettzell, Germany.

The estimated values of local ties using combined GNSS and SLR-to-GNSS observations might be used for validating the local ground measurements or can constitute additional data with full variance-covariance information as an input for future realization of TRF.

Key words GNSS, SLR, co-location, terrestrial reference frame, Galileo, GLONASS

Category: Symposium 1: Reference Frames => 1.3: Terrestrial and space geodetic ties for multi-technique combinations

178

S1-024

Large-scale dimensional metrology for geodesy - first results from the European GeoMetre Project

Florian Pollinger¹, Clément Courde³, Cornelia Eschelbach⁵, Luis Garcia-Asenjo⁷, Joffray Guillory⁹, Per Olof Hedekvist¹¹, Ulla Kallio¹³, Thomas Klügel¹⁵, Pavel Neyezhnikov², Damien Pesce⁴, Marco Pisani⁶, Jeremias Seppä⁸, Robin Underwood¹⁰, Kinga Wezka¹², Mariusz Wiśniewski¹⁴, for the GeoMetre Consortium¹⁶

1. Physikalisch-Technische Bundesanstalt (PTB), Bundesallee 100, 38116 Braunschweig, Germany
2. National Scientific Center "Institute of Metrology", Mironositskaya Str. 42, 61002 Kharkiv, Ukraine
3. Université Côte d'Azur, CNRS, Observatoire de la Côte d'Azur, IRD, Géoazur, 2130 Route de l'Observatoire, 06460 Caussols, France
4. Institut national de l'information géographique et forestière (IGN), 94160 Saint-Mandé, France
5. Laboratory for Industrial Metrology, Faculty of Architecture, Civil Engineering and Geomatics, Frankfurt University of Applied Sciences, Nibelungenplatz 1, 60318 Frankfurt am Main, Germany
6. Istituto Nazionale di Ricerca Metrologica (INRIM), Strada delle Cacce, 91, 10135 Torino, Italy
7. Departamento de Ingeniería Cartográfica, Geodesia y Fotogrametría, Universitat Politècnica de València, Camino de Vera s/n, 46022 Valencia, Spain
8. VTT Technical Research Centre of Finland Ltd, Centre for Metrology MIKES, PO Box 1000, 02044 VTT, Finland
9. Conservatoire National des Arts et Métiers (Cnam), Laboratoire commun de métrologie LNE-Cnam, 1 rue Gaston Boissier, 75015 Paris, France
10. National Physical Laboratory, Hampton Road, Teddington, TW11 0LW, United Kingdom
11. RISE Research Institutes of Sweden, Box 857, 501 15 Borås, Sweden
12. Faculty of Geodesy and Cartography, Warsaw University of Technology, Plac Politechniki 1, 00-661 Warsaw
13. Finnish Geospatial Research Institute, National Land Survey of Finland, Geodeetinrinne 2, 02430 Masala, Finland
14. Central Office of Measures, ul. Elektoralna 2, 00-139 Warszawa Poland
15. Geodetic Observatory Wettzell, Federal Agency for Cartography and Geodesy, 93444 Bad Kötzing, Germany
16. <https://www.ptb.de/empir2018/geometre/home/>

Terrestrial reference frames (TRFs) are based on space-geodetic observations and co-located sites local tie surveys results. Since 2019, 16 European institutions from geodesy as well as length and temperature metrology have been working together in the joint research project 'GeoMetre' to further reduce the TRF uncertainty, tackling two instrumental challenges:

(1) We seek for suitable references over several kilometers with an uncertainty level of 1 mm to support the instrumental development in SLR, VLBI, or GNSS.

(2) We develop and refine instrumentation, measurement methods and analysis strategies for the local tie vector determination, aiming at uncertainties of 1 mm in 3D.

So far, the surveying networks at the GGOS core stations Metsähovi, Finland, and Wettzell, Germany, have been expanded, e.g. by enabling seamless GNSS-terrestrial measurements. Two optical ranging systems are being developed with a targeted range of up to 5 km. Different strategies for refractive index compensation are being explored and compared. They will be applied to establish reference values for test fields, e.g. at the Calern site of the Observatoire de la Côte d'Azur (OCA) in France or the novel European large-scale reference base at the Pieniny Kippen Belt in Poland. For local tie metrology, they will reduce the uncertainty of the ground surveying network. A second focus is on reference point monitoring: we have explored photogrammetric methods and develop a complex telescope monitoring setup based on novel multilateration and temperature compensation systems. We also investigate the inclusion of the local gravity field to consider the deviations of the vertical in the data analysis. All those methods will be combined and evaluated in final joint measurement campaigns in the remaining project.

This project 18SIB01 GeoMetre has received funding from the EMPIR programme co-financed by the Participating States and from the European Union's Horizon 2020 research and innovation programme.

Key words Local Tie metrology, measurement technologies, terrestrial local tie measurements

Category: Symposium 1: Reference Frames => 1.3: Terrestrial and space geodetic ties for multi-technique combinations

228

S1-025

Determination of Galileo and GLONASS orbits based on combined SLR and GNSS data

Grzegorz Bury¹、Krzysztof Sośnica¹、Radosław Zajdel¹、Dariusz Strugarek¹、Urs Hugentobler²

1. Institute of Geodesy and Geoinformatics, Wrocław University of Environmental and Life Sciences

2. Institute for Astronomical and Physical Geodesy, Technical University of Munich

Modern satellites of the Global Navigation Satellites Systems (GNSS) are equipped with laser retroreflector arrays for Satellite Laser Ranging (SLR). As a two-way space geodetic technique SLR allows to measure ranges. Thanks to the different wavelengths, SLR observations (optical) are vulnerable to different systematic errors than GNSS observations (microwave). As a result, SLR observations to GNSS satellites typically serve as an independent tool for the validation of the GNSS-based orbit products. However, SLR observations can be used also for the determination of the GNSS orbit parameters.

In this study, we present the results for Galileo and GLONASS precise orbit determination using a combination of the GNSS and SLR-to-GNSS observations. The addition of the SLR-to-GNSS observations stabilizes the orbit solution especially for periods when the elevation of the Sun above the orbital plane is highest. The formal error of the semi-major axis of the Galileo satellites is diminished by up to 62%. As for the precision which is assessed based on the SLR residual analysis the STD of SLR residuals is diminished from 36.1 to 29.6 mm as compared to the GNSS-only solution. The combined SLR and GNSS orbit solution provides a promising prerequisite for the co-location onboard the GNSS satellites for the realization of the terrestrial reference frame and deriving global geodetic parameters.

Key words SLR, GNSS, co-location, precise orbit determination, Galileo, GLONASS

Category: Symposium 1: Reference Frames => 1.3: Terrestrial and space geodetic ties for multi-technique combinations

229

S1-026

Radar Corner Reflector installation at the OCA geodetic Observatory (France)

Xavier Collilieux^{1,7}, Clément Courde², Bénédicte Fruneau³, Mourad Aïmar⁴, Guillaume Schmidt^{7,8}, Isabelle Delprat^{7,8}, Damien Pesce⁵, Guy Wöppelmann⁶

1. Université de Paris, Institut de physique du globe de Paris, CNRS, IGN, Paris, France
2. Université Côte d'Azur, CNRS, Observatoire de la Côte d'Azur, IRD, Géoazur, Caussols, France
3. LaSTIG, Univ Gustave Eiffel, F-77454 Marne-la-Vallée
4. Université Côte d'Azur, CNRS, Observatoire de la Côte d'Azur, IRD, Géoazur, Caussols, France
5. Institut national de l'information géographique et forestière, Saint-Mandé, France
6. Laboratoire Littoral Environnement et Sociétés, UMR7266 – Univ La Rochelle and CNRS, La Rochelle, France
7. ENSG-Géomatique, IGN, Marne-la-Vallée, France
8. Enseignement Militaire Supérieur Scientifique et Technique, Ecole militaire, Paris, France

Geodetic observatories host several geodetic permanent instruments whose coordinates can be determined at the centimeter level or better. They comprise Global Navigation Satellite System (GNSS) permanent antenna/receivers, Satellite Laser Ranging (SLR) stations, Very Long Baseline Interferometry (VLBI) telescope and Doppler Orbitography Integrated by Satellite (DORIS) beacons. The Calern site of the Observatoire de la Côte d'Azur (OCA) is an example of such a multi-technique site located in the South of France. It hosts a DORIS beacon, a SLR/LLR station and two GNSS permanent stations.

In the process of determining coordinates of geodetic instruments in a unified reference frame, the relative positions of the instruments at co-location sites are integrated in the ITRF combination. Thanks to the additional measurements obtained from local surveys, it is possible to determine global biases between coordinates determined by individual space geodetic techniques, and express them in the same reference system. An additional fundamental assumption of the combination process is that stations located on the same site do not move with respect to each other. Spaceborne Synthetic Aperture Radar Interferometry (INSAR technique), is an interesting tool to evaluate that hypothesis as it allows measuring ground displacements in the line of sight of the satellite, and has been used only occasionally in the past for this purpose. Notably, the Persistent Scatterer (PS) Interferometry enables determining time series of ground displacements on particular

scatterers exhibiting phase stability in a stack of SAR images. To ensure the presence of such PS, artificial corner reflectors can be installed.

We present the procedure that we adapted from Parker et al. (2007) to install and validate the installation of a corner reflector at OCA observatory, close to the currently operating GNSS, SLR and DORIS stations, specifically designed for Sentinel-1 satellite. An initial local tie survey was carried out to assess the stability of the reflector through time.

Key words ITRF, local ties, InSAR

Category: Symposium 1: Reference Frames => 1.3: Terrestrial and space geodetic ties for multi-technique combinations

320

S1-027

Datum problem in terrestrial local ties

Ulla Kallio¹, Thomas Klügel², Simo Marila¹, Svetlana Mähler², Markku Poutanen¹, Torben Schüler², Heli Suurmäki¹

1. FGI, National Land Survey of Finland

2. BKG, Geodetic Observatory Wettzell

The datum problem is a fundamental issue in the network adjustment when connecting a local measurement network to an external reference frame. Datum elements in 3D networks are scale, translation, and orientation. We consider here the local tie network at geodetic core stations, where the external reference frame is the latest ITRF realization in the mean epoch of terrestrial observations.

Accurate distance measurements are used for the determination of the network scale. Thus the improvement of its accuracy and the inclusion of weather measurements to account for refraction errors are essential. For rotation and translation of the network, we need external information. Angle observations are related to the coordinate system of the instrument which is usually aligned to the plumb line. Instruments have different vertical orientation at every station point and the direction of the plumb line does not coincide with the normal vector of the reference ellipsoid. Horizontally the observed set of angles are oriented in arbitrary or approximately oriented directions.

External information which is needed for solving the orientation are datum points, providing the link to the global coordinate system, and correction terms for the vertical orientation (deflection of the vertical), which can be derived from combined terrestrial/GNSS observations, from a gravity based geoid model, or from astronomical observations.

In this article, we present the solutions/options for the datum problem in the framework of the EMPIR Geometre project using the example of the ITRF core stations Metsähovi and Wettzell. Beside the classical transformation, a transformation-free approach is presented. The inclusion of distant targets is promising, since at small networks even a millimetre change in the coordinates of a datum point can affect significantly a local tie vector. When using the vertical deflection or the dip of the geoid surface, the inclination should be known within 0.2 arc seconds.

Key words Datum problem, local ties, scale, orientation, network adjustment

Category: Symposium 1: Reference Frames => 1.3: Terrestrial and space geodetic ties for multi-technique combinations

341

S1-028

Multi-technique combinations using a closure in time

Jan Kodet¹、Ulrich Schreiber¹、Thomas Klügel²

1. Technical University München

2. Federal Agency for Cartography and Geodesy

Space Geodesy is based on accurate distance measurements, which are performed as signal delay measurements multiplied by the speed of light. VLBI and GNSS measure these delays with respect to the station clock; therefore, the pseudo-range must be corrected by a clock synchronization term in post-processing. In contrast, SLR is based on time of flight measurement, which does not require this computation step. To provide highly accurate geodetic products, the measurement can not be biased by error sources of unknown origin. They are more pronounced if the techniques are combined, showing correlation with clock synchronization parameters, as published in several studies. Since Space Geodesy relies on station clocks and time distribution, we consider a new measurement concept, probing and reducing systematic errors. It realizes a common clock for all geodetic space techniques operated at fundamental stations. In addition state of the art optical clocks are preferred to be used, which are such stable that no posterior clock adjustment is theoretically required. Applying this, we can consider a closure observation through the clock, where all discrepancies in signal propagation from source to the receiver are explicitly shown as an inconsistency in time. To enable such a measurement concept, we established an optical timing system at the Geodetic Observatory Wettzell. It uses drift-free timing dissemination to distribute timing signals to all space geodetic techniques. An integral part of the novel timing system is a calibration target, which combines all the instrumentations into a single reference point through a geometric tie and a closure measurement concept in time. In this calibration concept, the delays can be quantified independently by adding time as an additional quantity to the calibration procedure. When the closure is not zero, there is a systematic error in the measurement process. This talk updates on the concept and discusses the obtained results.

Key words VLBI, SLR, GNSS, Multi-technique combination, common clock, time in geodesy

Category: Symposium 1: Reference Frames => 1.3: Terrestrial and space geodetic ties for multi-technique combinations

374

S1-029

Close Range Photogrammetry for High Precise Reference Point Determination – A proof of concept at Satellite Observing System Wetzell

Michael Lösler¹, Cornelia Eschelbach¹, Thomas Klügel²

1. Frankfurt University of Applied Sciences

2. Federal Agency for Cartography and Geodesy

Local tie vectors are a crucial component within the combination of several space geodetic techniques. The vectors define the geometric relation between the space geodetic techniques, referring to the invariant reference points of such techniques. GGOS aims for an accuracy of 1 mm in the position on a global scale. In ITRF2014, about 50% of the used local ties show discrepancies of more than 5 mm w.r.t. the global solution. In the framework of the IAG/IERS Working Group on Site Survey and Co-location or joint research projects like the international GeoMetre project strategies to improve the reference point determination and the local ties are developed. Strategies mainly comprise the development or the recommendation for surveying instruments, developing approaches for transforming local measurements to the global frame, and deriving innovative analysis procedures to derive the reference point of space geodetic techniques.

In this contribution, we focus on the reference point determination. At the Geodetic Observatory Wetzell, a measurement campaign was carried out in September 2020 to evaluate the benefit of close range photogrammetry in the framework of reference point determination. For this purpose, the invariant reference point of a Satellite Laser Ranging telescope was derived several times using various configurations. The estimated reference point and the axis offset vary in a range of ± 0.1 mm and ± 0.02 mm, respectively. The resulting standard deviation of the coordinate components of the combined solution is 0.1 mm and impressively demonstrates the potential of the presented method.

Key words Reference point determination, Close range photogrammetry, Bundle adjustment, Satellite laser ranging, GeoMetre

Category: Symposium 1: Reference Frames => 1.3: Terrestrial and space geodetic ties for multi-technique combinations

489

S1-030

Combination of SLR observations to LEO, LAGEOS, LARES, and GNSS satellites

Dariusz Strugarek¹、 Krzysztof Sośnica¹、 Daniel Arnold²、 Adrian Jäggi²、 Grzegorz Bury¹、 Radosław Zajdel¹

1. Wrocław University of Environmental and Life Sciences

2. Astronomical Institute, University of Bern

The number of satellites equipped with retroreflectors dedicated to Satellite Laser Ranging (SLR) increases simultaneously with the development and invention of the spherical geodetic satellites, low Earth orbiters (LEOs), Galileo, and other components of the Global Navigational Satellite System (GNSS). SLR and GNSS techniques onboard LEO and GNSS satellites create the possibility of widening the use of SLR observations for deriving SLR station coordinates, which up to now have been typically based on spherical geodetic satellites.

We determine SLR station coordinates based on integrated SLR observations to LEOs, spherical geodetic, and GNSS satellites orbiting the Earth at different altitudes, from 330 to 26,210 km. We discuss the issues of handling range biases in multi-satellite combinations and the proper solution constraining and weighting. The weighted combination is characterized by a reduction of formal error medians of estimated station coordinates up to 50% and the reduction of station coordinate residuals. The combination of all satellites with optimum weighting increases the consistency of station coordinates in terms of interquartile ranges by 10% of horizontal components for non-core stations w.r.t LAGEOS-only solutions.

We show the possibility of using SLR observations to GNSS-based orbit solutions of LEO satellites for deriving station coordinates in SLR Precise Point Positioning mode, in analogy to GNSS-PPP methodology. The SLR-PPP solutions show a repeatability of all tested station coordinates at the level of less than 20, 15, and 12 mm for the Up, East, and North components, which corresponds well with the solution based on network constraining.

Key words SLR, GNSS, low Earth orbiters, Galileo, reference frame realization

Category: Symposium 1: Reference Frames => 1.3: Terrestrial and space geodetic ties for multi-technique combinations

496

S1-031

On DORIS and SLR simulation studies to single-satellite space-ties to achieve the Global Geodetic Observing System goals

Patrick Schreiner¹、Nicat Mammadaliyev²、Susanne Glaser¹、Rolf Koenig¹、Karl Hans Neumayer¹、Harald Schuh^{1,2}

1. Helmholtz Centre Potsdam GFZ German Research Centre for Geosciences

2. Technische Universität Berlin

In this study, we perform simulations for the techniques DORIS and SLR towards the co-location in space at a single satellite meeting the goals of the Global Geodetic Observing System (GGOS). Precise Orbit Determination (POD) to multiple existing missions starting from LAGEOS for SLR and TOPEX for DORIS to recent missions such as JASON-3 or Sentinel-6 is done to estimate individual station and receiver accuracy, availability, and further technique-specific effects. Realistic simulations of the existing missions are extended by simulations to six fictional orbit scenarios over a time span of seven years. For the fictional space-tie satellite scenarios, we included the formerly proposed NASA and ESA missions GRASP and E-GRASP, a modified version of E-GRASP with lower eccentricity, and three circular orbits with different inclinations reaching from near polar to 30 degrees. We generate terrestrial reference frame (TRF) solutions for the simulated observations to existing missions, for the six fictional orbit scenarios, and the combination of both. The effect on the TRF is quantified in terms of changes of the origin and scale, in terms of formal errors of adjusted ground station coordinates, and in terms of solved Earth rotation parameters. It can be shown that for instance a higher eccentricity of the orbit seems beneficial to improve the precision of length-of-day (LOD) from SLR. Based on all the scenarios, we will answer the questions which orbit is best suited for co-location in space fulfilling the important GGOS goals.

Key words simulations, space-ties, precise orbit determination, ggos, reference frame determination, doris, slr

Category: Symposium 1: Reference Frames => 1.3: Terrestrial and space geodetic ties for multi-technique combinations

525

S1-032

Differences in geocenter coordinate estimates delivered from GPS, GLONASS, and Galileo

Radosław Zajdel, Krzysztof Sośnica, Grzegorz Bury, Dariusz Strugarek, Mateusz Drożdżewski

Wrocław University of Environmental and Life Sciences

All satellites orbiting the Earth are naturally sensitive to the motion of the center of mass of the whole planet - the so-called geocenter motion. However, the geocenter coordinate estimates (GCC) based on the observations of the Global Navigation Satellite System (GNSS) satellites used to contain more orbital artifacts than the geophysical signals, especially for the Z component. The major source of the GCC-Z contamination is attributed to the orbit modeling deficiencies, especially the direct Solar Radiation Pressure (SRP).

This contribution conveys a discussion on the impact of SRP modeling on the geocenter motion estimates. To that end, three years of GPS, GLONASS, and Galileo observations (2017–2019) were processed. All possible individual system-specific solutions and combinations of the available constellations are tested in search of characteristic patterns in GCC. The impact of SRP modeling on GCC has been evaluated based on the analysis of different test cases applying both a priori box-wing models for the GNSS satellites and different variations of the Empirical CODE Orbit Model (ECOM).

Firstly, the analysis of the correlations between the estimated parameters confirmed the correlations between the GCC-Z and D2C, BC, and D0 terms from the ECOM model, with correlation coefficients reaching 0.8. Secondly, any system-specific GNSS estimates are affected by the orbital and draconitic signals. The analysis also revealed that the geocenter coordinates are best determined using two constellations: GPS and Galileo, whereas the GLONASS-based geocenter coordinates are of inferior quality. Finally, the amplitudes of the annual signal in the GNSS-based GCC-Z series are larger than those from the Satellite Laser Ranging observations to LAGEOS-1/2 and may reach up to 10 mm.

Key words GPS, GLONASS, Galileo, Geocenter motion, Network shift approach, Orbit modeling

Category: Symposium 1: Reference Frames => 1.3: Terrestrial and space geodetic ties for multi-technique combinations

631

S1-033

Towards tropospheric ties in the computation of terrestrial reference frames

Changyong He^{1,2}, Arnaud Pollet^{1,2}, David Coulot^{1,2}

1. Université de Paris, Institut de physique du globe de Paris, CNRS, IGN, F-75005 Paris, France

2. ENSG-Géomatics, IGN, F-77455 Marne-la-Vallée, France

To compensate for the limitations of the Terrestrial Reference Frames (TRFs) independently realised by different geodetic techniques (GPS, DORIS, VLBI and SLR), a multi-technique combination has been carried out to compute time series of global TRF solutions using the inter-technique ties. Currently, there are four types of ties, usable for such a computation of time series: the global ties of the Earth orientation parameters (EOPs), the local ties, the space ties and the tropospheric ties. However, the local ties are limited to both the total number and temporal resolution. The local ties are the links between the reference points of the instruments for two different techniques or of two stations for the same technique at the same geodetic site. The space ties are the global links of ground-based stations provided by some given satellites equipped with different instruments. As the tropospheric effects are the same on the microwave techniques (GPS, VLBI and DORIS), the ties of tropospheric delays and gradients, i.e., the tropospheric ties, can provide supplementary information to the computation of combined time series of TRF. In this study, we investigate the influence of tropospheric ties on the TRF combination using a batch least squares estimation at the observation level. The measurements of GPS, DORIS and VLBI from 2014-04-27 to 2014-05-31 (covering the continuous VLBI campaign of CONT14) are processed by the French GINS software developed by CNES/GRGS using the consistent correction and dynamical models. The ties of tropospheric delays and gradients are determined using the ERA-Interim and ERA5 reanalysis data provided by ECMWF. Also examined is the uncertainty level of tropospheric ties in the determination of station positions and EOPs.

Key words TRF, GPS, DORIS, VLBI, EOP

Category: Symposium 1: Reference Frames => 1.3: Terrestrial and space geodetic ties for multi-technique combinations

659

S1-034

Intra- and Inter-Technique Atmospheric Ties: Derivation, Implementation, and Results

Kyriakos Balidakis¹、 Daniela Thaller³、 Mateusz Drożdżewski⁷、 Claudia Flohrer³、
Changyong He⁵、 Robert Heinkelmann⁹、 Chaiyaporn Kitpracha^{9,13}、 Frank
Lemoine¹¹、 Lisa Lengert³、 Tobias Nilsson¹²、 Arnaud Pollet⁵、 Víctor Puente²、
Marcelo Santos⁴、 Benedikt Soja⁶、 Krzysztof Sośnica⁷、 Jungang Wang⁹、 Xiaoya
Wang⁸、 Dudy Wijaya¹⁰、 Florian Zus⁹、 David Coulot⁵

1. GFZ German Research Centre for Geosciences, Earth System Modelling, Potsdam, Germany
2. National Geographic Institute of Spain, Madrid, Spain
3. Federal Agency for Cartography and Geodesy, Geodesy, Frankfurt am Main, Germany
4. University of New Brunswick, Fredericton, Canada
5. IGN Institut Geographique National, Paris, France
6. ETH Zurich, Space Geodesy, Institute of Geodesy and Photogrammetry, Department of Civil, Environmental and Geomatic Engineering, Zurich
7. Institute of Geodesy and Geoinformatics, Wrocław University of Environmental and Life Sciences, Wrocław, Poland
8. Shanghai Astronomical Observatory, Chinese Academy of Sciences, Shanghai, China
9. GFZ German Research Centre for Geosciences, Space Geodetic Techniques, Potsdam, Germany
10. Institut Teknologi Bandung, Bandung, Indonesia
11. NASA Goddard Space Flight Center, Greenbelt, United States
12. Lantmäteriet, Geodetic Infrastructure, Gävle, Sweden
13. Technische Universität Berlin, Chair of Satellite Geodesy, Berlin, Germany

Atmospheric delay coefficients recovered by space geodetic data analysis at co-located sites differ systematically. These differences mainly depend upon the frequency of the signals employed, the relative station positions, and the observing system setup. Introducing external information regarding these differences, atmospheric ties, is useful in the intra- and inter-technique combination, especially under poor observation geometry. In this contribution, we present our progress regarding the determination of atmospheric ties based on high-resolution weather models such as ERA5 and ECMWF's operational model, the weighting strategy for atmospheric ties, and the multi-technique combination at the observation and normal equation level. Moreover, we discuss the organization of a combination benchmark campaign including station coordinates, Earth rotation parameters, and atmospheric delays.

Key words atmospheric ties, combination, ray-tracing

Category: Symposium 1: Reference Frames => 1.3: Terrestrial and space geodetic ties for multi-technique combinations

683

S1-035

A Study on Differencing Approaches for SLR Observations

Iván Herrera Pinzón, Markus Rothacher
ETH Zürich

In this contribution the precise estimation of geodetic parameters using single- and double-differenced SLR observations is investigated. Although the differencing of observables is a standard approach in GNSS data processing, double-differences of simultaneous SLR observations cannot be obtained due to the basic principle of operation of SLR. However, by extending the term "simultaneous" to observations that are further apart in time and with the availability of co-located SLR telescopes, forming SLR single- and double-differences is feasible. These differences are expected to be free of both, satellite- and station-specific error sources, and are shown to be a valuable tool to obtain relative coordinates and range biases, and to validate local ties. This approach is tested with the two co-located SLR telescopes at the Geodetic Observatory Wettzell (Germany) using SLR observations to GLONASS and LAGEOS. It is shown that it is possible to obtain parameters such as range biases at the stations and the local baseline vector with a precision at the millimetre level and an accuracy comparable to traditional terrestrial survey methods. The presented SLR differences constitute a valuable alternative for the monitoring of the local baselines and the estimation of geodetic parameters.

Key words Satellite Laser Ranging, Single and Double Differences, Local Ties

Category: Symposium 1: Reference Frames => 1.3: Terrestrial and space geodetic ties for multi-technique combinations

734

S1-036

SLR station range bias and coordinate determination using independent multi-LEO DORIS- and GNSS-based precise orbits

Heike Peter¹、 Daniel Arnold²、 Alexandre Couhert³、 Eléonore Saquet^{4,7}、 Flavien Mercier⁵、 Oliver Montenbruck⁶

1. PosiTim UG

2. Astronomical Institute, University of Bern, Bern, Switzerland

3. Centre National d'Etudes Spatiales, Toulouse, France

4. Collecte Localisation Satellites, Toulouse, France

5. Centre National d'Etudes Spatiales, Toulouse, France

6. DLR, Oberpfaffenhofen, Germany

7. Centre National d'Etudes Spatiales, Toulouse, France

Satellite Laser Ranging (SLR) has become an invaluable core technique in numerous geodetic applications. SLR measurements to spherical geodetic satellites essentially contribute to the determination of geocenter coordinates and global scale in the ITRF realizations.

Precise orbits for active satellites in Low Earth Orbit (LEO) are, on the other hand, mainly determined with microwave observation techniques based on GNSS or DORIS. SLR measurements to such satellites are in most cases used for independent validation of orbit solutions. This allows for the analysis of systematic orbit errors not only in radial direction (key to satellite altimetry applications), but in three dimensions.

Major error source and an obstacle to reach mm accuracy and stability goals of 0.1 mm/year are unavoidable SLR station biases and coordinate errors. Among the International Laser Ranging Service (ILRS) stations a large diversity of calibration accuracies and measurement qualities exists, and the calibration of biases and offsets for all stations is key to further exploit SLR data for geodetic applications.

Using two orbit sets of independent altimeter and gravity missions we estimate SLR range biases for all involved tracking stations on a yearly basis. We find that for many of the stations independently estimated sets of biases agree on a few-mm level and that the inclusion of satellites from multiple missions allows rendering the bias estimation more robust and in particular less prone to geographically correlated orbit errors. Non-negligible station coordinate corrections estimated in common with the range biases help to separate software-specific and reference frame-related (GNSS vs. DORIS) contributions from actual bias variations.

This study shows that microwave-derived high quality orbits of active LEO satellites can serve as interesting sources for SLR station calibration in demanding geodetic applications like, e.g., future ITRF realizations.

Key words Satellite Laser Ranging, Low Earth Orbit, range bias, coordinates, calibration

Category: Symposium 1: Reference Frames => 1.3: Terrestrial and space geodetic ties for multi-technique combinations

840

S1-037

Assessment of Local VLBI Baselines: The Wettzell Case

Iván Herrera Pinzón, Markus Rothacher
ETH Zürich

This work discusses the analysis of the short baseline between two co-located VLBI telescopes at the Geodetic Observatory in Wettzell (Germany). Geodetic VLBI sessions are processed using the VLBI capabilities of the Bernese GNSS Software to estimate station coordinates, troposphere zenith delays and clock parameters, where a strategy to work out the advantages of a short baseline is implemented. Results from this processing show a sub-millimetre agreement of the VLBI-derived baseline and the local ties. Zenith tropospheric delays compared to a co-located GNSS station show an agreement at the millimetre level, when considering the instrumental heights of the antennas. Moreover, our approach makes use of the actively stabilised two-way optical time and frequency distribution system (TWOTT), which provides a virtual common clock between the two telescopes, to distribute time and to make the estimation of clock corrections unnecessary (apart from one clock offset per session). The comparison between TWOTT-based local baseline length and the local tie shows a sub-mm agreement, demonstrating its potential to obtain stronger solutions. In turn, the proposed processing strategies represent a valuable tool for the continuous monitoring of systematic effects, the separation of VLBI technique-specific error sources and environmental effects, and provide an alternative to monitor the behaviour of the local baseline at the site.

Key words VLBI, Local Ties, Co-Location

Category: Symposium 1: Reference Frames => 1.3: Terrestrial and space geodetic ties for multi-technique combinations

863

S1-038

Demonstration of 1 mm Precision for Kilometer Co-location Ties at McDonald Geodetic Observatory

Jullian Rivera¹, Srinivas Bettadpur¹, John Griffin²

1. The University of Texas at Austin

2. John Griffin, Surveyors

This work illustrates the procedure in which 1 mm-level precision metrology surveys of the co-location baseline between the VLBI Global Observing System (VGOS) site and the Space Geodetic Satellite Laser Ranging (SGSLR) site at McDonald Geodetic Observatory (MGO) are conducted. MGO is located in Fort Davis, Texas, USA and spans a kilometer baseline and a 120 meter elevation change. This is a continuation of previous metrology work at MGO. We show surveys in which sub-millimeter post-fit residuals are achieved, demonstrating the capability for precision with sets of range and angle raw observations from a total station instrument. "Raw" in this context means that no internal corrections to the observations are made by the instrument and are instead modeled and corrected for in the processing of the output data. The sources of error and their effects on the post-fit residuals of the solution of the Local Ground Control Network at MGO are explored and incorporated into an error budget. Error sources include procedural errors in instrument stability, pointing, and leveling, deflection of the vertical, atmospheric effects on EDM lasers, and atmospheric angular refraction of EDM lasers.

Key words co-location ties, VLBI, SLR, GNSS, metrology, survey

Symposium 1: Reference Frames

S1.4: Regional reference frames and networks

Category: Symposium 1: Reference Frames => 1.4: Regional reference frames and networks

66

S1-039

GEODETIC DATUME TRANSFORMATION WITH THE MINIMUM CURVATURE SURFACE INTERPOLATION APPROACH in IRAQ

Yasir Ammar Abed Al-husseinawi¹、 Imzahim Abdul Al-Kareem²、 Ghydaa Abdul-Rehman³

1. State Commission of Survey
2. University of Technology
3. Ministry of water resources

This paper investigates a main and important problem related to the coordinates systems of Iraq. Maps of Iraq referenced to a local geodetic coordinate system while at the same time the technique of location observation and map production use the International Terrestrial Reference Frame (ITRF) as a base reference datum. Thus, it has become necessary to find an algorithm to convert between Iraq's local geodetic system (Karbala79) and (ITRF) simply because the (ITRF) is adopted globally and all GPS and GNSS devices use that datum to calculate positions.

In this study, we used a mathematical model that relates between the terrestrial coordinate system (Karbala 79) and ITRF08. Minimum curvature surface interpolation via geodetic coordinates approach is used to convert between (Karbala79) and (ITRF08).

We utilized 89 points from the old geodetic network (Karbala79) covering the whole area of Iraq and were observed using GNSS between 2007 and 2013. The observation time is 5 hours where the Static observation method was used. Computer software (IRAQCON) was developed with Matlab to achieve this conversion.

Precision of (0.03) meters in ΔE and (0.02) meters in ΔN were obtained when the results evaluated using test points. This approach can be recommended for the conversion and production of large-scale maps for Iraq which is necessary for agriculture, and oil production.

Key words minimum curvature interpolation ▪ international terrestrial reference frame (ITRF) ▪ geodetic datum▪

Category: Symposium 1: Reference Frames => 1.4: Regional reference frames and networks

72

S1-040

Recent achievements and current challenges in the maintenance of the geodetic reference frame of the Americas

José Antonio Tarrío¹、 Laura Sánchez²、 Sonia Alves³、 Alberto Silva³、 Jesarella Inzunza¹、 Gustavo Caubarrere⁴、 Alejandro Martínez⁵、 Óscar Rodríguez⁶、 Emilio Aleuy⁷、 Hernán Guagni⁸、 Guido González⁹

1. Universidad de Santiago de Chile, Chile

2. Deutsches Geodätisches Forschungsinstitut, Technische Universität München (DGFI-TUM), Germany

3. Instituto Brasileiro de Geografia e Estatística, Brasil

4. Instituto Geográfico Militar, Uruguay

5. Instituto Geográfico Militar, Ecuador

6. Instituto Geográfico Agustín Codazzi, Colombia

7. Instituto Geográfico Militar, Chile

8. Instituto Geográfico Nacional, Argentina

9. Instituto Nacional de Estadística y Geografía, Mexico

SIRGAS responds to the acronym of Geocentric Reference System for the Americas (Sistema de Referencia Geocéntrico para las Américas) and is a non-profit organization based on the contribution at the American level of organizations, universities, institutes, etc., with a close relationship with geodetic and geophysical activities. Its objective is to facilitate the member countries' access to a unified reference system as for the geometric component (densifying the ITRF) as for the physical component (densifying the IHRF). The geometric aspects are coordinated by the SIRGAS Working Group I (Reference system) at the continental level and by the SIRGAS Working Group II (SIRGAS at national level) at the national level. The physical height standardization is coordinated by the SIRGAS Working Group III (Vertical Datum). This contribution exposes the activities related to the Working Group I, whose main objectives are to maintain and to ensure the long-term stability of the SIRGAS reference frame. Presently, SIRGAS is realized by a network of about 440 continuously operating GNSS stations, which are processed on a weekly basis following the IERS conventions and the GNSS-specific guidelines released by the IGS. The main SIRGAS products are weekly station positions, multi-year solutions, surface deformation models, and tropospheric parameters in hourly intervals. This contribution summarizes recent achievements and open challenges in the maintenance and further development of the SIRGAS Reference Frame. Special care is given to the reprocessing of the SIRGAS reference network based on the ITRF2014 (IGS14 / IGB14) and the extension of the SIRGAS network to North America as a fundamental support for the activities of the GRFA (Geodetic Reference Frame for

Americas) working group, established in the framework of the Regional Committee of the United Nations on Global Geospatial Information Management for the Americas (UN-GGIM: Americas).

Key words Regional reference frames, GNSS permanent networks, frame densification,

Category: Symposium 1: Reference Frames => 1.4: Regional reference frames and networks

141

S1-041

Crustal block modelling using a combination of Euler pole and cluster analysis of GNSS velocities in Greece

Stylianos Bitharis, Christos Pikridas, Aristeidis Fotiou, Dimitrios Rossikopoulos
Aristotle University of Thessaloniki

In this study, we focused on GNSS velocities clustering using the Euler pole and clustering methodology for block modelling definition. Greece is characterized by an inhomogeneous geodetic velocity field due to complex tectonics and high deformation rates that effected to regional reference frames. We present an updated dense geodetic velocity field covering the Greek territory and the South Balkans. The velocity field derived using more than 220 continuously GNSS stations which are analyzed in a period of 16 years (2001-2016) using the GAMIT/GLOBK software suite. We identify 10 crustal blocks that appeared to move independently in Greek area applying the k-means clustering approach, Euler Pole estimation, and statistical criteria. Clustering technique contributes only to a pattern identification of GNSS sites that follows similar horizontal velocity motion without using any apriori information or assumption. For each n crustal block, we determine the best-fit Euler pole vectors and then we calculate the predicted residuals relative to n-1 other clusters. If the absolute value of the horizontal predicted residuals was smaller from the initial cluster, the GNSS station reassigned to another n-1 cluster. Statistical tests were applied in each Euler pole estimation of whether the goodness of the fit and the quality of the derived solution. Finally, the geometrical block boundaries definition obtained using Voronoi diagram methodology, providing polygons with the same kinematic behavior, without using any tectonics characteristics.

Key words GNSS, Euler Pole, Block modelling, Clustering

Category: Symposium 1: Reference Frames => 1.4: Regional reference frames and networks
435
S1-042

BEV DC 2.0

David Mayer, Philipp Mitterschiffthaler
Federal Office of Metrology and Surveying (BEV)

An important part of a large GNSS network is the collection and processing of GNSS data at a central location. This is usually done by Data Centers (DC). The Federal Office of Metrology and Surveying (BEV) operates one of these Data Centers for the EUREF network. A Data Center must be able to process large amounts of data and make it available to the end user in a short time. The BEV decided to renew the entire Data Center to meet these requirements.

The new Data Center provides a state of the art REST API interface which can be accessed via HTTPS. This interface can be used for both upload and download of GNSS data. Furthermore, a metadata search has been integrated to facilitate data access. The processing of the data is done in the backend of the application, where a standardized messaging queue is utilized to assure parallelization and redundancy.

In order to increase the reliability of the application, a microservice architecture with redundant components was chosen. The application was created using new container technology, which increases portability and allows automatic management of all components.

Key words Data Center, RINEX, HTTPS, GNSS

Category: Symposium 1: Reference Frames => 1.4: Regional reference frames and networks
503
S1-043

Approaches to time-dependent transformations between reference frames in deforming regions

Richard Stanaway
Quickclose

Conformal time-dependent transformations such as the 14-parameter Helmert transformation are widely used in geodetic practice but have limited application in deforming regions. To overcome this, a number of diverse approaches have been adopted by different geodetic agencies to enable coordinate transformation between a kinematic reference frame and regional or national reference frames within these deforming zones. The lack of a standardised approach and data format has been a major impediment to the uptake of precise and useable transformation models by many countries, positioning services and GIS vendors. As a consequence, the benefits of increasing positioning precision by a larger and wider spectrum of users is not being fully harnessed and in fact may lead to degradation of spatial data accuracy where deformation of the reference frame is not modelled or managed correctly.

This paper draws on the very substantial input of IAG Working Group 1.3.1 (Time-dependent transformations between reference frames in deforming regions) and closely allied working groups within the FIG and OGC. This collaborative effort is developing both a functional model for time-dependent transformations in deforming regions and an associated geodetic gridded data exchange format (GGXF) to enable the functional model to be used in practice. Highlights of the WG effort to date are presented.

This paper describes a schema for the implementation of time-dependent transformations in deforming zones whereby models of secular interseismic velocities, episodic coseismic displacements and postseismic decay can be managed and accommodated in the context of regional and national reference frames. Typical transformation scenarios are used to show how the schema can be applied within positioning systems and GIS.

Key words time-dependent transformation deformation GGXF reference frames

Category: Symposium 1: Reference Frames => 1.4: Regional reference frames and networks
506
S1-044

The North American Terrestrial Reference Frame of 2022: Its Definition and Plans for Adoption

Dru Smith¹, Mike Craymer², Daniel Roman¹

1. NOAA/National Geodetic Survey

2. Canadian Geodetic Survey

In the next few years, the United States will be updating its National Spatial Reference System (NSRS) based on four plate-fixed realizations of the forthcoming ITRF2020 that will cover four tectonic plates. As part of this effort and working through the IAG regional subcommission SC1.3c for North America (NAREF), the U.S. and Canada are developing the North American Terrestrial Reference Frame of 2022 (NATRF2022) to be suitable for adoption in both countries. The U.S. will also develop similar reference frames for the Caribbean (CATRF2022), Pacific (PATRF2022), and Mariana (MATRF2022) plates to cover U.S. territories in those regions. These models will also be developed collaboratively with other interests in each region, such as SIRGAS and APREF, respectively. Initially, all four plate-fixed models will be identical to ITRF2020 at the adopted reference epoch of 2020.0. The time-dependent coordinates of points in any of these four plate-fixed frames will be defined relative to the time-dependent coordinates in ITRF2020. The relative relationship will rely on a plate rotation model for the tectonic plate associated with each frame. This relationship will be based on rotation rates about the three ITRF axes representing the Euler pole parameters (EPPs) and be codified in a model called EPP2022. Each regional reference frame has its own unique issues, but NATRF2022 offers more challenge because of the extent of the common border between the U.S. and Canada (the longest land border in the world) and the desire for a common reference frame in both countries, the geophysical activity along the plate boundary deformation zone in the western portions of the continent, and the horizontal component of glacial isostatic adjustment (GIA) that affects much of the northern half of the continent. This presentation will primarily focus on current plans for development and implementation of NATRF2022 but also discusses the challenges with the other three regional reference frames.

Key words North America, NATRF2022, ITRF2020

Category: Symposium 1: Reference Frames => 1.4: Regional reference frames and networks

641

S1-045

On the impact of individual PCC errors on regional networks using different processing strategies

Tobias Kersten¹、Grzegorz Krzan²、Karol Dawidowicz²、Steffen Schön¹

1. Leibniz University Hannover

2. University of Warmia and Mazury

Various contributions in the past addressed the issue on the required quality of GNSS receiver antenna calibrations and the assessment of their effect on GNSS data processing. Thus, networks with and without individual phase centre corrections (PCC) were analysed at global and local scale. Together with different test strategies - starting from the observation domain up to the position domain - many questions arise regarding the required precision and accuracy of the receiver antenna PCCs. Comprehensive and fundamental answers to this, however, are difficult to achieve as complex interactions on the processing strategy prevent simple estimation.

In this paper, the authors present a closed concept for assessing the impact of receiver antenna patterns on a GNSS network geometry using generic patterns. A subset of Polish reference station network ASG-EUPOS applies as a sample for presenting the strategy in a step-by-step procedure. Two different approaches to GNSS processing are considered and investigated in detail, namely a network solution from Bernese and NAPEOS. We will show that and how specific generic pattern information - representing typical errors of PCCs - are spread over the network. The different estimated parameters, including the position solution, tropospheric parameters, and resolved ambiguities will be investigated for different GNSS in a heterogeneously equipped reference station network. The analyses reveal that repeatable offsets in the coordinate domain have to be expected, but also systematic deviations in the tropospheric parameters, which lead also to distortions of the derived meteorological products. In addition, a clear relationship was found with respect to the orientation of the baselines and to the density and distribution of the satellite sky distribution.

These analyses will support the quantitative assessment of different antenna calibration values and lead to a better understanding of their effects in the context of GNSS networks.

Key words carrier phase center corrections (PCCs); generic patterns; PPP; relative positioning; regional network

Category: Symposium 1: Reference Frames => 1.4: Regional reference frames and networks

668

S1-046

ADELA :Analysis of DEformation beyond Los Andes(2009-2021). The urgency to change from static to kinematic in any geodetic reference frame for Chile

José Antonio Tarrío Mosquera¹、 Jesarella Inzunza¹、 Fernando Isla¹、 Marcelo Caverlotti¹、 Catalina Cáceres¹、 Cristian Mardones²

1. University of Santiago de Chile, Chile

2. Servicio Nacional de Geología y Minería

The modern reference frames currently used in Chile are static, called SIRGASChile@2013 (Realization3) and SIRGASChile@2016 (Realization4). They are officially used to realize cadastre in the former and as an official reference frame for the second case. These reference frames are densification of the SIRGAS network for a specific fixed epoch; the time-dependent is not present beyond the moment of calculation, generating inconsistency in generating geospatial information from these frames over time. If we take into account that: the Iquique earthquakes of 2014 (8.4 Mw) and Coquimbo of 2015 (8.2Mw) produced a displacement in Realization3 of 1-2 m, that the average annual movement of the earth's crust in the area is 2 to 4 cm in different directions, this implies that the use of a static reference frame in Chile generates plenty of problems for the end-user and cannot be used to make correct political decisions, in aspects such as climate change.

In this work, from the USC geodetic analysis and processing center associated with SIRGAS, we propose a solution, through an analysis of the deformation of the crust over 12 years, using GNSS stations with information from 2009 to 2021; the study's name was ADELA: Analysis of DEformation beyond Los Andes. With the above analysis, we evidenced several aspects. Firstly, the Helmert transformations of 7 or 14 parameters do not manage to model the change of the different Chilean reference frames, and grids such as NTV2 are an intermediate solution that does not include the time-dependent variable. This research shows the creation of a deformation model based purely on geodetic observations, which integrate the interseismic, coseismic, and post-seismic components of the time series for the indicated period using a piecewise approximation. The advantage of this method lies in the inclusion of seismic events and the temporal variable, the disadvantage being, as in others, the dependence on the number of available GNSS stations.

Key words Regional reference frames, GNSS permanent networks, plate tectonic motion, frame alignment, time-dependent transformation models.

Category: Symposium 1: Reference Frames => 1.4: Regional reference frames and networks
671
S1-047

Extraction of common mode error of GNSS coordinate time series in Xinjiang with independent component analysis

Chuanjin Lei^{1,2}、Guanjun Wei^{1,2}、Maoning Gao^{1,2}、Pei Zhang^{1,2}

1. Faculty of Geomatics Lanzhou Jiaotong University
2. National-Local Joint Engineering Research Center of Technologies and Applications for National Geographic State Monitoring

The common mode error (CME) is one of the major error sources in the regional GNSS network. Aiming at the problem that GNSS time series is subject to non-Gaussian signals, and the principal component analysis (PCA) with second-order is inaccurately employed to separate the CME. In this contribution, the independent component analysis (ICA) introduces high-order statistics to extract the CME, the effectiveness of the method is validated by processing the data of 30 GNSS stations from 2011 to 2018 in Xinjiang, China, we analysis the influence of the CME for GNSS coordinate time series and the yearly signal of the CME. The results show that the CME mainly consists of the 6th independent components and can be attributed to satellite orbit, surface mass loading, and clock errors. After the ICA filtering, the reduction of mean RMS is 31.83%,32.29%,35.49% for the north, east, and up components, respectively, and the reduction of velocity uncertainty can achieve 44.14%,38.49%, and 35.49% in three components. In addition, the yearly and half-yearly amplitude of each GNSS station is more consistent than before spatiotemporal filtering, indicating that the ICA can effectively extract the CME and further improve the accuracy of coordinate time series.

Key words GNSS coordinate time series; Independent component analysis; Common mode error; Spatiotemporal filtering

Category: Symposium 1: Reference Frames => 1.4: Regional reference frames and networks
699
S1-048

ITRF densification in Cyprus

Chris Danezis¹, Miltiadis Chatzinikos¹, Christopher Kotsakis²

1. Cyprus University of Technology
2. Aristotle University of Thessaloniki

The aim of this paper is to present the first ITRF (International Terrestrial Reference Frame) densification in Cyprus and a preliminary estimation of its velocity field from the analysis of daily GNSS measurements in the CYPOS network. The CYPOS national network operates since 2008 in support of the Cyprus Positioning System under the auspices of the Department of Lands and Surveys, and it consists of seven permanent GNSS stations equipped with different types of receivers/antennas at an average distance of about 60 km. The NICO Cypriot station which belongs to the IGS (International GNSS Service) network is also included in the data processing, along with 34 additional reference stations from the EUREF-EPN and IGS networks which are located mostly in the continental part of Europe.

Daily RINEX files from the aforesaid stations, spanning a total period of seven years (2012-2019), were processed using the Bernese GNSS software. A number of auxiliary scripts were applied in the processing steps to investigate various data/network-quality metrics and the precision of the GNSS measurements at the Cypriot stations. The daily solutions obtained from Bernese (SINEX files) were used as input to a time-series stacking procedure in order to compute the final solution for the positions and velocities at the CYPOS stations in the latest ITRF frame realization. The results of our stacking solution are externally validated through comparisons with the official ITRF positions and velocities at the used EPN stations, showing an agreement level of 1-2 mm (for the positions) and < 1 mm/yr (for the velocities). This research was carried out in the framework of the CyCLOPS project (RIF/INFRASTRUCTURES/1216/0050), which is funded by the European Regional Development Fund and the Republic of Cyprus through the Research and Innovation Foundation.

Key words CYPOS, regional GNSS network, frame densification, time-series stacking

Category: Symposium 1: Reference Frames => 1.4: Regional reference frames and networks

733

S1-049

A three-dimensional crustal velocity field in mainland China from denser permanent GPS networks

Zhikai Li¹, Kaihua Ding², Peng Zhang¹

1. Geodesy Department, National Geomatics Center of China
2. School of Geography and Information Engineering, China University of Geosciences

Using measurements of 438 continuous stations since their installment to end of 2019 from permanent GPS networks, we derived a high-precision three-dimensional crustal velocity field in mainland China with a denser spatial resolution compared with previous studies. Due to the increased average station spacing of about 150 km, the horizontal velocity field with relative to stable Eurasia plate shows a clear image of large but complex crustal motions in western region and relatively small but uniform motions in eastern region, while the vertical velocity field is very related to locations that sites in Tien Shan, Junggar, Sichuan-Yunnan and Ordos regions are uplifting, whereas those in North China plain, Yangtze River delta are subsiding. In addition, different noise combination models are compared while solving for the velocity. It shows that the noise model should be considered because the noise of these continuously operating reference stations can best be characterized by white noise plus flicker noise or white noise plus power law noise, rather than white noise only preassumed in previous studies.

Key words permanent GPS networks; noise combination models; velocity field

Category: Symposium 1: Reference Frames => 1.4: Regional reference frames and networks

783

S1-050

GIANT-REGAIN: A comprehensive analysis of geodetic GNSS recordings in Antarctica for geodetic and geodynamic applications

Eric Buchta¹、Mirko Scheinert¹、Peter Busch¹、Matt A. King²、Terry Wilson³、
Christoph Knöfel¹、Eric Kendrick³、Demián Gómez³、Michael Bevis³、Martin
Horwath¹

1. Technische Universität Dresden

2. University of Tasmania, Australia

3. Ohio State University, USA

The IAG Subcommittee 1.3f deals with the utilization of geodetic GNSS measurements in Antarctica to realize and densify the terrestrial reference frame. Moreover, geodetic GNSS on bedrock allows to directly observe the solid Earth's response to past and present ice-mass changes. Therefore, GNSS derived deformation rates play an integral role for the modelling of glacial isostatic adjustment (GIA) by providing boundary conditions and evaluating existing models. The long-term stability of the adopted terrestrial reference frame is crucial to derive secular trends of coordinate changes associated with GIA in Antarctica.

To pursue these goals, the "Geodynamics in ANTArctica based on Reprocessing GNSS dAta INitiative" (GIANT-REGAIN) was initiated in close collaboration with SCAR (Scientific Committee of Antarctic Research). This project aims to re-process all available GNSS data acquired by episodic and permanent recordings at bedrock sites in Antarctica. These data cover a time span of 1995 to 2017. We will report on the data acquisition and on the treatment of metadata which are indispensable for a correct assignment of the hardware setup. For the processing different scientific software packages and strategies are applied (PPP and differential GNSS). We will present first results of the processing which will allow to infer consistent solutions of point coordinates and coordinate changes. We will assess the processing noise and the accuracy of the derived solutions.

Key words Terrestrial reference frame, GNSS, Antarctica, solid earth deformation

Category: Symposium 1: Reference Frames => 1.4: Regional reference frames and networks
809
S1-051

Towards an European Deformation Model

Elmar Brockmann, Simon Lutz
Federal Office of Topography swisstopo

The presentation highlights the recent developments of the EU Dense Velocity Working Group. Currently, more than 7200 individual site velocities are available for the area of Europe (6200 in the previous year) and more than 3600 sites (2000 sites status last year) are determined at least by two independent contributions. In addition to results from GNSS permanent networks, densified solutions stemming from GNSS campaigns, InSAR or levelling are also included. In some countries, as e.g. in the Nordic countries, velocity models are already in use. They can be integrated to indicate possible differences between modeled and observed velocities.

The web site (http://pnac.swisstopo.admin.ch/divers/dens_vel/index.html) provides feedback to the contributors and shows differences with estimates of other contributors. The web page was furthermore enhanced with dynamical visualizations (velocities as a wind field: (<http://geolabpasaia.org/gnss/agi/maps/EU-DenseVelocities.html#4/50.04/14.99>)). Whereas the horizontal velocities are on a level of clearly below 1 mm/yr for the stable part of the European plate, the velocities reach 3-4 mm/yr in Italy and 3-4 cm/yr in Greece and Turkey. The polygon covering the Nordic countries Norway, Sweden and Finland shows the NKG velocity grid. Another enhancement of the web page are strain calculations (http://pnac.swisstopo.admin.ch/divers/dens_vel/000.html#STRAIN). Since June 2020 the WG chair participates to an OGC working group "Deformation Models" which is focusing on standards and formats. We hope that these developments will soon lead to a European deformation model which is available for all European partners.

Key words Velocities, GNSS, Strain rates, Deformation models

Category: Symposium 1: Reference Frames => 1.4: Regional reference frames and networks
827
S1-052

Research on the realization of the regional reference frame

fan wang¹、DaNan Dong²

1. National Geomatics Center of China
2. East China Normal University

The surface load caused by non-tidal atmosphere, ocean and waters were not corrected in the GNSS observation data processing stage, which makes GPS station coordinate time series include significant seasonal patterns. A common approach to the analysis of GNSS observations is to compute a “fiducial-free” network first and then aligned it with a terrestrial reference frame by computing a HELMERT transformation. However, the implicit premise of HELMERT transform is that the networks should be geometrically similar. This means that the instantaneous station coordinate in the CM frame includes surface load, while the CF reference frame is usually a linear frame and does not involve surface load, in this case the un-modeled surface loading signals would alias into the transformation parameters. Transformations not done correctly can yield coordinate/velocity errors. This is even worse in the regional reference frame because of the heterogeneous GNSS station distribution. We study the effects of loading aliasing errors and network aliasing errors on the transformation parameters and station coordinate. Seasonal GNSS loading deformation is simulated by QOCA software. We used several different selections of global, regional and local transformation sites in order to assess how the transformation sites effect the transformation and geocenter motion. Local transformation sites cannot effetely realize the regional reference frame, and the load deformation will be absorbed by the geocenter motion. It is reasonable to use 75 IGS sites located in China’s neighboring regions as the for frame conversion, which can well separate the geocentric movement and greatly reduce the workload.

Seven-parameter transformation is usually used in HELMERT transformation, including the scale factor which represents the expansion and contraction of the network. The simulation results show that ignoring the scale factor is more reason for it decreased the RMS 50% in the horizontal direction and 80% in the vertical direction.

Key words Regional Reference Frame, Helmert, Geocentric movement

Category: Symposium 1: Reference Frames => 1.4: Regional reference frames and networks
864
S1-053

Frame accuracy of daily/weekly combined EPN solutions

Miltiadis Chatzinikos, Christopher Kotsakis
Aristotle University of Thessaloniki

The scope of this paper is to present an experimental quality assessment of the EPN (EUREF Permanent Network) daily and weekly combined coordinate solutions in relation to their frame realization accuracy. Specifically, the daily and weekly SINEX files from the EPN Analysis Combination Centre are analyzed in order to infer the origin, orientation and scale accuracy of the respective epoch solutions. Our investigation covers the entire operational period of EPN, starting from July 1996 up to present time, and it also extends to the daily/weekly coordinate solutions obtained from the completed reprocessing campaigns (EPN-repro1, EPN-repro2). Through the results of this study we shall be able to assess the effect of different factors and modeling options in GNSS data processing (e.g. tropospheric model, ionospheric corrections, inclusion of multi-GNSS measurements, antenna PCVs, choice of fiducial stations and alignment method) on the frame quality that is inherited by the daily/weekly combined EPN positions.

Key words EPN, daily/weekly coordinates, frame accuracy

Category: Symposium 1: Reference Frames => 1.4: Regional reference frames and networks
867
S1-054

Scientific goals and strategic actions of EUREF in a changing landscape

Martin Lidberg¹、Carine Bruyninx³、Elmar Brockmann⁵、Rolf Dach⁷、Ambrus Kenyeres⁹、Karin Kollo¹⁰、Juliette Legrand³、Tomas Liwosz¹¹、Rosa Pacione¹²、Martina Sacher²、Wolfgang Söhne²、Christof Völksen²、Zuheir Altamimi⁴、Alessandro Caporali⁶、Markku Poutanen⁸

1. Lantmateriet
2. Federal Agency for Cartography and Geodesy (BKG)
3. Royal Observatory Belgium
4. IGN France
5. Swiss Topo
6. University of Padova
7. University of Berne
8. Finnish Geospatial Research Institute
9. Satellite Geodetic Observatory Lechner nonprofit KFT.
10. Estonian Land Board
11. Warsaw University of Technology
12. ASI/CGS-Matera

EUREF's (IAG sub-commission 1.3a for Europe) primary mission is to define, realize and maintain the European Terrestrial Reference System 1989 (ETRS89) and the European Vertical Reference System (EVRS) for scientific and practical purposes in Europe. These systems are the basis for geo-referencing in Europe and have been endorsed by various European organizations and directives, e. g. the European Union INSPIRE directive (Infrastructure for Spatial Information in the European Community), Eurocontrol and EuroGeographics.

The realization, maintenance and development of the ETRS89 is primarily done through the EUREF Permanent GNSS Network (EPN), while the physical height system EVRS is realized through common adjustment of the Unified European Levelling Network (UELN). All contributions to EUREF are provided on a voluntary "best effort" basis, with more than 100 European bodies (agencies/research institutes) involved.

An overview of recent developments in the densified realizations of the ETRS89, the new EVRF2019 and the efforts towards the European velocity model will be given. The work done towards a strategy for EUREFs further development, including seven identified scientific challenges in geodesy will also be presented.

While the technical part is well established with infrastructure and processing chains generating, archiving, processing and analyzing geodetic observations all over Europe and new developments are under

discussion, e. g. the development of European geoid model, the future role of EUREF in the emerging and changing organizational landscape is challenging. For example, the UN-GGIM sub-committee on Geodesy has been established in 2016 to implement the road map for the GGRF (Global Geodetic Reference Frame), it is underpinned with regional (continental) structures and it is going to establish a Global Geodetic Center of Excellence this year to strengthen the geodetic infrastructure and capacity building all over the world. In the scientific part, the European Plate Observing System (EPOS), which is connecting various scientific disciplines and communities, and which has a formal and legal justification, has entered its pilot operational phase in 2020.

This calls for mutual collaborations in order to achieve common goals to the benefit for the wider user society, which will be discussed at the end.

Key words EUREF, regional reference frames, geodetic infrastructure

Symposium 1: Reference Frames

S1.5: Comparison and combination of space geodesy techniques for improving consistency between TRF, CRF and EOPs

Category: Symposium 1: Reference Frames => 1.5: Comparison and combination of space geodesy techniques for improving consistency between TRF, CRF and EOPs

149
S1-055

Astronomy VLBA campaign MOJAVE used in geodesy

Hana Krasna^{1,3}, Leonid Petrov²

1. TU Wien

2. NASA GSFC

3. Astronomical Institute of the Czech Academy of Sciences

The astronomy VLBA campaign MOJAVE-5 monitors jets in AGN with VLBA experiments. We investigate the dataset bl229 observed at 15 GHz in terms of its suitability for geodetic analysis in order to evaluate the MOJAVE-5 experiments to be a testbed for source structure investigations in geodetic and astrometric VLBI. We show that both geodetic metrics, i.e. the baseline length scatter and wrms of Earth orientation parameters are about a factor of 1.5 greater than from the dedicated geodetic dual-band 2.3/8.6 GHz RV and CN experiments conducted contemporary over the time span from September 2016 to July 2020. We isolate three major differences between the two datasets: a) the scheduling approach, b) treatment of the ionospheric delay, and c) selection of target radio sources. We show that the major factor that causes discrepancies between the baseline length repeatability and the EOP wrms is the more agile schedule of geodetic VLBI experiments that includes more scans at low elevations at shorter time intervals than the astronomical experiments. We conclude that MOJAVE-5 providing the baseline length repeatability under 1 ppb includes very low level of systematic errors which confirms this dataset to be an excellent testbed for investigations of source structure on astrometry and geodesy results in full detail.

Key words VLBA, MOJAVE, TRF, EOP

Category: Symposium 1: Reference Frames => 1.5: Comparison and combination of space geodesy techniques for improving consistency between TRF, CRF and EOPs

293

S1-056

Estimation of Earth rotation parameter UT from Lunar Laser Ranging observations

Liliane Biskupek¹, Vishwa Vijay Singh^{1,2}, Juergen Mueller¹, Mingyue Zhang^{1,3,4}

1. Institute of Geodesy, Leibniz University Hannover

2. Institute for Satellite Geodesy and Inertial Sensing, German Aerospace Center (DLR)

3. State Key Laboratory of Geodesy and Earth's Dynamics, Institute of Geodesy and Geophysics, APM, Chinese Academy of Sciences

4. University of Chinese Academy of Sciences, Beijing

Since 1969, Lunar Laser Ranging (LLR) data have been collected by different observatories and analysed by different analysis groups. In recent years, observations have been made with larger telescopes (APOLLO) and at infrared wavelengths, resulting in a better distribution of precise LLR data over the lunar orbit and the observed retro-reflectors on the Moon. In Germany, beginning in the early 1980s, the LUNAR software package was developed to study the Earth-Moon system and determine various related model parameters. Our research includes the physical libration and orbit of the Moon, the coordinates of observatories and retroreflectors, and, with special modifications, tests of Einstein's theory of relativity such as parameters related to the equivalence principle, the time variation of the gravitational constant, and for a selection of PPN (Parametrized Post-Newtonian) parameters. Providing the longest time series of any space geodetic technique for studying the Earth-Moon dynamics, LLR can also support the estimation of Earth Orientation Parameters (EOP), such as UT1. The increased number of high-accuracy LLR observations allows for more accurate determination of EOP compared to previous years. Here, we focus on Δ UT results from different constellations such as single or multi-station results and on results for a different number of normal points per night. The mean uncertainty of the determined corrections to the IERS C04 series are about 18 μ s. The findings are discussed in comparison to results from VLBI measurements. The Δ UT results of VLBI can be verified by LLR for selected nights.

This research was funded by the Deutsche Forschungsgemeinschaft (DFG, German Research Foundation) under Germany's Excellence Strategy – EXC-2123 QuantumFrontiers – 390837967. Further financial supports were from the Deutsches Zentrum für Luft- und Raumfahrt (DLR) and the Strategic Priority Research Program of the Chinese Academy of Sciences, the National Natural Science Foundation of China.

Key words Lunar Laser Ranging, Earth rotation, UT

Category: Symposium 1: Reference Frames => 1.5: Comparison and combination of space geodesy techniques for improving consistency between TRF, CRF and EOPs

563

S1-057

Multi-technique Integrated Processing on the Observation Level for Consistent Determination of TRF, CRF and EOPs

Jungang Wang^{1,2}、Maorong Ge^{1,2}、Susanne Glaser²、Robert Heinkelmann²、
Harald Schuh^{1,2}

1. Technische Universität Berlin, Institut für Geodäsie und Geoinformationstechnik

2. GFZ German Research Centre for Geosciences, Space Geodetic Techniques

The terrestrial and celestial reference frames (TRF and CRF) serve a foundation role in geodesy, while the Earth Orientation Parameters (EOPs) link TRF and CRF. The reference frames and EOP are determined by the space geodetic techniques, namely, Very Long Baseline Interferometry (VLBI), Satellite Laser Ranging (SLR), Global Navigation Satellite Systems (GNSS), and DORIS (Doppler Orbitography and Radiopositioning Integrated by Satellite). The CRF is determined by VLBI only, while the TRF is obtained by combining the techniques, where SLR provides the origin, VLBI and SLR provide the scale, and GNSS and DORIS contribute to the spatial and temporal densification. Although the current combination is performed on either the parameter or the normal equation level, the multi-technique integrated processing on the observation level allows fully consistent modelling and parameterization; so it can provide the TRF, CRF, and EOP with the best consistency, precision, and reliability. Aiming on the multi-technique integrated processing on the observation level, the Positioning And Navigation Data Analyst (PANDA) software has been upgraded recently to process VLBI and SLR observations and to combine the techniques.

In this study, we present preliminary results of the consistent TRF, CRF, and EOP determination with GNSS, VLBI, and SLR observations during the VLBI CONT05 to CONT17 campaigns. The ties which describe the relationship between the relevant parameters for different techniques, for example, the coordinates of co-located VLBI, SLR, and GNSS stations, play an important role in the combination. We therefore focus on the impact of global ties (EOP), local ties, and tropospheric ties on the precision of the reference frames and EOP. We demonstrate the improvement of the multi-technique integrated processing on the observation level in terms of the precision of the TRF, CRF, and the full set of EOP.

Key words TRF, CRF, EOP, multi-technique integrated processing, observation level

Category: Symposium 1: Reference Frames => 1.5: Comparison and combination of space geodesy techniques for improving consistency between TRF, CRF and EOPs

566

S1-058

Automatic detection of offsets in GNSS station position time-series using DIA and multivariate analysis algorithm

Jin Zhang^{1,2}, Lizhen Lian², Chengli Huang^{1,2,3}

1. CAS Key Laboratory of Planetary Sciences, Shanghai Astronomical Observatory, Chinese Academy of Sciences, Shanghai 200030, China.
2. CAS Key Laboratory of Planetary Sciences, Shanghai Astronomical Observatory, Chinese Academy of Sciences, Shanghai 200030, China.
3. School of Astronomy and Space Science, University of Chinese Academy of Sciences, Beijing 100049, China.

Offset detection, especially automated offset detection is still a main challenge in Global Navigation Satellite System (GNSS) station time series analysis. The Detection Identification Adaptation (DIA) and the Multivariate Analysis (MA) methods were applied to identify station position offsets and the detection performance of both were further investigated here. In addition, the binomial trees theory was adopted in the detection procedures, to segment the time series at offset moments, so we can avoid errors which may be injected from offset correction. First, the position time-series consisting of a linear trend, seasonal signals, offsets, and white noise were simulated for numerical comparison of DIA and MA algorithm in terms of efficiency in detecting offsets. The results showed that 72.2% and 82.71% of the offset detection rate could be achieved by the two aforementioned algorithms, respectively. Then the DIA and MA algorithm were also tested on the position time series of 649 GNSS stations which were used in ITRF2014. The results indicated that 72.73% and 87.54% of the existing offsets could be detected, respectively. After a combination of DIA and MA, the detection rate is increased to 89.72%. The detection performance of offsets caused by earthquake, unknown, antenna change, receiver change and nonlinearity are different. Most offsets due to earthquake, antenna change and unknown reasons could be detected; but for the offsets caused by nonlinearity, which indicates continuous rate changes, the detection performances of both methods are worse.

Key words ITRF, offset detection, DIA, Multivariate analysis

Category: Symposium 1: Reference Frames => 1.5: Comparison and combination of space geodesy techniques for improving consistency between TRF, CRF and EOPs

570

S1-059

The NTSC geodetic VLBI system and its application of UT1 measurements

Yuanwei WU

National Time Service Center of CAS

The NTSC geodetic VLBI system is consist of three 13-meter telescopes located in Jilin, Kashi and Sanya and a data analysis center located in Xi'an. The baseline length ranges from 3215 to 4018 km. The system has been used to measure the Universal Time UT1 and tracking Beidou Navigation satellites. Here we report this domestic geodetic VLBI system and its progress on determination of UT1.

Key words instrumentation: interferometers, methods: observational --- time --- Earth

Category: Symposium 1: Reference Frames => 1.5: Comparison and combination of space geodesy techniques for improving consistency between TRF, CRF and EOPs

572

S1-060

Identify the Multi-technology systematic errors: the relations among reference point determination, telescope pointing calibration and VLBI observing

Zhang Zhibin^{1,4}, Ma Xiaohui², Sun Zhongmiao², Zhang Ali³, Yuan Ye³, Sun Zhengxiong¹

1. Shanghai Astronomical Observatory

2. Xi'an Research Institute of Surveying and Mapping

3. Xinjiang Astronomical Observatory, Chinese Academy of Sciences

4. University of Chinese Academy of Sciences, Beijing 100049, China

The systematic errors among different technologies or facilities limit the accuracy of the multi-technology terrestrial reference frame (TRF). Identifying, monitoring, and correcting systematic errors are the premises for obtaining a high-precision TRF. However, the current research or discussion on multi-technology systematic errors are restricted to the consistencies of the atmospheric delays or reference point (RP) positions measured by different facilities at a co-location station. In order to maximize the methods to monitor and identify the systematic errors, we unify the models of VLBI RP determination (RPD) and VLBI telescope pointing calibration (PC). Hence, PC surveying with higher frequency is introduced as a common technical means to monitoring systematic errors. The relations among the RPD, PC, and the deviation of the vertical are also established.

In addition, we design an automatic RPD pipeline to evaluate the RP position of the Kunming 40-m (KM40) telescope. The result shows that the RP accuracy of the KM40 maybe reach up to the level of a centimeter, even though the formal error of the RP is in a sub-millimeter level.

Key words Systematic errors, Reference point determination, Pointing calibration, VLBI, Deflection of the vertical

Category: Symposium 1: Reference Frames => 1.5: Comparison and combination of space geodesy techniques for improving consistency between TRF, CRF and EOPs

596

S1-061

Combination of GNSS and VLBI data for consistent estimation of Earth Orientation Parameters

Lisa Lengert, Daniela Thaller, Claudia Flohrer, Hendrik Hellmers, Anastasiia Girdiuk

Federal Agency for Cartography and Geodesy (BKG)

We present the current activities of the Federal Agency for Cartography and Geodesy (BKG) towards a combined processing of VLBI and GNSS data. The main goal of the combined analyses of the two different space-geodetic techniques is the improvement of the consistency between the techniques through common parameters, i.e., mainly Earth Orientation Parameters (EOPs), but also station coordinates and tropospheric parameters through local ties and atmospheric ties, respectively.

Based on our previous combination studies using GNSS data and VLBI Intensive sessions on a daily and multi-day level, we generate a consistent, low-latency EOP time series with a regular daily resolution for polar motion and dUT1. We achieved in this way a significant accuracy improvement of the dUT1 time series and a slight improvement of the pole coordinates time series, comparing EOPs from the combined processing with the individual technique-specific EOPs.

We extend the combination of GNSS and VLBI Intensive sessions by adding VLBI 24-hour sessions in order to exploit the benefit of the combination to its maximum extend. We analyse the impact of the combination on the global parameters of interest, i.e., mainly dUT1, polar motion and LOD, but also on station coordinates.

BKG's primary interest is the combination of GNSS and VLBI data on the observation level. However, the current combination efforts are based on the normal equation level using technique-specific SINEX files as a starting point.

Based on the improved combination method, we generate a new operational BKG-EOP product. In this way, BKG is the first institution (according to the current status) which provides a complete and homogeneous combined EOP product with daily resolution and short latency (1-2 days) with open access for the international community.

Key words combination, VLBI, GNSS, EOP, consistency

Category: Symposium 1: Reference Frames => 1.5: Comparison and combination of space geodesy techniques for improving consistency between TRF, CRF and EOPs

602

S1-062

Earth rotation parameters estimation using satellite laser ranging measurements to multiple LEO satellites

Hongmin Zhang, Yongqiang Yuan, Qian Zhang, Jiaqi Wu, Wei Zhang, Yujie Qin, Xingxing Li

School of Geodesy and Geomatics, Wuhan University

Earth rotation parameters (ERP) are one of the key parameters in realization of the International Terrestrial Reference Frames (ITRF). At present, International Laser Ranging Service (ILRS) generates the SLR-based ERP products only using SLR observations to LAGEOS and Etalon satellites. Apart from these geodetic satellites, many low Earth orbit (LEO) satellites of Earth observation missions are also equipped with the laser retroreflector arrays and produce a large number of SLR observations, which are only used for orbit validation. In this study, we focus on the contribution of SLR observations from multiple LEO satellites to ERP estimation. The SLR observations of current seven LEO satellites (Swarm-A/B/C, GRACE-C/D, and Sentinel-3A/B) as well as LAGEOS are used. The impact of the LEO orbit characteristic and the precision of LEO orbits to ERP estimation is investigated. Meanwhile, we also discuss the contribution of different number of LEO satellites and the combination of LEO satellites and LAGEOS to ERP estimation. In addition, we investigate the feasibility of simultaneous estimation of LEO satellites and ERP, which named one-step method in this study.

The results show that the ERP estimation can benefit from the application of the ambiguity-fixed orbit. The accuracy of ERP can be improved gradually with the increase of LEO satellites included. We also find the combination of LEO satellites and LAGEOS can achieve best consistency with the IERS products, with RMS values of 0.4241 mas, 0.3161 mas and 0.0148 ms for X pole, Y pole and LOD. In addition, the result of one-step method shows an improvement for the precision of LEO orbits thanks to the inclusion of SLR observations, but lead to a degraded ERP solution compared to the two-step method.

Key words SLR; LEO; Polar motion; UT1-UTC; Precise orbit determination

Category: Symposium 1: Reference Frames => 1.5: Comparison and combination of space geodesy techniques for improving consistency between TRF, CRF and EOPs

649

S1-063

Combination of the VLBI, GNSS and LLR station coordinates using SINCOS software

Svetlana Mironova, Sergei Kurdubov, Iskander Gayazov
Institute of Applied Astronomy of the Russian Academy of Sciences

We constructed series of VLBI, GNSS and LLR station coordinates ("individual series") based on the SINEX files obtained by the number of analysis centers. We use SINCOS software for combination, the SINEX files were combined at the normal equation level. Individual series of different analysis centers were combined with each other in order to create combined series of coordinates for VLBI, GNSS and LLR stations. Using local ties connectivity, the combined station coordinates series of different analysis centers were combined with each other. The combination results were compared with the ITRF2014 catalog, IGS and IVS solutions.

Key words combination at the normal equation level, TRF, VLBI, GNSS, LLR

Category: Symposium 1: Reference Frames => 1.5: Comparison and combination of space geodesy techniques for improving consistency between TRF, CRF and EOPs

655

S1-064

Inter- and intra-technique evaluation of UT1-UTC estimates using Legacy S/X VLBI, VGOS and their combination with co-located GNSS. A case study comparing INT1 to VGOS-B sessions

Periklis-Konstantinos Diamantidis¹, Rüdiger Haas¹, Eskil Varenius¹, Matthias Schartner², Saho Matsumoto³

1. Chalmers University of Technology

2. Institute of Geodesy and Photogrammetry, ETH Zürich

3. Geospatial Information Authority of Japan

The VLBI Global Observing System (VGOS) with its increased temporal density of observations, improved sky coverage as well as its wideband capabilities, promises to deliver geodetic products of higher precision compared to the legacy S/X. We test this hypothesis by analyzing the so-called VGOS-B sessions. These are 1 h long observing sessions between the VGOS stations at Ishioka in Japan and the Onsala twin telescopes in Sweden, which were performed between December 2019 and January 2020 simultaneously to the legacy S/X intensive sessions (INT1). The derived UT1-UTC results and their agreement to the final values of the International Earth Rotation and Reference Frame Service (IERS) are presented for both types of sessions. Previous studies show that the VGOS-B give lower formal errors and slightly better agreement to the IERS products than the simultaneous INT1. We follow up this investigation using the multi-technique space-geodetic software c5++. In particular, we combine the two types of VLBI sessions with each other, and with co-located GNSS measurements on the basis of common tropospheric parameters using the combination on the observation level (COL) technique. The results of this inter- and intra-technique combination procedure are compared to single-technique VLBI and the differences are discussed.

Key words VGOS, Combination on the observation level, EOP, UT1, VLBI, GNSS, co-location

Category: Symposium 1: Reference Frames => 1.5: Comparison and combination of space geodesy techniques for improving consistency between TRF, CRF and EOPs

718

S1-065

Weekly Terrestrial Reference Frame realization from a combination of GNSS/SLR/VLBI/DORIS at the parameter level

Lizhen LIAN¹、Chengli HUANG^{1,3}、Jin ZHANG^{2,1}

1. Shanghai Astronomical Observatory, Chinese Academy of Sciences
2. School of Physical Science and Technology, Shanghai Tech University
3. School of Astronomy and Space Science, University of Chinese Academy of Sciences

The combination at the parameter level is still a standard approach, where technique-specific solutions are first estimated and then combined within a second least squares adjustment process. The terrestrial frame's origin and scale is usually realized using space geodetic observations spanning over two decades and subsequently constrain the time evolution to a linear model, besides non-linear station motions can reach a few centimeters. We investigate a new approach, which is based on weekly estimation of station positions and EOP from a combination of reprocessed solutions of GNSS, SLR, VLBI and DORIS, which can take any nonlinear station motion (periodic signals, abrupt position offsets, nonlinear local deformations, etc.) and nonlinear variation behavior of physical datum parameters (i.e., origin and scale) into account. Parameters of a similarity transformation are set up for each input solution and several necessary reliable local ties with high precision are introduced as pseudo-observations. The geodetic datum of the combined solution is realized by internal- constraint and minimal constraint. The resulting station position time series and consistently estimated EOP products are studied in detail and are compared with ITRF2014 and EOP 14 C04 series, respectively. The residual station positions in the weekly combined reference frame are usually at the millimeter level without any periodic characteristic, while that by deducting the regularized station position under ITRF2014 may reach a magnitude of a few centimeters and seem to have a significant annual signal.

Key words Terrestrial Reference Frame, geodetic datum, local ties, nonlinear motion

Category: Symposium 1: Reference Frames => 1.5: Comparison and combination of space geodesy techniques for improving consistency between TRF, CRF and EOPs

896

S1-066

Geodetic VLBI observations in single-frequency mode with 30-meter Warkworth radio telescope

Oleg Titov¹、Alexei Melnikov²、Sergey Gulyaev³、Stuart Weston Weston³、Tim Natusch³、Fengchun Shu⁴、Bo Xia⁴、Mikhail Kharinov²

1. Geoscience Australia

2. Institute of Applied Astronomy of the Russian Academy of Sciences

3. Auckland University of Technology

4. Shanghai Astronomical Observatory, Chinese Academy of Sciences

The geodetic VLBI operates in two frequencies (S-band, 2.3 GHz and X-band, 8.4 GHz) to provide a proper calibration of the ionospheric disturbance. However, its performance is violated due to a severe radio frequency interference (RFI) in S-band. We developed a method to calibrate for the ionosphere with the global total electron content (TEC) maps and applied it for several single frequency VLBI observations run by the Institute of Applied Astronomy of the Russian Academy of Science (IAA RAS). The VLBI array comprised of three radio telescopes of the "Quasar" VLBI network in addition of two other facilities: Seshan25 (China) and Wark30M (New Zealand). It should be noted that the 30-m telescope in New Zealand operates in single band, and for this experiment it operated in X-band only. The geodetic and astrometric results obtained during this short campaign are perfectly consistent with the results from the standard legacy S/X observations. Our presentation shows that application of the global TEC maps will help to overcome the annoying problem of the RFI in S-band.

Key words Geodetic VLBI observations

Symposium 1: Reference Frames

S1.6: Vertical Reference Systems: methodologies, realization, and new technologies

Category: Symposium 1: Reference Frames => 1.6: Vertical Reference Systems: methodologies, realization, and new technologies

253

S1-067

Geodetic SAR for Height System Unification and Sea Level Research - Observation Concept and Results in the Baltic Sea

Thomas Gruber¹, Jonas Ågren², Detlef Angermann³, Artu Ellmann⁴, Christoph Gisinger⁵, Jolanta Nastula⁶, Markku Poutanen⁷, Marius Schlaak¹, Faramarz Nilfouroushan², Sander Varbla⁴, Ryszard Zdunek⁶, Simo Marila⁷, Andreas Engfeldt², Timo Saari⁷, Anna Świątek⁶, Xanthi Oikonomidou¹

1. Technical University of Munich, Institute of Astronomical and Physical Geodesy

2. Lantmäteriet, Swedish Mapping, Cadastral and Land Registration Authority

3. Technical University of Munich, German Geodetic Research Institute

4. Tallinn University of Technology, School of Engineering

5. German Aerospace Center, Remote Sensing Technology

6. Centrum Badań Kosmicznych, Polskiej Akademii Nauk

7. Finnish Geospatial Research Institute

Traditionally, sea level is observed at tide gauge stations, which usually also serve as height reference stations for national leveling networks and therefore define a height system of a country. Thus, sea level research across countries is closely linked to height system unification and needs to be regarded jointly. One of the main deficiencies to use tide gauge data for geodetic sea level research and height systems unification is that only a few stations are connected to permanent GNSS receivers next to the tide gauge in order to systematically observe vertical land motion. As a new observation technique, absolute positioning by SAR using active transponders on ground can fill this gap by systematically observing time series of geometric heights at tide gauge stations. By additionally knowing the tide gauge geoid heights in a global height reference frame, one can finally obtain absolute sea level heights at each tide gauge. With this information the impact of climate change on the sea level can be quantified in an absolute manner and height systems can be connected across the oceans. First results from applying this technique at selected tide gauges at the Baltic coasts are promising but also exhibit some problems related to the new technique. The paper presents the concept of using the new observation type in an integrated sea level observing system and provides results for a test network in the Baltic sea area by combining geometric and physical heights with tide gauge readings.

Key words Height Systems Unification, SAR, Sea Level

Category: Symposium 1: Reference Frames => 1.6: Vertical Reference Systems: methodologies, realization, and new technologies

343

S1-068

Estimation of vertical datum parameters of Hong Kong using the GBVP approach based on combined global geopotential models

Panpan Zhang、Lifeng Bao、Lin Wu、Qianqian Li、Hui Liu

State Key Laboratory of Geodesy and Earth's Dynamics, Innovation Academy for Precision Measurement Science and Technology, Chinese Academy of Sciences

Unification of the global vertical datum has been a key problem to be solved for geodesy over a long period, the main challenge for a unified vertical datum system is to determine the geopotential value of local vertical datum based on the ITRS. For this purpose, the geodetic boundary value problem (GBVP) approach based on the remove-compute-restore (RCR) technique is used to determine the vertical datum parameters. The satellite missions of the GRACE and GOCE offer high accuracy medium-long gravity field information, but GRACE/GOCE-based GGMs are restricted to medium-long wavelengths because the maximum degree of their spherical harmonic representation is limited, which is known as an omission error. To compensate for the omission error of GRACE/GOCE-based GGM, a weighting method is used to determine the combined GGM by combining the high-resolution EGM2008 model and GRACE/GOCE-based GGM to effectively bridge the spectral gap between satellite and terrestrial data. An additional consideration for the high-frequency gravity signals is induced by the topography, and the residual terrain model (RTM) is used to recover the omission errors effect of the combined GGM. Finally, as a result of the GBVP solution based on the combined DIR_R6/EGM2008 model, RTM, and residual gravity, the geopotential values of the Hong Kong Principal Datum (HKPD) are estimated to be equal to $62636860.55 \pm 0.29 \text{ m}^2\text{s}^{-2}$ with respect to the global geoid $W=62,636,853.4 \text{ m}^2\text{s}^{-2}$. The vertical offsets of HKPD with respect to the global geoid is $-0.731 \pm 0.030 \text{ m}$, which means that the HKPD is about 73.1 cm below the global height datum.

Key words GRACE/GOCE; weighting method; the combined GGM; residual terrain model; geopotential value

Category: Symposium 1: Reference Frames =» 1.6: Vertical Reference Systems: methodologies, realization, and new technologies

697

S1-069

Chronometric Height: a genuine general relativistic definition of height measures

Dennis Philipp^{1,3}、Hu Wu²、Eva Hackmann^{1,3}、Claus Laemmerzahl^{1,3}、Juergen Mueller²

1. ZARM, University of Bremen, Germany

2. Institute of Geodesy (IfE), Leibniz University Hannover, Germany

3. Gauss-Olbers Center, c/o ZARM, University of Bremen, Germany

The Newtonian gravity potential is one of the main objects for conventional geodesy and employed for basic concepts, such as the definition of heights. A modern height definition in terms of geopotential numbers can offer a variety of advantages. Moreover, from the theoretical point of view, such a definition is considered more fundamental.

We know, however, that relativistic gravity (here General Relativity) requires to reformulate basic geodetic notions and to develop a consistent theoretical framework, relativistic geodesy, to yield an undoubtedly correct interpretation of contemporary and future (high-precision) measurement results. The new framework of chronometric geodesy that builds on the comparison of clocks at different positions in the gravitational field offers fundamental insight into the spacetime geometry if a solid theoretical formulation of observables is underlying all observations. For chronometry, high-performance clock networks, i.e., optical clocks connected by dedicated frequency transfer techniques, are capable to observe the mutual redshift with incredible accuracy.

Here we approach a genuine relativistic definition of the concept of height. Based on the relativistic generalization of geopotential numbers, a definition of chronometric height is suggested, which reduces to the well-known notions in the weak-field limit. This height measure is conceptually based on the so-called time-independent redshift potential, which describes the gravitoelectric degree of freedom in General Relativity.

We gratefully acknowledge the financial support by the Deutsche Forschungsgemeinschaft (DFG, German Research Foundation) under Germany's Excellence Strategy EXC-2123 "QuantumFrontiers" (Project-ID: 390837967). The study is also funded by the Deutsche Forschungsgemeinschaft (DFG, German Research Foundation) under the research program SFB 1464 "TerraQ - Relativistic and Quantum-based Geodesy" (Project-ID 434617780).

Key words relativistic geodesy, height, relativity, redshift, clock comparison

Category: Symposium 1: Reference Frames => 1.6: Vertical Reference Systems: methodologies, realization, and new technologies

804

S1-070

Using kriging interpolation for local geoid construction: accuracy evaluation in dependence of point density

Emanuele Alcaras, Pier Paolo Amoroso, Ugo Falchi, Claudio Parente
Parthenope University of Naples

The simplest way to represent a geoid model is given by the variability of the vertical separation between the ellipsoid and the geoid (geoid undulation), relative to the location expressed in a coordinate reference system, i.e. WGS84 ellipsoidal (longitude and latitude) coordinates. Global geoid models are available for free download, e.g. EGM96 and EGM2008, resulting in a grid of rows and columns with cell size of a few minutes, containing float values describing the difference between the WGS84 ellipsoid and the mean sea level.

National geoid models presenting higher resolution are generally derived by a combination of different datasets, integrating individual pure astrogeodetic, gravimetric and GPS/levelling solutions. To define local geoid, different interpolators may be applied starting from dataset of geoid undulation values. Several studies demonstrate the high performance of kriging methods (i. e. Universal kriging and Ordinary kriging). It is well known that the accuracy of the resulting models depends not only by interpolation method, but also by points numerosity and distribution. This article aims to analyse the performance of kriging approaches in dependence of the density of the dataset. The experiments are carried out on an already existing local geoid model: different subset are organized containing an increasing number of points in the same area and each of them is submitted to kriging interpolations. The resulting models are compared with the original one and residuals are calculated to evaluate the accuracy in dependence of point density. The results demonstrate the efficiency of the kriging methods, highlighting the possibility to achieve higher accuracy in dependence of opportune parameter settings; particularly, the choice of the type of semi-variogram, the mathematical function that graphically represents the spatial correlation between the input point values, permits to define the best performing model.

Key words local geoid, geoid undulation, interpolation, kriging, accuracy.

Symposium 2a: Earth's Static Gravity Field

S2a.1: Terrestrial, Marine and Airborne Gravimetry

Category: Symposium 2a: Earth's Static Gravity Field =» 2a.1: Terrestrial, Marine and Airborne Gravimetry

51

S2a-001

Determination Of The Vertical Gravity Gradient At A Few Sites Of The Absolute Gravity Network Of Algeria

Rabah HAMIDI¹, Mohamed HAMOUDI²

1. National Institute of Mapping & Remote Sensing/University of Algiers

2. University of Algiers

The gravity value g of an absolute gravimetric station measured by the new generation of absolute gravimeters with high precision ($1\mu\text{Gal}$) such as FG5, A-10 and other instruments must be reduced to the ground. In the case of Algeria, the absolute gravimetric network contains 12 absolute points observed by the NIMA's absolute gravimeter FG5-111 with accuracy ranging from $0.7\mu\text{Gal}$ (In Salah) to $2.9\mu\text{Gal}$ (Oran) [1], the gravity value g at each absolute gravimetric station is given at 130 cm. The aim of this work is to reduce a few absolute points to the ground.

The only and unique reduced technique is the one that uses the calculation of the vertical gradient (VG) between two levels, the ground level (level 0) and height level of the measurement given by the absolute gravimeter FG5-111 at 130 cm (level 1). For this purpose, four INCT's Lacoste&Romberg (LCR) gravimeters, G model type, G1140, G1152, G856 and G857, equipped with MVR (Maximum Voltage Retroaction) electronic system.

In this study and among the twelve (12) absolute gravimetric points, four (04) absolute points were used, CRAAG, Bechar, Ghardaïa and Oran sites. Including two gravimeters of LCR- G1140-G1152 type with eleven (11) series of measurements for each gravimeter at the CRAAG, four gravimeters of LCR- G857-G856-G1140-G1152 type with nine (09) series of measurements for each gravimeter at Bechar, two gravimeters of LCR-G1140-G856 type with eleven (11) series of measurements for each gravimeter at the CRAAG and two gravimeters of type LCR-G856-G1152 with 11 series of measurements for each gravimeter at Ghardaïa site.

Key words Gravimetry, Gravity, Absolute Gravimetry, Relative Gravimetry, Vertical Gradient.

Category: Symposium 2a: Earth's Static Gravity Field =» 2a.1: Terrestrial, Marine and Airborne Gravimetry

53

S2a-002

Current status and future improvements of digital zenith camera VESTA

Inese Varna, Ansis Zarins, Augusts Rubans
University of Latvia

The digital zenith camera VESTA (VERTical by STARs) was designed at the Institute of Geodesy and Geoinformatics (GGI) of the University of Latvia. By the end of 2020, vertical deflection measurements were carried out at more than 400 sites on the territory of Latvia. The typical accuracy of VESTA is ~0.1 arc seconds. Vertical deflections have been used as additional terrestrial data in combination with GNSS/levelling data and the EGM2008 global geopotential model for the improvement of the quasi-geoid of Latvia. Current research is focused on further improving the accuracy of VESTA, such as:

- testing the digital zenith camera under various conditions to investigate and mitigate the phenomenon of anomalous refraction at zenith;
- performance accuracy analysis in a permanent test site to estimate the spatial and temporal properties of the measured DoV values. Various instrumental settings will be tested during observations and post-processing.

This research has been supported by the European Regional Development Fund activity “Post-doctoral Research Aid”, project No. 1.1.1.2/VIAA/4/20/666 .

Key words digital zenith camera, deflections of vertical, anomalous refraction

Category: Symposium 2a: Earth's Static Gravity Field =» 2a.1: Terrestrial, Marine and Airborne Gravimetry

174

S2a-003

Preliminary Results of a Gravity Observing experiment at 848m under the earth surface

Xiaodong CHEN、 Miaomiao ZHANG、 Heping SUN、 Jianqiao XU、 Jiangcun ZHOU、 Xiaoming CUI

Innovation Academy for Precision Measurement Science and Technology, Chinese Academy of Sciences

Using simultaneous continuous tidal gravity observations from a Burris spring gravimeter in the -848 m deep tunnel and a LCR-ET20 spring gravimeter, surficial and underground gravity noise levels at the deep geophysical experimental field are preliminarily analysed. Analysis results show that the underground gravity noise level is lower than the surficial noise level below 1.7 mHz (period about 9.8 min); especially in the gravimeter sensitive frequency band (period over 3 h), the underground gravity noise level is lower by 2 orders of magnitude, which fully demonstrates the low noise of underground environment at the deep geophysical experimental field in Huainan, China. Our results further indicate that the -848 m deep tunnel can provide both an ultra quiet environment for deep multi-physical fields observations and a perfect condition for the detection of weak geophysical signals.

Key words Deep earth observation; Gravity noise level; Tidal gravity observations; Burris gravimeter; LCR-ET20 gravimeter.

Category: Symposium 2a: Earth's Static Gravity Field =» 2a.1: Terrestrial, Marine and Airborne Gravimetry

196

S2a-004

Extracting Long - Period Surface Waves Using Ambient Noise Data Recorded by Superconducting Gravimeters

Hang Li¹、 Xiaodong Chen¹、 Jianqiao Xu¹、 Heping Sun¹、 Jiangcun Zhou¹、
Qingchao Liu¹、 Miaomiao Zhang¹、 Lingyun Zhang²

1. State Key Laboratory of Geodesy and Earth's Dynamics, Innovation Academy for Precision Measurement Science and Technology, Chinese Academy of Sciences

2. North China University of Science and Technology

Surface waves are widely used in study of the deep internal structure of the Earth nowadays. With the ambient noise data on seismically quiet days sourced from the gravity tidal observations of 7 superconducting gravimeters (SGs) and the seismic observations for validation from 3 co-located STS-1 seismometers, long-period surface waves are successfully extracted by the phase autocorrelation (PAC) method. Group velocity dispersion curves at the frequency band of 2-7.5mHz are extracted and compared with the theoretical values calculated with the preliminary reference Earth model (PREM). The comparison shows that the best observed values differ about $\pm 2\%$ from the corresponding theoretical results and the extracted group velocities of the best SG are consistent with the result of the co-located STS-1 seismometer. The results indicate that reliable group velocity dispersion curves can be measured with the ambient noise data from SGs. Results in this study show that the SG, besides the seismometer, is proved to be another kind of instrument that can be used to observe long-period surface waves on seismically quiet days with a high degree of precision.

Key words Superconducting gravimeters; Long-period surface waves; Group velocity dispersion curves; Phase autocorrelation

Category: Symposium 2a: Earth's Static Gravity Field =» 2a.1: Terrestrial, Marine and Airborne Gravimetry

252

S2a-005

Recent Airborne Gravity Surveys in Denmark with Strapdown Technology

Tim Jensen, René Forsberg
DTU Space

In the recent years, a number of small-scale airborne gravity surveys have been carried out in Denmark in order to improve data coverage for an upcoming new Geoid model. These efforts have allowed for testing simple and easy-to-use strapdown gravity systems in small fixed-wing aircrafts flying at low altitude and low ground speed, allowing for an improved spatial resolution. The dense network of high-quality terrestrial gravity observations in Denmark allows for unique comparison with airborne observations and the possibility to constrain the long-wavelength information, which remains a challenge in strapdown gravity systems. The results of these new strapdown airborne surveys indicate that Geoid improvement of up to 5-10 cm are possible, especially in coastal regions, even in well-surveyed areas like Denmark.

Several airborne gravity surveys conducted over the years from 2018 to 2021 will be presented. The presentation will focus on the use of temperature stabilized strapdown gravity systems, but other gyro-stabilized platform systems will also be presented, such as the ZLS Dynamic Gravity Meter and the AT1A gravimeter from Dynamic Gravity Systems. The inter-comparison of airborne gravity systems and the comparison with terrestrial gravity observations allows for an in-depth analysis of the resulting gravity estimates and their errors

Key words Airborne gravimetry; Strapdown IMU

Category: Symposium 2a: Earth's Static Gravity Field =》 2a.1: Terrestrial, Marine and Airborne Gravimetry

260

S2a-006

The Airborne Gravity Measurement for Development of a New Precise Gravimetric Geoid Model in Japan

MASAHIRO NAKASHIMA、Kento Iio、Yasuhiro Iitsuka、Shinobu Kurihara、Kumikazu Ochi、Shuichi Omori、Tokuro Kodama、Masato Kuroyanagi、Masami Handa、Hiroaki Yamamoto、Takashi Toyofuku、Chiaki Kato、Koji Matsuo
Geospatial Information Authority of Japan

We, the Geospatial Information Authority of Japan (GSI) have made several attempts to improve the accuracy of the gravimetric geoid model in Japan, such as integration of additional gravity data of new satellite and improvement of methods to compute the model. However, due to lack of land gravity data in mountainous area and low accuracy of marine gravity data in coastal area, large discrepancies exist between the model and GNSS/leveling geoid heights. In addition, most of the land gravity data were obtained more than 30 years ago, and their location information was read from topographic maps. As a result, the quality of their location information is poor and this could be one of error sources in the model.

Therefore, we have started airborne gravity measurement since FY 2019 to tackle these challenges. Airborne gravity measurement is the method of efficiently acquiring homogenous gravity data over a wide area even in mountainous or coastal areas. Since the aircraft is equipped with a GNSS receiver, it is possible to obtain positions of the aircraft with centimeter accuracy. We are planning to complete the airborne gravity measurement covering the whole territory except for the outlying islands by FY 2022 and build a precise gravimetric geoid model with approximately 3 cm accuracy in FY 2023 by combining the airborne gravity data with existing land, marine and satellite gravity data.

As of December 2020, approx. 50% of data collection were completed. Comparison between the airborne gravity data and EGM2008 model gravity values reveals large differences in gravity values at some mountainous and coastal areas. In particular, differences of over 10 mGal are shown around Kashimanada Sea, Iyonada Sea, and Akaishi Mountain Range. This result indicates that the airborne gravity measurement could detect detailed gravity distribution which cannot be detected by EGM2008. We will report the progress of the measurement, data processing, and evaluation of the data quality.

Key words Airborne Gravity Measurement, Gravimetric Geoid Model

Category: Symposium 2a: Earth's Static Gravity Field =» 2a.1: Terrestrial, Marine and Airborne Gravimetry

355

S2a-007

Results from a car-based 3D-strapdown gravimetry campaign in the Bavarian Estergebirge

Peter Schack, Roland Pail, Thomas Gruber
Technical University of Munich

In 2019, a field campaign in the Northern Alps (Bavarian Estergebirge) was conducted to determine the 3D-gravity disturbance along a 23 km trajectory. A navigation-grade IMU, a geodetic GNSS receiver, a relative gravimeter and a zentih camera were applied to record observations in dynamic and static mode. With RMS errors of 0.2 - 0.5 arcsec for the vertical deflections and 1.5 mGal for the scalar gravity disturbance at an approximate spatial resolution of 200 m, it could be shown that high-quality gravity data can be generated with this measurement concept for local and regional gravity studies. These results are achieved by applying the indirect method using an Extended Kalman Filter and by incorporating GGMplus information. Apart from the results of the measurement campaign, this contribution also presents the impact of a temperature calibration onto the gravity disturbance estimates and investigates error components that deteriorate the results' quality.

Key words gravimetry, terrestrial, strapdown, moving-base, 3D-gravity disturbance

Category: Symposium 2a: Earth's Static Gravity Field =» 2a.1: Terrestrial, Marine and Airborne Gravimetry

377

S2a-008

A Magnetic Field Calibration Approach to Mitigate Accelerometer Errors in Strapdown Gravimetry

Felix Johann¹、 David Becker²、 Matthias Becker¹、 Matthias Hoss²、 Alexander Löwer²、 Christoph Förste³

1. Physical and Satellite Geodesy, Technical University of Darmstadt, Germany

2. iMAR Navigation GmbH, St. Ingbert, Germany

3. GFZ German Research Center for Geosciences, Dept. 1 Geodesy, Potsdam, Germany

Static experiments showed that the Earth's magnetic field significantly affects Q-Flex type accelerometer readings of strapdown gravimeters. In this study, a calibration function to reduce the resulting errors was developed and verified in several dynamic experiments.

In the static experiments, a navigation-grade inertial measurement unit (IMU) of the type iMAR iNAV-RQH-1003 with Honeywell QA-2000 accelerometers was placed in a 3-D Helmholtz coil, where it was exposed to various magnetic field directions and intensities. For the IMU under test, it was found that magnetic field intensities in the order of the Earth's magnetic field lead to systematic deviations in the accelerometer readings of several mGal ($1 \text{ mGal} = 10^{-5} \text{ m/s}^2$). The evaluation of the static experiments suggests that the extent of the accelerometer reading error depends on the intensity and direction of the magnetic field with respect to the input axis of the sensor. Based on these parameters, a calibration function was developed. Several shipborne and airborne strapdown gravimetry campaigns were re-processed applying this this calibration. The precision of the results improved depending on the local magnetic field intensity and trajectory characteristics by 7% to 82% in all campaigns. The bulk of the effect is suspected to be due to the Earth's magnetic field. Interfering magnetic fields caused by the carrier vehicles and their instrumentation were of minor significance and seem to be negligible.

The results show the importance of magnetic field consideration and the improvement that can be achieved due to its correction on Q-Flex based strapdown gravimeters. Analyses of the influence of the magnetic fields on further types of strapdown gravimeters are suggested.

Key words IMU, magnetic field, accelerometer, gravimetry, strapdown

Category: Symposium 2a: Earth's Static Gravity Field =» 2a.1: Terrestrial, Marine and Airborne Gravimetry

380

S2a-009

An approach to airborne vector gravimetry based on spherical scaling functions

Vadim Vyazmin

Lomonosov Moscow State University

Traditional airborne gravimeters (based on gyro-stabilized platforms) are well-suited for measuring the vertical component of the gravity vector. In contrast, strapdown airborne gravimeters have the potential for measuring all three components of the gravity vector. However, estimating the gravity vector from strapdown airborne gravimetry data remains challenging, since the gravity horizontal components (deflections of the vertical) are observed only in combination with systematic errors of the inertial measurement unit (IMU) of strapdown gravimeter. Postprocessing schemes for strapdown airborne gravimetry are based on IMU-GNSS integration and using an a priori gravity model. The traditional approach is based on modelling gravity in time.

This work presents an approach based on spatial gravity modelling. The primary idea exploited by the approach is that a priori information about the spatial behaviour of gravity in the survey flight area can improve observability of the gravity horizontal components. Namely, we parametrize the disturbing potential locally by the Abel-Poisson spherical scaling functions. Then the unknown parametrization coefficients are estimated along with the IMU systematic errors (terms of the error equations of inertial navigation) using the Kalman filter in the information form.

We present results of processing real data from a survey flight carried out by the DTU-Space with their iMAR strapdown gravimeter over the southern Kattegat in 2019. The flight data was kindly provided to the Navigation and Control Laboratory of MSU by prof. R. Forsberg (DTU-Space). Accuracy of the gravity horizontal component estimation was evaluated by comparing with EGM2008 and is at the level of 2 mGal (RMS), which can be considered very promising.

Key words airborne gravimetry, IMU/GNSS, deflections of the vertical, Kalman filtering

Category: Symposium 2a: Earth's Static Gravity Field =» 2a.1: Terrestrial, Marine and Airborne Gravimetry

609

S2a-010

Recent results of strapdown dynamic gravimeter on different platforms

KAIDONG ZHANG

Hunan INS Technology Co. Ltd

As a new kind of dynamic relative gravimeter, the accuracy and resolution of strapdown gravimeter developed by Hunan INS Technology Co., Ltd has improved a lot in recent two years. In this paper, the gravimeter is introduced in detail, and the results of some recent tests on different platforms are presented, including the Mount Everest airborne gravimetry campaign in May 2020. Tests showed that the accuracy of lake gravimetry is better than 0.1mGal, the accuracy of marine gravimetry is better than 0.3mGal, the accuracy of terrestrial gravimetry is better than 0.4mGal, and the accuracy of airborne gravimetry is better than 0.6mGal.

Key words strapdown dynamic gravimeter, marine gravimetry, terrestrial gravimetry, airborne gravimetry

Category: Symposium 2a: Earth's Static Gravity Field =» 2a.1: Terrestrial, Marine and Airborne Gravimetry

612

S2a-011

Gravity anomalies of large lakes from ICESAT-2 laser altimetry.

Ole Baltazar Andersen^{1,2}, Nielsen Karina¹, Forsberg Rene¹

1. DTU Space

2.

The data from NASA's Ice, Cloud, and Land Elevation Satellite-2 (ICESat-2) mission offer a unique opportunity to map rivers and lakes with an unprecedented number of observations in areas where previous missions have failed to provide valuable water level estimates. ICESat-2 carries just one instrument, the Advanced Topographic Laser Altimeter System (ATLAS), which is a green wavelength, photon-counting lidar, and several data products are available, such as the ATL03 product, which holds the photon data, and the ATL13 product which contains estimated inland water surface heights and statistics for water bodies across the world. The along-track resolution of the ATL03 product is less than 1 m, and with the three pairs of beams, i.e. six beams in total, the mission provides exceptional opportunities for inland water studies in areas with mountainous topography.

Deriving lake heights using altimetry in mountainous areas has proven to be a challenge for both conventional Low Resolution Mode (LRM) and Synthetic Aperture Radar (SAR) altimetry, causing issues not only with waveforms, but also the position of the range window.

With the un-precedented range precision offered by ICESAT-2 spatial lake elevation variations can be mapped with cm accuracy. This can be used to derive a map of the Mean lake elevation which will be a function of the mean dynamic lake topography (prevailing winds etc) and residual geoid signal and possible erroneous elevation and topography corrections.

In this study, we evaluate the first attempt to extract gravity anomalies over several large lakes and compare with airborne gravity to investigate if ICESAT-2 gravity anomalies can be used to augment global gravity data bases.

Key words ICESat2, Lake, Gravity mapping.

Category: Symposium 2a: Earth's Static Gravity Field =» 2a.1: Terrestrial, Marine and Airborne Gravimetry

646

S2a-012

Strapdown airborne gravimetry: postprocessing algorithms and some results

Vadim Vyazmin, Andrey Golovan, Yuri Bolotin
Lomonosov Moscow State University

Airborne gravimetry based on strapdown gravimetric systems has made progress over the last decade due to available high accuracy inertial sensors and thermal stabilization (e.g., strapdown systems by iMAR). A typical strapdown airborne gravity system includes an inertial measurement unit (IMU) and GNSS receivers. Processing strapdown gravimetry data is challenging as gravity estimates are influenced by the accelerometer systematic errors (bias, linear drift, etc.). Processing strategies use the inertial navigation approach based on IMU/GNSS integration. Generally, the horizontal and vertical channels are processed simultaneously.

We present strapdown airborne gravimetry algorithms that cover all postprocessing stages: GNSS raw data processing, IMU alignment, IMU/GNSS integration, and gravity estimation. The processing strategy has the following specific features. During the IMU alignment (before and after the survey flight), we determine not only the IMU orientation but also the values of the vertical accelerometer bias. This allows us to determine the linear drift of the vertical accelerometer. At the IMU/GNSS stage, we process only the horizontal channels and use the representation of inertial navigation errors (position and velocity errors) as a sum of so-called dynamic and kinematic errors (commonly used by the Navigation and Control Laboratory of MSU). The result of this stage are the attitude and inertial sensor bias estimates. Gravity disturbance is estimated at the last stage via Kalman filtering using the vertical channel alone and modelling gravity as a stationary process.

The developed algorithms were tested using data from a survey flight with the iMAR unit carried out in 2019 by the DTU-Space who kindly provided the data to the Navigation and Control Laboratory. We present characteristics of the iMAR unit in-flight accuracy and the results of gravity estimation and accuracy assessment.

Key words strapdown gravimetry, gravity, IMU/GNSS, Kalman filter

Category: Symposium 2a: Earth's Static Gravity Field =» 2a.1: Terrestrial, Marine and Airborne Gravimetry
679
S2a-013

The convergence of gravity change rates from repeated absolute gravity measurements

Mirjam Bilker-Koivula, Jaakko Mäkinen, Hannu Ruotsalainen, Jyri Näränen, Timo Saari

Finnish Geospatial Research Institute, National Land Survey of Finland

Repeated absolute gravity measurements are used to monitor changes in gravity, for example due to tectonics, uplift, or subsidence. Due to noise, caused for example by variations in local hydrology, long time series of absolute gravity measurements are needed to be able to determine reliable gravity change rates. How long time series are needed, depends not only on the noise of the data, but also on the desired accuracy level.

One way to determine if an obtained absolute gravity trend is reliable, is to look at the development of the trend in time when more measurements are added. This is done by calculating a time series of trends, starting with two measurements, and adding one measurement for each new trend calculation. In this approach we consider a trend reliable when its value is stable in time, i.e. it does not change significantly when adding new observations.

We analysed the convergence of trends of absolute gravity time series in Finland. Gravity in Finland changes due to the ongoing Fennoscandian postglacial rebound. Long absolute gravity time series were available. We used absolute gravity measurements of 7 stations, with time series lengths between 11 and 43 years. The time series measured with FG5 and FG5X absolute gravimeters generally stabilized within 10 years. When these data were combined with older measurements made with a JILAg gravimeter, the trend stabilized between 15 and 20 years, when an offset was applied for the JILAg gravimeter. At some stations the stabilization was even faster.

We conclude that looking at the development of a trend in time gives a good indication if a trend value is reliable or not. It is expected that the convergence to a stable trend can go faster when absolute gravity time series are corrected for changes in the local hydrology.

Key words absolute gravity, time series, change rates, trends, postglacial rebound, Finland

Category: Symposium 2a: Earth's Static Gravity Field =» 2a.1: Terrestrial, Marine and Airborne Gravimetry

690

S2a-014

Moving base gravimetry on a land vehicle: The first results from a short traverse drive in central Turkey

İlyas AKPINAR¹, Mehmet SİMAV¹, Kamil TEKE², Yunus Aytaç AKDOĞAN¹,
Hasan YILDIZ¹, Murat DURMAZ²

1. General Directorate of Mapping

2. Hacettepe University, Department of Geomatics Engineering

Although the traditional static terrestrial gravimetry offers better accuracy and precision in measuring the Earth's gravity field, it is very time and labor consuming to have adequate data coverage even with the most advanced instrumentation. SINS/GNSS integrated moving base gravimetric system, which has been extensively studied and successfully implemented primarily in the airborne gravimetry, appears to be an efficient option for providing high-resolution gravity data. It is a well-known fact that the airborne gravimetry is a band-limited technique and it suffers from relatively high-speed of the aircraft and ill-posed downward continuation operation. On the other hand, acquiring data on the Earth's surface with a ground vehicle having lower velocity may provide additional benefits. A study group of authors has started to develop a terrestrial mobile gravimeter prototype that may reveal these potential advantages. The platform will be a multi-sensor integrated land vehicle that may potentially improve navigation and gravity solutions. The first experiment has been performed with a thermally-stabilized iNAT-RQH navigation-grade strapdown inertial measurement unit aided with a single GNSS antenna over a 45 km-long traverse in Ankara. The integration has been achieved by loosely-coupled Extended Kalman Filter (EKF) having 18 state variables using indirect approach, which includes the vertical gravity disturbance in the system state vector and model the inertial sensor errors and gravity disturbance as stochastic processes. The well-surveyed gravity tie observations and the zero velocities at some parking positions along the traverse have been introduced as additional measurements to the EKF. The non-holonomic motion constraints have also been tested. The RTS-smoothed gravity solutions have been assessed at the available ground-truth control points to determine the gravity closure errors and the average long-term drift of the estimated gravity values.

Key words SIMU, GNSS, Sensor Fusion, EKF, Mobile Gravimetry, Land Vehicle

Category: Symposium 2a: Earth's Static Gravity Field =» 2a.1: Terrestrial, Marine and Airborne Gravimetry

728

S2a-015

Validation of the Hellenic gravity network in the frame of the ModernGravNet project

Vassilios Grigoriadis¹, Vassilios Andritsanos², Dimitrios Natsiopoulou¹

1. Laboratory of Gravity Field Research and Applications, Department of Geodesy and Surveying, Aristotle University of Thessaloniki
2. Department of Surveying and Geoinformatics Engineering, University of West Attica

In the frame of the “Modernization of the Hellenic Gravity Network - ModernGravNet” project, relative and absolute gravity measurements were carried out at selected 1st and 2nd order benchmarks of the Hellenic gravity network. These measurements are used first for the evaluation of the network while problems are identified related to the benchmark location and construction. Then, as the official network gravity values are referenced to the Potsdam gravity system, transformation parameters are determined for converting official values to the new gravity system as it is defined by the absolute gravity measurements. For this reason, different parametric models are utilized in an effort to identify possible biases and tilts. Moreover, global geopotential models are assessed at the network benchmarks as a first step towards the development of a new geoid model for Greece and successively the establishment of a national geoid-based vertical datum.

Key words Gravity network, Greece, gravity measurements

Category: Symposium 2a: Earth's Static Gravity Field =» 2a.1: Terrestrial, Marine and Airborne Gravimetry

780

S2a-016

Evaluation of the Muquans Absolute Quantum Gravimeter AQQ-A02 against a precise gravity reference

Julian Glässel, Hartmut Wziontek, Axel Rülke
German Federal Agency for Cartography and Geodesy (BKG)

Quantum gravimeters have been anticipated for decades as an alternative technology to measure absolute gravity. In recent years they have progressed from experimental lab setups to commercially available instruments suitable for routine operation and applications in geodesy and geosciences. We present an evaluation of the Muquans AQQ-A02, purchased in late 2018, from a user's perspective. We assess the absolute accuracy, repeatability and stability by comparing the instrument to the well-established precise absolute reference functions provided by superconducting gravimeters in combination with repeated absolute measurements at BKG's gravimetric stations at Wettzell and Bad Homburg, Germany. We conclude that, aside from occasional issues with susceptibility to environmental conditions and system reliability, the AQQ-A02 provides notable advantages, and, with few exceptions, delivers the specified accuracy of better than 100 nm/s^2 and precision of 10 nm/s^2 .

Key words absolute quantum gravimeter

Symposium 2a: Earth's Static Gravity Field

**S2a.2: Vertical Reference Systems:
methodologies, realization, and new
technologies**

Category: Symposium 2a: Earth's Static Gravity Field = » 2a.2: Vertical Reference Systems: methodologies, realization, and new technologies

145

S2a-017

Realization of the International Height Reference System in the region of Mount Qomolangma (Everest)

Tao Jiang¹、Yamin Dang¹、Chunxi Guo²、Chuanyin Zhang¹

1. Chinese Academy of Surveying and Mapping

2. Geodetic Data Processing Centre of Ministry of Natural Resources

On December 8, 2020, China and Nepal jointly announced that the orthometric height of Mount Qomolangma (Everest) in the International Height Reference System (IHRM) is 8848.86 m. For the first time, the IHRM was realized in the region of Mount Qomolangma through the establishment of a high precision gravimetric geoid model based on the IHRM standards and conventions. Due to the high altitude and extremely complex topography, there are lots of terrestrial gravity data gaps in this area. Airborne gravity survey at the average flight altitude of 10250 m and ground gravity measurement at the summit of Mount Qomolangma were carried out, which filled the gravity data gaps and significantly improved the accuracy of geoid model. Using the spectral combination approach and selecting EIGEN-6C4 as the reference gravity model, the local gravimetric quasigeoid was modeled by combining the airborne and terrestrial gravity data. This quasigeoid model agrees with the GPS leveling measured height anomalies at 61 benchmarks in ± 3.8 cm in terms of the standard deviation of discrepancies, while the standard deviation for the quasigeoid model computed solely from terrestrial gravity data is ± 7.8 cm, which demonstrates the accuracy improvement of 51.3% after the inclusion of airborne gravity data. Finally, the geoid height at the summit of Mount Qomolangma in the IHRM was determined from the interpolated height anomaly by applying the rigorous correction of geoid-quasigeoid separation (Flury and Rummel in *J Geod* 83:829–847, 2009).

Key words Airborne gravity, Gravimetric geoid, International Height Reference System, Mount Qomolangma

Category: Symposium 2a: Earth's Static Gravity Field = » 2a.2: Vertical Reference Systems: methodologies, realization, and new technologies

361

S2a-018

First attempt to establish connection between the Russian height system and the International Height Reference System (IHR)

Ilya Oshchepkov, Maria Gridchina
Center of Geodesy, Cartography and SDI

The connection between the existing height systems and the International Height Reference System/Frame (IHR/IHRF) has recently become one of the most important and interesting problems of modern geodesy. We are trying to establish this connection for the Russian height system which realised by the extremely spatially spreaded levelling network: it stretches by thousands of kilometres from the Baltic Sea to the Pacific Ocean and from the Arctic Ocean to the Caspian Sea. The levelling network is still realizing the Baltic Normal Height System 1977 (BHS77) which by definition has zero at the Kronstadt tide gauge. In fact, this single tide gauge was the only fixed point in the adjustment procedure in the 1970s and therefore it is expected for the levelling network to have an accumulated systematic errors, proportional to the distance from its zero point. These errors were never actually discovered and investigated properly before. In this study, we compute the reference potential value at the beginning of the BHS77 by using GNSS measurements on more than 800 levelling benchmarks. The height anomaly is computed from the global gravity field models. The computed W_0 values on all points were analyzed and it turned out that the levelling network has indeed a systematic error of about 0.05-0.07 mm/km which accumulates along the entire network. It results in the absolute errors of the normal heights of about 60-80 cm at the farthest east ends of the country. The systematic effect was also discovered independently by analyzing observations from several dozens tide gauges in comparison with Mean Dynamic Topography (MDT) model derived from the satellite altimetry. The final reference potential value at the beginning of the BHS77 can be used for the first approximate connection of the Russian and all other parts of the former USSR levelling network with the IHR/IHRF. However, due to the identified errors, this connection cannot be called completely reliable.

Key words height system, levelling network, IHR, height systems unification

Category: Symposium 2a: Earth's Static Gravity Field = » 2a.2: Vertical Reference Systems: methodologies, realization, and new technologies

401

S2a-019

Can the Earth Gravitational Model augmented by the Topographic Gravity Field Model realize the International Height Reference System accurately?

Jianliang Huang、 Marc Véronneau、 John W. Crowley、 Bianca D'Aoust、 Goran Pavlic

Canadian Geodetic Survey, Surveyor General Branch

Spatial resolution of the Earth Gravitational Model (EGM) has improved drastically for the last two decades. The highest-degree EGM augmented by the Topographic Gravity Field Model (TGFM) is up to spherical harmonic degree 5540, which corresponds to a spatial resolution of about 4 km. This resolution is close or identical to regional (quasi-)geoid models. In principle, the International Height Reference System (IHR) can be realized by either EGM+TGFM or regional (quasi-)geoid models. Either of the two approaches has advantages over the other. On the one hand, the former can ensure a consistent realization of IHR by a uniform mathematical representation, but may be subject to larger commission and omission errors than the latter primarily due to lack of complete coverage and availability of gravity data over some regions. On the other hand, the latter can be developed by experts from national agencies and universities with access to the best available gravity data, but may cause an uncertainty of several centimetres originating from methodology. The public availability of gravity data over Canada removed the data restriction on the former, thus allowing Canadian gravity data to be included in recent EGMs. In this study, we evaluate the suitability of EGM+TGFM for realization of IHR in Canada, and conclusions drawn are applicable for other regions as well.

Key words EGM, TGFM, IHR

Category: Symposium 2a: Earth's Static Gravity Field = » 2a.2: Vertical Reference Systems: methodologies, realization, and new technologies

502

S2a-020

An overview of SIRGAS activities towards the IHRF

Gabriel do Nascimento Guimarães¹、Ana Cristina Oliveira Cancoro de Matos²、Ayelen Pereira³、Ezequiel Darío Antokoletz^{4,8}、José Luis Carrión Sánchez⁵、Laura Sánchez⁶、SIRGAS WG III Team⁷

1. Federal University of Uberlandia

2. Studies Center for Geodesy

3. National University of Rosario

4. National University of La Plata

5. Ecuadoran Military Geographic Institute

6. Technical University of Munich

7. SIRGAS

8. Federal Agency for Cartography and Geodesy

Since 2015, when the International Association of Geodesy defined the International Height Reference System, SIRGAS has been focusing efforts on this topic. SIRGAS Working Group III “Vertical Datum” has the aim to establish, maintain and update a unified physical height system for the Americas and the Caribbean, following the recommendations of the International Association of Geodesy. For this reason, SIRGAS WG-III is in charge of this task and, since then, some activities related to the International Height Reference Frame (IHRF) have been carried out. This presentation has the purpose to show an overview of SIRGAS activities towards the IHRF, especially in Central and South America. National leveling networks based on geopotential numbers, international leveling crossings, and leveling connections with IHRF stations are an important task for the countries and part of the activities related to the IHRF. In the last years, SIRGAS has been promoting and supporting some capacities related to this topic. In terms of gravity data, the distribution and amount of data around the selected stations, as well as absolute gravity measurements in each place have been analyzed. To support the SIRGAS community, technical guides have been developed as well. These guides are related to strategies for the selection of the IHRF stations and gravity measurements around them, and also, to ensure the usability and long-term sustainability of the IHRF. Besides that, three activities are ongoing in the working group: the evaluation of the geoid models and GNSS/leveling stations available in Latin America using high-resolution gravity field models; the investigation related to the combination of satellite and ground-based data for the computation of geopotential values at the IHRF stations; and the first estimation of IHRF values using geoids and quasi geoids models available in the continent.

In summary, SIRGAS has been contributing to the establishment of the IHRF in the continent.

Key words IHRF, IHRS, SIRGAS, Vertical System

Category: Symposium 2a: Earth's Static Gravity Field = » 2a.2: Vertical Reference Systems: methodologies, realization, and new technologies

682

S2a-021

GEOPOTENTIAL NUMBER FOR THE IHRF ESTABLISHMENT IN BRAZIL

Valeria Silva¹、 Gabriel do Nascimento Guimarães²、 Denizar Blitzkow^{1,4}、 Ana Cristina Oliveira Cancoro de Matos⁴、 Iuri Bjorkstrom³

1. Universidade de São Paulo

2. Universidade Federal de Uberlândia

3. Geoverteentes

4. Centro de Estudos de Geodesia

The International Association of Geodesy (IAG) issued resolutions to modernize the gravimetric and altimetric references to establish a geodetic structure to monitor and to investigate Earth changes. In order to implement the International Height Reference Frame (IHRF) in Brazil, the Instituto Brasileiro de Geografia e Estatística (IBGE) selected 6 stations from the Brazilian Network for Continuous Monitoring of the GNSS System (RBMC), distributed along the country in the following cities: Brasilia (BRAZ); Fortaleza (CEFT); Cuiabá (CUIB); Imbituba (IMBT); Marabá (MABA) and Presidente Prudente (PPTTE). There is an effort to accomplish absolute gravity observations in these sites. At the moment BRAZ, CUIB and PPTTE have been already observed. The equipment used was A-10/032 gravimeter, from Instituto Geográfico e Cartográfico do Estado de São Paulo (IGC) with the efforts for data collection by Centro de Estudos de Geodesia (CENEGEO). RBMC is always at the top of a building or a pillar. The geodetic height of the stations was transferred from the top to the ground where absolute observations are carried out. The disturbing potential has been computed by Hotine integral using the numerical integration procedure. The potential $W(P)$ and the geopotential number $C(P)$ were computed for each station. The geopotential model XGM2019 ($n=m=250$) was adopted as a reference gravitational field. The $W(P)$ and $C(P)$ results were compared with the values obtained through the geoid heights of the official geoid models of Brazil: MAPGEO2015, MAPGEO2010 and MAPGEO2004.

Key words IGRS, IHRF, height.

Category: Symposium 2a: Earth's Static Gravity Field = » 2a.2: Vertical Reference Systems: methodologies, realization, and new technologies

693

S2a-022

An Investigation on the Geoid-Quasigeoid Separation with the Case Study in Colorado, U.S.

Mustafa Serkan Işık, Bihter Erol, Muhammed Raşit Çevikalp, Serdar Erol
Istanbul Technical University

The accurate determination of geoid-quasigeoid separation is of great importance for the realization of international height reference system (IHRs). The magnitude of the separation is highly dependent on the mass density variations and topographic roughness. In this study, we investigated the effects of different approaches for geoid-quasigeoid separation term on the accuracy of geoid modelling in Colorado, US where the topographic heights reach up to 4400 meters. Using geoid-quasigeoid separation terms modeled with the traditional approach (Heiskanen and Moritz, 1967), the so-called modern approach proposed by Flury and Rummel (2009) and a strict formulation by Sjöberg (2010), the quasi-geoid model, computed using the least squares modification of Stokes integral with additive corrections (LSMSA) method, is converted to the geoid model. The validation of the geoid models is carried out along the Geoid Slope Validation Survey 2017 (GSVS17) line where the GNSS/levelling measurements, astro-geodetic plump-line measurements and gravity measurements are available. The terrestrial and airborne gravity data used in this study is made available by National Geodetic Survey (NGS) for "The 1 cm Colorado geoid experiment" of IAG Joint Working Group (JWG) 2.2.2.

Heiskanen, W. A., Moritz, H., & Physical Geodesy, W. H. (1967). Freeman and Company. San Francisco.

Flury, J., & Rummel, R. (2009). On the geoid–quasigeoid separation in mountain areas. *Journal of Geodesy*, 83(9), 829-847.

Sjöberg, L. E. (2010). A strict formula for geoid-to-quasigeoid separation. *Journal of Geodesy*, 84(11), 699-702.

Key words Geoid, Quasigeoid, LSMSA, IHRs, GSVS17, Colorado

Category: Symposium 2a: Earth's Static Gravity Field = » 2a.2: Vertical Reference Systems: methodologies, realization, and new technologies

755

S2a-023

Status of the International Height Reference Frame (IHRF)

Laura Sanchez¹, on behalf of the IHRF Computation Team²

1. Deutsches Geodaetisches Forschungsinstitut, Technische Universitaet Muenchen
2. 30 geodesists working on the first solution for the International Height Reference Frame

The International Height Reference System (IHRF) was introduced by the International Association of Geodesy (IAG) in 2015 to provide a global standard for the precise determination of physical heights. The IHRF is based on the combination of a geometric component given by coordinates X referring to the International Terrestrial Reference Frame (ITRF), and a physical component given by the determination of potential values W_P at the positions P defined by the ITRF coordinates. The primary vertical coordinate is the geopotential number ($- \Delta W_P = C_P = W - W_P$), which may easily be converted to a metric physical height (orthometric, normal or dynamic height). The IHRF vertical datum is realised by the equipotential surface of the Earth's gravity field defined by the conventional value $W = 62\,636\,853.4 \text{ m}^2\text{s}^{-2}$. The realisation of the IHRF is the International Height Reference Frame (IHRF). The IHRF realises the IHRF in two ways: physically, by a set of globally distributed reference stations, and mathematically, by the precise determination of potential values at the reference stations. Thanks to a strong international cooperation hosted by the IAG, a first proposal for the IHRF reference network is completed. Present efforts concentrate on the determination of the potential values at the global IHRF reference stations. After evaluating different computation approaches, a standard procedure to determine potential values based on existing regional and global gravity field models was compiled and applied to release a first preliminary IHRF solution. This contribution summarises advances and present challenges in the establishment of the IHRF/IHRF.

Key words IHRF, IHRF, global unified height system, physical height standardisation

Symposium 2a: Earth's Static Gravity Field

S2a.3: Local and Regional Geoid and Gravity Modelling

Category: Symposium 2a: Earth's Static Gravity Field => 2a.3: Local and Regional Geoid and Gravity Modelling

88

S2a-024

Examining the optimal depth of the condensed topographic masses for precise geoid determination based on the Stokes-Helmert scheme – A case study in Colorado

Koji Matsuo

Geospatial Information Authority of Japan

In gravimetric geoid determination based on the Stokes-Helmert scheme, the topographic masses outside the geoid are condensed to an infinitely thin layer and stored on or below the geoid. Heck (2003) generalized the Stokes-Helmert scheme, and showed theoretically that the deeper the condensed topographic masses, the smoother the gravitational field becomes, while the larger the indirect effects becomes. The smooth gravity field alleviates the error in downward continuation process, while the large indirect effect leads to an unstable result of the geoid computation. Therefore, it is necessary to store the condensed topographic masses at the optimal depth for precise geoid computation. In this study, we examine the optimal depth of the condensed topographic masses for precise geoid determination based on the Stokes-Helmert scheme, as a case study in Colorado, USA. The basic methodology for geoid computation is the remove-compute-restore technique with the UNB Stokes-Helmert Scheme (Vaniček and Martinec, 1994; Huang and Véronneau, 2013). The evaluation of the computed geoid is performed by comparing with 222 GNSS/leveling geoid height data (Westrum et al., 2021). Consequently, the computed geoid heights are consistent with the GNSS/leveling geoid heights with a standard deviation of 2.38 cm when the condensation depth is set to 0 km, 2.20 cm when the depth is 25 km, 2.14 cm when the depth is 50 km, 2.37 cm when the depth is 75 km, and 3.16 cm when the depth is 100 km. In summary, the condensation depth of 50 km shows the best consistency with the GNSS/leveling geoid heights in the case of Colorado. In the most of the current studies using the Stokes-Helmert scheme, Helmert's second condensation method, which condense the topographic masses onto the geoid, is widely used. However, as demonstrated in this study, storing the condensed topographic masses below the geoid could produce more precise result of the geoid computation.

Key words Geoid, Gravity, Stokes-Helmert scheme

Category: Symposium 2a: Earth's Static Gravity Field => 2a.3: Local and Regional Geoid and Gravity Modelling

188

S2a-025

Local gravity field modelling in spatial domain using the FEM approach on the discretized Earth's surface: case study in Slovakia

Robert Cunderlik, Marek Macák, Zuzana Minarechová, Karol Mikula
Slovak University of Technology

We present detailed local gravity field modelling in Slovakia using the finite element method (FEM) and terrestrial gravimetric data. FEM as a numerical method is applied to solve the fixed gravimetric boundary-value problem in a spatial domain. The oblique derivative problem is treated directly at computational nodes that discretize the Earth's topography. The high horizontal resolution 100 x 100 m and non-uniform resolution in the radial direction results in a 3D unstructured mesh of finite elements with 5,287,500,000 unknowns. Large-scale parallel computations are performed on a parallel cluster using 1.5 TB of distributed memory. The obtained local quasigeoid model is tested at 396 GNSS-levelling benchmarks. The standard deviation of residuals 2.54 cm indicates its high precision. However, depicted residuals show their low-frequency character with amplitudes about ± 3 cm. As a by-product, the first and second derivatives of the obtained disturbing potential in the radial direction are also evaluated in several altitude levels as well as on the Earth's surface.

Key words local gravity field modelling, finite element method (FEM), fixed gravimetric BVP, oblique derivative problem, large-scale parallel computations

Category: Symposium 2a: Earth's Static Gravity Field =» 2a.3: Local and Regional Geoid and Gravity Modelling

271

S2a-026

Iterative refinement of regional marine geoid models by using sea surface height and dynamic topography datasets

Sander Varbla, Artu Ellmann
Tallinn University of Technology

Regional marine geoid models are needed for many research and engineering applications. The deficiencies in these models, however, may reach up to a few decimetres in the shorter wavelength spectrum due to gravity data void areas and/or inaccurate data. Accuracy of sea surface heights obtained through various data acquisition methods, such as satellite altimetry, thus often exceed that of marine geoid models. Furthermore, dynamic topography can also be accurately estimated when hydrodynamic model embedded data is used in conjunction with the tide gauge readings. This first means that the inaccuracies of hydrodynamic models are reduced by constraining these with the in-situ ground truth. Assuming that the tide gauges are connected to the geoid-based height system, then such an approach also eliminates hydrodynamic models' concealed biases with respect to the used vertical datum, which is an often overlooked deficiency of hydrodynamic models. By removing the estimated dynamic topography from the sea surface height measurements the geometric marine geoid heights are obtained. These heights hence represent the marine geoid independently from the usual gravity-based marine geoid models. This study therefore presents an iterative data assimilation approach for the refinement of gravity-based marine geoid models by using geometric marine geoid heights. Importantly, the approach also provides information on the accuracy of marine geoid models, which is often unknown as the conventional precise GNSS-levelling control points cannot be used for the validation purposes over the marine areas. It is concluded that the proposed iterative data assimilation approach can significantly improve the accuracy of marine geoid models, especially in the poor gravity data/gravity data void areas.

Key words Data assimilation; Dynamic topography; Geoid; Hydrogeodesy; Sea surface height

Category: Symposium 2a: Earth's Static Gravity Field => 2a.3: Local and Regional Geoid and Gravity Modelling
299
S2a-027

Gravimetric Geoid Modeling by Stokes and Second Helmert's Condensation Method in Yogyakarta, Indonesia

Brian Bramanto¹, Kosasih Prijatna¹, Muhammad Syahrullah Fathulhuda¹,
Arisauna Maulidyan Pahlevi²

1. Geodesy Research Group, Institut Teknologi Bandung
2. Geospatial Information Agency of Indonesia

Since the last decade, Indonesia has continuously improved the accuracy of the national geoid model by conducting rapid gravity acquisition using airborne and terrestrial-based gravimetry. As gravity data have been collected thoroughly in all regions, the time has come to carry out Indonesia's geoid modeling. We started our study by employing the Stokes and Second Helmert's condensation method to our terrestrial gravity data in Yogyakarta, Indonesia, with a test area of $1^\circ \times 1^\circ$. The computation was based on the commonly applied remove-compute-restore process. We used the satellite-only geopotential model to remove and restore the long-wavelength part of the gravity field within the modeling process. Numerical results show that few cm of geoid model accuracy was achieved when we compared it to the GNSS/leveling.

Key words Geoid modeling, Stokes, Helmert's second condensation

Category: Symposium 2a: Earth's Static Gravity Field => 2a.3: Local and Regional Geoid and Gravity Modelling

301

S2a-028

On the Optimum DHM Resolution for the Window Remove-Restore Technique: Case Study for Africa

Hussein Abd-Elmotaal¹, Norbert Kührtreiber²

1. Minia University, Faculty of Engineering, Civil Engineering Department, Egypt
(hussein.abdelmotaal@gmail.com)

2. Graz University of Technology, Institute of Geodesy, Graz, Austria
(norbert.kuehtreiber@tugraz.at)

In the framework of the activities of the IAG Sub-Commission on the gravity and geoid in Africa, it is needed to determine the optimum resolutions of the DHM used within the window remove-restore technique. The window remove-restore technique has been suggested by Abd-Elmotaal and Kührtreiber (2003) to get rid of the double consideration of the topographic-isostatic masses within the data window. Within the course of the window technique, one needs to compute the harmonic coefficients of the topographic-isostatic masses for the data window. The paper studies the effect of using DHM's with different resolutions on the computed harmonic coefficients of the topographic-isostatic masses as well as on the computed gravity anomalies and geoid. The needed precise formulas for computing the topographic-isostatic harmonic coefficients using the ellipsoid geometry are summarized with their associated approximations and expected relative errors. The African DHM of the finest resolution of 3" × 3" is used representing the topography of the test area. As this DHM covers a fairly large window ($-42^\circ \leq \varphi \leq 44^\circ$; $-22^\circ \leq \lambda \leq 62^\circ$), the needed CPU time to compute the topographic-isostatic harmonic coefficients plays an important role. The objective of the current study is to reduce the needed CPU time for such computations as much as possible without affecting the computed reduced anomalies and geoid. The results are presented and deeply discussed.

Key words window remove-restore technique, African geoid, DHM resolution

Category: Symposium 2a: Earth's Static Gravity Field => 2a.3: Local and Regional Geoid and Gravity Modelling
309
S2a-029

Preliminary results of the spatial distribution of tidal factors measured by recent continuous gravity stations

jin wei、Chongyang Shen、Mingzhang Hu、Ying Jiang、Ziwei Liu
Institute of Seismology, China Earthquake Administration

The spatial characteristics of tidal variation can be used to study the influence of earth shape, surface deformation, and the force characteristics of the different positions in the earth. Based on the data of 51 continuous relative gravimeters from 2015 to 2017, the spatial distribution of the main tide wave's tidal factor has been calculated by international standard tidal processing software and methods. To discussing the relationship between the spatial feature of tidal factor, the topography, and geophysics, the East-West and the North-South gravity tidal profile in China have been analyzed with Global Relief Model(ETOPO1) of 1'×1' and World Gravity Model(WGM2012) of 2'×2'. It is shown that (1) More than 90% of the Root Mean Square(RMS) of M_2 tidal factor is better than 0.001. The accuracy of CRG is comparable to that of the superconducting gravimeter(SG) in the 1980s-1990s. (2) The tidal factors of O_1 and K_1 waves in coastal stations are larger than those in inland; (3) The East-West M_2 wave tidal profile of Shiquanhe, Yushu, Songpan, Huangmei, Sheshan in Shanghai shows that, when the difference of elevation and Bouguer gravity anomaly(BGA) is more and 5km and $600 \times 10^{-5} \text{ms}^{-2}$, the difference of tidal factor in M_2 can be larger than 2%, moreover the tide factors are positively correlated with the elevation, especially, in Shiquanhe station, which is in the Tibet Plateau. However, the feature of positive correlation is not significant in the Songpan Ganzi plateau and Sichuan Basin, which should be related to the complex geomorphology and geological structure in the transitional region from East to West in China. (4) Comparing the elevation and the tidal factors in all gravity stations, it is found that the elevation of inland stations has more than 40% positive correlation with the tidal factor in M_2 and O_1 . The discrepancy of the spatial distribution in M_2 and O_1 which is comparable to that of coastline is related to the effect of crustal heterogeneity in China.

Key words The spatial characteristics of tidal factor; DDW; World Gravity Model in 2012; Gravity tidal profile in China; altitude effecton

Category: Symposium 2a: Earth's Static Gravity Field => 2a.3: Local and Regional Geoid and Gravity Modelling

317

S2a-030

Improved geoid models in Taiwan and its offshore islands

Huang Wenhsuan、Hwang Cheinway
National Chiao Tung University

The geoid is an important national infrastructure. Most countries invest many resources in order to create or high-quality geoid models. Taiwan has also invested resources to collect a large amount of high-resolution and high-accuracy gravity measurements for geoid modeling. Gravity data collected in airborne, shipborne and terrestrial surveys and those derived from satellite altimetry have been used to construct a high-resolution gravimetric-only geoid model in Taiwan. The gravimetric-only geoidal heights were combined with the ellipsoid heights at GPS/leveling benchmarks (called GPS/leveling data) to form a hybrid geoid model, which can be used to convert ellipsoid heights to orthometric heights in the TWVD2001 vertical datum. This conversion reduces the costs of projects that need orthometric height. This study extends the coverage of the current hybrid geoid model of Taiwan to its offshore island, including Kinmen, Matsu, Penghu, Liuqiu, Lyudao and Lanyu using new gravity data, new Digital terrain model (DTM) and GPS/leveling orthometric heights on these islands. The DTM is used to account for the short wavelength geoidal effects. The Helmert method condensation method is used to compute the gravimetric-only geoid. The GPS/leveling data are used to construct a hybrid geoid that covers the entire Taiwan and its offshore islands. Both the gravimetric-only and hybrid geoids are assessed by high-quality GPS/leveling data. Achieving cm-level geoid models in Taiwan and its offshore islands is a continuous effort here. The hybrid geoid can be used to determine the heights of offshore wind turbines and cross-sea bridges in the TWVD2001 vertical datum.

Key words geoid; gravity; Digital terrain model; TWVD2001; offshore island

Category: Symposium 2a: Earth's Static Gravity Field => 2a.3: Local and Regional Geoid and Gravity Modelling

349

S2a-031

Integrating NGS GRAV-D gravity observations into high-resolution global models

Philipp Zingerle¹, Xiaopeng Li², Martin Willberg¹, Roland Pail¹, Daniel R. Roman²

1. Technical University of Munich

2. NOAA National Geodetic Survey

Within this contribution we present a method that allows a smooth integration of in-situ ground gravity observations into high-resolution global models up to d/o 5400 (2' global resolution). The functionality is shown on the example of the airborne GRAV-D gravity dataset which is integrated into a global satellite-topographic spherical harmonic model. Conceptually, the method is divided into three steps: firstly, since the processing is based on residuals, a precursor model needs to be identified which is used for reducing the observations. In the actual example a combination between a satellite-only model (GOCO06s) and topographic model (EARTH2014) is chosen (named SATOP2) to ensure independency to the observations. Secondly, the previously reduced (GRAV-D) observations are gridded onto a regular geographic grid making use of the recently developed partition-enhanced least squares collocation approach (PE-LSC). PE-LSC allows an efficient collocation of virtually arbitrary large datasets using a partitioning technique that is optimized for computational performance and for minimizing fringe effects. As a third and last step, the obtained regular grid gets analyzed and combined with a satellite-only model (GOCO06s) on the normal equation level up to d/o 5400. This can be achieved efficiently by using a so-called kite-normal equation system which emerges when combining dense and block-diagonal normal equation systems (assuming equal accuracies for the ground gravity grid). The hereby obtained global gravity field model, named SGDT, is dominated by the satellite information in the lower frequencies (up to d/o 200), by GRAV-D in the mid-frequencies (d/o 200-2000) and by the topographic information in the high frequencies (above d/o 2000). The main purpose of the SGDT model is to validate the method itself and to allow a comparison of GRAV-D observations to pre-existing ground-gravity data by synthesizing SGDT to actual observation sites.

Key words Gravity, Global gravity field model, Local gravity field model, GRAV-D, Least squares collocation (LSC), Covariance function, Data combination

Category: Symposium 2a: Earth's Static Gravity Field => 2a.3: Local and Regional Geoid and Gravity Modelling
375
S2a-032

Gravimetric quasigeoid modelling by the GGI method in the Colorado mountains area

Marek Trojanowicz¹, Magdalena Owczarek-Wesołowska¹, Yan Ming Wang²,
Olgierd Jamroz¹

1. Wrocław University of Environmental and Life Sciences, Poland

2. National Geodetic Survey, USA

The study provides results of the development of the first gravimetric quasigeoid model based on the GGI method. The research was conducted on the basis of data used in the Colorado experiment, which included terrestrial and airborne gravity data, as well as the digital elevation model with a resolution of 3". In all calculations, the XGM2016 global geopotential model was adopted as the reference. Depending on the type of gravity data used, three versions of the quasigeoid models were determined: terrestrial-only (ζ_T), airborne-only (ζ_A), and combined (ζ_C), based on both terrestrial and airborne data. Calculations were preliminary provided for a large range of the assumed reference density model of topographic masses of 0-2670 kg/m³. The results of the calculations were compared to the mean quasigeoid heights (ζ_{mean}) obtained by the 13 approaches participating in the Colorado experiment and GNSS/levelling height anomalies ($\zeta_{\text{GNSS/lev}}$) at GSVS17 profile points. As a result of the research, an explicit dependency of the accuracy of the GGI model on the reference density model has been found. The version ζ_T turned out to be the most sensitive, giving the best results only in a very narrow range of densities of 2100-2200 kg/m³. The introduction of the airborne gravity data to the calculations had a positive effect on the final results. For two versions, i.e. ζ_A and ζ_C , the highest accuracies have been obtained for large ranges of reference densities (1500-2400 kg/m³ and 2000-2670 kg/m³ for ζ_A and the ζ_C version respectively). In addition, the version ζ_C turned out to be the most accurate. The obtained agreement of the particular versions of quasigeoid models with ζ_{mean} and $\zeta_{\text{GNSS/lev}}$ values, in terms of the standard deviation of their differences along the GSVS17 profile, were at the level of ± 0.9 cm, ± 1.5 cm and ± 1.7 cm for ζ_{mean} values, and ± 2.6 cm, ± 3.2 cm and ± 2.9 cm for $\zeta_{\text{GNSS/lev}}$ values (the stated standard deviations refer to the version: ζ_C , ζ_T and ζ_A respectively).

Key words Regional quasigeoid modelling, Terrestrial and airborne gravity data combination

Category: Symposium 2a: Earth's Static Gravity Field => 2a.3: Local and Regional Geoid and Gravity Modelling

404

S2a-033

Regularization parameter determination in case of combining different types of gravity data for regional gravity field refinement

Qing Liu, Michael Schmidt

Deutsches Geodätisches Forschungsinstitut der Technischen Universität München
(DGFI-TUM)

Low-resolution global satellite gravity observations can be combined with high-resolution regional gravity data from airborne, shipborne, or terrestrial measurements within a parameter estimation process for regional gravity refinement. In this process, regularization is in most cases inevitable, and choosing an appropriate value for the regularization parameter is a crucial issue. In this study, we investigate two frequently used procedures for determining the regularization parameter, namely the L-curve method and the variance component estimation (VCE), and discuss their drawbacks when different types of gravity data are to be combined.

Furthermore, to overcome the drawbacks, two 'combined approaches' are proposed, which combine the L-curve method and VCE. The first approach (VCE-Lc) starts with the calculation of the relative weights between the observation techniques by means of VCE. Based on these weights, the L-curve method is applied to determine the regularization parameter. In the second approach (Lc-VCE), the L-curve method determines first the regularization parameter, and it is set to be fixed during the calculation of the relative weights between the observation techniques by VCE. Numerical investigations show that these two proposed approaches deliver lower RMS errors with respect to validation data than the L-curve method and VCE do in different study cases.

Key words combination of heterogeneous observations; regularization parameter; the L-curve method; VCE

Category: Symposium 2a: Earth's Static Gravity Field => 2a.3: Local and Regional Geoid and Gravity Modelling
409
S2a-034

Application of 3-dimensional least-squares collocation for free-air vertical gravity gradient modelling

Yunus Aytaç Akdoğan¹, Gonca Okay Ahi², Hasan Yıldız¹

1. General Directorate of Mapping

2. Hacettepe University

Free-air vertical gravity gradients (VGG) are crucial both in geodesy and geophysics. Generally theoretical VGG (3086 Eötvös) is used in these studies due to the lack of measured VGG data which is quite challenging. In this study, the free-air VGG are modelled by 3-dimensional least-squares collocation using a high-precision satellite-based global geopotential model, point-wise terrestrial gravity measurements and a high-resolution digital elevation model. The study area is chosen in western Turkey where homogeneously scattered data sets of VGG measurements are previously collected under the frame of “Turkish Height System Modernization and Gravity Recovery Project (2015-2020)”. The available free-air VGG measurements are performed using a Scintrex CG5 instrument and a three-level platform and vary between 2306 and 4283 Eötvös. Differences between the measured and the theoretical VGG range from -25% to +39%, point out the necessity to consider the measured or the modelled VGG instead of the theoretical VGG values. The modelled free-air VGG in this study are validated using the available measurements at 159 benchmarks suggesting a very good agreement of about 190 Eötvös between the modelled and the measured VGG values ever obtained. The modelled free-air VGG may be used not only for the gravity reductions in geodesy but also for geophysical investigations as free-air VGG are known to be sensitive to density contrasts in the upper layers of the Earth.

Key words Free Air Vertical Gravity Gradient, Remove-Compute-Restore Method, Least-Squares Collocation.

Category: Symposium 2a: Earth's Static Gravity Field => 2a.3: Local and Regional Geoid and Gravity Modelling

447

S2a-035

On the computation of the complete geoid-quasigeoid separation term for the experiential geoid 2020

Yan Ming Wang¹、 Marc Veronneau²、 Jianliang Huang²、 Kevin Ahlgren¹、 Xiaopeng Li¹、 Jordan Krcmaric¹、 Ryan Hardy¹、 David Avalos³

1. National Geodetic Survey 1315 East West HYW Silver Spring MD 20910, USA
2. Canadian Geodetic Survey, Surveyor General Branch, Natural Resources Canada, 615 Booth Street, Ottawa, ON K1A 0E9, Canada
3. National Institute of Statistics and Geography of Mexico

The simple geoid-quasigeoid separation (GQS) term uses the Bouguer anomalies to approximate the difference between the mean gravity and normal gravity along the plumb line. More accurate formulas for computing the GQS term have been developed and called the complete GQS term hereafter. The computation starts in the area of the Colorado geoid computation experiment to show the magnitude of the improvement. The study shows that the largest error comes from the topographic potential correction, which reaches a maximum of 19.0 cm with a standard deviation of 1.8 cm over the area of 730 km by 550 km in Colorado. The gravity gradient correction is small: the RMS value is merely 0.3 cm, but varies between -2.5 to 2.0 cm in Colorado. In addition, the difference between the Bouguer gravity anomaly and disturbance causes about a cm bias and maximum value of 2 cm. The total correction ranges from -13.5 to 18.0 cm, with a root mean square of 1.9 cm for the region. The correction is significant for today's cm-geoid accuracy requirement. The complete GQS term is then computed for the experimental geoid xGEOID2020, which covers a region border by latitude 0° to 85° north, longitude 180° to 350° east.

Key words Geoid-quasigeoid separation, Bouguer disturbance, Bouguer anomaly, height anomaly and geoid computation

Category: Symposium 2a: Earth's Static Gravity Field => 2a.3: Local and Regional Geoid and Gravity Modelling

508

S2a-036

Modernization of the Danish Gravity Network in Preparation of the New 5 mm Danish Geoid

Hergeir Teitsson¹, René Forsberg¹, Gabriel Strykowski¹, Tim Enzlberger Jensen¹, Adolffientje Kasenda Olesen¹, Kristian Keller²

1. National Space Institute, Technical University of Denmark

2. The Danish Agency for Data Supply and Efficiency

In preparation for the upcoming Danish 5 mm geoid, an on-going nationwide survey has been conducted since 2018, consisting both of re-observation of older gravity data with modern instruments, as well as new supplementary airborne, marine and land surveys. The purpose is to validate the quality of the old terrestrial gravity network in the Danish gravity database, which consists of measurements dating back to the 1940's with long, and partly unknown, correction history. The representative data subset from the existing database is re-measured with the state-of-the-art relative gravimeters and RTK GNSS equipment in the different regions of Denmark. The results show that the accuracy of the older gravity data is generally satisfactory for precise geoid determination. Especially, when correctly transformed from the original national geodetic datum (map projection) to a modern datum.

The presentation will focus on the method of assessment based on comparing the Bouguer gravity anomaly of the old gravity data, to the re-measured gravity values at the original gravity point locations (where documentation is available), to identify systematic regional inconsistencies. The survey shows smaller and random inconsistencies across Denmark, with some smaller islands indicating significant biases. The overall results make good and clear conditions for a modernisation of the Danish relative gravity network, as well as for the ongoing development of a new national 5 mm geoid model.

Key words Quality-control, gravity-network, modernization, 5 mm geoid

Category: Symposium 2a: Earth's Static Gravity Field => 2a.3: Local and Regional Geoid and Gravity Modelling

554

S2a-037

A new model of the quasigeoid for the Baltic Sea area

Adam Łyszkowicz¹、 Adam Łyszkowicz²、 Janusz Zieliński³、 Monika Biryło⁴

1. Military University of Aviation

2. Space Research Centre PAS

3. Space Research Centre PAS

4. University of Warmia and Mazury in Olsztym

The Space Research Centre in Warsaw participates in the ESA program „ Geodetic SAR for Height System Unification and Sea Level Research”. For observing the absolute sea level and enabling unification of height systems physical heights of the tide gauge stations referring to a common equipotential surface (geoid) are needed. This paper describes the new geoid model determination for the area of the Baltic sea.

The quasigeoid calculation was carried out according to the Helmert method, in which the topography is condensed on a layer lying on the geoid. Aerial gravimetric anomalies from the Baltic area and terrestrial anomalies from Sweden, Finland, Denmark, and Poland were used.

The necessary terrain corrections have been computed from a digital terrain model based on the SRTM30. To calculate the long-wavelength part of quasigeoid the geopotential models GOCE-DIR6, GOCO06s and EIGEN-6C4 were used. All calculations were done in a zero-tide system. The new quasigeoid models are obtained on a regular 1.5' ×3.0' grid in the GRS80 reference system, covering the Baltic Sea and the surrounding area $52^{\circ} < j < 68^{\circ}$ and $11^{\circ} < l < 30^{\circ}$.

These gravimetric quasigeoids were compared to quasigeoid undulations derived at 29 GPS/leveling points of the ASG-EUPOS permanent network, located in the study area. Our calculations show that the accuracy of the calculated quasigeoid is almost the same in all three cases and is ± 0.03 meters. Finally, quasigeoid anomalies were interpolated at the Polish tide gauge stations. The new gravimetric geoid solution could be very important for height system unification, for geophysical purposes as well as for engineering purposes.

Key words gravity field, Stokes integral, quasigeoid,

Category: Symposium 2a: Earth's Static Gravity Field => 2a.3: Local and Regional Geoid and Gravity Modelling
565
S2a-038

Seamless Processing for Shipborne Gravity Data

Baogui Ke、Jinzhong Mi、Chuanyin Zhang、Yamin Dang、Hanjiang Wen
Chinese academy of surveying and mapping

The data of shipborne measurement is of great significance for the exploration of Marine geophysical resources and navigation of underwater weapons, but the data collection is a hard work that needs a lot of manpower and material resources, so it is very necessary to comprehensively utilize the existing gravity data.

The measurement data of the same department are consistent in terms of measuring equipment, measuring method and operating personnel, and the technical indexes such as data accuracy and reliability are consistent. But different department in the same test area, there will be a certain difference. In the course of the study, it is found that the discrepancy values of the measured data of different units at the intersection of the measured lines show systematic deviation, that is, the existence of gaps. With the accumulation of shipborne data, there are many situations such as overlapping of survey line data space coverage, crossing point of survey line, no crossing point of survey line in adjacent areas, etc. How to solve the inconsistency between different units of data has important engineering value.

In view of the data of adjacent survey areas without the intersection points of survey lines, the virtual survey line method is proposed for seamless Mosaic processing. The main steps include : (1) Set 1~3 virtual survey lines in the area connected by two survey areas, and give their longitude and latitude; (2) Gravity anomaly data of two adjacent regions were used to interpolate the gravity anomaly on the virtual survey line. (3) Compare the differences of gravity anomalies on the virtual survey line at the same point, and conduct statistics to determine the mean value of the differences. The average value is the gap value of data in adjacent areas; (4) Determine the gap value of each adjacent test area in a circular manner according to the above steps; (5) Select the data of a test area as reference, and calculate all gravity data according to the value of each gap; (6) Based on the reduced gravity anomaly data, the gravity anomaly grid is established. The experimental results show that this method can solve the consistency problem of data from different sources well and realize the seamless connection of data.

Key words Shipborne Gravity Data; Seamless Processing ; Marine ; systematic deviation

Category: Symposium 2a: Earth's Static Gravity Field => 2a.3: Local and Regional Geoid and Gravity Modelling
607
S2a-039

A 3-Dimensional Realization of Molodensky Heights

Robert Kingdon, Ismael Foroughi, Marcelo Santos
University of New Brunswick

The height of a point, P , in the Molodensky system, is the length along the normal plumbline from an ellipsoid to a point, P' . P' is above or below P and such that the normal potential at P' is equal to the gravity potential at P . This system has traditionally been realized either: (1) by determination of the geopotential number at levelling benchmarks in an area, and division by the mean normal gravity along the normal plumbline extending from the ellipsoid to P' ; or (2) by determination of the height anomalies at the surface of topography, which can then be subtracted from observed geodetic heights to determine Molodensky heights. Both methods are imperfect. In the case of method (1), as with all levelling-based realizations, users can only access the system at discrete levelling benchmarks. These must be maintained and may move over time. Any new height measurements must be connected to the benchmarks by time-consuming levelling observations, in a way inconsistent with modern GNSS surveying techniques. Method (2), often conceived as the production of a "quasigeoid", poses well-documented theoretical and computational challenges. Furthermore, the height anomalies comprising the quasigeoid are only valid for points at the topographical surface, and will be incorrect for any point not on the topographical surface, e.g. towers or mine shafts. These errors reach decimetres in magnitude. We propose that Molodensky heights can only be realized using height anomalies in a 3-dimensional space, instead of only at the topographical surface. We suggest a realization using height anomalies on the equipotential surface provided by a geoid model, that may be rapidly continued to any point outside of the geoid using Poisson upward continuation in a computation space where the disturbing potential is harmonic. In this method, the geodetic height of any point in space may be transformed accurately into either its normal or orthometric height.

Key words quasigeoid, geoid, Molodensky heights, height anomaly

Category: Symposium 2a: Earth's Static Gravity Field =» 2a.3: Local and Regional Geoid and Gravity Modelling

623

S2a-040

The improvement of global earth's gravity field model with airborne gravity data: case study in Maowusu

Wei Liang、Xinyu Xu、Jiancheng Li
Wuhan University

In this paper, we will present a method to improve global Earth's gravity field models in regional areas with airborne gravity data. The method is based on downward continuation with inverse Poisson's integral and block-diagonal least squares method. In this method, airborne gravity data is at first downward continued to the respective regional area on a sphere, then gravity data derived from a reference global model is used to fill the rest of the sphere. At last a new model is computed with block-diagonal least squares method using the global gravity data on the sphere. This method is also capable of improving global model with regional terrestrial gravity data. Four regionally improved gravity field models are computed with regional airborne gravity data and regional terrestrial gravity data respectively. The models are validated using regional GNSS/Leveling data in Maowusu and we will present the detailed analysis of the validation results.

Key words airborne gravity; regionally improvement; downward continuation; global gravity field model

Category: Symposium 2a: Earth's Static Gravity Field => 2a.3: Local and Regional Geoid and Gravity Modelling
687
S2a-041

Assessments on Terrestrial Gravity Data Grid Densification and Its Effects on Local Geoid Modeling Accuracy

Muhammed Raşit Çevikalp, Serdar Erol, Bihter Erol
İstanbul Technical University

In gravimetric geoid modeling, various factors have role on the accuracy of the calculated model. For the computational efficiency and optimal use of data processors, the gravity data are evaluated in grid form by majority of the geoid model computation algorithms. In this manner preparation of the data grids using appropriate type of gravity anomalies effects the performance of the modeling. In this manner, this study investigates different gravity reduction approaches and gridding through numerical experiments carried out with Colorado test dataset of the U.S. In the tests, the terrestrial gravity observations in a 550 km × 730 km area were reduced to the complete Bouguer gravity anomalies with conventional formula in planar approximation as well as the spherical approximation with using the topographic gravitational corrections from the SRTM2gravity high-resolution global model, respectively. The obtained complete Bouguer gravity anomaly datasets were gridded in 3', 1' and 30" resolutions. The restored free air gravity anomalies were employed in 'terrestrial-only' geoid model determination using the least squares modification of Stokes integral with additive corrections (LSMSA) method. The performances of the calculated geoid models were assessed and compared using the geoid undulation differences at the given GPS/leveling validation benchmarks in the area. Over the differences between the geoid model solutions, the contribution of the terrestrial gravity data reduced and gridded with different approaches on the local geoid model accuracy was clarified. The datasets which were used in this experimental study was provided by the National Geospatial Intelligence Agency (NGA) and National Geodetic Survey (NGS) for "1 cm Colorado Geoid Experiment" of IAG JWG 2.2.2.

Key words Terrestrial gravity data, gridding, gravity densification, local geoid accuracy, LSMSA, Colorado.

Category: Symposium 2a: Earth's Static Gravity Field => 2a.3: Local and Regional Geoid and Gravity Modelling

765

S2a-042

Gravimetric Geoid Modelling Using the Least Squares Modification of Hotine Integral in Turkey

Mustafa Serkan Işık, Bihter Erol, Fatıma Feyza Sakil, Muhammed Raşit Çevikalp, Serdar Erol

Istanbul Technical University, Department of Geomatics Engineering, 34469 Maslak, Istanbul, Turkey

With the dominance in the use of Stokes equation in gravimetric geoid modelling, the use of gravity anomaly is more common than gravity disturbance. The fact that the height information of most of the archived gravity measurements comes from the traditional levelling leads to the computation of gravity anomalies. The use of the GNSS technique together with the gravity measurements provides the opportunity for direct computation of the gravity disturbances. Hotine Integral enables the calculation of the gravimetric geoid model using gravity disturbances instead of gravity anomalies. Besides, the integral formula needs to be modified in order to minimize the expected mean square error of the geoid/quasi-geoid estimator by handling the absence of gravity measurements outside the geoid modeling area, and considering the errors introduced by the gravity measurements and the global geopotential model which is used as a reference for the long-wavelength gravity signal. In this study, we used the least squares modification of Hotine integral with additive corrections (LSMHA) method to model the gravimetric geoid in Turkey. Since the gravity anomaly data set is already gridded and raw gravity measurements are not available for this research, the gravity disturbance grid is computed from the gravity anomaly grid (1 ϕ spatial resolution) by using an existing geoid/quasi-geoid model. The best-fitting Hotine geoid is tested at 100 GNSS/leveling benchmarks and compared with the geoid model computed with the least squares modification of Stokes integral with Additive Corrections (LSMSA).

Key words Geoid modelling, Gravity disturbance, Hotine integral, LSMHA, LSMSA, Turkey

Category: Symposium 2a: Earth's Static Gravity Field => 2a.3: Local and Regional Geoid and Gravity Modelling

790

S2a-043

An improved regional gravity field solution for Antarctica for geodetic and geophysical applications

Mirko Scheinert¹, Philipp Zingerle², Theresa Schaller¹, Roland Pail², Martin Willberg²

1. Technische Universität Dresden, Germany

2. Technische Universität München, Germany

In the frame of the IAG Subcommittee 2.4f “Gravity and Geoid in Antarctica” (AntGG) a first Antarctic-wide grid of ground-based gravity anomalies was released in 2016 (Scheinert et al. 2016). At that time the grid space was 10 km, and the coverage reached about 73% of the Antarctic continent. Since then new data has been made available, mainly collected by means of airborne gravimetry, especially over the polar data gap originating from GOCE satellite gravimetry. Thus, to come up with an updated and enhanced regional gravity field solution we aim to improve several aspects in comparison to the AntGG 2016 solution: The grid spacing will be enhanced to 5 km. Instead of providing gravity anomalies only for parts of Antarctica, now the entire continent will be covered. In addition to the gravity anomaly further functionals of the disturbing potential will be provided (such as height anomaly and gravity disturbance).

The methodology applied in the analysis is based on the remove-compute-restore technique. Here we utilize the model SATOP1 (Zingerle et al. 2019) which is based on the global satellite-only model GOCO05s and the high-resolution topographic model EARTH2014. For the compute step the recently developed partition-enhanced least-squares collocation (PE-LSC) has been used (Zingerle et al. 2021). This method allows to treat all available data in one single computation step in an efficient and fast way. Thus, it becomes feasible to iterate the computations within short time once any input data or parameters are changed, and to easily predict the desirable functionals also in regions void of terrestrial measurements as well as at any height level.

We will discuss the results and give an outlook on the data products which shall be finally provided to present the new regional gravity field solution for Antarctica. Furthermore, implications for further applications will be discussed e.g. with respect to geophysical modelling of the Earth's interior.

Key words regional gravity field, Antarctica, terrestrial and airborne gravity surveys, least-squares collocation

Category: Symposium 2a: Earth's Static Gravity Field => 2a.3: Local and Regional Geoid and Gravity Modelling
852
S2a-044

Indian gravimetric geoid model: IndGG-CUT2021

Ropesh Goyal^{1,2}, Will Featherstone^{2,1}, Sten Claessens², Onkar Dikshit¹,
Nagarajan Balasubramanian¹

1. Department of Civil Engineering, Indian Institute of Technology Kanpur, Kanpur 208016, India
2. School of Earth and Planetary Sciences, Curtin University of Technology, GPO Box U1987, Perth WA 6845, Australia

In this study, we present the first nationwide results of Indian gravimetric geoid and quasigeoid models computed using the freely or commercially available gravity data and digital elevation models. The computations are done primarily based on Curtin University's approach with some minor modifications. We have computed both geoid and quasigeoid models to analyse their representativeness of the Indian normal-orthometric heights from differential levelling. Terrain corrections were found to reach a maximum of 187 mGal, Faye anomalies 617 mGal, and the geoid-quasigeoid separation 4.002 m, while the corresponding minimum values are 0 mGal, -300 mGal and -0.733 m, respectively. A hybrid geoid model for India has been computed with a standard deviation of ± 14.4 cm.

Key words Geoid, quasigeoid, India

Category: Symposium 2a: Earth's Static Gravity Field => 2a.3: Local and Regional Geoid and Gravity Modelling

860

S2a-045

Filtering and downward continuation of GOCE SGG data for regional geoid improvement

Dimitrios Natsiopoulos, Elisavet Mamagiannou, Eleftherios Pitenis, Georgios Vergos, Ilias Tziavos
Aristotle University of Thessaloniki

Within the GeoGravGOCE project, funded by the Hellenic Foundation for Research and Innovation, the overall goal is to utilize the original GOCE SGG data and combine them with local free-air gravity anomalies towards geoid determination. The main aim is to assess the improvement that SGG data can offer to local and regional geoid modeling, taking full advantage of all GOCE observations. In all related work, the combination with local data or the utilization of SGG grids is done either at the original satellite altitude or at a mean orbit (MO) through dedicated SGG grids. Thus, the novel approach within GeoGravGOCE refers to the downward continuation of GOCE observables to the surface of the Earth and the combination with local data. The original GOCE gravity gradients are filtered at the original altitude and then combined with a normal gravity field in order to form filtered second order derivatives of the disturbing potential. Hence, the determined observations are referred to a spectrally enhanced version of TIM-R6, so that the medium and long wavelengths of the spectrum are removed. After transformation from the Gradiometric Reference Frame (GRF) to the Earth Fixed Reference Frame (EFRF), via the provided kinematic orbits and quaternions, GOCE data are referred to a MO using Input Output System Theory (IOST). This is due to the fact that upward/downward continuation is considered as a convolution of the data and the Poisson kernel at a reference surface, similar to the Stokes convolution integral. Finally, after having determined the GOCE filtered SGG data to a MO, their downward continuation to the Earth's surface is carried out employing an iterative Monte Carlo simulated annealing method. In this process, XGM2019 and EGM2008 are used as ground truth terrestrial observations, so that through their power spectral density functions the upward/downward continuation can be carried out. Some first results from the entire processing chain are presented along with a first evaluation of the downward continued GOCE observations and their impact on geoid modeling. The validation is performed against a set of collocated GNSS/Leveling data over mainland Greece aiming to identify the impact that GOCE can have at various areas, given also the complexity of the topography.

Key words GOCE gradients, geoid modeling, IOST, downward continuation,

Category: Symposium 2a: Earth's Static Gravity Field => 2a.3: Local and Regional Geoid and Gravity Modelling
869
S2a-046

An oral rebuttal to “the shape of the quasigeoid”

Marcelo Santos¹、 Robert Kingdon¹、 Petr Vaníček¹、 Zdeněk Martinec²、 Ismael Foroughi¹

1. University of New Brunswick

2. Dublin Institute of Advanced Studies

In this oral presentation we will discuss the aftermath from an unfortunate affair that followed the IX Hotine – Marussi Symposium on Mathematical Geodesy, staged in Rome from June 18 to 22, 2018, involving the publication of a paper in the IAG Symposia Series. It is customary for either orals or posters presented in a conference to be part of the proceedings of that conference, as it is the meaning of conference proceedings: the published record of what happens during a conference. An oral by the first 3 authors, entitled “The shape of the quasigeoid”, was properly presented and discussed during the Hotine – Marussi Symposium but not submitted for publication in the proceedings. To our surprise, the proceedings possesses a paper (which was not part of the Hotine – Marussi Symposium), authored by a Mr. Popadyev, written with the aim of “analyzing the arguments in [our presentation]” and an implicit aim to create an impression that our thesis is suspect (viz the sub-title of his paper Once More on the Shape of Quasigeoid). Therefore, an unsuspecting reader might end up believing that Popadyev’s paper is a definitive and correct argument against “our questionable thesis presented at the Symposium”. In this oral presentation, we address some of Popadyev’s arguments and contextualize his paper as a contribution to the ongoing discussion between geodesists who believe in the validity of Molodensky height system and those who, like ourselves, believe in the superiority of the classical height system. We also clarify several apparent misconceptions contained in Popadyev’s paper. Our presentation ends highlighting what we consider a very important and enlightening statement by Popadyev: “A quasigeoid is not a vertical reference surface”. That is precisely what we have tried to prove.

Key words Molodensky height system, classical height system, quasigeoid

Symposium 2a: Earth's Static Gravity Field

S2a.4: Global Gravity Field Modelling

Category: Symposium 2a: Earth's Static Gravity Field => 2a.4: Global Gravity Field Modelling

129

S2a-047

Reconstruction of mathematical foundations for satellite gravimetry from tracking: solutions to problems incorrectly solved for 100 years

Peiliang Xu
Kyoto University

Earth's gravitational products have been routinely made from satellite tracking measurements of CHAMP and/or GRACE types by major institutions worldwide, for example, NASA Goddard Space Flight Center and German Research Center for Geosciences (GFZ). These global gravitational models have found widest possible multidisciplinary applications in Earth Sciences. The mathematical foundation used by these major institutions worldwide is essentially implemented by solving the differential equations of the partial derivatives of the orbit of a satellite with respect to the unknown harmonic coefficients under the conditions of zero initial values, which has been best known as the dynamical numerical integration method in geodesy and aerospace engineering. I prove that the method, originating from Gronwall on Ann Math almost 100 years ago and currently implemented and used in statistics, chemical engineering and satellite gravimetry and many other areas of science and engineering, is mathematically erroneous and physically not permitted.

I present three different methods to derive local solutions to the Newton's nonlinear differential equations of motion of satellites, given unknown initial values and unknown force parameters. They are mathematically correct and can be used to estimate unknown differential equation parameters, with applications in gravitational modelling from satellite tracking measurements. These solution methods are generally applicable to any differential equations with unknown parameters;

I develop the measurement-based perturbation theory and construct global uniformly convergent solutions to the Newton's nonlinear differential equations of motion of satellites, given unknown initial values and unknown force parameters. From the physical point of view, the global uniform convergence of the solutions implies that they are able to exploit the complete/full advantages of unprecedented high accuracy and continuity of satellite orbits of arbitrary length and thus will automatically guarantee theoretically the production of a high-precision high-resolution global standard gravitational models from satellite tracking measurements of any types; and finally,

I develop an alternative method by reformulating the problem of estimating unknown differential equation parameters, or the mixed initial-

boundary value problem of satellite gravimetry with unknown initial values and unknown force parameters as a standard condition adjustment model with unknown parameters.

Xu P (2018) Measurement-based perturbation theory and differential equation parameter estimation with applications to satellite gravimetry. *Commun Nonlinear Sci Numer Simulat*, 59, 515-543. DOI 10.1016/j.cnsns.2017.11.021

Xu P (2008) Position and velocity perturbations for the determination of geopotential from space geodetic measurements. *Celest Mech Dyn Astr*, 100, 231–249.

Xu P (2009) Zero initial partial derivatives of satellite orbits with respect to force parameters violate the physics of motion of celestial bodies. *Sci China Ser D*, 52, 562–566.

Xu P (2012) Mathematical challenges arising from earth-space observation: mixed integer linear models, measurement-based perturbation theory and data assimilation for ill-posed problems. Invited talk, joint mathematical meeting of American mathematical society, Boston, January 4–7.

Key words satellite gravimetry, mathematical foundation, measurement-based perturbation, perturbation, numerical integration method

Category: Symposium 2a: Earth's Static Gravity Field => 2a.4: Global Gravity Field Modelling

345

S2a-048

XGM202x: The impact of extending the dense modelling to d/o 1440

Philipp Zingerle, Roland Pail, Thomas Gruber
Technical University of Munich

Due to the improvements made in the scope of high-performance computing over the last decade, solving dense normal equation systems of global gravity field models beyond d/o 720 became feasible. Up until now, all XGM models published are limited to d/o 720 regarding the use of fully populated normal equations. Overcoming this limit poses one of the main subjects for future XGM models. Doubling the max. d/o from 720 to 1440 means to increase the computational complexity by a factor of 64 (~192 cpu-h) and the memory requirements by a factor of 16 (~32 TB). Such a computation is demanding even for modern high-performance computing systems. However, by now, it is not yet proven whether extending the dense modelling alters/improves the final solution at all. Hence, within this contribution, we will tackle this question by setting up a test-case scenario which targets to be as close as possible to the original XGM2019 model. Only difference shall be the increased spatial resolution of the weighed input grid to 7.5' (instead of 15') and the increase of the max. d/o to 1440 (i.e., the Nyquist frequency for 7.5'). The result is then compared to the original XGM2019 model. From this comparison conclusions are drawn whether and in which cases an extension of the maximum densely modelled d/o can impact or improve the obtained solution. Computations are carried out on the SuperMUC-NG HPC system provided by the Leibniz Supercomputing Centre (LRZ).

Key words Gravity, Combined gravity field model, Spherical harmonics, Full normal equation systems, High-performance computing

Category: Symposium 2a: Earth's Static Gravity Field => 2a.4: Global Gravity Field Modelling

420

S2a-049

Analysis of the potential contribution of the Tianwen-1 extended mission to the solution of Mars' low-order gravity field

Shanhong LIU、Jianguo YAN
Wuhan University

Tianwen-1 is China's first independent interplanetary exploration, aims to complete orbiting, landing, and roving in one mission, of which orbiting phase was designed as the polar orbit. This paper analyzed the possibility of improving the existing Mars gravity field model through the tracking data from Tianwen-1 extension mission. We simulated two type orbits, the polar orbit and the near equatorial large eccentricity orbit and recovered six gravity solutions when considering different error sources. By analyzing and evaluating the power spectrum of these gravity model, a month's tracking data from the polar orbit or the combined polar and near equatorial orbit can be used to reconstruct the Mars gravity field model with orders and degrees of 42 under the 0.1 mm/s measurement noise properly. After considering the influence of comprehensive error, it is found that the accuracy of gravity field solution of the two types of orbits is similar, and the orbit with large eccentricity near the equator has a slightly stronger constraint on more than 35 order and degree coefficients. This experiment provides a scientific reference for the future orbit selection of Tianwen-1 extended mission.

Key words Mars gravity field model; GGM-3; power spectrum; Tianwen-1

Category: Symposium 2a: Earth's Static Gravity Field => 2a.4: Global Gravity Field Modelling
470
S2a-050

DTU21 Global high resolution gravity field - first evaluation

Ole Baltazar Andersen¹, Adil Abulaitijiang¹, Shengjuin Zhang^{2,3}

1. DTU Space

2. Northeast University of China

3.

A newest DTU global high resolution global marine free air gravity field called DTU21 is presented in this presentation and the first evaluation against marine and airborne gravity performed.

A total of 14 years from geodetic missions including (7 years of Cryosat-2 (369 days repeat mission) as well as 3 years of Jason-1+2 end-of-life missions and 4 year of SARA/AltiKa drifting geodetic mission). Older geodetic missions (ERS-1 and GEOSAT) are now nearly retired.

All Geodetic missions have been fully retracked using the 2-pass retracker developed by Sandwell et al., (2013) to increase the range precision. Subsequently we derive 2-Hz altimetric observations from the 20/40 Hz retracked data using the Parks McClellan filter to avoid spectral leakage degrading the 10-40 km wavelength which is an effect of the box filter normally used to compute 1 Hz data.

In the Arctic Ocean we will present results from several new developments in high resolution gravity field modelling. One is a new dual-pass retracking of SARAL/AltiKa together with an new physical retracking system for Cryosat-2 derived at ESA called SAMOSA+. This was retracked using the ESA GPOD service.

A new medium wavelength correction based on altimetry and GOCE have been introduced to deal with problems in the older remove restore technology based on EGM2008. This is particularly important for Cryosat-2 due to its ability of provide new accurate sea surface height information for gravity field determination all the way up to 88N where no altimeters have measured before.

Key words altimetry, marine gravity

Category: Symposium 2a: Earth's Static Gravity Field => 2a.4: Global Gravity Field Modelling
593
S2a-051

Numerical Algorithm and Realization of Ellipsoidal Harmonic Expansion of the Earth Gravity Field

Cong Liu、Zhengtao Wang、Yang Xiao、Yonggang Zhang
Wuhan University

The degree of the international mainstream spherical harmonic model is now higher than 2160, we can predict that in the future gravity field models will reach a higher degree. However, spherical harmonic expansion faces divergence problem, which has little influence on 2160 degree models. The degree of gravity field model may be 10800 or higher in the future, the divergence problem needs to be paid attention, so the ellipsoidal harmonic expansion is studied. The main work and research results are as follows: 1) The convergence characteristics of spherical harmonic model and ellipsoidal harmonic model are compared on the reference ellipsoid. The results show that high-degree spherical harmonic model has divergence problem. Its convergence is related to latitude. And there is no problem in the convergence of high-degree ellipsoidal harmonic model; 2) Ellipsoidal harmonic analysis is carried out with the help of SHTOOLS package. The accuracy of the two analysis methods of SHTOOLS is compared. The results show that the accuracy of Gauss-Legendre quadrature is better than Driscoll/Healy quadrature. 3) A set of Fortran program is compiled to realize ellipsoidal harmonic synthesis. Based on OpenMP parallel technology and FFT technology, the program realizes the fast calculation of regular grid and scattered point; 4) The accuracy of model B is evaluated by using the measured vertical deflection DEFLEC96 and the gravity anomaly data NGS99 given by NGS. The results show that the accuracy of the vertical deflection calculated by model B in Continental United States is generally good, but there is still a large error in the local area, and the accuracy of gravity anomaly of model B in America is good on the whole, but the local error is large; 5) The trial calculation of 10800 degree ellipsoidal harmonic model of gravity field is carried out. The results show that the algorithm fully supports the analysis and synthesis of 10800 degree ellipsoidal harmonic model.

Key words 10800 degree gravity field model; ellipsoidal harmonic analysis; ellipsoidal harmonic synthesis; quadrature techniques; FFT

Category: Symposium 2a: Earth's Static Gravity Field =» 2a.4: Global Gravity Field Modelling

605

S2a-052

Joint modelling of the lithospheric and deep Earth gravity field to study the density structure of the lithosphere

Bart Root¹、Javier Fullea²、Zdenek Martinec³、Jörg Ebbing⁴、Sergei Lebedev³

1. Delft University of Technology

2. Universidad Complutense de Madrid

3. Dublin Institute for Advanced Studies

4. Christian Albrecht University

Different multi-data joint inversions are using this dataset together with other terrestrial geophysical data to determine the physical characteristics of the lithosphere. The gravitational signal from the deep, sub-lithospheric Earth is usually removed by high-pass filtering, or by appropriately selecting gravity field components insensitive to the deep mantle density distribution. However, any long-wavelength signal inherent to lithosphere is neglected. An optimal approach to remove the sub-lithospheric gravity signal is still missing. An alternative approach is to forward model the gravitational signal of these deep situated mass anomalies and subtract it from the observed data. Global seismic tomography provides shear-wave velocity mantle models. These need to be converted to density anomalies, with uncertain conversion factors related to temperature and composition. Understanding the sensitivity of these effects helps in determining the interaction of the deep Earth and the lithosphere.

In our study, the density anomalies of the mantle as well as the effect of CMB undulations are forward modelled to determine their gravitational potential field. Matching the remaining lithospheric related gravity field signal after subtracting the deep signal requires extreme lithospheric thermochemical models. A possible explanation is that dynamic topography associated with mantle convection has a large compensating that needs to be added to the lithosphere model to appropriately account for the deep gravity signal. Here, we present different modelling approaches to add the remaining dynamic topography effect in lithosphere models. This results in new realistic lithospheric thermal and compositional (density/seismic velocity) models able to explain both seismic observations and gravimetric measurements. The introduction of these dynamic forces is a step forward in understanding how to properly use global gravity field data in joint inversions of lithosphere models.

Key words Lithosphere modelling, mantle convection, global gravity field, 3D Earth

Category: Symposium 2a: Earth's Static Gravity Field => 2a.4: Global Gravity Field Modelling
660
S2a-053

On the Fast Computation of Model Gravity Gradient Tensor

Zhibin Xing¹、Shanshan Li²、Yao Meng¹、Na Yang¹、Qian Li¹、Jianchen Shan²

1. Space Engineering University

2. Information Engineering University

When recovering the Earth gravity field model from satellite gravity gradient data, the gravity gradient of satellite orbits needs calculating. While point-by-point calculations will take a lot of time, the spherical grid gravity gradient values of different height layers can be generated and interpolated the gravity gradient values of satellite orbits. To balance calculation efficiency and accuracy, the form of vector and matrix of model gravity gradient expressions as well as the vectorization technique was studied. The Fast Fourier Transform expressions of model gravity gradient taking into account the coordinates of the starting calculation point were deduced. Combined vector operations and FFT technique, using mixed programming method and cubic spline interpolation method, fast and accurate calculation of model gravity gradient values of satellite orbits can be realized. Compared with the traditional method, the computational efficiency of our method of calculating the global grid gravity gradient tensor can be increased up to nearly 20 times. The efficiency of calculating the gravity gradient tensor of 1200,510 points of satellite orbits can be increased by nearly 600 times.

Key words Gravity gradient tensor, Vector form, Matrix form, Vector operations, FFT, Mixed programming, Cubic spline interpolation

Category: Symposium 2a: Earth's Static Gravity Field => 2a.4: Global Gravity Field Modelling
758
S2a-054

Establishment of the global geoid model 2021 (GGM2021)

Wenbin Shen^{1,3}, Youchao Xie¹, Jiancheng Han², Jiancheng Li¹

1. Time and Frequency Geodesy Center, Department of Geophysics, School of Geodesy and Geomatics, Wuhan University, Wuhan, China
2. Institute of Geophysics, China Seismological Bureau, Beijing, China
3. State Key Laboratory of Information Engineering in Surveying, Mapping and Remote Sensing, Wuhan University, Wuhan, China

Abstract: We will release a $5' \times 5'$ global geoid model based on the shallow layer method (Shen 2006). We choose an inner surface S below the gravity field model EGM2008 global geoid, and the layer bounded by the inner surface S and the Earth's geographical surface E is referred to as the shallow layer. The Earth's geographical surface E is determined by the digital topographic model DTM2006.0 combining with the DNSC2008 mean sea surface. We formulate a 3D $5' \times 5'$ shallow-layer density model (SLDM) using a refined $5' \times 5'$ crust density model from CRUST1.0. Based on the SLDM and the given EGM2008 defined outside the Earth, we determine a gravity field model EGM2008S defined outside the inner surface S , the definition domain of the gravity field being extended. Based on EGM2008S and the definition of the geoid, $W(P) = W_0$, where W_0 is the geopotential constant on the geoid and P is the point on the geoid G , we determined the $5' \times 5'$ global geoid model 2021 (GGM2021). Comparisons show that GGM2021 fits the globally available GPS/leveling points better than the EGM2008 global geoid. This study is supported by National Natural Science Foundation of China (NSFC) (grant Nos. 42030105, 41721003, 41631072, 41874023, 41804012), and Space Station Project (Grant No. 2020-228).

Key words Shallow Layer Method, Shallow-Layer Density Model, Gravity Field, Global Geoid Model.

Symposium 2a: Earth's Static Gravity Field

S2a.5: Satellite Altimetry and Oceanography

Category: Symposium 2a: Earth's Static Gravity Field =» 2a.5: Satellite Altimetry and Oceanography
202
S2a-055

Performance of Five Satellite Altimetry Observations in Marine Gravity Inversion over the Gulf of Guinea

Richard Annan, Xiaoyun Wan

School of Land Science and Technology, China University of Geosciences (Beijing)

The geophysical performance of five altimetry missions (HY-2A/GM, Envisat, Cryosat-2, Jason-1/GM and SARAL/AltiKa) has been assessed by constructing a gravity anomaly model over the Gulf of Guinea (15°W to 5°E, 4°S to 4°N). The gravity anomalies were derived from vertical deflections computed directly from sea surface heights without the influence of a global geopotential model. In terms of standard deviation of errors, the east component's accuracy was lower than that of the north component by approximately 3 times. The adopted remove-compute-restore method allowed for individual assessment of the satellites, which showed that the north component of vertical deflection can be resolved by each satellite almost equally. On the other hand, each satellite resolved the east component differently; with the dominant satellites Cryosat-2, Jason-1/GM and SARAL/AltiKa respectively establishing ~34%, ~28% and ~24% of the east component. This may be attributed to the unprecedented spatial resolution of Cryosat-2, the 66° inclination of Jason-1, and the high range accuracy of SARAL/AltiKa's Ka-band signal. The impact of accuracy disparity of the vertical deflection components on the gravity anomalies were minimized through weigh assignment, where the north and east components were assigned weights of 0.687 and 0.313 respectively. The gravity anomaly model compares well with DTU13 and SIOv28 models used as references. Also, it compares well with shipborne gravimetry in deep ocean areas.

Key words Sea surface heights, Vertical deflection, Gravity anomaly, Remove-restore technique, Gulf of Guinea

Category: Symposium 2a: Earth's Static Gravity Field =》 2a.5: Satellite Altimetry and Oceanography
265
S2a-056

Altimeter-derived marine gravity variations reveal the magma mass motions within the subaqueous volcano

Qianqian Li^{1,2}、Lifeng Bao^{1,2}、Lin Wu^{1,2}、Panpan Zhang^{1,2}、Hui Liu^{1,2}
1. Innovation Academy for Precision Measurement and Technology, CAS
2. University of the Chinese Academy of Sciences

Volcanic activity is one of the important factors affecting global climate change and how to investigate and study it is a hot topic. Many techniques have been used to detect and study evolutions of magma mass motions only for land volcanoes, just like absolute gravimeters. For the submarine volcanic activities, the correlative research is grossly insufficient. Variations of marine gravity reflect mass changes in Earth's interior, including magma motions during volcanic eruption, which manifest in submarine mass transports. Here for the first time, we used radar altimeter-derived time-varying marine gravity fields, corresponding to before, during and after the Nishinoshima volcanic eruption, Izu–Bonin arcs near Japan, to quantify the evolution of undersea volcanic magma mass motions. The magma depths were observed to become shallower and <2 km, which are almost in exact accordance with seismic results. We find that the magma volume decreased beneath the Nishinoshima volcano, while increased or being fed by deeper reservoirs to the east and northeast of Nishinoshima. We conclude that the magmas of Nishinoshima volcanic eruption may derived from the subduction of the Pacific Plate westwards beneath the Philippine Sea Plate and the Nishinoshima volcano may continue to be active in the future. This study highlights the use of satellite radar altimetry as an innovative and viable tool to study subaqueous volcanism.

Key words Satellite altimetry; Gravity anomaly; Subaqueous Volcano; mass motion;

Category: Symposium 2a: Earth's Static Gravity Field => 2a.5: Satellite Altimetry and Oceanography
279
S2a-057

Optimal gravity anomaly and vertical gravity gradient in the South China Sea from multi-altimeter data

Daocheng Yu、Cheinway Hwang
National Yang Ming Chiao Tung University

The South China Sea (SCS) is a semi-closed sea with a complex gravity field and bathymetry, receiving intensive studies in oceanography and marine geophysics. Gravity anomalies have been widely used in examining the lithospheric structures of the SCS. The marine gravity field of the SCS has been steadily improved thanks to the advancement of satellite altimetry. Vertical gravity gradient (VGG), which can also be derived from satellite altimetry, is the vertical component of gravity gradient and is useful for detecting seafloor linear features and the continent-ocean boundaries (COB) in the South China Sea. We produce an optimal gravity field and a VGG field in the SCS from multi-altimeter data. Different satellites use different orbit positioning techniques and different radar altimeters, resulting in different footprint sizes, ranging accuracies, and along-track spatial resolutions of sea surface heights (SSH). Ideally, the best marine gravity field from multi-mission is one that combines all data by optimally calibrating weights across these missions and by reducing systematic and random errors in the altimeter data. We test for outliers of the along-track geoid gradients iteratively to locate blunders and select qualified gradients. Using the estimation of variance components, we calibrate cross-satellite error variances of geoid gradients to form the north and east geoid gradients. The gridded geoid gradients are used to compute gravity anomalies and vertical gravity gradients by the methods of inverse Vening-Meinesz (IVM) and numerical differentiation of gradients. The assessment using the shipborne gravity data indicates that altimeter-derived gravity anomalies are improved.

Key words gravity anomaly; vertical gravity gradient; inverse Vening-Meinesz; South China Sea; satellite altimeter

Category: Symposium 2a: Earth's Static Gravity Field => 2a.5: Satellite Altimetry and Oceanography
360
S2a-058

Estimating Snow Depth in Arctic Using the Sea Ice Surface Height from Heterologous Altimeter Satellites

Wenxuan Liu, Taoyong Jin, Hailan Huang
Wuhan University

The combination of Heterologous altimeters operating at two frequencies is a useful attempt to obtain large-scale snow depth on the Arctic sea ice. We estimate snow depth on the Arctic sea ice from October 2018 to April 2021 by differencing the sea ice freeboard and sea ice surface height from the laser altimetry ICESat-2 and the radar altimetry CryoSat-2 respectively. Comparison with in-situ measurements from Operation Ice Bridge mission, the snow depths retrieved by differencing the sea ice surface height show a better consistency with a RMSE of 4 cm. And affected by the monsoon and water vapor, the snow depth in northern Greenland and the Beaufort Sea is deeper (about 40 cm), and the snow spreads outward and extends to the vicinity of the Bering Strait and gradually becomes thinner. The results also show that the retrieved snow depth suggests a thinner snow cover (~54%) than the Warren climatology dataset. Combined with meteorological data, it is found that temperature changes and wind force changes play an important role in snow depth. The atmospheric temperature anomaly of the Arctic sea surface is negatively correlated with snow depth and sea ice thickness. Furthermore, the retrieved snow depths are used to estimate the sea ice thickness, and which is also closer to in-situ measurements from Operation Ice Bridge mission than that retrieved by Warren99 dataset. So the way to estimate snow depth in Arctic by combining two Heterologous altimeters operating at different frequencies or by dual-frequency altimeter in the future (e.g. CRISTAL) will obtain more accurate observations than earlier sea ice monitoring altimeters.

Key words ICESat-2; Arctic snow depth; CryoSat-2; Sea ice thickness

Category: Symposium 2a: Earth's Static Gravity Field => 2a.5: Satellite Altimetry and Oceanography
471
S2a-059

DTU21 Mean Sea Surface for Vertical Offshore Reference Frame

Ole Baltazar Andersen¹、 Adil Abulatijiang¹、 Shengjuin Zhang²、 Stine Kildegaard
Rose¹

1. DTU Space

2. Northeastern University China

A new Mean Sea Surface (DTU21MSS) for referencing sea level anomalies from satellite altimetry is presented. The major new advance leading up to the release of this MSS the use of 5 years of Sentinel-3A and an improved 10 years Cryosat-2 LRM+SAR+SARin record including retracked altimetry in Polar regions using the SAMOSA+ physical retracker via the ESA GPOD facility.

A new processing chain with updated editing and data filtering has been implemented. The filtering implies, that the 20Hz sea surface height data are filtered using the Parks-McClellan filter to derive 1Hz. This has a clear advantage over the 1 Hz boxcar filter in not introducing sidelobes degrading the MSS in the 10-40 km wavelength band. Similarly, the use of consistent ocean tide model for the Mean sea surface improves the usage of sun-synchronous satellites in high latitudes.

The presentation will also focus on the difficult issues to consolidating Cryosat-2 and Sentinel-3 onto a past 20 year mean sea surface. This is implemented using simultaneous estimation of the mean, sea level trend and annual and semi-annual variations in sea level.

Key words Satellite Altimetry, Mean Sea Surface

Category: Symposium 2a: Earth's Static Gravity Field => 2a.5: Satellite Altimetry and Oceanography
488

S2a-060

The mean dynamic topography and geostrophic current estimation based on a Least-square method

Hongkai Shi^{1,3}、Yihao Wu²、Ole Andersen³、Xiufeng He²

1. School of Earth Sciences and Engineering, Hohai University, Nanjing, China

2. Hohai University

3. DTU Space, Technical University of Denmark, 2800 Lyngby, Denmark

The mean dynamic topography (MDT) can be derived based on from the combination of the mean sea surface (MSS) and geoid. The traditional modelling method would require a filtering procedure for a smooth solution in this combination due to the spectral inconsistency, which leads to a distortion of the MDT and signal attenuation in the geostrophic current. This study introduces a Least-square-based (LS) algorithm to assimilate heterogeneous altimetry and gravimetry data for MDT and associated geostrophic current estimation. The algorithm parameterizes the MDT by Lagrange basis functions (LBFs) and geoid height using spherical harmonics (SHs) from global geopotential models (GGMs). The design matrix and the error models are rigorously constructed. In addition, the performance of LBFs consisting of 4 parameters in the MDT modelling is investigated, and the deduced geostrophic current is validated based on the in-situ data.

The numerical experiment shows that the LS-based algorithm separate the MDT signals better, especially near the current region. The misfits between the estimate and a Gaussian filtered MDT solution against the comparison data show comparable standard deviation. The GOCE-based satellite-only GGM contributes more geoid signals when the spatial resolution of the MDT increases from 1° to 0.5°. More importantly, the signals of the deduced geostrophic current are significantly enhanced compared with the Gaussian filtered solution.

Key words Mean dynamic topography; GOCE; Signal reconstruction; Geostrophic current; Gulf stream

Category: Symposium 2a: Earth's Static Gravity Field => 2a.5: Satellite Altimetry and Oceanography
568
S2a-061

Inversion of gravity anomalies in the South China Sea and Hawaii area derived from ICESat-2 ocean products

Hang Li, Shengjun Zhang
Northeastern University

The Ice, Cloud, and land Elevation Satellite-2 (ICESat-2) satellite uses a synchronized multi-beam photon-counting method to collect data from three pairs of synchronous ground tracks. The sampling rate along the ground tracks is designed to be ~0.7 m, much smaller than that used in conventional radar altimeters. Hence, it is reasonable to expect an improvement in marine gravity recovery over coastal zones using ICESat-2 data. ICESat-2 provides valid sea surface height (SSH) measurements and standard ocean products (ATL12). This led us to consider the possibility of investigating its ability to calculate the deflection of vertical (DOV) and marine gravity anomalies in coastal and open ocean areas.

We process ATL12 data about 24 months over the South China Sea (0°–23°N, 103°–120°E) and the Hawaii area (15°–30°N, 188°–208°E). The results show that the ICESat-2 SSHs have a similar centimeter-magnitude accuracy level with Jason-2 data. Furthermore, the accuracy of both cross-track deflection of vertical (CTDOV) and along-track deflection of vertical (ATDOV) calculated between synchronized beams is valid. Accordingly, the accuracy of calculated prime components is significantly improved by combining CTDOV and ATDOV at along-track points, while the enhancement is weak for the meridional components. After that, we calculated DOV components at 2'×2' gridding points and recovered ICESat-2 single-mission derived marine gravity anomalies based on the inverse Vening-Meinesz formula and Remove-Restore procedure. Verifications with shipborne measurements and XGM2019 model show that the standard deviations (STD) are ~1.35 mGal and ~2.47 mGal in South China Sea, and ~0.87 mGal and ~1.23 mGal in Hawaii area. To sum up, ICESat-2 deserves the attention of the altimetry community, and its advantages are expected to make it an alternative data source for multi-mission fusion inversion of the ocean gravity field in the future.

Key words ICESat-2; cross-track; deflection of vertical; gravity anomaly

Category: Symposium 2a: Earth's Static Gravity Field => 2a.5: Satellite Altimetry and Oceanography
579
S2a-062

Radar Altimeter-Based Water Level and Wind Speed Monitoring Over the Laurentian Great Lakes

Yuanyuan Jia¹, Philip Chu², C.K. Shum¹

1. The Ohio State University

2. NOAA/GLERL

The Laurentian Great Lakes is the world's largest freshwater lakes, consisting of Lakes Superior, Michigan, Huron, Erie, and Ontario, located on the Canada-United States border and shared by these two countries. They provide drinking water, recreations, to over 35 million people and billions of dollars in economic benefits to the people around them. The Great Lakes have a significant influence on regional climate and weather patterns that sensitive to a number of climate variable or indicators, including lake surface height, wave and wind speed, ice coverage and thickness change, and temperature, etc. In addition, more severe and extreme weather events arguably intensified in the Great Lakes region, such as storm surges, meteotsunamis and lake-effect snowstorms. In order to provide long-term protection of the Great Lakes' ecology and environment, many observing and forecasting systems are developed. Some novel passive and active remote sensing techniques have been used in recent research for in land water observing and forecasting. In this study, we used observables acquired from multi-mission satellite radar altimetry, including ERS-1/-2, Envisat, GFO, TOPEX/Poseidon, Jason-1/-2/-3, SARAL/Altika, CryoSat-2, Sentinel-3A/B, for water level and wind speed monitoring over the entire Great Lakes. These altimeters continuously measuring the Great Lakes, and provide about three decades records, from 1991 to present. Here, we also estimated the Great Lakes mean lake surface, and detected storm signals from radar altimetry. These results could complement existing NOAA CoastWatch satellite products and be used to improve Great Lakes environmental monitoring and forecasting models, possible monitoring of abrupt weather events.

Key words Great Lakes, radar altimetry, water level, wind speed

Symposium 2a: Earth's Static Gravity Field

S2a.6: Gravity Inversion for Solid Earth

Category: Symposium 2a: Earth's Static Gravity Field => 2a.6: Gravity Inversion for Solid Earth

116

S2a-063

Correlation between gravitational and magnetic anomalies and crustal susceptibility in the Three Gorges area, China

Yi Zhang^{1,4}、Yunlong Wu^{1,4}、Chao Chen²、Kai Sun³、Jiapei Wang¹

1. Institute of Seismology, China Earthquake Administration

2. China University of Geosciences

3. Taiyuan University of Technology

4. Institute of Disaster Prevention

In this study, four major magnetic anomalies in the Three Gorges area were identified from RTP aeromagnetic anomalies: Shaanxi Zhenping-Chongqing Wuxi-Hubei Badong, Hubei Zhongxian, Shishou-Jili, and Zigui-Yichang. The former two are mainly caused by uplift of the magnetic basement, while the latter two result from the intrusion of magmatic rocks.

Combining the Bouguer gravity anomaly and its gradient, gravity and magnetic correspondence analysis was performed. The results show that the main magnetic anomaly in the Three Gorges area is caused by intrusive rocks in the core of Huangling Anticline, and its magnetic and gravity anomaly have the same source. We also inverted the magnetic susceptibility in the region using the inversion results of crustal density as a constraint. The results reveal the magnetic susceptibility distributions of four rock masses (Sandouping, Huanglingmiao, Dalaoling, and Xiaofeng) in the core of the Huangling Anticline. The bottom depth of the Sandouping rock mass is basically the same as the emplacement depth estimated from amphibole barometry. In comparison, the Huanglingmiao rock mass is deeper, the Dalaoling rock mass is shallower, and the Xiaofeng rock mass depth is significantly greater than the original estimated emplacement depth. In addition, we suggest that the abnormally low magnetism and high density of the Huanglingmiao rock mass results from the combined effects of weathering and erosion of the top of the magnetic body and tectonic activity in a ductile shear zone at the bottom.

Key words Three Gorges; Huangling Anticline; Aeromagnetic anomaly; Correspondence analysis; Susceptibility inversion

Category: Symposium 2a: Earth's Static Gravity Field => 2a.6: Gravity Inversion for Solid Earth

180

S2a-064

Possible Deep Structure and Composition of Venus with Respect to the Current Knowledge from Geodetic Data

Chi Xiao¹、 Fei Li²、 Jianguo Yan²、 Michel Gregoire³、 Weifeng Hao⁴、 Harada Yuji⁵、
Mao Ye²、 Jean-Pierre Barriot⁶

1. Hubei Earthquake Agency
2. State Key Laboratory of Information Engineering in Surveying, Mapping and Remote Sensing, Wuhan University
3. Géosciences Environnement Toulouse, Observatoire Midi-Pyrénées Université Paul Sabatier Toulouse III-CNRS-CNES-IRD
4. Chinese Antarctic Center of Surveying and Mapping, Wuhan University
5. Space Science Institute, Macau University of Science and Technology
6. Geodesy Observatory of Tahiti

Almost no in situ seismic data are available for Venus; therefore, we can constrain the deep structure of this planet only from the geodetic data obtained by spacecraft. Of particular interest is Venus's core-mantle boundary, which holds clues about the origin and evolution of this celestial body. In this study, we build a series of different mantle/core models of Venus based on several mantle composition models and compare their associated Love numbers k_2 with the observed values. Due to the large uncertainty in the observed values of k_2 , the state of Venus's core cannot be reliably constrained. However, the expected precision of k_2 obtained by the EnVision mission will sufficiently reduce the acceptable model space and contribute to estimating the mantle viscosity structure. Based on current geodetic data, we find that the bottom of Venus's mantle may not feature a phase transition from perovskite to post-perovskite if the FeO content of the mantle is less than 8.1 wt%; this region may be different from Earth's D" layer. Furthermore, we find that the combination of observed k_2 and Q can be used to distinguish whether the lowermost part of Venus's mantle is a high-temperature basalt layer or a thin thermal boundary layer if observations of Q can be obtained.

Key words interior structure, equation of state, tidal Love number, tidal dissipation factor, Venus

Category: Symposium 2a: Earth's Static Gravity Field => 2a.6: Gravity Inversion for Solid Earth

217

S2a-065

Research on the basement depth of Sichuan basin with real gravity data

Menglong Xu^{1,2,3}、Yabin Yang^{1,2,3}、Chengye Sun^{1,2,3}、Liang Chen^{1,2,3}、Gengen Qiu^{1,2,3}

1. Institute of Geophysical and Geochemical Exploration, Chinese Academy of Geological Science
2. National Research Center of Geo-Exploration Technology
3. Key Laboratory of Geophysical Electromagnetic Probing Technologies of Ministry of Natural Resources

The research of the basement tectonic morphology of the southern margin of the Sichuan Basin is of great significance to the deep structure, the distribution and delineation of the paleo-uplift, the evolution of regional tectonic changes, and the relationship between the late evolution of the basin. However, the lack of geophysical data in the southern margin of the Sichuan Basin has already limit the deepgoing understanding. In this paper, we achieve 1:250 000 measured gravity data, and 7 MT profiles and seismic profiles are collected to construct the initial basement depth model. The interface inversion method proposed by Granser (1987) and Cordell (1968) was used to fit the regional isostatic gravity anomaly, and the inversion basement depth is obtained. The result shows that the sedimentary thickness is up to 10km, and that in the outside of Sichuan Basin, the sedimentary thickness is less than 5km. Basement uplift belt existed around Gongxian, Wenxing and Gulin, and there are large sedimentary sags on the south side of the uplift belt. There is a basement uplift zone (Xishui - Gulin) in the basin-mountain transition zone between Sichuan Basin and the northern Guizhou. The thin sedimentary thickness in Dafang-Jinsha-Zunyi area reflects the lack of some strata in the central Guizhou paleo-uplift. The preliminary result of the basement can provide geophysical basis for further understanding of the tectonic framework, deep dynamics process and deep potential resource prospects.

This research is supported by the National Key R&D Program of China (No. 2018YFE0208300), the China Geological Survey Program (No. DD20190032).

References

Cordell, L. and Henderson, R.G., 1968. Iterative three-dimensional solution of gravity anomaly data using a digital computer. *Geophysics* 33, 596-601.

Granser, H., 1987a. Three - dimensional interpretation of gravity data from sedimentary basins using an exponential density – depth function. *Geophysical Prospecting* 35, 1030-1040.

Key words Sichuan Basin; Basement depth; Real gravity data; Interface inversion.

Category: Symposium 2a: Earth's Static Gravity Field => 2a.6: Gravity Inversion for Solid Earth
222
S2a-066

Crustal geological provinces seen by gravity field data: an automatic Bayesian approach applied to the Central Eastern Mediterranean area

Martina Capponi, Daniele Sampietro
Geomatics Research & Development srl

The indirect investigation of the Earth's interior, with methods based on the analysis of gravity field data, is quite common nowadays. This is because dedicated satellite gravity missions provided observations spread worldwide that, combined with terrestrial data, have been used to realize high resolution models from global to regional scales. One of the applications of gravity field data, regards the use of interpretation algorithms to unveil information about the Earth crust classification. The classical approach is qualitative and strongly affected by the expertise of the operator. In fact, it generally consists in the application of a filter to the gravity data (to reduce short/long wavelengths due to sedimentary layers and mantle respectively) on which, then, a visual matching with the known geological crustal features is performed.

Within this work, we present the application on a real case study of an automatic method, based on a Bayesian probabilistic approach, that starting from a set of a-priori information infers the boundaries of the main geological crustal provinces. It has been developed in the framework of the Gravity for Lithosphere Architecture Determination and Analysis (GIADA) project, funded in 2020 by the European Space Agency. One of the advantages of this method is that it does not only retrieve the most probable classification but also an estimate of the predicted accuracy as well as of the average density of each crustal province. It has been tested over the Central Eastern Mediterranean area to delineate the boundaries of the principal basins. To apply the algorithm it was necessary to define an a-priori geological model in terms of main horizons and a rough basins classification. The algorithm then modified the shape of the initial crustal provinces in order to be coherent with the gravity observations, namely the second radial derivatives of the anomalous potential. The results, here summarized, are a valuable starting point to understand the geological evolution history of the area.

Key words gravity interpretation, Bayesian probabilistic approach, automatic method, crustal geological provinces, Central Eastern Mediterranean case study

Category: Symposium 2a: Earth's Static Gravity Field =》 2a.6: Gravity Inversion for Solid Earth
310
S2a-067

The contribution of gravity to crust and upper mantle structure modeling – an example in Tibet Plateau

Jiakuan Wan、 Zhicai Luo
Huazhong University of Science and Technology

Seismic tomography in Tibet Plateau suffers from the poor and uneven distribution of seismic stations, resulting in low resolution and unreliable models of crust and upper mantle. While current gravity models (e.g. EIGEN6C4) are of high resolution and precision and may lead to better understanding of subsurface structure of Tibet Plateau. In this work, we conduct the joint inversion of gravity and surface dispersion data for crust and upper mantle structure modeling. The results of simulation experiments demonstrate remarkable lateral resolution improvement in joint inversion comparing to the inversion of seismic data only. And constrains of the gravity data contribute more to the modeling of density structure than to the seismic wave velocity when the bias in the empirical formula of velocity and density is taken into consideration. Then, we present a density model of crust and upper mantle in Tibet Plateau from the joint inversion. The density model, combined with the velocity models from seismic tomography, may shed light on the tectonic debates in Tibet Plateau.

Key words crust and upper mantle, joint inversion, Tibet Plateau

Category: Symposium 2a: Earth's Static Gravity Field => 2a.6: Gravity Inversion for Solid Earth

403

S2a-068

Mapping the upper mantle thermochemical heterogeneity from coupled geophysical-petrological inversion of seismic waveforms, heat flow, surface elevation and gravity satellite data

Javier Fullea^{1,2}, Sergei Lebedev², Zdenek Martinec², Nicolas Celli²

1. Facultad de Fisica, Universidad Complutense de Madrid (UCM)

2. Dublin Institute for Advanced Studies (DIAS) Ireland

Here we present a new global thermochemical model of the lithosphere-upper mantle (WINTERC-grav) constrained by state-of-the-art waveform tomography, satellite gravity, surface elevation and heat flow data. WINTERC-grav is based upon an integrated geophysical-petrological approach where seismic velocities and density are computed within a thermodynamically self-consistent framework. The complementary sensitivity of our input data sets allow us constraining the geometry of the lithosphere-asthenosphere boundary, separating temperature and composition mantle anomalies, and estimating dynamic vs isostatic surface elevation contributions. Our model shows that the thickest lithosphere is mostly associated with cratons but also some active areas. We identify considerable differences in cratonic temperatures and compositions. The N. American and Siberian cratons appear to be thick (>260 km) and compositionally refractory, whereas the Sino-Korean, Aldan and Tanzanian cratons are defined by a thinner and averagely fertile lithosphere similar to younger continental lithosphere elsewhere. WINTERC-grav shows a progressive thickening of oceanic lithosphere with age, with significant lateral differences: the mantle beneath the Atlantic and Indian oceans is, on average, colder, more fertile and denser than that in the Pacific Ocean. Our results also suggest that mantle composition, temperature and density are correlated to spreading rates up to values < 50-60 mm/yr. The 1D average of WINTERC-grav corresponds to a mantle geothermal gradient of 0.55-0.6 C/km and a potential temperature of 1300-1320 C for depths>200 km. Our predicted isostatic residual topography values, a proxy for dynamic topography, are large (>1 km) mostly in active subduction settings. The residual isostatic bathymetry from WINTERC-grav is remarkably similar to the lateral pattern independently determined based on extensive oceanic crustal data compilations. The amplitude of our predicted continental residual topography is relatively large (>500m) in the East European Craton, Greenland, and the Andes and Himalaya cordilleras. Our results show that part of the topography signal that has been previously identified as residual (or dynamic) can be explained isostatically by lithospheric density variations.

Key words Composition and structure of the mantle; Gravity anomalies and Earth structure; Joint inversion; Seismic tomography; Cratons; Mid-ocean ridge processes

Category: Symposium 2a: Earth's Static Gravity Field => 2a.6: Gravity Inversion for Solid Earth

415

S2a-069

A Method of Determining Moho Topography from On-orbit GOCE Gravity Gradients: A Case Study in Tibetan Plateau

Chuang Xu

Department of Surveying Engineering, Guangdong University of Technology,
Guangzhou 510006, China

State Key Laboratory of Geodesy and Earth's Dynamics, Innovation Academy for
Precision Measurement Science and Technology, CAS, Wuhan 430077, China

Gravity data is widely applied to determine Moho topography due to global dense and homogeneous gravity observations. Gravity gradients, which can reveal more details of Moho structure in both horizontal and vertical directions, are more competitive. However, during the inversion gravity gradients must be transformed into gravity data, which causes loss of some high-frequency signals. Thus, an improved method by constructing direct function relation between Moho topography and gravity gradients is proposed in this paper. Subsequently, a simulation test is designed to verify our improved method. Without consideration of errors, the improvement is at least 31.8% for inverted precision and 33.3% for spatial resolution. After considering errors from uncertainty of crustal density, improvements for precision and spatial resolution are still at least 18.3% and 17.3%, respectively. At last, a case study in Tibetan Plateau is conducted using this improved method, and a new Moho topography with higher spatial resolution and precision is determined. More refined tectonic implications can be also revealed from this new Moho topography: (1) the prevailing wavelengths of detected Moho folds are approximately 578 km - 722 km in the east-west direction and approximately 540 km - 708 km in the north-south direction, which are close to Jin et al. (1994) of 500 km - 700 km; (2) two lower crustal mass flow channels can be identified clearly according to the traces leaving on Moho topography in the southeastern Tibetan Plateau, which are in good agreement with previous seismic results; (3) clearer Moho subsidence, approximately 5 km, can be observed in the central Tarim Basin.

This study is supported by the National Natural Science Foundation of China (Grant no. 41974014) and State Key Laboratory of Geodesy and Earth's Dynamics, Innovation Academy for Precision Measurement Science and Technology, CAS, Wuhan 430077, China.

Key words Moho topography; GOCE; Gravity gradient; Tibetan Plateau

Category: Symposium 2a: Earth's Static Gravity Field => 2a.6: Gravity Inversion for Solid Earth

767

S2a-070

Improving the GEMMA inversion algorithm towards a new release of the GOCE-based crustal model

Lorenzo Rossi¹、 Mirko Reguzzoni¹、 Biao Lu²、 Islam Fadel²、 Daniele Sampietro³、
Mark van der Meijde²
1. Politecnico di Milano
2. University of Twente
3. Geomatics Research & Development srl

Since its discovery in 1909, the Moho was routinely studied by the seismological method. However, from the fifties, a possible alternative was introduced by gravimetric inversion. Thanks to the satellite gravity missions launched from the beginning of the 21st century, a global inversion became feasible, e.g. leading to the computation of the GEMMA model in 2012. Here, the GOCE gravity gradients were inverted in spherical harmonic domain by a Wiener filter, linearizing the forward of the anomalous signal produced by a two-layer model with lateral and vertical density variations. Moreover, seismic information was introduced in the inversion to deal with the joint estimation/correction of both density and geometry. This study aims at revising the GEMMA algorithm from the theoretical point of view, also introducing a cleaner formalization, and studying the used approximations more thoroughly. The updates are on: 1) the forward operator, directly computing the gravitational signal of the different layers in terms of spherical harmonics; 2) the management of the approximations due to the forward linearization required for the inversion; 3) the regularization of spherical harmonic coefficient in the inversion by proper modelling the Moho signal and the gravity error covariances; 4) the regularization in the least-squares adjustment when introducing seismic information to correct the density model. Thanks to these updates, a significant improvement from the computational point of view is achieved too, thus the convergence of the iterative solution by closed-loop tests can be assessed, showing the algorithm performance in retrieving the simulated “true” Moho. Finally, the algorithm is applied on the last release of the GOCE global gravity model by using the same geophysical/geological information of the original GEMMA model. Those tests are performed in view of producing an updated version of this model, where also new geophysical/geological information will be integrated.

Key words global inversion, GOCE, global gravity model, GEMMA, Wiener Filter, Moho discontinuity

Category: Symposium 2a: Earth's Static Gravity Field => 2a.6: Gravity Inversion for Solid Earth
889
S2a-071

Crustal configuration of the West and Central African Rift System from gravity and seismic data analysis

Franck Eitel Kemgang Ghomsi¹、 Robert Tenzer²、 Rebekka Steffen³、 Emmanuel Njinju⁴

1. National Institute of Cartography, P.O. Box 157, Yaoundé, Cameroon

2. Department of Land Surveying and Geo-Informatics, Hong Kong Polytechnic University, Hong Kong

3. Lantmäteriet, Lantmäterigatan 2, 80182 Gävle, Sweden

4. Department of Geosciences, Virginia Tech, Blacksburg, VA, USA

The West and Central African Rift System is the only stable continental geological structure on Earth that is formed by large - scale topographic massifs (swells). The scarcity of high - resolution geodynamical studies of the lithospheric structure beneath this atypical region is liable for the ongoing discussion about the crustal architectonics of Cenozoic volcanism and the mechanism behind the formation of the African hotspot. Since active seismic experiments are rare in this part of Africa, we use the gravity information from satellite gravity missions to interpolate the Moho depth information where seismic data are sparse or absent. In particular, we use the XGM2016 global gravitational model for a determination of the Moho depth constrained by seismic Moho depth estimates at only 41 seismological stations. Our result reveals a regional Moho deepening to ~40 km beneath the Hoggar, Air and Tibesti Massifs. In addition, a regional Moho deepening is detected beneath the Congo Craton and the Adamawa Plateau. The Moho geometry beneath the Chad basin, the Chad Shear Zone and the Termit basin is relatively smooth with Moho depth variations between 24 and 26 km only. The significant Moho deepening as well as the large Moho depth variations mostly within 32-45 km beneath the Saharan Metacraton and the Congo Craton (especially under its northern margin) reflect the metacratonization processes which occurred during the Neoproterozoic. The Niger delta and the Benue Through are characterized by a very thin continental crust with Moho depth varying from ~20 km in the south along the Atlantic coastline to about 24 km in the northeast branch of the Cretaceous Benue Through around the Garoua-Yola Rift.

Key words West and Central African Rift System; gravity; inversion; Moho; seismic data

Symposium 2a: Earth's Static Gravity Field

S2a.7: Topography and Bathymetry Gravity Modelling

Category: Symposium 2a: Earth's Static Gravity Field => 2a.7: Topography and Bathymetry Gravity Modelling

109

S2a-072

Marine Gravimetry, Ship Sounding and Ocean Bottom Topography Estimation in the South-western Coastal Area of the Baltic Sea

Biao Lu¹、Chuang Xu²、Jinbo Li²、Bo Zhong³、Mark van der Meijde¹

1. Department of Earth Systems Analysis, Faculty of Geo-Information Science and Earth Observation (ITC), University of Twente

2. Department of Surveying Engineering, School of Civil and Transportation, Guangdong University of Technology

3. School of Geodesy and Geomatics, Wuhan University

Marine gravimetry provides high-accuracy and high-resolution gravity measurements in the Baltic Sea, especially in coastal areas. After the updating of new sensors in GFZ's air-marine gravimeter Chekan-AM, the gravimetry measurements showed a significant improvement from the first new campaign on-board the research vessel DENEBO in 2017. The RMS of the gravity differences at crossover points is 0.3 mGal in this campaign. The corresponding accuracy (standard deviation of a single measurement) is about 0.21 mGal @ 1 km (approximately spatial resolution, half-wavelength) according to the law of error propagation which reaches the highest accuracy level of marine gravimetry at current. Together with the gravimeter, a sonar system on-board the research vessels measured the ship-sounding data at a high-accuracy level of 0.15 m with a high-spatial resolution of several meters. Then, these measurements are used in the geodetic and geophysical studies, e.g., combined gravity anomalies from satellite altimetry and marine gravimetry together with sounding data are used to estimate the ocean bottom topography by using the gravity-geologic method in the south-western part of the Baltic Sea. Our estimated model is more accurate than existing digital elevation datasets like EMODnet, SRTM and SIO models and furthermore shows some more detailed and accurate ocean bottom topography information, e.g., the RMS of depth differences of our estimated model at checking points is 0.64~m while that of other existing models (EMODnet, SRTM and SIO) are 0.73~m, 1.90~m and 2.06~m, respectively. The marine gravimetry and sounding measurements as well as the estimated ocean bottom topography are crucial for future geoid determination, 3 D-navigation and resource exploration in the Baltic Sea.

This research is supported by the Dutch Research Council (Grant No. ALWGO.2017.030) and also supported by the National Natural Science Foundation of China (Grant No. 41974014, 41974015, 42061134007).

Key words Marine Gravimetry; Ocean Bottom Topography Estimation, Baltic Sea

Category: Symposium 2a: Earth's Static Gravity Field => 2a.7: Topography and Bathymetry Gravity Modelling

181

S2a-073

The omission error modelling of global gravity field models using different digital terrain models

Martin Pitonak¹, Matej Varga², Michal Sprlak¹

1. NTIS – New Technologies for the Information Society, Faculty of Applied Sciences, University of West Bohemia

2. Institute of Geodesy and Photogrammetry, GSEG, ETH Zürich, Switzerland

The launch of gravity field dedicated satellite missions such as CHAMP, GRACE and GOCE at the beginning of the new millennium led to a significant improvement of global gravity field models resolution and accuracy. Theoretically, the gravity potential can be expressed by an infinite series of spherical harmonic coefficients. Practically, such series has to be truncated at a certain degree and order. The newest high-frequency global gravity field models (GGMs), e.g., SGG-UGM-2 (Liang et al. 2020), XGM2019e_2159 (Zingerle et al. 2019) or GECO (Gilardoni et al. 2016) represent Earth's gravity field with a relatively high spatial resolution of 5 arc-minutes (~9 km). Each GGM contains two types of errors, the commission error and the omission error. The commission error is caused by the inaccurate input data used in development of GGM, whereas the omission error comes from the loss of high frequencies due to the finite maximum degree and order.

The main goal of this contribution is to compare different approaches of spectral- and spatial-domain forward gravity field modelling of omission error, which is known to be one of the error sources in global and regional geoid determination. To do so gravity disturbances are employed over three study areas, namely, Czechia, Slovakia and southern Colorado (USA). Firstly we subtract the high-frequency part of the gravity field generated from the XGM2019e_2159 model up to the degree 2190 terrestrial datasets. Then the omitted signal is modelling in XGM2019e_2159 by: (i) the topographic gravity field model dV_ELL_Earth_5480 (Rexer et al. 2017), (ii) the Earth's short-scale gravity field model ERTM2160 (Hirt et al., 2014) and (iii) the forward modelling of residual topographic masses in the spatial domain. Residual gravity disturbances will be represented as differences between selected global (or near-global) digital elevation models such as AW3D30 (Tadano et al. 2014), SRTM 4.1 (Jarvis et al. 2008) or MERIT DEM (Yamazaki et al. 2017) and EARTH2014 (Hirt and Rexer 2015). Finally, residual gravity disturbances will be statistically compared and discussed.

Key words Forward modelling, omission error, RTM effect

Category: Symposium 2a: Earth's Static Gravity Field => 2a.7: Topography and Bathymetry Gravity Modelling

529

S2a-074

Topographic gravity field modelling for improving high resolution global gravity field models

E. Sinem Ince, Christoph Foerste, Oleh Abrykosov, Frank Flechtner
GFZ-Potsdam

Topographic gravity field models represent the gravitational potential generated by the attraction of the Earth's topographic masses. The gravity is computed based on the shape of the topography (e.g., digital elevation model) and the mass-density knowledge. Assuming that the high-frequency gravity field components are mainly caused by the topography, such models can then be used to complement high-resolution combined static gravity field models for the very high-frequency components of the gravity field.

The performance of our preliminary model (ROLI_EllApprox_SphN_3660) expanded up to spherical harmonic degree 3660 developed in a previous contribution (Abrykosov et al. 2019) has been assessed w.r.t. other similar models and independent ground truth data (Ince et al. 2020). The mass-source information used is provided by the 1 arcmin resolution Earth2014 relief model (Hirt and Rexer 2015). The calculation of the potential is performed outside of all the masses on the bounding ellipsoid and the integration is computed for every single shell that are arranged 5 m distance apart starting from the lower boundary ellipsoid (e.g. Mariana trench). The gravitational potential is expanded for each shell and then summed up to represent the complete gravitational potential of the topography.

In this contribution we will present the impact of different shell thicknesses to the numerical stability and computation time and we will expand the model representation up to d/o 5400. Different lower boundaries will be investigated based on the needs of different disciplines. For geoid calculation, topography above the mean sea level will be considered. Finally, EIGEN-6C4 model will be enhanced with the high frequency components retrieved from the topographic model and differences w.r.t. EIGEN-6C4 will be presented.

Our preliminary model is available on the ICGEM Service (http://icgem.gfz-potsdam.de/tom_reltopo) and can be freely downloaded from <http://doi.org/10.5880/ICGEM.2019.011>.

Key words Topographic gravity field modelling, high resolution gravity field models, ellipsoidal approximation, enhanced high resolution gravity field models, new generation gravity field model, ICGEM

Category: Symposium 2a: Earth's Static Gravity Field => 2a.7: Topography and Bathymetry Gravity Modelling
712
S2a-075

Bathymetry of northeast Greenland revealed by Oceans Melting Greenland (OMG) airborne gravity

Junjun Yang¹、Zhikai Luo¹、Liangcheng Tu^{2,1}

1. Huazhong University of Science and Technology
2. Sun Yat-sen University

Seafloor topography shapes the pathways of ocean currents transporting ocean heat and thus is a fundamental boundary condition for modeling ocean-ice interactions. However, few ship bathymetric data are available on the inner continental shelf of northeast Greenland due to the year-round presence of sea ice. We infer seafloor topography of this region from airborne gravity anomaly measured by National Aeronautics and Space Administration's Oceans Melting Greenland mission through a nonlinear inversion method called simulated annealing, and results in a model with 1.95~3.9 km resolution and 52 m accuracy. The model provides a view of the seafloor near Zachariæ Isstrøm, and reveals new topographic features which have never been measured by traditional ship-based echo sounders, such as a 370~560 m deep trough that is well below the range of observed warm water depths and provides potential access of warm Atlantic water to Zachariæ Isstrøm.

Key words Bathymetry, Airborne Gravity, Greenland, Gravity Inversion

Category: Symposium 2a: Earth's Static Gravity Field =» 2a.7: Topography and Bathymetry Gravity Modelling

717

S2a-076

Harmonic Correction for Residual Terrain Modelling (RTM) Technique in Physical Geodesy Applications

Meng Yang¹、Xiao-Le Deng²、Wei Feng^{1,3}、Chang-Qing Wang³、Min Zhong^{1,3}

1. School of Geospatial Engineering and Science, Sun Yat-Sen University, Zhuhai, 519082, China

2. Department of Earth and Space Sciences, Southern University of Science and Technology, Shenzhen, 518055, China

3. State Key Laboratory of Geodesy and Earth's Dynamics, Institute of Geodesy and Geophysics, Innovation Academy for Precision Measurement Science and Technology, Chinese Academy of Sciences

The harmonic correction (HC) is one of the key parameters when using residual terrain modelling (RTM) for high-frequency gravity field modelling. As one classical approach, the condensation method has been widely used for HC computation over the past decades. However, the classical condensation method based on an unlimited Bouguer plate approximation suffers from various approximations, e.g., mass inconsistency and planar assumption. In this study, we derive expressions of HC terms for RTM geoid height, RTM gravity anomaly, and RTM radial tensor component under three different assumptions separately: residual masses approximated by an unlimited Bouguer plate (named HC-UBP), residual masses approximated by a limited Bouguer plate which overcomes the mass inconsistency effect (named HC-LBP), and residual masses approximated by a Bouguer shell which overcomes the effect of planar approximation (named HC-BS). The errors due to various approximations in HC terms are investigated through a comparison between HC-UBP, HC-LBP, and HC-BS; HC terms are computed by means of an expansion up to degree and order 2,159, defining a reference surface evaluation. Besides HC for RTM gravity anomaly with values up to 303 mGal, our results outline the significance of HC for RTM geoid height, with values up to 10 cm, in cm- and mm-level geoid determination. The HC for RTM radial tensor component is of a constant value of 2239 E. With integration masses extending up to a distance of 1° from the computation point for the determination of RTM geoid height and gravity anomaly, and 0.5° for RTM gradient, the errors due to an unlimited Bouguer plate approximation are negligible. The validation through comparison with terrestrial measurements and a baseline solution of RTM technique proves that the HC terms provided in this study can improve the accuracy of RTM-derived gravitational functionals and are expected to be useful for applications of the RTM technique in regional and global gravity field modelling.

Key words Harmonic correction (HC), Residual Terrain Modelling (RTM), RTM Geoid Height, RTM Gravity Anomaly/Disturbance, Radial Tensor Component

Symposium 2b: Earth's Time- variable Gravity Field

S2b.1: Analysis Techniques

Category: Symposium 2b: Earth's Time-variable Gravity Field =» 2b.1: Analysis Techniques

167

S2b-001

Monthly low-degree gravity field models from Swarm GPS data for the last 7 years

Joao Encarnacao^{1,7}, Daniel Arnold², Ales Bezdek³, Christoph Dahle⁴, Junyi Guo⁵, Jose van den IJssel¹, Adrian Jaeggi², Jaroslav Klokocnik³, Sandro Krauss⁶, Torsten Mayer-Guerr⁶, Ulrich Meyer², Josef Sebera³, CK Shum⁵, Pieter Visser¹, Yu Zhang⁵

1. Delft University of Technology
2. Astronomical Institute of the University of Bern
3. Astronomical Institute of the Czech Academy of Sciences
4. GFZ German Research Centre for Geosciences
5. School of Earth Science of the Ohio State University
6. Institute of Geodesy of the Graz University of Technology
7. Center for Space Research, University of Texas at Austin

Since the end of 2013, the GPS data collected by the Swarm constellation, consisting of a lower pair of satellites flying in formation and one higher flying satellite, makes it possible to estimate monthly Earth gravity field models that represent large-scale mass transport processes, relevant also for improving our understanding of Earth's climate. With the support of the European Space Agency and the International Combination Service for Time-variable Gravity Fields (COST-G), a team from the Astronomical Institute of the University of Bern, the Astronomical Institute of the Czech Academy of Sciences, the Delft University of Technology, the Institute of Geodesy of the Graz University of Technology and the School of Earth Sciences of the Ohio State University publishes these models on a quarterly basis. The models are independent of any other source of gravimetric data and are free of a priori temporal and spatial correlations. The models are produced from different gravity inversion strategies, combined into a final model at the solution level, and they have been demonstrated to be consistently of higher quality.

These models represent land surface mass changes with a ~30-50% better agreement than in ocean areas, when compared to a GRACE/GRACE-FO-derived parametric model. We present the time series of large water storage basins and illustrate the good agreement with dedicated gravimetric data, showing crucial continued monitoring across the gap between GRACE and GRACE-FO. Moreover, the Swarm monthly gravity field solutions help validating the accuracy of the initial GRACE-FO data with transplanted onboard accelerometer modeling over various regions of the world.

Key words Swarm, gravity, mass transport, hl-sst

Category: Symposium 2b: Earth's Time-variable Gravity Field =》 2b.1: Analysis Techniques

211

S2b-002

Status of temporal gravity field modeling at HUST

Hao Zhou、 Zhicai Luo、 Lijun Zheng、 Yaozong Li、 Kang Wang
Huazhong University of Science and Technology

The way to reach the prelaunch baseline accuracy is still one of crucial issues for GRACE temporal gravity field model determination. In this work, we will present the current progress of GRACE temporal gravity field modeling at Huazhong University of Science and Technology (HUST). Based on the previous work related to HUST-Grace2019, we update our software via the new background force models (mainly include the AOD RL06 and linear mean pole model) and the new L1B V03 dataset. The updated force models have passed the so-called benchmark test, i.e., our force models agree with those packages in the COST-G service at a level of less than $10\text{--}11\text{ ms}^{-2}$. Using the updated force models and dataset, the new developed model HUST-Grace2020 shows superior performance than our HUST-Grace2019 model, and comparable performance of the official RL06 model developed by SDS.

Acknowledgement: This research was funded by the National Key Research and Development Program of China (No. 2018YFC1503503, 2018YFC1503504) and the National Natural Science Foundation of China (No. 41931074, 42074018, 42061134007, 41704012)

Key words GRACE; Temporal gravity field model; HUST; new force model; new dataset

Category: Symposium 2b: Earth's Time-variable Gravity Field => 2b.1: Analysis Techniques

243

S2b-003

Angular velocity recovery method based on satellite gravity gradient measurement based on quaternion joint of astrometry

Yunlong Wu

Institute of seismology, China Earthquake Administration

In the preprocessing of L1b data in satellite gravity gradient measurement, the satellite inertial angular rate needs to be accurately measured to recover the high-precision gravity gradient component. The traditional method calculates the angular velocity noise of a single star tracker's attitude data is relatively large and will be transmitted to other angular velocity components, thereby affecting the calculation accuracy of the entire gravity gradient component. Based on the noise characteristics of the star tracker, this paper constructs the noise distribution weighting matrix of each axis of the star tracker, and jointly solves the best attitude quaternion of the attitude quaternions of two or more star trackers, and provides precise attitude control for the subsequent angular velocity recovery. The calculation results show that the angular rate of the star tracker calculated by the implementation of the multi-star tracker joint method has achieved a significant improvement in the entire power spectral density. Compared with the single star tracker calculation method, multiple star tracker in joint optimal attitude angular rate data component w_y , w_z accuracy reached 10^{-5} orders of magnitude, and will not be single star tracker visual axis component measurement accuracy is low, the influence of can effectively restrain the error caused by the coordinate transformation of variable transmission, at the same time, based on the star tracker joint method to calculate the gravity gradient tracing value, compared with the single star tracker method, shows more significant improvements.

Key words Star trackers; Attitude quaternion calibration; Attitude quaternion combination; Satellite gravity gradiometry

Category: Symposium 2b: Earth's Time-variable Gravity Field =» 2b.1: Analysis Techniques

268

S2b-004

Time-variable Gravity Signals in Reprocessed GOCE Gradient Data

Betty Heller¹、 Frank Siegismund¹、 Roland Pail¹、 Thomas Gruber¹、 Roger Haagmans²

1. Technical University of Munich

2. European Space Agency

The 2018/2019 reprocessing of the satellite gravitational gradiometry (SGG) data from the Gravity field and steady-state Ocean Circulation Explorer (GOCE) satellite mission reduced the low-frequency noise in the data. This resulted in a noise reduction in derived gravity field models at spatial scales of several 100 km, at which the temporal variations of the Earth's gravity field have their largest amplitudes. In this contribution, the reprocessed GOCE SGG data are tested for their ability to resolve temporal gravity signals such as glacier melting and earthquake-induced mass displacement signals. For the gravity field processing, we apply and compare a conventional spherical harmonics (SH) approach using the time-wise processing method, and a mass concentration (mascon) approach that uses point masses as base elements, which are grouped to land or ocean mascons by taking into account the coastlines. Although their global signal-to-noise ratio is smaller than 1, SH GOCE SGG-only models resolve the strong regional signals due to the deglaciation in Greenland and Antarctica and the 2011 moment magnitude 9.0 earthquake in Japan, thereby providing an estimation of these gravity signals that is independent of Gravity Recovery and Climate Experiment (GRACE) data. Based on the ice mass trend signals in Greenland and Antarctica, the benefit of combined GRACE/GOCE SGG models is tested. We show that the incorporation of GOCE SGG data does not provide a signal contribution additional to the GRACE models, but a numerical stabilization of the related normal equation systems.

Key words GOCE; time-variable gravity; combination; mascon; spherical harmonics; satellite gravitational gradiometry

Category: Symposium 2b: Earth's Time-variable Gravity Field =» 2b.1: Analysis Techniques

269

S2b-005

HUST-ERA5: A new 1-hourly atmosphere de-aliasing product for satellite gravity mission

Fan Yang, Zhicai Luo

Huazhong University of Science and Technology

The current state-of-the-art of satellite gravity data processing makes use of de-aliasing products to reduce high-frequency mass anomalies. For example, the most recent official Atmosphere and Ocean De-aliasing products (AOD1B-RL06) are applied for the Gravity Recovery and Climate Experiment (GRACE) and GRACE-Follow On (GRACE-FO) missions. The temporal resolution of AOD1B-RL06 is 3 hours, and spectrally, they are computed up to degree and order 180. In this study, we explore a refined, i.e., geometrically, physically, and numerically improved, mass integration approach that is important for computing the atmosphere part of these products. Besides, the newly available ERA-5 climate data are used to produce a new set of non-tidal atmosphere de-aliasing product (HUST-ERA5) that is computed hourly up to degree and order 100, covering 2002 onwards. Despite an overall agreement with AOD1B-RL06 (correlation>0.99), considerable discrepancies still exist between HUST-ERA5 and AOD1B-RL06. The possible reasons are therefore analyzed, and we find the input climate data, sampling rate and integration method may result in a product difference of ~0.3, ~0.15 and ~0.05 millimeter geoid height, respectively. The total differences between HUST-ERA5 and AOD1B-RL06 can lead to a mean variation of ~7.34 nm/s on the LRI (Laser Ranging Interferometry) range-rate residuals, for example during January 2019, which is already close to the LRI precision. This impact is invisible for the GRACE(-FO) gravity inversion because of the less accurate on-board KBR (K-band ranging) instrument, however, it will be non-negligible and should be considered when the LRI completely replaces the KBR in the future gravity missions.

Acknowledgement: The authors acknowledge financial supports through the National Natural Science Foundation of China (Grant No.41804016 and Grant No.41931074), and National Key Research Development Program of China with project No.2018YFC1503503.

Key words AOD, ERA5, Gravity mission, GRACE(-FO)

Category: Symposium 2b: Earth's Time-variable Gravity Field =» 2b.1: Analysis Techniques
289
S2b-006

Treatment of ocean tide background model errors in GRACE/GRACE-FO data processing

Petro Abrykosov¹, Roman Sulzbach^{2,3}, Roland Pail¹

1. Institut für Astronomische und Physikalische Geodäsie, Technische Universität München, Arcisstraße 21, 80333 München
2. Deutsches GeoForschungsZentrum (GFZ), Telegrafenberg, 14473 Potsdam
3. Institut für Meteorologie, Freie Universität Berlin (FUB), Carl-Heinrich-Becker-Weg 6-10, 12165 Berlin

Due to its high-frequency, high-amplitude nature the ocean tide (OT) signal poses a core limitation within the GRACE/GARCE-FO data processing, as its temporal undersampling ultimately results in the typical striping pattern. To some degree this issue can be resolved by employing a-priori de-aliasing based on an OT background model. However, due to model errors and imperfections some residual effects inevitably remain within the resulting gravity product.

So far, the background models have been assumed as error-free within the data processing. Since ocean tide models feature distinct, time-invariant spatial error patterns (low uncertainties in open oceans, high uncertainties in coastal and high-latitude regions), it is reasonable to assume that weighting the observations based on the underlying spatial error shall result in a more homogenous gravity solution.

Thus, error co-variance matrices are derived for the spherical harmonic coefficients representing the eight principal tides based on a set of five modern-day OT models and propagated onto the level of observations. This error information is then employed within the least-squares parameter estimation for the final gravity product. The functionality of this approach is verified through closed-loop simulations and its limitations are discussed.

Key words GRACE, GRACE-FO, de-aliasing, ocean tides, background models

Category: Symposium 2b: Earth's Time-variable Gravity Field =» 2b.1: Analysis Techniques

440

S2b-007

Combination Service for Time-variable Gravity fields (COST-G): operations and new developments

Ulrich Meyer¹、 Martin Lasser¹、 Adrian Jäggi¹、 Frank Flechtner⁴、 Christoph Dahle⁴、
Eva Boergens⁴、 Christoph Förste⁴、 Torsten Mayer-Gürr⁷、 Andreas Kvas⁷、 Saniya
Behzadpour⁷、 Jean-Michel Lemoine⁹、 Stephane Bourgoigne¹⁰、 Igor Koch¹²、 Jakob
Flury¹²、 Andreas Groh¹⁴、 Annette Eicker¹⁶、 Benoit Meyssignac²、 Ingo Sasgen⁵、
João de Teixeira da Encarnação^{8,18}、 Heike Peter¹¹、 Hao Zhou¹³、 Zhengwen Yan¹⁵、
Qiujie Chen¹⁷、 Xiang Guo³、 Wei Feng⁶、 Changqing Wang⁶

1. University of Bern

2. Laboratoire d'Etudes en Geophysique et Oceanographie Spatiales

3. Wuhan University

4. GFZ German Research Centre for Geosciences

5. Alfred-Wegener-Institute Bremerhaven

6. Chinese Academy of Sciences

7. Graz University of Technology

8. Center for Space Research, University of Texas at Austin

9. Centre National d'Etudes Spatiales

10. Stellar Space Studies

11. PosiTim UG

12. Leibniz University Hannover

13. Huazhong University of Science and Technology

14. Technical University of Dresden

15. Southern University of Science and Technology

16. HafenCity University Hamburg

17. Tongji University Shanghai

18. Delft University of Technology

Since its start of operations in July 2019, IAG's Combination Service for Time-variable Gravity fields (COST-G) has been providing a complete time-series of combined monthly gravity fields from GRACE, as well as regularly updated time-series of monthly gravity fields derived from kinematic Swarm orbits. Starting November 2020, the COST-G product line has been extended by a time-series of operationally combined, monthly updated GRACE-FO gravity fields. All these combinations are performed by variance component estimation at solution level.

We report on new developments, such as a planned extension of COST-G to include GRACE and GRACE-FO analysis centres from China, a revisit of the combination strategy to better focus on the range of spherical harmonic coefficients most relevant for the users, and the potential application of COST-G products for orbit determination of altimeter satellites.

Key words GRACE, GRACE-FO, Swarm, satellite gravimetry, gravity field combination

Category: Symposium 2b: Earth's Time-variable Gravity Field =» 2b.1: Analysis Techniques

532

S2b-008

On the combination of gravity field time series derived from kinematic positions of Low Earth Orbiting satellites

Thomas Grombein, Martin Lasser, Daniel Arnold, Ulrich Meyer, Adrian Jäggi
Astronomical Institute, University of Bern

The Earth's time-variable gravity field provides important information for the monitoring of changes in the Earth's system. Dedicated satellite missions like GRACE and GRACE-FO use ultra-precise inter-satellite ranging observations to derive time series of monthly gravity field solutions. Alternative gravity field information can be obtained from the analysis of GPS-based kinematic orbit positions of Low Earth Orbiting (LEO) satellites. Although this technique is less sensitive, it can provide mostly uninterrupted time series, which is particularly valuable for those months where no inter-satellite ranging measurements are available from GRACE or GRACE-FO. Furthermore, the increasing number of operational LEO satellites makes it attractive to produce combined Multi-LEO gravity field solutions that will take advantage of a large number of observations and the variety of complementary orbital configurations. At the Astronomical Institute of the University of Bern (AIUB) GPS-based kinematic orbits have been generated for various LEO satellites like GRACE and GOCE or are routinely processed for operational missions like GRACE-FO, SWARM, Sentinel or Jason. In this contribution, we will use these kinematic LEO positions to perform gravity field recovery with the Celestial Mechanics Approach and to derive monthly gravity field time series. By evaluating mass trends and changes in Greenland, Antarctica and the Amazon river basin, the time series of different LEOs are compared with respect to superior solutions based on inter-satellite ranging. Finally, we will combine the gravity field solutions of different LEO satellites either on solution level using variance component estimation or on normal equation level and investigate their individual contribution and the additional value of the combination.

Key words time-variable gravity field, combination, Low Earth Orbiting satellites, GRACE/-FO, Celestial Mechanics Approach

Category: Symposium 2b: Earth's Time-variable Gravity Field =» 2b.1: Analysis Techniques

557

S2b-009

Combined gravity solution from SLR and GRACE/GRACE-FO

Zhigui Kang, John Ries, Srinivas Bettadpur, Himanshu Save
Center of Space Research, The University of Texas at Austin

The recovery of Earth's time variable gravity field from satellite data relied heavily on Satellite Laser Ranging (SLR) before missions like the Gravity Recovery and Climate Experiment (GRACE) and GRACE Follow-On (FO). Currently, the monthly gravity solutions from GRACE/GRACE-FO provide amazing information about the temporal variations of gravity field. However, there are some low-degree coefficients derived from GRACE/GRACE-FO that are unreliable, primarily due to various issues with the accelerometer data. These low-degree coefficients, on the other hand, can be reasonably well determined using SLR data and can be used to replace the unreliable values from GRACE/GRACE-FO. Currently, the coefficients C20 and C30 from GRACE-FO monthly gravity solution, are replaced by SLR-based estimates, but a more rigorous and consistent approach is to combine SLR and GRACE/GRACE-FO directly. This study presents some combination strategies for gravity field recovery from SLR and GRACE-FO combined at the information equation level with optimal weighting. Preliminary results show that the combined products are improved in comparison with the nominal GRACE-FO solutions.

Key words GRACE , GRACE-FO, SLR, Time-variable Gravity Field

Category: Symposium 2b: Earth's Time-variable Gravity Field => 2b.1: Analysis Techniques

564

S2b-010

Determination of Terrestrial Water Storage without Stripes using Grace-Like Geopotential Models

Hussein Abd-Elmotaal, Ayman Hassan, Mostafa Abd-Elbaky
Minia University, Faculty of Engineering, Civil Engineering Department

GRACE and GRACE-FO are considered highly valuable tools to monitor mass redistribution within the Earth's system with a spatial resolution of ~300 km (half wavelength). This can be used to estimate water storage changes over an entire region or basin, with higher accuracy at larger spatial scales. GRACE-like geopotential models have been developed by employing time-dependent harmonic coefficients of the global gravity field models. The GRACE-like models can also be used to estimate the water storage changes. The advantage of using the GRACE-like coefficients to estimate water storage changes is that no smoothing is needed. Therefore, no signal attenuation will take place. The GRACE/GRACE-FO and GRACE-like models are compared at the frequency domain as well as at the space domain (TWS). The results are shown and widely discussed.

Key words GRACE, GRACE-FO, time-dependent harmonic coefficients, GRACE-like, Terrestrial Water Storage (TWS)

Category: Symposium 2b: Earth's Time-variable Gravity Field =» 2b.1: Analysis Techniques

615

S2b-011

Data-Driven Self-De-Aliasing approach for monthly GRACE and GRACE-FO gravity retrieval

Michael Murböck¹、Petro Abrykosov²、Christoph Dahle³、Frank Flechtner^{1,3}、
Roland Pail²

1. TU Berlin

2. Technical University of Munich

3. GFZ German Research Center for Geosciences

The NASA-GFZ GRACE-FO mission is successfully continuing the GRACE time series of mass transport measurements. In addition to continuity, the international Earth system science community is seeking for improved accuracy as well as improved spatial and temporal resolutions of mass transport data. Therefore the research unit NEROGRAV (New Refined Observations of Climate Change from Spaceborne Gravity Missions), funded by the Deutsche Forschungsgemeinschaft, is currently investigating the capability of improving mass transport data from GRACE, GRACE-FO and the Next Generation Gravity Mission.

In this talk, we present the main outcome of the real data analyses on improving the spatio-temporal parameterization, which is one of the main objectives of NEROGRAV. Based on promising simulation results, a data-driven self-dealiasing approach for monthly GRACE and GRACE-FO gravity retrieval is investigated. In contrast to an earlier published method by Wiese et al. (2011), where gravity field parameters of high temporal and low spatial resolution are co-estimated, we assess the use of daily GRACE/GRACE-FO gravity fields as additional de-aliasing products. This additional de-aliasing product is then used in the standard GFZ GRACE/GRACE-FO Level-2 processing scheme to reduce temporal aliasing errors.

We show results based on different daily solutions with different weighting and filtering schemes in terms of the signal content of the daily solutions themselves and of the effects on the monthly solution. The results are discussed in the spectral and spatial domain for time series of monthly GRACE and GRACE-FO solutions in comparison with the standard GFZ RL06 solutions. Using this new approach, the noise in high spherical harmonic degrees and orders is significantly reduced.

Wiese D, Visser P, Nerem R (2011) Estimating low resolution gravity fields at short time intervals to reduce temporal aliasing errors, *Advances in Space Research*, 48 (6), p1094-1107, DOI 10.1016/j.asr.2011.05.027

Key words GRACE/GRACE-FO gravity retrieval; data-driven de-aliasing; daily solutions

Category: Symposium 2b: Earth's Time-variable Gravity Field =» 2b.1: Analysis Techniques

686

S2b-012

LOW-DEGREE GRAVITY FIELD ESTIMATION FROM THE SLR DATA PROCESSING OF SPHERICAL SATELLITES

Linda Geisser, Ulrich Meyer, Thomas Grombein, Daniel Arnold, Adrian Jäggi
Astronomical Institute Of The University Of Bern, Switzerland

Nowadays, the determination of the time-variable Earth's gravity field is mostly based on dedicated gravimetry satellite missions, i.e., Gravity Recovery And Climate Experiment (GRACE) and GRACE Follow-on. Nevertheless, some of the low-degree gravity field coefficients, especially the zonal harmonic coefficient C_{20} , and C_{30} in case of GRACE Follow-On, can be better determined by the geodetic technique of Satellite Laser Ranging (SLR). In this study, multi-satellite SLR solutions are analyzed, where the orbits are determined in 7-day arcs together with spherical harmonic (SH) coefficients of the Earth's gravity field up to d/o 4/4. We investigate the optimal orbit parametrization to simultaneously estimate the SH coefficients with station coordinates and other geodetic parameters as the Earth Rotation Parameters (ERPs), namely the polar motion and length-of-day. Hence, these solutions cover all 'three pillars' of geodesy, i.e., geokinematics, Earth rotation and the Earth's gravity field, and ensure a highest possible level of consistency. We analyze the quality of all parameters by internal and external quality metrics, e.g., by comparing the co-estimated SH coefficients with the COST-G Level-2 products and GPS-only gravity field solutions from Swarm, GRACE/GRACE-FO and their combination.

Key words low-degree gravity field coefficients, Satellite Laser Ranging

Category: Symposium 2b: Earth's Time-variable Gravity Field =» 2b.1: Analysis Techniques

696

S2b-013

On Validating the Swarm Data to Fill-in the GRACE/GRACE-FO Gap Employing Artificial Neural Networks Applied to Africa

Hussein Mohasseb¹、WenBin Shen²、Mostafa Ashry¹、Hussein Abd-Elmotaal³

1. State Key Laboratory of Information Engineering in Surveying, Mapping and Remote Sensing (LIESMARS), Wuhan University, Wuhan, China

2. School of Geodesy and Geomatics, Wuhan University, Wuhan, China

3. Civil Engineering Department, Faculty of Engineering, Minia University, Minia, Egypt

The missions Gravity Recovery and Climate Experiment (GRACE) and the GRACE Follow-On (GRACE-FO) and the mission Swarm play an important role for study of the Earth's gravity field with unprecedented high-precision and high-resolution measurements. The aim of our study is to use Swarm data to fill-in the data-gap between GRACE and GRACE-FO missions from July 2017 to May 2018 employing the artificial Neural Networks. The artificial Neural networks are used to fit the Swarm data to GRACE/GRACE-FO data, and hence to fill-in the GRACE data gaps. An artificial model is created using the GRACE data. Four hidden layers are used in the fitting process. Africa has been chosen as the area of study. We used the available data from the triple GRACE processing centers CSR, GFZ and JPL, in addition to the Swarm TVGF data provided by the Czech Academy of Sciences (ASU) and the International Combination Service for Time-variable Gravity (COST-G). The GRACE and Swarm data are tested in the frequency and space domains. For the frequency domain, the data were assessed in two different levels: the potential degree variances and the harmonic coefficients themselves. To evaluate the adopted fitting process, an artificial gap - simulating the gap between GRACE and GRACE-FO – has been made in the GRACE data from July 2015 to May 2016, and the Swarm-detrended model has been compared versus the GRACE data at that period. The results are presented and deeply discussed. This study is supported by the National Natural Science Foundations of China (NSFC) under Grants 42030105, 41721003, 41804012, 41631072, 41874023, Space Station Project (2020)228.

Key words GRACE, GRACE-FO, Swarm, Artificial Neural Network, TWS

Category: Symposium 2b: Earth's Time-variable Gravity Field =» 2b.1: Analysis Techniques

747

S2b-014

High-precision Light Time Correction Model in GRACE and GRACE Follow-On Mission

Yihao Yan^{1,3}、 Vitali Müller²、 Changqing Wang³、 Min Zhong^{3,4}、 Wei Feng^{3,4}、 Lei Liang³

1. School of Physics, Huazhong University of Science and Technology, Wuhan, 430074, China
2. Max-Planck-Institut für Gravitationsphysik (Albert-Einstein-Institut) and Institut für Gravitationsphysik of Leibniz Universität Hannover, 30167 Hannover, Germany
3. Innovation Academy for precision Measurement Science and Technology, CAS, Wuhan, 430077, China
4. School of Geospatial Engineering and Science, Sun Yat-Sen University, Zhuhai, 519082, China

The GRACE/GRACE-FO mission is a revolutionary advancement in gravity field measurement. It provides for the first time high-precision, all-weather global, mid-to-long space-scale and monthly resolution time-varying gravity field information. The key observation is the biased inter-satellite range, which is measured primarily by a K-Band Ranging system (KBR) in GRACE and GRACE Follow-On. The GRACE Follow-On satellites are additionally equipped with a Laser Ranging Interferometer (LRI), which provides measurements with lower noise compared to the KBR. The true propagation time of microwaves or lasers between satellites is delayed by the high-speed movement of satellites, the residual atmosphere in the space, and path curvature caused by the effect of general relativity, the differences between the true propagation time and the instantaneous propagation time is called light time correction (LTC). We revisit the calculation of the LTC from the photon motion equation considering general relativistic effects and state-of-the-art models of Earth's potential field. The novel analytical expressions for the LTC of KBR and LRI can circumvent numerical limitations of the classical approach. The dependency of the LTC on geopotential models and on the parameterization is studied, and afterwards the results are compared against the LTC provided in the official datasets of GRACE and GRACE Follow-On. It is shown that the new approach has a significantly lower noise, well below the instrument noise of current instruments, especially relevant for the LRI, and even if used with kinematic orbit products. This allows calculating the LTC accurate enough even for the next generation of gravimetric missions and even other space missions.

Key words GRACE, GRACE-FO, Light time correction, general relativity

Category: Symposium 2b: Earth's Time-variable Gravity Field =» 2b.1: Analysis Techniques

792

S2b-015

Evaluating the regional reanalysis COSMO REA6 vs ERA Interim for dealiasing analysis of the GRACE/GRACE-FO Datasets

Shashi Dixit, Petra Freidrichs, Andreas Hense
MIUB, Institute of Geosciences, University of Bonn

This work is a part of German Research Foundation (DFG) Research Group (RG) "New Refined Observations of Climate Change from Spaceborne Gravity Missions (NERO GRAV)". The RG develops new analysis methods and modeling approaches to improve the observations of the GRACE and GRACE-FO mission. The RG central hypothesis is: by Improvement and better understanding of -sensor data, - background dealiasing models, - processing strategies of satellite gravimetry, the mass transport and mass variations time series obtained from satellite gravimetry can be significantly increased.

The aim of the presentation is (1). Transform the idealised COSMO-REA6 simulations to the realistic world representation for a better comparability with the satellite observations (2). To evaluate and assess scale effects of the all processes being simulated in a regional, high resolution, non-hydrostatic model with respect to its representation of the atmospheric mass. The analysis puts an emphasis on the contributions of the atmospheric hydrological cycle and the non-hydrostatic effects in two views: the systematic mass effects based on the differences of means of a full year and on variability mass effects based on an EOF analysis of hourly data. The region considered is the CORDEX (North Atlantic, European region) domain. It is interesting to see non-hydrostatic case because very few studies are available in this context. We also expect that GRACE-FO could be sensitive to the water mass variability because high resolution atmospheric modelling intensifies the water cycle components. This can lead to more localised mass variability of the water component which can have a systematic as well as a variability effect.

Key words GRACE-FO, Background Daalising models

Symposium 2b: Earth's Time- variable Gravity Field

S2b.2: Spaceborne and terrestrial gravimetry for hydrology

Category: Symposium 2b: Earth's Time-variable Gravity Field => 2b.2: Spaceborne and terrestrial gravimetry for hydrology

136

S2b-016

Sub-regional groundwater storage recovery in North China Plain after the South-to-North water diversion project

Chong Zhang¹、Qingyun Duan²、Pat J.-F. Yeh³、Yun Pan⁴

1. Beijing Normal University

2. Hohai University

3. Monash University (Malaysia Campus)

4. Capital Normal University

The South-to-North water diversion Middle Route Project (MRP) is expected to alleviate the long-term groundwater storage (GWS) depletion in North China Plain (NCP) after the beginning of its operation in December 2014. This study aims to investigate the effect of MRP on GWS by comparing GWS changes before (2003–2014) and after (2015–2018) the MRP operation. The analysis was conducted by using groundwater level data from 617 wells in NCP, and then evaluated against satellite-based water storage data from Gravity Recovery and Climate Experiment (GRACE) and its Follow-On missions. On average in NCP, a decreasing trend of -19.1 ± 5.1 mm/yr was seen in GWS based on well observations during 2003–2014, but a recovery trend of $+1.8 \pm 0.7$ mm/yr was found during 2015–2018. The GWS recovery was most prominent in subregions where groundwater over-utilization had occurred in NCP. GRACE exhibited the capacity to detect the regional GWS depletion during 2003–2014, but difficult to distinguish the sub-regional GWS recovery during 2015–2018. The potential causes for GWS recovery were found to be complicated, not only caused by the reduction of groundwater pumping as accelerated by MRP-diverted water, but also the increasing precipitation recharge of aquifers and the enhanced management of groundwater system. The findings highlight that GWS in NCP has started a gradual transition from unsustainable depletion to sub-regional recovery as benefit from the MRP water diversion.

Key words Groundwater recovery, Groundwater depletion, GRACE, South-to-North water diversion, North China Plain

Category: Symposium 2b: Earth's Time-variable Gravity Field => 2b.2: Spaceborne and terrestrial gravimetry for hydrology

233

S2b-017

Gravity response to a monsoonal rain event in the Pingtung Plain, southern Taiwan

KUAN-HUNG CHEN, Cheinway Hwang
National Yang Ming Chiao Tung University

We installed an absolute gravity site to monitor gravity changes due to groundwater changes in an aquifer system in Pingtung, a county in southern Taiwan, for 1.5 years since May 2019. The annual peak-to-peak gravity change here was 135 μgal as recorded by the absolute gravimeter. A monsoonal rain in May 2020 introduced large gravity changes from our hourly gravity measurements during this rain event. In the first 30 hours of this event, the total rainfall was 397 mm, followed by a rainfall of 178 mm in 10 hours. The gravity changes finally reached 45 μgal and the groundwater level increased by 5 m after 10 days since the event started. Unlike the steady increase of groundwater level, the gravity values underwent three stages of changes: a rapid rise, followed by nearly zero changes for 2 days, and finally a gentle rise consistent with the groundwater level. The rapid gravity rise in the first-stage gravity was caused by the fast and steady accumulated infiltrated water held in the unsaturated zone at the end of the dry season. Thus, our gravity experiment demonstrates that absolute gravity observations can verify the progress of surface water infiltrated into an unsaturated zone to recharge the saturated zone in the aquifer system below the gravity site. Soil water change in a 30-m thickness in the unsaturated zone induced 18 μgal of gravity change during this rain event. A gravity-based aquifer storage coefficient can be overestimated due to varying rates of gravity changes and groundwater level changes right after heavy rains.

Key words gravity, groundwater, rain, recharge, unsaturated zone

Category: Symposium 2b: Earth's Time-variable Gravity Field => 2b.2: Spaceborne and terrestrial gravimetry for hydrology

292

S2b-018

Retrieving daily terrestrial water storage changes based on an independent component analysis-based inversion method

Zhongshan Jiang, Dingfa Huang
Southwest Jiaotong University

Based on the elastic response of the solid Earth to hydrological loads, the Global Navigation Satellite System (GNSS) provides a powerful tool for retrieving temporal and spatial changes of terrestrial water storage on a regional scale. Here, we implement the inversion method based on independent component analysis to examine the changes in water storage and hydrological extremes in Yunnan. Our time-varying inversion can reproduce the temporal and spatial evolutionary history of terrestrial water storage changes. Three independent components (ICs) are selected in the time-varying inversion model. The first two ICs contribute to 93.3% and 5.8% of the data variance, respectively, and they both reveal the annual water storage changes at different temporal scales. The third IC slightly explains the network time series and shows the spatial signals related to latitude. The multi-annual seasonal average water storage changes based on GNSS, GRACE, and GLDAS have good consistency in the spatial pattern. All the data show that from the northeast to the southwest, seasonal water storage changes show a gradually increasing trend. The annual peak amplitude in the water thickness inferred by GNSS is larger than the annual peak amplitude of the GLDAS and GRACE models. The GNSS results also indicate that the drought event in 2019 is most serious according to the lowest amplitude of terrestrial water storage. Daily water estimates under both wet and dry conditions have a good correlation between GNSS- and GLDAS-based results, which also agree with rainfall anomalies. Our research results confirm that a GNSS network can remotely monitor the daily evolution of water storage associated with extreme weather. These findings can further broaden the applications in operational hydrological monitoring and contribute to understanding climate extremes.

Key words GNSS; Hydrologic loading; Terrestrial water storage; Hydrometeorological extremes; Drought characterization

Category: Symposium 2b: Earth's Time-variable Gravity Field => 2b.2: Spaceborne and terrestrial gravimetry for hydrology

311

S2b-019

Quantifying water storage change over Lake Baikal using GRACE and GRACE Follow-On

Min Wei、 Hao Zhou、 Zhicai Luo、 Min Dai、 Siyou Xu
Huazhong University of Science and Technology

As the largest and deepest freshwater lake in the world, the changes of water storage over Lake Baikal have significant impacts on its surrounding ecological environment. In this study, GRACE and GRACE Follow-On (GRACE-FO) products are used to quantify the terrestrial water storage (TWS) variations over Lake Baikal during 2003-2020. To improve the accuracy of the TWS estimates over Lake Baikal, a modified forward-modeling method is introduced, and the simulation results demonstrate the reliability of our method in retrieving TWS variations over this region. Based on the RL06 products of GRACE and GRACE-FO, the TWS in Lake Baikal shows completely opposite trend between 2014-2016 and 2017-2020. The driving factors of this unique characteristic are then discussed.

Acknowledgement: This research was funded by the National Key Research and Development Program of China (No. 2018YFC1503503, 2018YFC1503504) and the National Natural Science Foundation of China (No. 41931074, 42074018, 42061134007, 41704012)

Key words GRACE and GRACE Follow-On, Lake Baikal, forward-modeling method, terrestrial water storage

Category: Symposium 2b: Earth's Time-variable Gravity Field => 2b.2: Spaceborne and terrestrial gravimetry for hydrology

316

S2b-020

Reconstructing Climate-driven Water Storage Anomalies using GRACE Satellite Data

Bingshi Liu^{1,2}, Xiancai Zou¹, Shuang Yi², Nico Sneeuw², Jianqing Cai²,
Jiancheng Li¹

1. School of Geodesy and Geomatics, Wuhan University, Wuhan, China

2. Institute of Geodesy, University of Stuttgart, Stuttgart, Germany

Hydrological changes, which are affected by climate variability and human activities, pose challenges to the sustainable management and conservation of water resources. As such, it is important to improve our understanding of how climate and anthropogenic activities impact land water storage. Previous studies using Gravity Recovery and Climate Experiment (GRACE) satellite data have struggled to effectively separate the impacts of climate variability and human activities on water storage. Here, we propose a statistical model that simulates natural dynamically driven changes in water storage to reconstruct climate-driven water storage anomalies (CWSAs) at basin scales. The proposed model shows a good performance for both predicting and reconstructing CWSAs. Compared with water storage anomalies calculated using land surface models, our reconstruction results are closer to GRACE observations, especially in humid basins with few human interventions. The median of correlation coefficient and Nash–Sutcliffe efficiency of reconstructed CWSAs in 55 basins are 0.89 and 0.71, respectively. And these results are similar to the results based on machine learning-based methods. Our method presents a viable alternative to machine learning-based methods for bridging the data gap between GRACE and GRACE-Follow on missions and for extrapolating water storage anomaly outside of the GRACE period in basins where water storage changes are dominated by climate variability. The results of this study provide a method to effectively reconstruct and monitor CWSAs, thereby providing information for better protection and utilization of water resources.

Key words GRACE; Reconstruction; Water storage anomaly; Climate variability;

Category: Symposium 2b: Earth's Time-variable Gravity Field => 2b.2: Spaceborne and terrestrial gravimetry for hydrology

400

S2b-021

Reconstruction of Water Storage Change and Drought Monitoring in the Yangtze River Basin Combining Satellite Gravity and Hydrological Data

Xiaolong Li, Taoyong Jin
Wuhan University

Terrestrial Water Storage Change is one of the most important part of global water cycle. Compared with traditional approach, the method based on GRACE and GRACE-FO satellites provides a new idea for obtaining large-scale water storage change series. However, there is an 11-months interval between GRACE and GRACE-FO missions, which affects the continuity analysis of water storage changes. So, we propose a simple algorithm to complete this gap period based on the characteristics of water balance in the basin combining with multi-source hydrometeorological data. Validation results show that the reconstruction method has high stability and accuracy. The reconstructed time series not only accurately reflected the long-term water storage change of the Yangtze River basin, but also monitored the drought event in the southern part of the Jinshajiang River basin in the spring of 2018. Further research shows that not only the reconstruction method has strong predictive potential for TWSC, but when the input month is more than 90, the prediction accuracy will converge to a very high level (the correlation coefficient is about 0.92).

Based on reconstructed TWSC series, the GRACE drought index (GRACE-DSI) was obtained, and used to identified the drought events in the Yangtze River basin using the run theory effectively. Results show that from GRACE-DSI, there were 17 severe drought events in the Yangtze River basin from 2002 to 2020, among which the most severe drought occurred in the middle-lower Yangtze River basin and part of the upper reaches during the winter of 2010 to the winter of 2011. This drought lasted 13 months, and the intensities of GRACE-DSI and SPI reached 18.23 and 6.63, respectively. The drought reached the vertices in April and May 2011, that 56.25% and 58.23% regions of the Yangtze River basin reached the standard of extreme drought, respectively, and the proportions were reached to 96.31% and 94.64% in the middle-low Yangtze River basin.

Key words the Yangtze River basin; GRACE; GRACE-FO; Terrestrial Water Storage Change; reconstruction; drought monitoring

Category: Symposium 2b: Earth's Time-variable Gravity Field => 2b.2: Spaceborne and terrestrial gravimetry for hydrology

416

S2b-022

Inversion of Regional Surface Mass Anomalies using GRACE Geopotential Differences Based on Slepian Basis Functions

Jiangtao Tan¹、Bo Zhong^{1,2}、Xianpao Li¹、Tao Liu¹

1. School of Geodesy and Geomatics, Wuhan University, 129 Luoyu Road, Wuhan 430079, China

2. Key Laboratory of Geospace Environment and Geodesy, Ministry of Education, Wuhan University, 129 Luoyu Road, Wuhan 430079, China

Surface mass anomalies estimated by mascon approach using GRACE Level-1B data generally present higher spatial resolution than the spherical harmonic solutions, due to the longitudinal stripes and high-frequency noise are suppressed by applying constraints. However, it is a great challenge to mascon approach in regional surface mass anomalies inversion that the process of downward continuation from satellite altitude to the Earth's surface will amplify the noises of gravity signal and cause serious ill-posed problem. Hence, we present an improved mascon approach based on the Slepian basis functions to invert regional surface mass anomalies by using GRACE intersatellite geopotential differences. Firstly, the surface mass anomalies are expressed as the Slepian coefficients and corresponding Slepian basis functions. With the concentration of gravity signals in the region of interest, the advantage of Slepian localization is that it can fully express regional surface mass anomalies with less Slepian coefficient. Secondly, the Slepian coefficients are estimated as intermediates through the linear relationship between GRACE geopotential differences and surface mass anomalies by using constraints. Finally, surface mass anomalies can be recovered from the estimated Slepian coefficients and corresponding Slepian basis functions. Because fewer Slepian coefficients were estimated during the inversion, the ill-posed problem would be weaker and the recovered surface mass anomalies were more stable and reliable. To demonstrate the effectiveness of our improved method, we carried out a closed-loop simulation experiment on the inversion of surface mass anomalies over South America by using GRACE intersatellite geopotential differences simulated from GLDAS hydrological model. The simulation results show that our regional solutions based on Slepian basis functions are closer to the true GLDAS-derived surface mass anomalies, compared to the tradition spherical harmonic solutions.

Key words regional surface mass anomaly; Slepian basis function; geopotential difference; mascon solution; GRACE

Category: Symposium 2b: Earth's Time-variable Gravity Field => 2b.2: Spaceborne and terrestrial gravimetry for hydrology

504

S2b-023

Drought Events over the Amazon River Basin (1993-2019) as Detected by the Climate-driven Total Water Storage Change

Kunjun Tian、 Zhengtao Wang、 Fupeng Li、 Yu Gao、 Yang Xiao、 Cong Liu
Wuhan University

The Gravity Recovery and Climate Experiment (GRACE) mission has measured total water storage change (TWSC) and interpreted drought patterns in an unparalleled way since 2002. Nevertheless, there are few sources that can be used to understand drought patterns prior to the GRACE era. In this study, we extended the gridded GRACE TWSC to 1993 by combining principal component analysis (PCA), least square (LS) fitting, and multiple linear regression (MLR) methods using climate variables as input drivers. We used the extended (climate-driven) TWSC to interpret drought patterns (1993–2019) over the Amazon basin. Results showed that, in the Amazon area with the resolution of 0.5°, GRACE, GRACE follow on, and Swarm had correlation coefficients of 0.95, 0.92, and 0.77 compared with climate-driven TWSCs, respectively. The drought patterns assessed by the climate-driven TWSC were consistent with those interpreted by the Palmer Drought Severity Index and GRACE TWSC. We also found that the 1998 and 2016 drought events in the Amazon, both induced by strong El Niño events, showed similar drought patterns. This study provides a new perspective for interpreting long-term drought patterns prior to the GRACE period.

Key words Amazon river basin; climate-driven; drought; GRACE; GRACE follow on; TWSC

Category: Symposium 2b: Earth's Time-variable Gravity Field => 2b.2: Spaceborne and terrestrial gravimetry for hydrology

505

S2b-024

Using Swarm to Detect Total Water Storage Changes in 26 Global Basins (Taking the Amazon Basin, Volga Basin and Zambezi Basin as Examples)

Zhengtao Wang、 Kunjun Tian、 Fupeng Li、 Si Xiong、 Yu Gao、 Lingxuan Wang、
Bingbing Zhang
Wuhan University

The Gravity Recovery and Climate Experiment (GRACE) satellite provides time-varying gravity field models that can detect total water storage change (TWSC) from April 2002 to June 2017, and its second-generation satellite, GRACE Follow-On (GRACE-FO, <https://gracefo.jpl.nasa.gov/>), provides models from June 2018, so there is a one-year gap. Swarm satellites are equipped with Global Positioning System (GPS) receivers, which can be used to recover the Earth's time-varying gravitational field. Swarm's time-varying gravitational field models (from December 2013 to June 2018) have been solved by the International Combination Service for Time-variable Gravity Field Solutions (COST-G, <https://www.issibern.ch/teams/gravityfieldsolution/>) and the Astronomical Institute of the Czech Academy of Sciences (AUS). on a timely scale, Swarm has the potential to fill the gap between the two generations of GRACE satellites. In this paper, using 26 global watersheds as the study area, first we explored the optimal data processing strategy for Swarm and then obtained the Swarm-TWSC of each watershed based on the optimal results. Second, we evaluated Swarm's accuracy in detecting regional water storage variations, analyzed the reasons for its superior and inferior performance in different regions, and systematically explored its potential in detecting terrestrial water storage changes in land areas. Finally, we constructed the time series of terrestrial water storage changes from 2002 to 2019 by combining GRACE, Swarm, and GRACE-FO for the Amazon, Volga, and Zambezi Basins. The results show that the optimal data processing strategy of Swarm is different from that of GRACE. The optimal results of Swarm-TWSC were explored in 26 watersheds worldwide; its accuracy is related to the area size, runoff volume, total annual mass change, and instantaneous mass change of the watershed itself, among which the latter is the main factor affecting Swarm-TWSC. Knowledge of the Swarm-TWSC of 26 basins constructed in this paper is important to study long-term water storage changes in basins.

Key words GRACE; Swarm; GRACE follow on; gap; TWSC; global basins

Category: Symposium 2b: Earth's Time-variable Gravity Field => 2b.2: Spaceborne and terrestrial gravimetry for hydrology

519

S2b-025

Method for GRACE/GRACE-FO data de-stripe based on image processing perspective

Peng-Hui Wang、 Hao Zhou、 Zhi-Cai Luo、 Lu Tang
Huazhong University of Science and Technology

The unavoidable stripe noise limits the geoscience application scope of GRACE and GRACE Follow-On (GRACE-FO) time-variable gravity field models. How to reduce the stripe noise is still one of the crucial issues for GRACE and GRACE-FO data processing. Heuristic observation shows that the distributions of these stripes have roughly the same pattern, which reminds us that de-stripe processing may draw on the experience of texture removal problem in computer vision or image processing. In the perspective of image processing, all images can be regarded as the superposition of different modal signals. Taking the above considerations, this study attempts to use VMD (Variational Mode Decomposition), CEEMDAN (Complete Ensemble Empirical Mode Decomposition with Adaptive Noise) and other signal decomposition algorithms to decompose the equivalent water height image of GRACE monthly solution to several modal signals. Each signal after decomposition contains different features and meanings. Therefore, deducting the specific modal signals may help eliminate stripe errors. The preliminary results show the potential of this method in removing stripes.

Acknowledgement: This research was funded by the National Key Research and Development Program of China (No. 2018YFC1503503, 2018YFC1503504) and the National Natural Science Foundation of China (No. 41931074, 42074018, 42061134007, 41704012).

Key words GRACE, GRACE Follow-On, Image Processing, De-stripe

Category: Symposium 2b: Earth's Time-variable Gravity Field => 2b.2: Spaceborne and terrestrial gravimetry for hydrology

552

S2b-026

Detect Songhua River Basin Groundwater Spatiotemporal Variation Characteristics by GRACE and Multi-source Hydrological Data

Zhiming XU、 Zhengtao WANG

School of geodesy and geomatics, Wuhan University

Songhua River Basin is located in high latitude area, as one of the most important food-producing areas in China. Exploring and analyzing groundwater reserve changes in this region is of great significance to reveal the characteristics of regional groundwater change, to ensure the sustainable development of the social economy and to protect the regional ecological environment. In this paper, we use GRACE satellite data released by CSR, combined with GLDAS hydrological model and GPM precipitation data to retrieve the groundwater change of Songhua River Basin in the period of 2002-2017. The sustainability index SI is also introduced to detect the spatial and temporal sustainability of groundwater quantitatively before being compared with precipitation, temperature and measured well data. The results show that: In the study period, groundwater of Songhua River Basin increases continuously with the rate of 0.34cm/a, besides the recovery rate of groundwater increases from south to north; Groundwater system of Songhua River Basin shows poor sustainability throughout the period; A significant time lag could be found when the groundwater is compared with precipitation and temperature data; satellite inverse result appears to show the same trend with the in-situ well data and appears to have a time lag between them.

Key words GRACE; Songhua River Basin; groundwater storage; sustainability

Category: Symposium 2b: Earth's Time-variable Gravity Field => 2b.2: Spaceborne and terrestrial gravimetry for hydrology

594

S2b-027

Hydrological Load Effect in the Tibetan Plateau: from GRACE or Hydrological data?

Weilong Rao, Wenke Sun

University of Chinese Academy of Sciences

The uplift state of the Tibetan Plateau (TP) is determined by tectonic deformation and hydrological load deformation. However, it is unknown how much the load effect contributes to the uplift of the plateau. In this study, we used hydrological data to calculate the vertical deformation of the hydrological loading. The results show that the average hydrological load deformation rate is 0.23 ± 0.10 mm/yr. Furthermore, the average uplift rate of the TP estimated from the Global Positioning System (GPS) velocities is 0.90 ± 0.22 mm/yr, so the contribution of the loading to the TP's uplift is 26%. In addition, we used the Gravity Recovery and Climate Experiment (GRACE) spherical harmonic coefficients (SHs) data to estimate the load contribution, and we obtained average load deformation rate of -0.08 ± 0.02 mm/yr. We found that the large difference between the loading values calculated using GRACE data and hydrological data is mainly due to the effect of the tectonic signals. Because the mass changes recovered using GRACE data are not entirely due to the hydrological mass change, and the mass change caused by tectonic movement is obvious on the TP.

Key words the Tibetan Plateau, hydrological load, tectonic deformation, GRACE

Category: Symposium 2b: Earth's Time-variable Gravity Field => 2b.2: Spaceborne and terrestrial gravimetry for hydrology

597

S2b-028

Monitoring groundwater storage change in China by satellite gravimetry

Xiaotao Chang, Guang Zhu, Wei Liu, Miao Zhou, Haozhe Zhang, Qingliang Que
Land Satellite Remote Sensing Application Center, Ministry of Nature Resources

Groundwater is an important nature resource. Being the primary source of fresh water, groundwater storage change and its spatial distribution are vital to its rational utilization. In this study, the groundwater storage change of nine typical regions in China are studied using GRACE and GRACE Follow-On data from 2003 to 2019. Moreover, correlation between meteorological data and groundwater storage change is investigated. Results show that groundwater reserves in most parts of southeastern China has an upward trend, which is recharged mostly by precipitation. In comparison, the loss of groundwater in densely populated areas such as the North China Plain is serious during the study period, for which precipitation can only alleviate the rate. Glacier areas such as the Tianshan Mountains and Nyainqentanglha Mountains have good correlations with temperature anomalies, therefore, glacier melting may be the main reason for mass loss in these areas.

Key words groundwater, storage change, satellite gravimetry

Category: Symposium 2b: Earth's Time-variable Gravity Field => 2b.2: Spaceborne and terrestrial gravimetry for hydrology

617

S2b-029

Recent Changes in Surface and Groundwater in Large Arctic River Basins

Hong Lin、Xiao Cheng、Lei Zheng
Sun Yat-sen University

Surface and groundwater in large Arctic river basins are changing to varying degrees due to significant climate warming and permafrost thawing in Arctic region. Given that Arctic surface and groundwater have major implications for terrestrial hydrology, ocean, ecosystem and economy, it is imperative to assess Arctic surface and groundwater changes. GRACE satellite data has been widely used to evaluate groundwater storage (GWS) changes at large scale. However, groundwater evaluation at basin scale in Arctic are limited. In this study, we derived GWS changes over 15 years (2002–2017) from combining multi-source remote sensing data: GRACE, GlobSnow v3.0 SWE and updated ground-based monitoring runoff data in five large Arctic river basins (Lena, Ob, Yenisei, Mackenzie and Yukon) and calculated the proportion of the main surface water (SW) transition area between 1984 and 2019 in each basin by using JRC Global Surface Water Transition data. Results show decreasing GWS trends of 16 km³ in Lena, 92.6 km³ in Mackenzie and 163.8 km³ in Yukon over 15 years while the increasing GWS trends of 80.1 km³/15 yr and 108.6 km³/15 yr are detected respectively in Ob and Yenisei. Transition proportion results suggest new seasonal and permanent SW are the primary contributors to SW transition in most basins, accounting for more than or near 50% in area of the main transition categories in each basin. Moreover, significant seasonal SW losses of 18.4% in area of the main transition categories and 7.5% in area of basin are discovered in Ob. We infer that these surface and groundwater changes are closely related to Arctic lake and river dynamics, permafrost thawing and development of talik and thermokarst. By using the latest SWE with bias-correction and extending the evaluation period, we also anticipate the groundwater evaluation in this study should be more accurate and insightful.

Key words Arctic, basin, surface water, groundwater, permafrost, GRACE

Category: Symposium 2b: Earth's Time-variable Gravity Field => 2b.2: Spaceborne and terrestrial gravimetry for hydrology

688

S2b-030

Machine Learning approach to study groundwater depletion in Central Valley, California using GRACE and other hydrological data

VIBHOR AGARWAL^{1,5}, Orhan Akyilmaz², CK Shum^{5,6}, Wei Feng⁶, Ehsan Forootan³, Umesh Haritashya¹, Tajdarul Syed⁴

1. Department of Geology and Environmental Geosciences, University of Dayton, Dayton OH, USA
2. Department of Geomatics Engineering, Istanbul Technical University, Istanbul, Turkey
3. Geodesy and Earth Observation Group, Department of Planning, Aalborg University, Aalborg, Denmark
4. Department of Earth Sciences, Indian Institute of Technology Kanpur, Kanpur, India
5. Division of Geodetic Science, School of Earth Sciences, The Ohio State University, Columbus, OH, USA
6. State Key Laboratory of Geodesy and Earth's Dynamics, Innovation Academy for Precision Measurement Science and Technology, Chinese Academy of Sciences, Wuhan, China

California's Central Valley (CV) watershed, covering an area of 160,000 km², is one of the most agriculturally productive regions in the world. CV's aquifers are affected considerably by climate change and anthropogenic stresses. Gravity Recovery and Climate Experiment (GRACE) and its follow-on GRACE-FO satellite missions represent a novel technology from space capable of sensing shallow and deep global groundwater storage (GWS) change at a large-scale, provided that the signals due to surface water and other storage components are separated suitably from GRACE derived total terrestrial water storage (TWS). We use Random Forest (RF) and Artificial Neural Network (ANN) Machine Learning (ML) models to establish an empirical relationship between GRACE-derived TWS along with other hydrological variables, and GW level (GWL) for the period Oct 2002 - Sep 2016. The objective is to downscale GWS at 5 km resolution for practical water resource management. Both RF and ANN models achieved good accuracy for modeling in CV, however, we chose the RF model which is able to identify some important predictor variables for the modeling/reconstructions of GWS and GWL. Modeled GWL changes were also compared with independent vertical deformation data from Global Positioning System (GPS), Interferometric Synthetic Aperture Radar (InSAR), and Cryosat-2 (CS2), which can help compute the inelastic storage coefficient (S_{kv}), an important aquifer mechanical property. We assessed the temporal variations in GWS during the study period and noted that CV lost up to 25 km³ GWS which is consistent with

past studies. Maximum GWS losses are obtained during the drought periods of Jan 2007 - Dec 2009 and Oct 2011 - Sep 2015 respectively, while other time periods experienced GWS gains. The downscaled GWS trend maps show that the GW depletion is mostly concentrated in southern San Joaquin Valley in the CV, which is also the region experiencing severe land subsidence due to GW over-withdrawal.

Key words GRACE, Machine Learning, Groundwater Storage Changes, InSAR, GPS, altimetry, downscaling

Category: Symposium 2b: Earth's Time-variable Gravity Field => 2b.2: Spaceborne and terrestrial gravimetry for hydrology

784

S2b-031

Monitoring fast water storage variations in Karst through gravimetry: a study case from the Classical Karst

Tommaso Pivetta¹、Carla Braitenberg¹、Franci Gabrovšek²、Bruno Meurers³、
Gerald Gabriel^{4,5}

1. Department of Mathematics and Geosciences, University of Trieste, Via Weiss 2, 34128 Trieste, Italy
2. Karst Research Institute ZRC SAZU, Titov trg 2, 6230 Postojna, Slovenia
3. Department of Meteorology and Geophysics, University of Vienna, Althanstraße 14, UZA II, 1090 Wien, Austria
4. Leibniz Institute for Applied Geophysics (LIAG), Stilleweg 2, 30655 Hannover, Germany
5. Institute of Geology, University of Hannover, Callinstraße 30, 30167 Hannover, Germany

The Classical Karst is an almost 600 km² karstic region shared between Italy and Slovenia. The aquifer consists of a complex network of conduits and voids fed by both autogenic and allogenic components. The allogenic contribution is provided by the Reka river which enters the karstic system in the Škocjan caves and then continues its underground flow for over 30 km, finally reaching the Adriatic Sea. Variations in the discharge of the Reka river cause fast water level fluctuations in several caves along the underground water path, with water level excursions exceeding 100 m which lead to temporary accumulation of huge water volumes in the voids. The hydrodynamics of the system has been mostly depicted relying on classical hydrologic prospections, taking advantage of a network of pressure sensors deployed in some of the known and accessible cave systems.

Since July 2018 a continuous recording gravimeter has been installed nearby the Škocjan caves in order to get more insights into the water mass balance of this cave system, which is prone to accumulate $>10^6$ m³ of water during the flood events of the Reka river. In order to obtain quantitative estimates of the water mass fluxes in the system we integrate all the available hydrologic and gravity observations into a unified 4D hydrodynamic model that simulates the response of the cave system to the Reka discharge variations. The model is able to explain both the gravity transients as well as the water levels observed in the cave system and improves the previous mass estimates which were based relying only on hydrologic data. Our joint hydraulic gravimetric model confirms the dominant role of the allogenic contribution in Škocjan in comparison to the autogenic recharge.

Our innovative integrated approach can be extended to less known areas of the Classical Karst as well as more generally to other karstic contexts where the allogenic contribution is similarly dominating.

Key words Classical Karst, hydrogravimetry, hydraulic models, karst

Category: Symposium 2b: Earth's Time-variable Gravity Field => 2b.2: Spaceborne and terrestrial gravimetry for hydrology

828

S2b-032

Bridging the gap between GRACE and GRACE-FO by simulating GRACE-like terrestrial water storage anomalies using deep machine learning tools

Merve Keleş¹, Tuğçe Ay¹, Bihter Tandoğdu¹, Metehan Uz¹, Yu Zhang², Orhan Akyilmaz¹, C.K. Shum², Kazım Gökhan Atman³

1. Dept. of Geomatics, Istanbul Technical University, Istanbul, Turkey

2. School of Earth Sciences, The Ohio State University, Columbus, Ohio, USA

3. Dept. of Physics, Faculty of Science, Ege University, Izmir, Turkey

GRACE and its successor GRACE-FO have provided invaluable information on the spatio-temporal variation of total (surface and groundwater) terrestrial water storage (TWS) for various geophysical and hydrological applications, including assimilative hydrological modelling where the large-scale GRACE/-FO observed TWS anomaly (TWSA) are used to constrain the water balance equation. GRACE/-FO derived TWSA data set is available at global scale with monthly sampling. However, there is 11-months of data gap between GRACE/-FO periods. The lack of such TWSA data during this period may degrade the assimilation studies and the resulting hydrological models may include large uncertainties as well as biases. Thus, it is crucial to fill this gap with realistic simulations of GRACE-like TWSA. Recent studies have shown that there are strong, though nonlinear, relationships between hydro-/climatic observations (e.g. precipitation, temperature, evapotranspiration, surface runoff, soil moisture etc.) and the TWSA. In this study, we use state-of-the-art deep machine learning (DML) algorithms to retrieve the complicated transformation parameters from the input hydro-/climatic observations (from ECMWF reanalysis data product, ERA-5) to reconstruct the global TWSA maps. In addition to the hydro-/climatic observations, we include the coarse resolution Swarm temporal gravity field solutions as additional input data in order to capture the long wavelength component of the TWS variations. The monthly TWSA solutions have served as the target TWSA to be approximated by the DML. In contrast to previous studies, we applied neither de-trending nor de-seasoning process to the input-output data series in order to avoid biasing the simulations considering the temporal variability of the climate-induced extreme weather episodes. The simulation results of different DML models are compared to each other as well as to the hydrological model outputs both at global and basin scales for selected major basins. Acknowledgements: This research is partially supported by the

Scientific and Technological Research Council of Turkey (TÜBİTAK)
under Grant No. 119Y176

Key words GRACE, GRACE-Follow on, Swarm, deep machine learning, terrestrial water storage anomaly

Category: Symposium 2b: Earth's Time-variable Gravity Field => 2b.2: Spaceborne and terrestrial gravimetry for hydrology

834

S2b-033

Regional inversion of GRACE/-FO KBRR/-LRI observations to estimate high resolution total water storage changes

Metehan Uz¹, Yu Zhang², Orhan Akyilmaz¹, Junyi Guo², C.K. Shum²

1. Dept. of Geomatics, Istanbul Technical University, Istanbul, Turkey

2. School of Earth Sciences, The Ohio State University, Columbus, Ohio, USA

Since April 2002, with an ~ 11 months of interruption in-between, GRACE and its successor GRACE-FO missions have provided unique observations of Earth's temporal gravity field. Their most commonly used data set are the so-called Level-2 (L2) and Level-3 (L3) which include the monthly spherical harmonic coefficients (SHC) of the global gravity field and the total water storage changes (TWSC) retrieved from post-processing of L2 data, respectively. However, the spatial and temporal resolutions of the L3 TWSC solutions are usually limited due to the truncation of SHC at certain degree/order as well as the applied filtering to remove/reduce the errors in high degree SHC. In this study, we directly estimate the TWSC over selected basins represented by $2^{\circ} \times 2^{\circ}$ (~ 200 km ground resolution) grids using the in situ potential difference observations between the twin satellites estimated by improved energy balance approach. The ill-posed downward continuation problem has been solved (i) by iterative least squares (LS) estimation with internal calibration of the initial covariance matrix of unknowns assuming first order Gaussian process and (ii) by single step regularized LS estimation using a covariance matrix retrieved from land hydrology models as light constraints. In order to reduce the edge effects, we tested several weighting strategies of the in situ observations depending on the relative positions of the ground tracks within the study regions. The numerical experiments are performed at regions which are selected such that to include both high (e.g. Amazon, Greenland) and low (e.g. Anatolia) hydrological variability. The regional solutions are compared to the latest release of official L3 solutions as well as to CSR (Center for Space Research) mascons both in spatial and time domain. Finally, some practical hints are given in particular for the initialization of the regional inversion process considering the approximate TWSC signal power within and outside the regions.

Acknowledgements: This research is partially supported by the Scientific and Technological Research Council of Turkey (TÜBİTAK) under Grant No. 119Y176

Key words GRACE, GRACE-Follow on, total water storage anomaly, regional gravity inversion, downward continuation, energy balance approach

Category: Symposium 2b: Earth's Time-variable Gravity Field => 2b.2: Spaceborne and terrestrial gravimetry for hydrology

836

S2b-034

Inter-annual terrestrial water storage changes over the Lake Victoria region from GRACE/GFO and satellite altimetry observations

Jin Li¹, Song-Yun Wang¹, Jianli Chen², Xiaogong Hu¹

1. Shanghai Astronomical Observatory, Chinese Academy of Sciences

2. Center for Space Research, University of Texas at Austin

As the largest lake in Africa, the terrestrial water storage (TWS) changes of the Lake Victoria region are observable by satellite gravimetry, including the Gravity Recovery and Climate Experiment (GRACE) and GRACE Follow-On (GFO) missions. Affected by regional extreme climate events, the TWS of Lake Victoria region exhibits strong inter-annual changes in recent years. Using the GRACE and GFO RL06 monthly solutions, we retrieve the TWS change signals over the Lake Victoria region from 2002 to 2020. The GRACE/GFO results from both the SH (Spherical Harmonic) and Mascon (Mass concentration) products show some dramatic decreases and increases in the recent ten plus years, which agrees with the estimation based on satellite altimetry observations, land surface models and precipitation data. Comparison with global climate index series suggests that the inter-annual TWS changes over this region are correlated with the El Niño and La Nina events in recent years. In addition, we find that the differences between GRACE/GFO and satellite altimetry observations become distinctly larger and systematic during the late stage of GRACE mission and into the GFO era, which is consistent with the latest finding by estimating the global mean ocean mass change in a recent study.

Key words GRACE; GRACE Follow-On; satellite altimetry; terrestrial water storage; Lake Victoria

Category: Symposium 2b: Earth's Time-variable Gravity Field => 2b.2: Spaceborne and terrestrial gravimetry for hydrology

857

S2b-035

Flood monitoring over the Yangtze River basin using GLDAS daily data products based on GRACE data assimilation

Xiao Yan, Bao Zhang, Yibin Yao
Wuhan University

A severe flood occurred around the middle and lower reaches of the Yangtze River (MLYR) in 2020 and caused great terrestrial water storage (TWS) surpluses. It is important to understand this flood process and assess its impacts. We combine the Gravity Recovery and Climate Experiment (GRACE) observations and Global Land Data Assimilation System (GLDAS) -2.2 daily outputs based on GRACE data assimilation to thoroughly investigate this flood event. Evaluation using ground-based measurements shows the TWS data from GLDAS agree well with that from GRACE and the water budget estimate in the MLYR basin and its sub-basins at the monthly or daily scales, which provides confidence in the use of GLDAS-simulated TWS for monitoring floods around the MLYR at the daily scale. TWS results from GLDAS suggest that this flood event started in early July in the northern MLYR, peaked in the end of July with TWS surplus of ~223 mm in the MLYR, and then decline rapidly until early September, influencing a vast area of $\sim 3.0 \times 10^5$ km² around the MLYR. The flood center first appeared in the MLYR mainstream, then moved northward to the north of the MLYR, and finally stayed to the south of the MLYR mainstream. GRACE results exhibit similar spatiotemporal characteristics to the GLDAS results but with larger magnitudes. These two TWS results together identify and assess this severe flood event, providing us a quantitative understanding of it. The water budget analysis demonstrates that above-normal precipitation around the MLYR during June-July 2020 is generally the main drivers of this flood. Using the ERA5 atmospheric reanalysis, we show that the precipitation increase is mainly due to anomalies in low-latitude atmospheric circulation, including the anomalous extensions of the Western Pacific subtropical high and South Asia high, anomalous low-level southwesterlies, and upper-level westerlies. And the precipitation increase is also closely associated with the anomalous blocking high and cold air activities in the extra-tropical latitudes.

Key words Yangtze flood; Terrestrial water storage; Global Land Data Assimilation System; GRACE; Precipitation

Category: Symposium 2b: Earth's Time-variable Gravity Field =» 2b.2: Spaceborne and terrestrial gravimetry for hydrology

882

S2b-036

Satellite Gravimetry-based Monitoring System for Natural Hazards and Water Resources Management

C K Shum ^{1,2*}, Yu Zhang ¹, Orhan Akyilmaz ³, Ehsan Forootan ⁴, Metehan Uz ³

1. School of Earth Sciences, The Ohio State University, Columbus, Ohio, USA

2. . Innovation Academy for Precision Measurement Science and Technology, Chinese Academy of Sciences, Wuhan, China

3. Dept. of Geomatics, Istanbul Technical University, Istanbul, Turkey

4. Geodesy and Earth Observation Group, Dept of Planning, Aalborg University, Denmark

The advent of dedicated Earth gravity satellite missions during the Decade of the Geopotential, in to 2000, revolutionized measurements of gravity signals and mass transports within the Earth system, with pioneering satellite missions, CHAMP, GRACE, and GOCE. Temporal satellite gravimetry missions, Gravity Recovery And Climate Experiment (GRACE), 2002–2017, and GRACE-Followon (GRACE-FO) twin-satellite missions, 2018–, are innovative sensors cable of observing global mass transport signals within the Earth system at monthly sampling and spatial scale longer than 333 km (half wavelength). The onset of climate change and its ensuing effects exacerbate adverse impacts on global environmental and ecological regimes, and natural or anthropogenic hazards such as abrupt climate/weather episodes, surface and groundwater depletion, storms, cyclones, large floods, and prolonged droughts. Timely monitoring of climate or hazardous weather variables governing these complex processes at an adequately downscaled spatio-temporal resolutions provide a means for applications to improve water resources management and hazards response. GRACE/GRACE-FO temporal gravity fields augmented by a high-resolution GOCE static gravity field model enabled novel characterizations of Earth's mass transports by accurately measuring minute changes of gravity from space. Here we postulate the plausible spatio-temporal downscaling of GRACE/GRACE-FO data inverted Earth's mass change would enable accurate monitoring of the aforementioned natural hazards and surface/groundwater sensing for improved water resources management and disaster response, and present preliminary results.

Acknowledgements. This research is supported by the National Science Foundation Division of Industrial Innovation and Partnerships under Grant No. AWD-109695.

Key words Satellite gravimetry, GRACE/GRACE-FO, Natural hazards, Water resources

Symposium 2b: Earth's Time- variable Gravity Field

S2b.3: Cryospheric changes from gravity data

Category: Symposium 2b: Earth's Time-variable Gravity Field => 2b.3: Cryospheric changes from gravity data

77

S2b-037

Advanced estimation of regional ice mass losses in Greenland from GRACE data

Linyang XIN、Jiangjun RAN

Southern University of Science and Technology

Mascon products derived from GRACE satellite gravimetry data are widely used to study the Greenland ice sheet (GrIS) mass balance. However, the products released by different research groups – JPL, CSR and GSFC – show noticeable discrepancies. To understand them, we compare those mascon products with mascon solutions computed in-house using a varying regularization parameter. We show that the observed discrepancies are likely dominated by differences in the applied regularization. Furthermore, we present a numerical study aimed at an in-depth analysis of regularization-driven biases in the solutions. We demonstrate the ability of our simulations to reproduce 60-80% of biases observed in real data, which proves that our simulations are sufficiently realistic. After that, we demonstrate that the quality of mascon-based estimates can be increased by a proper modification of the applied regularization: no correlation between mascons is assumed when they belong to different drainage systems. Using both simulations and real data analysis, we show that the improved regularization mitigates signal leakage between drainage systems by 11-56%. Finally, we validate various mascon solutions over the SW drainage system, using the RACMO model as the source of independent information, since mass variations in SW are mostly explained by surface mass balance (the contribution of ice discharge is small). In general, our trend estimates obtained with the improved regularization are as consistent with RACMO-based ones as the estimates based on the CSR and JPL solutions. Over the time intervals 2003-2014 and 2003-2006, our solutions yield the estimates that are the closest to the RACMO-based ones.

Key words Greenland ice sheet; surface mass balance; GRACE; mascon products

Category: Symposium 2b: Earth's Time-variable Gravity Field => 2b.3: Cryospheric changes from gravity data

201

S2b-038

Performance of Tongji-RegGrace2019 Solution over Major Mountain Glaciers

Wei Wang、 Yunzhong Shen、 Qiuji Chen
Tongji University

The new high spatial resolution monthly gravity field solution Tongji-RegGrace2019 is with spherical harmonic coefficients up to degrees and orders 180, spanning from April 2002 to December 2016. The performance of the Tongji-RegGrace2019 solution over major mountain glaciers is evaluated and compared to the CSR and JPL mascon solutions. At first, the mass change trends and amplitudes of Tongji-RegGrace2019 and CSR mascon solutions are shown in terms of equivalent water height at the continental scale. Then the spatiotemporal characteristics of mass changes over major mountain glaciers are analyzed in detail with the Tongji-RegGrace2019 solution compared to the CSR and JPL mascon solutions. The results show that the mass changes derived from Tongji-RegGrace2019 have good consistency with mascon solutions in the studied area. Moreover, compared to the two mascon solutions, Tongji-RegGrace2019 demonstrates a relatively higher spatial resolution and stronger signal, which have the potential to retrieve signals at the studied mountain glaciers.

Key words satellite gravimetry; mountain glaciers; high-resolution monthly harmonic solutions

Category: Symposium 2b: Earth's Time-variable Gravity Field => 2b.3: Cryospheric changes from gravity data

221

S2b-039

New Constrains on Glacier Mass Balance on High Mountain Asia

Qiuyu Wang, Shuang Yi, Wenke Sun
University of Chinese Academy of Sciences

Glacier melt in High Mountain Asia (HMA) is an indicator of climate change and has a major impact on the regional hydrology and freshwater supply. We determined the recent status of HMA glaciers based on the analysis of Ice, Cloud, and Land Elevation Satellite-2 (ICESat-2) data. We used the Gravity Recovery and Climate Experiment (GRACE) and GRACE Follow-On (FO) data to complement ICESat-1,2 data and validate them independently. We find a good agreement between ICESat-1,2 and GRACE/GRACE-FO data, which demonstrates the high reliability of results. Based on our results, the continuous glacier mass change from 2003–2019 is $-28 \pm 6 \text{ Gt yr}^{-1}$, which is more negative than stereo imagery-based studies. The regional variability of the glaciers ranges from $-1.07 \pm 0.10 \text{ m yr}^{-1}$ in southeastern Nyaingentanglha to $+0.16 \pm 0.10 \text{ m yr}^{-1}$ in West Kunlun. ICESat-2 data enable new insight into the continuous measurement of HMA glacier elevation change.

Key words GRACE; mass balance; High Mountain Asia

Category: Symposium 2b: Earth's Time-variable Gravity Field => 2b.3: Cryospheric changes from gravity data

277

S2b-040

An Investigation on the Ice Mass Loss in Antarctica Using Different Geosensors Data

Bilal Mutlu, Serdar Erol, Bihter Erol

Istanbul Technical University, Geomatics Engineering Department, 34469, Maslak, Istanbul, Turkey.

In the last decades, a severe decrease of the glacial masses is observed in the Polar Regions due to the increasing effect of global warming. Continuous observations in these regions are required for quantifying the loss in the glacier mass and monitoring the increase in mean sea level. Besides, as a consequence of the glaciers mass loss, an uplift occurs (the post-glacial rebound (PGR) effect) in the affected areas and should be monitored as well. In this context, the geosensors including GNSS (Global Navigation Satellite System), satellite radar altimetry, Earth gravity satellite missions as well as the tide-gauges are widely used and contribute to studies of these dynamic phenomena. Within the scope of this study, the variations of the glacial mass within a time period in the Antarctic region are investigated using the geosensors data. Regarding this, the GNSS stations of the UNAVCO (University NAVSTAR Consortium) and IGS (International GNSS Service) networks data, the GRACE/GRACE-FO (The Gravity Recovery and Climate Experiment) solutions, CryoSat-2 and ICESat-2 (Ice, Cloud, and Land Elevation Satellite) satellite radar altimetry data in addition to the tide-gauge observations are used to carry out the analyzes through the generated time series. Thus, the mass loss in the study area is clarified from a broad perspective relying on the comparative results of different geosensors' data.

Key words Mass Loss Monitoring; Geosensors; GNSS; GRACE; Satellite Altimeter; Tide-Gauge; PGR.

Category: Symposium 2b: Earth's Time-variable Gravity Field => 2b.3: Cryospheric changes from gravity data

281

S2b-041

Inter-annual variability in the Antarctic ice sheets using multi-technique geodesy and modeling

Athul Kaitheri¹, Anthony Mémin¹, Frédérique Rémy²

1. Université Côte d'Azur, CNRS, Observatoire de la Côte d'Azur, IRD, Géoazur, 250 rue Albert Einstein, 06560 Valbonne, France

2. Laboratoire d'Etude en Géophysique et Océanographie Spatiales, Observatoire Midi-Pyrénées, 14 avenue Edouard Belin, 31400, Toulouse cedex 9, France

Quantifying the mass balance of the Antarctic Ice Sheet (AIS), and the resulting sea-level rise, requires an understanding of the inter-annual variability and associated causal mechanisms. The Gravity Recovery and Climate Experiment (GRACE) and its follow-on mission have been monitoring changes in the AIS since 2002. Alongside gravity change estimates from GRACE missions, we have elevation change measurements from altimetry Envisat (2002 – 2010). Similar estimates of the changes are made using weather variables (surface mass balance (SMB) and temperature) from a regional climate model (RACMO2.3p2) using a firn compaction model. For the period 2002 – 2010, we then extract inter-annual height change patterns using for the first time an empirical mode decomposition followed by a principal component analysis to investigate for influences of climate anomalies on the AIS. Investigating the inter-annual signals in these regions revealed a 4 to 6 year periodic signal in the height change patterns especially along the coasts in East Antarctica. This is likely due to the influence of El Niño Southern Oscillation, a climate anomaly that alters, among other parameters, moisture transport, sea surface temperature, precipitation, in and around the AIS at a similar frequency by alternating between warm and cold conditions. This periodic behavior in the height change patterns is altered in the Antarctic Pacific sector possibly by the influence of multiple climate drivers like the Amundsen Sea Low and the Southern Annular Mode. We also observe height change anomaly propagating eastwards from Coats Land to Pine Island Glacier regions passing through Dronning Maud Land and Wilkes Land in 6 to 8 years. This is representative of climate anomaly propagation due to the Antarctic Circumpolar Wave. Altogether, inter-annual variability in the SMB of the AIS is found to be modulated by multiple competing climate anomalies.

Key words Mass balance, GRACE, Envisat, RACMO2.3p2, El Niño Southern Oscillation, Antarctic Circumpolar Wave

Category: Symposium 2b: Earth's Time-variable Gravity Field => 2b.3: Cryospheric changes from gravity data

290

S2b-042

Antarctica Ice-Mass Variations on Intraseasonal-Interannual Timescale: East-West Coastal Dipole and Eastward Circumpolar Wave

Zhen Li¹, Benjamin Fong Chao², Hansheng Wang¹

1. Innovation Academy of Precision Measurement of Science and Technology, CAS

2. Institute of Earth Sciences, Academia Sinica

Constituting by-far the largest body of freshwater on Earth and sensitive to climatic changes, the Antarctica ice has been undergoing accelerated melting. The target is the non-secular, non-seasonal, intraseasonal-interannual ice-mass redistribution over the Antarctica continent, as observed by the satellite mission GRACE (Gravity Recovery and Climate Experiment) for the period from 2003 to 2015. We employ the empirical orthogonal function (EOF) and complex EOF (CEOF) methods on the GRACE monthly time-variable gravity in the form of the mascon data. We find two separate phenomena on different timescales: (1) EOF Mode 1 represents an interannual standing “seesaw” pattern of some 70 gigatons of ice-mass redistribution largely concentrates along the coast, which we refer to as the Antarctica East-West Coastal Dipole (EWCD), reversed its polarity twice during 2003-2015, coincident with ENSO events caused by precipitation anomaly, relative to atmospheric pressure and sea surface temperature over Antarctica surrounding oceans, whereas Mode 2 correlates with the Antarctica Oscillation (AAO), suggesting AAO connects ice-mass variations by Amundsen Sea blocking. (2) CEOF Mode 1, referred to as the Eastward Circumpolar Wave (ECW), strongest in West Antarctica, represents a propagating pattern at intraseasonal periodicity of ~5 months (that cycles around the Antarctica in ~3 years) with a clear semi-annual modulation in amplitude, two 1-2-year hiatuses in the phase cycling of ECW happened around 2007 and 2011, again in close proximity to the timing of the ENSO events. ECW may be induced by a coupling mechanism of surface net radiation and Antarctica Circumpolar Wave.

Key words Antarctica, GRACE, Empirical Orthogonal Function, East-West Coastal Dipole, Eastward Circumpolar Wave

Category: Symposium 2b: Earth's Time-variable Gravity Field =» 2b.3: Cryospheric changes from gravity data

294

S2b-043

Two decades of Antarctic surface elevation changes from multi-mission satellite altimetry and gravimetry

Lianzhe Yue、Nengfang Chao、Shuai Wang、Ying Hu、Yanze Zhang
China University of Geosciences

The Antarctic ice sheet (AIS) plays a role in the current rising of the global sea level. Precise measurements of surface height changes (SEC) can improve estimates of the mass balance of AIS and global sea-level changes. We developed a multi-mission satellite altimetry analysis over the AIS which include ICESat, CryoSat-2, and ICESat-2. The monthly grids of multi-mission SEC were obtained using the crossover and repeat-track methods during 2003-2020. We also examine mass change estimates from the Gravity Recovery and Climate Experiment (GRACE), GRACE Follow-On (GFO) data, SECs and densities. The result showed that (1) there was a large SEC decline on the Antarctic Peninsula and the coastal regions of the East Antarctic; (2) the Amundsen Sea Embayment was the largest mass losses of the AIS, and the maximum annual variation rate was larger than -10 m/yr; (3) the AIS increased mass loss after 2006 and accelerated after 2010. The multi-mission satellite altimetry and gravimetry can enhance mass balance estimates in the AIS, and coincident results of altimeter and gravimetry are important for research of the contributions of snow and ice to mass balance in the AIS.

Key words Antarctic Ice Sheet; Surface Elevation Change; crossover and repeat-track; ICESat/Cryosat-2/ICESat-2; GRACE/GRACE-FO

Category: Symposium 2b: Earth's Time-variable Gravity Field => 2b.3: Cryospheric changes from gravity data

384

S2b-044

Mass Variations of the Greenland Ice Sheet based on GRACE/GARCE Follow-On Satellite Gravimetry and Mass Budget Method

Peisi Shang, Xiaoli Su, Zhicai Luo
Huazhong University of Science and Technology

In recent years, the melting of glaciers and ice sheets associated with global warming contributes a lot to global mean sea level rise and has posed a serious threat to the environment over coastal regions. As the second largest ice sheet on the Earth, the Greenland ice sheet is experiencing melting heavily. Based on GRACE/GRACE Follow-On Satellite Gravimetry and Mass Budget Method, we find that the monthly mass variations are in good agreement with each other by comparing the consistency over the Greenland Ice Sheet. Here we examine further the melting of Greenland Ice Sheet, by analyzing gravity satellite data. We find that the melting was the most serious in 2012 and 2019 approaching to 470 Gt year^{-1} and 490 Gt year^{-1} . Moreover, the melting amounts are close to nearly 330 Gt mon^{-1} and 280 Gt mon^{-1} and the melting area covered almost the entire Greenland ice sheet in August of 2012 and 2019 alone.

Acknowledgement: This research is funded by the National Natural Science Foundation of China, grant number 41804014, and also supported by the National Key R&D Program of China, grant number 2018YFC1503503.

Key words GRACE and GRACE Follow-On, Mass Budget Method, Greenland Ice Sheet, Mass variations.

Category: Symposium 2b: Earth's Time-variable Gravity Field => 2b.3: Cryospheric changes from gravity data

390

S2b-045

Low Degree Spherical Harmonic Influences on Polar Ice Sheet Mass Change Derived from GRACE/GRACE-FO Gravimetry

Xiaoli Su¹、Junyi Guo²、C.K. Shum²、Zhikai Luo¹、Lin Liu¹

1. Institute of Geophysics, Huazhong University of Science and Technology

2. Division of Geodetic Science, School of Earth Sciences, The Ohio State University

The accuracy of low degree spherical harmonic coefficients is vital to accurately estimate polar ice sheet mass variations using monthly gravity field solutions from the Gravity Recovery and Climate Experiment (GRACE) and GRACE-Follow-On (GRACE-FO) data. Currently, there are estimates of these low degree spherical harmonic coefficients such as degree one terms, degree two zonal term and in different versions available for proper science application in satellite gravimetry community. Here we assess the impact of degree one terms, SLR-based and estimates on GRACE- and GRACE-FO-derived polar ice sheet mass variations. We report that degree one terms recommended for GRACE Release 06 (RL06) data have an impact of 2.5 times more than those for GRACE RL05 data on the mass trend estimates over the Greenland and the Antarctic ice sheets. The latest recommended solutions in GRACE Technical Note 14 (TN14) affect the mass trend estimates of ice sheets in absolute value by exceeding 50% larger, as compared to those in TN11 and TN07. The SLR-based replacement has some impact on the Antarctic ice sheet mass variations, mainly depending on the length of the study period. This study emphasizes that reliable solutions of low degree spherical harmonics are crucial for accurately deriving ice sheet mass balance from satellite gravimetry.

Acknowledgments: This research is funded by the National Key R&D Program of China, grant number 2018YFC1503503, and also supported by the National Natural Science Foundation of China, grant number 41804014.

Key words Satellite Gravimetry; Polar ice sheets; Mass change; Low degree spherical harmonic coefficients

Category: Symposium 2b: Earth's Time-variable Gravity Field => 2b.3: Cryospheric changes from gravity data

452

S2b-046

Bridging the data gap between GRACE and GRACE-FO using artificial neural network in Greenland

Bao Zhang, Yulin He, Yibin Yao
Wuhan University

Gravity Recovery and Climate Experiment (GRACE) has provided an entirely new way to measure mass changes on the Earth with unprecedented accuracy and resolution. However, the delayed launch of GRACE Follow On (FO) mission led to an approximately 1-year data gap between GRACE and GRACE-FO, breaking the continuity of the observations and limiting its further application. Excellent efforts have been made to bridge this data gap in major river basins, but few was done on ice sheets. To address this limitation, we use three artificial neural networks (ANN) to reconstruct the GRACE-like mass change at basin scales in Greenland with precipitation, runoff, evapotranspiration, and ice discharge as input data. The optimal settings of the ANNs are automatically determined by minimizing the posterior Root Mean Square (RMS) error. To test the reconstruction performance, we propose a sliding window testing method for this particular case. The testing results show that the Back Propagation Neural Network (BPNN) outperforms the Deep Belief Network (DBN) and Multiple Linear Regression (MLR) by having a predicting RMS error of 1.4 cm in term of equivalent water height for the pan Greenland and 1.5-3.4 cm (2.3 cm in average) for the six basins of Greenland. All the correlation coefficients (CC) between the predicted mass change and GRACE-inferred ones exceed 0.98. Given the fact that GRACE has an uncertainty of ~2 cm in measuring mass change, the reconstruction accuracy is rather impressive. The relatively poor accuracy in basins of SW (3.2 cm) and SE (3.4 cm) is mainly due to the mass leakage problem between adjacent basins and can be improved by simply merging basins. This work bridges the data gap between GRACE and GRACE-FO and thus provides continuous GRACE-like ice mass change data at basin scales for Greenland studies.

Key words Greenland; GRACE; Gap filling; Artificial neural network

Category: Symposium 2b: Earth's Time-variable Gravity Field => 2b.3: Cryospheric changes from gravity data

523

S2b-047

Filling the data gaps within GRACE missions using Singular Spectrum Analysis

Shuang Yi¹, Nico Sneeuw²

1. Institute of Geodesy, University of Stuttgart

2. University of Stuttgart

Dozens of missing epochs in the monthly gravity product of the satellite mission Gravity Recovery and Climate Experiment (GRACE) and its follow-on (GRACE-FO) mission greatly inhibit the complete analysis and full utilization of the data. Despite previous attempts to handle this problem, a general all-purpose gap-filling solution is still lacking. Here we propose a non-parametric, data-adaptive and easy-to-implement approach—composed of the Singular Spectrum Analysis (SSA) gap-filling technique, cross-validation, and spectral testing for significant components—to produce reasonable gap-filling results in the form of spherical harmonic coefficients (SHCs). We demonstrate that this approach is adept at inferring missing data from long-term and oscillatory changes extracted from available observations. A comparison in the spectral domain reveals that the gap-filling result in the same signal intensity as the product of GRACE missions for spherical harmonic degrees below 30. As the degree increases above 30, the degree variance of the gap-filling result decreases more rapidly than that of GRACE/GRACE-FO SHCs, demonstrating effective suppression of noise. As a result, our approach can reduce noise in the oceans without sacrificing resolutions on land. The quality of the gap-filling product is evaluated through comparison with a surface-mass-balance-based estimate in Greenland, Swarm gravity solutions and a climate-driven water storage model, all of which confirm the good performance of our results. This study makes a ready-to-use gap-filling product in the form of SHCs together with proper error estimates available. Nonetheless, our method is also applicable to smoothed gridded observations.

Key words GRACE; data gap; gap filling; singular spectrum analysis;

Category: Symposium 2b: Earth's Time-variable Gravity Field => 2b.3: Cryospheric changes from gravity data

743

S2b-048

Extraction of GRACE/GRACE-FO Observed Mass Change Patterns across Antarctica via Independent Component Analysis (ICA)

Tianyan Shi¹, Yoichi Fukuda², Koichiro Doi^{2,1}, Jun'ichi Okuno^{2,1}

1. Graduate University for Advanced Studies, SOKENDAI

2. National Institute of Polar Research

Here we qualitatively analyze the mass change patterns across Antarctica via independent component analysis (ICA), a statistics-based blind source separation method to extract signals from complex datasets, in an attempt to reduce uncertainties in the glacial isostatic adjustment (GIA) effects and improve understanding of Antarctic Ice Sheet (AIS) mass-balance. We extract the six leading independent components from gravimetric data acquired during the Gravity Recovery and Climate Experiment (GRACE) and GRACE Follow-On (GRACE-FO) missions. The results reveal that the observed continental-scale mass changes can be effectively separated into several spatial patterns that may be dominated by different physical processes. Although the hidden independent physical processes cannot be completely isolated, some significant signals, such as glacier melt, snow accumulation, periodic climatic signals, and GIA effects, can be determined without introducing any external information. We also observe that the time period of the analyzed dataset has a direct impact on the ICA results, as the impacts of extreme events, such as the anomalously large snowfall events in the late 2000s, may cause dramatic spatial and temporal changes in the ICA results. ICA provides a unique and informative approach to obtain a better understanding of both AIS-scale mass changes and specific regional-scale spatiotemporal signal variations.

Key words GRACE; GRACE-FO; ICA; Antarctica; GIA

Symposium 2b: Earth's Time- variable Gravity Field

S2b.4: Satellite Altimetry and Oceanography

Category: Symposium 2b: Earth's Time-variable Gravity Field =» 2b.4: Satellite Altimetry and Oceanography

146

S2b-049

Quantitative Analysis of Global Sea-Level Budget Based on GRACE, Satellite Altimetry and Argo Observations

Fengwei Wang、 Yunzhong Shen、 Qiujiu Chen
Tongji University

The global sea-level budget is theoretically closed between the Gravity Recovery and Climate Experiment (GRACE) solution, Satellite Altimetry and Argo observations. Five GRACE solutions (CSR RL06, GFZ RL06, JPL RL06, ITSG-Grace2018 and Tongji-grace2018) are used to estimate the Global Mean Ocean Mass (GMOM) change and demonstrate the sea-level budget relative to Altimetry-Argo. The results show that the GMOM change from the new Tongji-Grace2018 solution can reduce the misclosure by 0.10~0.16 mm/year compared to the other four GRACE solutions over the period January 2005 to December 2016. When the same missing months as the GRACE solution are deleted from altimetry and Argo data, the resulted misclosure will be reduced by 0.06 mm/year. Once retained the GRACE C20 term, the linear trends from Tongji-Grace2018 and ITSG-Grace2018 are 2.62 ± 0.16 and 2.64 ± 0.16 mm/year, closer to the linear trend of 2.62 ± 0.14 mm/year from Altimetry-Argo than the three RL06 official solutions. We further analyze the contribution of low Spherical Harmonic (SH) coefficients to GMOM change by truncating different Degrees and Orders (d/o), and find that the linear trends from the SH coefficients truncated to d/o 15 and 20 are very close to those of using all d/o 60 SH coefficients with the contribution over 90%. The averaged square root of accumulated geoid degree variances of Tongji-Grace2018 solution from January 2005 to December 2016 are 8.44, 7.90 and 6.92 mm when the SH coefficients are truncated to d/o 20, 15 and 10, respectively, larger than those of the other four GRACE solutions, indicating that the low SH coefficients of Tongji-Grace2018 solution contain more GMOM change signals. Therefore, Tongji-Grace2018 can reduce the misclosure between Altimetry, Argo and GRACE data, regardless of whether the C20 term is replaced or not, since the low coefficients of Tongji-Grace2018 can capture more signals.

Key words GRACE; Global ocean mass change; Sea level budget; Altimetry; Argo

Category: Symposium 2b: Earth's Time-variable Gravity Field =» 2b.4: Satellite Altimetry and Oceanography

424

S2b-050

The ways to improve the accuracy of determining the height of the geoid using GNSS signals reflected from the ocean surface

Vladislav Lopatin, Vyacheslav Fateev
VNIIFTRI

A geoid is a surface of equal gravitational potential on the Earth's figure, containing a point, taken as the beginning of counting heights. The surface of the geoid coincides with the surface of the World Ocean in the absence of disturbing forces.

Currently, measurements of the ocean surface height are carried out using active satellite altimetry methods. Satellite altimetry based on monolocators has a high accuracy (1-2 cm) and will allow to avoid expensive gravimetric surveys in all parts of the World Ocean. At the same time, satellite active altimetry has the following disadvantages:

- the on-board altimeter requires a high-power power supply device and large dimensions of a spacecraft (SC);
- limited coverage area, since only one observation track of the current altitude profile is realized in one pass of the SC.

A promising method of expanding the coverage area is to use the bistatic method of satellite altimetry, based on GNSS-reflectometry. This method is based on the principle of detecting GNSS signals reflected from the Earth's surface and processing them in order to determine the properties of the surface. In one pass of the SC with the onboard GNSS-reflectometry system, it is possible to simultaneously obtain up to 20-30 tracks of the geoid height profile - according to the number of visible navigation satellites GLONASS/GPS/Galileo/BeiDou. With this method of height measurement, the onboard transmitter with all its disadvantages is completely excluded.

The errors of the code, interferometric and phase methods of GNSS altimetry were analyzed. Ways to improve the accuracy of determining the height of the ocean surface by choosing the optimal integration time and using all frequency channels in processing are proposed.

Experiments were carried out to measure height using a GNSS-altimeter from the roof of a building, from a bridge over the river, and also in an anechoic shielded chamber.

Key words GNSS-R, altimetry, geoid

Category: Symposium 2b: Earth's Time-variable Gravity Field =» 2b.4: Satellite Altimetry and Oceanography

431

S2b-051

Leading Edge Identification with Prior Information (LEIPI): a new approach to retracking inland altimetry waveforms

Nico Sneeuw, Sajedah Behnia, Mohammad Tourian
University of Stuttgart, Institute of Geodesy

Almost in parallel to the decline of in situ gauging stations over the past few decades, satellite altimetry has proven effective in filling in for this gap to a meaningful extent. Despite both theoretical and methodological developments, however, inland altimetry is still hindered by many factors, an important one being land contamination. Inland waveforms in general, and the more contaminated ones especially, do not follow a typical shape. This effect complicates the retracking process, and plays usually a degrading role in the final accuracy and precision of the altimetry retrieved water heights.

To tackle the problem, a wide range of retracking algorithms have been developed so far. What is noticeable, however, is that the claimed precision of satellite altimetry (~2 cm) has never been achieved over inland waters. In effect, none of the existing methods can deal with all complexities caused by inland processes. In what may be termed as a classic approach, waveform retracking is a case-independent problem with a universal solution. Any such approach implicitly ignores the defining role of the morphological properties and seasonal regime of the water body of interest.

We argue that the aforementioned factors affect the inland water level time series oftentimes in a systematic manner; meaning that a prior time series analysis should let us infer the common types of contamination during the radar acquisition, and hence, the way they are translated into the waveform properties. As opposed to what has been done so far, we believe that retracking of inland waters yields the most precise results only if it is performed with reliable prior information. Our proposed method, therefore, relies on the outputs of an iterative outlier identification procedure, where at each iteration i) a model of the input time series is generated, ii) the greatest outlier is rejected and iii) replaced with the model value. The algorithm eventually outputs both outlier flags and the ensemble of models. The deviation of the outlying measurement from the model value is then translated into radar bin units. As long as this deviation falls into the covered range spectrum of the waveform, it is possible to reconsider the retracking results. The rationale

here is that an expected value coming from a time series analysis is reliable enough to bound the searching area where the leading edge can be located.

LEIPI is expected to not only retrieve true height values from the so-called outliers, but also to provide more reliable estimations for trivially contaminated measurements. From a theoretical point of view, the latter potentially alters our understanding of both accuracy and precision of altimetry missions over inland waters. On the practical side, it yields denser and more reliable inland time series.

Key words satellite altimetry, lakes and reservoirs, retracking, outlier rejection, time series

Category: Symposium 2b: Earth's Time-variable Gravity Field =» 2b.4: Satellite Altimetry and Oceanography

522

S2b-052

Data quality analysis of Argo float observations from 2016 to 2020

Lu Tang¹、Jin Li²、Hao Zhou¹、Zhikai Luo¹、Penghui Wang¹

1. Huazhong University of Science And Technology

2. Shanghai Astronomical Observatory, Chinese Academy of Sciences

The steric sea level change caused by thermohaline effects is one of the main results for the ocean response to climate change process. Based on the Argo (Array for Real-Time Geostrophic Oceanography) observations, many researchers have made efforts to quantify the contribution of temperature and salinity to the steric sea level change, as well as the contribution of steric sea level change to the global sea level change in past decades. However, there are obvious discrepancies among different Argo gridded products, which inevitably enlarge the uncertainties of steric sea level change estimation. In this study, we carry out comprehensive analysis on the uncertainties of the JAMSTEC、SIO and IPRC Argo gridded data from 2016 to 2020. Moreover, we compare the Argo estimates with the observations from Satellite Altimetry and Satellite Gravimetry (including GARCE and GRACE Follow-On). Results indicate that the steric sea level change estimation uncertainties play an important role in the closure of global sea level budget during the period 2016 - 2020. Acknowledgement: This research was funded by the National Key Research and Development Program of China (No. 2018YFC1503503, 2018YFC1503504) and the National Natural Science Foundation of China (No. 41931074, 42074018, 42061134007, 41704012)

Key words Argo float; Steric sea level change; Error analysis; Satellite Altimetry; Satellite Gravimetry

Category: Symposium 2b: Earth's Time-variable Gravity Field =» 2b.4: Satellite Altimetry and Oceanography

575

S2b-053

Quantifying the precision of retracked Jason-2 sea level data in the 0-5 km Australian coastal zone

FUKAI PENG¹、Xiaoli Deng²、Xiao Cheng¹

1. Sun Yat-Sen University

2. The University of Newcastle, Australia

This paper aims to quantify the precision of retracked Jason-2 altimeter sea level data (2008-2016) in the 0-5 km Australian coastal zone. A new retracking strategy has been developed to achieve the highest possible precision of coastal sea-level data. Coastal waveforms were classified into four groups according to the adaptability of dedicated coastal retrackers, from which each group was reprocessed using an optimal retracker. A modified Brown model was introduced to reprocess the quasi-specular waveforms over calm waters. A seamless transition of sea surface heights from different retrackers was achieved by estimating and removing the significant wave height dependent height differences. In order to generate the 20-Hz sea level anomaly (SLA) and total water level envelope (TWLE) at the coast, the regional along-track mean sea surface (MSS) with a high spatial resolution (~300 m) was estimated. Compared to the global MSS model, the use of the along-track MSS has dramatically reduced the SLA variance by 140 cm² in the 0-15 km coastal strip.

The results from the evaluation of data precision for Jason-2 ground tracks and the validation against tide gauges show that this new retracking strategy can retrieve more reliable sea level data nearshore. The precision of 20-Hz sea level data in the 0-5 km Australian coastal strip ranges typically from 5 cm to 6 cm in most coastal areas, which is only ~1 cm lower than that beyond 5 km off the coastline. However, in Northwest Australian and some coastal regions, the data precision drops to ~7 cm due partly to the specific coastal sea states and topography. In addition, it is found that the altimeter and tide gauge TWLE time series have a high correlation (>0.8) in the 0-5 km distance band, indicating that coastal sea-level data are useful for applications such as estimation of river plumes, long-term variation of water level in lakes and rivers, and the analysis of storm surges.

Key words Satellite altimetry, sea level anomaly, total water level envelope, Jason-2, Australian coastal zone, data precision, validation

Category: Symposium 2b: Earth's Time-variable Gravity Field =» 2b.4: Satellite Altimetry and Oceanography

626

S2b-054

Global Ocean Mass Change Estimates in 1993~2004 from LEO Gravity Field Models Determined at Tongji University

Qiujie Chen¹、Xingfu Zhang²、Fengwei Wang¹、Yunzhong Shen¹

1. Tongji University

2. Guangdong University of Technology

Due to the lack of gravity field models like GRACE/GRACE Follow-on which can directly estimate the global ocean mass change (GOMC) during the period January 1993 to March 2002, one only can estimate GOMC in terms of its components such as polar ice sheets, mountain glaciers and variations of Terrestrial water storage (TWS), and close the sea level budget with the estimated results using Altimetry and Steric observations (Altimetry-Steric). In this work, a preliminary time series of gravity field models named Tongji-LEO up to degree and order 40 for the period 1993 to 2004 are derived from observations of LEO satellites including SPOT2, SPOT3, SPOT4, ERS1, ERS2 and TP. Using the LEO gravity field models, we estimate the GOMC over the period from 1993 to 2004, and investigate the closure of global sea level budget with respect to Altimetry-Steric. During our analysis, DDK and Gaussian smoothing with different filtering strength are used for noise suppression. In addition, a 500km buffer zone is applied to reducing signal leakage from lands to oceans. The GIA effects are accounted for by the ICE6G - D model. Our results show that the linear trend of global Mean Ocean Mass (GMOM) change ranges 0.83 ± 0.22 mm/yr to 1.06 ± 0.21 mm/yr when using different filtering strategies. To further study the global sea level budget from 1993 to 2004, Altimetry and steric observations are used to estimate the GMOM change indirectly. After deducted the ensemble mean steric sea level change rate 1.55 ± 0.15 mm/year from the ensemble mean GMSL rate 2.66 ± 0.15 mm/year (after correcting TOPEX-A drift), we derive the GMOM linear trend of 1.11 ± 0.15 mm/year, which is consistent with the estimates from Tongji-LEO solutions. Therefore, Tongji-LEO gravity field solutions are useful for both providing an independent measure for directly quantitatively estimating GMOM change and understanding the global sea level change.

Key words LEO Satellites, Gravity field solution, Global ocean mass change, Altimetry, Steric

Category: Symposium 2b: Earth's Time-variable Gravity Field = » 2b.4: Satellite Altimetry and Oceanography

637

S2b-055

Spatial-temporal prediction of regional sea level changes from the ocean Climate Data Records

Ruiyang Cai, Jian Zhao
China University of Petroleum (East China)

The first global ocean Climate Data Records (CDRs) of China were used to analyze and predict the sea level changes in the Yellow Sea with obvious seasonal variability. Based on the singular spectrum analysis (SSA) method, the spatiotemporal series of sea level anomaly (SLA) from the CDRs data of the Yellow Sea are de-noised and decomposed to obtain the empirical orthogonal functions (EOFs) and the corresponding principal components (PCs). Then the PCs were modeled by the long short-term memory (LSTM) neural network to predict the future trends. The prediction results of PCs were then reconstructed to obtain the final nonlinear sea level variability in the Yellow Sea from the gridded SLA spatiotemporal series. Compared with the conventional methods, the prediction accuracy of SSA-LSTM combined model is significantly improved with a minimum RMSE of 40.74 mm. The sea level trends in the Yellow Sea are highly consistent and significantly related to the season and latitude. The rate of sea level rise in the Yellow Sea will reach up to about 3.65 ± 0.79 mm/year in the next decade. The results suggest that, more accurate sea level trend estimates in coastal area can be obtained using the SSA-LSTM combined model, and the ocean CDRs data can be devoted to the studies of regional sea level change and associated coastal impacts.

Key words Climate Data Records; sea level anomaly; spatiotemporal series; singular spectrum analysis (SSA); long short-term memory (LSTM); Yellow Sea

Category: Symposium 2b: Earth's Time-variable Gravity Field =» 2b.4: Satellite Altimetry and Oceanography

656

S2b-056

Mechanism of Interannual Variability of Ocean Bottom Pressure in the South Indian Ocean

Yuting Niu, Jianhuang Qin, Xuhua Cheng
Hohai University

The study of ocean bottom pressure (OBP) helps to understand the barotropic processes that contribute to sea level rise, and it is of great significance to the study of sea level change and the prediction of climate change. In this study, the characteristic and mechanism of interannual OBP in the South Indian Ocean are examined using GRACE satellite data from 2003 to 2016. The result shows that there are two energetic OBP centers (45~60°S, 80~120°E and 50~60°S, 30~60°E) in the South Indian Ocean on seasonal to interannual time scales. It is found that the atmospheric forcing plays an important role in local OBP variability, that is high (low) sea level pressure (SLP) benefits to positive (negative) OBP anomalies, via the convergence (divergence) of Ekman transport driven by local wind stress curl. Such SLP anomalies are related to Indian Ocean dipole (IOD) and El Niño–Southern Oscillation (ENSO). The positive SLP anomalies occur over the South Indian Ocean during the positive IOD, leading to convergence Ekman transport and positive OBP there. Moreover, ENSO has a positive relationship with SLP and OBP anomalies in the South Indian Ocean only during austral winter, when ENSO is strongest. These results are validated by a mass conservation (non-Boussinesq) ocean model, which is expected to not only better understanding of OBP mechanisms in a longer time, but also predict OBP variation on the global scale.

Key words GRACE; ocean bottom pressure; the South Indian Ocean; Ekman transport

Category: Symposium 2b: Earth's Time-variable Gravity Field =» 2b.4: Satellite Altimetry and Oceanography

703

S2b-057

High-resolution water level changes in coastal and estuarine regions in North Sea and Baltic

Luciana Fenoglio¹、 Joanna Staneva²、 Salvatore Dinardo³、 Jürgen Kusche¹、
Jerome Benveniste⁴、 Matthias Gärtner¹、 Bernd Uebbing¹

1. University of Bonn, Germany

2. Helmholtz Zentrum Geesthacht, Germany

3. CLS (Collect Localisation Satellites), Toulouse, France

4. ESA

Estuaries are the natural transition from rivers to the coastal ocean and, together with coastal zone, are threatened by erosion due to rising sea level, long-term change in river discharge and extreme events. The monitoring of water level change in estuaries and at the coast is today not optimal due to the limitations of current satellite altimetry near land. These limitations are exacerbated in the estuaries, where ocean modelling is difficult due to tides and to complex hydrodynamics.

We use satellite SAR altimetry and simulated SWOT observations to study small scale processes in the river-to-ocean continuum, together with in-situ and model data along the North Sea and Baltic German coast.

We have first investigated the quality of coastal water level height. Coastal sea level is recovered with up to 2-3 cm accuracy at 3-4 km from coast from the satellite altimetry in SAR mode. However, in estuaries and in coastal zone with high tidal regimes the accuracy of height deteriorates and is 30 cm in the Elbe estuary at Otterndorf. Ocean models, the BSHcmod and the Geestacht COAstal model SysTem GCOAST have comparable accuracy.

The future SWOT mission will provide observations of higher spatial and temporal resolution (HR). Time sampling is up to 4 in 21-day at our latitudes during the science phase and once a day in the calval phase. Short-scale spatial processes will be monitored with these HR data in coastal zone.

In this study we simulate the SWOT observations of both mission phases using an HR ocean model and attempt to separate the ocean tide and the discharge contributions. Further work will consider upwelling, mesoscale circulation and extreme events.

Key words sea level change, short scale processes, SAR altimetry

Category: Symposium 2b: Earth's Time-variable Gravity Field =» 2b.4: Satellite Altimetry and Oceanography

735

S2b-058

Detecting regional deep ocean warming below 2000m based on altimetry, GRACE, Argo, and CTD data

Yuanyuan Yang¹、Min Zhong^{1,3}、Wei Feng^{1,3}、Dapeng MU²

1. Innovation Academy for Precision Measurement Science and Technology,
Chinese Academy of Sciences

2. Institute of Space Sciences, Shandong University

3. School of Geospatial Engineering and Science, Sun Yat-sen University

The deep ocean below 2000m is a large water body with the sparse data coverage, challenging the closure of sea level budget and the estimation of the Earth's energy imbalance. Whether the deep ocean below 2000m is warming globally has been debated in the recent decade, since the global warming signal is not significant due to its large uncertainty. Considering the regional warming signals are generally larger than global average, here we adopt an indirect method that combines altimetry, GRACE, and Argo data to examine the regional deep ocean temperature changes below 2000m. Assuming that the deep steric change is dominated by the temperature change, significant deep ocean warming in Middle East Indian Ocean, subtropical North Pacific, subtropical Southwest Pacific, and Northwest Atlantic, and deep ocean cooling in Northwest Atlantic are detected by "Altimetry–Argo–GRACE" from 2005 to 2015. The high-quality conductivity-temperature-depth (CTD) data from repeated hydrographic sections also confirmed the validity of the indirect method.

Although the indirect method has the potential to detect regional deep ocean warming, it is difficult to accurately estimate deep ocean warming or cooling quantitatively. Due to the significant difference in spatial and temporal resolution between the two methods, the amplitude of steric trend estimated indirectly is quite larger than that calculated from CTD observations. Therefore, we recommend using independent methods and multiple data to estimate and confirm deep ocean warming.

The significant-signal regions detected by multi-source data can also be used as the basis for the Deep Argo deployment. More multi-source geodetic and oceanographic datasets with higher precision and spatiotemporal resolutions in the near future can further deepen our understanding of changes in ocean heat content and steric sea-level in deep oceans.

Key words Deep ocean warming, GRACE, Argo, GO-SHIP, Altimetry

Category: Symposium 2b: Earth's Time-variable Gravity Field =» 2b.4: Satellite Altimetry and Oceanography

837

S2b-059

Retracking of radar altimetry waveforms over inland water bodies

Xiaoli Deng¹, Andrew Marshall², Fukai Peng³

1. The University of Newcastle, Australia

2. The University of Newcastle

3. Sun Yat-Sen University, China

This paper estimates water surface level variations over inland water bodies, including lakes in the Tibetan plateau (TP) and Dianchi Lake in China, as well as the middle Fly River floodplain and Lake Murray in Papua New Guinea, using waveform data from multi-satellite altimetry missions (e.g., Envisat, Saral/Altika and CryoSat-2). Different retrackers and the dedicated data editing procedure have been developed that enable routine, accurate and reliable extraction of water surface elevations from LRM, SAR and SARIn modes of radar altimeters over heterogeneous inland waters. The lake level estimations are indirectly validated against those from Jason-2 in TP and from in-situ data in Dianchi Lake, both showing good agreement with strong correlation coefficients >0.74 . The results suggest that the official ICE retracker for LRM data and APD-PPT retracker for SARIn-mode waveforms are the most appropriate retrackers over Dianchi Lake and TP lakes, respectively. The trend estimates of the time series derived by both retrackers are 61.0 ± 10.8 mm/yr for lakes in TP, and 30.9 ± 64.9 mm/yr for Dianchi Lake, indicating that the lake levels over three plateau lakes were continuously rising over the study period. In Papua New Guinea, the derived water surface elevation (WSE) from retracking has been validated against an external reference, both in-situ gauge WSE time series and discrete survey WSE measurements. The validation results show that the standard deviation for Envisat RA-2 has consistently been in the range ± 5 to 6 cm for both river WSE and lake WSE investigations, although extended to ± 8 cm for the narrow river site in the upper reaches of the middle Fly River. The results of this study show that our dedicated retracking methodologies have the capabilities of estimating the precise WSE and water level variations over heterogeneous inland water bodies.

Key words Waveform retracking, altimetry, water surface elevation, lakes and rivers

Category: Symposium 2b: Earth's Time-variable Gravity Field = » 2b.4: Satellite Altimetry and Oceanography

846

S2b-060

Impact of hydrological loading signals on the tide gauge observations of sea level

Balaji Devaraju, Milaa Murshan
Indian Institute of Technology Kanpur

It is well known that many tide gauge stations around the world undergo vertical land motion and that they have to be corrected to estimate the rise/decline in sea-level. It is also well known that the Earth's crust responds elastically to mass changes, especially hydrological, ocean and atmospheric mass changes. Therefore, the tide gauge locations can also respond to hydrological loading. In this study, we compare the seasonal signals obtained from satellite altimetry with tide-gauge observations after removing the vertical land motion signal at four locations in the Indian coast - Chennai, Haldia, Cochin and Okha. We find significant discrepancies between the frequencies of the seasonal signals sensed by the tide gauge and the satellite altimeters. To this extent we investigate the influence of hydrological loading signals at the tide gauges to see if they can explain the discrepancies. We use data from hydrological models and the Gravity Recovery and Climate Experiment (GRACE) and its GRACE Follow On to conduct the investigation.

Key words Tide gauges, Satellite altimetry, Hydrological loading, Elastic deformation, GRACE/GRACE-FO

Category: Symposium 2b: Earth's Time-variable Gravity Field = » 2b.4: Satellite Altimetry and Oceanography

850

S2b-061

Spatio-temporal variations of the steric sea level in the seas around India during the GRACE era

Balaji Devaraju, Gaurav Jiwan, Shivam Chaudhary, Yasir Malik
Indian Institute of Technology Kanpur

Sea-level rise is confirmed by satellite altimeter measurements, and with the advent of Gravity Recovery and Climate Experiment (GRACE) satellite mission we have been able to separate the sea-level variations into steric and mass components. On an average, globally, the steric sea level changes dominate the mass changes, but they can vary regionally. In recent studies it has been indicated that in the seas around the Indian coast the steric sea level dominate the ocean mass changes. In this study, we investigate the spatio-temporal variations of the steric sea level changes in the Arabian sea, Bay of Bengal and the northern Indian Ocean adjoining the south Indian coast and Srilanka. We use monthly sea surface height data derived from satellite altimetry, monthly gravity variations from GRACE/GRACE-FO missions and steric sea level changes from Argo float network data. We use empirical orthogonal function analysis to identify the dominant spatial patterns of the steric sea level changes. In addition we also look at the closure of the sea level budget in the study area.

Key words SSH, Steric sea level, GRACE, Satellite altimetry, Argo floats

Symposium 2b: Earth's Time- variable Gravity Field

S2b.5: Gravity Inversion for Solid Earth

Category: Symposium 2b: Earth's Time-variable Gravity Field => 2b.5: Gravity Inversion for Solid Earth
190
S2b-062

Vertical Deformation Analysis with GNSS and GRACE Data in North China Using Independent Component Analysis

Tengfei Feng, Yunzhong Shen, Qiujie Chen
Tongji University

Vertical deformations of the GNSS permanent sites are composed of tectonic and non-tectonic deformations, which can be estimated from the vertical coordinate time series of the GNSS daily solutions. The non-tectonic deformation is induced by various mass loading variations, mainly including atmospheric pressure, terrestrial water storage, and non-tidal ocean loading, these mass loading variations can be detected with time-variable gravity field solutions from the satellite mission of Gravity Recovery and Climate Experiment (GRACE). In this contribution, the modified Independent Component Analysis (ICA) approach is employed to analyze the Independent Components (ICs) of vertical deformation from the GNSS coordinate time series of 24 stations in North China. The ICs of mass loading deformation components are then extracted from the time series of GRACE spherical harmonic solutions of Tongji-Grace2018 and CSR RL06 also by using the ICA approach. The ICs derived from two GRACE solutions show similar spatial/temporal characteristics, however different for different stations. By Comparing the results from GNSS with that from GRACE, the ICs of GNSS vertical deformations are partly related to the ICs of mass loading deformation in North China, which is mainly caused by groundwater depletion, including the groundwater pumping by human activities, such as agricultural irrigation.

Key words Vertical deformation; GNSS regional networks; ICA; GRACE

Category: Symposium 2b: Earth's Time-variable Gravity Field => 2b.5: Gravity Inversion for Solid Earth
439
S2b-063

Comparison of GRACE and GNSS seasonal load displacements considering regional averages and discrete points

Lan Zhang, He Tang, Wenke Sun
University of Chinese Academy of Sciences

The global navigation satellite system (GNSS) and gravity recovery and climate experiment (GRACE) are two independent geodetic technologies that can detect geometric and gravity deformations, respectively. The signals observed by the two technologies mainly include the internal tectonic movement and surface mass loading effects. The former generally exhibits a long-term stable linear trend, whereas the latter exhibits strong seasonality. Many studies have compared seasonal deformations between GRACE and GNSS or combined them to study the water cycle or tectonic signals. However, whether GRACE and GNSS are comparable and what the magnitude of their differences is still remains unclear. In this study, we present simulations and a case study to address this ambiguity. The loading deformations were simulated in response to load masses with varying resolutions and distributions. We tested the simulation in the Amazon basin and found that the displacements that typically deviated from GRACE data underestimated the load displacement response to a single load mass of approximately 30%–50% on a spatial average, and this underestimation could be increased by several times at individual stations. For more complex and detailed mass distributions, the discrepancies might become smaller but still cannot be ignored (5%–20%). The vertical and horizontal deformations exhibited the same performance on the whole spatial average, while the latter performed worse in the loaded area of a single mass or as a result of a more complex mass distribution. We demonstrate that the difference between GRACE and GNSS is significant for both regional average and single-point analyses. Moreover, we found that inconsistent resolution was not the reason for the different vertical and horizontal deformation behaviors.

Key words GRACE, GNSS, seasonal loading, Amazon basin

Category: Symposium 2b: Earth's Time-variable Gravity Field => 2b.5: Gravity Inversion for Solid Earth
652
S2b-064

Data-driven separation of past and present-day surface loading from GRACE and GNSS observations

Yann Ziegler¹, Bramha Dutt Vishwakarma¹, Aoibheann Brady¹, Stephen Chuter¹,
Sam Royston¹, Jonathan Rougier², Richard Westaway¹, Jonathan Bamber¹
1. School of Geographical Sciences, University of Bristol
2. Rougier Consulting Ltd.

Both past and present loading of the Earth surface induce changes in the Earth shape, gravity field and rotation. Therefore, to better understand the Earth system's response to ongoing climate change, we must separate geodetic signals from the past and the present, which is one of the biggest challenges in using geodetic data for climate research. Fortunately, these signals have distinct physical and spatiotemporal characteristics that may help us achieve source separation. Present-day surface loading induces instantaneous vertical land motion (VLM) that results from the elastic response of the solid Earth, whereas loading and unloading from past glacial cycles result in a VLM due to the long-term response of the visco-elastic Earth mantle, the Glacial Isostatic Adjustment (GIA). The total signal from both processes is recorded by different geodetic observation systems such as GNSS (VLM) and GRACE (mass change), and to separate them we usually rely on forward models that suffer from large uncertainties. This has led to a few attempts at data-driven signal separation that does not rely on poorly known ice loading history and approximate Earth rheology. In this work, we describe two new data-driven approaches, a least-squares framework that relies on geophysical relations between observations and variables of interest, and a Bayesian hierarchical modelling framework that takes advantage of the differences in the spatiotemporal characteristics of the GIA and present-day mass change fields. We compare these two approaches and highlight their merits and limitations. Overall, we obtain a good agreement between these methods, but some differences remain that require further investigations.

Key words GRACE, GNSS, surface loading, VLM, GIA, hydrology

Category: Symposium 2b: Earth's Time-variable Gravity Field => 2b.5: Gravity Inversion for Solid Earth

711

S2b-065

Coseismic gravity changes of the Wenchuan earthquake observed by surface gravimetry

Hongtao Hao、Minzhang Hu

Key Laboratory of Earthquake Geodesy, Institute of Seismology, China Earthquake Administration

Coseismic gravity changes have important reference significance for studying the mechanisms of great earthquakes and deepening the fault model study. In this paper, the coseismic gravity changes were obtained with the data of Chengdu Gravimetric network and the absolute gravity results at the Pixian station before and after the Wenchuan earthquake; Simulation of coseismic gravity changes was conducted based on the half-space dislocation theory using the fault model obtained by Wang et al. through inversion with multiple types of geodetic survey data, and the results were compared with the observed results. The results show that the observed results and the simulation results are basically consistent, the significant changes are mainly concentrated in the near rupture zone in the hanging wall of the Yingxiu-Beichuan fault, and the changes decrease rapidly away from the rupture zone. The changes exhibit a positive to negative trend from east to west in the footwall of the Yingxiu-Beichuan fault and have a distribution characteristic of alternate positive and negative changes in the hanging wall of the fault. The result demonstrates the reliability of the observed results in this paper and the reasonableness of the fault model used.

In the near rupture zone on the west and east sides of the Yingxiu-Beichuan fault, there are still some differences between observed and simulation results. The spatial distribution trends of differences exhibit a deviation similar to "phase delay", in other words, a observed result has a deviation with corresponding simulation result in respect of spatial position, which is speculated to be caused by the errors of the geometric parameters and slip distribution of the fault model. After the slip distribution of Pengguan fault model was modified based on the actual surface rupture distribution, the simulation result at the Hongjiawan station near the eastern boundary of the fault model is more consistent with the observed result.

Key words Wenchuan earthquake, coseismic gravity change, fault model

Category: Symposium 2b: Earth's Time-variable Gravity Field => 2b.5: Gravity Inversion for Solid Earth
820
S2b-066

Horizontal deformation of GNSS on the improvement of mass load inversion

Song-Yun Wang¹、Jin Li^{1,3}、Jianli Chen²、Pengfei Wang¹

1. Shanghai Astronomical Observatory, Chinese Academy of Sciences
2. Center for Space Research, University of Texas at Austin
3. University of Chinese Academy of Sciences

The Global Navigation Satellite System (GNSS) three dimensional time series include the elastic response of the Earth to surface mass redistribution signals. We carry out the synthetic experiment of regional mass load inversion using GNSS vertical and horizontal deformation. The gridded checkerboard mass model and the model based on Gravity Recovery and Climate Experiment (GRACE) data are used individually. Our experiments show that using horizontal displacements can significantly improve the quality of inversion results when number of sites larger than one third of the number of grids, especially for the region with insufficient GNSS sites. We also analyze three cases of site's location in each grid, and quantify their differences. Through comparison between experiments using two synthetic models, we conclude that the selection of roughness factor defined in the mass inversion theory is related to the spatial resolution of the mass model, and will affect the quality of inversion results.

Key words Mass inversion, GNSS, GRACE, Load deformation

Category: Symposium 2b: Earth's Time-variable Gravity Field => 2b.5: Gravity Inversion for Solid Earth
871
S2b-067

Time-Space Characteristics of Viscoelastic Post-Seismic Deformations Corresponding to Different Rheology Models

He Tang, Wenke Sun
University of Chinese Academy of Sciences

On a long time (> 1 yr) scale, the viscoelastic properties of mantle media significantly affect post-seismic deformation. The stress field disturbance in viscoelastic medium caused by fault slip gradually relax, and the relaxation process and its temporal-spatial characteristics are determined by the viscoelastic model. In this paper, we assume that the mantle media are types of common linear rheological models, i.e., the Burgers body, the standard linear solid, and the Maxwell body, and we calculate the dislocation Love number and Green function for a spherically symmetric, non-rotating, viscoelastic, and isotropic (SNRVEI) Earth model. The characteristics of the post-seismic relaxation deformations corresponding to the different models are compared. Our results show that for a short time period, the Burgers body and standard linear solid are similar; while for the long time period, the Burgers body and Maxwell body are similar. This suggests that the observations of post-seismic deformation on the surface have a great potential for the inversion of underground viscoelastic structures. However, the potential of using surface displacement to distinguish between different rheological models is limited when the observation period is not long enough.

Key words Post-seismic deformation; Dislocation Love numbers; Viscoelasticity

Symposium 2b: Earth's Time- variable Gravity Field

S2b.6: Future Gravity Mission Concept

Category: Symposium 2b: Earth's Time-variable Gravity Field =» 2b.6: Future Gravity Mission

Concepts

206

S2b-068

The expected performance of the inclined satellite formation mission for temporal gravity field determination

Hao Zhou, Zhicai Luo

Huazhong University of Science and Technology

The prerequisite of implementing a Bender-type mission by two institutions is to ensure the combination as well as the independency of the missions in the PSF (polar satellite formation) scenario as well as in the ISF (inclined satellite formation) scenario. In this work, we will present the performance of the stand-alone ISF mission via a close-loop simulation. The ISF mission presents its superior capability in detecting the Earth's mass variations within its observational areas than the PSF mission. In addition, the general better performance of gravity estimations via ISF may promote the potential geoscience applications over the small river basins, the coastal ice sheet and the earthquake areas with better accuracy and finer resolution. The simulation results demonstrate the feasibility of implementing a stand-alone mission in the inclined orbits, and the further possibility of promoting a Bender-type mission via a profound cooperation by two institutions.

Acknowledgement: This research was funded by the National Key Research and Development Program of China (No. 2018YFC1503504, 2018YFC1503503) and the National Natural Science Foundation of China (No. 42061134007, 42074018, 41931074)

Key words Inclined satellite formation, Temporal gravity field, Future gravity mission

Category: Symposium 2b: Earth's Time-variable Gravity Field =» 2b.6: Future Gravity Mission Concepts
359
S2b-069

Simulation studies for a Mass change And Geosciences International Constellation (MAGIC) – An ESA/NASA joint mission concept in preparation

Roland Pail¹、 Frank Flechtner²、 Sean Bruinsma³、 Pieter Visser⁴、 Andreas Güntner²、 The MAGIC Science Team⁵

1. Technical University of Munich, Chair of Astronomical and Physical Geodesy
2. GFZ German Research Centre for Geosciences
3. Centre national d'études spatiales, Space Geodesy Office
4. Delft University of Technology, Astrodynamics and Space Missions
- 5.

In November 2020 it was decided at ESA's Ministerial Conference to investigate a European next-generation gravity mission (NGGM) in Phase A as first Mission of Opportunity in the FutureEO Programme. The Mass-change And Geoscience International Constellation (acronym: MAGIC) is a joint investigation with NASA's MCDO study resulting in a jointly accorded Mission Requirements Document (MRD) responding to global user community needs. On NASA side, a pre-Phase A study to address these needs is expected to start in summer 2021. On ESA side, the MAGIC concept will be investigated in two parallel industry Phase A studies, complemented by a science support study.

In the frame of this science study, several potential mission constellations will be investigated and numerically simulated in great depth. This includes Bender-type double pair mission concepts and single/multiple pendulum configurations, with realistic error assumptions regarding the key payload products, in close interaction with the parallel industry studies. Methodological improvements of processing strategies, for example the co-estimation of short-term gravity field models with various resolution, and the optimum treatment of long-term signals and tailored post-processing techniques, will be investigated. Further aspects such as the benefit of including DORIS for improving satellite orbits to support accelerometer calibration and contributing to gravity retrieval, and advanced methods for accelerometer calibration, shall be studied. The results of these studies will be evaluated by an associated science expert panel, leading to potential modifications of the MRD.

In this contribution, we will outline the motivation and set-up of this study, present first results of full-fledged numerical simulations of potential MAGIC constellations, and evaluate them against the results of a multitude of previous studies such as the ESA ADDCON project.

Key words next-generation gravity missions; MAGIC; constellation; double pair; gravity field applications

Category: Symposium 2b: Earth's Time-variable Gravity Field =» 2b.6: Future Gravity Mission Concepts
430
S2b-070

Laser space gravity gradiometer with free test mass

Ruslan Davlatov^{1,2}, Vyacheslav Fateev¹

1. VNIIFTRI

2. MIIGAiK

The second gradient of the potential of the Earth's gravitational field in the space is calculated by measurements of the changing distance between the test masses (TMs). Spacecrafts (projects: CHAMP, GRACE, GRACE-FO) or masses inside a spacecraft (SC) can be used as TMs.

In this report we will consider the laser space gravity gradiometer with free TMs moving inside the spacecraft. The idea of a gradiometer was first proposed in this article [1]. The gradiometer uses the principle of a ballistic gravimeter. Two TMs are located along each axis of the orbital coordinate system. They go into the state of a free movement and return to their original state after a set time interval with the help of special devices - arresters. Due to the action of gravitational gradients, the TMs will approach (or move away) along the corresponding spacecraft axis. The TM, which is located on the OZ axis, passing through the spacecraft and the center of the Earth, moves away from the spacecraft's center of mass with an acceleration proportional to the distance from the center of mass. Test masses placed on the other two axes - converge. The magnitude of the mutual displacement is recorded by laser interferometers.

A mathematical model and its software realization was developed to study the characteristics of a new type of gradiometer. The paper presents the results of the study of the main parameters of the gradiometer and formulates the requirements for its elements: parameters of the orbit of the spacecraft carrier, discreteness of data, accuracy of the onboard laser interferometer. A data processing technique is proposed to refine the model of the Earth's gravitational field.

1. V.F. Fateev. Space measuring instrument of the gravitational field parameters// Almanac of modern metrology, 2015, No. 3, pp. 32-62.

Key words Gravity gradiometer, free test mass, laser interferometer.

Category: Symposium 2b: Earth's Time-variable Gravity Field =» 2b.6: Future Gravity Mission Concepts

445

S2b-071

Multi-satellite formations and constellations of CubeSats and their potential in NGGMs

Nikolas Pfaffenzeller, Roland Pail
Technical University of Munich

In the context of an increased public interest in climate-relevant processes, a number of studies on Next Generation Gravity Missions (NGGMs) have been commissioned to better map mass transport processes on Earth. On the basis of the successfully completed gravity field missions CHAMP, GOCE and GRACE as well as the current satellite mission GRACE-FO, different concepts were examined for their feasibility and economic efficiency. The focus is on increasing the spatiotemporal resolution while simultaneously reducing the known error effects such as the aliasing of temporal gravity fields due to under-sampling of signals and uncertainties in ocean tide models. An additional inclined pair to a GRACE-like satellite pair (Bender constellation) is the most promising solution.

This contribution focuses on alternative concepts for the medium-term future in the form of different constellations and formations of CubeSats, making benefit of the ongoing miniaturization of satellites and relevant sensors. In the frame of the DFG-project CubeGrav, such concepts of CubeSats are investigated in a feasibility study regarding their potential for gravity field retrieval. Among others this includes the evaluation of different aspects like orbit parameters, the amount of satellites including link strategies for pairs or pearl-of-strings configurations as well as instrument performance.

With numerical closed loop simulations and based on realistic error assumptions for current or near-future miniaturized payload, optimal solutions are assessed and compared to state-of-the-art of other NGGM concepts. Especially the impact of higher temporal resolutions obtained from a constellation of multiple satellites is analysed. Furthermore, the resulting gravity field solutions are further evaluated based on different solutions approaches in which short-term temporal gravity fields or ocean tides parameters are co-parametrized.

Key words NGGM, CubeSats, simulation study, time-variable gravity field

Category: Symposium 2b: Earth's Time-variable Gravity Field =» 2b.6: Future Gravity Mission Concepts

501

S2b-072

GRACE-I mission for gapless observation of mass transport and biodiversity

Frank Flechtner¹、 Christoph Dahle¹、 Markus Hauk²、 Josefine Wilms¹、 Michael Murböck³

1. GFZ German Research Centre for Geosciences, Potsdam, Germany

2. Max-Planck-Institute for Gravitational Physics, Hannover, Germany

3. TU Berlin, Institute for Geodesy and Geoinformation Science, Germany

The actual NASA Earth Science Decadal Survey Report highlights mass transport monitoring as one of five top priorities in earth observation for the next decade. To realize such a Mass Change Mission, NASA is seeking international partnership.

In November 2020 it was decided at ESA's ministerial conference to investigate a next generation gravity mission as first mission of opportunity as defined in the FutureEO program. This Mass-change And Geoscience International Constellation (MAGIC) will be investigated jointly with NASA. On ESA's side, two parallel industry Phase A studies and a science support study have recently kicked-off. In the initial part the complete design space will be explored, including two pairs in Bender configuration or hybrid configurations with two pairs at different altitude and possibly deployed in a staggered manner.

In March 2021 a Phase-0 study was kicked-off by the DLR to investigate a "GRACE-I" mission based on a GRACE-like concept combined with an optional ICARUS (International Cooperation for Animal Research Using Space) payload. The study will be closely discussed with JPL/NASA as a future continuation of the very successful GRACE/GRACE-FO technological and scientific partnership is in the involved partners' interest. GRACE-I will be a single pair mission based on a fully redundant Laser Ranging Interferometer at 490 km or, preferably, at 420 km altitude and drag compensation with a launch not later than 2027 to guarantee data continuity and moderate accuracy improvements w.r.t. GRACE-FO. GRACE-I could then be a component of a hybrid Bender constellation if combined with a second pair.

We will present the GRACE-I mission architecture and first simulation results performed at GFZ which are based on realistic assumptions of background models and errors as well as instrument noise characteristics. These assumptions conform with MAGIC's mission

requirements in order to be comparable with results obtained in the science support study.

Key words GRACE-FO, GRACE-I, MCM, MAGIC, mass transport

Category: Symposium 2b: Earth's Time-variable Gravity Field =» 2b.6: Future Gravity Mission Concepts

604

S2b-073

Mass change And Geosciences International Constellation (MAGIC) – An ESA/NASA joint mission in preparation

Ilias Daras¹, Lucia Tsaoussi², Charley Dunn³, Roger Haagmans¹, Günther March¹, Luca Massotti¹, Bernardo Carnicero¹, Charles Webb², Pierluigi Silvestrin¹

1. ESA, ESTEC, Noordwijk, the Netherlands

2. NASA, HQ, Washington DC, USA

3. NASA, JPL, Pasadena, CA, USA

ESA and NASA are currently intensifying their long-term efforts on a collaborative implementation of a next generation mass change and gravity monitoring satellite mission. The NASA-ESA Joint Programme Planning Group initiated an activity to investigate ideas for observing mass transport from space in the future. An Interagency Gravity Science Working Group (IGSWG) with experts from US and ESA member states was established in 2013, which delivered a report in 2016 "Towards a sustained observing system for mass transport to understand global change and to benefit society". The global user community document of the International Union of Geodesy and Geophysics (IUGG) served as a basis for the report. In the meantime, the most recent Decadal Survey was released in 2017 in the US and identified Mass Change (MC) as one of the five Designated Observables (DO) recommended for implementation. The MCDO study was issued by NASA at the end of 2018 to answer to Decadal Survey science questions, whilst ESA completed Phase 0 of Next Generation Gravity Mission (NGGM). In order to bring both activities together ESA and NASA established a science expert group with 5 US and 5 ESA member state scientists to consolidate science questions and user needs for the Mass-change And Geosciences International Constellation (MAGIC) incorporating elements from NGGM and MCDO. This resulted in the Mission Requirements Document (MRD) for MAGIC which summarizes the requirements of the global scientific community (which include requirements from the IGWSG report, IUGG, MCDO, etc.) and serves as the starting point for mission design in both agencies. The target and threshold user requirements consolidated by science expert group are provided in form of spatio-temporal resolution and accuracy for the individual disciplines of hydrology, cryosphere, oceanography, solid Earth and climate. Currently, ESA starts a Phase A and NASA pre-Phase A which are coordinated and aim at designing a constellation which provides on one hand enhanced continuity towards a climate series and on the other hand a better space-time resolution with homogeneous quality to serve the

community needs for science and applications. In this presentation the science questions and requirements of MAGIC will be explained and the status of the studies will be reviewed.

Key words MAGIC, Gravity Mission, ESA, NASA, NGGM, MCDO

Category: Symposium 2b: Earth's Time-variable Gravity Field =» 2b.6: Future Gravity Mission Concepts
676
S2b-074

Climatological, tectonic and volcanic gravity signals compared to the sensitivity of the proposed MOCAS^T+ gravity mission

Carla Braitenberg, Alberto Pastorutti, Tommaso Pivetta
University of Trieste

The significance of an innovative satellite gravity mission depends on the enhancement in the detection of mass variations in the earth system. In our study we calculate the expected gravity field for glaciers, lakes, earthquakes for the High Mountains of Asia and Andes, with the aim to obtain a realistic estimate of the gravity field changes in time to be compared with the noise level of an innovative gravity mission.

In particular, we consider MOCAS^T+ (MONitoring mass variations by Cold Atom Sensors and Time measures) which proposes the integration of a payload of atomic interferometry gravity sensors with the measurement of time/frequency with optical clocks. The study is funded by the Italian Space Agency (ASI) and will be presented in Migliaccio et al. (2021).

The simulations in the hydro-glacio-tectono and volcanic sphere aim to define the sensitivity of an innovative gravity mission, by considering the noise spectral curves or more generally the noise budget. The research relates to the evaluation of a proposed satellite mission, where it is central to define the trade-off based on the noise spectral curves of the payload depending on the instrumental choice and on the satellite constellation. We create a database of relevant geophysical signals and assess what is the optimal method to evaluate the instrumental performance in relation to the simulated signals. A first approach to this endeavor is described in Pivetta et al. (2021). The realistic performance obtained from mission simulations requires an accurate investigation of the method used in comparing the spectral curves of the localized field in space and time, with the error characteristics of the satellite. The assessment of a satellite constellation and the instrument will take into account the impact of the observations, measured in terms of the completeness level of the detected geophysical phenomenon. The results define the parameters needed to give a thoughtful choice of instrumental payload and satellite constellation. Our simulations could be the basis for a flexible software: an end-to end simulation tool, aimed at evaluating the geophysical performance of different satellite constellations and payloads of the next generation gravity mission.

References

Migliaccio F., Reguzzoni M., Braitenberg C., Mottini S., Rosi G., Sorrentino F., Tino G.M., Batsukh K., Koç Ö., Rossi L., Pivetta T., Pastorutti A. (2021) The MOCAS+ study: proposal of a quantum gravimetry mission integrating atomic clocks and cold atom gradiometers. IAG Scientific Assembly 2021, Beijing 28.06-02.07 2021, Session 6.4

Pivetta T., Braitenberg C., Barbolla D.F. (2021) Geophysical challenges for future satellite gravity missions: assessing the impact of MOCASS mission, under Review in Pure and Applied Geophysics.

Key words New generation gravity mission, Geophysical signals, Sensitivity, Scientific Readiness Level

Category: Symposium 2b: Earth's Time-variable Gravity Field =» 2b.6: Future Gravity Mission Concepts

746

S2b-075

Simulations of the Next Generation Gravity Field Missions Based on Multi-Pair Constellations and Status of Chinese TianQin Mission

Wei Feng^{1,2}、Changqing Wang¹、Yihao Yan¹、Min Zhong^{1,2}、Hou-Tse Hsu¹、Meng Yang²、Hsien-Chi Yeh²

1. Innovation Academy for Precision Measurement Science and Technology (APM), Chinese Academy of Sciences (CAS)

2. Sun Yat-sen University

GRACE satellites have revolutionized our understanding of the Earth's temporal gravity fields and the inferred mass transport and redistribution. Large-scale terrestrial water storage variations and co-/post-seismic gravity changes have been successfully observed by GRACE and advanced the respective scientific disciplines, but spatio-temporal resolutions are limited to hinder further advances. In the future, Next Generation Gravity Missions (NGGMs) are expected to enhance our knowledge of mass transport processes in the Earth system, including hydrological signals and solid Earth signals. In a joint initiative of Chinese and European study teams, full-fledged robust numerical simulation studies on NGGMs based on double-pair and multi-pair constellations of GRACE-type satellites but also equipped with laser-ranging interferometers (LRIs) are performed. The Chinese space gravitational-wave project "TianQin" contains a pathfinder LEO mission with LRI, and high-precision drag-free control, which is proposed to be one pair of the NGGM constellation. The added value compared to double-pair scenarios from the Chinese TianQin-II mission with various inclined orbits is investigated. Hydrological signals with various spatial and temporal resolutions, and gravity changes due to earthquakes with different fault types and magnitudes are simulated, and used to assess the accuracy along with the spatio-temporal resolutions of the retrieved gravity fields for NGGMs.

Key words NGGM, TianQin, hydrology, LRI

Category: Symposium 2b: Earth's Time-variable Gravity Field =» 2b.6: Future Gravity Mission Concepts

830

S2b-076

Simulations on gravity field recovery from potential differences and gravity gradients for the MOCAS^T+ quantum mission proposal

Öykü Koç, Khulan Batsukh, Lorenzo Rossi, Mirko Reguzzoni, Federica Migliaccio
Politecnico di Milano

The goal of the MOCAS^T+ project is to investigate the performance of a gravity field mission based on a spacecraft having both an atomic clock and a single-axis cold atom gradiometer onboard. The former, in combination with the clock on board another spacecraft, provides measurements of potential differences; the latter provides gravity gradient observations, assuming that gradiometers onboard different spacecrafts can be oriented along different directions. Several mission scenarios, e.g., considering different noise levels, orbit altitudes, inter-satellite distances, and sampling rates, have been processed by exploiting the so-called space-wise approach. In the framework of MOCAS^T+, this approach consists of estimating the long wavelengths of the field from the potential differences and then using this estimation to reduce the already filtered gravity gradients. These residuals are processed by a local collocation gridding procedure with the aim of retrieving the shorter wavelengths. The conversion from gridded values to spherical harmonic coefficients is finally performed by discretization of the quadrature formula. For each scenario, the error budget is evaluated by Monte Carlo simulations.

The results of this analysis show that a Bender-like configuration with two pairs of satellites with a long baseline is required to get results comparable or better than GRACE performances at low harmonic degrees, and therefore to address time-variable gravity field investigations. As for the high harmonic degrees, the lower noise level of the cold atom gradiometer with respect to the electrostatic one gives the possibility of improving the GOCE performances in static gravity field determination, if the orbit altitude is not too high. A further comparison against the expected performance of the NGGM mission has been performed with the aim of investigating if and in which degree range MOCAS^T+ might provide additional information.

Key words Earth gravity field, Cold atom interferometry, Atomic clock, Space-wise approach

Symposium 3: Earth Rotation and Geodynamics

S3.1: Earth rotation, low-degree gravitational change and mass transport in geophysical fluids

Category: Symposium 3: Earth Rotation and Geodynamics =» 3.1: Earth rotation, low-degree gravitational change and mass transport in geophysical fluids

187

S3-001

Influence of core-mantle topographic coupling on the frequency of the free core nutation

Huifeng Zhang¹、Wenbin Shen²

1. School of Geodesy and Geomatics, Wuhan University

2. State Key Laboratory of Information Engineering in Surveying, Mapping and Remote Sensing, Wuhan University

Free core nutation (FCN) is one of the free rotational modes of the Earth and associated with the dynamic ellipticity of the Earth's fluid core and core-mantle coupling. Considering the core-mantle topographic coupling, we further improve the theory of triaxial three-layered Earth rotation and find that different core-mantle boundary (CMB) topography models mainly affect the frequency of the FCN. Based on four models of the CMB topography, we obtain the corresponding periods of the FCN as $-(329.83 \pm 28.12)$, $-(457.54 \pm \sim)$, $-(428.23 \pm 1.09)$ and $-(470.76 \pm 12.07)$ mean solar days, respectively. Taking into account the normal modes of the triaxial three-layered Earth rotation, the results of the CMB topography obtained by seismic tomography can be constrained in the future to a certain extent. In this study, considering the topographic coupling with the appropriate CMB topography model and by fitting the theoretical and observational values of the FCN, the estimates for the dynamic ellipticity of the fluid core lie between 0.0026340 and 0.0026430, values that are 3.56 % higher than the hydrostatic equilibrium value, while the previous result is 3.8 % higher than that value. This study was supported by the National Natural Science Foundation of China (NSFC) (Grant Nos. 41631072, 41721003, 41874023, 41574007 and 41429401).

Key words core-mantle boundary; free core nutation; topographic coupling

Category: Symposium 3: Earth Rotation and Geodynamics = » 3.1: Earth rotation, low-degree gravitational change and mass transport in geophysical fluids

296

S3-002

Why the Earth accelerates its rotation since 2016?

Leonid Zotov¹、Olesya Marchukova²、Christian Bizouard³、Nikolay Sidorenkov⁴

1. National Research University Higher School of Economics

2. Institute of natural and technical systems, RAS

3. SYRTE, Paris observatory

4. Hydrometcenter of Russia

Year 2020 has been recognized by the scientific climate community as one of the hottest year on record in the last decades. At the same time the anomalous velocity of the Earth rotation has been observed. The length of day LOD reached its minima, which can force to subtract second from the Universal Time Coordinated UTC. It would be interesting to know, why since 2016 the Earth rotation started to accelerate. The processes in the atmosphere, ocean and Earth's interior, leading to the exchange of angular momentum between the planet systems, as well as tides, changing the figure of the Earth, influence Earth rotation velocity. If tidal and atmospheric processes are mostly related to the annual and subannual variations, interdecadal LOD changes are mostly caused by the processes in the ocean and Earth's interiors. It was found out that oscillations in the ocean and atmosphere, such as El Nino Southern Oscillation (ENSO), Atlantic Multidecadal Oscillation (AMO) etc. put their fingerprints on the Earth rotation. They are also related with climate. We would like to attract attention to ENSO and alternations of El Nino and La Nina. Strong El Nino of 1972-73, 1997-98, 2015-16 happened almost on the maxima of LOD, after which the transition to acceleration happened. La Nina are often related to the minima of LOD. Large decadal variations of LOD happen with quasi 20 and 60-year periods, which could be not only related to magnetic field changes, but also with 18-year precession of the Moon, AMO and variations of the Chandler wobble amplitude. In our talk we will compare climatic factors, multidecadal processes and angular momentum of the atmosphere and ocean, trying to uncover some regularity of the events mentioned above.

Key words Earth rotation, LOD, Climate oscillations

Category: Symposium 3: Earth Rotation and Geodynamics =» 3.1: Earth rotation, low-degree gravitational change and mass transport in geophysical fluids

379

S3-003

Preparations for a Second Earth Orientation Parameters Prediction Comparison Campaign

Jolanta Nastula¹、Henryk Dobslaw²、Justyna Śliwińska¹、Tomasz Kur¹、
Małgorzata Wińska³、Aleksander Partyka¹

1. Space Research Centre, Polish Academy of Sciences, Warsaw, Poland

2. GFZ German Research Centre for Geosciences, Potsdam, Germany

3. Faculty of Civil Engineering, Warsaw University of Technology, Warsaw, Poland

The precise transformation between the celestial and terrestrial reference frames, which is needed for many advanced geodetic and astronomical tasks, requires precise Earth Orientation Parameters (EOP) data and their predictions. Various institutions worldwide therefore maintain capacities to rapidly process space geodetic observations to obtain estimates for the EOPs with short latencies as a basis for the subsequent prediction.

Between 2006 and 2008, the first EOP Prediction Comparison Campaign provided a comprehensive assessment of the capabilities of different EOP prediction methods. However, since that time, much progress has been made in terms of improved geodetic data processing, reduced VLBI latency, and routine availability of model-based forecasts of effective angular momentum functions for geophysical fluids. In light of those developments, a re-assessment of the various EOP prediction capabilities will be pursued in the frame of the 2nd Earth Orientation Parameters Prediction Comparison Campaign (2nd EOP PCC), which will start under the auspices of the IERS (International Earth Rotation and Reference Systems Service) in summer 2021. The campaign will be supervised and led by the office maintained by the Space Research Centre of the Polish Academy of Sciences (CBK PAN) in Warsaw in cooperation with GeoForschungsZentrum (GFZ) in Potsdam.

This presentation provides information on the 2nd EOP PCC technical preparations and comparison methods. The main idea of the campaign is to compare the various methods, models and strategies that can be used to predict EOP. Each predicted time series will be evaluated by the same statistical methods concerning mean prediction error, correlation, mean value, standard deviation, and other, to indicate the most appropriate and trusted prediction methods. The campaign is open to all participants and predictions of each EOP are welcome.

Key words EOP, Prediction

Category: Symposium 3: Earth Rotation and Geodynamics = » 3.1: Earth rotation, low-degree gravitational change and mass transport in geophysical fluids

406

S3-004

Oceanic mass-related excitation of polar motion: an assessment based on GRACE and multi-mission satellite altimetry

Franziska Göttl¹、Dharani Jyothi Nandagopalakrishnan²、Sam Royston³、Michael Schmidt¹、Christian Schwatke¹、Florian Seitz¹

1. DGFI-TUM

2. TUM

3. University of Bristol

Mass redistributions in the oceans affect the orientation of the Earth's spin axis with respect to an Earth-fixed reference system (polar motion). Mass changes in the oceans can be derived from both time variable gravity field solutions from GRACE (Gravity Recovery And Climate Experiment) and sea level anomalies (SLA) observed from satellite altimeter missions. While the accuracy of GRACE oceanic mass change estimates is limited by signal noise (meridional error stripes), leakage effects and uncertainties of the glacial isostatic adjustment (GIA) models, the accuracy of satellite altimetry derived oceanic mass changes is limited by waveform retracking, adjustment method and the reduction of the volume changes (steric effect) from the sea level anomalies.

In this study we use different spherical harmonic (CSR RL06, JPL RL06, GFZ RL06, ITSG-Grace2018, GRGS RL05) and mascon GRACE gravity field models (CSR RL06M, JPL RL06M) as well as satellite altimetry data (from AVISO and DGFI-TUM) to assess the accuracy of the gravimetry and altimetry derived polar motion excitation functions for the oceans. We compare these geodetic results with oceanic mass-related excitations from geophysical ocean models (ECCO and MPIOM). Furthermore we show that due to a combination of gravimetry and altimetry solutions systematic and random errors of the individual solutions can be reduced and the robustness of the geodetic derived oceanic mass-related polar motion excitation functions can be increased.

Key words Oceanic polar motion excitation, GRACE, satellite altimetry

Category: Symposium 3: Earth Rotation and Geodynamics = » 3.1: Earth rotation, low-degree gravitational change and mass transport in geophysical fluids

408

S3-005

Characterization of a noise level of hydrological and cryospheric angular momentum determined from GRACE and GRACE Follow-On data

Justyna Śliwińska¹、Małgorzata Wińska²、Jolanta Nastula¹、Aleksander Partyka¹、Tomasz Kur¹

1. Space Research Centre, Polish Academy of Sciences, Warsaw, Poland

2. Faculty of Civil Engineering, Warsaw University of Technology, Warsaw, Poland

The pole coordinates, as one of the Earth Orientation Parameters, are needed to define the relationship between the celestial and terrestrial reference frames. Therefore, the variations in polar motion (PM) should be monitored regularly and interpreted in order to assess the role of geophysical processes in this phenomenon.

In the contemporary geodesy, quantifying and interpreting the role of continental hydrosphere and cryosphere in PM excitation is an important but also challenging task. This can be done by analysing time series of hydrological angular momentum (HAM) and cryospheric angular momentum (CAM), commonly treated together as HAM/CAM. HAM/CAM can be obtained from variations of the gravity field resulting from changes in global mass redistribution provided by the Gravity Recovery and Climate Experiment (GRACE) and GRACE Follow-On (GRACE-FO) missions. A number of institutes around the world process and deliver GRACE/GRACE-FO datasets, which involve both spherical harmonic coefficients of geopotential (Level-2 data) and terrestrial water storage (TWS) maps (Level-3 data). However, the non-negligible differences between HAM/CAM estimates derived from various GRACE/GRACE-FO solutions exist.

The purpose of this work is to build an objective criterion that justifies the use of one GRACE/GRACE-FO solution to estimate HAM/CAM. To do that, we determine the quality of HAM/CAM obtained from different GRACE/GRACE-FO solutions by making an estimation of their noise level, using a generalized formulation of the “three-cornered hat method”. We show the correlation between the noise of the each GRACE/GRACE-FO-based HAM/CAM time series and series of hydrological plus cryospheric signal in observed (geodetic) excitation called geodetic residuals. After that, we construct a combined HAM/CAM series for which the noise level will be minimal. We then determine the influence a minimal noise level on the correlation between HAM/CAM and geodetic residuals.

Key words GRACE, GRACE Follow-On, polar motion excitation

Category: Symposium 3: Earth Rotation and Geodynamics = » 3.1: Earth rotation, low-degree gravitational change and mass transport in geophysical fluids

511

S3-006

Long-Range Predictability of the Length of Day and Extratropical Climate.

Adam Scaife

Met Office / University of Exeter

Angular momentum is fundamental to the structure and variability of the atmosphere and hence regional weather and climate. Total atmospheric angular momentum (AAM) is also directly related to the rotation rate of the Earth and hence the length of day. However, the long-range predictability of fluctuations in the length of day, atmospheric angular momentum and the implications for climate prediction are unknown. Here we show that fluctuations in AAM and the length of day are predictable out to more than a year ahead and that this provides an atmospheric source of long-range predictability of surface climate. Using ensemble forecasts from a dynamical climate model we demonstrate predictable signals in the atmospheric angular momentum field that propagate slowly and coherently polewards into the northern and southern hemisphere due to wave-mean flow interaction within the atmosphere. These predictable signals are also shown to precede changes in extratropical surface climate via the North Atlantic Oscillation. These results provide a novel source of long-range predictability of climate from within the atmosphere, greatly extend the lead time for length of day predictions and link geodesy with climate variability.

Key words Atmospheric angular momentum, predictability, length of day, eddy feedback, climate

Category: Symposium 3: Earth Rotation and Geodynamics = » 3.1: Earth rotation, low-degree gravitational change and mass transport in geophysical fluids

634

S3-007

The Earth and Mars' Variable Rotations Excited by Surficial Fluids

Yonghong Zhou¹、Xueqing Xu¹、Cancan Xu¹、Zhaoyang Kong¹、Xianran An¹、
Xinhao Liao¹、Jianli Chen²、David Salstein³

1. Shanghai Astronomical Observatory, Chinese Academy of Sciences, Shanghai
200030, China

2. Center for Space Research, University of Texas at Austin, Austin, TX 78759, USA

3. Atmospheric and Environmental Research, Lexington, MA 02421, USA

The dynamic interactions that occur between the solid Earth and surficial fluids are related globally by conservation of angular momentum in the Earth system. Owing to this condition, the surficial fluids have shown to be main excitation sources of the Earth's variable rotation on time scales between a few days and several years. Likewise, the Mars' rotation changes due to variations of atmospheric circulation and surface pressure, and the variable Martian polar ice caps associated with the CO₂ sublimation/condensation effects. Here, we present our recent progresses on excitations of the Earth and Mars' rotational variations on multiple time scales: (1) analyses among the LOD change, AAM and ENSO, and the 2020~2021 La Nina event, and (2) the Mars' LOD change/Polar motion with relation to the dust cycles during the Martian Years 24-33. Investigations of the Earth and Mars' rotations by surficial fluids will further our understandings of the Earth and planetary global dynamics.

Key words Earth rotation; Mars's rotation; Surficial fluids.

Category: Symposium 3: Earth Rotation and Geodynamics = » 3.1: Earth rotation, low-degree gravitational change and mass transport in geophysical fluids

684

S3-008

On improved precession-nutation models

Jose M. Ferrandiz¹, Miguel A. Juárez¹, Santiago Belda², Tomás Baenas³,
Sadegh Modiri⁴, Robert Heinkelmann⁵, Alberto Escapa^{6,1}, Harald Schuh^{5,7}

1. University of Alicante

2. Image Processing Laboratory (IPL) - Laboratory of Earth Observation (LEO),
University of Valencia, Spain

3. University Centre of Defense, MDE-UPCT, Murcia, Spain

4. Federal Agency for Cartography and Geodesy (BKG), Department Geodesy,
Frankfurt am Main, Germany

5. Helmholtz Centre Potsdam, GFZ German Research Centre for Geosciences,
Potsdam, Germany

6. Department of Aerospace Engineering, University of León, Spain

7. Technische Universität Berlin (TU Berlin), Germany

In the last two years a few research groups have developed new estimations of nutation amplitudes or precession parameters, corrections to some of the inconsistencies existing between the nutation and precession theories IAU2000 and IAU2006, and new empirical models for the free core nutation (FCN) as well. A part of their results has been already published in journals, whereas another has been presented at main meetings. Research on those subjects was encouraged by Resolution 5 of the 2019 General Assembly of the International Association of Geodesy (IAG). Besides, the GGOS/IERS Unified Analysis Workshop held in October 2019 recommended that effort to be prioritized among the tasks of the current IAU/IAG Joint Working Group on Improving Theories and Models of the Earth's rotation (JWG ITMER). This presentation includes an assessment of the last semi-empirical and semi-analytical precession-nutation models developed by the authors, together with comparisons with the alternative models proposed so far.

Key words Earth rotation - precession and nutation - analytical and empirical models - free core nutation

Category: Symposium 3: Earth Rotation and Geodynamics = » 3.1: Earth rotation, low-degree gravitational change and mass transport in geophysical fluids

838

S3-009

Effects of the observed Earth's oblateness variation on precession-nutation: A first assessment

Jose M. Ferrandiz¹、Alberto Escapa^{2,1}、Tomás Baenas³、Ahmed Z. Zerifi¹、Isabel Vigo¹

1. University of Alicante

2. Dept. of Aerospace Engineering, University of León, Spain

3. University Centre of Defense, MDE-UPCT, Murcia, Spain

The current IAU2000 nutation theory considers the Earth's dynamical ellipticity as a constant, whereas the IAU2006 precession theory uses a linear model for it. Apart from the problems of consistency between the two theories, whose full solution was proposed recently although is not yet implemented in the conventional standards, the fundamental issue, namely whether the observed time variation of the Earth's gravity field can affect the Earth's rotation to a non-negligible extent, remains untreated. This is one of the topics that should be considered in the investigation of future Earth rotation models as encouraged by Resolution 5 of the 2019 General Assembly of the International Association of Geodesy (IAG).

This presentation is intended to share some preliminary results concerning precession and nutation. The variation of the Earth's dynamical ellipticity is modelled from observed time-varying Stokes coefficients, and its effects on the longitude are computed following a new method introduced by the authors to that purpose. The found variations are above the accuracy goals of GGOS, the Global Geodetic Observing System of the IAG, adopted by the IAG Working Group 3.1 on Improving theories and models of the Earth rotation (JWG ITMER), joint with the International Astronomical Union.

Key words Earth rotation - precession and nutation - time-varying gravity

Category: Symposium 3: Earth Rotation and Geodynamics = » 3.1: Earth rotation, low-degree gravitational change and mass transport in geophysical fluids

862

S3-010

Chandler wobble excitation by external geophysical fluids estimated from GRACE gravity data

Aleksander Brzezinski^{1,2}, Justyna Sliwinska²

1. Warsaw University of Technology

2. Space Research Centre, Polish Academy of Sciences

We investigate the excitation of the free Chandler wobble by the large-scale processes taking place in the external fluid layers of the Earth, including the atmosphere, the oceans and the land hydrology. The mass term of excitation is expressed by the so-called gravimetric excitation function estimated from time variation of degree-2, order-1 harmonics of the Earth gravity field, derived from Gravity Recovery and Climate Experiment (GRACE) data. We compare the excitation results based on the geodetic observations of polar motion and the most recent GRACE solutions. In addition, we estimate to which extent the Chandler wobble excitation balance can be improved when adding the motion term of excitation derived from the output fields of the global circulation models of external geophysical fluids.

Key words polar motion, Chandler wobble, geophysical excitation, GRACE data

Category: Symposium 3: Earth Rotation and Geodynamics = » 3.1: Earth rotation, low-degree gravitational change and mass transport in geophysical fluids

874

S3-011

Internal co-seismic displacement and strain changes inside a homogeneous spherical Earth

Jie Dong¹、Pengfei Cheng¹、Hanjiang Wen¹、Wenke Sun²

1. Chinese Academy of Surveying & Mapping

2. University of Chinese Academy of Sciences

In this study, we devised a new set of analytical foundation solutions to compute the internal co-seismic displacement and strain changes caused by four independent point sources (strike-slip, dip-slip, horizontal tensile, and vertical tensile) inside a homogeneous spherical Earth model. Our model provides constraints on the deformation properties at depth, and reveals that the internal co-seismic deformation is larger than that on the surface. The deformation near the source is convergent with our formulae. For the internal deformation at radial section plane, the patterns of horizontal displacements u_θ , u_ϕ and strain changes e_{rr} , $e_{\theta\theta}$, $e_{\phi\phi}$, $e_{\theta\phi}$ caused by strike-slip and tensile sources appear symmetric at the equidistance above and below the source. Their amplitudes are not identical but with a small discrepancy actually. Unlike these, the patterns of radial displacements for strike-slip and tensile sources exhibit point symmetry with the equidistance from the source. Also, the corresponding amplitudes are slightly different. The displacements u_θ , u_ϕ and strain changes e_{rr} , $e_{\theta\theta}$, $e_{\phi\phi}$, $e_{\theta\phi}$ caused by dip-slip also appear the same properties as u_r of strike-slip source. The magnitudes of the displacements and strain changes depend on the source types. The curvature effect on the near-field surface deformations is small, and it increases with the studied depth. But for the far-field deformation caused by the strike-slip source ($d_s = 20$ km), the curvature effect can be as large as 77% when the epicentral distance approximates to 1778 km.

Key words analytical foundation solutions; internal deformation; spherical Earth model

Symposium 3: Earth Rotation and Geodynamics

S3.2: Observations and modeling of deformation related to changing ice loads

Category: Symposium 3: Earth Rotation and Geodynamics => 3.2: Observations and modeling of deformation related to changing ice loads

137

S3-012

Spatiotemporal glacial isostatic model resolution testing for small ice loads: Input parameter recommendations and examples for mountain glaciers in southcentral and southeast Alaska

Kimberly DeGrandpre, Jeffrey Freymueller
Michigan State University

Small glaciers (surface areas <30,000 km²) are rarely included in global or regional models for glacial isostatic adjustment because their individual signals are considered to be insignificant. When such glaciers are included, they are often smoothed to an arbitrary resolution in both time and space over a generally glaciated region. While these small glaciers are individually not voluminous, they frequently exhibit rapid and dynamic accumulation and loss that can have a significant effect on local glacial isostatic adjustment model predictions when totaled across many such loads. Detailed ice histories for these glaciers are generally unavailable as their remote nature prohibits direct measurement and small spatial extents limit spaceborne observations, but sparse measurements does not necessarily mean that their influence is negligible.

We address these questions: How much ice is missing from current models and what effect does this missing ice have on rate and displacement predictions? How precisely does the space-time load history need to be known to make accurate predictions of geodetic observables? We conducted a series of synthetic tests for disk loads of various sizes using the TABOO postglacial rebound calculator. Results will be summarized for several test loads representative of glaciers of varying sizes in southcentral and southeastern Alaska, including Columbia Glacier, the Bering Malaspina glacier system, the Juneau Ice Field, and a generic glacially filled fjord. Loading histories are evaluated for up to 3000 years after the complete removal of a volume of ice to identify the temporal extent of signals from these smaller loads, with particular interest in changes over the past 200 years, simulating volumes related to the Little Ice Age. Recommendations for model input parameter values and the most appropriate use and resolution of various datasets concerning these small, densely distributed loads are provided.

Key words glacial isostatic adjustment, ice loads, TABOO, Alaska, benchmarking, little ice age

Category: Symposium 3: Earth Rotation and Geodynamics => 3.2: Observations and modeling of deformation related to changing ice loads

154

S3-013

GNSS observations and GIA modelling of vertical crustal motion in the Lützow-Holm Bay region, East Antarctica

Junichi Okuno^{1,2}, Akihisa Hattori², Takeshige Ishiwa¹, Yoshiya Irie¹, Yuichi Aoyama^{1,2}, Koichiro Doi^{1,2}, Yoichi Fukuda¹

1. National Institute of Polar Research

2. SOKENDAI

Geodetic and geomorphological observations in the Antarctic coastal area generally indicate the uplift movement of the crust associated with the Antarctic Ice Sheet (AIS) change since the Last Glacial Maximum (LGM). This trend is called the glacial isostatic adjustment (GIA), the Earth's viscoelastic response due to the surface load changes. The current crustal motion, which the GNSS observation indicates, includes the elastic component due to the present-day surface mass balance of AIS in addition to the viscoelastic response. To reveal the secular crustal movement associated with the GIA, the separation of both components due to the current mass balance and last deglaciation is essential.

Recently geomorphological study in the Lützow-Holm Bay region, East Antarctica, reported that the rapid ice thinning of about 400 m for 3000 years has occurred in the early-to-mid Holocene. This melting may influence the crustal deformation through the viscoelastic response due to rapid ice load change. Therefore, we examine the GIA component due to this melting on the current crustal deformation rate using numerical modeling. Results indicate that the viscoelastic relaxation due to the abrupt ice thinning depends significantly on the upper mantle viscosity profile. This presentation will discuss the dependence of the AIS retreat history and mantle viscosity structure on the GIA-induced crustal movement based on the numerical experiments.

Key words GIA, GNSS, Antarctic Ice Sheet, Holocene rapid melting

Category: Symposium 3: Earth Rotation and Geodynamics => 3.2: Observations and modeling of deformation related to changing ice loads

159

S3-014

Dependence of upper mantle viscosity profile on GIA-induced gravity change in Antarctica

Yoshiya Irie¹、Jun'ichi Okuno^{1,2}、Takeshige Ishiwa¹、Koichiro Doi^{1,2}、Yoichi Fukuda¹

1. National Institute of Polar Research

2. The Graduate University for Advanced Studies, SOKENDAI

The Antarctic ice mass loss is accelerating due to recent global warming. Changes in Antarctic ice mass have been observed as the gravity change by GRACE (Gravity Recovery and Climate Experiment) satellites. However, the gravity signal includes both the component of the ice mass change and the component of the solid Earth response to surface mass change (Glacial Isostatic Adjustment, GIA). Namely, to constrain the ice mass change from the gravity observation, viscosity structure of the Earth's mantle and ice history from the last deglaciation are required with sufficient accuracy. Here we examine spatial and temporal patterns of gravity field changes in Antarctica using GIA modeling. We also explore the sensitivities of the gravity field change to mantle viscosity structure and ice history. Results indicate that the gravity field change mainly depends on the upper mantle viscosity profile. In particular, the long - wavelength gravity field changes in the adoption of viscosity models with a low viscosity layer beneath the elastic lithosphere become dominant. On the other hand, short - wavelength components become dominant for models with a low viscosity layer above the 670 km phase boundary. Moreover, results indicate that the gravity field change significantly depends on the end of Holocene deglaciation. In particular, the gravity field change for W12 is less sensitive to the low viscosity layer than that for ICE-6G. This is because the postglacial period for W12, which is shorter than that for ICE-6G, is not enough time to reflect the viscous relaxation process related to the low viscosity layer. In this presentation, we intend to discuss the verification of whether GRACE data can detect the impacts of low viscosity layer on the gravity field change.

Key words GIA, GRACE

Category: Symposium 3: Earth Rotation and Geodynamics => 3.2: Observations and modeling of deformation related to changing ice loads

313

S3-015

The mid-Holocene sea-level highstand and Glacial Isostatic Adjustment modelling

Tanghua Li¹、 Hansheng Wang²、 Stephen Chua¹、 Nicole Khan³、 Patrick Wu⁴、 Benjamin Horton^{1,5}

1. Earth Observatory of Singapore, Nanyang Technological University

2. State Key Laboratory of Geodesy and Earth's Dynamics, Innovation Academy for Precision Measurement Science and Technology, Chinese Academy of Science

3. Department of Earth Sciences and Swire Marine Institute, University of Hong Kong

4. Department of Geoscience, University of Calgary

5. Asian School of the Environment, Nanyang Technological University

Holocene relative sea-level (RSL) records from regions distal from ice sheets (far-field) are commonly characterized by a mid-Holocene highstand, when RSL was higher than present level. Both the magnitude and timing of the mid-Holocene highstand vary spatially due to hydro-isostatic processes (e.g., ocean syphoning and continental levering). However, the timing, magnitude and source of ice-equivalent sea level in the middle to late Holocene are not well determined.

Here, we compare Glacial Isostatic Adjustment (GIA) model predictions to a standardized database of sea-level index points (SLIPs) from Southeast Asia where we have near-complete Holocene records. The database has more than 130 SLIPs that span the time period from ~9.5 ka BP to present. We investigate the sensitivity of mid-Holocene RSL predictions to variations in GIA parameters, including the lateral lithospheric thickness variation, mantle viscosity (both 1D and 3D), and deglaciation history from different ice sheets (e.g., Laurentide, Fennoscandia, Antarctica).

We compute gravitationally self-consistent RSL histories from the GIA model with time dependent coastlines and rotational feedback using the Coupled Laplace-Finite Element Method. The preliminary results show that the timing of the highstand is mainly controlled by the deglaciation history (ice-equivalent sea level), while the magnitude is dominated by Earth parameters (e.g., lithospheric thickness, mantle viscosity). We further investigate whether there is meltwater input during the middle to late Holocene and whether the RSL records from Southeast Asia can reveal the meltwater source (e.g., Antarctica).

Key words Sea-level change; Glacial Isostatic Adjustment; mid-Holocene highstand.

Category: Symposium 3: Earth Rotation and Geodynamics => 3.2: Observations and modeling of deformation related to changing ice loads

474

S3-016

Vertical Land Motion From Present - Day Deglaciation in the Wider Arctic

Carsten Bjerre Ludwigsen, Ole Baltazar Andersen
DTU Space

A high-resolution ice model (2x2 km) for Arctic glaciers and Greenland Ice Sheet has been constructed from 2003-2015 to calculate yearly elastic VLM-rates in the wider Arctic region (roughly north of 30N). The high resolution makes it possible to use the elastic VLM in both in the proximity of glacial ice change and in the far field (e.g. Northern Europe).

The elastic VLM-model is combined with a GIA-model and is corrected for non-secular geocenter motion effects, as well as rotational feedback, to construct a complete VLM-model that is comparable with yearly GNSS-measured VLM-rates. Furthermore, are far field elastic VLM-estimates from Antarctica added to the model (about -0.1 mm/y in the Arctic area).

Averaged over time, does the VLM-model correlate well with GNSS-sites - in particular in the far field and clearly outperforms a GIA-only model. Residuals between GNSS and the combined VLM-model is used to quantify the effect of ongoing seismic activity (Alaska), low-viscosity areas (Iceland) or ongoing rebound from Little Ice Age (Svalbard) on VLM.

Generally, it shows that VLM from present-day ice melt of in particular Greenland, is far-reaching and even in the North Sea region or along the North American coast show uplift rates in the order of 0.4-0.7 mm/y. Interestingly, this is comparable to Greenland's sea level contribution for the same period, thereby is elastic VLM, in parts, 'neutralizing' the barystatic sea level contribution of Greenland and glaciers. As Arctic ice mass loss continues to accelerate, the elastic uplift will have increased importance for coastal regions and future relative sea level projections.

Key words Vertical Land Movement,

Category: Symposium 3: Earth Rotation and Geodynamics => 3.2: Observations and modeling of deformation related to changing ice loads

543

S3-017

Bedrock uplift in response to recent ice-mass variability on northern Marguerite Bay, Antarctic Peninsula

Nahidul Hoque Samrat^{1,3}, Matt King¹, Christopher Watson¹, Andrea Hay¹,
Valentina Barletta², Andrea Bordonì²

1. University of Tasmania

2. Technical University of Denmark

3. Central Queensland University

Glaciers in the Antarctic Peninsula have been thinning and retreating over the 20th and 21st centuries due to surface and ocean warming and ice shelf collapse. This results in a solid Earth deformation measurable by GPS fixed to bedrock, which provides insight into solid Earth rheology when combined with models. We investigate ice-mass change and bedrock deformation in the northern Marguerite Bay (NMB) region of the Antarctic Peninsula from ~2002 to 2015 in order to provide new constraints on Earth rheology. The mass balance estimation over this region suggests that the ice mass loss reduced around the Rothera research station (ROTH) since ~2012 and the Muller Ice Shelf since ~2009 compared to 2004-2012 and 2002-2009, respectively. GPS time series recorded at nearby ROTH station reveals bedrock uplift of $\sim 1.6 \pm 0.8$ mm/year (1999.1-2005.0) increasing to $\sim 5.9 \pm 0.9$ mm/year (2006.0-2010.0) before reducing to $\sim 4.6 \pm 0.6$ mm/year (2010.0-2016.0) and now $\sim 1.8 \pm 1.3$ mm/year (2016.0-2020.0). This cannot be explained by purely elastic deformation. A comparison between ROTH and modeled viscoelastic deformation up to 2015 suggests the change can be explained by a model with an upper mantle viscosity of $\sim 0.1-9 \times 10^{18}$ Pa s with $\sim 10-95$ km of effective elastic lithosphere thickness for NMB. Analysis of a nearby site at San Martin (SMRT) over 1999.3-2009.2 permits a wider range of lithosphere thickness ($\sim 10-130$ km) and upper-mantle viscosity ($\sim 0.1-20 \times 10^{18}$ Pa s) but in agreement with the ROTH analysis. This viscosity estimate is consistent with a north-south gradient in viscosity suggested by previous studies focused on specific regions within the Antarctic Peninsula and adds further evidence of low viscosity upper mantle in the northern Antarctic Peninsula.

Key words Dynamics of lithosphere and mantle, Rheology: crust and lithosphere, Rheology: mantle, Antarctica, Space geodetic surveys

Category: Symposium 3: Earth Rotation and Geodynamics => 3.2: Observations and modeling of deformation related to changing ice loads

555

S3-018

A study of sea level change around Greenland based on multi-source data

Jiachun An、 Baojun Zhang、 Zemin Wang、 Songtao Ai、 Yu Feng、 Hong Geng
Wuhan University

In this study, we analyzed the sea level changes in Greenland by using observations of GPS stations, tide gauges, gravity satellite and altimetry satellite, as well as glacier isostatic adjustment models, and revealed the profound impact of Greenland ice sheet melting under global warming. We dealt with the observations of more than 50 GPS stations in and around Greenland from 2007 to 2018, and used principal component analysis to eliminate common mode errors. The results show that all the stations in Greenland have an upward trend, and the stations in the southern region rise faster. The GPS-derived vertical velocities corrected by the glacier isostatic adjustment model fit well with the GRACE-derived vertical velocities caused by the mass changes of the Greenland ice sheet. At the same time, the absolute sea level change around Greenland is analyzed in combination with the relative sea level obtained from tide stations and the crustal rise rate obtained from GPS stations, and verified by the altimetry satellite observations. The results show that the sea level around Greenland has decreased significantly and there are large spatial differences in different regions.

Key words sea level change, Greenland, GPS, tide gauge

Category: Symposium 3: Earth Rotation and Geodynamics => 3.2: Observations and modeling of deformation related to changing ice loads

707

S3-019

Quantitative Analysis of Arctic Ice Flow Acceleration with Increasing Temperature

Zemin Wang^{1,4}、Boya Yan^{1,4}、Songtao Ai^{1,4}、Kim Holmén²、Jiachun An^{1,4}、
Hongmei Ma³

1. Wuhan University

2. Norwegian Polar Institute

3. Polar Research Institute of China

4. Chinese Antarctic Center of Surveying and Mapping

This study explores the ice flow acceleration (21.1%) of Pedersenbreen during 2016–2017 after the extremely warm winter throughout the whole Arctic in 2015/2016 using in situ data and quantitatively analyses the factors contributing to this acceleration. Several data sets, including 2008–2018 air temperature data from Ny-Ålesund, ten-year in situ GPS measurements and Elmer/Ice ice flow modelling under different ice temperature scenarios, suggest that the following factors contributed to the ice flow acceleration: the softened glacier ice caused by an increase in the air temperature (1.5°C) contributed 2.7%–30.5%, while basal lubrication contributed 69.5%–97.3%. The enhanced basal sliding was mostly due to the increased surface meltwater penetrating to the bedrock under the rising air temperature conditions; consequently, the glacier ice flow acceleration was caused mainly by an increase in subglacial water. For Pedersenbreen, there was an approximately one-year time lag between the change in air temperature and the change in glacier ice flow velocity.

Key words ice flow velocity, Arctic temperature rising, Pedersenbreen, Elmer/Ice, meltwater

Category: Symposium 3: Earth Rotation and Geodynamics => 3.2: Observations and modeling of deformation related to changing ice loads

715

S3-020

Surface mass balance loading displacement as a dominant source of error in GPS estimates of Antarctic glacial isostatic adjustment and its relevance to a critical sector of East Antarctica

Matt King, Christopher Watson
University of Tasmania

We show that varying surface mass balance (SMB) induces a dominant source of noise in Antarctic bedrock GPS time series, an effect more widespread than the effects of dynamic ice mass change concentrated within some regions of fast ice flow. Using models of SMB anomalies and an elastic Earth model, we show that SMB loading displacement power spectra are approximated by a random walk process with the greatest power at lowest frequencies. The power at the lowest frequencies easily exceeds that of atmospheric loading displacements. If SMB loading displacement is not considered at GPS bedrock sites in Antarctica, biases can reach $> \pm 2$ mm/yr over periods up to 11 years with the largest biases in the Antarctic Peninsula and Marie Byrd Land. We explore the impact of SMB loading on new GPS time series of bedrock uplift from the Totten-Denman glacier region of East Antarctica where GIA models disagree, glaciers appear to be losing mass, and few GIA model data constraints exist. SMB loading induces uplift rate bias of up to 2.2 mm/yr over 2014-2019 in this region which, after correcting for it and common mode error, shows that the bedrock in this region is likely subsiding or near zero. The exception is the Totten Glacier region where residual uplift of $\sim 1-2$ mm/yr is evident when correcting for either SMB loading displacements or those derived from ice altimetry that also include a dynamic ice mass change component. The results suggest closest agreement with the W12a GIA model in this region and disagreement with some empirical solutions of bedrock uplift which suggest strong uplift.

Key words glacial isostatic adjustment (GIA), GPS, bedrock uplift, surface mass balance

Category: Symposium 3: Earth Rotation and Geodynamics => 3.2: Observations and modeling of deformation related to changing ice loads

724

S3-021

Monitoring glacier mass balance of the West Kunlun Mountains over the past 20 years by ICESat-2 altimetry and bistatic InSAR

Tao Li、Liming Jiang

State Key Laboratory of Geodesy and Earth's Dynamics, Innovation Academy for Precision Measurement Science and Technology, Chinese Academy of Sciences

Mass balance of mountain glaciers is an important parameter of glacier changes, which is of great significance to climate change research, ecological environment protection and water resources management. In recent years, ice melting of mountain glaciers in the Qinghai-Tibet Plateau has accelerated response to atmospheric warming, but the glaciers in West Kunlun Mountains have shown a stable or even increasing ice volume during the early 21st century, and is considered as the center of the "Karakoram anomaly", however, the recent changes in the glacier mass balance of this region are still unclear.

During the past decade, space-borne geodesy technologies (e.g. gravimetry, altimetry and InSAR) have been widely used to estimate regional-scale mass balance in High Mountain Asia (HMA). In this study, we combined ICESat-2 satellite laser altimetry and bistatic InSAR observation to monitor the changes of glacier thickness and mass balance in the West Kunlun Mountains from 2000 to 2018/19, and analyzed its temporal and spatial characteristics. Glacier surges were also analyzed.

The results show that: (1) From 2013 to 2018/19, the average annual increase rate of glacier thickness in the West Kunlun Mountains was 0.274 ± 0.061 m/a, and the mass balance was 0.233 ± 0.054 m w.e./a; (2) During 2000-2018/19, the glacier presented a positive trend, and the mass accumulation rate during 2013-2018/19 was higher than that during 2000-2013 (0.173 ± 0.029 m w.e./a); (3) Glacier surges in the West Kunlun Mountains were still widely distributed during 2013-2018/19. The 5Y641F0073 glacier and West Kunlun glacier were active. A new surge-type glacier (5Y641F0046) was found, which elevation change presents anomalous spatial characteristics and the ice flow velocity changes sharply.

The results preliminarily verified the feasibility and reliability of TanDEM-X global DEMs and ICESat-2 laser altimeter measurements for estimating the mass balance of mountain glaciers.

Key words ICESat-2; Satellite altimetry; Bistatic InSAR; West Kunlun Mountains; Glacier mass balance

Category: Symposium 3: Earth Rotation and Geodynamics => 3.2: Observations and modeling of deformation related to changing ice loads

787

S3-022

Spatio-temporal evolution of the Greenland ice sheet and associated deformation of the Earth: a multi-technique geodetic approach

Ana Sanchez^{1,4}、 Laurent Métivier^{4,5}、 Luce Fleitout²、 Marianne Greff⁴、 Kristel Chanard^{4,5}、 Romain Hugonnet^{3,6,7}、 Etienne Berthier³

1. Centre national d'études spatiales (CNES), France.
2. Laboratoire de Géologie de l'École Normale Supérieure, PSL Research University, UMR CNRS 8538, 75231 Paris, France
3. LEGOS, Université de Toulouse, CNES, CNRS, IRD, UPS, Toulouse, France.
4. Université de Paris, Institut de physique du globe de Paris, CNRS, IGN, F-75005 Paris, France.
5. ENSG-Géomatique, IGN, F-77455 Marne-la-Vallée, France.
6. Laboratory of Hydraulics, Hydrology and Glaciology (VAW), ETH Zürich, Zürich, Switzerland.
7. Swiss Federal Institute for Forest, Snow and Landscape Research (WSL), Birmensdorf, Switzerland.

The evolution of the Greenland Ice Sheet (GIS) is an important indicator of climate change and driver of sea level rise. However, providing accurate GIS ice mass balance remains a challenge today. Here, we propose to combine geodetic measurements to improve our knowledge of the GIS spatial and temporal evolution. We attempt to reconcile satellite altimetry observations of ice volume variations with regional GNSS velocities estimates and time variable space gravity measurements over the 2003-2009 and 2011-2015 periods. The GIS mass variations are inferred from satellite altimetry for large ice sheets (ICESat-1 and CryoSat-2) and digital elevation models generated from multiple satellite archives for peripheral glaciers, associated with IMAU-FDM firn model. The spatial and temporal variations of the gravity field are measured by the GRACE mission for which we use an improved solution, based on a combination of solutions from various analysis centers, where smaller wavelength signals are preserved.

To resolve short wavelength load variations affecting the displacement of nearby GNSS stations, we use Green's functions for vertical crustal displacements assuming purely elastic Earth properties. We show that vertical elastic displacements are in good agreement with observations in some regions, but models disagree in the South-eastern and the Northern parts of Greenland. We show that shorter wavelengths load variations of peripheral glaciers are essential to compute deformation close to GNSS stations but are not sufficient to fully explain GNSS observations.

We also compare a mass variation model combining altimetry with a firm model (FDM) to one using a constant density with gravity field variations observed by the GRACE mission. We show that the model with FDM underestimates ice mass loss by a large factor.

We then explore the potential viscoelastic response of the asthenosphere to recent ice and little ice age mass loss to further explain observed GNSS displacements.

Key words Greenland Ice Sheet, ice mass balance, GNSS, GRACE, satellite altimetry, peripheral glaciers

Category: Symposium 3: Earth Rotation and Geodynamics => 3.2: Observations and modeling of deformation related to changing ice loads

895

S3-023

Glacier velocity monitoring and the potential points of geological hazards monitoring in A'nyemaqen Glacier

Zhaoxia Miao^{1,2}, Lin Bai^{1,2}, Zhenhong Li^{1,2}, Longyan Wang^{1,2}, Chenglong Zhang^{1,2}

1. College of Geological Engineering and Geomatics, Chang'an University, Xi'an 710054, China.
2. Key Laboratory of Western China's Mineral Resource and Geological Engineering, Ministry of Education, Xi'an 710054, China

Glaciers is the important freshwater resource, and may lead to geological disasters due to glaciers melting caused by global warming. In this paper, we use the Sentinel-1A data to monitor the surface velocity of A'nyemaqen glacier during 2016~2020 with offset tracking method. The results show that the maximum velocity reaches 6 m/a, with a higher velocity in the warm season (May to September) and a lower velocity in the cold season (October to April of the next year). Then, the potential points of geological hazards around A'nyemaqen glacier are identified by ground deformation derived by SBAS-InSAR and optical image. Most of the potential points of geological hazards are located in the surrounding areas of the A'nyemaqen glacier. The most likely reason is that the sustained glacier melting increases the soil moisture, and reduces the strength of the rock and soil, resulting in the geological hazards such as landslides and collapses. The study is meaningful for the prevention and reduction of geological disasters caused by glaciers melting.

Key words Glacier velocity; SAR offset tracking; geological hazards; SBAS-InSAR; A'nyemaqen glacier

Symposium 3: Earth Rotation and Geodynamics

S3.3: Geodetic observations in volcanic and tectonically active areas

Category: Symposium 3: Earth Rotation and Geodynamics => 3.3: Geodetic observations in volcanic and tectonically active areas

183

S3-024

Horizontal and vertical deformation rates linked to the Magallanes-Fagnano Fault System, Tierra del Fuego: interpretation of the geodetic observations in the context of geological evidence and the current seismic cycle

Luciano Pedro Oscar Mendoza^{1,3}, Andreas Richter^{3,4,1}, Eric Rodolfo Marderwald^{3,1}, José Luis Hormaechea^{2,5,3}, Gerardo Connon^{2,3}, Mirko Scheinert⁴, Reinhard Dietrich⁴, Raúl Anibal Perdomo^{5,3}

1. MAGGIA, FCAG, Universidad Nacional de La Plata (UNLP), La Plata, Argentina

2. Estación Astronómica Río Grande (EARG), Río Grande, Argentina

3. Consejo Nacional de Investigaciones Científicas y Técnicas (CONICET), Buenos Aires, Argentina

4. Institut für Planetare Geodäsie (IPG), Technische Universität Dresden (TUD), Dresden, Germany

5. Facultad de Ciencias Astronómicas y Geofísicas (FCAG), Universidad Nacional de La Plata (UNLP), La Plata, Argentina

We present results which are based on 24 years of GNSS observations at Tierra del Fuego, since 1994. The data analysis is based on a reprocessing of all data with up-to-date models and satellite products. We apply a precise point positioning (PPP) processing strategy, made possible by the recent availability of highly accurate and consistent GNSS satellite orbits and clocks. The 54 stations included in the analysis allow a detailed investigation of horizontal and vertical velocity rates which provide a sound basis to study the deformation associated with the Magallanes-Fagnano Fault System, i. e. the transform boundary between the South American and Scotia plates at the southern tip of Patagonia. A deeper geophysical modelling has been performed which points to a seismogenic layer thickness of 15 ± 3 km and to fault planes inclined 64 ± 4 deg at the uppermost ends of the fault segments. Furthermore, we model the current seismic cycle from the great 1949 M_w 7.7 earthquake to the present, including the ongoing postseismic viscoelastic relaxation process. We identify a seismic moment deficit rate and a cumulative seismic moment which is at present equivalent to an earthquake of magnitude $M_w \sim 7$.

Key words Tierra del Fuego, GNSS, seismic cycle, Magallanes-Fagnano Fault System

Category: Symposium 3: Earth Rotation and Geodynamics => 3.3: Geodetic observations in volcanic and tectonically active areas

197

S3-025

Crustal rheology and heterogeneity impact on tectonic stress characteristics of North China revealed by GNSS observations

Yuan Gao¹、Wei Qu^{1,2}、Qin Zhang¹、Hailu Chen¹、Shichuan Liang¹

1. Chang'an University

2. State Key Laboratory of Geohazard Prevention and Geoenvironment Protection, Chengdu University of Technology

North China is characterized by significant lithosphere heterogeneity and numerous faults due to continuous Indo-Asia collision and subduction from the Pacific plate, with the occurrence of many historical devastating earthquakes. To further understand the mechanisms of seismicity and fault activity in this domain, a three-dimensional viscoelastic finite element model based on the lithospheric lateral heterogeneity of physical properties across the north–south gravitational lineament (NSGL), spatial distribution of tectonic faults, and interseismic global navigation satellite system (GNSS) velocities (1999–2018) was established. Then the stress accumulation characteristics across the NSGL and its relationship with seismicity were analyzed. Finally, the temporal and spatial variations of stress along major faults were explored and potential relationships between the stress components and rupture mechanisms of typical faults were further analyzed. The results showed that high maximum shear stress corresponded well to the focal depth in eastern North China (ENC) and western North China (WNC), which suggests that the different brittle crustal thicknesses across the NSGL may be one of the major factors that dominates earthquake depth in North China. Maximum shear stress is significantly accommodated on faults around the Ordos Block in WNC and northern faults in ENC, which is consistent with frequent seismic activity in these domains. The relationship between stress components and rupture mechanisms of typical faults imply that the differential tectonic loading from neighboring blocks may be one of the major dynamic factors for seismogenic processes in North China.

Key words North China; GNSS observation; Viscoelastic finite element model; North–south gravitational lineament; Stress characteristic; Tectonic fault

Category: Symposium 3: Earth Rotation and Geodynamics => 3.3: Geodetic observations in volcanic and tectonically active areas

199

S3-026

Spatiotemporal functional modeling of postseismic deformation after the 2011 Tohoku-Oki earthquake

Satoshi Fujiwara, Mikio Tobita, Shinzaburo Ozawa
Geospatial Information Authority of Japan

Postseismic deformation continues for a long duration after major earthquakes. A previous study has shown that temporal changes in postseismic deformation can be approximated through simple functions. Almost 10 years have passed since the 2011 M9 Tohoku-Oki earthquake, and data at continuously operating GNSS stations have accumulated. We performed statistical processing of the data on postseismic deformations of this earthquake and obtained and verified their spatiotemporal distribution. We were able to approximate the postseismic deformations over a wide area with a standard deviation of 1 cm for approximately 10 years using two logarithmic and one exponential functions. However, the residuals from the functional model showed a sharp deviation from 2015. Although the pattern of postseismic deformation did not change after the earthquake, a change in steady-state velocity occurred from 2015 and continues till date. By improving the functional model to incorporate this steady-state velocity, we can reduce the overall standard deviation of the residuals of more than 200 stations distributed over more than 1000 km to less than 0.4 cm in the horizontal component. Furthermore, the spatial distributions of the coefficients of each time constant are not random and have a natural spread, which makes it possible to grid model them in terms of a spatial function. The spatial distributions of the short- and long-period components of the functional model and the afterslip and viscoelastic relaxation calculated by a physical model are similar to each other, respectively. Each time function has a meaning related to the physical processes in the underground, which provides an understanding of the physical phenomena involved in seismogenesis. Additionally, there are the other purposes of using the spatiotemporal functional model developed in this study: discerning small variations other than those of the postseismic deformation, and modeling for precise positioning such as ITRF.

Key words 2011 Tohoku-Oki earthquake, crustal deformation, postseismic deformation, slip, global navigation satellite system time series, predicting model

Category: Symposium 3: Earth Rotation and Geodynamics => 3.3: Geodetic observations in volcanic and tectonically active areas

230

S3-027

On the detection of structural breaks in GNSS station coordinate time series caused by earthquakes using machine learning

Laura Crocetti, Matthias Schartner, Benedikt Soja
ETH Zurich

The Global Navigation Satellite System (GNSS) continuously monitors station positions all around the world with a high accuracy. This high accuracy, together with the dense global coverage, makes GNSS observations sensitive to geophysical phenomena such as earthquakes. Earthquakes are geohazards that are characterized by an abrupt occurrence and cause deformations of the Earth's surface. These deformations are reflected in the GNSS station coordinate times series as structural breaks. For various applications, such as the estimation of velocity fields, a precise knowledge of the time an earthquake, and thus a structural break, occurred in the time series is crucial for achieving highest accuracy.

In this study, we tried to detect structural breaks caused by earthquakes using novel machine learning (ML) algorithms. We used big data GNSS station coordinate time series from the Nevada Geodetic Laboratory database to build a supervised machine learning model. After a sophisticated data preparation process, several ML algorithms were applied and compared based on their performance. The results revealed that by using Random Forest, up to 80% of all earthquakes causing significant displacements could be detected. This confirms that ML is a capable technique to inspect GNSS station coordinate time series. Extracting reliable information from GNSS signals could be of great benefit to geosciences and society.

Key words GNSS, earthquakes, machine learning

Category: Symposium 3: Earth Rotation and Geodynamics => 3.3: Geodetic observations in volcanic and tectonically active areas

266

S3-028

Grey Wolf Optimal Combination Algorithm for Inversion of Seismic Source Parameters: A Case Study of the Bodrum-Kos earthquake in 2017

Longxiang Sun, Leyang Wang

Faculty of Geomatics, East China University of Technology

The determination of the seismic source parameters is an essential component of earthquake investigations. Due to the high precision of modern geodetic technologies, it leads to the higher requirements for the inversion algorithm of seismic source parameters. In view of this problem, we successfully develop a novel Grey Wolf Optimization (GWO) algorithm to invert the seismic source parameters. The GWO algorithm with the strategy of the nonlinear decreasing convergence factor based on the cosine law is proposed to instead that of the original linear decreasing. Subsequently, a combination approach with the improved weighted GWO algorithm and the Simplex algorithm is configured and the introduction of the latter algorithm is to stabilize the performance of the proposed GWO algorithm. Thus, the combination algorithm has better advantages for both convergence and stability. Finally, we achieve synthetic tests to evaluate the performance of the basic weighted distance GWO algorithm, the genetic algorithm and the combination algorithm. The simulated experimental results show that the estimation of seismic source parameters via the proposed algorithm is superior to the weighted distance GWO algorithm, which expresses excellent stability and accuracy. On the other hand, the stability of seismic source parameters is validated between the combination algorithm and the genetic algorithm, and we find the superiority of the combination algorithm. Furthermore, the availability of the combination algorithm is tested by the 2017 Bodrum-Kos earthquake. The results show that the combination algorithm can not only achieve the inversion precision of genetic algorithm, but also exhibit better parameters stability. Considering that the accurate determination of seismic source parameters is conducive to earthquake investigations, our algorithm has potential applications in the inversion of seismic source parameters.

Key words Global Positioning System; Seismic source parameter inversion; Grey Wolf Optimization algorithm; Simplex algorithm; Bodrum-Kos earthquake.

Category: Symposium 3: Earth Rotation and Geodynamics => 3.3: Geodetic observations in volcanic and tectonically active areas

282

S3-029

Retrieving 3D coseismic deformation of the 2016 Mw 7.8 Kaikoura earthquake using different combinations of SAR and optical data

Ajian Zou、Leyang Wang
East China University of Technology

Co-seismic deformation monitoring is of great significance for the interpretation of Co-seismic deformation characteristics and intuitive understanding of fault geometric characteristics. For large earthquakes with surface rupture, GPS technique has a low spatial resolution, and InSAR technology will cause phase decorrelation due to large deformation gradients, it is impossible to obtain specific fault near-field deformation. Optical image correlation(OIC) and pixel offset tracking(POT) based on sub-pixel cross-correlation can solve these problems well. This paper takes the 2016 Kaikoura Mw 7.8 earthquake as an example. We first obtained the EW and NS directions deformation using Sentinel 2 data, and obtained the range and azimuth directions deformation using Sentinel 1 data. Both results can provide the specific deformation near the fault and the geometric characteristics of the fault. In addition, in order to determine the most reliable combination of Sentinel 1 SAR data and Sentinel 2 optical data to obtain the 3D deformation field, these deformation types are divided into different combinations, and the least square method is used to compute the 3D deformation. The results show that weighting various kinds of data can enhance the accuracy of some combination results, especially the accuracy of the NS deformation. The vertical deformation obtained by combining the optical data with the SAR data of ascending or descending orbit is not in good agreement with the actual situation. The NS deformation obtained by the SAR data is quite different from that obtained by the optical data, but the EW deformation has a good consistency. The combination of optical data and SAR data, the combination of optical data and range deformation of SAR data can obtain better 3D deformation. Combined with the different kinds of observation data, the effect and precision of 3D deformation can be controlled well, which can provide a reference for the study of 3D surface deformation.

Key words Optical images correlate; SAR pixel offset tracking; kaikoura earthquake; Three-dimensional deformations

Category: Symposium 3: Earth Rotation and Geodynamics => 3.3: Geodetic observations in volcanic and tectonically active areas

322

S3-030

Coeruptive and posteruptive crustal deformation associated with the 2018 Kusatsu-Shirane phreatic eruption based on PALSAR-2 time series analysis

Yuji Himematsu¹, Taku Ozawa¹, Yosuke Aoki²

1. National Research Institute for Earth Science and Disaster Resilience

2. The University of Tokyo

We report coeruptive crustal deformation associated with the 2018 Kusatsu-Shirane phreatic eruption detected by time series analyses of L-band satellite SAR (ALOS-2/PALSAR-2) data. Cumulative deformation maps derived from SAR time series analyses show that subsidence and eastward displacement dominate the southwestern side of an eruptive crater with a spatial extent of approximately 2 km in diameter. Although we were unable to identify any significant deformation signals before the 2018 eruption, posteruptive deformation on the southwestern side of the crater has been ongoing until the end of 2019. This prolonged deformation implies the progression of posteruptive physical processes within a confined hydrothermal system, such as volcanic fluid discharge, similar to the processes observed during the 2014 Ontake eruption. Although accumulated snow and dense vegetation hinder the detection of deformation signals on Kusatsu-Shirane volcano using conventional InSAR data, L-band SAR with various temporal baselines allowed us to successfully extract both coeruptive and posteruptive deformation signals. The extracted cumulative deformation is well explained by a combination of normal faulting with a left-lateral slip component along a southwest-dipping fault plane and an isotropic deflation. Based on the geological background in which the shallow hydrothermal system develops across Kusatsu-Shirane volcano, the inferred dislocation plane can be considered as a degassing pathway from the shallow hydrothermal system to the surface due to the phreatic eruption. We reconfirmed that SAR data are a robust tool for detecting coeruptive and posteruptive deformations, which are helpful for understanding shallow physical processes associated with phreatic eruptions at active volcanoes.

Key words Satellite SAR, Phreatic eruption, Crustal deformation, Volcano, Hydrothermal system

Category: Symposium 3: Earth Rotation and Geodynamics => 3.3: Geodetic observations in volcanic and tectonically active areas

370

S3-031

Measuring the Recent Status of Land Subsidence in Bandung Basin, Indonesia, by InSAR and GPS methods

Irwan Gumilar¹, Teguh Purnama Sidiq¹, Gigih Pambudi¹, Brian Bramanto^{2,1},
Hasanuddin Zainal Abidin¹

1. Geodesy Research Group, Institut Teknologi Bandung

2. Faculty of Science and Technology, Norwegian University of Life Sciences

Land Subsidence in Bandung Basin has been historically detected and possibly caused by several factors, including groundwater withdrawal. It is presumed that the land subsidence is still occurring and causing broad impacts to several aspects, e.g., infrastructures and building damaged. This study aims to determine the current status of the land subsidence in Bandung Basin using the Interferometric Synthetic Aperture Radar (InSAR) and Global Positioning System (GPS).

The Synthetic Aperture Radar (SAR) imageries used in this study are Sentinel-1 imagery in 2016, 2017, 2018, and 2019. The land subsidence was then estimated using the Interferometric Synthetic Aperture Radar (InSAR) method and validated with the GPS results. The largest land subsidence in Bandung Basin occurred in the Gedebage, Kopo, and Dayeuhkolot districts, as interpreted from the InSAR results. The average annual land subsidence in these districts was estimated to 15 cm, and a number of considerable damages due to land subsidence were also found. InSAR-derived land subsidence showed a good agreement with the GPS-derived land subsidence. In conclusion, the land subsidence is still occurring and tends to be more severe in Bandung Basin.

Key words SAR Imagery, validation, land subsidence impact, Sentinel

Category: Symposium 3: Earth Rotation and Geodynamics => 3.3: Geodetic observations in volcanic and tectonically active areas

437

S3-032

Earthquake Risk Analysis of Anqiu-Juxian Section of Yishu Fault Zone

Cunpeng Du¹、 Haitao Yin²

1. Shandong university of Science and Technology

2. Shandong Earthquake Agency

The Yishu fault zone is the boundary structure of the western Shandong fault block and eastern Shandong fault block, the Anqiu-Juxian fault is the main active fault in the Yishu fault zone. In this paper, we collected the earthquake catalog data from 1970 to 2018 and used the maximum likelihood method to scan the three-dimensional b value along the Yishu belt, and calculated the b value at different depths. By using the velocity data of each station of 2011~2019 and a dislocation model, we inverted the distribution of fault locking degree and slip rate deficit on the Yishu fault. The results show that 262 earthquakes with $ML > 2.0$ have occurred in the Juxian-Tancheng segment since 1970, and 66 earthquakes have occurred in the Anqiu segment, which only accounts for one-fourth of the Juxian-Tancheng segment. Moreover, the small earthquake activity in the Anqiu segment of the Anqiu-Juxian fault presents an abnormally sparse trend, which has similar characteristics of the seismicity gap, reflecting that the fault is in a locked state of elastic strain energy accumulation. There is an area with an abnormally low b-value north of the Anqiu-Juxian fault, about 0.6, and a depth of about 30km, reflecting the relatively high-stress level in this area. The south of Zhucheng County of Anqiu-Juxian fault is basically in creep state, and there is no accumulation of slipping rate deficit; the fault north of Zhucheng county has a relatively high locking degree, with a locking depth of about 26km. The extrusion deficit rate is large, manifested as a right-lateral slip deficit, with a deficit rate of 0.6mm/a~0.84mm/a. From north of the Zhucheng to Changyi segment, the coupling rate is higher, which is the unruptured section of the Tancheng earthquake. More importantly, the seismic hazard should pay more attention to the sparse micro-seismicity, which is beneficial to accumulate the stress.

Key words Anqiu-Juxian fault, b-value, slip deficit, locking fault

Category: Symposium 3: Earth Rotation and Geodynamics => 3.3: Geodetic observations in volcanic and tectonically active areas

457

S3-033

Research on Integrating Multi-track InSAR Deformation Maps

Jun Hua^{1,4}、Xinjian Shan¹、Wenyu Gong¹、Zhenjie Wang¹、Lingyun Ji²、Chuanjin Liu²、Yongsheng Li³、Dezheng Zhao¹

1. Institute of Geology, China Earthquake Administration
2. Second Monitoring and Application Center, China Earthquake Administration
3. National Institute of Natural Hazards, Ministry of Emergency Management
4. College of Marine and Space Information in China University of Petroleum

With the rapid development of Interferometric Synthetic Aperture Radar (InSAR), massive high-quality Synthetic Aperture Radar (SAR) imagery makes the surface deformation monitoring over a larger area become available. It is necessary to process and integrate SAR acquisitions from different tracks. While for many geophysical applications, the deformation sources combined from lateral or 3D directions rather than simple subsidence, the side looking and limited swath length introduces inconsistencies in multi-track measurements. In this research, we first generated the simulated dataset and quantitatively analyzed the error sources in integrating the multi-track InSAR deformation products into large scale deformation maps. We investigated optimal strategies to reduce impacts from incidence angle variation and also from the inconsistent local geo-reference frame of the side looking InSAR system. Taking the south-east Tibetan Plateau as an experimental region, we integrated the three-track InSAR deformation rate fields reconstructed by Sentinel 1 satellite to verify our result. The GPS velocity was used as ground control points to correct the geo-reference and evaluate accuracy. This research presented solutions to reduce incidence angle and other error impacts to refine the multi-track deformation maps. Our result proved the reliability of development methods in integration when the region is dominated by lateral displacement.

Key words Multi-temporal InSAR; GPS; Integration; Multi-track; Errors analysis; Incidence angle

Category: Symposium 3: Earth Rotation and Geodynamics => 3.3: Geodetic observations in volcanic and tectonically active areas

459

S3-034

InSAR observation and inversion of the seismogenic fault for The 2009 Yao'an Ms6.0 earthquake in China

Bing Zhang¹、Yongchao Ma¹、Guochang Xu¹、Zhiping Lv^{1,2}

1. Institute of Space Science and Applied Technology, Harbin Institute of Technology (Shenzhen)

2. Information Engineering University

An earthquake with Ms6.0 occurred in Yao'an County, Yunnan Province on June 9, 2009. In this paper, two L-band ALOS PALSAR ascending images are used, combined with the aftershock precision positioning results, and the coseismic deformation field of this earthquake is obtained using InSAR technology. The coseismic slip distribution was inverted and the static Coulomb stress changes in the aftershock distribution area and surrounding faults were calculated. Finally, the seismogenic structure was analyzed and discussed. The results show that: 1) The rupture direction of the earthquake is basically a straight line, and the length of the rupture exceeds 10km; 2) The coseismic dislocations are dominated by right-handed strike-slip, aftershocks are concentrated in 3-12km, and the maximum slip is about 75cm at a depth of 7km; 3) Most of the aftershocks occurred in the area where the Coulomb stress increased. The earthquake increased the Coulomb stress of some faults in the surrounding area of the epicenter, such as the Chuxiong-Nanhua fault, the Huajiaoyuan fault and the Mouding fault. The future seismic risk of the Huajiaoyuan fault is worthy of attention; 4) This earthquake is an extension of the 2000 Yao'an Ms6.5 earthquake in the NW direction.

Key words Yao'an; InSAR; Coseismic sliding distribution; Coulomb stress change; Maweijing fault

Category: Symposium 3: Earth Rotation and Geodynamics => 3.3: Geodetic observations in volcanic and tectonically active areas

486

S3-035

Complementary afterslip process following the 2016 Mw 7.8 Kaikoura earthquake from ~4 years GPS observations and its implication for seismic hazard

Lupeng Zhang^{1,2}, Dingfa Huang¹, CK Shum²

1. Faculty of Geosciences and Environmental Engineering, Southwest Jiaotong University, Chengdu 611756, China

2. Division of Geodetic Science, School of Earth Science, Ohio State University, Columbus, OH 43210, USA

Large subduction earthquakes always lead to significant postseismic deformation during the months and years thereafter, and it is commonly assumed that afterslip plays the dominant role for the postseismic transients. Yet knowledge of the characteristics of space-time evolution of afterslip is still insufficient. Here, we investigate the postseismic afterslip process following the 2016 Kaikoura earthquake using the ~4 years Global Positioning System (GPS) observations. Results show that afterslip mainly occurs around the coseismic high-slip regions appearing a complementary pattern. The seismic moment of afterslip is $\sim 2.87 \times 10^{21}$ N·m, equivalent to an Mw ~ 7.60 earthquake event, whose peak slip is ~ 0.70 m. The time-dependent afterslip evolution suggests that the afterslip rate rapidly decreases with time, consistent with the state- and rate-strengthening frictional law. Nearly 64.4% of the afterslip occurs in the first six months with a seismic moment of ~ 7.44 . Cumulative positive Coulomb stress changes induced by co- and postseismic slips of the 2016 Kaikoura event indicate that the Wairarapa fault and Kekerengu fault have been brought closer to failure. Ongoing postseismic afterslip further increases the seismic hazard on the Wellington region. It highlights the importance of understanding the afterslip for early postseismic disaster relief and future seismic hazard assessment.

Key words GPS; Kaikoura earthquake; Postseismic deformation; Complementary pattern; Seismic hazard

Category: Symposium 3: Earth Rotation and Geodynamics => 3.3: Geodetic observations in volcanic and tectonically active areas

494

S3-036

Preliminary forecast model of crustal earthquakes in southwest Japan based on GNSS data

Takuya Nishimura
Kyoto University

The present model for crustal earthquakes in Japan relies on geological and geomorphological data of active faults and never use geodetic data, whereas contemporary deformation of the Japanese Islands has been monitored by a dense GNSS network. Here, we attempt to develop a preliminary forecast model of crustal earthquakes using GNSS data.

We follow the procedure of Shen et al.(2007) to calculate the forecast model. The GNSS velocities from April 2005 to December 2009 are used in southwest Japan. Smoothed strain rate field is calculated from the velocity corrected for elastic deformation due to interplate coupling along the subduction zone. The strain rates are converted to geodetic moment rates by a formula proposed in Savage and Simpson (1997). The thickness of a seismogenic layer, rigidity, b value of the Gutenberg-Richter law, and magnitude of the maximum earthquake are assumed to be 12 km, 30 GPa, 0.9, and 7.5, respectively. They are uniform in the modeled region. Previous studies revealed that geodetic strain rates were larger than seismological ones in Japan because geodetic strain includes both elastic and inelastic strain. Elastic strain rates presumably equal to seismological ones on a long-term average. We estimated a ratio of seismic moment rates released by shallow historical earthquakes since AD1586 to the geodetic moment rates and it was 0.16 in southwest Japan. Applying 0.16 for calculating elastic rates and the stationary Poisson process of the earthquake occurrence, the maximum probability of $M \geq 6$ earthquakes for 30 years is 5.1 % in a 0.2° cell. We verify this probability model by using shallow (Depth ≤ 20 km) $M \geq 5$ earthquakes occurred in 2010-2019, which is a period after the used GNSS data. About 58 % of the earthquakes occurred with 25 % of the area with the highest strain rates, which suggests many crustal earthquakes occur in high strain-rate regions. The verification suggests the preliminary forecast model has predictive power.

Key words GNSS, probabilistic hazard assessment earthquake

Category: Symposium 3: Earth Rotation and Geodynamics => 3.3: Geodetic observations in volcanic and tectonically active areas

537

S3-037

InSAR-derived earthquake catalog: Source locations and focal mechanisms of 30+ earthquakes (Mw4.1-6.6) in west China from time-series Sentinel-1 SAR images

Teng Wang¹、 Heng Luo²、 Shengji Wei³、 Mingsheng Liao²

1. Peking University

2. Wuhan University

3. Nanyang Technological University

Small-to-moderate size earthquakes occur much more frequently than large ones but are general less studied by InSAR, despite that they also provide critical information about the physics of faulting and earthquake mechanisms. The weak coseismic deformations contaminated by severe atmosphere turbulences make them difficult to be studied by single interferogram. The high-temporal sampling rate of Sentinel-1 data produce sufficient images for the stacking process to greatly reduce the local atmospheric turbulence. This procedure allows the extraction of very weak coseismic deformation (i.e. sub-centimeter) for small-to-moderate size earthquakes and systematical static slip inversions of the earthquakes.

Here we report this stacking method and a new downsampling strategy based on quadtree mesh obtained from preliminary slip model to efficiently reduce the number of unwanted data points. Applying the proposed methods, we successfully retrieve coseismic deformations for 33 earthquakes (Mw4.1-Mw6.6) occurred in west China from Nov, 2014 to Jul 2020. Among these earthquakes, the smallest peak Line-of-Sight coseismic deformation is only ~6 mm. These InSAR-based earthquake catalogs show robust and precise absolute location (latitude, longitude and depth), therefore can be used as benchmark events to calibrate seismic based catalogues. However, strong trade-offs between earthquake source parameters (e.g. fault size vs slip) exist when the earthquake magnitude is small (in general smaller than Mw5.5). Such trade-offs are rooted due to the smaller deformation gradient in comparison with larger earthquakes. We suggest to combine geodetic and seismic datasets for more comprehensive and accurate earthquake source parameter inversions.

Key words InSAR coseismic deformation stacking

Category: Symposium 3: Earth Rotation and Geodynamics => 3.3: Geodetic observations in volcanic and tectonically active areas

581

S3-038

Monitoring The Activity of Changbaishan Tianchi Volcano with Time Series InSAR and Geophysical Modeling

Jiaqi Zhang¹、Lianhuan Wei¹、Guoming Liu²、Cristiano Tolomei³、Guido Ventura³、Elisa Trasatti³、Christian Bignami³、Stefano Salvi³、Tiejun Gao¹、Francesca Romana Cinti³

1. Northeastern University

2. Changbaishan Volcano Observatory

3. Istituto Nazionale di Geofisica e Vulcanologia

Changbaishan Tianchi volcano is located at the border of China and North Korea, which is the most active volcano with eruption potential in China. During the period from 2002 to 2005, the frequency and magnitude of seismicity in Tianchi volcano area increased significantly, indicating the volcanic activity entered an active period. After the active period, volcanic activity has returned to previous level. However, a volcanic swarm suddenly appeared on December 22, 2020, with 38 volcanic seismicity events of various types occurred. On March 5, 2021, another earthquake with magnitude of ML3.1 occurred, which is the largest VT (Volcanic-tectonic) type earthquake event after active volcanic disturbance period. These phenomena show that the volcanic seismic activity after December 2020 is beyond the background level, and monitoring of Tianchi volcano should be conducted continuously.

In this study, 19 ALOS-2 images from November 2018 to October 2020 were processed to estimate the surface deformation of Tianchi volcano area based on SBAS-InSAR technology. Due to the large topographic inequality in the volcanic area, obvious vertical stratified atmospheric phase and topographic residual are detected and removed from the interferometric phase. The results show that the ground surface of Tianchi volcano is uplifting slightly during this period, and the closer to the crater, the more obvious the uplift. Geophysical modeling based on Mogi point source was also conducted using the SBAS-InSAR results, indicating a point source at the depth of approximately 3km. The modeled depth is in agreement with the depth of seismic events, which is possibly where hydrothermal activity is happening in the shallow magma chamber. Generally, this study provides data support for the monitoring of volcanic activity and future disaster assessment in Changbaishan Tianchi volcano, and verifies the feasibility of time series InSAR and geophysical modeling in applications of active volcanoes.

Key words Tianchi volcano, SBAS-InSAR, deformation, Mogi point source

Category: Symposium 3: Earth Rotation and Geodynamics => 3.3: Geodetic observations in volcanic and tectonically active areas

584

S3-039

Estimation and correction of error sources in MTInSAR

Hongyu LIANG、 Lei ZHANG

College of Surveying and Geo-Informatics, Tongji University

InSAR technique has been widely used in mapping and quantifying crustal deformation on the solid Earth. However, InSAR observations suffer from several error sources, which should be carefully treated to avoid unreliable deformation results. In this study, we propose a step-by-step approach to model and estimate the error sources in MTInSAR, including decorrelation noise, topographic error, and atmospheric delays. We develop an iterative weighted least squares method to suppress the decorrelation noise and reconstruct the interval unwrapped phase. The topographic error is treated as a fixed pattern in space and is further isolated by using independent component analysis. We correct atmospheric delays by using a quadtree-based joint model, which simultaneously estimates stratified tropospheric delays with the parameters of displacement. The effectiveness of the error source correction is demonstrated using both simulated and real experiments.

Key words InSAR, decorrelation noise, topographic error, atmospheric delays, error source estimation

Category: Symposium 3: Earth Rotation and Geodynamics => 3.3: Geodetic observations in volcanic and tectonically active areas

589

S3-040

Detecting transient signals in GPS time series using machine learning

Xueming Xue
Michigan State University

Detecting transient-deformation signals in GPS time series is very important to study its underlying geophysical processes such as fault slip or volcanic unrest. The development of the GPS network within the past two decades has led us to a large volume of dense and continuous time series dataset. It has become impossible to manually locate and extract transient signals from all the GPS sites. Therefore, many methods have been proposed as an automated tool for this task. Here we show a simple model based on the machine learning technique that can be used to detect transient signals in GPS time series. We first generate plenty of synthetic data based on the realistic noise characteristics, seasonal and transient terms. The synthetic data are then used to train and test the model. Lastly, as an example, we applied the model on a real dataset that capture the slow slip transients on the Cascadia subduction interface. In addition to the major events which have been reported previously, we find more transient signals that could be some smaller events.

Key words transient detection; machine learning; slow slip events

Category: Symposium 3: Earth Rotation and Geodynamics => 3.3: Geodetic observations in volcanic and tectonically active areas

638

S3-041

Causative fault geometries of two blinded dip-slip earthquakes in the interior of Asia Continent revealed by InSAR

Yuqing He¹, Teng Wang¹, Lihua Fang², Li Zhao¹

1. School of Earth and Space Sciences, Peking University

2. Institute of Geophysics, China Earthquake Administration

Intra-continental dip-slip earthquakes often occur in the orogen and rift zones with complex tectonics accompanying large vertical deformation. Such earthquakes are less studied due to the sparse seismological and geodetic observations. However, such blinded dip-slip earthquakes raise concerns for seismic risk and provide rare opportunities to illuminate the deformation and evolution of the continental structures. Here, we report the fault geometries of two dip-slip earthquakes recently occurred in Southern Tian Shan and Mongolia-Baikal rift zone revealed from the radar imaging geodesy.

The first one is the 2020 Mw6.0 Jiashi earthquake occurred in the Keping-tage fold-thrust belt in southwest Tian Shan. This region is seismically active, yet most well-recorded earthquakes occurred south of the mountain front, hindering our understanding of the orogenic process to the north. The 2020 earthquake is an important event with surface deformation in the nappe structure well illuminated by InSAR. We combine InSAR deformation measurements and relocated aftershocks to investigate the faults responsible for this earthquake. Tests of different fault models show that the combination of a shallow thrust fault and two deeper faults can best explain the surface deformation and aftershock distribution. Stress analysis suggests that slips on the shallow fault reactivated the older basement structure at depth. Our results reflect the basement-involved shortening activated by a thin-skinned thrust faulting event with the surface deformation implying the basin-ward orogenic process of the southwest Tian Shan.

The second one is the 2021 Mw6.7 Lake Hövsgöl earthquake occurred in the Mongolia-Baikal rift zone (MBRZ), which is located in the northern tip of the Asian tectonic region, and is bounded by the Tibet Plateau orogenic belt and the Siberian Platform. This region is one of the most active tectonic regions in the world (Tapponnier and Molnar, 1979). We collected Sentinel-1 SAR images spanning the earthquake from descending DT04 track and extracted the surface deformation field for this event. Combining the LOS deformation field and previous geological

studies, we find that the causative faults of this event is complex with at least two segments. Using the Bayesian inversion method we derive two shallow normal faults with opposite dipping directions. Normal faults with opposite directions near the lake boundary play an important role in controlling the formation and development of the Hövsgöl rift. Since the catastrophic M8+ earthquakes in 1905, no large earthquakes have occurred in this region, thus the attention should be paid to the Coulomb stress changes on adjacent faults due to this event.

Reference:

Tapponnier, P., & Molnar, P. (1979). Active faulting and Cenozoic tectonics of the Tien Shan, Mongolia, and Baykal regions. *Journal of Geophysical Research*, 84(B7), 3425-3459.

Key words Intra-continental dip-slip earthquakes; southwest Tian Shan; Mongolia-Baikal rift zone; 2020 Mw6.0 Jiashi earthquake; 2021 Mw6.7 Lake Hövsgöl earthquake.

Category: Symposium 3: Earth Rotation and Geodynamics => 3.3: Geodetic observations in volcanic and tectonically active areas

694

S3-042

COSEISMIC DEFORMATION DUE TO THE EARTHQUAKE IN SAN JUAN (ARGENTINA) OF JANUARY 18, 2021 (MW 6.4) AS MEASURED BY CONTINUOUS GNSS DISPLACEMENTS

Juan Navarro^{1,2}, Silvia Miranda¹, Alfredo Herrada^{1,2}

1. Departamento de Geofísica y Astronomía, Facultad de Ciencias Exactas, Físicas y Naturales, Universidad Nacional de San Juan

2. Facultad de Ingeniería, Universidad Nacional de San Juan

Today more and more high seismic activity sites are instrumented with continuous GNSS receivers because this technique provides the possibility of precisely and speedily observing the coseismic deformation. San Juan Province is in central-western Argentina, in a region characterized by the subhorizontal subduction of the Nazca plate under the South American plate, whose convergence gave rise to a particular style of deformation and high seismic activity. It is mainly in the Precordillera and Western Pampean Ranges where the main crustal seismogenic structures are located (5-35 km depth). On January 18, 2021, at 23 h 46 m local times, there was an earthquake of intermediate intensity, which according to INPRES (National Institute of Seismic Prevention) had a magnitude of 6.4 MW, with an epicenter in the Eastern Precordillera ($-31,854^\circ$ latitude, $-68,963^\circ$ longitude), about 57 km southwest of the San Juan city and at a depth of 8 km. Related to the seismic event, it has reported damage to non-seismic resistant structures and ground surface ruptures. We used continuous GPS/GNSS measurements to determine and analyze the static coseismic displacement field associated with this earthquake. To this end, we processed the time series of daily positions in the three coordinate components of 10 permanent GNSS sites located around the epicentral area. In processing, we used the static Precise Point Positioning GPS technique using the GipsyX package (Jet Propulsion Laboratory). The resulting displacement vector map shows, for the site closest to the epicenter (station CSJ1), up to 8 mm of coseismic displacement in the horizontal component (N-NW direction) and 2 mm in the vertical one. In addition, we processed four months of GNSS observations to detect displacements related to the earlier post-seismic deformation. It is possible that this event, close to the epicentral zone of the earthquake of June 11, 1952, is associated with an active fault system recognized in the Eastern Precordillera.

Key words coseismic deformation, GPS displacements, San Juan

Category: Symposium 3: Earth Rotation and Geodynamics => 3.3: Geodetic observations in volcanic and tectonically active areas

710

S3-043

Time-dependent Modeling of the Long-lasting Afterslip due to the 2016 Moderate Earthquakes along Chaman Fault using InSAR Time Series

Masato Furuya¹, Matsumoto Fumiko²

1. Hokkaido University

2. PASCO, Japan

Postseismic-to-co-seismic moment ratios (PCMR) for large earthquakes greater than M6 are roughly around 0.3 or less, but those for moderate to even smaller earthquakes could be greater than 1 or more (Alwahedi and Hawthorne, 2019). However, there have been limited estimates on those ratios for moderate earthquakes. Of those few estimates on PCMR, the one reported by Furuya and Satyabala (2008) is exceptionally large, nearly 6, in which a long-lasting afterslip due to an M5.0 earthquake in 2005 along Chaman Fault was detected. Chaman Fault is the western transform plate boundary between Indian and Eurasian plates and is well known for its low seismicity, which was interpreted as either a long-recurrent interval of large earthquakes or steady creep. On May 13 and July 10, 2016, moderate earthquakes occurred along the Chaman Fault, and are the largest earthquakes since the 2005 M5.0 event. The USGS reports that the 1st event on May 13 consists of the triplet at almost the same hypocenter with Mw 5.2, 4.7, and 5.5, and that the 2nd event ~20 km to the northeast was mb 4.7. Our goals are to examine if the Chaman Fault is anomalous in terms of its frictional properties and/or if the PCMR for moderate earthquakes will always get larger. To estimate the PCMR for these events, we examine the surface deformation associated with these moderate earthquakes, using 75 Sentinel-1A SAR images from October 2014 to August 2018 to generate 428 interferograms. We perform InSAR time-series analysis, using the LiCSBAS package by Morishita et al (2020). We have found:(1) The PCMR for the smaller mb 4.7 earthquake was ~8, whereas that for the larger Mw5-class events to the south was ~0.7.(2) Slips on the fault for the mb4.7 earthquake reached the surface, whereas those for the Mw5 events did not. (3) Significant gap in the slip patches between the M5-class events and the mb4.7 event is located around the ruptured area by the 1892 M6.6 earthquake.

Key words Chaman Fault, InSAR, Afterslip

Category: Symposium 3: Earth Rotation and Geodynamics => 3.3: Geodetic observations in volcanic and tectonically active areas

738

S3-044

Mapping vertical crustal deformation over Weihe Basin, China using Sentinel-1 and ALOS-2 ScanSAR imagery

Yufen Niu¹、Feifei Qu²、Wu Zhu²、Qin Zhang²、Chaoying Zhao²、Wei Qu²、Yuxuan Hu³

1. School of mining and Geomatics Engineering, Hebei University of Engineering
2. College of Geology Engineering and Geomatics, Chang'an University
3. The Second Monitoring and Application Center, China Earthquake Administration

Weihe Basin is located in Shaanxi Province, central China, and spanning 350km from east to west. Hundreds of active faults were discovered over the basin in history, and most of these deeply buried faults criss-crossed the basin. The main faults that control the sedimentary basin formation include Beishan Piedmont fault, Guanshan fault, Qinling North Piedmont fault, Chang'an-Lintong fault, and Lishan Piedmont fault. Weihe Basin is characterized by intense crustal activity, and more than 25 earthquakes have been recorded with magnitude larger than 5.0 since 1177. One Ms 8.0 earthquake occurred in Huaxian was recorded in 1556, however, there are no documented cases greater than MS 5.5 since the 20th century. In order to understand the structure and slip rate of the known fault zones, identify potential active faults as well as their activity intensities, and compensate for the existing discrete located GPS and leveling measurements in Weihe Basin, 92 scenes ascending Sentinel-1 and 6 scenes descending ALOS-2 ScanSAR datasets were utilized to derive LOS deformation velocity respectively. The geoid offset correction between EGM96 datum and WGS84 datum was applied to the SRTM DEM. GACOS atmospheric products are employed to reduce the effects of tropospheric delay. Then the deformation components in the east-west and vertical directions are estimated using the descending and ascending InSAR images together over the entire basin. InSAR measurements allow us to position not only the previously known faults, but also new active fault not previously revealed, which indicates that the complex internal motion within the Weihe Basin could be controlled by multiple faults. Finally, we calculate the slip rates and blocking depths of the Longxian-Mazhao fault, Puyang-Lantian, the southern part of Weihe fault, and the Kouzhen-Guanshan fault, and evaluate their potentials to arise large earthquakes.

Key words Weihe Basin, InSAR, Crustal deformation, Tectonic activity

Category: Symposium 3: Earth Rotation and Geodynamics => 3.3: Geodetic observations in volcanic and tectonically active areas

754

S3-045

Earthquake triggering by tidal stresses at global scale

Laurent Métivier^{1,2}, Marianne Greff-Lefftz¹, Gwendoline Pajot-Métivier^{1,2}, Kristel Chanard^{1,2}

1. Institut de Physique du Globe de Paris (IPGP)

2. Institut national de l'information géographique et forestière (IGN)

Earthquakes occur when fault stresses build to levels that exceed a critical threshold for fault rupture. Thus, applying additional stress to a fault system that is near failure may initiate the rupture process that produces an earthquake. Tidal attractions, exerted by the Moon and Sun, induce elastic deformation of the solid Earth on a sub-daily basis. Solid tides might therefore trigger earthquakes, producing excess seismicity near the Earth tide maximum.

Small correlations between earthquake occurrence and the tidal gravity potential at diurnal and semi-diurnal periodicities, have been shown in previous studies. But the mechanism that initiates the triggering remains unclear and only a small proportion of seism seems to correlate with tidal maxima. It has been suggested that the earthquake initiation is linked to a diminution of tidal normal stresses at the time of the earthquake. Yet the importance the tidal shear stresses may be also fundamental here.

We investigate a global earthquake database (USGS earthquake database) that references about 900 000 earthquake events, worldwide located, with magnitudes between 2-10. Using modelling of tidal ground displacements, gravity and elastic stresses, we systematically investigate the timing of the earthquakes with respect to tidal extrema, in particular for shear and dilatational tidal stresses. Statistical analyses have been conducted with respect to earthquake locations, magnitudes and focal mechanisms (when provided). If previous conclusions with smaller earthquake databases are confirmed here with respect to tidal potential periodicities, the impact of tidal shear stresses is also clearly evidenced and discussed.

Key words Solid tides, Seismicity, Deformation modelling

Category: Symposium 3: Earth Rotation and Geodynamics => 3.3: Geodetic observations in volcanic and tectonically active areas

760

S3-046

Extraction of crustal deformation by using InSAR and GPS at the eastern margin of Tibet Plateau

Weiwei Bian、 Jicang Wu

College of Surveying and Geo-Informatics, Tongji University, Shanghai 200092, China;

This research reports our InSAR experiment results by using ALOS-2 ScanSAR images, and velocities of GPS stations in the east margin of Tibet Plateau. Especially, we have calculated the crustal deformation in Yunnan by using ALOS-2 SAR images and compared it with that by GPS observation in the same area. we find that GPS has a high temporal resolution, and InSAR has a high spatial resolution. We hope to obtain high spatiotemporal resolution crustal deformation results through the combination of GNSS and InSAR observations. The rate of high-resolution crustal deformation and local geological information are combined to analyze the stress accumulation around the active faults, so as to achieve the effect of preliminary prediction and early warning of geological disasters.

Key words crustal deformation; geological disasters; InSAR; GPS; active faults

Category: Symposium 3: Earth Rotation and Geodynamics => 3.3: Geodetic observations in volcanic and tectonically active areas

829

S3-047

The GNSS observed modulated seasonal signals in Yunnan, southwest China

Weijie Tan, Junping Chen

Shanghai Astronomical Observatory, Chinese Academy of Sciences

Global Navigation Satellite System (GNSS) provides detail information of crustal deformation induced by different geophysical processes, including the plate motion, post-glacial rebound, mass redistributions and thermal expansions. Those effects can be usually explained by the GNSS site velocities and annual variations. The un-modelled processes, such as modulated seasonal signals are still not clear. Here, we apply the SSA (Singular spectrum analysis) to extract the modulated seasonal signals in Yunnan, which may have a time-variable amplitude and phase. The first two recovered principal components were treated as the modulated seasonal signals according to the spectra analysis, which explain ~50% of data variance. We also compare our SSA-derived results to those obtained using least-squares analysis. Our results demonstrate that SSA can effectively extract modulated oscillations in Yunnan, which is highly correlated with the precipitation anomalies.

Key words SSA, modulated seasonal variation

Category: Symposium 3: Earth Rotation and Geodynamics => 3.3: Geodetic observations in volcanic and tectonically active areas

847

S3-048

Modeling of the volcano-tectonic activity of Deception Island (Antarctica) from 30 years of GPS observations (1991-2021)

Belén Rosado¹、 Manuel Berrocoso¹、 Javier Antonio Ramírez-Zelaya¹、 Alberto Fernández-Ros¹、 Jorge Gárate¹、 Gonçalo Prates²、 Amós de Gil¹

1. University of Cadiz

2. University of Algarve

Deception Island (South Shetland Islands) is one of the most active volcanoes in Antarctica. More than 20 explosive eruptions have been recorded on this volcanic island over the last two centuries, concentrated in three main periods of activity: 1818–1828, 1906–1912 and 1967–1970. Since 1991, and within the limitations of its inhospitable Antarctic environment and scarce human presence, Deception Island is being mostly monitored by recording seismic activity and ground displacements. In order to monitor the island's tectonic and volcanic behavior, a GPS geodetic network has been deployed, consisting of 15 geodetic marks distributed around Deception Island's inner bay, known as Port Foster. Two additional geodetic benchmarks were installed off Deception Island to be used as reference for the differential positioning strategy. Since 1991-1992 Spanish campaign in Antarctica, geodetic ground displacement velocities between the successive austral summer Antarctic campaigns have been computed and analyzed.

Deception Island's volcanic behavior is shown by the evolution in time of the ground-displacement velocity, real strain, shear-strain, pressure source and maximum geodetic deformation models calculated for the whole period 1991–2021. From the study of the data obtained during this period, it is possible to identify some different inflation and deflation phases separated by transitional (or mixed) stages characterized by extension without uplift and compression without subsidence. The most representative inflation and deflation periods were analyzed in detail, to understand their correlation with high and low seismic activity, respectively.

Correlation between inflation processes with the increase of seismic activity as well as the increase of the soil temperature indicates the transitional mixed phases may be considered precursors of possible volcanic crisis.

Key words Volcano geodesy, Deception Island Volcano, Volcano-tectonic model 4D, deformation models

Category: Symposium 3: Earth Rotation and Geodynamics => 3.3: Geodetic observations in volcanic and tectonically active areas

861

S3-049

GNSS-GPS Time Series Analysis: Application to the southern region of the Iberian Peninsula and North Africa.

Javier Antonio Ramírez Zelaya¹、 Manuel Berrocoso Domínguez¹、 Belén Rosado Moscoso¹、 Alejandro Pérez Peña¹、 Jorge Gárate Pasquín¹、 Amos de Gil ¹、 Alberto Fernández-Ros¹、 Gonzalo Prates²、 Paola Barba¹、 Sonia Pérez-Plaza¹、 Fernando Fernández-Palacín¹

1. University of Cádiz

2. University of Algarve

The application of surface deformation in the geodynamic study of a region has evolved from classical geodetic procedures to methodologies based on GNSS (Global Navigation Satellite Systems), specially GPS (Global Positioning System). Horizontal and vertical ground-displacements are obtained from repeated observations through continuous data recording receivers (CGPS) or through episodic measurements, GPS observations are posteriorly analyzed to achieve millimetric accuracy in the obtained daily positions.

In this work, various techniques and strategies are evaluated and applied for the analysis of time series translated into CGPS coordinates, to determine the deformation of the horizontal model. These strategies incorporate a preliminary study of the time series to clean out the outliers, then Wavelet, Kalman, ARMA and ARIMA techniques are applied to the same series to reduce dispersion, filtering the solutions and decompose the signal, in order to determine the models of displacement, stress and deformation at each site. The analyzed data correspond to 60 continuously recording GPS stations located in the southern region of the Iberian Peninsula and northern Africa (SPINA Network). The results show four different zones: the south-east of the Iberian Peninsula, the south of Iberia and the north of Africa, the north of Andalusia and the south of Portugal. The general trend is in the NE-SW direction. The geodynamic deformations in the region of northern Andalusia are associated with the convergence of the Eurasian plate.

Key words Time series analysis, strain and stress analysis, geodynamic deformation

Symposium 4: Positioning and applications

S4.1: Geodetic Remote Sensing

Category: Symposium 4: Positioning and applications => 4.1: Geodetic Remote Sensing

103

S4-001

Estimation of 4D Atmospheric Water Vapor from GNSS and Infrared Sensor Data: A Combined Tomography Approach

Wenyuan Zhang^{1,3}、Nanshan Zheng¹、Gregor Moeller³、Nan Ding²、Shubi Zhang¹

1. School of Environment Science and Spatial Informatics, China University of Mining and Technology

2. School of Geography, Geomatics and Planning, Jiangsu Normal University

3. Institute of Geodesy and Photogrammetry, Swiss Federal Institute of Technology Zurich

Atmospheric water vapor is an important greenhouse gas and its spatio-temporal variations significantly impact the thermodynamics of the Earth system. Global Navigation Satellite System (GNSS) tomography is a promising technique for reconstructing the water vapor fields. In the last decades, it has been developed rapidly to a cost-efficient technique with all-weather availability, high spatio-temporal resolution, and wide-coverage. However, due to the inconsistency between the inverted cone-shaped GNSS signals and the box-shaped tomographic domain, common tomography models are faced with the problem of an uneven distribution of observations and many invalid voxels (without any GNSS rays crossing). Currently, remote sensing (RS) infrared (IR) water vapor products, with high spatial resolution and global coverage, show great potential for the retrieval of positive cone-shaped slant water vapor (SWV) observations to complement the single GNSS acquisition geometry. In this paper, we propose a combined tomography method based on GNSS, MODIS and MERSI based water vapor products to further improve the accuracy of tomographic water vapor fields. Therefore, precipitable water vapor (PWV) observations from MODIS and MERSI and multi-GNSS data over Xuzhou region are utilized to validate the proposed method. Concerning the geometric distribution, the average number of observations and the mean number of the crossed voxels are increased by 38.4% and 55.6%, respectively. Compared to the radiosonde and ERA5 data, the mean root-mean-square error of the tomography derived water vapor profiles decreases from 2.19 g/m³ to 1.54 g/m³, and thus, the overall accuracy of 3D water vapor distribution is improved by 20.3%. Such improvements highlight that the combination of GNSS with IR products using tomographic principles has significant potential to retrieve a more accurate and reliable 4D atmospheric water vapor distribution.

Key words Global Navigation Satellite System (GNSS); Remote Sensing (RS); Troposphere tomography; Slant water vapor (SWV); Radiosonde; ERA5

Category: Symposium 4: Positioning and applications => 4.1: Geodetic Remote Sensing

111

S4-002

Evaluation of shipborne GNSS precipitable water vapor from six cruises based on multiple datasets

Zhilu Wu¹、Cuixian Lu¹、Yuxin Zheng¹、Yang Liu²、Yanxiong Liu²、Qihua Tang²

1. Wuhan University

2. First Institute of Oceanography, Ministry of Natural Resources, Qingdao

Atmospheric water vapor plays an essential role in climate change and weather forecasting. However, monitoring water vapor with high spatial and temporal resolutions remains a challenge, especially over ocean regions where observations are insufficient. Shipborne global navigation satellite systems (GNSS) contribute to enriching water vapor measurements over oceans and also can help validate satellite observations. Due to the lack of long-time serial observations, the performance of shipborne GNSS-derived precipitable water vapor (PWV) is inadequately evaluated on the global ocean scale. In this study, an overall assessment of shipborne GNSS PWV over global oceans is performed based on six voyages from 2014 to 2018. In coastal areas, the PWV differences of shipborne GNSS with respect to (w.r.t.) ground-based GNSS and ground-launched radiosonde data are 2.64 mm and 2.98 mm in RMS, respectively. In open oceans, compared to ship-launched radiosonde profiles and satellite measurements, shipborne GNSS PWV shows RMS of differences of 2.54 mm and 2.53 mm, respectively. In addition, the RMS of PWV differences between the whole track of shipborne GNSS PWV and ERA5 products is 2.86 mm. The inter-technique validations demonstrate the accuracy of shipborne GNSS PWV is superior to 3 mm, which meets the requirements of climate research and numerical weather prediction (NWP). Furthermore, larger biases between shipborne GNSS PWV values and ERA5 products are revealed in low-latitude and coastal areas due to the relatively lower accuracies of satellite measurements that are assimilated into ERA5 in these areas, indicating the necessity of assimilating shipborne GNSS data into NWP models.

Key words Shipborne GNSS; Water Vapor; Uncertainty; Radiosonde; ERA5; Satellite-borne Microwave Radiometer

Category: Symposium 4: Positioning and applications => 4.1: Geodetic Remote Sensing

131

S4-003

Soil moisture retrieved using multi-constellation and multi-frequency GNSS signals

Nikolaos Antonoglou^{1,2}, Jens Wickert^{2,3}, Bodo Bookhagen¹

1. University of Potsdam, Germany

2. GFZ German Research Centre for Geosciences, Germany

3. Technische Universität Berlin, Germany

The Global Positioning System (GPS) and later, more general, the Global Navigation Satellite Systems (GNSS) were initially designed to provide high accuracy Position Velocity and Time (PVT) for military or civilian purposes. While precise positioning applications presuppose the elimination of both systematic and random errors, in GNSS remote sensing one or multiple errors are isolated and exploited. In soil moisture estimation, we focus on the multipath effect and we use the patterns of the signal-to-noise ratio (SNR) observations created by the interference between the direct and the reflected signal.

There were various experiments in the past showing the effectiveness of this method using only single-frequency GPS signals. The main advantage of this constellation is its ground track repeat cycle, which is equal to one sidereal day (the period is approximately 23h 56m). Since soil moisture estimation requires comparison of two or more interference patterns that occur in the same location, it is possible to achieve relative measurements almost every day. On the other hand, Globalnaya Navigacionnaya Sputnikovaya Sistema (GLONASS) and Galileo reflections are repeated every eight and ten sidereal days respectively. Our approximation combines observations from the three constellations mentioned above and all frequencies (L1, L2 and L5) in a least-squares adjustment (LSA). We use observations from two stations located in northeast Germany (Marquardt and Fürstensee) and we use data from time-domain reflectometry (TDR) for control. We have tried various combinations and, in the best case, our solutions show a correlation of 0.91 and a root-mean-square error (RMSE) of 2.53% vol/vol.

Key words Reflectometry, Interferometry, GNSS, GNSS-R, GNSS-IR, Soil moisture

Category: Symposium 4: Positioning and applications => 4.1: Geodetic Remote Sensing

139

S4-004

Remote Sensing of Soil Moisture using Spaceborne GNSS Relectometry Measurements

Mina Rahmani¹, Jamal Asgari¹, Milad Asgarimehr²

1. Department of Geomatics Engineering, Faculty of Civil Engineering and Transportation, University of Isfahan, Isfahan, Iran
2. German Research Centre for Geosciences GFZ, Potsdam, Germany

GNSS signals not only play an important role in navigation and positioning, but also they are applied for a variety of remote sensing applications. Global Navigation Satellite System Reflectometry (GNSS-R) as an innovative remote sensing technique, operates based on the GNSS reflected signals from the Earth's surface. It has emerged since the late 80s. Every point on the Earth's surface has being monitored by multi GNSS satellites which result in high global coverage; also, GNSS transmitted signals can propagate in all weather conditions including cloudy and rainy atmosphere. Providing high spatial resolution over the globe in all weather conditions is so desirable for remote sensing applications. Furthermore, high temporal sampling rate of CYGNSS (U.S eight-satellite constellation fully dedicated to space-borne GNSS-R mission) offer new opportunities in monitoring a wide variety of geophysical applications. Despite the initial objective of this mission, monitoring of oceans and wind speed in tropical regions, the sensitivity of GPS L-band to soil moisture leads to a new direction toward GNSS-R soil moisture monitoring. Along with mentioned advantages for soil moisture monitoring using CYGNSS, especially high spatial and temporal sampling rate, this investigation has limitations that must be considered to improve this mission's data products. In this presentation, we will have an overview of the current state of GNSS-R soil moisture remote sensing. We will also present the statistical analysis on the sensitivity of CYGNSS measurements to soil moisture and finally the estimations from these observations.

Key words GNSS-R, Soil moisture, CYGNSS, Bi-static GNSS reflection, geophysical applications

Category: Symposium 4: Positioning and applications => 4.1: Geodetic Remote Sensing

140

S4-005

Alternative ionospheric correction algorithm for Galileo single frequency users

M Mainul Hoque, Juan Andrés Cahuasquí
German Aerospace Center (DLR)

Recently DLR developed an ionosphere prediction model for single frequency Galileo users. The model can be driven by the same Az coefficients transmitted by Galileo satellites to operate the NeQuick-G ionosphere model. The compact model approach uses only 12 model coefficients and a few empirically fixed parameters. The required ionospheric delay or total electron content values can be computed at any location and time without using any spatial or temporal interpolation of parameters. This makes the new model very fast running in operational applications when compared with the NeQuick-G model. The global performance analysis with reference Vertical Total Electron Content (VTEC) data from the International GNSS Service (IGS) shows that the performance of the model is better than that of NeQuick-G. Our investigation in the position domain considering test stations at high, middle and low latitude regions shows that the new model performance is better than the GPS Klobuchar model and similar to the NeQuick-G model. For determining the Single Point Positioning (SPP) solution we used the gLAB software tool developed by the research group of Astronomy and Geomatics (gAGE) which provides precise modelling of GNSS observables at the centimetre level, allowing standalone SPP positioning as well as Precise Point Positioning (PPP). The current publicly available version of gLAB includes the GPS Klobuchar model for SPP computation. In order to perform the new model validation, we implemented our model and NeQuick-G to the modelling capacities of gLAB. The source code of NeQuick-G is obtained from the European space software repository and integrated into the gLAB.

Key words GNSS, Galileo, ionosphere correction model, single point positioning

Category: Symposium 4: Positioning and applications => 4.1: Geodetic Remote Sensing

147

S4-006

Application of the Total Variation Method in near real-time GNSS Tropospheric Tomography

zohreh adavi, Robert Weber
TU Wien

GNSS tomography is an all-weather remote sensing technique to capture the spatiotemporal behavior of the atmospheric water vapor using the standing infrastructure of GNSS satellites and networks. In this method, the troposphere is discretized to a finite number of 3D elements (voxel) in horizontal and vertical directions. Then, the wet refractivity in these voxels is reconstructed using the Slant Wet Delay (SWD) observations in the desired tomography domain by means of the discrete inverse concept. Due to the insufficient spatial coverage of GNSS signals in the voxels within the given time window, some of the voxels are intersected by a few signals or plenty of signals, and others are not passed by any signals at all. Therefore, the design matrix is sparse, and the observation equation system of the tomography model is mixed-determined. Therefore, some constraints or external data sources should be added to the tomography problem in order to reconstruct the wet refractivity field. Moreover, the GNSS tomography is a kind of discrete ill-posed problem. Therefore, all singular values of the structure matrix (A) in the tomography problem decay gradually to zero without any noticeable gap in the spectrum. Hence, slight changes in the measurements can lead to extremely unstable parameter solutions. In consequence, the regularization method should be applied to stabilize the inversion process and ensure a stable and unique solution for the tomography problem. In this presentation, the Total Variation (TV) method is suggested to retrieve a regularized solution. TV is a nonlinear technique, which efficiently preserves discontinuities in the model and resists noise. This method can also reconstruct the promising wet refractivity field without any initial field in a shorter time span. For this purpose, observation data from the EPOSA (Echtzeit Positionierung Austria) GNSS network located in the eastern part of Austria is processed within the period DoYs 232-245 in 2019. Then, the TV method is performed in six different tomography windows (10 minutes to 60 minutes) with a time step of 10 minutes by focusing on near-real-time applications. Finally, radiosonde measurements in the area of interest are utilized to compare the estimated wet refractivity field in order to obtain the accuracy of the proposed method.

Key words GNSS, Tomography, Total Variation Method

Category: Symposium 4: Positioning and applications => 4.1: Geodetic Remote Sensing

158

S4-007

Extracting ionospheric phase scintillation index from 1 Hz GNSS observations

Dongsheng Zhao、 Wang Li、 Kefei Zhang
China University of Mining and Technology

The ionospheric scintillation, as one of the astronomical disasters occurring frequently in Arctic regions, poses great challenges to GNSS positioning navigation and timing (PNT) services. This calls for an urgent need in studying and effectively monitoring the scintillation to overcome its adverse impact. With the capability of high frequency sampling, ionospheric scintillation monitoring receivers (ISMR) are usually required to monitor the ionospheric scintillation, but the distribution of ISMR restricts the comprehensive monitoring in larger areas (such as the Arctic region). Therefore, based on GNSS observations with 1 Hz sampling, this paper studies the relevant empirical parameters and methods of extracting the ionospheric scintillation signal from the carrier phase observations by using geodetic detrending, precise point positioning and wavelet transform techniques, to construct a new phase scintillation index, which can be used to monitor the ionospheric scintillation. Its effectiveness and accuracy are verified by 188-day observations from 11 stations provided by the Canadian High Arctic Ionospheric Network (CHAIN). The results show that, compared with the commonly used ROTI index, both the scintillation index proposed in this paper and ROTI can effectively detect the occurrence of ionospheric scintillation, but the scintillation index proposed in this paper has a better correlation with the phase scintillation index given by ISMR, especially during periods with strong ionospheric scintillation, indicating that the proposed scintillation index has better ionospheric scintillation monitoring capability.

Key words GNSS, ionosphere scintillation monitoring, scintillation index

Category: Symposium 4: Positioning and applications => 4.1: Geodetic Remote Sensing

235

S4-008

An operational GNSS processing system for near-real-time tropospheric ZTD and IWV monitoring in South America: breaking the 2-hour lateness barrier!

Juan Manuel Aragón Paz, Luciano Pedro Oscar Mendoza, Laura Isabel Fernández
Laboratorio MAGGIA. Facultad de Ciencias Astronómicas y Geofísicas - Universidad Nacional de La Plata - CONICET. Argentina.

The observation of atmospheric Water Vapor (WV) is fundamental in the study of the evolution of meteorological weather, especially in severe phenomena. Until recently, there was no operational systems in South America that could offer continuous WV observations, with sufficiently low latencies, and significant density and geographic coverage, to allow their implementation in nowcasting meteorological models. On the other hand, Global Navigation Satellite Systems (GNSS) have shown to have the capacity to fill this gap in the study of atmospheric WV. In this work we present such an operational system for South America. The unattended system process GNSS data streams and produces Integrated Water Vapor (IWV) observations for more than 40 sites in this region, in near-real-time (i.e., a timelines lower than 2-hours is achieved). In practice, the system produces estimates of the tropospheric Total Zenith Delay (ZTD), for sites in Argentina, Uruguay and southern Brazil, from the analysis of the GNSS observations provided by the regional Cartographic Agencies. The IWV observations are then obtained by incorporating surface meteorological data, also distributed in near-real-time by the regional Weather Services. All the products obtained during the processing are immediately and openly accessible by the whole community. The products have been compared with a posteriori results from several international GNSS Analysis Centers, at several common sites, and also with regional observations by independent techniques (e.g., radiosounding), to reliable quantify their quality and usefulness. The evaluation highlights their advantages in terms of temporal sampling and spatial resolution, with uncertainties falling within standard thresholds. Thus, the operational system provides IWV observations with adequate quality, and sufficient low latency, to be implemented in assimilation models for short-term forecasting, which are under development at several regional Weather Services.

Key words IWV, Near-Real-Time, GNSS, Water Vapor

Category: Symposium 4: Positioning and applications => 4.1: Geodetic Remote Sensing

237

S4-009

Using the spaceborne GNSS-R coherent signals to detect the flood of South Asia

Qi Liu¹, Shuangcheng Zhang^{1,3}

1. Chang'an University

3. State Key Laboratory of Geo-Information Engineering

Flood is arguably most common, devastating, and frequent natural hazard in the globe and the destruction from its impacts is getting worse due to recent climate change. The Global Navigation Satellite System-Reflectometry (GNSS-R) measurement provides a new solution for flood monitoring. At present, GNSS-R mainly uses the threshold method to separate reflectivity and detect flood inundation, ignoring land surface conditions and signal scattering mechanism. This work introduces a new method of coherent signal detection based on Cyclone Global Navigation Satellite System (CyGNSS) raw counts Delay-Doppler Map (DDM), and then based on the sensitivity of space-borne GNSS-R signals to floods using coherent signal detection to study the spatial and temporal changes of floods in South Asia. The research results show that, compared with the flood detection results of Soil Moisture Active Passive (SMAP), the monitoring range of the two methods in the dry season is similar; while in the rainy season, the detection range of the surface reflectivity is larger about 6.69%, and the detection range of the power ratio is smaller about 3.6%. This method is consistent with soil moisture and rainfall in time series. Therefore, the method of using GNSS-R coherent signals to detect floods is more accurate than the surface reflectivity, and this method does not need to consider the influence of surface characteristics on the incoherent scattering power. It is a simple and effective method for flood detection.

Key words CyGNSS; Floods; Coherent Signal; SMAP; Raw Counts DDM

Category: Symposium 4: Positioning and applications => 4.1: Geodetic Remote Sensing

255

S4-010

IAG JWG 4.3.1 Real-time Ionosphere Monitoring and Modeling: Status during 2019-2021

Ningbo Wang¹、 Zishen Li¹、 Yunbin Yuan⁴、 Manuel Hernández-Pajares⁷、 Alexis Blot¹⁰、 Andrzej Krankowski¹²、 Andre Hauschild¹⁴、 Alberto Garcia-Rigo⁷、 Andreas Goss¹⁶、 Attila Komjathy¹⁸、 Cheng Wang²、 Eren Erdogan¹⁶、 German Olivares⁵、 Kenji Nakayama⁸、 Libo Liu¹¹、 Nicolas Bergeot¹³、 Qile Zhao¹⁵、 Raul Orús¹⁷、 Reza Ghoddousi-Fard¹⁹、 Wookyoung Lee³、 Xingliang Huo⁶、 Xiaodong Ren¹⁵、 Zhizhao Liu⁹

1. Aerospace Information Research Institute, Chinese Academy of Sciences

2. BUAA, China

3. KASA, South Korea

4. IGG/CAS, Wuhan

5. GA, Australia

6. IGG/CAS, Wuhan

7. UPC-IonSAT, Spain

8. NICT, Japan

9. PolyU, China Hongkong

10. CNES, France

11. IGG/CAS, Beijing

12. UWM, Poland

13. ROB, Belgium

14. DLR/GSOC, Germany

15. WHU, China

16. TUM/DGFI, Germany

17. ESA/ESTEC, Netherland

18. NASA/JPL, USA

19. NRCan, Canada

For many decades the International GNSS Service (IGS) is delivering high-precision ionospheric products for various scientific applications. The Ionosphere Associated Analysis Centers (IAAC), for instance, provide routinely maps of the Vertical Total Electron Content (VTEC), i.e. the integral of the electron density along the height to correct measurements for ionospheric influences, usually disseminated with latencies of days to weeks and based on post-processed observations. Precise GNSS applications, however, such as autonomous driving or precision farming, require the use of high-precision and high-resolution ionospheric correction models in real-time. Hence, the Joint Working Group 4.3.1 “Real-time Ionosphere Monitoring and Modeling” was launched together with IGS and Global Geodetic Observing System (GGOS) within IAG sub-commission 4.3.

The structure and objectives of IAG JWG 4.3.1 during 2019-2023 are described at first. Progress of the JWG during 2019-2021, are then presented in detail, which can be summarized as follows:

- (1) Discussion of “Ultrarapid”, “Rapid” and “Final” time scales for designing /delivering different types of IGS ionospheric State Space Representation (SSR) messages.
- (2) Finalization of global ionosphere corrections in IGS RT-WG proposed SSR data format, which had been released in early October 2020 (Phase 1).
- (3) Continue working on the IGS experimental RT-combination of CAS, CNES and UPC-IonSAT RT-GIMs, and routine generation of IGS RT-GIM.
- (4) Discussion on delivering ionospheric corrections using alternative base functions (e.g. B-Splines) together with accuracy information or quality indicator.
- (5) Working with IRI-WG on the assimilation of IGS RT-GIM into IRI model.

Finally, the next-step work of JWG 4.3.1 in the generation, comparison, combination, and dissemination of experimental two- and/or three-dimensional ionospheric information in support of real-time ionospheric monitoring and associated scientific applications are given.

Key words GNSS, Ionosphere, Total Electron Content, Real-time Global Ionospheric Map

Category: Symposium 4: Positioning and applications =» 4.1: Geodetic Remote Sensing

280

S4-011

Fast Snow Water Equivalent estimation with GPS interferometric reflectometry (GPS-IR) snow depth

Jiatong Wang^{1,2}、Yufeng Hu^{1,2}、Zhenhong Li^{1,3,2}、Chenglong Zhang^{1,2}、Miaomiao Zhang^{1,2}、Jing Yang^{1,2}、Wandong Jiang^{1,2}

1. College of Geological Engineering and Geomatics, Chang'an University, Xi'an 710054, China.
2. Big Data Center for Geosciences and Satellites, Chang'an University, Xi'an 710054, China.
3. Key Laboratory of Western China's Mineral Resource and Geological Engineering, Ministry of Education, Xi'an 710054, China

Snow Water Equivalent (SWE) is an important environmental variable. It governs energy and water fluxes. GPS interferometric reflectometry (GPS-IR) has been proven to be a powerful tool to monitor snow depth changes. In this paper, an efficient framework is developed to estimate SWE rapidly from GPS-IR-derived snow depth. It is applied to a plate boundary observatory (PBO) GPS station located in Idaho, USA. First, the daily snow depth series are obtained by GPS-IR and compared to the in-situ observations from SNOTEL. Second, a site-specific SWE conversion model is constructed using snow depth, SWE and climate observations of SNow TElemetry (SNOTEL) stations from 2011 to 2014. Finally, with the climate forecast data from the winter of 2015 provided by ClimateNA project, the daily GPS snow depth series are promptly converted to SWE. Our framework provides a fast way to convert the snow depth to SWE, which enhances the existing GPS network and improves accumulated snow products. The main contributions of this study are as follows:

(1) GPS-IR is employed to determine a reliable snow depth time series ($R^2 = 0.98$, RMSE = 11.1 cm, Bias = -3.7 cm).

(2) A regression model is constructed using observations from SNOTEL stations, and the performance of the model is evaluated. The results show the model has high temporal and spatial stability with the residuals of about 5 cm and the peak probability density close to 0 cm.

(3) Using the climate forecast data as parameter constraints, the daily GPS snow depth was rapidly converted to SWE ($R^2 = 0.98$, RMSE = 4.2 cm, Bias = -2.5 cm). The performance of this model is slightly worse (9 mm increase in bias) than the SWE model with SNOTEL observations as parameter constraints.

(4) The SWE is estimated by GPS-IR snow depth and climate observed variables of SNOTEL stations. The results show that the height

has greater impact on the SWE conversion compared with the horizontal distance.

Key words GPS-IR; Snow depth; Snow water equivalent; Fast estimation

Category: Symposium 4: Positioning and applications => 4.1: Geodetic Remote Sensing

295

S4-012

From spaceborne to ground-based polarimetric observations: Is precipitation detectable in GNSS reflected signals?

Milad Asgarimehr¹、Mostafa Hoseini²、Maximilian Semmling³、Markus Ramatschi¹、Adriano Camps^{4,6}、Hossein Nahavandchi²、Rüdiger Haas⁵、Jens Wickert^{1,7}

1. German Research Centre for Geosciences (GFZ), 14473 Potsdam, Germany.
2. Department of Civil and Environmental Engineering, Norwegian University of Science and Technology, 7491 Trondheim, Norway.
3. Institute for Solar-Terrestrial Physics, German Aerospace Center (DLR), 17235 Neustrelitz, Germany.
4. CommSensLab-UPC, Department of Signal Theory and Communications, UPC BarcelonaTech, 08034 Barcelona, Spain.
5. Department of Space, Earth and Environment, Chalmers University of Technology, 41296 Gothenburg, Sweden.
6. Institut d'Estudis Espacials de Catalunya (IEEC/CTE), Universitat Politècnica de Catalunya (UPC), 08034 Barcelona, Spain.
7. Institute of Geodesy and Geoinformation Science, Technische Universität Berlin, 10623 Berlin, Germany.

GNSS Reflectometry (GNSS-R) offers remote sensing of numerous surface and atmospheric parameters. “GNSS is an all-weather system”, nevertheless, can the signals detect precipitation? In this presentation, we will have an overview of recent studies addressing this question and theorizing the physical approach.

Although GPS signals are insignificantly attenuated by raindrops in the atmosphere, the splash effect, i.e. altered ocean/sea surface roughness by the impinging raindrops, is detectable when the signals are weakly diffused. This condition is met either over oceans induced with winds lower than 6 m/s or in coastal regions with a similar condition and where the coastline shelters the sea, leaving a limited fetch for winds.

The precipitation signatures, a significant drop in the power of the GNSS reflected signals, were observed in spaceborne measurements of UK TechDemoSat-1 for the first time. A plausible physical explanation by simulations based on a recent scattering model was provided. The GNSS-R spaceborne missions operate with a nadir LHCP antenna.

Recently, we investigated the signatures using a coastal experiment providing GNSS-R observations at RHCP and LHCP from side-looking antennas. We will discuss monitoring of the modifications in the surface roughness by rain splash as well as the surface salinity change by the accumulation of freshwater on the sea surface. It will be presented how the precipitation leads to significant decreases in RHCP and LHCP power, the magnitude of which is dependent on the elevation angle. The average LHCP power decreases by ≈ 5 dB at an elevation angle of 45° .

The roughness shows a steady increase with the rain rate. The derived surface salinity shows a decrease at rain rates higher than 10 mm/h. The sensitivity difference in the LHCP and RHCP signals and the technical/environmental limitations are discussed. This study confirms the potentials of GNSS-R, especially polarimetric measurements, for tracking precipitation events.

Key words GNSS-reflectometry (GNSS-R) , polarimetric observations , rain , sea surface salinity (SSS) , surface-roughening, TechDemoSat-1

Category: Symposium 4: Positioning and applications => 4.1: Geodetic Remote Sensing

297

S4-013

Multi-GNSS Meteorology: Computation of tropospheric delays and gradients at GFZ Potsdam

Karina Wilgan^{1,2}, Galina Dick², Florian Zus², Jens Wickert^{2,1}

1. Technische Universität Berlin (TUB)

2. German Research Centre for Geosciences (GFZ)

Heavy precipitation is the most dangerous and difficult to predict weather phenomena in Europe. Improving the precipitation predictions could lead to better warning systems e.g., against flash floods, debris falls or landslides. One way of improving the forecasts is the assimilation of external data. Many weather services operationally assimilate the Global Navigation Satellite Systems (GNSS) data. However, this impact is still limited due to focusing almost exclusively on GPS-only products in zenith direction, i.e. zenith tropospheric delays (ZTDs) or integrated water vapor (I WV). Assimilation of more advanced products, such as Slant Total Delays (STDs) from more satellite systems may lead to improved forecasts.

In this study we show the computation of multi-GNSS tropospheric products at GFZ Potsdam, i.e. the ZTDs, STDs and tropospheric gradients. The obtained parameters are compared with two global Numerical Weather Models (NWM): ERA5 reanalysis and a forecast model ICON. The results show that for ZTDs and horizontal gradients, all considered GNSS solutions show similar level of agreement with the NWM data. For STDs, the multi-GNSS solution has the highest agreement with ERA5. When only the Galileo observations are considered, the biases are reduced by ~25% compared to the GPS-only solution. This study shows that all systems are of comparable quality, however adding more systems in the operational data assimilation results in adding more observations, especially for low elevation and azimuth angles, which can improve the meteorological forecasts.

Key words multi-GNSS meteorology, troposphere modeling, tropospheric delays, weather models,

Category: Symposium 4: Positioning and applications => 4.1: Geodetic Remote Sensing

298

S4-014

Bounding the Residual Tropospheric Error by Interval Analysis

Jingyao Su, Steffen Schön
Leibniz Universität Hannover

GNSS integrity monitoring requires proper bounding to characterize all ranging error sources. Unlike classical approaches based on probabilistic assumptions, the alternative integrity approach depends on deterministic interval bounds as inputs. The intrinsically linear propagated intervals are adequate to describe the remaining systematic uncertainty.

In this contribution, we will make a proposal on how to derive the required intervals in order to quantify and bound the residual error for empirical troposphere models. We revise and refine the alternative approach based on interval analysis. The sensitivity analysis of the troposphere models is first implemented via interval arithmetic. The resulting sensitivities, together with carefully estimated uncertainties of model influence factors, are used to construct deterministic intervals. To this end, long-term statistics against on-site measurements are performed to estimate the interval bounds of meteorological parameters that are needed as input to the troposphere models.

Following this strategy, we evaluated the Saastamoinen model with a priori ISO standard atmosphere. In addition, the results with on-site measurements as inputs are also assessed for comparison. To this end, experiments using measurements from IGS and Deutscher Wetterdienst (DWD) stations are conducted. We obtain consistent and complete enclosure of residual ZPD errors w.r.t IGS ZPD products. Uncertainty interval maps in Germany for meteorological parameters and residual ZPD errors are generated as by-products thanks to the DWD dense network. These experimental results and products are finally validated, taking advantage of the high-quality tropospheric delays estimated by the Vienna Ray Tracer. Overall, the results indicate that our strategy based on interval analysis is feasible for the bounding of tropospheric model uncertainty. This will contribute to a realistic uncertainty assessment of GNSS-based single point positioning.

Key words Global Navigation Satellite Systems, integrity, interval analysis, residual tropospheric error, troposphere bounding

Category: Symposium 4: Positioning and applications => 4.1: Geodetic Remote Sensing
303
S4-015

Tomographic fusion strategies for the reconstruction of atmospheric water vapor

Gregor Moeller¹、 Chi Ao³、 Zohreh Adavi⁵、 Riccardo Biondi⁷、 Hugues Brenot⁹、
André Sá¹⁰、 George Hajj³、 Natalia Hanna⁵、 Chaiyaporn Kitpracha^{11,12}、 Eric
Pottiaux²、 Witold Rohm⁴、 Endrit Shehaj¹、 Estera Trzcina⁴、 Kuo-Nung Wang³、
Karina Wilgan^{11,12}、 Wenyuan Zhang⁶、 Kefei Zhang⁸

1. ETH Zürich, Switzerland
2. Royal Observatory, Belgium
3. Jet Propulsion Laboratory, California Institute of Technology, USA
4. Wroclaw University of Environmental and Life Sciences, Poland
5. TU Wien, Austria
6. China University of Mining and Technology
7. University of Padova, Italy
8. Royal Melbourne Institute of Technology, Australia
9. Royal Belgian Institute for Space Aeronomy, Belgium
10. Polytechnic Institute of Guarda, Portugal
11. Technische Universität Berlin, Germany
12. German Research Centre for Geosciences (GFZ) Potsdam, Germany

Geodetic GNSS networks are the backbone for tropospheric tomography studies. In addition, InSAR interferograms, GNSS radio occultation or microwave radiometer profiles are valuable assets, which can provide important complementary information for stabilizing the tomography system and further increase the spatio-temporal resolution of the reconstructed water vapor field. The combination of sensing techniques is a challenging task and requires a profound understanding of the underlying observation principles. Furthermore, tomographic fusion requires a strategy for observation selection and a weighting scheme for a reliable handling of the redundant information. Thus, over the last two decades of tomographic research, a series of methods has been established for the optimal combination of space geodetic and related sensing techniques – sensitive to the water vapor distribution in the lower atmosphere. Within the IAG working group 4.3.6, a review of integrated fusion strategies has been carried out. In this presentation we will provide an overview about the major findings – categorized according to the type of sensor combination and integration level.

Key words GNSS tomography; water vapor; sensor fusion; IAG working group 4.3.6

Category: Symposium 4: Positioning and applications => 4.1: Geodetic Remote Sensing
307
S4-016

A New Method of Predicting the Global Ionospheric Map

Yan ZHANG、Ningbo WANG、Zishen LI

Aerospace Information Research Institute, Chinese Academy of Sciences

This paper proposes a global ionospheric prediction model based on the theory of maximum posterior estimation. Based on the rapid ionospheric product of the Ionospheric Analysis Center of the Chinese Academy of Sciences (CAS), we realize the prediction of global ionospheric map (GIM) of 1 day, 2 days and 5 days. Taking the final GIM of the International GNSS Service Organization (IGS), the ionospheric TEC of Jason-2 altimetry satellite, and the measured ionospheric total electron content (TEC) of the reference station as reference, we evaluate the accuracy of the ionospheric predict products of CAS in global continent and ocean in 2008-2020, cooperated with the predict products of the European Orbit Determination Center (CODE), the European Space Agency (ESA) and the Polytechnic University of Catalonia (UPC) in Spain. Compared with IGS-GIM TEC, the accuracy of CAS prediction products is 2 TECu; compared with the altimetry satellite TEC, the accuracy of CAS prediction products is 5.1-6.6 TECu; compared with the TEC measured by the reference station, the accuracy of CAS prediction products is 2.40-2.91 TECu. The accuracy of CAS ionospheric prediction products is equivalent to the CODE prediction products.

Key words global ionospheric map; ionospheric TEC prediction; spherical harmonic function; maximum post-test estimate

Category: Symposium 4: Positioning and applications => 4.1: Geodetic Remote Sensing

332

S4-017

Near Real-Time Global Ionospheric Modeling Based on Multi-GNSS and Virtual Observation Stations

Xulei Jin^{1,3}, Shuli Song²

1. Shanghai Astronomical Observatory, Chinese Academy of Science, Shanghai, China
2. Shanghai Astronomical Observatory
3. University of Chinese Academy of Sciences, Beijing, China

Influenced by factors such as the sun and the magnetic activities and constantly coupled with other earth's layers, the ionosphere shows the attributes of nonlinear, time-varying, and disorder, therefore it is difficult to achieve accurate prediction of the ionosphere. Real-time positioning navigation and timing (PNT) and ionosphere monitoring rely on global ionospheric models of high timeliness and precision. However, The International GNSS Service (IGS) provides high-precision global ionosphere maps (GIMs) with delays ranging from nearly a day (rapid GIMs) to several weeks (final GIMs), which makes it difficult to meet the requirements mentioned above. Hence, we utilize multi-GNSS (GPS/GLONASS/Galileo/BEIDOU) observations of IGS hourly observations and real-time data stream to generate data sliding windows of 24 hours, adopt spherical harmonic function expansion and generate hourly ionospheric ultra-rapid GIMs (SHUG). The timeliness of SHUG is better than two hours. In order to solve local anomalies in GIMs caused by inhomogeneous distribution of GNSS stations, we establish several virtual observing stations (VOSs) with help of International Reference Ionosphere-2016 model (IRI-2016). GNSS and VOSs Bias (GVB) parameters are added to each VOS's observation equation to deal with the large biases between these two kinds of observations. The SHUG (day of year from 001 to 100, in 2021) are validated by IGS products. Taking IGSG as a reference, the RMSs of SHUG, C1PG, C2PG, UPCG, CASG, EMRG, SHAG, CODG, ESAG and JPLG are 0.72, 0.78, 0.91, 0.56, 0.59, 0.61, 0.65, 0.66, 0.86 and 1.18 total electron content unit (TECu) respectively. The results show that the precision of SHUG is basically between the IGS forecast and final GIMs and the timeliness are improved from several days to about two hours, and SHUG can not only meet the requirements of near-real-time PNT and ionosphere monitoring, but provide priori TECs and DCBs for real-time ionospheric modeling and forecasting.

Key words Near-real-time ionospheric modeling, Multi-GNSS, VOSs, TEC, Ultra-rapid GIMs

Category: Symposium 4: Positioning and applications => 4.1: Geodetic Remote Sensing

333

S4-018

ASHAK: Adjusted Spherical Harmonic and Kriging method for Regional Ionospheric TEC Modeling

Ang Liu、 Zishen Li、 Ningbo Wang、 Yan Zhang、 Hong Yuan
Aerospace Information Research Institute, Chinese Academy of Sciences

Considering that the applicability of conventional regional ionospheric VTEC models is limited, such as a strong dependence on the evenly distribution of local monitoring stations in interpolation methods, complex calculations of tomographic methods which puts a heavier burden on real-time services and lower correction efficiency of empirical model, a new approach based on Adjusted Spherical Harmonic and Kriging method (ASHAK) is proposed in this work, in which the deterministic component is fitted by the adjusted spherical harmonic function, and the stochastic component is estimated based on the Kriging method. This method can reduce the dependence on the station's distribution and calibrate the boundary distortion effect caused by function fitting. The accuracy analysis of the new model in China and surrounding regions carried out in the real-time processing mode in the two periods with different geomagnetic activity levels, with multi-GNSS data of IGS and CMONOC. Results shows that new method has increased by 8.8-40% and 4.0-20% compared with IDW and ASH, respectively; and the improvement is more obvious at the edge of the area. Compare with the GNSS-TEC, its rms is 1.0-2.0 TECu and 2.0-3.0TECu in the quiet and active periods, respectively, which is better than other products, including the regional ionospheric map (IOSR), and the global ionospheric map (C1PG, C2PG, CORG, UPCG).

Key words Total Electron Content (TEC); Regional Ionospheric TEC Modeling; Real-time; adjusted spherical harmonic; Kriging;

Category: Symposium 4: Positioning and applications => 4.1: Geodetic Remote Sensing

337

S4-019

BDS/GNSS Atmospheric Monitoring And Retrieval Terminal (BDSMART): Progress and Experiment

Zishen Li, Ningbo Wang, Liang Wang, Kai Zhou, Hong Yuan
Aerospace Information Research Institute, Chinese Academy of Sciences

Benefiting from the real-time high-rate multi-GNSS technique, BDS/GNSS ionospheric Monitoring And Retrieval Terminal (BDSMART) had been developed at the Aerospace Information Research Institute, Chinese Academy of Sciences (AIR/CAS) for ionospheric total electron content (TEC), scintillation and irregularity monitoring. BDSMART supports to track GPS L1/L2/L5, GLONASS L1/L2, Galileo E1/E5a/E5b, BDS-2 B1I/B2I/B3I and BDS-3 B1I/B3I/B1C/B2a signals, with the capabilities of 1) calibration of receiver differential code biases (DCBs), 2) retrieval of absolute ionospheric total electron contents (TECs), 3) calculation of phase and amplitude scintillation indexes and 4) computation of ionospheric TEC disturbance indicators, including ROTI, AART and home-developed RRROT indexes. New features of BDSMART compared to the commonly used Ionospheric Scintillation (IS) monitoring receivers are first presented, followed by the analysis of the estimated receiver DCBs, the extracted multi-GNSS Slant TECs (STECs), the generated phase and amplitude scintillation indexes as well as TEC disturbance indicators. The performance of BDSMART has been routinely assessed by the co-located Septentrio PolaRx5S IS monitoring receiver at CAS Miyun/Beijing observation site (mid-latitude), and more tests will be done at CAS Snaya/Hainan observation site to check the sensitivity of BDSMART to ionospheric amplitude and phase scintillations.

Key words BDSMART, Ionospheric monitoring, Total Electron Content (TEC), Ionospheric scintillation, Ionospheric disturbance, Real-time Multi-GNSS

Category: Symposium 4: Positioning and applications => 4.1: Geodetic Remote Sensing

342

S4-020

An enhanced atmospheric model of integrating GNSS CORS network and ERA5 for augmenting PPP-RTK

Yaxin Zhong、Cuixian Lv、Xingxing Li、Zhilu Wu、Yuxin Zheng、Bo Wang
Wuhan University

In the conventional PPP-RTK positioning, atmospheric corrections from nearby reference stations are interpolated at the clients based on linear combination algorithm. However, these interpolated tropospheric corrections reveal insufficient accuracy and reliability under the circumstance of complex terrain, which constrains the high-precision applications of PPP-RTK. In this study, an enhanced atmospheric model which integrates the continuous CORS network tropospheric parameters and the European Centre for Medium - Range Weather Forecasts (ECMWF) ERA5 dataset is established, in order to further augment the capabilities of PPP-RTK. In the augmented PPP-RTK, the slant path delay (SPD) derived from the proposed atmospheric model are taken as the a priori information to constrain the normal equation. The performance of the atmospheric model augmented PPP-RTK are investigated in terms of success rate of ambiguity fixing, convergence time and positioning accuracy, according to experiments in Chongqing and Sichuan CORS networks where the topography is relatively complicated. The results show that the proposed atmospheric model, which takes advantages of both ERA5 and GNSS CORS network tropospheric data, exhibits excellent capabilities in reducing the tropospheric delay effects resulting from the complex terrain environment and in improving the PPP-RTK positioning performance.

Key words PPP-RTK; atmospheric model; CORS network; ERA5; tropospheric delay

Category: Symposium 4: Positioning and applications => 4.1: Geodetic Remote Sensing

362

S4-021

Analysis of tropospheric estimates from multi-frequency low-cost GNSS receivers

Katarzyna Stępniaak, Jacek Paziewski, Radosław Baryła
University of Warmia and Mazury in Olsztyn

Water vapour is a key variable of the water cycle that plays a special role in many atmospheric processes controlling the weather and climate. Previous studies proved that the Global Navigation Satellite System (GNSS) is one of the few tools that can be used as an atmospheric water vapour sensor and therefore may provide continuous, precise and robust information on the atmosphere condition. This is possible taking advantage of the global network of permanent stations equipped with high-grade receivers and choke-ring antennas. Recently we have witnessed a remarkable progress in the performance of low-cost GNSS equipment that, in turn, opens the door to novel applications. One of the applications that may especially benefit from an ubiquity of low-cost receivers is the troposphere sensing. This motivated us to draw a special attention to the quality of the tropospheric estimates derived from low-cost receiver data processing.

In this study we investigate the usability of multi-frequency low-cost receivers for climate applications. Experiment is based on GNSS data collected over three consecutive days at three collocated stations equipped with low-cost u-blox ZED F9P receivers and high-grade Trimble Alloy one. The processing was performed using Bernese GNSS Software v.5.2 in Precise Point Positioning mode. We analyse the zenith total delays and horizontal tropospheric gradients obtained from GNSS data processing and afterwards converted integrated water vapour. The tropospheric parameters obtained from ERA5 reanalysis were compared to GNSS estimates to validate and assess the quality of the low-cost GNSS solution. The results show that the low-cost receivers can provide accurate GNSS tropospheric parameters time series that was confirmed by a validation against the data from climate reanalysis.

Key words GNSS; low-cost receiver; Zenith Tropospheric Delay; ERA5

Category: Symposium 4: Positioning and applications => 4.1: Geodetic Remote Sensing

396

S4-022

Based on InSAR Monitoring and Discrete Element Numerical Simulation Research on the Damage Trend Mountain Deformation in Jinsha River Basin

Xiong Guohua、 Yang Chengsheng、 Lv Sen、 Dong Jihong、 He Guoqiang
College of Geological Engineering and Geomatics, Chang'an University

Landslide disaster is widely distributed in the mountainous area of Southwest China. In this paper, taking the Jinsha River Basin as the research area, and using the Interferometric Synthetic Aperture Radar (InSAR) technology to identify and monitor the potential landslide groups in Gongjue County, Changdu city. According to the geometric relationship of the image, the one-dimensional deformation of the radar line of sight is projected to the slope direction, and the time series of slope direction deformation is obtained. At the same time, this paper decomposes and analyzes the deformation characteristics of landslide group. Finally, based on the drilling data, DEM data, simulating the two-dimensional deformation process of Sela landslide by using the discrete element software. The following conclusions are obtained: (1) From the results of time series deformation of slope direction, the landslide group in Gongjue county showed uniform deformation from November 2017 to November 2018. In November 2018, the Baige landslide formed a barrier lake and dredged in the upper reaches of Jinsha river, and all the landslides in the area experienced accelerated deformation. According to the results of periodic term and trend term of time series deformation decomposition of landslide front point, the deformation of the landslide cycle term fluctuated greatly in November 2018, and the trend term deformation presented uniform deformation as a whole; (2) Using MatDEM to simulate the Sela landslide in the landslide group. The simulation results show that the front sliding mass slides firstly, which leads to the instability of the rear sliding mass. It is determined that the Sela landslide is a tractive landslide, which corresponds to the deformation characteristics of InSAR.

Key words Jinsha River, InSAR, Deformation trend, Wavelet analysis , MatDEM

Category: Symposium 4: Positioning and applications => 4.1: Geodetic Remote Sensing

421

S4-023

Near Real-time Regional Ionospheric Modeling and Navigation Enhancing

Chunyuan Zhou¹、Ling Yang¹、Bofeng Li¹、Xiaoning Su²

1. Tongji University

2. Lanzhou Jiaotong University

As one of the main errors that Global Navigation Satellite Systems (GNSS) suffer from, the ionospheric delay can significantly degrade the accuracy of navigation and positioning, of which the impact can reach several meters or more. Although the empirical ionosphere model and Global Ionosphere Map (GIM) products are available, the immediacy and reliability of the model cannot be satisfied in the real-time high-precision requirements. With that in mind, a near Real-time Regional Ionosphere Model (RRIM) is proposed, the root-mean-square (RMS) maps of residuals are also provided to determine the reasonable weight of ionospheric pseudo-observations in Precise Point Positioning (PPP) model. Taking China and its surroundings as experimental areas, a near RRIM is established by using the polynomial model with dual-frequency observations and verified in the uncombined single-frequency PPP. The experimental results show that the performance of single-frequency PPP is obviously improved after using the RRIM products and determining the weight probably. In pseudo-dynamic uncombined single-frequency PPP experiments, the time required for the convergence of the E, N and U directions to 0.2 m, 0.2 m and 0.4 m is shortened by almost 4 times, only taking about 9 minutes, and the final positioning accuracy can reach centimeter level. In dynamic uncombined single-frequency PPP experiments, the positioning accuracy can reach instantaneous sub-meter level, which provides the possibility for the realization of automatic driving and lane level positioning.

Key words GNSS; Ionosphere; Near real-time modeling; PPP

Category: Symposium 4: Positioning and applications => 4.1: Geodetic Remote Sensing

442

S4-024

Sensitivity of ship-borne GNSS troposphere retrieval to processing parameters

Aurélie Panetier¹, Pierre Bosser², Ali Khenchaf³

1. Lab-STICC/PIM UMR 6285 CNRS, ENSTA Bretagne

2. Lab-STICC/M3 UMR 6285 CNRS, ENSTA Bretagne

3. ENSTA Bretagne

Water vapor is a key variable in meteorology and climate studies. Since the late 90s, GNSS estimates from ground antennas are commonly used for its description. Indeed, the estimation of propagation delays due to the transit of the signal through the atmosphere is a crucial step that is needed for the precise GNSS positioning. Integrated Water Vapor (IWV) contents are then derived from these delays and help to describe the distribution of water vapor.

However, severe meteorological phenomena often originated over the oceans and could strongly affect coastal regions. These phenomena are often less well described or forecasted because of the small number of observations available in these regions. In this context, the potential of ship-borne GNSS measurements has already been highlighted.

This work aims at investigating the impact of GNSS processing parameters such as cutoff angle, random walk of the estimated delays, and observation weighting, on IWV retrieval from a ship-borne antenna in PPP mode. Data were collected for 2 months in 2018 by the GNSS antenna of a vessel operating in the Bay of Brest, France. The impact of the different parameters is assessed by comparing the GNSS-derived IWV to the IWV estimated from a close GNSS ground station, and those computed by the ERA5 reanalysis and operational radiosonde profiles from the nearest Météo-France station. The most satisfying parameterization is shown to have RMS differences of 0.6 kg/m², 1.0 kg/m², and 1.8 kg/m² compared to GNSS ground station, ERA5, and radiosonde, respectively. These conclusive results are also confirmed by comparing the GNSS height estimates to the measurements from the Brest tide gauge, with an RMS difference of 5.0 cm.

In the future, these results should be confirmed with a more representative dataset, covering a more extended period, and collected in open seas (offering a broader range of sea states), in order to assess ship-borne GNSS IWV retrieval in less favorable conditions.

Key words Ship-borne GNSS, IWV, meteorology, climatology, PPP

Category: Symposium 4: Positioning and applications => 4.1: Geodetic Remote Sensing

446

S4-025

Development of the next-generation GNSS-Meteo stations

Matthias Aichinger-Rosenberger, Alexander Wolf, Philippe Limpach, Gregor Moeller

ETH Zürich, Switzerland

The last years we have seen a rapid growth in the number of low-cost GNSS sensors available on the market. Alongside the increase in the number of products, capabilities of these sensors are also permanently extended (e.g. to dual-frequency operation). This makes them usable also for typically high-accuracy applications like remote sensing of atmospheric water vapor.

At the group of Mathematical and Physical Geodesy (MPG), ETH Zürich we operate a series of GNSS sensor stations for the monitoring of permafrost/rock glacier movements and landslides. A current research focus of the group is the extension and upgrade of this station network for troposphere monitoring. Therefore, different setups and station payloads as well as processing strategies are currently under investigations.

The present study explores prerequisites for the setup and operation of a next-generation, low-cost GNSS station to be used for meteorological/climatological monitoring. We introduce detailed investigations on the benefits of upgrading individual components for GNSS signal tracking, maintenance and data transfer – designed for the operation of stations in remote areas. In this regard, the capabilities of the power-efficient u-blox ZED F9P receiver module for estimation of tropospheric parameters are analysed using different antenna setups (patch or geodetic antennas). First results from a test campaign indicate that, up till today, high-grade antenna solutions are still the preferable choice for GNSS meteorology as typical error sources like multipath effects can be mitigated more efficiently. The GNSS receiver and antenna combination investigated in this study might also serve as a possible solution for the upgrade of automatic weather stations using GNSS. This would allow for the build-up of collocated GNSS/Meteo stations which come with a huge number of scientific benefits (e.g. in-situ cross-validation of observations), not only for meteorological purposes.

Key words low-cost GNSS, water vapor, climate monitoring, remote areas

Category: Symposium 4: Positioning and applications => 4.1: Geodetic Remote Sensing

465

S4-026

Spatial-Temporal Characteristics of the Tropopause Height over Global Tropical and Subtropical Regions Using COSMIC-2 Radio Occultation Data

Jiaqi Shi, Kefei Zhang

School of Environment Science and Spatial Informatics, China University of Mining and Technology

The tropopause height (TPH) of lapse rate (LRT) and cold point (CPT) can be used to obtain the TPH from temperature profiles. The recently launched COSMIC follow-on (Constellation Observing System for Metrology Ionosphere and Climate-2) temperature data from Dec 2019 to Feb 2021 were used in the investigation of the spatial-temporal characteristics in global tropical and subtropical regions ($45^{\circ}\text{S} - 45^{\circ}\text{N}$) using a $2.5^{\circ} \times 2.5^{\circ}$ grid. The diurnal variation of TPH in the Qinghai-Tibet Plateau and the Sahara Desert was also studied. The radiosonde data and Metop-A/B/C (Meteorological Operational-A/B/C) RO data were used to evaluate TPH obtained from the COSMIC-2 data using the collocation criteria and Gaussian weighting functions. It is shown that the TPH negatively correlates with latitude and is mainly concentrated in the 15–18 km altitude range in $25^{\circ}\text{S} - 25^{\circ}\text{N}$. Similarly, the TPH decreases with the increase of latitude in $25^{\circ}\text{S} - 40^{\circ}\text{S}$ and $25^{\circ}\text{N} - 40^{\circ}\text{N}$, and it can decrease to 12 km at 40°S and 40°N . The temperature and pressure distribution at the TPH are opposite to the height distribution. Meanwhile, the TPH shows strong seasonal correlation in subtropical regions, it is higher in summer and lower in winter. It is found that the LRT is high accuracy than CPT in comparison with the radiosonde data.

Key words Radio Occultation; COSMIC-2; Tropopause Height

Category: Symposium 4: Positioning and applications => 4.1: Geodetic Remote Sensing

477

S4-027

GNSS-R coastal sea level altimetry with an open-source low-cost sensor: initial evaluation of high elevation angle satellites

Manuella Fagundes, Felipe Geremia-Nievinski
Federal University of Rio Grande do Sul

The ground-based GNSS reflectometry is a geodetic remote sensing technique capable of performing coastal sea level altimetry away from the water. The combination of coherent direct and reflected reception results in an interference pattern in signal-to-noise ratio (SNR). SNR-based GNSS-R enables the retrieval of geophysical parameters such as water level. While geodetic antennas dampen the SNR interference pattern, low-cost antennas make it possible to observe the SNR oscillations at higher elevation angles. Such observations are desirable because they have the potential of alleviating sky visibility requirements that are stringent near the horizon. Furthermore, as reflection points will be closer to the antenna, it would allow the retrieval of water height from smaller water bodies, such as narrow rivers and ponds. We have evaluated elevation angles up to 65 degrees collected with an open-source GNSS-R sensor based on an external patch antenna installed by the Guaíba Lake (30.0277° S, 51.2287° W) in Brazil. Satellites at lower elevation angles experience more atmospheric errors and suffer more influence from the earth's curvature. Our aim was to quantify and correct for such systematic experimental errors. Besides, we hope to obtain accurate results in water level closer to the antenna.

Key words GNSS-R; low-cost; altimetry.

Category: Symposium 4: Positioning and applications => 4.1: Geodetic Remote Sensing

545

S4-028

Comparison of the Effective Isotropic Radiate Power parameter in CYGNSS v2.1 and v3.0 level 1 data and its impact on soil moisture estimation

Paulo de Tarso SETTI JUNIOR¹, Tonie VAN DAM^{2,3}

1. University of Luxembourg

2. Interdisciplinary Center for Security and Trust, University of Luxembourg

3. Department of Geology & Geophysics, University of Utah

The effective isotropic radiated power (EIRP) of the Global Positioning System (GPS) is a function of the transmitted Right-Hand Circularly Polarized (RHCP) power and the gain of the transmitting antenna. The EIRP determines the power incident on the surface of the Earth. In Global Navigation Satellite Systems Reflectometry (GNSS-R), the EIRP is a fundamental parameter for estimating surface reflectivity. The Cyclone Global Navigation Satellite System (CYGNSS) is a mission consisting of eight small satellites measuring the reflected GPS L1 signals with the primary objective of measuring wind speed in hurricanes and tropical cyclones. Reflections over land have the potential to be used to estimate near-surface soil moisture if properly treated and modelled. For CYGNSS v2.1 level 1 data, available since March 2017, the EIRP was computed assuming a static value for the power level of the L1 signal transmitted by the GPS satellites. In the v3.0 level 1 data, available since August 2018, a dynamic EIRP calibration algorithm was introduced, with the variations in GPS transmit power being tracked using the direct signal power measured by the navigation receivers. In this contribution, we compare the values of the estimated EIRP from CYGNSS versions 2.1 and 3.0 in the year of 2020. To analyze the impact of the EIRP parameter for estimating soil moisture. We correlate the estimated surface reflectivity with reference soil moisture observations from the Soil Moisture Active Passive (SMAP) mission. The correlation is slightly improved when using the CYGNSS v3.0 data.

Key words CYGNSS; EIRP; GNSS-R; soil moisture

Category: Symposium 4: Positioning and applications =» 4.1: Geodetic Remote Sensing

561

S4-029

Sea-ice signatures in coherently reflected GNSS signals: Findings from the MOSAiC expedition

Maximilian Semmling¹、 Jens Wickert^{2,4}、 Frederik Kreß^{2,4}、 Mainul Hoque¹、 Dmitry Divine³、 Sebastian Gerland³

1. German Aerospace Center DLR-SO

2. German Research Center for Geosciences GFZ

3. Norwegian Polar Institute

4. Technische Universität Berlin

Sea ice is a crucial parameter in the Earth climate system. Its high albedo compared to water influences the oceans' radiation budget. The importance of monitoring arises from the high variability of sea-ice state and amount induced by seasonal change and global warming. GNSS reflectometry can contribute to global monitoring of sea ice. Properties like ice salinity, temperature and thickness can affect the signal reflection. The MOSAiC expedition (Multidisciplinary drifting Observatory for the Study of Arctic Climate) gave us the opportunity to conduct reflectometry measurements under different sea-ice conditions in the central Arctic. A dedicated setup was mounted, in close cooperation with the Alfred-Wegener-Institute (AWI), on the German research icebreaker Polarstern that drifted during nine months with the Arctic sea ice.

Here, results from the expedition's first leg in autumn 2019 are presented. They refer to the Siberian Sector of the Arctic (from about 85°N to 87°N). Profiles of sea-ice reflectivity are derived with daily resolution considering reflection data recorded at left-handed (LH) and right-handed (RH) circular polarization. Respective predictions of reflectivity are based on reflection models of bulk sea ice or a sea-ice slab. The latter allows to include the effect of signal penetration down to the underlying water. Results of comparison between LH profiles and bulk model confirm that the reflectivity decreases (about 10 dB) when the drifting ship enters compact sea ice.

Anomalies in the reflectivity signatures occur when sea ice in the central Arctic is reached. The comparison of signatures and applied models (bulk and slab) indicate the role of coherent signal penetration into the ice. Sea ice salinity and temperature can alter these signatures. We conclude that monitoring of ice type/salinity and temperature can benefit from grazing angle GNSS reflectometry. Future studies will proceed to investigate these signatures in coherent observations.

Key words GNSS reflectometry, sea-ice properties

Category: Symposium 4: Positioning and applications => 4.1: Geodetic Remote Sensing

562

S4-030

Detection of earthquake and tsunami signatures in the ionosphere from the combination of different observation techniques

Michael Schmidt¹, Andreas Goss¹, Eren Erdogan¹, Wojciech Jarmołowski², Pawel Wielgosz², Anna Krypiak-Gregorczyk², Beata Milanowska², Manuel Hernández Pajares³, Alberto García-Rigo³, Enric Monte-Moreno³, Victoria Graffigna³, Heng Yang³, Anna Belehaki⁴, Ioanna Tsagouri⁴, Evangelos Paouris⁴, Roger Haagmans⁵

1. Technical University Munich

2. University of Warmia and Mazury in Olsztyn

3. Universitat Politecnica de Catalunya

4. National Observatory of Athens

5. European Space Agency

In the frame of the ESA funded project COSTO we investigated the responses of the electron density within the ionosphere to the seismic activity and the propagation of a tsunami caused by an earthquake (EQ) of magnitude 8.3 in the Chile-Illapel region at September 16, 2015, 22:54 UTC. This study means a wide review of available ground and satellite data available to detect seismically induced traveling ionospheric disturbances (TID) and small-scale irregularities. They occur before, shortly after or later well after the main earthquake and can be detected in the immediate vicinity but also far away from the epicenter. The data we used include several types of ground and satellite-based observations from low-Earth orbit (LEO) satellite missions such as GRACE and Swarm. The applied modelling techniques include spectral analysis of LEO along-track data and terrestrial GNSS measurements. For the analyses we focused on the days September 16 and 17, 2015. We partly extended the time span to adjacent days, if an enhanced seismic activity has been recorded.

In this presentation several examples of seismically triggered TIDs will be shown. Their possible detection results from the combination of observations from more than one measurement system and the application of different evaluation techniques, e.g. the wavelet transform. Applying a combination procedure weaknesses of individual techniques can be compensated by the strengths of others. The combination of satellite data from LEOs and terrestrial data, e.g. from local GNSS receiver networks or ionospheric HF sounders looks promising, especially in view of the nearby availability of CubeSat constellations equipped with instruments for ionosphere sounding. An important conclusion of this study is the need of spectral analysis techniques in the processing of LEO along-track data and the requirement of validating

LEO observations with information from other independent LEOs or terrestrial data.

Key words electron density, travelling ionospheric disturbances, earthquakes, tsunamis

Category: Symposium 4: Positioning and applications => 4.1: Geodetic Remote Sensing
573
S4-031

High-precision SLR tropospheric zenith delay prediction

haoyue zhang
chinese academy of surveying & mapping

The troposphere is an important part of the earth's low-altitude atmosphere, and the atmospheric refraction caused by it is the main factor restricting the accuracy of satellite laser ranging. The establishment of a model to reduce the atmospheric refraction delay error as much as possible is a key step to improve the accuracy of satellite laser ranging data processing. It is also the use of satellite laser ranging data to accurately determine the orbit of space targets, maintain the geodetic reference frame, and determine the earth's rotation parameters. Important Guarantee. This paper analyzes and compares the time series of the tropospheric zenith delay model of a single station, that is, using the BJFS station IGS tropospheric zenith delay product and weather record data from 2014 to 2020, analyzes and compares the difference between the Marini-Murray model and the tropospheric product released by the IGS, through the time series Analyze and establish the time variation law of tropospheric delay at BJFS station, and use IGS products that have not participated in the modeling to test it. The results show that the deviation between the IGS-MM model and the ZPD of IGS is about -0.19mm, and the standard deviation is about 19.2mm. In the work of SLR data processing, space geodetic survey, etc., the IGS-MM model can be used to obtain higher precision and more stable ZTD, and weaken the influence of the troposphere on SLR technology.

Key words SLR; GNSS; Zenith tropospheric delay; time series analysis;

Category: Symposium 4: Positioning and applications => 4.1: Geodetic Remote Sensing

580

S4-032

Improving the global estimation of zenith wet delay and weighted mean temperature with machine/deep learning methods

Zhangyu Sun, Bao Zhang, Yibin Yao
Wuhan University

The modeling of tropospheric delay and weighted mean temperature (T_m) by conventional methods is unable to reflect complicated temporal variations caused by synoptic variations or irregular climate fluctuations, which brings uncertainties in Global Navigation Satellite System (GNSS) tropospheric delay correction and water vapor retrieval. Machine and deep learning methods provide us new powerful tools to further improve the estimation accuracy of tropospheric delay and T_m due to their strong nonlinear fitting capability and data-adaptive modeling property. In this study, three machine learning methods, i.e., the backpropagation neural network (BPNN), the generalized regression neural network (GRNN), and the random forest (RF), and one deep learning method, i.e., the deep belief network (DBN), are employed to improve the estimation of zenith wet delay (ZWD) and T_m over the globe. The basic idea is to use the machine and deep learning methods to simulate the complex relationship between ZWD/ T_m and surface meteorological elements, and further incorporate geographical and temporal information to calibrate and optimize this relationship in space and time. Validating results show that the proposed machine and deep learning methods in this study significantly improve the ZWD and T_m accuracies by approximately 20% and 30%, respectively, compared with conventional models. Among these four machine/deep learning models, the DBN model performs the best owing to its relatively high accuracy and low requirement for computational cost. The achievement of this study could potentially contribute to the high-accuracy GNSS positioning and meteorology.

Key words Global Navigation Satellite System; zenith wet delay; weighted mean temperature; backpropagation neural network; generalized regression neural network; random forest; deep belief network

Category: Symposium 4: Positioning and applications =» 4.1: Geodetic Remote Sensing

586

S4-033

A global latitude zone weighted mean temperature (T_m) augment method for empirical T_m model

Fei Yang¹、Di Zhang²、Ming Chen³、Jiming Guo²、Xiaolin Meng⁴

1. China University of Mining and Technology-Beijing

2. Wuhan University

3. National Geomatics Center of China

4. Global Geospatial Engineering Ltd. and the Sino-UK Geospatial Engineering Centre

The atmospheric water vapor information retrieved by Global Navigation Satellite System (GNSS) techniques provides abundant basic data for meteorology. In this process, the weighted mean temperature (T_m) is regarded as the most critical parameter which ensures the conversion from the GNSS tropospheric delays to precipitable water vapor (PWV). The existing T_m empirical models, which fed only by coordinates of the site and the time, can provide T_m estimates and guarantee the rapid PWV retrieval, but the accuracy is limited, especially the existence of the regional differences. With more and more GNSS sites are installed with meteorological sensors, abundant ground weather data can be collected together with GNSS observation data. Therefore, this paper explores the relationship of the T_m changing with the collected surface temperature, divides the world into different latitude zones, introduces surface temperature into the existing T_m empirical models, and proposes a global latitude zone T_m augment method. The proposed augment method utilizes the data of the globally distributed radiosonde, obtains the augment coefficients of each latitude zone adopting the least square method, and achieves the error compensation effect for estimating T_m. The formula of the proposed method is simple, which can be quickly extended to any empirical T_m model, and provides a guarantee for real-time GNSS-PWV with high precision.

Key words GNSS meteorology, troposphere delay, weighted mean temperature, precipitable water vapor

Category: Symposium 4: Positioning and applications => 4.1: Geodetic Remote Sensing

627

S4-034

Sea level estimation using signal strength indicator data based on GNSS multipath reflectometry

Nazi Wang, Tianhe Xu, Fan Gao

Institute of Space Sciences, Shandong University, Shandong, China.

Sea level estimation based on GNSS multipath reflectometry (GNSS-MR) can be seen as GNSS tide gauge, because it can provide low-cost and long-time sea level data. Comparing with traditional tide gauge, sea level estimations based on GNSS-MR are also not susceptible to crustal subsidence. Signal-to-noise ratio (SNR) observables in GNSS files are commonly used for GNSS-MR, and this method is usually referred to as SNR method. However, the SNR observables are not always exist, especially in early GNSS files. Several literatures proposed to use different combinations of code and carrier-phase for GNSS-MR as a substitute to extract sea level. But cycle slip detection or dual-frequency even triple-frequency observations are needed to isolate multipath signals by using these methods, which reduce the applicability of the method. Here, we propose a new sea level estimation method using signal strength indicator (SSI) data in RINEX files based on GNSS-MR, which can be seen as an alternative for existing method because SSI data are always exist even for early GNSS files. In order to verify the proposed method, we use one-year GNSS data from AT01 station in Alaska to monitor sea level. By comparing with tide gauge data, sea level estimations with RMSE of 17-26 cm and correlation coefficient of more than 0.78 were retrieved. S5Q for GPS, S8Q for Galileo and S7I for BDS achieve better performance than other signals. Meanwhile, the precisions of retrieved sea level are similar with that based on SNR method. Additionally, synthetic SSI data are also used to estimate the implications of station height and data sampling rate on the precision of GNSS-derived sea levels. We find that the data sampling rate have a bigger influence than station height for proposed method. The proposed method makes it more feasibility to integrate early GNSS observation files for studying long-time sea level variations using GNSS-MR technology, and increases the diversity of sea level monitoring methods.

Key words sea level estimation, signal strength indicator (SSI), GNSS-MR, SNR

Category: Symposium 4: Positioning and applications => 4.1: Geodetic Remote Sensing
654
S4-035

Determination of water vapor content using low-cost dual-frequency GNSS receivers

Tomasz Hadas^{1,2}、Grzegorz Marut²、Jan Kapłon^{2,3}、Witold Rohm²

1. Institute of Navigation, University of Stuttgart

2. Wrocław University of Environmental and Life Sciences

3. U+Geo Ltd, Poland

With Global Navigation Satellite Systems (GNSS), the near real-time remote sensing of water vapor content in the troposphere is performed in Europe under the E-GVAP (<http://egvap.dmi.dk/>) program, but the spatial resolution is limited by the density of permanent GNSS stations. However, low-cost receivers are a promising solution to the problem of densifying GNSS networks, while the availability of multi-GNSS real-time corrections allows reducing the temporal latency, i.e. to switch to real-time processing. Although the performance of dual-frequency low-cost receivers was investigated in several geoscience applications, their use in GNSS meteorology has not been well documented yet.

We used prototype dual-frequency low-cost units for GNSS meteorology and co-located them with the International GNSS Service (IGS) station WROC. During a test period of several weeks, we investigated the accuracy of real-time and near real-time Zenith Total Delay (ZTD) with respect to the IGS Final products. Several processing strategies and hardware configurations were investigated, that varied e.g. in GNSS selection, antenna model, and ground plate application. In best cases, we achieved accuracy better than 5 mm and 9 mm with survey-grade and patch antenna, respectively, despite the dynamic weather conditions. Finally, we deployed a network of 17 low-cost receivers in and around the city of Wrocław, Poland. From estimated ZTDs and atmospheric parameters derived from a high-resolution numerical weather model WRF (Weather Research and Forecasting), we determined Integrated Water Vapor (IWV). We estimated the IWV uncertainty at a 95% confidence level of 2.3 kg per m². We observed significant under- or over-determination of the IWV for the entire test area, as well as small-scale IWV variations with respect to WRF forecasts. Therefore we conclude, that low-cost receivers have a great potential of monitoring weather phenomena at a high spatio-temporal scale and support nowcasting application.

Key words GNSS, troposphere, low-cost, water vapor

Category: Symposium 4: Positioning and applications => 4.1: Geodetic Remote Sensing

658

S4-036

An improved method for real-time tropospheric delay modeling with a regional GNSS network

Hongxing Zhang, Yunbin Yuan

Innovation Academy for Precision Measurement Science and Technology, Chinese Academy of Sciences

The real-time GNSS-derived tropospheric delays have become increasingly valuable for tropospheric delay modeling with increasing number of GNSS networks. Previous studies on GNSS-based regional tropospheric delay modeling mainly focused on how to well characterize tropospheric delays in spatial domain using simulated perfect real-time GNSS-related data (state-space-representative, broadcast ephemeris and observation), which leads two deficiencies: (1) the temporal information of regional troposphere state are not fully explored in modeling; (2) the stream-based GNSS-related data always experience greater uncertainties in “true” real-time mode, which make the modeling processing more complicated in practice than simulated cases. In this study, we reveal the weakness of the customary modeling method in imperfect real-time GNSS-data conditions and present an improved method by making fully use of the temporal information of regional troposphere state in modeling. Our improved method seek to derive the model coefficients recursively epoch-by-epoch by using a robust extended Kalman filtering (REKF-TROP) rather than the single-epoch-based least-squares adjustment used in customary method (LSE-TROP). This feature enables the REKF-TROP two main advantages: (1) fully utilizing the properties of temporal smooth variations of the regional troposphere state in modeling; (2) effectively minimizing the impacts of temporary uncertainties of real-time GNSS-related data on tropospheric delay modeling. The REKF-TROP is evaluated over a four-week period at two typical regional GNSS network. The results indicate that the REKF-TROP is more accurate (with an average accuracy improvement of ~10%) and robust than the conventional LSE-TROP, especially in unfavorable real-time data conditions including temporary SSR accuracy degradation, outlier occurrence and temporary sparse GNSS stations in modeling.

Key words global navigation satellite system (GNSS); real-time zenith tropospheric delay (RT-ZTD); regional tropospheric delay modeling, robust extended Kalman filter (EKF);

Category: Symposium 4: Positioning and applications => 4.1: Geodetic Remote Sensing

666

S4-037

Cross-polarization Correction for Soil Moisture Retrieval Using GNSS SNR data

Mutian Han、 Dongkai Yang、 Bo Zhang、 Xuebao Hong
Beihang University

Soil moisture monitoring using GNSS-Interferometric Reflectometry (GNSS-IR) technique was studied. Previous studies have shown that, under the interference of the soil reflected signal, the Signal-to-Noise Ratio (SNR) measured by the receiver shows cosine-like variation pattern. And three metrics extracted from the SNR data are used to retrieve soil moisture including the amplitude, frequency and initial phase. Due to the complexity of these metrics, empirical models are preferred for retrieval. However, the parameters of the empirical models are highly dependent on the experiment scenario, which are not universally applicable. Besides, long-term experiment data are needed to train the model before it can be used.

To overcome those disadvantages, we re-examined the theoretical SNR model, based on which a semi-empirical SNR model was proposed in 2018. By directly fitting this model with the raw SNR data, the power of the direct and reflected signal can be estimated, based on which well-established theoretical model could be used to retrieve soil moisture. However, we soon realized that further studies should be carried out in order to improve the accuracy of the retrieval. We focused on reducing the errors on the estimated power of the reflected signal, among which the most significant one comes from the cross-polarization leakage of the GNSS antenna. In order to correct its influence, we reformulated the theoretical SNR model by taking the antenna cross-polarization into account. Although similar model has already been derived by V. U. Zavorotny et al. in 2010, their derivation has not reached the final usable form and has not been used for this purpose. In combination with the retrieval method we proposed before, we showed how this model could be used for correction through both simulation and experiment data processing. The results showed that the mean retrieval error could be reduced by about $0.16 \text{ cm}^3\text{-cm}^{-3}$ after cross-polarization correction.

Key words Global Navigation Satellite System (GNSS), Signal-to-Noise Ratio (SNR), Cross-polarization, Soil Moisture, Remote Sensing

Category: Symposium 4: Positioning and applications => 4.1: Geodetic Remote Sensing

669

S4-038

Further evaluation of a GNSS-R synthetic vertical array for high-rate water level altimetry

Mauricio Yamawaki, Felipe Geremia-Nievinski
UFRGS

Due to sea-level rise and its combination with extreme events, coastal sea level monitoring is a growing necessity worldwide. Conventional tide gauges are well-known solutions but can be difficult to install and expensive to maintain. With the growth of global navigation satellite system (GNSS) constellations, GNSS Reflectometry (GNSS-R) is becoming increasingly more reliable for water level altimetry. The GNSS-R sensor can be installed on land, away from the water, which is an important advantage for sandy beaches where a pier would otherwise need to be constructed to support a conventional tide gauge. Past studies have shown that GNSS-R can achieve centimeter-level precision. One of the weaknesses of GNSS-R is its time resolution, which is tens of minutes per independent measurement, depending on the satellite movement. Recently we have demonstrated that a vertically-sweeping antenna could retrieve surface height within 5 minutes. This artificial displacement synthesizes a vertical array that imprints an interference pattern on top of the interference pattern normally found for a static antenna. Interferometric phase can be retrieved via nonlinear fitting for each sweeping cycle, from which reflector height can be retrieved based on a simple linear regression over several cycles. The proof-of-concept experiment was limited to ground reflectors, had some horizon obstruction, and power supply issues. A geodetic antenna had been employed, dampening the multipath interference pattern. To further evaluate the synthetic vertical array, we conducted an improved field experiment. It lasted for longer (6 hours), over a water surface (a well leveled and homogeneous target), on a site with little horizon obstruction employing a high-capacity battery, and a non-geodetic antenna (for improved reflection reception). We will report the preliminary results of this second experiment.

Key words GNSS, GNSS-R, Tide-gauge

Category: Symposium 4: Positioning and applications => 4.1: Geodetic Remote Sensing

701

S4-039

Mitigating Long Wavelength Ocean Tide Loading Effects on InSAR Observations Over Wide Regions

Chen Yu¹, Nigel Penna², Zhenhong Li^{3,4}

1. School of Engineering, Newcastle University, Newcastle upon Tyne, NE1 7RU, UK

2. Newcastle University

3. College of Geological Engineering and Geomatics, Chang'an University, Xi'an 710054, China

4. Key Laboratory of Western China's Mineral Resources and Geological Engineering, Ministry of Education, Xi'an, 710054, China

Recent advances in Interferometric Synthetic Aperture Radar (InSAR), such as Sentinel-1 and the planned GEOSAR, enable the Earth's deformation being measured over extreme large spatial extents so that large scale deformation signals caused by tectonic and groundwater storage variations may now be mapped in unprecedented detail. However, errors within InSAR measurements increase with distance and may completely mask these geophysical signals at such scale. Previous researches have focused on the tropospheric and ionospheric effects, but the Ocean Tide Loading (OTL) effect receives little attention. The only solid investigation was in 2008 using simulated datasets of outdated SAR missions and the OTL effect on real measurements was not shown. Therefore, OTL effects have not usually been modeled to date, as the need has not previously been shown.

In this contribution, we aim to demonstrate for the first time the importance of the OTL effect on the abovementioned geophysics studies, and on those seeking to generate nationwide or continent-wide deformation products using InSAR, given the fact that the future InSAR mission (e.g., GEOSAR) may have a spatial extent of over 1000 km. Over five years, we evaluate the OTL effect globally on interferograms from Sentinel-1 and suggest substantial contamination arises over most coastal and many tectonically active regions. As a result of this demonstration of the need to model OTL, we anticipate Earth observation scientists, geophysicists, and geologists needing to change their analysis approaches in order for InSAR to be used to obtain millimetric level geophysical signals over wide regions, to enable InSAR to be used for studies of Glacial Isostatic Adjustment, inter-seismic tectonic strain accumulation, post-seismic relaxation, slow slip events and creeping of fault systems, continental rifting, and groundwater storage variations.

Key words Ocean tide loading; InSAR; Atmospheric delay; Tectonic

Category: Symposium 4: Positioning and applications =» 4.1: Geodetic Remote Sensing

720

S4-040

An empirical zenith wet delay model using piecewise height functions based on a sliding window algorithm for China

Ge Zhu^{1,3}、Liangke Huang^{1,3}、Lilong Liu^{1,3}、Si Xiong²、Junyu Li²、Chao Ren^{1,3}

1. College of Geomatics and Geoinformation, Guilin University of Technology

2. School of Geodesy and Geomatics, Wuhan University

3. Guangxi Key Laboratory of Spatial Information and Geomatics

Tropospheric delay is an important factor affecting high-precision satellite navigation positioning, and its variation in the vertical direction is much greater than that in the horizontal direction. The water vapor at different heights shows different trends, which changes rapidly with respect to height. Thus, the zenith wet delay (ZWD) with direct relation to water vapor has complex spatio-temporal variations in the vertical direction. ZWD is also a key parameter for GNSS precipitable water vapor (PWV) sounding. It is worthwhile undertaking research aimed at developing a high precision zenith wet delay (ZWD) model. Some shortages still exist in current ZWD models, such as only single function as well as gridded data is used for modeling. A new approach, the sliding window algorithm, is proposed to develop a ZWD model using piecewise height functions. Based on the analysis of vertical variations of ZWD, the troposphere is divided into three height intervals (below 2 km, 2 to 5 km, and 5 to 10 km). Besides, the fitting functions are also determined within these height intervals. In this work, an empirical zenith wet delay model using piecewise height functions considering spatiotemporal factors is developed based on the second Modern-Era Retrospective analysis for Research and Applications (MERRA-2) data, which is named the CZWD model. Radiosonde data is treated as reference values to evaluate the performance of the CZWD model which is compared to the canonical GPT3 model. Validated by the radiosonde data in 2017, the CZWD model achieves the higher performance compared with GPT3 model, which is improved by 2.8mm in bias and 1.2mm in RMS. Thus, the applicability of this model could be enhanced in GNSS precipitable water vapor sounding and GNSS precise position.

Key words Sliding window algorithm; GNSS meteorology; Zenith wet delay; Piecewise

Category: Symposium 4: Positioning and applications => 4.1: Geodetic Remote Sensing

730

S4-041

Satellite-based GNSS-R: A New Tool for Flood Monitoring —— Flood monitoring of the Yangtze River Basin in 2020 using CYGNSS data

Wenxiao Ma^{1,2}、Xuerui Wu^{1,2,3}

1. Shanghai Astronomical Observatory, CAS

2. University of Chinese Academy of Sciences

3. School of Resources, Environment and Architectural Engineering, Chifeng
University

Flood is one of the most serious natural disasters in the world, and the analysis of flood inundation is of great significance for climate change research, environmental monitoring, and the protection of people's lives and property. Remote sensing technology is an effective means of flood monitoring. However, the traditional remote sensing methods have their own limitations, the timeliness of optical remote sensing monitoring is poor, often can not measure the flood, because during the flood, the earth's surface is usually covered by clouds, while optical remote sensing can't penetrate the clouds. The satellite-based synthetic aperture radar (SAR) technology works in the more penetrating microwave band, which allows the advantage of higher spatial resolution without cloud interference, but revisit times tend to be longer. After more than 30 years of development, GNSS-R technology has been improving its theoretical system and application fields, and the scope has been transitioned from ocean remote sensing to land remote sensing. The observation platform has been changed from ground-based or shore-based platform to airborne or satellite-based platform. Among the current satellites in orbit, CYGNSS's (Cyclone Global Navigation Satellite System) eight near-Earth orbit satellites are equipped with radar receivers to receive both direct signals from GPS satellites and reflected signals from the Earth's surface. Analysis of June to August floods in the Dongting Lake area of the Yangtze River basin (28°N-30°N, 112°E-114°E) in the summer of 2020 using CYGNSS . It is found that the surface reflectivity (SR) of the signal is sensitive to the change of water inundation extent, and the SR data can be used to efficiently monitor the flooded area. The results of the CYGNSS study were compared and verified with Sentinel-1A satellite images, and the consistency between them is good. It is confirmed that GNSS-R will be an effective new method for flood monitoring.

Key words CYGNSS; GNSS Reflectometry(GNSS-R); Flood; Surface Reflectivity(SR)

Category: Symposium 4: Positioning and applications => 4.1: Geodetic Remote Sensing

745

S4-042

An alternative MTInSAR framework for deformation retrieval over areas with heavy decorrelation

Lei Zhang、 Hongyu Liang
Tongji University

Decorrelation is inherent in InSAR measurements, which could be raised by changes of ground features and large deformation gradient. It is especially serious in vegetated areas undergoing rapid deformation, degrading the ability of InSAR for geohazards (e.g., landslides and sinkholes) identification. Although phase linking technique is gaining popularity for reducing the decorrelation and thereby improving the density of InSAR measurements in recent years, it is still insufficient to retrieval deformation in heavily decorrelated areas. We propose here an alternative MTInSAR processing framework that can work satisfactorily in such areas. The main innovations of the proposed framework lie in that (1) local correlation serves as a constraint for phase optimization and coherence matrix is no longer needed; (2) Phase ambiguity can be simultaneously resolved during the phase optimization; (3) It has less requirement on the number of interferograms. Several case studies related to the monitoring of tailing dam and natural slopes with Sentinel-1 data demonstrated the performance of the proposed method.

Key words InSAR, Multi-Temporal InSAR

Category: Symposium 4: Positioning and applications => 4.1: Geodetic Remote Sensing

752

S4-043

Spatial-temporal evolutionary behaviors of global ionospheric response to severe storms on 7-8 September 2017 using the GNSS, SWARM, COSMIC and TIE-GCM techniques

Wang Li, Dongsheng Zhao, Kefei Zhang
China University of Mining and Technology

Geomagnetic storms on September 7-8, 2017 triggered severe ionospheric disturbances that had a serious effect on satellite navigation and radio communication. This study utilizes multiple observations derived from Global Navigation Satellite Systems (GNSS) receivers, Earth's Magnetic Field and Environment Explorers (SWARM) and Constellation Observing System for Meteorology, Ionosphere & Climate (COSMIC) to investigate the three-dimensional (3D) ionospheric behaviors under storms. The results indicate that the electron density in the Asia-Australia, Europe-Africa and America sectors suddenly changed with the Bz southward excursion, and the ionosphere in the sunlit hemisphere was more easily to be affected by the disturbed magnetic field. The observations of SWARM and COSMIC demonstrated that the ionospheric perturbations had a remarkable double-peak structure. The magnitude of enhancements in F2 layer was maximum, but the bottom-side disturbances were more sensitive. Besides, Thermosphere-Ionosphere -Electrodynamics General Circulation Model (TIE-GCM) simulations further concluded the storms also triggered significant Polar disturbances that were dependent on geographic position and altitude. The Polar disturbances had a latitudinal excursion associated with the offset of geomagnetic field. The storms also triggered bottom-side enhancements that were only observed in the auroral zone and middle latitudes ($>47.5^\circ\text{N/S}$). Furthermore, the equatorial electrojet, thermospheric density ratio O/N₂ and TIE-GCM are used for explaining the 3D behaviors. A combination of equatorial electrojet and thermospheric composition change may be responsible for the equatorial-middle latitudinal ionospheric perturbations. The enhanced neutral vertical winds and O⁺ increment dominated the topside Polar disturbances, and the bottom-side positive perturbations were controlled by the neutral zonal, meridional winds and O₂⁺ ion density enhancements.

Key words magnetic storms, ionospheric disturbances, thermospheric composition changes, TIE-GCM, hemispheric asymmetry

Category: Symposium 4: Positioning and applications =» 4.1: Geodetic Remote Sensing

770

S4-044

The Study of the Coupling relationship between Land subsidence and Resources and Environmental carrying capacity in Plain area of Beijing

Rui Liu

Shandong University of Science and Technology

Land subsidence is one of the main geological disasters in Beijing plain area, which seriously threatens the ecological environment and human social security. And it brings great pressure to the resources and environment. Groundwater overdraft is the main cause of land subsidence. In this paper, the groundwater index is added to build the evaluation system of resources and environment carrying capacity. The P-S model is used to evaluate the resources and environment carrying capacity of the nine districts in Beijing plain areas, and the coupling relationship between land subsidence and resources and environment carrying capacity is further explored. The results show that: (1) In the six districts of Beijing City, except Haidian District, the carrying capacity of resources and environment in the other five districts is on a downward trend from 2012 to 2019. Haidian District, Tongzhou District and Shunyi District show an upward trend. Daxing District shows a downward trend from 2012 to 2015, and an upward trend from 2016 to 2019. (2) The coupling degree of subsidence area is mostly in antagonistic stage from 2012 to 2019, and the coupling degree decreases with the ground subsidence slowing down, and the coupling degree of non-subsidence area is low. The results of the study can provide a scientific basis for the policy-making of the Beijing Municipal Government.

Key words land subsidence; the resources and environment carrying capacity; P-S model; coupling relationship

Category: Symposium 4: Positioning and applications => 4.1: Geodetic Remote Sensing

778

S4-045

InSAR modeling and deformation estimation for drilling soluble rock salt mine based on CT-PIM function

Xuemin Xing、Xiangbin Liu、Tengfei Zhang、Yikai Zhu、Wei Peng
Changsha University of Science and Technology

Long-term dynamic deformation monitoring of rock salt mines is extremely important in preventing potential geological damages. Building deformation models consistent with reality is a crucial step for time-series deformation monitoring induced by mining activities. However, most InSAR deformation models for mining-induced deformation monitoring are empirical mathematical models, lacking consideration of the underground mining mechanisms. In this paper, the Coordinate-Time (CT) function, which can describe the Dynamic Probability Integral Model (DPIM) for mining area, is introduced into the time-series InSAR deformation modeling. A novel time-series InSAR model, namely InSAR-CTPIM, considering the probability integral prediction parameters, is proposed. The unknown parameters of the model can be estimated based on the InSAR time series phase observations, which can be utilized to generate the time-series deformation for the mining area. Both simulated and real data experiments over Xinhua (a typical rock salt mine in Hunan province, China) have been investigated to assess the feasibility and accuracy of the proposed CT-PIM model. The Root Mean Square Error for the deformation was estimated as ± 13 mm in the simulation compared to the simulated true values. In the real data experiment, 24 Sentinel-1A SAR satellite images were used to estimate the time series subsidence of the rock salt mine, and finally the time series deformation from June 15, 2015 to January 11, 2017 was obtained. The maximum settlement of the mine was estimated as 211 mm, and the RMSE was ± 31 mm compared with external leveling measurements.

Key words Novel deformation model; Time-series deformation; Rheological properties; Environmental factors; Seasonal variation; Soft clay; Highway

Category: Symposium 4: Positioning and applications => 4.1: Geodetic Remote Sensing

791

S4-046

Detection of snow depth on the Tibetan Plateau by satellite-based GNSS-R

Wenxiao Ma^{1,2}、Xuerui Wu^{1,2,3}

1. Shanghai Astronomical Observatory, CAS

2. University of Chinese Academy of Sciences

3. School of Resources, Environment and Architectural Engineering, Chifeng University

Snow cover is a fundamental component of the global energy and water cycle, which is of great importance for regional climate change, water resources utilization and natural disaster monitoring. The Tibetan Plateau is an area with the highest average altitude in the world, rich in snow, glaciers and underground ice resources, known as the "Third Pole of the World" and the "Water Tower of Asia", and is a sensitive area and ecologically fragile area for climate change. The snow cover on the Tibetan Plateau has an impact not only on the atmospheric circulation and weather systems in East Asia, but also on the climate of mainland China. Therefore, the study of snow cover in this area has important hydrological and climatic significance. The field observation time of the former field stations is not continuous, which couldn't meet the need of the study of the distribution characteristics of large area snow cover. Satellite observation is an effective way to monitor snow cover. Visible light depends on sunlight and is heavily influenced by cloud. It can not work in high latitudes and cloudy weather. Passive microwave remote sensing data is one of the main means to monitor the change of snow cover. In recent years, the emerging GNSS-R technology is the combination of navigation technology and remote sensing technology, using the reflected signals of navigation satellites for remote sensing. The results show that the daily time series of surface reflectivity is similar to the snow depth time series. Besides, the sampled data have higher spatial and temporal resolution compared with traditional remote sensing satellites.

Key words CYGNSS; GNSS Reflectometry(GNSS-R); snow depth ; Tibetan Plateau

Category: Symposium 4: Positioning and applications => 4.1: Geodetic Remote Sensing
801
S4-047

The gridded tide corrections of the long-strip differential InSAR measurements estimated using the GPS network and tide models

Wei Peng

Changsha University of Science & Technology

The multi-frame imageries based long-strip interferometric synthetic aperture radar (InSAR) method provides larger spatial-scale interferograms for ground deformation monitoring, and the coastal ground displacements caused by solid Earth tide (SET) and ocean tide loading (OTL) effect reaches decimeters. To evaluate and correct the SET and OTL effect on the long-strip differential interferograms, we proposed a gridded tide correction model that integrates the solid Earth tide model, 1038 continuous GPS sites, global and regional ocean tide models. The gridded tide corrections were tested using the long-strip differential interferograms of 9 Sentinel-1B SLC imageries along the west coast of the United State. The experiment results demonstrated that the SET and OTL effect on the long long-strip differential interferogram can reach 140mm, the error of the grid tide model based on multi-source tide displacements is less than 1mm, and the improvement of the long-strip differential interferograms are more than 40% after tide correction.

Key words InSAR; Ocean tide loading; Solid Earth tide; GPS-PPP

Category: Symposium 4: Positioning and applications => 4.1: Geodetic Remote Sensing

808

S4-048

Based on Sentinel-1A images revealing the co-seismic and post-seismic deformation mechanism of the Ms6.4 Jiashi earthquake in Xinjiang in 2020

Ting Wang、 Chengsheng Yang
Chang'an University

On January 19, 2020, an Ms6.4 earthquake occurred in Jiashi County, Kashgar Prefecture, Xinjiang Province. Prior to this, a series of earthquake warm-up activities occurred in the area, including the Ms5.6 Kuqa earthquake on January 16, 2020, and the Ms5.4 Jiashi foreshock on January 18, 2020. Monitoring and inversion of the coseismic and post-earthquake deformation of the earthquake will help to further understand the geometry of the tectonic belt in this area. In this paper, Sentinel-1A images of the ESA are used to obtain and analyze coseismic and post-earthquake deformation after 449 days. Okada elastic dislocation model were inverted the slip distribution of the coseismic and post-seismic deformation, then two-dimensional slip distribution of coseismic and the time series of the two-dimensional slip distribution of the post-earthquake were obtained, and the slip process on the post-earthquake were analyzed, the post-earthquake deformation mechanism was revealed; Finally, Coulomb stress Change of coseismic deformation and 449d after the earthquake were obtained. Co-seismic deformation fields showed that maximum uplift and subsidence deformations from the ascending tracks were 55mm and 66mm, respectively, maximum uplift and subsidence deformations from the ascending tracks were 73mm and 70mm, respectively. Co-seismic slip distribution showed that this earthquake was a mainly thrust earthquake. The moment magnitude was Mw6.1, the average slip amount was 40mm, and the average slip angle was -152.38° . The post-earthquake deformation showed that the earthquake caused a subsidence near the epicenter. Within 449 days after the earthquake, the subsidence there reached 7cm. The post-earthquake deformation mechanism was mainly after-slip.

Key words Jiashi earthquake, coseismic deformation, post-earthquake deformation mechanism, Coulomb stress, coseismic slip distribution

Category: Symposium 4: Positioning and applications => 4.1: Geodetic Remote Sensing

817

S4-049

The inversion, characterization and assessment of 3-D water vapor using tomography during typhoon weather over Hong Kong

Laga Tong, Kefei Zhang
China University of Mining and Technology

GNSS (Global Navigation Satellite Systems) tomography is a well-recognized technique for the determination of regional atmospheric water vapor that can achieve a high spatial and temporal resolution. This is mainly due to the advantages of GNSS systems since it can be performed in real-time, high precision and all-weather operability. Numerous studies have been carried out utilizing this technology to inverse the three-dimensional distribution of the water vapor under both normal and rain weather conditions. However, the research in using the tomography technique under tropical cyclone weather conditions is very limited. In this study, three-dimensional water vapor field is investigated during six typhoons with different intensities in 2017 over Hong Kong region by the GNSS tomography technique. The vertical profile of the water vapor derived from 3D tomography using ground-based CORS (Continuously Operating Reference Stations) stations was then evaluated by comparing with radiosonde data in HK. It is concluded that the 3D tomographic inversion technique to be effective and useful information can be obtained. Preliminary results showed that, water vapor density was significantly increased during the typhoon and its maximum value was about 25g/m^3 occurs under 1km in altitude and its rate of increase was influenced by the typhoon intensity.

Key words GNSS tomography, 3-D water vapor, typhoon

Category: Symposium 4: Positioning and applications => 4.1: Geodetic Remote Sensing

818

S4-050

Recent activities of the JWG 4.3.4 - Validation of VTEC models for high-precision and high resolution applications

Anna Krypiak-Gregorczyk¹, Attila Komjathy³, Beata Milanowska¹, Wojciech Jarmołowski¹, Paweł Wielgosz¹, Qi Liu⁵, Haixia Lyu⁵, Manuel Hernández-Pajares⁵, Andreas Goss⁷, Eren Erdogan⁷, Michael Schmidt⁷, Mainul Hoque⁹, Gu Shengfeng¹¹, Reza Ghoddousi-Fard¹³, Raul Orus-Perez¹⁴, Bruno Nava², Dieter Bilitza⁴, Tam Dao⁶, Shuanggen Jin⁸, Yunbin Yuan¹⁰, Heather Nicholson¹²

1. University of Warmia and Mazury in Olsztyn, Poland
2. International Centre for Theoretical Physics, Telecommunications/ICT for Development Laboratory (T/ICT4D), Italy
3. NASA - Jet Propulsion Laboratory, USA
4. Department of Physics and Astronomy, GeorgeMason University, USA
5. Universitat Politècnica de Catalunya (UPC-IonSAT), Barcelona, Spain
6. Royal Melbourne Institute of Technology (RMIT) University, Australia
7. German Geodetic Research Institute of the Technical University of Munich (DGFI - TUM), Munich, Germany
8. Nanjing University of Information Science & Technology, China
9. German Aerospace Center (DLR), Germany
10. Chinese Academy of Sciences, Wuhan, China
11. Wuhan University, China
12. University of New Brunswick, Canada
13. Natural Resources Canada
14. European Space Agency (ESA), Noordwijk, the Netherlands

The global and regional ionospheric maps are often used for a wide range of applications in geosciences, in particular to support precise positioning, but also for geophysical and atmospheric studies. There are currently many analysis centers and research groups providing operational and test VTEC maps. However, IGS ACs and other groups use different mathematical models and estimation techniques resulting different resolutions, accuracies and time delays of their products. Therefore, there is a need to compare and validate existing VTEC models.

In this presentation, we present the recent progress of the IAG Joint Working Group (JWG 4.3.4) on validation of VTEC models for high-precision and high resolution applications. Among others, we evaluated (1) the accuracy and consistency of the IAAC GIMs during high and low solar activity periods of the 24th solar cycle, (2) the accuracy the two most popular ionospheric mapping functions - SLM and MSLM, (3) deterministic and stochastic approaches to VTEC modelling, (4) GIMs performance in single point and precise point positioning GNSS applications.

Key words TEC; GIM; ionosphere; GNSS; altimetry; NeQuick

Category: Symposium 4: Positioning and applications => 4.1: Geodetic Remote Sensing
821
S4-051

TropNet: A deep spatio-temporal model for tropospheric parameters forecasting

Yuxin Zheng, Cuixian Lu, Zhilu Wu
School of Geodesy and Geomatics, Wuhan University

Precise forecasting of tropospheric parameters including zenith total delay (ZTD), zenith wet delay (ZWD), zenith hydrostatic delay (ZHD), and tropospheric gradients is essential to weather monitoring as well as GNSS real-time precise positioning. However, due to the changeable and unpredictable atmospheric conditions and lack of fine-resolution meteorological information, precise tropospheric forecasting in a high spatiotemporal resolution remains a challenging task. The numerical forecasting products from NCEP operational Global Forecast System (GFS) are capable of providing estimates for a set of meteorological quantities on a global grid and the Geostationary Operational Environmental Satellite (GOES) - R Series operated with a low time latency can offer meteorological observations of high spatiotemporal resolution. Therefore, the fusion of the GFS products and GOES-R observations provides a promising opportunity to enhance high-resolution tropospheric parameters forecasting. In this study, we formulate tropospheric parameters forecasting as a spatiotemporal sequence forecasting problem and propose a deep spatio-temporal model (TropNet) based on the method of deep learning to tackle this problem. The TropNet is based on an encoding-forecasting framework, which consists of an encoder for learning feature representation and five forecasters for predicting multiple outputs including ZTD, ZWD, ZHD, North and East tropospheric gradients. Specifically, the encoder is constituted by stacking multiple convolutional long short-term memory (ConvLSTM) layers to aggregate spatio-temporal information from GFS products and GOES-R observations. This model forecasts tropospheric parameters up to 6 hours at a high spatial resolution of 2 km and a temporal resolution of 1 hour. The performance of TropNet is evaluated and validated with GNSS tropospheric products. In addition, this model is also promising for general spatiotemporal sequence forecasting problems.

Key words GNSS, tropospheric parameters forecasting, deep learning, encoding-forecasting framework, GFS, GOES-R

Category: Symposium 4: Positioning and applications => 4.1: Geodetic Remote Sensing

831

S4-052

Current status of the IAG working group 4.3.7 on geodetic GNSS-R

Sajad Tabibi¹、Felipe Geremia-Nievinski⁴、Nikolaos Antonoglou^{7,21}、Karen Boniface¹²、Estel Cardellach¹⁴、Clara Chew¹⁷、Rüdiger Haas¹⁹、Thomas Hobiger²、Chung-Yen Kuo⁵、Kristine Larson⁸、Wei Liu¹⁰、Manuel Martín-Neira¹³、Jihye Park¹⁵、Dave Purnell¹⁸、Joerg Reinking²⁰、Ole Roggenbuck²⁰、Maximilian Semmling³、Rashmi Shah⁶、Kegen Yu⁹、Jens Wickert^{11,22}、Simon Williams¹⁶

1. University of Luxembourg
2. University of Stuttgart, Germany
3. German Aerospace Center, Germany
4. Federal University of Rio Grande do Sul, Brazil
5. National Cheng Kung University, Taiwan
6. Jet Propulsion Laboratory, USA
7. German Research Centre for Geosciences GFZ, Germany;
8. University of Colorado, USA
9. China University of Mining and Technology, China
10. Shanghai Maritime University, China
11. German Research Centre for Geosciences GFZ, Germany
12. European Commission, , Joint Research Centre, Italy
13. European Space Agency, Netherlands
14. Institute of Space Sciences (ICE-CSIC, IEEC), Spain
15. Oregon State University, USA
16. National Oceanography Centre, UK
17. National Center for Atmospheric Research, USA
18. McGill University, Canada
19. Chalmers University of Technology, Sweden
20. Jade University of Applied Sciences, Germany
21. University of Potsdam, Germany
22. Technical University of Berlin, Germany

The reflected radio signals of opportunity at L-band broadcasted by Global Navigation Satellite Systems (GNSS) have been used for ground-based sea level studies at several locations in recent years. The geodetic GNSS-R working group 4.3.7 of the International Association of Geodesy (IAG) with 21 members, is a part of Sub-Commission 4.3 Atmosphere Remote Sensing under the IAG Commission 4 on positioning and applications. The main objective of the working group is to further demonstrate and consolidate the value of GNSS-R for the geodesy, oceanography, cryosphere, and hydrology communities. The first inter-comparison campaign on SNR (signal-to-noise ratio)-based GNSS-R for sea level monitoring was established in the IAG period 2015 – 2019 under the JWG (Joint Working Group) 4.3.9 using the Onsala GNSS-R tide gauge station. The second inter-comparison campaign on geodetic GNSS-R with eight research groups was launched in July 2020 to address further the impacts of large tidal range and multi-GNSS revisit

time on tidal constituents on GNSS-R sea level retrievals. Data from two different GNSS stations with 5-m and 9-m tidal ranges with 10-m and 8.5-m reflector heights in the Netherlands and France were provided to all research groups. In addition, the processing settings were also provided to the eight groups to have comparable observation conditions in all processing centers. Five groups submitted their solutions for the inter-comparison campaign, but three groups have withdrawn their submissions at their discretion. Here, we present results of two different GNSS-R sea level solutions (GPS-L1-C/A; combined GPS-L1-C/A and GLONASS-R1-C/A) that are compared to tide gauge records 2-m from the GNSS antennas. Investigation of external corrections to the sea level solutions such as atmospheric effects is planned for the future activity of the geodetic GNSS-R working group.

Key words GPS; GLONASS; GNSS-R; Reflectometry; Geodetic GNSS-R; Sea Level; Altimetry

Category: Symposium 4: Positioning and applications => 4.1: Geodetic Remote Sensing

832

S4-053

Multi-mode multi-frequency GNSS-IR combination method for water level retrieval

Xiaolei Wang、 Xiufeng He
Hohai University

Accurate water level monitoring is important for water resource regulation and disaster monitoring. With the development of Global Navigation Satellite System (GNSS), multipath effect, which was once considered as an error source, has been found able to monitor water level. Gradually, it developed into a water level retrieval technology named GNSS-Interferometry Reflectometry (GNSS-IR). Currently, the multi-mode multi-frequency signals of GPS, GLONASS, Galileo and Beidou have all been demonstrated can used for GNSS-IR water level retrieval. However, the multi-GNSS retrievals introduce a new question that is how to combine the multi-mode multi-frequency GNSS-IR sea level retrievals. So, we developed a multi-GNSS combination algorithm to formulate a 10-min sea level time series based on an altimetry observation equation set. Data of 9 sites in different environment such as calm water, tidal water and water in storm surge were used. Results of multi-GNSS combined retrievals shown an approximately 50% accuracy improvement compared to individual signal sea level retrievals; and it can even achieve mm-level monitoring accuracy for calm water. In addition, if a state-transition equation is established, the altimetry observation equations can be solved by Kalman filtering method; results of Kalman filtering retrievals can further improve the retrieval accuracy and realize near real-time water level monitoring.

Key words Remote sensing; GNSS-IR; water level retrieval; multi-mode multi-frequency combination

Category: Symposium 4: Positioning and applications => 4.1: Geodetic Remote Sensing

841

S4-054

Land subsidence monitoring in Tongzhou and Three Northern Counties of Langfang based on time series InSAR Technology

Sun GuangTong
Institute of Disaster Prevention
Liaoning Technical University

After the relocation of Beijing Administrative Center, it is of great significance to further promote the coordinated development of Tongzhou District and Three Northern Counties of Langfang for the construction of Beijing Sub Center. But for a long time, due to the over exploitation of groundwater and other reasons, Beijing-Tianjin-Hebei region has developed into one of the most serious areas of land subsidence in China, and the situation of land subsidence in Tongzhou and Three Northern Counties of Langfang is more severe. Land subsidence can cause a series of problems, such as subgrade subsidence, bridge deformation, pipeline fracture and so on, which directly threaten the safety of people's lives and property. Traditional survey methods, such as leveling and GPS survey, have high precision, but it is difficult to form a high-density survey control network. In this paper, time series InSAR technology is used. By processing the stable points with high coherence in time series, it overcomes the influence of temporal and spatial incoherence of traditional InSAR technology, weakens the error components caused by atmospheric delay, achieves millimeter level monitoring accuracy, and achieves the purpose of large-scale and high-precision monitoring. Based on the sentinel-1a satellite data of 20 scenes covering Tongzhou District and Three Northern Counties of Langfang from April 16, 2019 to April 22, 2020, this paper uses time series InSAR technology to carry out time series inversion on the settlement distribution of the study area, and obtains the average settlement rate map and cumulative settlement map of the study area, The inversion results, the development of land subsidence and the causes of land subsidence are analyzed. The results can be used for early warning and assessment of regional disasters, and provide help for regional sustainable planning and development in the future.

Key words Land Subsidence; Time Series InSAR; Tongzhou and Three Northern Counties of Langfang

Category: Symposium 4: Positioning and applications => 4.1: Geodetic Remote Sensing

849

S4-055

Research on segmented fitting ranging model based on multiple filter

Wang Minmin、Deng Yang、Jian Wang
Beijing University of Civil Engineering and Architecture

In the process of Low Power Bluetooth (BLE) indoor positioning, the path loss exponent is greatly affected by the complex indoor environment. Aiming at the problem of BLE signal instability and low ranging accuracy, an RSS segmented fitting ranging model based on multiple filter method is proposed in this paper. Firstly, using BLE of different wireless standards, the experimenters collect 30 groups of RSS every 0.3m, and compared the RSS values of the same distances. Then, the RSS value is optimized based on Gaussian-median-mean filter, and this method can reduce the influence of outliers. Last, on this foundation, according to the distance, the experimental scene is divided into several parts, and the path loss exponent of different distance regions are fitted and calculated respectively. Distance is taken as unknown variable, least square (LS) estimates the path loss exponent, and this paper propose a segmented fitting ranging model method. The experimental results show that different wireless standards receive different RSS in the same environment, and the segmented fitting method proposed in this paper has high flexibility and high ranging accuracy compared with the traditional methods.

Key words BLE; the path loss exponent; RSS

Category: Symposium 4: Positioning and applications => 4.1: Geodetic Remote Sensing
851
S4-056

Analysis of the BDGIM Performance in BDS Single Point Positioning

Guangxing Wang¹、Zhihao Yin¹、Zhigang Hu²、Yadong Bo¹
1. China University Geosciences, Wuhan
2. Wuhan University

The broadcast ionospheric model is mainly used to correct ionospheric delay error for single-frequency users. Considering that the BDGIM is a novel broadcast ionospheric model for BDS-3, this study adopted single point positioning (SPP) to analyze the positioning performance of the model. Twenty-two IGS/iGMAS stations that can simultaneously receive B1C, B2a, B1I and B3I signals were selected for the SPP experiments. The DCB parameters were used to correct the hardware delays in the signals of B1C and B2a. The results showed that the BDGIM performs the best in high-latitude areas, and can effectively improve the positioning accuracy compared with the Klobuchar model. The average 3D positioning accuracy of the four civil signals can reach 3.58 m in high-latitude areas. The positioning accuracies with the BDGIM in the northern hemisphere are better than those in the southern hemisphere, and the global average 3D positioning accuracy of the four civil signals is 4.60 m. The positioning performance of the BDGIM also shows some seasonal differences. The BDGIM performs better than the Klobuchar model on the days of spring equinox and winter solstice, while the opposite is true on the days of summer solstice and autumn equinox. On the day of winter solstice, the average 3D accuracies with the BDGIM on the signals of B1C, B2a, B1I and B3I are 4.13m, 5.32m, 4.40m and 4.49m, respectively. Although the SPP accuracies are to some extent affected by the geomagnetic storm, the BDGIM generally performs better and are more resistant to the geomagnetic storm than the Klobuchar model.

Key words BDS; BDGIM; Klobuchar; Single point positioning (SPP); Differential Code Bias (DCB)

Category: Symposium 4: Positioning and applications => 4.1: Geodetic Remote Sensing
853
S4-057

Landslide Detection and Segmentation Using Mask R-CNN with Simulated Hard Samples

WanDong Jiang、 JiangBo Xi、 XinYu Dou、 LiGong Yang
Chang'an University

With the advance in artificial intelligence, the use of high-resolution imagery to identify geological hazards has gradually become a research hotspot. Visual interpretation of landslides heavily relies on expert experience and conventional automatic landslide detection approaches are sensitive to the presence of bare land, roads and other ground objects, and hence a Mask R-CNN with simulated hard samples is presented in this paper for landslide detection and segmentation. The background areas of landslides are extended, and then hard landslide samples are simulated by combing the shapes, colors, textures, and other characteristics of landslides. Finally, the original imagery and simulated hard samples are fed into the Mask R-CNN for landslide detection and segmentation. Since the number of landslides is often limited in reality, small sample learning in the frequency domain is also presented in this paper to reduce the input data, and ensure the accuracy of detection and segmentation. The application to Bijie landslide, Guizhou Province, shows that the detection and the average pixel segmentation accuracies of the proposed Mask R-CNN method with simulated hard samples are as high as 94.0% and 90.3%, respectively. It shows that the proposed method has high performance on landslide detection and segmentation with low false alarm rates. In addition, the performance of the proposed small-sample-based learning method in frequency domain can be improved even with a half of the data input. Finally, the effectiveness of the proposed Mask R-CNN method is further proved by the successful detection of TianShui landslides in Gansu Province.

Key words Deep learning; Landslide detection; Mask R-CNN; Hard samples; Frequency domain

Category: Symposium 4: Positioning and applications => 4.1: Geodetic Remote Sensing

883

S4-058

Feasibility of GNSS-R Altimetry Using CyGNSS 8-Satellite Constellation Mission Data

C K Shum ^{1,2*}, Yuchan Yi ¹, Weiqiang Li ³, Yihang Ding ¹, Haibo Ge ⁴, Maorong Ge ⁵, Yu Zhang ¹, Chungyen Kuo ⁶, Chi-Ming Lee ⁶, Estel Cardellach ³, Yuanyuan Jia ¹, Yixin Xiao ¹, Xiaochun Wang ⁷

1. School of Earth Sciences, The Ohio State University, Columbus, Ohio, USA

2. Innovation Academy for Precision Measurement Science and Technology, Chinese Academy of Sciences, Wuhan, China

3. Institut de Ciències de l'Espai (ICE-CSIC/IEEC), Barcelona, Spain

4. College of Surveying and Geo-Informatics, Tongji University, Shanghai, China

5. Deutsches GeoForschungs Zentrum GFZ, Helmholtz Zentrum Potsdam, Germany

6. Department of Geomatics, National Cheng Kung University, Tainan, Taiwan

7. Joint Institute for Regional Earth System Science and Engineering, University of California at Los Angeles, California, USA

NASA's Cyclone Global Navigation Satellite System (CyGNSS) 8-satellite constellation mission has the primary objectives to quantify wind fields with improved temporal and spatial sampling during the evolution of Tropical Cyclones (TC) and measure all-weather wind speed within the eyes of the cyclones, to enhance the understanding of physics and mechanisms governing TC towards improving cyclone forecasting. Here, we conduct feasibility studies with the goal to exploit CyGNSS single-frequency bistatic radar, or GNSS-Reflectometry (GNSS-R), to enable interferometric phase altimetry (Level 0 raw Intermediate Frequency data), and code range (group delay) altimetry (Level 1 DDM or Delay-Doppler Maps, waveform retracked data), for ocean and lake altimetry. Precision orbit determination (POD) methodologies are developed using GPS L1 C/A (pseudorange) data, incorporating 2-layer ionosphere, troposphere corrections, and other geophysical corrections, to improve the CYGNSS 8-constellation constellation radial orbit accuracy for altimetry application. We present results using the CYGNSS GNSS-R grazing angle phase altimetry and the DDM derived code range altimetry over lakes and underneath hurricane passes in the Gulf of Mexico during the Atlantic hurricane seasons in 2019 and 2020. The retrieved GNSS-R altimetry are compared with available *in situ* tide gauge water/sea-level, and with *in situ* GNSS-R SNR retrieved sea-level altimetry.

Acknowledgements. This research is supported by National Aeronautics and Space Administration CyGNSS Program Grant No. 80NSSC18K0703.

Key words CyGNSS, GNSS-R SNR altimetry, Phase altimetry, Code range altimetry, Bistatic radar, Hurricanes

Category: Symposium 4: Positioning and applications => 4.1: Geodetic Remote Sensing

890

S4-059

GNSS-R monitoring of St. John river water levels: implementation and first results

Alexander Turner¹, Marcelo Santos¹, Thalia Nikolaidou¹, Felipe Nievinski²

1. University of New Brunswick

2. Federal University of Rio Grande do Sul

Like many provinces in Canada, New Brunswick suffers from property damage by yearly spring floods due the fast thawing of winter snow and ice. Water levels are currently monitored by a sparse network of water level gauges. To increase the spatial coverage with a comparable accuracy and decrease in total cost of ownership (including installation and maintenance), we are testing the feasibility of water level monitoring using GNSS-R stations. For that purpose, we have assembled a GNSS-R unit and installed it on the roof of the New Brunswick Art Gallery overlooking a portion of St. John river in Fredericton, the capital city of New Brunswick, which is highly impacted by yearly floods. This unit started operating in January of this year (2021). In this poster we will describe the characteristics of the GNSS-R unit and discuss the early data collection.

Key words GNSS-R, Reflectometry, Natural Disaster, Societal Impact

Symposium 4: Positioning and applications

S4.2: Next Generation Positioning

Category: Symposium 4: Positioning and applications => 4.2: Next Generation Positioning

75

S4-060

Kinematic determination of state-space representation corrections for unified RTK and PPP-RTK solutions

Yanming Feng, Wenzong Gao
Queensland University of Technology

GNSS real time kinematic (RTK) and precise point positioning (PPP)-RTK solutions are derived with observation-space representation (OSR) and state-space representation (SSR) messages, respectively. However, the current OSR and SSR algorithms do not theoretically result in consistency between RTK and PPP-RTK state solutions. This paper presents a single-receiver computing approach to the generation of SSR corrections for satellite-specific uncalibrated hardware delays (UHD) in GNSS code and phase signals as well as ionosphere- and troposphere-delays. These SSR corrections are determined with respect to a set of given GNSS orbits and clocks and based on geometry-free and ionosphere-free combinations. As a result, the computing can be easily implemented within a receiver hardware processor. Theoretically, the single-epoch phase UHDs, ionosphere-delays, and troposphere are determined to the precision of phase observables, while the single-epoch code UHD solutions are to the precision of code measurements. Mathematically, applying the single-epoch SSR corrections to calibrating the same delays in the user observations will result in double-differenced (DD) equations for RTK processing. Applying the fitted SSR corrections to the user observation will result in single differenced (SD) observation equations for PPP-RTK treatments. Inter-receiver code-offsets can also be determined with respect to a reference receiver and should be calibrated for user code observation equations. Numerical analysis confirmed the precision of code and phase UHD solutions and their consistence from different stations. RTK results from three baselines preliminarily show SSR calibration and inter-receiver code-offsets directly improve the RTK state solutions from code measurements, thus improving the ambiguity resolution. Overall, the new SSR approach unifies RTK and PPP-RTK services with the SSR corrections and improves the positioning performance to a certain extend.

Key words GNSS, space state representation corrections (SSR), uncalibrated hardware delays, Real Time Kinematic positioning

Category: Symposium 4: Positioning and applications => 4.2: Next Generation Positioning

132

S4-061

Multipath Characterization using Ray-Tracing in Urban Trenches

Lucy Icking, Fabian Ruwisch, Steffen Schön
Institut für Erdmessung, Leibniz Universität Hannover

Multipath in urban environments still represents a great challenge for Global Navigation Satellite System (GNSS) positioning as it is a degrading factor which limits the attainable accuracy, precision and integrity. In an urban trench, the dense building structures in the vicinity of the antenna cause reflections of the satellite rays resulting in multipath errors. Various work has been presented for simulating reflections for stations under laboratory conditions, yet the simulative analysis of multipath propagation in urban environments is still missing. In this contribution, we enhanced an existing ray-tracing algorithm which identifies potentially multipath affected satellite signals. So far, it calculates reflection points on a plane ground and estimates the resulting multipath error. We extended it for the urban area case by introducing a 3D city building model with possible reflections on all surfaces of the buildings. Based on the geometry between the antenna position, satellite position and the reflection surface, the extra path delays, the characteristics of the propagation channel and the signal amplitudes are calculated. The resulting multipath errors are then estimated from the discriminator function using state of the art correlator parameters and antenna models. In a second step, the simulation results are validated. We conducted real world GNSS measurements using parked cars in dense urban areas. Different approaches of combining observations (multipath linear combination, code-minus-carrier combination, double difference processing) for determining the multipath error are compared. Finally, the empirically derived multipath errors are evaluated with the multipath errors from our simulation tool.

Key words GNSS, multipath, ray-tracing, urban navigation

Category: Symposium 4: Positioning and applications => 4.2: Next Generation Positioning
305
S4-062

VISION BASED NAVIGATION IN INDOOR ENVIRONMENT: EVALUATION OF PERFORMANCE USING SMARTPHONE SENSOR

Fickrie Muhammad^{1,2}, Reiner Jäger²

1. Hydrography Research Group, Faculty of Earth Sciences and Technology, Bandung Institute of Technology, Indonesia
2. Laboratory for GNSS and Navigation, Faculty of Information Management and Media, Hochschule Karlsruhe, Germany

Robot navigation in an unknown environment usually implements GNSS positioning techniques. As the robot travels in an Indoor environment some signal interruption may occur such as multipath that leads to positioning accuracy degradation or even position loss. The vision-based navigation (VbN) offers a beneficial solution for robot (body) positioning in indoor environment or GNSS-denied area where GNSS-based navigation can no longer be used. VbN algorithm focuses on the robustness of feature (object) tracking and camera (robot) positioning using an existing Visual Odometry (VO) method, which is based on Simultaneous Localization and Mapping (SLAM) algorithm. In estimating 3D robot position, a quasi-continuous structure from motion (SfM) that estimates 2D points position from 3D space with transformation function from previously tracked feature points was used in SLAM.

In this research, the navigation solution with VbN system's setting for indoor environments is evaluated. The system's setting was running with a compact 27 mm lens from a standard smartphone camera. In order to publish image output to consumer laptop, a connection via wireless streaming was used and able to capture circa 10 – 20 frames per second. A fiducial marker-based system with millimeters accuracy of reprojection error was used as a trajectory's true value (ground truth). To analyze the accuracy, comparison between marker and VO trajectories has been transformed to a common coordinate system with least-squared method. Our small-scale experiments showed that the VbN system with a standard smartphone camera can do the navigation task with centimeters accuracy. However, the wireless stream connection often leads to delaying image output that can cause increasing CPU load and position loss.

Key words Indoor navigation, Vision-based Navigation, Visual Odometry, SLAM

Category: Symposium 4: Positioning and applications => 4.2: Next Generation Positioning

338

S4-063

Analysis of BDS Two-way Time Synchronization

Bin Wang¹、Jie Cui^{2,1}、Junping Chen^{1,2,4}、Binghao Wang³

1. Shanghai Astronomical Observatory, Chinese Academy of Sciences

2. School of Astronomy and Space Science, University of Chinese Academy of Sciences

3. Beijing Navigation Center

4. Shanghai Key Laboratory of Space Navigation and Positioning Techniques

Time synchronization is of vital importance for GNSSs. GNSSs are based on strict time-keeping system, and excellent atomic clocks are onboard the GNSS satellites, as well as in the stations of ground monitoring network. Clock measurement, estimation and predictions are the important work of GNSS ground control segment. Traditionally, orbit determination and time synchronization (ODTS) are used for the time synchronization of the GNSS, such as GPS, GLONASS and Galileo.

But this is different for BDS. In order to make up the disadvantage of limited satellite-tracking ability of regional monitoring stations network, and also to get the precise satellite clock offsets, the independent time synchronization system of BDS is established. In this system, two way time transfer (TWTT) techniques such as L-band two-way radio time transfer (TWTT), C-band two-way satellite time and frequency transfer (TWSTFT), and Ka-band inter-satellite link (ISL) two-way time transfer are used.

Two-way time transfer of BDS provides another method for the time synchronization of GNSS. For each time-comparison link, there is also a parallel ODTS link available. The TWTT and ODTS links are redundant to each other. For ODTS, radial orbit errors and the clock parameters are highly correlated, and these errors are also visible as a bump in the allan deviation (ADEV) of the GNSS satellite clocks at the orbital frequency. TWTT provides the opportunity of performance evaluation of BDS satellite clock in orbit and the monitoring of ODTS orbit error, and it can be valuable for the orbital dynamics model refinement. Considering that TWTT apparent clocks is less affected by the satellite orbit errors, some periodic variations of L-band clocks is actually the variation of L-band orbits.

Through the comparison of two types of satellite clocks respectively estimated by TWTT and ODTS method, we analyze the unique time synchronization system of BDS from three aspects, time synchronization between stations, between satellites and ground, and between satellites. The separation of time-comparison-link noise from the apparent clock is performed using three-cornered hat method, and we obtain the near-true

performance of BDS satellite clock on orbit, which lay the foundation for high-precision satellite-ground time transfer and the refinement of orbital dynamics models.

Key words Beidou navigation satellite system; two-way radio time transfer; two-way satellite time and frequency transfer; inter-satellite link

Category: Symposium 4: Positioning and applications => 4.2: Next Generation Positioning

369

S4-064

Investigation of the informativeness of the gravity field for indoor navigation

Dmitry Bobrov
FSUE VNIIFTRI

Existing navigation systems based on the use of GNSS signals are not always capable to provide high-precision positioning of the consumer in conditions of dense urban development and indoors. One of the possible ways to solve the problem of consumer navigation under the above conditions is to use the derivatives of the gravitational potential - the values of the free fall acceleration (FFA) and gravity gradients (GG). Such fields are stable over time and are not affected by interference.

The article discusses the variability of the FFA and GG fields using the example of mathematical modeling of the distribution of their parameters within a typical three-story building. The estimation of the mathematical modeling uncertainty is calculated from the results of experimental measurements inside a room with known parameters. The assessment of the navigation information content of the FFA and GG fields was carried out according to the obtained results. Preliminary requirements were formed for the set and parameters of the consumer equipment for indoor navigation with an uncertainty no more than 1 m.

Additionally, studies of the navigation information content of the FFA and GG fields were carried out using the example of mathematical modeling of the distribution of their parameters along a city street with typical buildings.

Key words gravity, gravity gradients, indoor navigation

Category: Symposium 4: Positioning and applications => 4.2: Next Generation Positioning

407

S4-065

Fusion of GNSS/INS and Maps for lane-level vehicle navigation

Emerson Cavalheri, Marcelo Santos
University of New Brunswick

In this work, we present a GNSS/INS with Maps of the road integration to provide robust lane-level vehicle navigation. Current lane-level navigation algorithms are mostly relying on imagery technology, prone to failures in extremely bright or dark environments, or using learning algorithms that can be limited to the area of the trained data. The main problem we try to solve is to accurately track vehicle position on its lane of navigation in any environment, for this, a common approach is to use a GNSS/INS sensor fusion. These two sensors have a complementary nature and can provide accurate solutions anywhere on the Earth's surface. However, during long GNSS outages, INS alone cannot offer a reliable solution due to its inherent errors. We solve this limitation by providing a third piece of information, a map of the lanes. These data are combined on a TC GNSS/INS and loosely coupled (LC) INS/MAP and it was tested on a challenging urban environment. In comparisons with a Precise Point Positioning (PPP) and a tightly coupled (TC) GNSS/INS, the proposed architecture was able to maintain solutions within the correct trajectory in several situations such as driving under a walking bridge, underpasses, and streets with tall buildings, where GNSS signals were lost for as long as 20 seconds. The proposed filter had an increase in solution availability of 12% over PPP. The average solution bounds, with 95% confidence, were 3 and 1 cm. Signal multipath seems to be a major issue that can be misleading inform a good GNSS and confuse the map matching and subsequent LC+MAP integration. Another challenge is to provide reliable velocity information, which by relying on GNSS can be, again, misleading during multipath environment and it can disrupt the ability of LC+MAP to maintain a correct velocity estimation. Due to these challenges, LC+MAP had an average of 45 cm in along-track for the whole experiment. PPP and TC GNSS/INS achieved 17cm and 63 cm in along-tracks, respectively.

Key words Sensor fusion, GNSS/INS, Map of lanes

Category: Symposium 4: Positioning and applications => 4.2: Next Generation Positioning

458

S4-066

Robust constrained Kalman filter with GNSS/INS vehicle tightly coupled navigation application

Meng Zhang、 Cheng Yang、 Yan Liu、 Xingyu Long
China University of Geosciences (Beijing)

This paper proposed a constrained method to improve the robustness of the GNSS/INS tightly integrated navigation system by using a fixed distance between the antennas. A robust constraint target function of Kalman filter is proposed. The IGGIII robust model is applied to reduce the influence of the observation outliers. The proposed method is resistant to GNSS outliers, and has less affected by random errors of GNSS. The field test is carried out to verify to proposed method. The results indicate the constraint Kalman filter improved the positioning accuracy by 13% compared with that of conventional Kalman filter. The robust constraint Kalman filter further improved the positioning accuracy by 6% by reducing the influences of GNSS outliers.

Key words GNSS/INS, constrained, robust, tightly integrated navigation

Category: Symposium 4: Positioning and applications => 4.2: Next Generation Positioning

516

S4-067

GNSS positioning accuracy of smartphones and sports watches

Piotr Patynowski, Marcin Mikoś, Krzysztof Sośnica, Kamil Kaźmierski
Wrocław University of Environmental and Life Sciences

The continuous development of technology and the needs of users have contributed to the miniaturization of everyday objects. Until recently, it was hard to imagine a cell phone or a sports watch being able to determine the user's position using Global Navigation Satellite Systems. Thanks to tremendous progress, the number of widely available positioning devices is constantly growing. Low-budget GNSS signal receivers are successfully used, for example, in navigation, in rescuing services, or in sports training. With the proper computational strategy and the provision of convenient measurement conditions, low-cost devices provide the user location with meter-level accuracy.

In this work, two types of low-cost devices were evaluated in the context of their positioning accuracy: mobile devices - Samsung Galaxy Note 10, Huawei Mate 30 PRO, Xiaomi mi 8, Huawei P10, and sports watches - Polar M430, Polar V800, Suunto Ambit2, Suunto Ambit3, Garmin Forerunner 610, Garmin Forerunner 310XT, Garmin Forerunner 735XT, Garmin Vivoactive 3 Music. The obtained results for all tested low-cost receivers are compared with reference GNSS RTK position computed based on the observations stored by the professional geodetic devices.

The best results in the case of smartphones are obtained for Huawei Mate 30 PRO and Xiaomi Mi 8, for which the position accuracy oscillate between 0.50 - 1.00 m for 5h static absolute positioning sessions. In terms of the sports watches, the best results are obtained for Polar M430, Garmin Forerunner 735XT, and Garmin Vivoactive 3 Music, where about 50% of the value of linear deviations obtained on the test route was within 1 m. Additionally, some hardware delays are observed, which may be connected with the time needed to calculate and obtain a smoothed position by sports watches.

Key words GNSS positioning, Smartphones, Sports watches

Category: Symposium 4: Positioning and applications => 4.2: Next Generation Positioning
600
S4-068

Facial Feature Recognition Based on Deep Neural Network

Yihan Yang, Wei Sun
Liaoning Technical University

Facial feature recognition, as an important part of biometrics technology, has become a research hotspot in various industries in recent years. In order to improve the accuracy of facial feature recognition, a method of facial feature recognition based on deep convolutional neural network was proposed. In view of the interference of noise and light on the image to be recognized, BEEMD noise reduction method and Retinex image brightness enhancement method were proposed in order to provide clear and distinguishable facial feature information for facial feature recognition. In addition, the principle of face detection method in facial feature recognition was studied and the framework of multi-task convolutional neural network algorithm was used to detect facial features. At the same time, the principle and method of face recognition were studied, and the FaceNet algorithm was used to recognize the features of the detected facial images. The experimental results of image preprocessing showed that the BEEMD method can effectively reduce image noise, the Retinex method effectively improved the brightness of darker image, and the image after preprocessing was used for facial feature recognition, multi angle and multi hole facial feature recognition experimental results showed that the proposed method could effectively improve the accuracy and reliability of facial feature recognition.

Key words BEEMD image denoising; Retinex brightness enhancement; Multi-task convolutional neural network; FaceNet facial feature recognition

Category: Symposium 4: Positioning and applications => 4.2: Next Generation Positioning

629

S4-069

A cloud platform and hybrid positioning method for Indoor location service

Jinzhong Bei、 Dehai Li

Chinese Academic of Surveying and Mapping

In order to deal with the discontinuity and deficient availability of indoor positioning, a private cloud platform of location service was built in this paper, and a hybrid positioning technology was realized. In this platform, dynamic deployment, elastic computing, and on-demand cloud computing services was implemented by the hardware resource virtualization. The limits in large users online service and data communication were overcome by utilizing microservices management and its cloud-push-service component. In the hybrid cloud positioning, a method of beacon node correction and autonomous trajectory estimation was proposed. This method could improve continuity and usability of indoor positioning, and reach a positioning accuracy of 2 m approximately. At last, by integrating indoor map and hybrid indoor positioning, the cloud software and terminal application had been developed for public location service.

Key words cloud platform; indoor hybrid positioning; beacon node correction; autonomous trajectory estimation; location service

Category: Symposium 4: Positioning and applications => 4.2: Next Generation Positioning

650

S4-070

Geomatics and Soft Computing techniques for road infrastructure monitoring: a case study

Antonino Fotia, Vincenzo Barrile
Mediterranea University

In the context of the monitoring and control of the Italian transport infrastructure heritage, both in terms of existing network and infrastructure works, an experiment has been developed that combines geomatic and soft computing techniques in order to produce a system aimed at the one hand at solving Early Warning problems, and on the other able to generate a forecasting system on the infrastructure's behavior over time, mainly exploiting geomatics parameters.

The proposed integrated/early warning predictive system is based on the initial realization and integration of multiple models (geometric/structural) representative of the object of study (infrastructure) necessary for training and subsequently in the implementation of a neural network that requires in input only displacements, which can be acquired from the "sensors" positioned on the infrastructure to produce different hazard levels. Particular attention has been paid to the displacement measurement phase by GPS (Global Position System) signal.

The experimentation of the proposed integrated predictive system was carried out on the Viaduct "Annunziata" in Reggio Calabria (Southern Italy), already used as a case study in the context of other research activities conducted by the Geomatics laboratory of DICEAM (Civil, Energetic, Environmental and Material Engineering Department - Mediterranean University of Reggio Calabria).

Key words Monitoring, Sensors, GPS, Neural Network

Category: Symposium 4: Positioning and applications => 4.2: Next Generation Positioning
651
S4-071

A 3D map based place recognition solution for underground positioning using laser scanning

Liu Jingbin、Dong Xu、Yifan Liang、Hongyu Qiu
a State Key Laboratory of Information Engineering in Surveying, Mapping and
Remote Sensing, Wuhan University,

Underground positioning is a challenging topic as GNSS is not available, and one of potential solutions is 3D map based global localization using laser scanning. Place recognition is a critical procedure for 3D map based global localization, which provides an initial position for fine registration. However, the existing LiDAR based place recognition solutions are not robust under the changed viewpoint conditions. In addition, different types of LiDAR sensors cannot be used directly for 3D map creation and online query localization with the existing place recognition solutions. This paper presented a 3D map based place recognition solution, which allows for the use of different types of LiDAR in the processes of 3D map generation and localization, to provides initial position for underground positioning. At first, a novel multiple scale spin image (MSSI) descriptor with rotation-invariance feature and high descriptive for place recognition is generated. To resolve the difficulty that the applicability of existing methods as it is of high probability that different types of sensors are used in mapping and localization processes, the 3D artificial technology generating synthetic point cloud is presented subsequently. Finally, we integrated MSSI descriptor and 3D artificial technology into the proposed solution. The proposed MSSI descriptor and solution were evaluated using several popular benchmark datasets and our own dataset. Comprehensive experiments demonstrated that the MSSI descriptor have higher descriptiveness, and is robust to the changed viewpoint scenes, which are shown by the comparison of PR curve using datasets of multiple scenes. The proposed place recognition solution has high success rates of up to 100% in the evaluation. Therefore, the results show that it is feasible to achieve robust place recognition using 3D map under GNSS-denied and bad-light spaces. In future work, the approach of global localization will be developed based our result of place recognition.

Key words place recognition, 3D map, underground positioning, laser scanning.

Category: Symposium 4: Positioning and applications => 4.2: Next Generation Positioning

756

S4-072

A State-Domain Robust Fault Detection Algorithm for GNSS/INS Integration Positioning

Zhangjun Yu, Qiuzhao Zhang, Nanshan zheng
China University of Mining and Technology

Aiming at the abrupt fault in GNSS/INS integrated system in complex environment, classical fault detection algorithms are mostly developed from the measurement domain. A robust fault detection algorithm based on the state domain is proposed in this paper. The fault detection statistic is built based on the difference between prior state estimation and posterior state estimation in Kalman filtering. To improve the calculation stability, singular value decomposition (SVD) is used to factor the covariance matrix of the difference. The relevant formulas of the proposed method were theoretically derived, and the relationship between the proposed method and the existing innovation chi-square test method was revealed. Theoretical derivation proves that the proposed method is equivalent to the innovation chi-square test method when the state dimension and measurement dimension are equal. The proposed method was compared with the innovation chi-square test method and verified by GNSS/INS integration positioning experiments using simulation data and real data. In the simulation experiment, some abrupt faults were artificially added to the measurements of three different time instants. In the real data experiment, abrupt faults were simulated by deleting latitude, longitude and altitude values at the track. The experimental results show that the proposed method (a) directly works in the state domain, (b) does not require the known real system state, (c) has good robustness for the integrated navigation system with higher state dimension, (d) accurately detects the abrupt fault like the innovation chi-square test method.

Key words State Domain; Singular Value Decomposition; Fault Detection; Integration Positioning

Category: Symposium 4: Positioning and applications => 4.2: Next Generation Positioning

785

S4-073

Towards collaborative positioning of pedestrian and UAS platforms by integrating vision, UWB, and IMU data

Andrea Masiero¹、 Paolo Dabove²、 Vincenzo Di Pietra²、 Antonio Vettore³、 Charles Toth⁴、 Vassilis Gikas⁵、 Harris Perakis⁵、 Jelena Gabela⁶、 Laura Ruotsalainen⁷

1. University of Florence

2. Politecnico di Torino

3. University of Padua

4. Ohio State University

5. National Technical University of Athens

6. RMIT University

7. University of Helsinki

Nowadays, it is becoming increasingly important to deliver high quality positioning (accuracy, robustness, integrity, etc.) for various mobility applications: in this context, numerous efforts have recently been undertaken in order to guarantee high continuity of the positioning solution on consumer devices even in GNSS-denied environment. Starting from these considerations, this paper aims at investigating the performance of pedestrian positioning systems based on the data fusion of several sensors: smartphone inertial sensors, an Ultra-Wide-Band (UWB) ranging system, and a camera mounted on an Unmanned Aerial Vehicle (UAV) flying over the test area. The solutions provided by dual frequency GNSS receivers carried by the pedestrians serve as reference trajectories. The UWB positioning system exploits a static infrastructure of anchors, which provide range measurements to the rovers carried by the pedestrians. In addition, a dynamic anchor was mounted on the UAV, hence improving the network geometry. Test results show that the stand-alone UWB solution exhibits a median 2D positioning error less than 0.50 m. Nevertheless, the UWB positioning solution was sporadically unstable due to occasional observation outliers. The integration of inertial data with UWB significantly reduced these instabilities. The vision-based approach reached better positioning results for those segments the pedestrians were visible in the video frames, resulting to a median 2D positioning error less than 0.25 m. However, in order to ensure continuity in the solution obtained outside of the area monitored by the UAV deems necessary the integration of vision with the other sensors. Despite the average performance is similar as for the vision-based solution, this setup reduces remarkably the discontinuity issues. Also, the implementation of a collaborative positioning approach showed to reduce the discontinuity issues. This is a preliminary study towards collaborative pedestrian-UAV positioning.

Key words Positioning, sensor fusion, vision, UWB, UAS, IMU

Category: Symposium 4: Positioning and applications => 4.2: Next Generation Positioning

822

S4-074

Decentralized information filter with delayed states for cooperative location of UUVs

Zhenqiang Du、 Hongzhou Chai、 Xiao Yin、 Minzhi Xiang、 Fan Zhang
Information Engineering University

The cooperative work of unmanned underwater vehicle (UUV) can extend the sensing range of single UUV and realize the complex tasks that it is difficult to accomplish. Due to the complexity of underwater environment and the limitation of UUV sensors, the traditional Kalman filter method for UUVs cooperative localization needs strict time synchronization, and causes huge communication burden. To solve the problem, a new decentralized filter method for UUVs cooperative positioning is proposed, which is based on the information filter with delayed states. Each UUV establishes its own state chain according to the local sensor data, broadcasts its ranging observation information, and cooperates to complete the Cholesky correction. Based on rigorous mathematical theory, the consistency between the proposed decentralized filter and centralized filter is proved. The comparison experiment between the new method and traditional Kalman filter is carried out. Compared with the traditional methods that caused the observation of the single UUV or the observation between the two UUV will result in the observation updating of the whole UUVs, the new method realizes the observation update only related to the UUV directly involved in the observation. The proposed method obviously reduces the communication payloads, and has good expansibility for observation information.

Key words UUV; cooperative location; information filter with delayed states; Decentralized; Cholesky

Symposium 4: Positioning and applications

S4.3: Techniques and Applications in High Precision GNSS

Category: Symposium 4: Positioning and applications => 4.3: Techniques and Applications in High Precision GNSS

79

S4-075

Network RTK performance analysis on moving vehicle in challenging environments

Ali Karimidoona, Steffen Schön
Leibniz Universität Hannover

Currently, automatic applications of navigation are increasing rapidly. Autonomous moving agents e.g. cars and UAVs, are instances of these kinds of applications. The best achievable accuracy using GNSS in kinematic mode is based on Real Time Kinematic (RTK) solutions. RTK solution is limited when the distance from reference station increases. On the other hand, Network RTK can model the biases in a larger area than single RTK. The performance of the navigation systems depends on accuracy, continuity, availability and integrity. Because of the complicated moving environments for the autonomous platforms and the importance of safety issues especially in urban areas, integrity monitoring is of great importance in navigation systems. However, we notice that the integrity monitoring concept has not yet been well developed for Network RTK.

In this contribution, we will evaluate the performance of different commercial N-RTK systems in order to assess the integrity. We conducted static and kinematic experiments running several commercial RTK receivers in parallel. In static mode, these receivers were mounted on a stationary pillar with very good satellite visibility and gathered N-RTK solution as well as raw observations for 2 hours in 10 Hz and 2 days in 30 s. In the next step, the receivers were mounted on the roof top of a van. The van drove a 13 km urban trajectory including both areas with good and also difficult satellite visibility conditions, repeating 1 km loop six times and then another 7 km loop. The quality measures of the raw data (code and phase) e.g. satellite visibility, signal strength, signal continuity, multipath, NLOS and M-W linear combination will be investigated. The quality of the N-RTK solution also will be evaluated by looking at the solution type (fixed, float, DGNSS), CQ of the solution, along-track and cross-track deviations of the RTK from the reference trajectory obtained from GNSS-IMU and reliability analysis in form of Stanford diagrams.

Key words Real Time Kinematic, Network RTK, vehicle positioning, urban environment, integrity

Category: Symposium 4: Positioning and applications => 4.3: Techniques and Applications in High Precision GNSS

115

S4-076

Virtual Reference Station Technology in Geological Hazard Monitoring

Qinglan Zhang^{1,3}、Ming Chen³、Junli Wu³、Chaoqian Xu²、Fan Wang³

1. GNSS Center, WuHan University

2. WuHan University

3. National Geomatics Center of China

The surveying and mapping administrative competent departments in 31 provinces (autonomous regions and municipalities) have built provincial-level satellite navigation and positioning reference stations and data centers, and provided CORS services. This provides a good condition for exploring the application of geological hazard monitoring and early warning using Virtual Reference Station (VRS) service based on CORS. At present, The layout mode of "one point one reference station" is usually adopted, when GNSS is used for geological disaster monitoring and early warning. However, the high deployment cost of this plan limits its large-scale promotion and application. Using the existing CORS service resources of natural resource system, this paper carried out the application experiment of virtual reference station in geological hazard monitoring application at Huanglongya geological hazard monitoring site in Shaanxi Province, and assessed the virtual reference station data quality, comparative analyzed the precision of static baseline processing results and GNSS real-time deformation monitoring results. The experimental results show that the overall quality of virtual reference station data is better than that of the monitoring station, and the accuracy of the static baseline calculation results is better than 1.0cm in the X direction, and better than 2.0cm in the Y direction and Z direction, which is similar to the static baseline calculation results formed by the physical reference station. The accuracy of the baseline results of real-time observation data calculation is better than 5mm in horizontal RMS and 15mm in vertical RMS. Therefore, it can be seen that the virtual reference station is feasible to be used as the reference station for geological disaster monitoring. In addition, the application experiment of network RTK real-time dynamic single epoch positioning mode is also carried out in geological hazard monitoring. The experimental results show that the RMS values of all three directions are $\pm 3.7\text{mm}$, $\pm 9.2\text{mm}$ and $\pm 5.0\text{mm}$ respectively, which meet the precision requirements of GNSS disaster monitoring. Therefore, it is also a feasible scheme for geological disaster monitoring and early warning.

Key words CORS, Geological Disaster Monitoring and Early Warning, GNSS, VRS

Category: Symposium 4: Positioning and applications => 4.3: Techniques and Applications in High Precision GNSS

138

S4-077

Adaptive Stochastic Model Based on LS-VCE for GNSS Kinematic Precise Point Positioning

Qieqie Zhang¹、Long Zhao¹、Bin Wang²

1. Beihang University

2. Shanghai Astronomical Observatory

For kinematic precise point positioning, the stochastic model plays an important role in optimizing float trajectories and improving float solution convergence. However, the stochastic model currently used is mainly an empirical function model, which cannot accurately reflect the true error level of observations in complex environments in real time. To address this problem, an adaptive stochastic model based on least-squares variance component estimation (LS-VCE) method is proposed in this paper. The coefficients of the stochastic model are adaptively adjusted by real-time estimation of the unit weight variance factor of the pseudorange and carrier-phase observations. The optimal estimation of the positioning result is achieved by fusing LS-VCE and Kalman filter. The effectiveness of the proposed method is verified by both static and kinematic tests. The results show that the proposed method can significantly improve the positioning accuracy and stability of precise point positioning.

Key words adaptive stochastic model; least-square variance component estimation; precise point positioning; Kalman filter

Category: Symposium 4: Positioning and applications => 4.3: Techniques and Applications in High Precision GNSS

143

S4-078

Integer-estimable FDMA model as an enabler of GLONASS PPP-RTK

Baocheng Zhang

Innovation Academy for Precision Measurement Science and Technology, CAS

PPP-RTK extends the precise point positioning (PPP) by incorporating the idea of integer ambiguity resolution underlying the real-time kinematic (RTK) technique, making rapid initialization and high accuracy attainable with a standalone receiver.

While PPP-RTK has been well achieved by using global navigation satellite system (GNSS) code division multiple access (CDMA) observables, GLONASS PPP-RTK is nonetheless challenging due to the nature of frequency division multiple access (FDMA) observables. In this work, we present a GLONASS PPP-RTK concept that takes advantage of the integer-estimable FDMA (IE-FDMA) model recently proposed in Teunissen (in *GPS Solutions* 23(4):1-19, 2019. <https://doi.org/10.1007/s10291-019-0889-0>) to guarantee rigorous integer ambiguity resolution and simultaneously takes care of the presence of the inter-frequency biases (IFBs) in homogeneous and heterogeneous network configurations. When conducting GLONASS PPP-RTK based on a network of homogeneous receivers, code and phase observation equations are used to construct the IE-FDMA model, in which the IFBs are implicitly eliminated through reparameterization. For a network consisting of heterogeneous receivers, we exclude the code observables and develop a phase-only IE-FDMA model instead, thereby circumventing the adverse effects of IFBs. For verification purposes, we collect a set of five-day global positioning system (GPS) and GLONASS data from two regional networks: one equipped with homogeneous receivers and another with heterogeneous receivers. The results show that the GLONASS-specific network corrections, including satellite clocks, satellite phase biases, and ionospheric delays estimated by the two networks, are as precise as those of their GPS-specific counterparts. Via satellite clock and phase bias corrections, we succeed in fixing both GPS and GLONASS ambiguities, shortening the convergence time to 5 (12) minutes, compared to 11 (18) minutes of ambiguity-float positioning in the case of a homogeneous (heterogeneous) network with a data sampling rate of 30 seconds. For ambiguity-fixed positioning, the convergence time defined in this work also indicates the time to first fix since the positioning error converges to the centimeter level once successful integer ambiguity

resolution is achieved. Adding ionospheric corrections further speeds up the initialization in the two networks, with the convergence time being reduced to 0.5 (3) minutes. Compared with GPS-only positioning, the integration of GPS and GLONASS yields an improvement of 8%-34% in accuracy and leads to a reduction of 25%-50% in convergence.

Key words GLONASS; PPP-RTK; Integer-estimability; Frequency division multiple access (FDMA); Inter-frequency bias (IFB); Integer ambiguity resolution (IAR)

Key words GLONASS; PPP-RTK; Integer-estimability; Frequency division multiple access (FDMA); Inter-frequency bias (IFB); Integer ambiguity resolution (IAR)

Category: Symposium 4: Positioning and applications => 4.3: Techniques and Applications in High Precision GNSS

151

S4-079

Accuracy analysis of GNSS multi-system single point positioning algorithm with different cut-off altitude angles

Guanpeng Yin¹, Meng Gao²

1. Geodetic survey center

2. Satellite Navigation Center, Liaoning Technical University

This paper puts forward the deep research about the mathematical model of pseudo range single point positioning and the processing of the error term, resolving the difference between the precision and performance of pseudo range single point positioning of BDS single system, GPS single system, GLONASS single system and BDS / GPS / GLONASS combination system in the case of different cut-off elevating angle and the pseudo range single point positioning of different system. First of all, this paper introduces the data processing methods of pseudo range single point positioning of Beidou satellite navigation system, global positioning system, GLONASS satellite navigation system and the navigation combined by three system. The data experiments of pseudo range single point positioning of single system and combined system are carried out in different stations selected in the world, which shows that the precision of pseudo range single point positioning of Beidou navigation and positioning system is slightly lower than that of the global positioning system, while the precision of pseudo range single point positioning of combined system is higher than that of Beidou system, besides, when the cut-off elevating angle increases, the number of visible satellites is becoming more with a stability which is better than that of GPS. The E, N and U directions of GLONASS satellite navigation system show a large deviation, which is unstable due to the small number of visible satellites.

Key words pseudo-range single point positioning ; group system ; BDS ; GPS ; GLONASS ; precision analysis

Category: Symposium 4: Positioning and applications => 4.3: Techniques and Applications in High Precision GNSS

157

S4-080

BDSBAS-B1C Service Performance Evaluation Model and Experimental Analysis

xiancai Tian、longping Zhang、haichun Wang、shiming Gu、dezhi Zhang
Piesat Information Technology Co.,Ltd

BDS-3 single-frequency SBAS service broadcasts GPS satellite error correction and integrity information on B1C signals through three GEO satellites, aiming to provide users in China and its surrounding areas with single-frequency (SF) services in line with ICAO standards. Firstly, this paper introduces the development of BDSBAS and foreign SBAS system; Then, the error correction and integrity calculation models of SBAS are given, including satellite orbit error, clock error, ionospheric correction model and integrity protection level calculation model; Finally, the SBAS orbit, clock error, grid ionospheric correction accuracy and positioning accuracy are evaluated. At the same time, the Stanford graph model is constructed to judge the security level of the system positioning results, and the protection level coverage in the service area is calculated. The experimental results show that the satellite orbit correction accuracy (RMS) in R, T and N directions is 0.50m, 1.00m and 0.80m respectively, and the clock error correction accuracy (RMS) is 1.02ns; The horizontal and elevation positioning accuracy (95%) is about 1.20m and 2.6m respectively; The HPL and VPL (95%) are about 6m and 10m respectively. According to the safety level results of Stanford diagram, it can fully meet the requirements of ICAO for APV-I.

Key words SBAS; Integrity; Protection Level; Ionospheric Delay; Positioning Accuracy; Stanford

Category: Symposium 4: Positioning and applications => 4.3: Techniques and Applications in High Precision GNSS

160

S4-081

Quality control of outlier detection, identification and adaptation in GNSS positioning

Ling Yang、 Yunzhong Shen、 Bofeng Li
Tongji University

Outlier detection, identification and adaptation (DIA) is a harsh problem for GNSS positioning in urban environment. The least squares method (LS), typically applied to GNSS positioning, is BLUE (best linear unbiased estimator) and MVUE (minimum variance unbiased estimator) if measurement errors follow the normal distribution. Outliers or misspecifications in the functional model generally result in LS estimators that are biased. The DIA method, together with its associated internal and external reliability measures has been conventionally implemented in various GNSS data processing software.

The DIA method firstly makes hypothesis testing between the original/null and a group of alternative hypothesis models. The most trustworthy model is selected and considered to exclude any unmodelled misspecifications. Then, estimation is conducted under the identified model aiming to remove the potential bias on the unknown parameters. However, missed detection, false alarm, and wrong identification, usually cannot be avoided due to the geometry of the observation model, the separability among hypothesis models, the selected test statistics and the predetermined critical values for testing. These incorrect decisions would still introduce biases in the final parameter estimation, which has been rarely discussed and considered in current data processing procedure.

In this work, the author define three groups of indices that measure the quality of the DIA estimator under the unconditional case where the parameter estimation combines the estimators from multiple hypothesis models determined by different testing decisions. Firstly, the confidence levels of the testing decisions are proposed by grouping the hypothesis testing into correct acceptance and false alarm under the null hypothesis, into correct detection, missed detection, correct identification, and wrong identification under a specified alternative hypothesis. Secondly, the reliability indices are redefined and formulated to describe the capability of the specified alternative hypothesis in terms of resistance to the null hypothesis, to another alternative hypothesis, and to all other hypotheses in the group. Finally, the expectations, squared variances, and protection levels of the estimated parameters are determined to measure the biasedness, dispersion and integrity of the estimator by considering the

uncertainty of the testing decisions, the model reliabilities, and the parameter distribution properties. Numerical examples of a dual-constellation GNSS Single Point Positioning (SPP) are used to demonstrate the quality control of and comparison among three conventional DIA methods.

Key words outliers, DIA, hypothesis testing

Category: Symposium 4: Positioning and applications => 4.3: Techniques and Applications in High Precision GNSS

177

S4-082

Ambiguity-fixed relative positioning with GNSS dual-frequency observations of Huawei Mate20 smartphones

Weikai Miao
Tongji university

Most of previous studies on smartphone positioning are mainly with single-frequency signals and for low-accuracy positioning. The availability of GNSS dual-frequency measurements in smartphone in recent several years gives great opportunities to achieve high-precision positioning. In this paper, we comprehensively evaluate the characteristics of GNSS dual-frequency observations from Huawei Mate20 smartphone using both embedded and external antennas, including the C/N0 values, signal availability, random noises and real-time kinematic positioning etc. The results show that the embedded antenna is the key limitation for signal quality, which has smaller C/N0 values and lower positioning accuracies compared to external antennas. In addition, the performance is also affected by the smartphone posture, and it is the best when the antenna faces upwards. Although the double-differenced (DD) carrier-phase ambiguities are fixable, the constant offsets exist and differ from systems and frequency bands. For simulated kinematic positioning with static data, the positioning errors of Mate20 are all smaller than 10 cm by 95% for three antenna postures. For real kinematic vehicle positioning, the positioning errors are smaller than 0.12 m and 0.22 m by 68% and 95%, respectively.

Key words Smartphones; GNSS dual-frequency observations; External antenna; Ambiguity resolution

Category: Symposium 4: Positioning and applications => 4.3: Techniques and Applications in High Precision GNSS

203

S4-083

ADDTID: An Efficient Tool for Characterizing Travelling Ionospheric Disturbances

Heng Yang^{1,2,4}、 Enrique Monte-Moreno⁴、 Manuel Hernández-Pajares^{2,3}

1. School of Electronic Information and Engineering, Yangtze Normal University, 408100 Chongqing, China
2. Department of Mathematics, IonSAT, Universitat Politècnica de Catalunya, 08034 Barcelona, Spain
3. IEEC-CTE-CRAE, Institut d'Estudis Espacials de Catalunya, 08034 Barcelona, Spain
4. Department of Signal Theory and Communications, TALP, Universitat Politècnica de Catalunya, 08034 Barcelona, Spain

The traveling ionospheric disturbances (TIDs), constituting the most frequent ionospheric wave signatures, affects Global Navigation Satellite System (GNSS) signals. This effect can be exploited to use the GNSS system as a global ionospheric sensor (or “ionoscope”) for detecting and characterizing the TIDs. A blind detection method is to be proposed, referred as Atomic Decomposition Detector of TIDs (ADDTID), for the detection and characterization of simultaneous TIDs and its application to figure out the relationship to the origins. The TID information comes from regional detrended vertical total electron content maps which are obtained on line of sight from GNSS satellites to receivers. The featured contribution is the detection of the exact number of independent TIDs from a nonuniform sampling of the ionospheric pierce points. The solution to the problem is set as the estimation of the representative perturbations from a dictionary of atoms that span a linear space of possible TIDs. The estimate is done by a sparse decomposition based on the solution of improved Least absolute shrinkage and selection operator. Four case studies by means of ADDTID are to characterize the detailed propagations of TIDs regarding different sources, where the highlights are the following: (1) Simultaneous medium scale TIDs exhibit the complex behaviour regarding different sources during 2011 Japan Spring Equinox day; (2) TIDs produced by the 2017 U.S. total solar eclipse exhibits a double bow wave phenomenon, the wavelength evolution of which depends on the solar zenith angle of the umbra center; (3) Anisotropic propagation of TIDs regarding 2011 Japan Tohoku earthquake provide clues to the location of tsunami wavefront, which could be used as the indicator of early warning; (4) The location information of strong TIDs can be used to indicate the propagation of tsunami, by characterizing the ionospheric response to 2015 Chile Illapel earthquake through a small number of GNSS networks.

Key words Traveling Ionospheric Disturbances; Global Navigation Satellite Systems

Category: Symposium 4: Positioning and applications => 4.3: Techniques and Applications in High Precision GNSS

205

S4-084

A new ambiguity resolution method for single-receiver LEO precise orbit determination

Xingyu Zhou、 Hua Chen、 Weiping Jiang、 Yan Chen、 Tianjun Liu、 Mingyuan Zhang
Wuhan University

Ambiguity Resolution (AR) is an effective approach in Global Navigation Satellite System (GNSS) based Low Earth Orbit (LEO) satellite Precise Orbit Determination (POD). For single-receiver AR, there are typically two types of AR methods including the Single-Difference (SD) AR and the Track-to-track (T2T) AR. The SD AR approach requires Fractional Cycle Bias (FCB) or Integer Recovery Clock (IRC) products in addition to the GNSS precise orbits and clocks, while the T2T AR is hampered by the receiver hardware delay variations. In this study, a new AR method called SD T2T (SDT2T) is proposed. The SDT2T AR is to recover the integer nature of the ambiguities by the differences between GNSS satellites and LEO orbit tracks without external information. After differencing the biases from the receiver and GNSS satellites sequentially, the SDT2T ambiguities can be fixed to integers successfully. The performance of the new method is assessed by the Gravity Recovery and Climate Experiment Follow On (GRACE-FO) twin satellites and three SWARM satellites. The results from the Reduced Dynamic POD (RDPOD) and the Kinematic POD (KPOD) show that the SDT2T AR has a very high and stable AR success rate, and the orbits are found to be comparable to that from the SD AR. Therefore, it is recommended that the SDT2T AR can be adopted in LEO missions for orbit refinement.

Key words GNSS, LEO, Ambiguity Resolution, GRACE-FO, SWARM

Category: Symposium 4: Positioning and applications => 4.3: Techniques and Applications in High Precision GNSS

208

S4-085

A New Underwater Positioning Model Based on Average Sound Speed

Yixu Liu¹、Shengli Wang¹、shuqiang Xue²、Xiushan Lu¹

1. Shandong University of Science and Technology

2. Chinese Academy of Surveying and Mapping

The marine navigation, positioning, and the development of marine resources are increasingly concerned for most of the countries around the world. The research on underwater navigation and positioning technology has become increasingly mature. The construction of the submarine geodetic reference network is extremely difficult, and the technical requirements for the calibration of reference points are rigorous. The layout of seafloor datum points is the key to constructing the seafloor geodetic datum network, and a reliable underwater positioning model is the prerequisite for achieving precisely deployment of the datum points. However, due to the particularity of the water environment, underwater positioning has the characteristics of dynamic and non-repeatability compared to land positioning. Thus, the sound speed error is the main factor affecting the positioning accuracy. The traditional average sound speed positioning model is generally adopted in underwater positioning due to its simple and efficient algorithm, but it is sensitive to the incident angle-related errors, which lead to the unreliable positioning results. Based on the relationship between the incident angle and the sound speed, the sound speed function model considering the incident angle is established. Results show that the accuracy of positioning is easily affected by the errors related to the incident angle; the new average sound speed correction model based on the incident angle proposed in this paper is used to significantly improve the underwater positioning accuracy.

Key words Underwater Positioning; Average Sound Speed; Sound Speed Profile; Incident Angle

Category: Symposium 4: Positioning and applications => 4.3: Techniques and Applications in High Precision GNSS

209

S4-086

The evaluation of position and attitude accuracy for MS GNSS receiver with SD algorithm

Chenglong Zhang^{1,2}, Wen Chen^{1,2}, Danan Dong^{1,2}

1. East China Normal University

2. Engineering Center of SHMEC for Space Information and GNSS, East China Normal University

As a new type of receiver, the multi-antenna synchronized (MS) Global navigation satellite system (GNSS) receiver is widely used in position and attitude determination. With the help of the synchronized technology, the single-difference (SD) of MS GNSS receiver is equivalent to double-difference. But most MS receivers still keep the DD algorithm due to the uncalibrated phase delay (UPD). We propose the ambiguity substitution approach (ASA) to isolate UPD and fix the SD ambiguities into integers. To evaluate the accuracy of MS receiver with SD algorithm under ideal conditions. Multipath hemispherical map (MHM) is used to eliminate the multipath and finally we obtain the clean vector. Static and ship experiments results show that, while determining the millimeter baseline solution and 0.2° attitude solution, the dispersity of baseline vector and attitude obtained by SD algorithm is not only equivalent to DD algorithm in the horizontal direction but is at least twice less than DD in the vertical direction. In addition, the vehicle experiment gives evidence that MS receiver with SD algorithm can detect small ups and downs like inertial navigation system which the DD algorithm cannot do. These advantages of MS receiver with SD algorithm should be paid more attention to and applied to marine surveying and other fields that need high precision positioning and attitude.

Key words GNSS; single difference; uncalibrated phase delay; integer ambiguity resolution; multi-antenna synchronized receiver

Category: Symposium 4: Positioning and applications => 4.3: Techniques and Applications in High Precision GNSS

216

S4-087

Establishing a new method for heavy precipitation detection using optimal anomaly-based thresholds of predictors derived from GNSS-PWV

Haobo Li^{1,2}, Xiaoming Wang², Kefei Zhang¹, Suqin Wu¹, Jinglei Zhang², Cong Qiu²

1. School of Environment Science and Spatial Informatics, China University of Mining and Technology
2. Aerospace Information Research Institute, Chinese Academy of Sciences

In recent years, the rapid system deployment and super successful development of the Global Navigation Satellite Systems (GNSS) has revolutionized the atmospheric remote sensing technology due to its high spatio-temporal resolution, high accuracy, all-weather capability and low costs. Recognized as an essential climate variable by World Meteorological Organization Global Climate Observing System (WMO-GCOS), the precipitable water vapor (PWV), derived from ground-based GNSS tracking stations, has advanced its usages in meteorological applications such as the predictions of weather events. Among all the models using the continuous PWV time series for heavy precipitation detection, the widely used threshold-based model is a typical extrapolation method, which uses a threshold value as a trigger for detecting an extreme weather event. Moreover, the anomaly series of any meteorological variable that represents the departure of the variable from its long-term mean value, is widely and effectively used in minimizing its data range and quantitatively estimating its variations in meteorological studies. Therefore, in this study, a new model for detecting heavy precipitation using anomaly-based thresholds of seven predictors derived from GNSS-derived PWV time series is established. The seven predictors including PWV value, PWV increment and decrement, rate of PWV increment and decrement, and hourly PWV increment and decrement, which reflect not only the ascending and descending trends, but also long-term and short-term variations in the PWV time series. Prior to determining the reliable anomaly series of predictors used in the model, the mean values of different predictors were calculated using their respective data in the 12-h time windows before the onset of all the heavy precipitation events happened at three pairs of co-located GNSS/weather stations in Hong Kong over an 8-year period of 2010-2017. Then an optimal set of thresholds for the predictors for each summer month was determined based on hourly precipitation records and the anomaly series of PWV-derived predictors using the

widely accepted percentile method. The new model was evaluated by comparing its prediction results against the hourly precipitation records for the summer months in 2018 and 2019. Results showed that 98.5% of heavy precipitation events can be correctly detected with a lead time of 3.86 h and the seasonal false alarm rate was greatly reduced to only 25.3%. These results suggest that it is promising to use the new model proposed to obtain better detection results for heavy precipitation events and the new model also has the potential to be used as a complementary tool to the operational models for the very short-range forecasting (VSRF) of severe precipitation events.

Key words Global Navigation Satellite System (GNSS); precipitable water vapor (PWV); heavy precipitation detection; natural hazards prevention; geosciences

Category: Symposium 4: Positioning and applications => 4.3: Techniques and Applications in High Precision GNSS

240

S4-088

BDS-3 SISRE assessment as well as comparison between D1 and B-CNAV (B-CNAV1, B-CNAV2 and B-CNAV3) navigation messages

Zhenghua Dong, Songlin Zhang
Tongji University

Based on precise ephemeris products from Wuhan University Multi-GNSS (WUM), the orbit, clock error and SISRE of 18 medium earth orbit (MEO) satellites' D1 and B-CNAV (B-CNAV1, B-CNAV2 and B-CNAV3) navigation messages of BDS-3 are computed, analyzed and compared. Their annual evolution processes of the whole year of 2019 are studied. The root mean square (RMS) values of BDS-3 broadcast ephemeris orbit error are 0.069 m, 0.275 m and 0.318 m in radial, cross and along direction, respectively. And the 3D RMS value of it is 0.420 m. Thanks to the use of new orbit parameters in the B-CNAV (B-CNAV1, B-CNAV2 and B-CNAV3) navigation message of BDS-3, the satellite orbit accuracy of it is obviously better than that of the D1 navigation message in radial direction, and the percentage of its accuracy improvement is 14.2%. With respect to clock errors, the timescale differences between the two clock products are eliminated to assess the accuracy to broadcast ephemeris clock error. The standard deviation value of 0.288 m shows a good performance as a result of the use of the two new types atomic clocks, but the RMS value is 0.513 m due to a nonzero mean bias. For the new hydrogen and rubidium atomic clocks, their RMS and standard deviation are 0.539 m, 0.266 m and 0.493 m, 0.306 m respectively. The RMS value of SISRE of BDS-3 broadcast ephemeris is 0.516 m, and the value is 0.904 m when it with 95% confidence level. While after deducting the influence of the clock error, the value of SISRE_ORB is 0.090 m. Since the satellite clock error is much larger than orbit radial error, the SISRE is mainly affected by the clock error and the annual evolutions of them are consistent. Because of the improvement of the B-CNAV (B-CNAV1, B-CNAV2 and B-CNAV3) navigation message in orbit radial accuracy, it has a significant effect on improving the accuracy of SISRE_ORB, and the percentage of the accuracy improvement is 5.5%.

Key words BDS-3; D1 and B-CNAV (B-CNAV1, B-CNAV2 and B-CNAV3) navigation messages; Orbit and clock errors; SISRE

Category: Symposium 4: Positioning and applications => 4.3: Techniques and Applications in High Precision GNSS

247

S4-089

The estimation of inter-receiver pseudorange biases and its impact on the BDS-2 GEO satellite precise orbit determination

Ran Li¹、 Ningbo Wang¹、 Jiatong Wu²、 Zishen Li¹、 Kai Li³、 Yang Li^{1,4}

1. Aerospace Information Research Institute, Chinese Academy of Sciences (CAS)

2. Map Supervision Center, Ministry of Natural Resources, China

3. Shanghai Astronomical Observatory, Chinese Academy of Sciences

4. University of Chinese Academy of Sciences

The ground receivers with different configurations, different front-end bandwidth or different correlator spacing, exist inconsistent pseudorange biases for same navigation signal. The issue of inter-receiver pseudorange biases becomes particularly obvious when satellite orbit parameters are created based on observations from a network containing mixed receiver types. In this contribution, we investigate the effects of inter-receiver pseudorange biases on the regional BeiDou navigation satellite system (BDS-2) satellite precise orbit determination (POD). The results showed that the existence of the inter-receiver pseudorange biases cause along-track bias in GEO satellite orbit determination. By correcting the inter-receiver pseudorange biases, the RMS values of 24-h POD overlap improvement corresponding to along-track components are 16%. The inter-receiver pseudorange bias corrections can effectively improve the precise orbit determination accuracy of the BDS-2 GEO satellite, especially for the along-track accuracy.

Key words Precise Orbit Determination; Inter-receiver pseudorange biases; BDS-2; Geostationary Earth Orbit

Category: Symposium 4: Positioning and applications => 4.3: Techniques and Applications in High Precision GNSS

251

S4-090

Assessments on multi-GNSS real-time precise point positioning

Ruohua Lan、Jie Lv、Junyao Kan、Zhouzheng Gao

School of Land Science and Technology, China University of Geosciences Beijing

Precise Point Positioning (PPP), based on multi-constellation Global Navigation Satellite Systems (GNSS) measurements and real-time precise satellite products, is regarded as a potential high-accuracy positioning mode for most of mass-market applications in the future. In this paper, the methods of real-time multi-GNSS (GPS/BDS/GLONASS/Galileo/QZSS) PPP are described firstly. Then, to evaluate the performance of real-time multi-GNSS PPP at present, real-time precise satellite orbit and clock products provided by International GNSS Service (IGS) centers (i.e., CAS, CNES, DLR, GFZ, GMV, and WHU) are collected by using BNC software. After evaluating the quality of real-time satellite products from different IGS centers by comparing with that of final products, those products are applied to the proposed uncombined undifferenced multi-GNSS PPP with using measurements from both static and kinematic experiments. Results illustrate that (1) the accuracy of real-time orbit and clock products is close to that of final products, which makes high-accuracy positioning by PPP in real-time possible; (2) the accuracy of GPS's orbit and clock products from those IGS centers is higher than that other GNSS systems; (3) the positioning performance of real-time PPP is almost the same with that of the post-processing mode; (4) while using the multi-GNSS together, both position accuracy and convergence time can be improved significantly.

Key words Multi-GNSS; Real-time; Precise Point Positioning (PPP)

Category: Symposium 4: Positioning and applications => 4.3: Techniques and Applications in High Precision GNSS

256

S4-091

On the Limits of State-of-the-art GNSS Receivers in Frequency Transfer

Thomas Krawinkel, Steffen Schön
Leibniz University Hannover

Today, frequency transfer (FT) based on Global Navigation Satellite System (GNSS) measurements is used as a standard technique. Within the frame of the Collaborative Research Centre “TerraQ - Relativistic and Quantum-based Geodesy”, it is our goal to push the limits of GNSS FT to the 10^{-17} instability range. As a first step, we want to explore the minimum achievable frequency link instability between two GNSS receivers. For this, the receivers are set up in a zero-baseline, common-clock measurement configuration in a controlled environment. In addition, the signal paths, and thus the induced delays, from the antenna to both receivers must be identical. Such an environment is available at Physikalisch-Technische Bundesanstalt (PTB), Germany’s national metrology institute. Since all error sources affecting the satellite signals are the same for both receivers, they cancel when forming receiver-to-receiver single differences (SDs). Due to the fact that the remaining SD carrier phase ambiguities can be easily fixed to integer values, the relative receiver clock bias is the only parameter to be estimated. Both receivers are connected to the same frequency source, in this case UTC(PTB), whose instability is significantly smaller than that of any GNSS carrier phase observable. Thus, the resulting instability virtually provides a lower bound for GNSS FT in general, since it is almost exclusively caused and dominated by the hardware delay instability of the receivers in use. In our contribution, we will present and discuss the results of such a dedicated experiment carried out for ten days in April 2021 at PTB with a total of four receivers: two Septentrio PolaRx5TR, and two Javad Omega. We will focus on GPS and Galileo signals, with an emphasis on new signals like GPS L1C, L2C and Galileo AltBOC. Furthermore, we will analyze potential benefits of receiver clock modeling in GNSS FT.

Key words GNSS, frequency transfer, Allan deviation, receiver clock modeling

Category: Symposium 4: Positioning and applications => 4.3: Techniques and Applications in High Precision GNSS

258

S4-092

A modified global tropospheric delay model considering diurnal variation

Guolin Liu, Lei Li, Xin Chen, Ying Xu
Shandong University of Science and Technology

The tropospheric delay is one of the main error sources that degrades the accuracy of global navigation satellite system (GNSS) high-precision positioning. It is difficult to model the tropospheric delay all over the world accurately due to the limitation of the number of reference stations and the time resolution of zenith tropospheric delay (ZTD). Numerical weather prediction (NWP) provides global distribution grid meteorological reanalysis data and forecast data. The ZTD estimated by integral method using NWP data has high accuracy and time resolution. In order to solve the issue that the characteristic of daily variation of ZTD is ignored or incompletely considered by the existing global tropospheric delay model without meteorological parameters, this study provides a modified global tropospheric delay model ZTD-DV (ZTD-Diurnal Variation) by using non phase function fitting model with daily variation, annual period and half year period. The ZTD of global grid point with the spatial resolution of $2.5^{\circ} \times 2^{\circ}$ used in this model are estimated with integral method using the ERA5 and ERA5-Land data sets with high time resolution provided by ECMWF from 2015 to 2018. The ZTD estimated by NWP data of the global grid point (NWP-ZTD) in 2019 and high-precision ZTD of 330 IGS stations (IGS-ZTD) evenly distributed in the world are used to assess the performance of ZTD-DV model and the experimental results show that the proved ZTD-DV model has higher precision than that of GPT3 model. The specific performance is as follows: the mean deviation and RMS of the difference between of ZTD estimated by the ZTD-DV model (Model-ZTD) and the NWP-ZTD are -1.04mm and 36.64mm respectively. The mean deviation and RMS of the difference between the Model-ZTD and the IGS-ZTD are 1.28mm and 38.46mm respectively, which is slightly better than GPT3 ($1^{\circ} \times 1^{\circ}$) (mean deviation:-2.24mm,RMS:38.41mm),and is significantly better than GPT3 ($5^{\circ} \times 5^{\circ}$),UNB3,UNB3m and EGNOS model.

Key words global navigation satellite system; zenith tropospheric delay; numerical weather forecast; diurnal variation; integration method

Category: Symposium 4: Positioning and applications => 4.3: Techniques and Applications in High Precision GNSS

272

S4-093

Precise orbit determination for FY3D satellite using onboard BDS and GPS observation data and orbit forecast accuracy analysis

Mingming Liu^{1,2}, Yunbin Yuan¹

1. Innovation Academy for Precision Measurement Science and Technology,
Chinese Academy of Sciences, China

2. University of Chinese Academy of Sciences, China

FY3D satellite were successfully launched in 2017, with the aim of achieving all-weather and multi-spectral observations of the global atmosphere and geophysical elements, and it is equipped with an onboard BDS/GPS receiver. How about accuracy performance of Low-Earth-Orbit satellite (LEO) precise orbit determination (POD), which is worth studying and analyzing. Thus, we use onboard GPS and BDS data to carry out LEO POD research, assess orbital accuracy, and make the orbital forecast studies. Some conclusions can be derived as follows: (1) FY3D satellite receiver antenna phase center variation (PCV) is modeled using LEO onboard data. The three-dimensional (3D) root-mean-square (RMS) of overlap orbit differences (OOD) for FY3D with onboard GPS-only data is 0.0161 m. The 3D RMS and 1D RMS of orbital differences for BDS-2-only POD results relative to onboard GPS orbits for FY3D are 0.1516 and 0.0875 m, respectively. The 3D RMS mean of orbital differences for joint POD (GPS+BDS-2 solution) relative to onboard GPS orbits is 0.0306 m. As more and more LEO satellites are equipped with onboard BDS-3 receivers, the accuracy of LEO POD is higher than that of the current FY3D satellite, which will be greatly improved in the future. (2) Using 24-hour precise orbit of FY3D satellite to forecast the orbits of 2h, 6h, 12h, and 24h respectively, the accuracy evaluation results show that the averaged RMS of 2h orbit forecast is centimeter level, and the averaged RMS of 6h, 12h, and 24h orbit forecast is decimeter level, and the RMS of 24h orbit forecast in most days is within 1 m. Generally speaking, with the increase of forecast time, the orbit forecast accuracy RMS decreases gradually, and the 24-hour orbit forecast accuracy of the FY3D satellite can reach decimeter level.

Key words GPS, BDS-2, LEO, FY3D, onboard GPS/BDS, joint POD, orbit forecast, accuracy, RMS.

Category: Symposium 4: Positioning and applications => 4.3: Techniques and Applications in High Precision GNSS

286

S4-094

Estimation and Validation of Codephase Center Correction using the Empirical Mode Decomposition

Yannick Breva, Johannes Kröger, Tobias Kersten, Steffen Schön
Leibniz University Hannover, Institut für Erdmessung

In high precision GNSS applications, it is necessary to take phase center corrections (PCC) into account. Beside these corrections for carrier phase measurements, also corrections for the codephase exist, so called codephase center corrections (CPC). The CPC, also known as group delay variations (GDV), are antenna dependent delays of the receiving codephase, which are varying with azimuth and elevation of the incoming GNSS signal.

A concept for estimate absolute CPC and PCC for multi GNSS signals has been established by the Institut für Erdmessung (IfE). A robot is used to precisely rotate and tilt an antenna under test (AUT) around a specific point in space. By using an external frequency standard, time differenced single differences (dSD) with a sample rate of 1 Hz are calculated, which are used to estimate CPC and PCC with spherical harmonics (8,8). This approach works well for PCC, however, there are some challenges for estimating repeatable CPC patterns. The main drawback is the significantly higher noise to pattern ratio in the dSD.

In this contribution, we present an alternative processing strategy to highly reduce the noise by maintaining all pattern information in the input observations of the estimation process. By increasing the sample rate to 10 Hz, the empirical mode decomposition (EMD) can be used. This method was introduced by Huang et. al. (1996) and allows the decomposition of any complicated data set into finite number of intrinsic mode functions (IMF). By preprocessing the dSD with the EMD, the repeatability of the estimated CPC pattern can be significantly increase. An analyse for a LEIAR20 LEIM antenna shows an improvement in the RMS of 75 %, from 44 mm to 12 mm. We present the estimated multi GNSS CPC of different antennas with the new processing strategy. A further validation of the estimated CPC pattern will be shown in the observation domain for short baselines.

Key words multi GNSS antenna calibration, codephase center corrections, empirical mode decomposition

Category: Symposium 4: Positioning and applications => 4.3: Techniques and Applications in High Precision GNSS

291

S4-095

Optimal kernel functions of Gaussian process regression for TEC prediction on the Ring of Fire region

Nhung Le Thi^{1,3,5}, Benjamin Männel¹, Pierre Sakic¹, Thai Chinh Nguyen^{1,4}, Hoa Thi Pham^{2,5}, Harald Schuh^{1,3}

1. GFZ German Research Centre for Geosciences, Potsdam, Germany

2. School of Earth and Planetary Science, Spatial Science Discipline, Curtin University, Perth, Australia

3. Technische Universität Berlin, Germany

4. Hanoi University of Mining and Geology, Vietnam

5. Hanoi University of Natural Resources and Environment, Vietnam

Total Electron Content (TEC) data plays a significant role in monitoring GNSS-based navigation, meteorological phenomena, and related seismic activities. The TEC forecasts are also used for early warning systems of ionospheric disturbances. In this study, we investigate ten kernels of Gaussian Process Regression (GPR) to select optimal functions for TEC model forecast on the Ring of Fire region. We use TEC time series with one-minute, daily, and monthly intervals, that are computed from GNSS (Global Navigation Satellite Systems) data during the 2004 - 2020 period. TEC anomaly values in time series are eliminated based on the quartile algorithm (probability 95%) and then filter noise by the moving median average (probability 99.7%). The Makima (Modified Akima Piecewise Cubic Hermite) interpolation algorithm is also used to fill out the determined TEC outliers. The performance of models is represented by validation RMSE (Root Mean Squared Error) values of the trained models, and evaluations of the final models for different kernel covariance functions. Our preliminary results show that Exponential GPR produces the best TEC estimates with RMSE of ~3.4, 4.5, and 5.7 TECU on the data patterns with monthly, daily, and one-minute intervals, respectively; followed by Matern and Rational Quadratic functions. The forecast model evaluations on the TEC time series' sparse data (monthly intervals) also show the highest reliability. In general, GPR is best suited to small TEC datasets, and the exponential kernel functions have the highest accuracy and reliability for TEC forecast.

Key words Gaussian process regression, Machine learning, TEC forecast, Optimal kernel function, Exponential kernel

Category: Symposium 4: Positioning and applications => 4.3: Techniques and Applications in High Precision GNSS

318

S4-096

Disturbance analysis of underwater locating sound line and design of piecewise exponential weight function

Xin pu WANG¹、Shu qiang XUE²、Guo qing QU¹、Yi xu LIU³、Wen long YANG²

1. Shandong University of Technology

2. Chinese Academy of Surveying and Mapping

3. Shandong University of Science and Technology

The sound velocity error is an important error source of underwater positioning, which mainly includes the uncertainty of sound velocity measurement and the sound velocity error caused by the temporal-spatial variation of the sound speed field. Based on the constant gradient sound ray tracking model, we derive a mathematical model for the sound ray disturbance analysis about the incident angle, sound velocity gradient and water depth. The results show that, for the same water depth and sound velocity error, the greater the incident angle is, the greater the impact of incident angle perturbation on the sound ray, and the greater the impact of sound ray bending will be. According to the derived function response relation between incident angle disturbance and acoustic ray disturbance, a piecewise exponential function stochastic model of underwater positioning based on incident angle correlation is established. The positioning results of the piecewise-exponential function random model are compared with the equal weight model. The piecewise-cosine weighting model is also validated, but the model in this article will retain more observation information.

Key words incident angle; sound ray propagation; underwater positioning; random model

Category: Symposium 4: Positioning and applications => 4.3: Techniques and Applications in High Precision GNSS

335

S4-097

Integrity monitoring of precise satellite orbit and clock products for real-time precise point positioning

Jiaojiao Zhao、Zishen Li、Ningbo Wang

Aerospace Information Research Institute, Chinese Academy of Sciences

The integrity of real-time precise point positioning (PPP) is the key constraint for its application in autonomous driving, drones, and other life-safety-related scenarios. The integrity monitoring of real-time precise orbit and clock products is the basis of the integrity of the PPP service. Currently, there are limited research on the integrity of real-time precise orbit and clock products. The conventional integrity monitoring method based on pseudo-range can't satisfy the integrity requirements of high-precision application based on carrier phase observations. In view of this, this contribution first analyzed the fault characteristic of real-time precise orbit and clock products, then the real time precise orbit and clock integrity monitoring method based on ionospheric-free carrier-phase observation were presented. Finally, experiments based on a one month of real data were carried to verify and estimate the performance of the proposed method. The results show that with simulation fault, the false alert rate for CLK93 is lower than 1×10^{-6} for both GPS and BDS. As for CAS SSR, the false alert rate is lower than 1×10^{-6} for GPS and 1×10^{-5} for BDS. This work can provide an important knowledgebase for the real-time PPP integrity theory and has important theoretical and practical significance.

Key words Global Navigation Satellite System; real-time precise point positioning; precise orbit and clock products; integrity monitoring

Category: Symposium 4: Positioning and applications => 4.3: Techniques and Applications in High Precision GNSS

336

S4-098

A Modified Interpolation Method for Regional Tropospheric Delay Modeling in Network RTK

Yakun Pu^{1,2}, Yunbin Yuan¹, Min Song¹

1. Innovation Academy for Precision Measurement Science and Technology,
Chinese Academy of Sciences

2. University of Chinese Academy of Sciences

Abstract

Due to the advantages of a simpler implementation and higher efficiency, the traditional interpolation algorithm with the linear interpolation method (LIM) is widely used to obtain the atmospheric delay correction at the virtual reference station (VRS) near the rover in the network real-time kinematic (NRTK) positioning. However, the traditional interpolation algorithm based on the LIM only models the atmospheric error in the horizontal direction. It ignores the atmospheric error distribution in the elevation direction, especially for the tropospheric error. When the reference stations and rover's height are not at the same level, and the height difference between reference stations and the rover is significant, due to tropospheric error and height are strongly correlated, the performance of the traditional method is unsatisfactory for tropospheric delay interpolation at the VRS. Therefore, considering the height difference between the reference stations and the rover, an improved linear interpolation method is proposed in this study. In order to validate the performance of the proposed method, the data from the American NOAA continuously operating reference stations network were used for experiments, and the results of the traditional interpolation algorithm and the proposed method were compared and analyzed. The experimental results showed that the interpolation accuracy of the double-differenced tropospheric delay was improved obviously by the proposed method. The modified algorithm performed better than the traditional algorithm, especially for satellites with lower elevation angles. The positioning accuracy of the proposed method was also enhanced in the horizontal and vertical direction, especially significant in the vertical direction. When the height difference between the master reference stations and the rover is relatively small, the traditional interpolation algorithm met the accuracy requirements of traditional NRTK both in tropospheric interpolation accuracy and positioning accuracy. In the case of a considerable height difference situation, we require correction for tropospheric delay systematic errors in NRTK.

Key words Keywords: GPS; NRTK; VRS; tropospheric delay; interpolation

Category: Symposium 4: Positioning and applications => 4.3: Techniques and Applications in High Precision GNSS

340

S4-099

Characteristics of BDS-3 multipath effect and its mitigation methods in precise point positioning

Ran Lu, Wen Chen, Danan Dong, Lei Li, Luyao Huang
East China Normal University

The comprehensive completion of BeiDou Navigation Satellite System (BDS) provides more available satellites and more abundant frequency resources for BDS precise point positioning (PPP) in urban environment. Similar to GPS, multipath effect is also one of the bottlenecks that restrict BDS PPP to achieve decimeter to millimeter positioning accuracy in urban occlusion environment. In addition to the B1I and B3I signals inherited from BeiDou Regional Navigation Satellite System (BDS-2), BeiDou Global Navigation Satellite System (BDS-3) also broadcast new open service signals B1C and B2a. We comprehensively analyze the multipath characteristics of BDS-3 open service signals, and compare them with GPS and Galileo compatible and interoperable signals. Based on the anti-multipath optimal signal, we utilize PPP ionospheric-free combination mode (PPP-IF) to extract the pseudorange and carrier phase residuals of three orbits (GEO, IGSO, MEO) of BDS-3. The results indicate that BDS-3 satellites with different orbital types have different orbital repetition times. Therefore, it is difficult to utilize the time domain repeatability of multipath for BDS-3 multipath mitigation. At present, the method based on multipath spatial domain repeatability has the advantages of simple algorithm, easy implementation and real-time correction of multipath error. Among them, the original multipath hemispherical map (MHM) can only effectively alleviate the low-frequency multipath error, but can not effectively correct the high-frequency multipath inside the grid. The trend surface analysis-based MHM (T-MHM) makes up for the defect of MHM. T-MHM introduces the trend surface analysis method to model the multipath changes within the grid, which effectively alleviates the high- and low-frequency multipath errors. Therefore, this paper proposes a PPP multipath correction method based on T-MHM to alleviate the multipath error of BDS-3. We evaluate the multipath correction effect of T-MHM and analyze the error characteristics of PPP before and after multipath correction. The experimental results show that the positioning accuracy of T-MHM in North, East, Up, and 3D can be improved by 65.6, 79, 69.5, 70.5%, and the convergence time can be reduced by 58.9, 92.9, 89.3, 83.9% in scenes with rich multipath effects.

Key words BDS-3; Precise point positioning (PPP); Multipath mitigation; Spatial repeatability; Trend surface analysis

Category: Symposium 4: Positioning and applications => 4.3: Techniques and Applications in High Precision GNSS

344

S4-100

Measurement of Dynamic Structural Parameters of Super High-rise Buildings Based on Beidou-3 System

Xuece Miao¹、Keliang Ding¹、Qijie Luo²、Tianzong Xue³

1. Beijing University of Civil Engineering and Architecture

2. Yunnan Institute of Water & Hydropower Engineering Investigation, Design and Research

3. China Institute of Geotechnical Investigation and Surveying

After Beidou-3 system is established and put into service, the relevant problems of measuring dynamic structure parameters of super high-rise buildings using Beidou-3 data are explored and studied. Based on the long-term monitoring data of Beidou-3 of Beijing Olympic Tower, this paper analyzes the quality of monitoring data of Beidou-3. Normal time-frequency transform was used to extract structural parameters, and the least square fitting method was used to fit the motion law of the monitoring points. It was obtained that the overall motion of the tower was approximately ellipse under normal conditions, with the amplitude of swing ranging from 3-4mm and the natural frequency ranging from 3-5Hz.

Key words BDS; Normal Time-Frequency Transform; High-rise Building Monitoring; Swing Monitoring; Time Series Modeling

Category: Symposium 4: Positioning and applications => 4.3: Techniques and Applications in High Precision GNSS

371

S4-101

INS/Visual Odometry aided GNSS data gap repairmen in urban environment

Tianxia Liu^{1,2}, Bofeng Li¹, Ling Yang¹

1. Tongji University

2. The Hong Kong Polytechnic University

The high-precise and reliable positioning technology is becoming more and more important for various applications in urban environment. Traditionally, the Global Navigation Satellite Systems (GNSS) can provide high-precise positioning results with carrier phase observations. However, in complex urban environment, the frequent signal blockage and data interruption will lead to frequent re-initialization of the ambiguities hence significantly deteriorate the availability of precise positioning. The initial measurement unit (IMU) that provides short-term high accuracy is often integrated with GNSS to enhance the cycle slip detection and data gap repairmen. However, the systematic bias will rapidly accumulate and significantly hinders its application when long-time GNSS data gap occurs. Thus, in this research, the visual odometry (VO) that provides more stable relative poses with consecutive captured images is involved in the integrated system to enhance the positioning when large GNSS data gap occurs. Moreover, poses provided by the integration of VO/INS are employed as a relative constraint, to avoid the ambiguity re-initialization and to ensure the high-precise and reliable positioning results in GNSS-adverse conditions.

The INS, VO and GNSS are integrated by an Extended Kalman Filter (EKF). The relative pose solved by INS/VO between two adjacent GNSS epochs is employed as a constraint in GNSS cycle slip estimation. Then, the associate ambiguity can be fixed and holden after cycle slip repairmen hence to ensure the high-precise positioning even after a large data gap. Experimental tests with the septentrio AsteRx-i GNSS receiver with an onboard ADIS MEMS and the synchronous stereo Grey Point cameras were carried out. The results show that with the aid of INS/VO, the re-initialization of the ambiguity unknowns are avoids so that the availability of precise GNSS positioning is significantly improved after the GNSS data gap.

Key words GNSS; INS; VO; data gap repairmen

Category: Symposium 4: Positioning and applications => 4.3: Techniques and Applications in High Precision GNSS

382

S4-102

PPP with raw GNSS observation data of smartphones

Marcus Franz Glaner, Klaus Gutleiderer, Robert Weber
Higher Geodesy, TU Wien

Precise Point Positioning (PPP) is one of the most promising processing techniques for Global Navigation Satellite System (GNSS) data and well-established for geodetic receivers. Unlike relative positioning methods, PPP does not rely on nearby reference stations or a regional reference network. PPP is characterized by the use of precise satellite products (orbits, clocks, and biases) and the application of sophisticated algorithms to estimate the user's position. Typically, code and phase observations on multiple frequencies are required to build the ionosphere-free linear combination. Since the release of Android 7.0 in 2016, the raw GNSS measurements of smartphones operating with Android can be accessed. Therefore, the smartphone's GNSS observations are processed directly to estimate the user position with specialized self-developed algorithms and correction data. However, smartphones provide challenging, low-quality GNSS measurements because they are equipped with simple, cost-effective GNSS chips and antennas. Furthermore, they mainly offer GNSS measurements on only one frequency, which prevents to build the ionosphere-free linear combination. In this contribution, we discuss the necessary adaptations of PPP to handle the demanding raw GNSS observations from smartphones in the best way. Therefore, we present various strategies and the application of the uncombined PPP model with ionospheric constraint. This flexible PPP model avoids building the ionosphere-free linear combination, is suitable for any number of frequencies, and allows the utilization of ionosphere models as an ionospheric constraint. In this way, a position accuracy at the decimeter level is achieved. The PPP calculations are performed with our self-developed in-house software raPPPid.

Key words GNSS, PPP, smartphone

Category: Symposium 4: Positioning and applications => 4.3: Techniques and Applications in High Precision GNSS

383

S4-103

On the Potential of Image Similarity Metrics for Comparing Phase Center Corrections

Johannes Kröger, Tobias Kersten, Yannick Breva, Steffen Schön
Leibniz Universität Hannover, Institut für Erdmessung

In order to obtain highly precise and accurate positioning and navigation solutions with GNSS, it is mandatory to take all error sources adequately into account. This includes phase center corrections (PCC), composed of a phase center offset (PCO), elevation-dependent phase center variations (PCV) and a constant part. These corrections are provided by different calibration facilities and are published in the official IGS antenna exchange format (ANTEX) file for several geodetic antennas.

Currently, discussions in the framework of the IGS antenna working group (AWG) are ongoing on how to accept new calibration facilities as an official IGS calibration facility. Therefore, requirements have to be set for comparing different sets of PCC for the same type of antenna.

Since the three-dimensional PCC are usually mapped on a regular grid, they can be interpreted as a two-dimensional image, where the actual grey-scale value of a pixel is equivalent to the metric correction value for a specific azimuth and elevation angle. Therefore, image similarity metrics like the structural similarity (SSIM) index are an appropriate way to describe the differences between different sets of PCC. In this contribution, we present alternative methods to compare PCC at the pattern level. To this end, different measures and concepts are presented which perform independently of the respective datum definition and take care of allowed transformations. Furthermore, the used similarity metrics take the neighbourhood of the respective pixels into account. Consequently, local discrepancies between different sets of PCC can be detected. This can help to reveal weak spots in the calibration procedure which could be caused by insufficient number of observations at a certain area of the antenna hemisphere.

Key words GNSS receiver antennas; phase center corrections; similarity metrics

Category: Symposium 4: Positioning and applications => 4.3: Techniques and Applications in High Precision GNSS

391

S4-104

A de-noising method of landslide deformation monitoring data based on CEEMDAN and enhanced multi-scale permutation entropy

Hao Xu^{1,2,3}、Li Wang^{1,2,3}、Bao Shu^{1,2,3}、Chen Yi^{1,2,3}、Yunqing Tian^{1,2,3}

1. College of Geological Engineering and Geomatics, Chang'an University

2. State Key Laboratory of Geographic Information Engineering

3. Key Laboratory of Western China's Mineral Resources and Geological Engineering

In order to solve the problems of inaccurate analysis and low prediction accuracy of landslide deformation caused by the interference of various noises in GNSS monitoring data, a new method based on Complete Ensemble Empirical Mode Decomposition with Adaptive Noise (CEEMDAN) and Enhanced Multi-scale Permutation Entropy (EMPE) is proposed in this study. Firstly, the landslide monitoring data series are decomposed by CEEMDAN to obtain multiple intrinsic mode functions (IMF). Second, calculate the EMPE value of each IMF to determine the high and low frequency boundary value C . Finally, we use wavelet analysis to denoise the high frequency IMF, and reconstruct the denoised signal with the low frequency IMF to get the denoising result. The results of simulation signals and GNSS monitoring data of Faer landslide show that the RMSE and SNR of denoised data are better than those of empirical mode decomposition method and wavelet denoising, which can provide reliable basis for subsequent deformation analysis and prediction research.

Key words CEEMDAN;Enhance multi-scale permutation entropy;Landslide monitoring;De-noising

Category: Symposium 4: Positioning and applications => 4.3: Techniques and Applications in High Precision GNSS

422

S4-105

Methods and assessments on the integration of inter-satellite differential BDS PPP and INS

Yu Min、Jie Lv、Qiaozhuang Xu、Zhouzheng Gao

School of Land Science and Technology, China University of Geosciences Beijing

Currently, BeiDou Navigation Satellite System (BDS) has got the capability to provide both standard positioning service and precise positioning service for users over the world. Wherein, the Precise Point Positioning (PPP) based on the information from B2b frequency, has been one of the hottest research topics after July 2020. However, its drawbacks such as slow initial positioning accuracy, long re-convergence time, and signals easily unlocked will lead to low reliability and continuity. In order to overcome some of those drawbacks in conventional PPP mode, this paper firstly introduces the inter-satellite differential into BDS ionosphere-free combination measurements, which is to eliminate the receiver related common errors and upgrade the initial positioning accuracy and improve the re-convergence time. Besides, Inertial Navigation System (INS) is furtherly adopted to integrate with PPP, which forms a new inter-satellite differential BDS PPP/INS integration system with providing a capability to bridge the BDS solutions before and after outages. This benefits from the characters of high-accuracy in short-term and autonomous navigation without external observations of INS. In this paper, the methods of inter-satellite differential BDS PPP/INS integration are described in detail and evaluated by sets of experiment data. According to the results, it can be found that the convergence time and initial positioning accuracy can be improved significantly by using the proposed BDS PPP model comparing with that of conventional PPP mode. Then, the positioning accuracy of the proposed integration method is consistent with those of inter-satellite differential PPP under the open-sky conditions. However, the performance of the integration method could be improved visibly while suffering satellites signal partial/complete outages.

Key words BeiDou Navigation satellite system (BDS); inter-satellite differential; Precise Point Positioning (PPP); Inertial Navigation System (INS)

Category: Symposium 4: Positioning and applications => 4.3: Techniques and Applications in High Precision GNSS

423

S4-106

A DIA Method based on Maximum A Posteriori Estimate for Multiple Outliers

Yangkang Yu, Yang Ling, Yunzhong Shen
Tongji University

The DIA method based on datasnooping (DIA-datasnooping) is commonly used for the detection, identification and adaptation of the outlier or mismodelling errors in Gauss-Markov model. However, effectiveness of the DIA-datasnooping usually degrades when dealing with multiple outliers.

Since the DIA for multiple outliers would be hampered by overfitting and masking effects. On the one hand, if the maximum number of outliers to be detected is large, the statistical test tends to declare more outliers than there are. On the other hand, multiple outliers can mask each other easily, which increases the difficulty of detection and identification. In this paper, the Maximum A Posteriori estimate (MAP), a classic Bayesian statistic approach, is applied to the DIA estimator, and the DIA based on MAP (DIA-MAP) method is proposed. Based on the prior distribution of outliers, the alternative hypothesis with the max posterior probability can be derived via DIA-MAP. Compared to the conventional DIA-datasnooping method, the proposed DIA-MAP outperforms on following aspects. Firstly, the prior of outlier model is introduced to handle the model selection among multiple alternative hypotheses with different suspected outlier numbers. Secondly, the prior could be adjusted flexibly according to the specific geodetic applications, rather than fixing to uniform distribution. Besides, a set of new confidence level indices is introduced for multiple outliers, which concerns both the correct detection of all outlying observations and the correct acceptance of each normal observation. Experimental results of a GNSS Single-Point Positioning example verified that performance of the proposed DIA-MAP method is superior to the DIA-datasnooping when dealing with multiple outliers. There are around 20%, 50% and 60% improvement when the outlier size is 20 times of the observation std, the outlier occurrence probability is 0.01, 0.05 and 0.1 respectively.

Key words Detection, Identification and Adaption (DIA); datasnooping; Maximum A Posteriori estimate;

Category: Symposium 4: Positioning and applications => 4.3: Techniques and Applications in High Precision GNSS

432

S4-107

Antarctic GNSS station of the National Geographic Institute of Spain. Geodetic purposes

Esther Azcue, Unai Quintana, Sergio Calvo, Víctor Puente
National Geographic Institute of Spain

The National Geographic Institute of Spain participated in the 2020 Antarctic Campaign with the aim of installing a GNSS permanent station named BJCI, close to the Spanish Antarctic Base Juan Carlos I in Livingston Island.

This permanent station was conceived as a multipurpose station whose data will be used in different, geodetic and non geodetic, applications.

The installation process, status, future goals and scientific purposes of BJCI station will be presented in the following publication.

Key words GNSS station Antarctica

Category: Symposium 4: Positioning and applications => 4.3: Techniques and Applications in High Precision GNSS

434

S4-108

A new strategy of tropospheric gradient estimation and its application in GNSS PPP

Di Zhang¹、Fei Yang²、Lv Zhou³、Jiming Guo¹

1. School of Geodesy and Geomatics, Wuhan University

2. College of Geoscience and Surveying Engineering, China University of Mining and Technology-Beijing

3. College of Geomatics and Geoinformation, Guilin University of Technology

Horizontal gradients have been used to model the asymmetry part of the tropospheric delay for decades. However, due to the similarity of the hydrostatic and wet gradient mapping functions, only the total gradient parameters can be estimated in most GNSS analyses. In this paper, hydrostatic and wet gradient parameters were estimated separately, together with coefficients of mapping function based on ray-traced tropospheric delays derived from the high spatio-temporal resolution NWM. Compared with an estimation of total gradients parameters, the accuracy of fitted slant delays is improved significantly. In GNSS PPP, by fixing the ZHD and hydrostatic gradients derived from ray-traced delays as a priori value, the ZWD and wet gradients were estimated as a random walk. Results show that the novel methodology's positioning accuracy, especially the height repeatability, is superior to the traditional strategy.

Key words tropospheric gradient; PPP; ray-trace; NWM; random walk

Category: Symposium 4: Positioning and applications => 4.3: Techniques and Applications in High Precision GNSS

436

S4-109

Research on LEO constellations enhancing GNSS orbit determination and precise point positioning

junjun yuan^{1,2}、shanshi zhou¹、xiaogong hu¹、kai li¹、min liao¹

1. Shanghai Astronomical Observatory, Chinese Academy of Sciences

2. University of Chinese Academy of Sciences

The multi-navigation constellations represented by GPS/GLONASS/GALILEO/BDS are constantly building and updating. To meet the need of modernization of navigation satellites and provide high-precision Positioning Navigation and Timing (PNT) service, it is necessary to further improve the orbit determination accuracy of GNSS satellites. On the other hand, Precise Point Positioning (PPP) technology needs to solve the problems of slow convergence time and unavailability in special environment, such as city canyons or indoor environment. Low Earth Orbit (LEO) satellites operating in 200~2000 km are expected to solve those issues with multi-source spaceborne GNSS observations, rapid spatial structure change and high intensity signal.

Firstly, we use LEO satellites as space-based stations and process the integrated data of LEO and ground-stations to determinate precise GPS orbit. When we just use 48 ground stations, the average RMS precision at R, T, N and 3D direction is 5.43, 11.91, 8.40, 15.57 cm respectively. After adding one LEO (GRACE-A) data, the average RMS precision at R, T, N and 3D direction is 4.97, 9.43, 6.66, 12.58 cm respectively, with increasement by 8.46%, 20.69%, 20.27%, 19.01% respectively. After adding two LEO (GRACE-A&B) data, the average RMS precision at R, T, N and 3D direction is 4.89, 9.08, 6.56, 12.23 cm respectively, with increasement by 9.97%, 23.59%, 21.49%, 21.21% respectively. The results show that the GPS Orbit is significantly improved by adding LEO data. Then, we verify the possibility of using GPS/LEO satellites to provide high-precision, real-time PNT service with simulation data. When we only use GPS observations from ground-stations, the final position precision in N, E, U direction is 0.040, 0.013, 0.045 m and the convergence time is 18 min. After adding one LEO's observations, the final position precision in N, E, U direction is -0.038, 0.022, 0.034 m and the convergence time is 8.4 min. After adding two LEO's observations, the final position precision in N, E, U direction is 0.010, 0.014, 0.017 m and the convergence time is 4.8 min. Obviously, the combination of GNSS and LEO data can help ground PPP users reduce convergence time and improve positioning accuracy. This study can provide reference for exploring more functions of LEO satellites.

Key words LEO; GNSS; navigation enhancement; orbit precision; PPP

Category: Symposium 4: Positioning and applications => 4.3: Techniques and Applications in High Precision GNSS

453

S4-110

The mean dynamic topography model MDTVN2020 on Vietnam sea surface

Thanh Thach Luong¹、 An Dinh Nguyen²、 Van Hai Tran²、 Dinh Thanh Nguyen³、
Nhưng Le Thi^{4,1}

1. Hanoi University of Natural Resources and Environment, Vietnam

2. Surveying and Aerial Mapping Co., Ltd, Vietnam

3. Vietnam Association of Geodesy, Cartography and Remote Sensing

4. GFZ German Research Centre for Geosciences, Potsdam, Germany

The Vietnam sea surface is located in a highly complex tidal area with variations in surface waves, internal waves, and currents. Thus, using a local topography model as the basis of geographic information to adjust depth measurements is necessary. In this study, we establish the Mean Dynamic Topography Model MDTVN2020 as a national reference system to transfer seabed topographic measurements, manage national marine geographic information systems, and connect with Southeast Asia regional seabed topographic maps. Based on the relationship between the global gravity geopotential and the local closest to the mean sea surface at the “0” tide gauge station - HONDAU in Vietnam, we transfer the global mean dynamic topography model (DTU15MTD) to the national mean dynamic topography model. The ArcGIS software is applied to match the local mean dynamic topography model to the global mean sea surface based on 98 tide gauge stations across the coastline and small islands in Vietnam. We use independently 23 tidal monitoring stations observed continuously for 30 days to evaluate the accuracy of the MDTVN2020 model. Based on statistic algorithms, we detect and adjust the systematic errors due to transferring DTU15 MDT to MDTVN2020. The algorithm of spline with barriers is also applied to map the MDTVN2020 model with the average accuracy of ± 0.075 m. The MDTVN2020 model is presented on a 1:2000000 scale map with grids of 1' x 1'. The findings of the study contribute to the national database for the management of marine natural resources and research of the continental shelf.

Key words Mean Dynamic Topography, Mean Sea Surface, Tide Gauge Station, MDTVN2020

Category: Symposium 4: Positioning and applications => 4.3: Techniques and Applications in High Precision GNSS

472

S4-111

An improved tropospheric mapping function modeling method for space geodetic techniques

Yaozong Zhou, Yidong Lou, Weixing Zhang, Jingna Bai, Zhenyi Zhang
GNSS Research Center, Wuhan University

Tropospheric mapping function modeling method determines the modeling accuracy of mapping functions, and is very important for space geodetic data processing and applications. In the past decades, the 'fast' method instead of the rigorous least-square methods was dominantly used for the development of mapping functions, such as the Vienna Mapping Functions 1 (VMF1) and VMF3, considering the convergence issue and computation efficiency. We reconsidered the suitability of the rigorous least-square methods in operational mapping function development, and presented a new mapping function modeling method where the number of to-be-estimated coefficients in the mapping function continued fraction is automatically determined according to the convergence in the least-square fitting. The modeling accuracy of the new method was evaluated during Global Positioning System (GPS) week 2130 at globally distributed 905 Global Navigation Satellite Systems (GNSS) stations. Significant improvement of the new method to the 'fast' method was found, with hydrostatic and wet mapping function modeling Mean Absolute Errors (MAEs) of about 0.3 and 0.4 mm for the new method, and of about 2.2 and 2.5 mm for the 'fast' method, respectively. Multi-GNSS Precise Point Positioning (PPP) of the new method was conducted at 115 International GNSS Service (IGS) Multi-GNSS Experiment (MGEX) stations. Effectiveness of the new method was also found for the PPP station height and zenith total delay estimation. The new method is therefore recommended for new mapping function development for pursuing higher accuracy in the future.

Key words Space geodetic technique; Tropospheric mapping function; Modeling method; Modeling accuracy; Multi-GNSS PPP

Category: Symposium 4: Positioning and applications => 4.3: Techniques and Applications in High Precision GNSS

476

S4-112

Multi-GNSS code biases: from the perspectives of DCB and OSB

Fei Guo, Yuanfan Deng, Xiaohong Zhang
School of Geodesy and Geomatics, Wuhan University

The proper handling of code biases is essential for realizing precise ionospheric modeling, positioning and timing. It is common to treat code biases in a differential mode as a differential code bias (DCB). Firstly, a new series of (over 20 types of) DCBs is derived from BDS multi-frequency and multi-channel signals. Due to the influence of error propagation, the accuracy and reliability of DCB obtained by linear transformation are not as good as DCB estimated directly. With the modernization of GPS and GLONASS and the implementation of Galileo and BDS, the traditional DCB calibrations are complex and not easily extendable to different frequencies and modulations. An alternative treatment of code biases is to use observable-specific signal biases (OSBs). In this contribution, all possible OSBs are estimated for the latest GNSS and analyzed from the perspectives of precision, consistency and stability. The precisions of the GPS and Galileo OSBs are significantly better than those of the GLONASS and BDS OSBs. Considering the inter-frequency bias (IFB) of GLONASS and the inter-system bias (ISB) of BDS can improve the precisions of their OSB estimates. OSB comparisons among different agencies reveal that GPS and Galileo show good agreement at the level of 0.2-0.3 ns, while the differences of the GLONASS and BDS OSBs reach 0.5-1.0 ns. In addition, agreement of 0.4-0.5 ns is demonstrated for IGSO and MEO OSBs, while the consistency of GEO OSBs is worse by a factor of 2-3. The stability of the OSB estimates is at the level of 0.03-0.09 ns for GPS, 0.10-0.25 ns for Galileo, 0.14-0.48 ns for GLONASS, and 0.16-0.44 ns for BDS. In general, the BDS-3 OSB estimates show better stability than the BDS-2 OSBs. Moreover, the code biases at the same or at a close central frequency show similar performance. This is particularly obvious for Galileo and BDS, which adopt the dual-frequency constant envelope multiplexing (DCEM) technique.

Key words Multi-GNSS; code bias; Observable-specific signal bias (OSB); Inter-frequency bias (IFB); Inter-system bias (ISB)

Category: Symposium 4: Positioning and applications => 4.3: Techniques and Applications in High Precision GNSS

487

S4-113

Precise Orbit Determination of Low, Middle and High Satellite Network Based on Regional Ground Stations

Xuwen Gong、Jizhang Sang、Fuhong Wang、Xingxing Li
Wuhan University

In recent years, with the gradual upgrade and deployment of Global Navigation Satellite Systems (GNSS) such as GPS, GLONASS, Galileo and BDS on the medium and high Earth orbits (MEO/HEO), the development of multi-purpose low Earth orbit (LEO) constellation has gradually become a research focus in various countries. The navigation augmentation to the existing GNSS is a core service capability of such a LEO constellation. Being used as a position reference of GNSS navigation and LEO augmentation system, the high-precision orbits of satellites are fundamental for the navigation performance enhancement, and it would require a globally well-distributed network of a large number of ground tracking stations (GTS). However, for China to deploy and maintain a global GTS network could be difficult due to unreasonable international concerns and possible adverse interference.

Hence, this research focuses on the precise orbit determination (POD) of all satellites in the HEO/MEO/LEO network (HML-Net) based only on a regional GTS network. The designed POD solution purses all GNSS satellites and some LEO satellites in an integrated orbit determination (IOD) manner by multi-level data fusion of GNSS observations from a China-region GTS network and those IOD-participating LEO satellites, Inter-Satellite-Links (ISL) ranging measurements between GNSS satellites, Ka-Band Ranging (KBR) measurements between LEO satellites, and Satellite Laser Ranging (SLR) observations, etc.. And then, based on the GNSS orbit and clock products generated in the first step, each of the remaining LEO satellites is processed individually in the POD process to obtain their highly precise orbits. Key factors limiting the accuracy of GNSS/LEO IOD only with regional GTSS and LEO POD with the inaccurate GNSS ephemeris are raised and analyzed in detail. Accordingly, a series of processing refinement methods are proposed to deal with these factors. On the basis of the refined processing methods, a complete POD experiment of the entire satellite network is performed by using GTS/LEO/ISL/KBR/SLR real data. The results show that, with several (5~8) regional GTSS, the average orbit accuracy of the GEO/IGSO/MEO/LEO satellites could reach 5~15 cm level. The methods and experiments in this research are helpful for the construction of space-based reference frame with regional ground stations in the future.

Key words HEO/MEO/LEO satellite network; integrated precise orbit determination; multi-level data fusion; refined processing method; space-based reference frame

Category: Symposium 4: Positioning and applications => 4.3: Techniques and Applications in High Precision GNSS

491

S4-114

A method to compensate for the missing of real time phase bias products from CNES

Shi Du¹、Guanwen Huang¹、Yulong Ge³、Bao Shu¹

1. Chang' an University

2. Nanjing Normal University

With the real-time (RT) multi-frequency phase bias products for multi-GNSS constellations, which are provided freely by the Centre National d'Etudes Spatiales (CNES). The RT precise point positioning (RT-PPP) with ambiguity resolution (AR) technique has changed from theory to reality. However, because of the unstable network transmission, bandwidth delay and incomplete service product, the RT phase biases products are frequently missing. There are generally three kinds of missing cases: 1) all RT phase biases products of all satellites in all constellations are lost in a short time, which will lead to the re-convergence of positioning; 2) some satellites have no RT phase biases in some epochs, which may make positioning results of corresponding epochs suddenly jitter; 3) The RT phase biases of some satellites are missing for a long time. If the number of satellites involved in the positioning is too low in this period, the positioning accuracy will be significantly affected. Therefore, it is very necessary to propose a simple and effective method to compensate the RT phase biases product missing. In this paper, 35 days of CNES RT phase biases products are used to calculate the data integrity rate, and analyze the stability of the RT phase biases products by using different sliding windows. According to the statistical results, the size of the sliding window of the phase biases of different navigation systems is different. Using the above method, we conduct the RT-PPP with AR ambiguity of different systems in 50 MGEX stations for 35 days. The statistical results show that compared with the positioning results without RT phase biases compensation, the above method can effectively avoid the impact of RT phase biases product missing. At the same time, the fixed rate of ambiguity and positioning accuracy are improved.

Key words PPP; PPP-AR; CNES

Category: Symposium 4: Positioning and applications => 4.3: Techniques and Applications in High Precision GNSS

509

S4-115

Triple-frequency ambiguity resolution of BDS/Galileo precise point position with raw GNSS data

Jin Wang¹、Shengli Wang²

1. Shandong University of Science and Technology, College of Geodesy and Geomatics

2. Shandong University of Science and Technology, College of Ocean Science and Engineering

Multi-frequency and multi-GNSS Precise Point Positioning (PPP) is an available method to obtain the high precision global location service. The critical processing of providing reliable and stable positioning is Ambiguity Resolution (AR) technology. To achieve ambiguity-fixed solutions, the Fractional Cycle Biases (FCBs) should be corrected to recover the integer characters of float ambiguities. For conventional approach, the wide-lane and narrow-lane ambiguities are adopted to fix the dual-frequency ionosphere-free combined ambiguity. To flexible realize the multi-frequency ambiguity resolution, the uncombined method using raw GNSS data is proposed to estimate the FCBs and achieve triple-frequency PPP AR. In this study, the uncombined float ambiguities on each frequency are estimated from the undifferenced and uncombined PPP model. These raw float ambiguities are recombined with the integer coefficient vector, proposed as (4, -3, 0), (1, -1, 0), (0, 1, -1) which are named as Narrow-Lane (NL), Wide-Lane (WL), Extral-Wide-Lane (EWL) combinations, respectively, to be the measurements of FCBs estimation. For BDS and Galileo data, the variations of Inter-Frequency Clock Biases (IFCBs) are neglected. The triple-frequency FCBs of BDS and Galileo are estimated with the supplementary of dual-frequency GPS FCBs. The FCBs accuracy is firstly evaluated by the RMS of posterior residuals. For BDS, the RMS is 0.063, 0.091, 0.020 cycle for NL, WL, EWL combinations, respectively. For Galileo, it is 0.058, 0.045, 0.005 cycle for NL, WL, EWL combinations, respectively, which is performed better than that of BDS. Then, the PPP AR is processed with GPS, BDS and Galileo FCBs using 29 stations from MGEX. For triple-frequency PPP AR, the convergence time is 55.5 minutes for BDS which is improved 45.0% compared with float solutions, and is 12.5 minutes for Galileo which is improved 39.0% compared with float solutions. The positioning accuracy is 3.6 cm for BDS PPP AR which is improved 41.5% compared with float solutions 6.2 cm, while it is 1.5 cm for Galileo which is improved 26.5% compared with float solutions 2.1 cm. For ambiguity

fixing success rate, it is 95.6% and 90.5% for BDS and Galileo after 1-hour positioning, respectively.

Key words Triple-frequency Precise Point Positioning; BDS; Galileo; Fractional Cycle Bias; Ambiguity Resolution

Category: Symposium 4: Positioning and applications => 4.3: Techniques and Applications in High Precision GNSS

510

S4-116

Improvement of ISLs on BDS-3 Orbit Determination and Time Synchronization

Xia Ren¹, yufei Yang²

1. Xi'an Research Institute of Surveying and Mapping
2. Beijing Satellite Navigation Center

Inter-satellite Links are newly equipped payloads on BDS-3 satellites with ranging and communication functions. ISLs contribute to the improvement of BDS-3 standard positioning and timing performance, and the implementation of global services, such as global short message communication service, MEO satellite-based search and rescue service. This paper mainly analyzes the contribution of ISLs to the improvement of BDS-3 orbit determination and time synchronization. The results show that, with only regional tracking stations, the accuracy of BDS-3 estimated orbits is 0.6 m, and that of the predicted orbits is 0.75 m. With the support of ISLs, the accuracy of determined and predicted orbits is 0.25 m and 0.23 m, respectively. The improvement of ISLs on orbit determination is 50% to 60%. For time synchronization, the average standard deviation of the broadcast clocks is 0.55 ns.

Key words BDS-3, inter-satellite link, orbit determination, time synchronization

Category: Symposium 4: Positioning and applications => 4.3: Techniques and Applications in High Precision GNSS

512

S4-117

Precise Orbit Determination of CubeSats Using a Proposed Observations Weighting Model

Amir Allahvirdizadeh, Ahmed El-Mowafy

School of Earth and Planetary Sciences, Curtin University, Perth, Australia

CubeSats are small low-cost and low-power satellites that can be used for many space missions. Some missions require precise location determination of the CubeSats, such as radio-occultation, Interferometric Synthetic Aperture Radar (InSAR), satellite altimetry, and gravity field recovery. Therefore, precise orbits and clocks of CubeSats are essential to achieve the required accuracy. They are also essential for future mega-constellations Low Earth Orbit (LEO) satellites that are proposed as augmentation systems for positioning and navigation. The Precise Orbit Determination (POD) methods are well developed for large LEO satellites during the last two decades. However, CubeSats are mainly built from commercial off-the-shelf (COTS) components and have their own characteristics, which need new investigations. In this paper, seventeen 3U-CubeSats, launched in different orbits in the Spire Global Constellation, are analyzed in terms of precise orbits and clocks. The orbits generated from both the reduced-dynamic and the kinematic POD methods are validated internally with the overlap analysis, the posterior covariance factors, and the residuals. One-month processing of these CubeSats revealed that around 90% of precise orbits have decimeter accuracy, while 50% are at centimeter-level. This accuracy fulfills most of the abovementioned space and earth science applications. The limitations in using elevation-dependant weighting models for CubeSats POD are discussed and, as an alternative, a weighting model based on signal-to-noise ratio has been proposed and tested. The impact of crossing CubeSats from the eclipse region, as well as the near-filed multipath due to the CubeSat structure and the signal direction in space, are also considered in the proposed weighting model. Results show improvement in the POD accuracy and residuals.

Key words CubeSats, Precise Orbit Determination, Weighting Model, Mega-Constellations LEO Satellites

Category: Symposium 4: Positioning and applications => 4.3: Techniques and Applications in High Precision GNSS

514

S4-118

Robust RTK method for short baselines with high sample rate

Zhiteng Zhang、Bofeng Li
Tongji University

Real-time kinematic (RTK) positioning is a commonly used high-precision positioning method outdoors. Unmodelled errors such as multipath delays always degrade the positioning performance of RTK. This paper proposes an RTK method by imposing the curve constraints amongst multiple epochs. For the new method, high-precision coordinates of next epochs are predicted based on the curve constraints to improve the positioning performance. The covariance matrix of RTK positioning and the covariance matrix of the coordinate differences between adjacent epochs are derived. Based on which, the improvements of RTK precision and stability and the ability for resisting multipath delays are deeply analyzed. The Finally, some real data are utilized to illustrate the performance of RTK results of the new method. The results confirm that the proposed curve-constrained RTK method is robust to multipath delays and can realize the RTK positioning with 1mm between-epoch relative accuracy.

Key words Real-time Kinematic, curve constraint, robust, relative accuracy, multipath

Category: Symposium 4: Positioning and applications => 4.3: Techniques and Applications in High Precision GNSS

528

S4-119

Comprehensive assessment Precise position and velocity determination for airborne gravimetry over long baselines

Min Li, Tianhe Xu
Shandong University

In an airborne gravimetry experiment, precise position is critical for all measuring instruments mounted on the same platform, and accurate velocity especially the upward component is used to separate the GNSS oscillation acceleration from the gravity measurements. This paper first comprehensively evaluated the performance of precise position and velocity determination with BeiDou global navigation system (BDS) and integrated GPS/GLONASS/Galileo/BDS. In this contribution, we propose an extended PPP method which is independent of precise clock information as the satellite clock offsets and drifts are estimated "on-the-fly" with a wide network of stations. This approach is based on a stand-alone receiver and is especially suitable for positioning in remote areas such as in the pacific ocean, Antarctica or Arctica where there is a sparse distribution of reference stations. A static multi-GNSS experiment demonstrates that the estimated BDS clock offsets and drifts are in good accordance with the IGS MGEX orbits inside the network. Results show that the accuracy of the estimated velocity by BDS-only solutions can be within 1 mm/s and is comparable with GPS. This approach has better performance both than the double-difference and PPP approaches when applied in a long baseline over than 2000 km. Kinematic vertical velocity with accuracy of mm/s can be achieved with four-system observations.

Key words PPP; differential GPS; position; velocity; clock offsets and drifts; airborne gravimetry

Category: Symposium 4: Positioning and applications => 4.3: Techniques and Applications in High Precision GNSS

534

S4-120

Recognition of periodic signals in coordinate time series from GPS, GLONASS, and Galileo Precise Point Positioning

Radosław Zajdel, Kamil Kaźmierski, Krzysztof Sońnica
Wrocław University of Environmental and Life Sciences

Periodic signals in the GNSS-derived global geodetic parameters should reflect mainly the well-known phenomena such as unmodelled solid Earth tides, residual ocean tidal and non-tidal loading, atmospheric pressure loading. However, the time series of the GNSS-based parameters also contains effects of inadequate satellite orbit modelling, the errors in the background models, or multipath. The orbit modeling errors reveal the periods strongly related to the orbital characteristics of individual GNSS constellations, especially the satellite revolution period and the GNSS draconitic year.

This contribution examines the sub-daily coordinate spectral characteristics for 15 GNSS sites, based on the time series of site coordinates estimated every 30 seconds using Precise Point Positioning for GPS, GLONASS, and Galileo observations. Depending on the GNSS constellation used, the coordinate time series are affected by spurious signals with the periods arising from the linear combination of satellite revolution and Earth rotation periods. The strong spurious signals appear with the periods of 95.7 h, 21.3 h, 10.6 h, 7.4 h for GLONASS, and 59.8 h, 34.2 h, and 17.1 h for Galileo, and ~24 h, ~12 h, ~8 h for GPS. The unmodeled GNSS-related sub-daily signals with amplitudes up to 15 mm propagate into the most commonly used 24 h solutions. The propagated aliased signals are mainly visible close to 2.5 days, 8 days, and annual/semi-annual periods for Galileo, GLONASS, and GPS estimates, respectively. The amplitudes of the aliased signals reach up to 10 mm for GLONASS and single millimeters for both GPS and Galileo.

The periodic signals discussed in this contribution are entirely a function of the orbital design of GNSS constellations, the existence of orbital errors, and the selection of the processing session length. However, the presence of spurious signals in the GNSS time series can lead to erroneous findings when recovering geodynamical signals.

Key words PPP, GPS, GLONASS, Galileo, systematic errors, multi-GNSS

Category: Symposium 4: Positioning and applications => 4.3: Techniques and Applications in High Precision GNSS

535

S4-121

An ADOP-based integrating multi-GNSS algorithm for fast and high-precision positioning

Xin Liu、 Shubi Zhang、 Qiuzhao Zhang
China University of Mining and Technology

The multiple global navigation satellite systems (multi-GNSS) can improve the positioning accuracy and success rate. However, its large number of visible satellites makes the positioning more time-consuming. Hence, how to use the useful observed information of multi-GNSS to achieve the fast and high-precision positioning with large success rate is an urgent problem. The single-frequency single-epoch (SFSE) positioning performances of global positioning system (GPS), Beidou navigation satellite system (BDS), and Galileo system are analysed firstly. By introducing ambiguity division of precision (ADOP), a novel integrating multi-GNSS positioning algorithm based on ADOP is proposed to address the above problem of multi-GNSS. The BDS and Galileo satellites with highest elevation angle are added to GPS until the ADOP of the GPS and the added satellites satisfies the given ADOP. The SFSE relative positioning experimental results of GPS, BDS, and proposed method show that the proposed algorithm can achieve the success rate 100.0%, which can improve the SFSE success rate of single system; it can achieve high positioning accuracy close that of multi-GNSS; it can realize fast positioning and greatly improve the positioning efficiency of multi-GNSS by larger than 50.0%.

Key words ADOP, Multi-GNSS, Fast and high-precision positioning, success rate

Category: Symposium 4: Positioning and applications => 4.3: Techniques and Applications in High Precision GNSS

536

S4-122

Performance Analysis of Multi-GNSS Real-Time Kinematic Timing

Baoqi Sun^{1,3,4}、 Jiawei Liu^{1,3,4}、 Xiaosong Dong^{2,1,3}、 Zhe Zhang^{1,3,4}、 Haiyan Yang^{1,3}、
Xuhai Yang^{1,3,4}

1. National Time Service Center, Chinese Academy of Sciences

2. Shandong University of Technology

3. Key Laboratory of Precise Positioning and Timing Technology, Chinese Academy of Sciences

4. University of Chinese Academy of Sciences

Time plays an important role in modern society. The new technologies such as the new generation of wireless communication put forward higher requirements for the precision of time synchronization. Similar to real-time kinematic positioning which has been widely used, real-time kinematic timing can also be carried out based on GNSS. This timing method can achieve sub-nanosecond accuracy by using the carrier phase observations. Because GNSS real-time kinematic timing only uses broadcast ephemeris, and does not rely on precise ephemeris, it is more convenient for users to implement. GNSS real-time kinematic timing can provide a high-precision and low-cost solution for time synchronization between reference stations in 5G network, indoor positioning, Internet of Things and other fields. Using the multi-day observation data of the receivers at time laboratories, the multi-GNSS real-time kinematic timing experiment over short baselines was carried out. The timing precision and convergence time under different constellation combinations and different user dynamic modes were analyzed.

Key words Carrier phase, precise timing, broadcast ephemeris, real-time kinematic, multi-GNSS

Category: Symposium 4: Positioning and applications => 4.3: Techniques and Applications in High Precision GNSS

538

S4-123

A simplified reduced dynamic orbit determination for LEOs with orbit variation constraints

Shoujian Zhang¹、 Jiancheng Li¹、 Geng Gao²、 Kemin Zhu¹、 Hui Wei¹

1. Wuhan University

2. WU

Dynamic orbit determination is the most precise orbit determination method for Low Earth Orbit (LEO) satellites, currently. In the method, all kinds of force models must be handled precisely, which leads to the complicated data processing. In this contribution, we proposed a new simplified reduced dynamic orbit determination. Firstly, we derived the second-order time-differenced orbit variations from three-consecutive point-wise accelerations. Then, the above equations are treated as constraints of the geometric observations. The constraint equations between orbits and accelerations have the same function with the traditional equation of satellite motion, but is more simplified. Theoretical and numerical analyses show that, in order to obtain orbit variation at the level of 1 cm accuracy for 30 s sampling interval, only forces with magnitude greater than 10^{-5}m/s^2 are required. Thus, non-conservative forces, like solar radiation pressure and atmospheric drag can be ignored. At last, we solved orbits for GRACE using one week GPS observations, results illustrated that the orbits of the simplified reduced dynamic method are more precise and smoother than the kinematic solution. Compared with the JPL scientific orbits, the RMS of the orbits are 1.5, 1.5 and 2.0 cm in radial, along and cross directions, respectively. Results showed that the proposed method could be an alternative orbit determination method for LEOs.

Key words POD, acceleration constraint, GRACE

Category: Symposium 4: Positioning and applications => 4.3: Techniques and Applications in High Precision GNSS

547

S4-124

GNSS real-time troposphere monitoring

Jan Douša, Pavel Václavovic

Research Institute of Geodesy, Topography and Cartography

Near real-time GNSS double-difference network processing is a traditional method still used within the EUMETNET EIG GNSS Water Vapour Programme (E-GVAP) for the atmosphere water vapour content monitoring in support of Numerical Weather Prediction. The standard production relies on estimating zenith tropospheric path delays (ZTDs) for GNSS ground stations with a 1h time resolution and a latency of 90 minutes. The Precise Point Positioning (PPP) method applied in real-time mode has recently reached the reliability and the accuracy fully comparable to the near real-time solution. The effectiveness of the PPP method relies on exploiting undifferenced observations from individual receivers, thus optimal use of tracking systems and signal bands, a possible in-situ processing, a high temporal resolution of all estimated parameters (e.g. 5-min) and almost no latency. The solution may implicitly include horizontal tropospheric gradients and slant tropospheric path delays for enabling the monitoring of a local asymmetry of the troposphere around each individual site. We have been estimating ZTD and gradients in real-time continuously since 2015 with a limited number of stations. Recently, the solution has been extended to a pan-European and global production consisting of approximately 200 stations. We implemented an 'all-in-one' processing strategy including multi-GNSS PPP for both real-time and near-real time modes for simultaneously estimating ZTDs, gradients and slant path delays. The solution has been operationally submitted to the E-GVAP since May 2021 and provides the basis for the development of specific fog and storm demonstrators.

Key words GNSS, real-time, troposphere

Category: Symposium 4: Positioning and applications => 4.3: Techniques and Applications in High Precision GNSS

551

S4-125

Comparison of the RAIM availability performance of the maximum value method and the matrix maximum eigenvalue method under the condition of double-satellite faults

Xiaping Ma¹、Qinzhen Li²、Ershen Wang³、 Xiaoxing He ⁴

1. Xi'an University of Science and Technology

2. Southwest Jiaotong University

3. Shenyang Aerospace University

4. Jiangxi University of Science and Technology

Receiver Autonomous Integrity Monitoring (RAIM) fault monitoring and identification needs to judge the geometric distribution of currently visible satellites based on performance indicators, and determine whether it is suitable for integrity monitoring, that is, to determine the availability of the RAIM algorithm. On the basis of summarizing the existing Matrix Maximum Eigenvalue Method (MMEM) of RAIM availability evaluation, the mathematical model in the existing RAIM availability method under double-satellite faults conditions is improved, and the extremes of Maxima Method (MM) of RAIM availability evaluation are proposed. Maxima Method (MM). Based on the GNSS measured data provided by 8 tracking stations in China provided by the International GNSS Monitoring & Assessment System (IGMAS) on May 1, 2021, the two methods are used to calculate the Horizontal Protection Level (HPL) under the condition of double-satellite faults, to compare and analyze the RAIM availability performance of BDS. The results show that in China, the RAIM availability of BDS double-satellite faults calculated by these two methods can meet the needs of Non-precision Approach (NPA), Terminal, Route and Ocean; overall the RAIM availability of MM calculation is lower than that of MMEM calculation, HPL calculated by MM is about 4m larger than MMEM on average, and it takes more time. The MM-based RAIM availability evaluation method has rigorous theory, simple mathematical model, and easy to program design. It is another RAIM availability evaluation method outside of MMEM.

Key words Double-satellite faults; RAIM Availability; MM; MMEM; HPL

Category: Symposium 4: Positioning and applications => 4.3: Techniques and Applications in High Precision GNSS

569

S4-126

LEO's Contribution on Ambiguity and Positioning Convergence in Urban Canyons

Yanning Zheng、Bofeng Li、Haibo Ge
Tongji University

Low Earth Orbit (LEO) enhanced Global Navigation Satellite System (LeGNSS) has been a research hot spot of the next-generation of navigation system. Currently, most LeGNSS Precise Point Positioning (PPP) simulations show that the convergence time can be significantly shortened compare to that of GNSS PPP. However, the mechanics of this improvement haven't been thoroughly investigated as well as the benefit of LEO satellites under complex environment, such as urban canyons. In this study, we demonstrated the contributions of LEO satellites on the estimation of each parameters, especially for ambiguities. Moreover, the performance of LeGNSS in urban canyons is also tested. One data segment with no change in observed satellites is selected to verify the advantage of LEO satellites. Kinematic PPP is conducted for GPS+Galileo and GPS+LEO, where the number of Galileo and LEO satellites is the same. Convergence of both position error and variance is compared, and Chi-square test is conducted to demonstrate consistency between error and variance. Then ambiguity error, ambiguity variance, ADOP, and other factors are analyzed to show the convergence difference between GNSS and LeGNSS. It shows that ambiguities for GPS in LeGNSS converge faster than that in GNSS, which proves the contribution of LEO. All factors of LeGNSS ambiguities are smaller than those of GPS+Galileo within 1 minute. Kinematic PPP with LeGNSS and GNSS in urban canyons are conducted. Several scenarios of urban canyons are tested. It shows that LEO can improve convergence time and positioning precision in urban canyons, and the improvement is dependent on elevation angle. Moreover, the influence of elevation angle to LEO's contribution to PPP in urban canyons is discussed.

Key words Low Earth Orbit (LEO); Precise Point Positioning (PPP); Simulation

Category: Symposium 4: Positioning and applications => 4.3: Techniques and Applications in High Precision GNSS

577

S4-127

BDS2 / BDS3 / GPS Multi-Frequency and Multi-System Fusion Long-Baseline Relative Positioning Analysis

Xiaoting Lei、Huizhong Zhu、Jingfa Zhang
Liaoning Technical University

BDS3 reached global coverage in June 2020. In order to study the precision relative positioning performance of the BDS3 single system and the improvement effect of adding BDS3 satellites on the precision relative positioning performance of BDS2 and GPS. This paper selects the data of 033-039d provided by the International GNSS service MGEX in 2021. BDS2 / BDS3 / GPS fusion data were used for static and simulated dynamic high-precision long-baseline calculation experiments, the influence of BDS2 / BDS3 / GPS single system and BDS2 and GPS added into BDS3 satellites on precision relative positioning convergence speed and positioning accuracy were analyzed respectively. The experimental results show that the current BDS3 positioning effect (convergence speed and positioning accuracy) is similar to GPS, and add the BDS3 satellites can effectively improve the positioning convergence speed of BDS2 and GPS. In the static mode, after adding the BDS3 satellites, the positioning accuracy of the single GPS and the BDS2 + GPS combination system only increases by 20 % in the U direction, and for BDS2 single system the positioning accuracy of E, N and U is increased by 60%, 71% and 65% respectively. In the dynamic mode, after the introduction of BDS3 satellites, the positioning accuracy of GPS single system and GPS + BDS2 combined system in the three directions of E, N and U can be improved by about 15 %, 23 % and 23 %, and BDS2 single system can be improved by about 46 %, 38 % and 36 % in three directions of E, N and U.

Key words BDS3; baseline solution; Multi-system Fusion; convergence speed; positioning accuracy

Category: Symposium 4: Positioning and applications => 4.3: Techniques and Applications in High Precision GNSS

585

S4-128

A deformation monitoring system based on BDS-2/BDS-3 PPP with optimal stochastic model

Chenhao Ouyang、Junbo Shi、Jiming Guo
Wuhan University

Considering the relative high cost of GNSS deformation monitoring system based on the differential positioning technique which requires at least two receivers, we designed a precise point positioning (PPP) technique-based system which only requires a single receiver. BDS-2/BDS-3 mixed observations are adopted in the designed system. Due to BDS's multi-type satellite orbits including Geostationary Earth orbit (GEO), Inclined Geosynchronous Satellite Orbit (IGSO) and Medium Earth Orbit (MEO), two major concerns arise for this deformation monitoring system. Firstly, BDS GEO, IGSO and MEO satellites differ in code/phase observation noise, and thus lead to non-homogeneous observation weights. Moreover, this deflection is enlarged by various orbit/clock product qualities. Secondly, due to the stationary status of GEO satellites and regional coverage of IGSO satellites, the slow spatial geometry variation of GEO and IGSO satellites leads to long PPP convergence time. To address these two concerns, we developed an optimal stochastic model taking the observation noise and orbit/clock error into account. More importantly, these factors are individually selected for BDS-2 and BDS-3 GEO, IGSO and MEO satellites. In the meantime, external troposphere and ionosphere corrections are adopted to reduce the atmosphere effect and subsequently speed up the convergence time. Experiment was carried out to assess the deformation sensitivity of designed system. We set the GNSS antenna on a mm-level displacement testing platform. 1/5/10/15/20/25 cm horizontal and vertical displacements are simulated to the receiver antenna every 30 mins. Numerical results indicated that the developed deformation monitoring system can provide mm-cm level horizontal and cm-level vertical monitoring precisions.

Key words BDS-2/BDS-3; PPP; deformation monitoring; stochastic model; convergence time

Category: Symposium 4: Positioning and applications => 4.3: Techniques and Applications in High Precision GNSS

587

S4-129

Characteristics analysis of raw multi-GNSS measurement from Huawei P30 and positioning performance

Chen Yi^{1,2,3}、Li Wang^{1,2,3}、Bao Shu^{1,2,3}、Hao Xu^{1,2,3}、Yunqing Tian^{1,2,3}

1. Chang'an University

2. State Key Laboratory of Geographic Information Engineering

3. Key Laboratory of Western China's Mineral Resources and Geological Engineering

Global Navigation Satellite System (GNSS) chipset is now embedded in almost all Android smartphones. In May 2016, Google announced that the developers could access some Android GNSS raw measurements. Providing GNSS application developers the opportunity to develop advanced processing algorithms for accurate position estimation using pseudorange, doppler and carrier phase observations. Compared with measurement receivers, smartphones have poorer data quality and it is difficult to obtain reliable positioning results using traditional methods. In this paper, a comprehensive analysis of the quality of raw GNSS observations of Android smartphones is conducted in terms of the tracking capability of the satellite, signal-to-noise ratio, pseudorange noise, phase minus code and velocity estimation. An improved positioning algorithm based on time difference filtering is proposed. This method uses extended kalman filtering to remove gross errors from smartphone GNSS data and optimize the observation equation noise model based on the estimated noise results of the observations. Then the time-differenced carrier phases filtering is used to obtain high-precision speed information and construct the speed constraint equation. Evaluate the proposed method by collecting static and dynamic test data, The results show that compared with the traditional single point positioning method, the positioning accuracy and usability of the improved filtering method in the horizontal and elevation directions are significantly improved and the positioning accuracy is increased by more than 20%.

Key words Smartphones; GNSS raw observation; Quality assessment; Time differenced filter

Category: Symposium 4: Positioning and applications => 4.3: Techniques and Applications in High Precision GNSS

620

S4-130

High-precision deeply-coupled GNSS/INS positioning technology and its application for survey vehicle

Baoguo Yu^{1,2}、Cailun Wu^{1,2}、Teng Long^{1,2}、Song Xie^{1,2}、Yixiong Sun^{1,2}

1. The 54th Research Institute of CETC

2. State Key Laboratory of Satellite Navigation System and Equipment Technology

In the urban environment, satellite navigation signals are severely attenuated due to the shelter of trees, buildings and bridges. It results in discontinuous signal tracking and affects the RTK solution of the receiver. For the traditional GNSS/INS integrated navigation system based on RTK, the positioning accuracy is significantly reduced in this condition. In order to further improve the environmental adaptability and positioning accuracy of the GNSS/INS integrated navigation, a deeply-coupled GNSS/INS method based on vector tracking is proposed in this paper. This method combines the code tracking and carrier phase tracking of all channels and introduces INS information assistance, which greatly improves the continuous carrier phase tracking ability of weak signals. In this paper, the structure of the vector tracking loop, the design of navigation filter, the processing of weak signal channel and the hardware implementation are introduced in detail. Finally, the effectiveness and navigation accuracy of the proposed method are verified through vehicle navigation experiments. The developed high-precision deeply-coupled GNSS/INS positioning terminal is demonstrated in the mobile survey vehicle, which lays a good foundation for unmanned driving and high-precision map acquisition.

Key words high-precision; deeply-coupled GNSS/INS; vector tracking; survey vehicle

Category: Symposium 4: Positioning and applications => 4.3: Techniques and Applications in High Precision GNSS

621

S4-131

Positioning performance with low-cost GNSS receivers

Kamil Kazmierski¹, Kamil Dominiak¹, Krzysztof Sośnica¹, Tomasz Hadas^{2,1}

1. Wrocław University of Environmental and Life Sciences

2. Institute of Navigation, University of Stuttgart

GNSS receiver market is evolving and tends to the improvement in all aspects, also GNSS receivers are currently crucial in everyday life. The broad potential application spectrum of GNSS technology also brings miniaturization of the receivers. This contributes to the production costs and intensifies activities in developing positioning techniques employing the so-called low-cost GNSS receivers. Limitation of the cost may be an excellent opportunity to densify the local GNSS network and bring benefits to all GNSS users. However, cost reduction is also related to a lower standard of the components used during the production process. Additionally, low-cost antennas are also susceptible to local signal noise. In this work, the performance of the low-cost instruments is evaluated in the context of practical use in the geodetic network establishment. We show results from a test of different processing strategies of multi-GNSS data collected by low-cost receivers. The influence of the selection of GNSS observations and the distance of points on the obtained results are tested. We evaluate the different session lengths for various baselines and different observation interval storage to check the actual low-cost GNSS receiver positioning usefulness. In this context, a field experiment with two sets of receivers was conducted. The tested set of receivers includes a low-cost receiver with the results referred to the professional geodetic GNSS identical geometry network. Additional PPP tests are also performed for the local low-cost GNSS network located in the area of Wrocław, Poland.

The obtained results show that the low-cost GNSS receivers provide mean positioning accuracies of 2.1, 2.5 cm for the vertical and horizontal components, respectively, in terms of the differences with respect to the professional GNSS receivers. The smallest 3D position difference equals 3.5 cm, whereas the maximum value equals 5.9 cm when referring to the professional GNSS equipment.

Key words low-cost GNSS receiver, positioning, geodetic networks

Category: Symposium 4: Positioning and applications => 4.3: Techniques and Applications in High Precision GNSS

632

S4-132

Precise positioning using low-cost dual-frequency GNSS receivers

Tomasz Hadas^{1,2}, Natalia Wielgocka², Adrian Kaczmarek², Grzegorz Marut²

1. Institute of Navigation, University of Stuttgart

2. Wrocław University of Environmental and Life Sciences

Global Navigation Satellite Systems (GNSS) allow for determining position coordinates with centimeter-level precision in real-time or up to sub-millimeter accuracy in post-processing solutions. The relative positioning, including the Real-Time Kinematic (RTK) or Network RTK (NRTK) modes, and the absolute positioning, dominated by the Precise Point Positioning (PPP) technique, are commonly used in positioning application. High accuracy positioning takes advantage of carrier phase measurements, whereas PPP and long-baseline RTK requires the acquisition of two frequencies. Although for many years such features were limited to geodetic-grade receivers, low-cost multi-frequency receivers have become available on the market recently. The positioning performance declared by the manufacturers is impressive, but initial studies reported, that it is limited to a favorable environment. In this contribution, we evaluate a low-cost dual-frequency multi-GNSS receiver and low-cost antenna in terms of the signal acquisition performance and positioning accuracy under RTK, network RTK and PPP. Signal acquisition is on average 7 dB Hz weaker than with a geodetic-grade receiver and is unsatisfactory for elevation angles lower than 10°. In open-sky conditions, a 1-hour long static session allows us to achieve horizontal accuracy of few centimeters and 80% fixed ambiguities and a similar accuracy can be achieved with the PPP for a session length of 2.5 hours. We notice a distinct disagreement between positioning accuracy and estimated uncertainty, which we justify by the stochastic modeling, which is not tuned for measurements performed by a low-cost receiver. With RTK (with geodetic grade base-station) and Network RTK, we achieve horizontal and vertical accuracy better than 5 cm and 8 cm, respectively. However, in the RTK between two low-cost receivers, the change of relative antenna orientation results in height determination errors exceeding 10 cm.

Key words GNSS, low-cost, positioning, RTK, PPP

Category: Symposium 4: Positioning and applications => 4.3: Techniques and Applications in High Precision GNSS

642

S4-133

Multi-GNSS satellite inter-frequency clock bias estimation based on IGS clock datum in the multi-frequency context

Lei Fan、Chuang Shi
Beihang University

The inconsistency of Global Navigation Satellite System (GNSS) multi-frequency data must be considered in high-precision GNSS applications. However, current methods of dealing with this inconsistency, e.g., differential code bias provided by International GNSS Service (IGS) analysis centers, are in weak consistency with the IGS clock product. In view of this, we develop a unified model for multi-GNSS satellite inter-frequency clock bias (IFCB) estimation based on IGS clock datum. By means of accurate modeling of both satellite phase-based IFCB (PIFCB) variation and code-based IFCB (CIFCB), a set of independent satellite IFCBs are estimated in a full-rank multi-GNSS and multi-frequency uncombined model where IGS orbit and clock products are taken as input. The proposed model is validated using two month's GPS, BDS and Galileo multi-frequency observations collected from 18 globally distributed stations. By choosing L1W/L2W (GPS), B1I/B3I (BDS) and E1/E5a (Galileo) as reference frequencies, periodic analysis results suggest that a 4th-order and 2nd-order periodic function are suitable for modeling GPS (L5X) and BDS-2 (B2I) satellite PIFCB variations respectively, where the root mean square of posteriori phase residuals are reduced by 35% and 4% when compared to those without PIFCB modeling. Yet there is no need to introduce periodic function into BDS-3 and Galileo satellite PIFCB variations. The stability of the CIFCB for GPS (L5X), BDS-2 IGSO (B2I) and BDS-3 (B2a, B2b) satellites are at the same level, which standard deviation (STD) is about 0.10 ns. The CIFCB of Galileo (E5b) satellite achieves the smallest STD of 0.06 ns, while that of BDS-2 GEO and MEO (B2I) satellites are 0.24 and 0.17 ns. However, the STD of BDS-3 (B1C) satellite is 3.08 ns which is much larger than other satellites and frequencies. A major reason for the large STD is that the frequency value of B1C is very close to the reference frequency B1I which would significantly amplify data noises.

Key words BDS-3; Multi-GNSS; Inter-frequency clock bias; Multi-frequency; Uncombined model

Category: Symposium 4: Positioning and applications => 4.3: Techniques and Applications in High Precision GNSS

643

S4-134

Multi-level augmentation and highly reliable BeiDou/GNSS precise cloud positioning and space atmospheric effect control

Yunbin Yuan

State Key Laboratory of Geodesy and Earth's Dynamics, Innovation Academy for Precision Measurement Science and Technology, Chinese Academy of Sciences

In the context of multi-level augmentation, a series of problems need to be solved to achieve highly reliable precise cloud positioning and space atmospheric effect control. First, the multi-level enhanced satellite positioning based on cloud platform needs the unified processing of the whole network and distributed. This is reflected in the implementation mode, interface and information sharing mechanism of various high-precision global navigation satellite system (GNSS) positioning technologies (single point positioning (SPP), precise point positioning (PPP), real-time kinematic (RTK) positioning and real-time differential (RTD) positioning) need to be unified and optimized. Second, massive multi-constellation and multi-frequency GNSS observations from different regions need to be combined in the cloud (server-end) and the user (user-end). Therefore, it is necessary to establish a more rigorous theoretical undifferenced and uncombined BeiDou/GNSS data processing method, so as to realize the real-time synchronous optimal estimation of satellite orbit, clock error, ionosphere and troposphere correction information. Third, new concepts and methods with high reliability are also necessary to high-precision enhanced GNSS positioning. It is significant to realize the synergistic enhancement between the server-end and the user-end, which is beneficial to ensure the atmospheric effect control in precise positioning when abnormal events occur. Fourth, the combination of different types of correction information on the user-end needs to be reasonably designed so as to serve users with different precision needs. In addition, in order to serve the high-precision and high-reliability industrial demonstration application, it is also important to realize the precise positioning of multi-sensor fusion such as GNSS and inertial navigation system (INS).

Key words GNSS, RTK, PPP, cloud positioning

Category: Symposium 4: Positioning and applications => 4.3: Techniques and Applications in High Precision GNSS

647

S4-135

BDS-3 multi-frequency PPP-RTK for vehicle navigation in urban environments

Bo Wang¹、Xin Li¹、Jiixin Huang²、Hongbo Lv¹、Guolong Feng¹、Xingxing Li¹

1. School of Geodesy and Geomatics, Wuhan University

2. Technische Universitat Berlin (TUB)

In order to integrate advantages of precise point positioning (PPP) and real-time kinematic (RTK), PPP-RTK method has been proposed to achieve centimeter-level positioning with rapid integer ambiguity resolution and implemented in some commercial systems such as Trimble RTX-Fast, NavCom StarFire etc. But it doesn't work well for vehicle navigation in urban environment. BDS-3 was formally commissioned on July 2021, with 3 GEO, 3 IGSO and 24 MEO satellites on orbit. In addition to the legacy B1I and B3I signals, BDS-3 satellites are capable of transmitting several new navigation signals, including B1C, B2a, B2b and B2a+b. Multi-frequency observations bring more possibilities for enhancing the performance of BDS-3 PPP-RTK. We develop a multi-frequency BDS-3 PPP-RTK system aimed at realizing precise positioning for vehicle navigation in urban environments. On the server side, we estimate extra-wide-lane(EWL), wide-lane(WL) and narrow-lane(NL) UPDs and extracting precise atmospheric delays based on multi-frequency observations. Then these corrections are distributed to users to achieve PPP rapid ambiguity resolution with the five-frequency EWL-WL-NL successive ambiguity fixed method. Vehicle experiments in different scenarios such as suburbs, overpasses, tunnels are conducted to validate the proposed method. Our results indicate that centimeter-level positioning accuracy can be achieved with the time to first fix of 6s and fixing percentage of 95%. In the urban environments where signals are interrupted frequently, a fast ambiguity recovery can be achieved within 5s. Moreover, the PPP-RTK performance is significantly improved with multi-GNSS and multi-frequency observations. Compared to GPS-only solution, multi-frequency and multi-GNSS solution is more precise and reliable with accuracy improved by 75%, fixing percentage improved by 25%.

Key words Multi-frequency;Multi-GNSS;PPP-RTK;UPD;Ambiguity resolution

Category: Symposium 4: Positioning and applications => 4.3: Techniques and Applications in High Precision GNSS

648

S4-136

High-rate hourly ultra-rapid multi-GNSS precise clock estimation

Guoqiang JIAO^{1,2}, Shuli SONG¹, Qinming CHEN¹

1. Shanghai Astronomical Observatory, Chinese Academy of Sciences

2. School of Astronomy and Space Science, University of Chinese Academy of Sciences

With the development of GNSS, the requirement for the latency and accuracy of precise products are also gradually improving in terms of positioning, navigation, timing (PNT) and atmospheric retrieval. The hourly updated ultra-rapid products is of great interest in GNSS real-time and near-real-time field. Due to the estimation of a large number of ambiguity parameters, the computation is time-consuming. It is hard to achieve the high-rate hourly updated precise clock estimation (PCE). At present, the highest sampling interval of ultra-rapid clock provided by IGS and iGMAS analysis AC is 5 min. The sampling interval of precise clock offsets affects the accuracy of clock prediction and precise point positioning (PPP). To meet the real-time and near-real-time demands of subscribers, we introduce an efficient methods and design a new software framework for high-rate hourly updated ultra-rapid PCE. By using the epoch-difference (ED) model, OpenMP and Intel MKL technology, the 1-hourly updated clock offsets with the sampling interval of 30 s can be estimated in less than 20 minutes using GPS, BDS-2, BDS-3, GLONASS and Galileo observations. Further, in the observation session, the root mean square (RMS) of the ED clock for GPS, BDS-2 (GEO), BDS-2 (Non GEO), BDS-3, GLONASS and Galileo are better than 20 ps, 60 ps, 40 ps, 30 ps, 40 ps and 20 ps compared with Helmholtz-Centre Potsdam - German Research Centre for Geosciences (GFZ) rapid products, respectively. Due to the improvement of the sampling interval of clock, the original clock of the prediction and observation sessions has been improved to different degrees. The achievement of the high-rate 1-hourly updated ultra-rapid clock effectively improves the convergence time and positioning accuracy of PPP users and promotes the application and research of real-time or near-real-time users.

Key words High-rate; hourly ultra-rapid clock; precise clock estimation (PCE); epoch-difference (ED); precise point positioning (PPP).

Category: Symposium 4: Positioning and applications => 4.3: Techniques and Applications in High Precision GNSS

657

S4-137

A Real-time Ionospheric Estimation Method Based on Undifferenced and Uncombined Precise Point Positioning

Changxin Chen、 Xu Lin、 Wei Li、 Lin Cheng、 Hongyue Wang、 Qingqing Zhang
Chengdu University of Technology

Undifferenced and uncombined model is considered as an ideal precise point positioning(PPP) model without error propagation. However, in the undifferenced and uncombined model, there are many weak observations, such as strong coupling between the ionosphere and the hardware delay of the receiver and the satellite terminal. Even in the case of using the final ionospheric grid product, it is difficult to separate it due to the influence of the accuracy of the ionospheric product. In this paper, a global ionospheric model based on spatial-temporal distribution is established by using multiple MGEX stations to observe the global ionosphere. By bringing the model into the observation equation, the influence of ionospheric delay on PPP can be effectively reduced, and the coupling between ionospheric delay and hardware delay can be reduced, so as to effectively eliminate the influence of ionosphere and hardware delay on non-difference non-combined precision point positioning.

Key words precise point positioning; Ionosphere model; GNSS

Category: Symposium 4: Positioning and applications => 4.3: Techniques and Applications in High Precision GNSS

672

S4-138

Optimization of GNSS PDOP assessment and monitoring algorithm based on equal-area grid models

Zhitao Wang、 Shuli Song

Shanghai Astronomical Observatory, Chinese Academy of Sciences

PDOP is one of the key parameters for assessing the performance of GNSS. With the development and standardization of GNSS monitoring and assessment, it is necessary to study a feasible and efficient PDOP calculation strategy for GNSS monitoring. This research mainly focuses on studying of equal-area grid models, including the equal-arch-length Grid (GRID_EAL) and the Icosahedron-Based Grid (GRID_IB), to optimize the PDOP calculation. The differences between these two equal-area grid models and typical grid model with equal-interval of longitude and latitude (GRID_ELL) are analyzed. With the same total volume of grid points, these two equal-area grid models have notable reduction of the excessive grid points in high-latitude regions. These three grid models are used to simulate the global PDOP and PDOP availability. The simulations indicate that when these three grid models reach the same effect for monitoring and assessment of GNSS, the GRID_EAL and GRID_IB can both reduce the total number of grid points to improve computing efficiency obviously. The excessive grid points weight of GRID_ELL in high-latitude regions will lead a bias to the statistics of GLONASS global PDOP availability. However, because GRID_IB is complicated to change the intervals, GRID_EAL model is recommended for PDOP calculation. In this article, further research was carried out on GRID_EAL model with different grid intervals. The results show that, with the GRID_ELL of 1 degree as reference, GRID_EAL of 5 angular degree is enough to describe the performance of GNSS and with suitable efficiency. Comparing to GRID_ELL in 5 degrees, the computing efficiency of GRID_EAL in 5 angular degrees can be improved by 34% and the storage occupation can be reduced by 33%.

Key words PDOP, Assessment and Monitoring, Computing efficiency

Category: Symposium 4: Positioning and applications => 4.3: Techniques and Applications in High Precision GNSS

677

S4-139

How much does the price matter? Real-time geohazard monitoring with low-cost GNSS

Roland Hohensinn, Raphael Stauffer, Reto Spannagel, Yara Rossi, Iván Dario Herrera Pinzón, Gregor Moeller, Markus Rothacher
ETH Zurich, Institute of Geodesy and Photogrammetry

Over the recent years, measurement devices with low-cost dual-frequency GNSS chips became available, at a price of a few hundred Dollars. This is considerably cheaper than geodetic-grade receivers, that still cost around 10.000 Dollars or more. Two years ago, the Swiss company u-blox presented a low-cost GNSS module, that is capable of tracking multiple GNSS constellations in two different frequency bands (e.g. GPS L1/L2). Furthermore, the Chinese company Xiaomi launched the world's first smartphone that is capable of collecting multi-GNSS phase observations in two different frequency bands (L1/L5). In the meantime, this dual-frequency capability became available for many GNSS devices that are on the market.

In this contribution we want to give answers, if this new GNSS sensor technology can meet the requirements of GNSS high-precision applications regarding the real-time detection and the monitoring of geohazards, such as earthquakes or induced vibrations of structures. For these applications, it is necessary to monitor dynamic movements with displacement rates from a few cm/s down to mm/s. Based on experiments with a mobile robot arm, we have tested different kinds of such motions, and collected the data with the GNSS equipment mounted on top. For these robot tests, a very precise ground truth is available as well. For the GNSS data processing we used real-time Precise Point Positioning (PPP), as well as phase-enabled GNSS velocimetry. For the case of the u-blox receiver positioning, we also investigated the added value of introducing patch antenna calibrations in the processing.

We demonstrate that with these sensors it is possible to resolve movements at the level of centimeters and centimeters per second, and even reaching the millimeter level is possible. The main differences in quality are found to be caused by the quality and the type of the GNSS antenna. However, this new low-cost technology is very beneficial for a variety of GNSS geomonitoring applications.

Key words High-precision GNSS, Low-cost GNSS, Real-time GNSS, GNSS Antennas, Estimation and Detection, Natural Hazards, Geomonitoring

Category: Symposium 4: Positioning and applications => 4.3: Techniques and Applications in High Precision GNSS

689

S4-140

Assessment of the Galileo System Contribution on RT-PPP Using Different Real-Time Correction Services in the Antarctic Region

Serdar Erol, Bilal Mutlu, Bihter Erol

Istanbul Technical University, Geomatics Engineering Department, 34469, Maslak, Istanbul, Turkey.

IGS Real-Time Service (RTS) provides GPS-only or GPS+GLONASS real-time precise orbit and clock products for RT-PPP applications. On the other hand, some IGS analysis centers (ACs) provide real-time precise products for Multi-GNSS RT-PPP within the scope of the IGS-Multi-GNSS EXperiment (MGEX) project. In addition, the Spaceopal GmbH, the prime contractor responsible for the Galileo operations, launched a new worldwide real-time correction service known as NAVCAST in October 2018. This service provides GPS+Galileo real-time precise orbit and clock products based on the RETICLE algorithm developed by the German Aerospace Centre (DLR). This study aims to test the convergence and accuracy performance of the RT-PPP method using the IGS-MGEX and Spaceopal NAVCAST RTS products separately in the Antarctica continent with different constellations. For this purpose, the RT-PPP solutions have been carried out for GPS-only, Galileo-only, and GPS+Galileo constellations by using the real-time data from OHI300ATA0 IGS-MGEX RT station in the Antarctica continent together with the mentioned RTS products. In the study, real-time corrections of DLR were used as MGEX RTS products. The obtained results were compared by means of both the contributing satellite systems and the used RTS products. In the result, the horizontal and vertical position accuracies were found centimeter and around one decimeter level, respectively for the single constellation RT-PPP solutions using the NAVCAST and IGS-MGEX RTS products. By using the two constellations together, the convergence time was shortened and the horizontal and vertical position accuracies were improved by approximately 40% and 30%, respectively. These accuracies were obtained for an 8-hour observation period with approximately 30-60 minutes convergence time. In conclusion, the NAVCAST-RTS provided almost equal RT-PPP accuracies with IGS-RTS for the single- and multi-constellation data of an IGS-RT network station in the Antarctic region.

Key words RT-PPP; NAVCAST; Galileo; IGS-MGEX; Antarctica.

Category: Symposium 4: Positioning and applications => 4.3: Techniques and Applications in High Precision GNSS

702

S4-141

Continuous multipath and partial obstruction monitoring in high-precision GNSS base stations

Marco Mendonca, Marcelo C. Santos
University of New Brunswick

With a growing number of network RTK (NRTK) providers and users as well as recent advances in PPP-RTK, the real-time quality control of GNSS base station observations has become a central issue to alleviate the processing burden in both correction providers' computers and in, often, low-cost mass-market rover receivers. Given the densification of networks and the diverse antenna location characteristics, continuous monitoring of possible partial obstructions and multipath sources is one way to improve such quality control. This paper proposes an iterative method based on the wavelet spectral analysis of a 14-day observation buffer, employing the signal-to-noise ratio (SNR) and the code-minus-carrier (CMC) metrics. Taking advantage of the periodicity of the GNSS orbits and the multiple satellites in the same orbital plane, this analysis over multiple signals and constellations allows the real-time identification of sections of the sky where the signal quality is sub-par and could be removed from the filter in high-precision applications. Results from three reference stations in different latitudes show that this method can yield improved accuracy and integrity metrics with the proposed signal-specific quality control, allowing the use of observations with lower elevation angles. For RTK, the accuracy gains were between 3% and 12%, while the considered integrity metric was improved between 5% and 8%.

Key words GNSS, multipath, wavelet

Category: Symposium 4: Positioning and applications => 4.3: Techniques and Applications in High Precision GNSS

705

S4-142

Performance Analysis of a Low-cost MARG Sensor/Single-antenna GNSS System for Land Vehicle Attitude Estimation

Wei Ding, Yang Gao

Department of Geomatics Engineering, Schulich School of Engineering, University of Calgary, Calgary, AB, Canada, T2N 1N4

Low-cost MARG (magnetic, angular rate, and gravity) sensors have gained more and more attention for land vehicle attitude estimation in the last two decades. MARG consists of magnetometers, gyros, and accelerometers. On the other hand, the global navigation satellite system (GNSS) with single-antenna can derive the pitch and heading angles of a land vehicle using the position changes between two adjacent epochs, and the time differenced carrier phases (TDCP) can provide high accuracy of delta position estimation.

Both MARG and GNSS have pros and cons as a stand-alone navigation system as summarized herein: 1) Gyro can provide continuous attitude after initialization but suffers from time-varying drift error; 2) Accelerometer coupled with magnetometer can determine absolute attitude but are sensitive to external accelerations and magnetic anomalies, respectively; 3) Single-antenna GNSS provides absolute pitch and heading estimates but the results are unreliable when the vehicle is static or slowly moving; 4) Besides, GNSS signals are vulnerable to problems like signal blockage, cycle slips, and low observation quality.

This paper investigates the performance of a low-cost MARG sensor/single-antenna GNSS system for land vehicle attitude estimation. A right-multiplied error quaternion-based error state Kalman filter (ESKF) has been applied for the fusion of MARG and GNSS data. The vehicular attitude information is represented using quaternion, whereas the attitude error is interpreted as a small rotation vector. The Kalman filter state consists of attitude error and gyro bias variation. The angular rates are integrated to continuously propagate attitude based on the quaternion kinematic equation, accelerations and magnetic field measurements are applied to estimate gyro bias and correct attitude under scenarios without external disturbances. The single-antenna GNSS-based pitch and heading are derived and used as measurements when the vehicle is non-stationary.

Key words Attitude estimation; low-cost MARG sensor; single-antenna GNSS; time-difference carrier phases

Category: Symposium 4: Positioning and applications => 4.3: Techniques and Applications in High Precision GNSS

709

S4-143

Study on crustal movement characteristics before Yutian MS6.4 earthquake in 2020 based on GNSS

Zhiguo Zhu

Earthquake Administration of Xinjiang Uygur Autonomous Region

Altyn Tagh fault area has strong neotectonic activity. The MS6.4 earthquake occurred in Yutian County of Hotan area at 5:05 on June 26, 2020. The focal area of the earthquake is located at the end of the western segment of Altyn Tagh fault zone. The strike of the seismogenic fault is nearly north-south and tends to the west, mainly normal fault with strike slip component. Using the GNSS data from Chinese mainland tectonic environment monitoring network 2015~2019, the horizontal velocity field in the focal area before the Yutian Ms6.4 earthquake is obtained by GAMIT/GLOBK software. The partial derivative relationship between horizontal displacement and strain of regional velocity field is established by using the least square collocation method, and the apparent strain field image of focal area is obtained by solving the strain parameters; By using the Green's function method, the relationship between the ground observations and the earth's internal stress field variables is established through the crustal physical model, and the crustal tectonic stress field at 10km in the source area is inversely calculated. The analysis shows that the velocity field image reflects that the Tibetan Plateau has absorbed the northward pushing energy of some Indian plates, and the crustal material in the southeast of the plateau tends to be squeezed eastward. The distribution of strain field shows that the epicenter of Yutian MS6.4 earthquake is at the edge of plane expansion rate and shear strain rate. The shear strain rate in the source area is nearly equal to the surface expansion rate, and there is a "locking" phenomenon. The crustal tectonic stress field at 10km of the crust reflects that the focal area is at the edge of the crustal stress field, and there is a high tensile maximum principal stress in the west of the focal area, which provides favorable conditions for the extensional fault activity in the focal area.

Thanks to Xinjiang Natural Science Foundation (2020D01A85)

Key words GNSS, Yutian earthquake, velocity field, strain rate and stress field

Category: Symposium 4: Positioning and applications => 4.3: Techniques and Applications in High Precision GNSS

713

S4-144

Validation and Evaluation of BDS-3 PPP-B2b service

Haibo Ge, Bofeng Li, Yuhang Bu, Yanning Zheng
Tongji University

BDS-3 began to provide global service since 1st August, 2020. Precise Point Positioning (PPP) Service Signal PPP-B2b is the first high-precision service signal released by BDS-3, which aims to realize real-time PPP in China and surrounding areas. However, few research has been done on this subject. This article systematically studies the use of PPP-B2b service, including raw data decoding, product characteristics analysis, and algorithm processing. Finally, static and kinematic PPP experiments are carried out with eight iGAMS stations in August 2020.

Broadcasting through satellite communications, PPP-B2b products are not restricted by the interruption of internet network, which makes the service more stable. Currently, PPP-B2b can provide BDS-3 and GPS real-time correction information, which mainly includes orbit offset, clock offset, and Different Code Bias (DCB) correction. The results show that the average positioning accuracy of BDS-3 single system in E, N and U directions is 2.35, 1.52 and 5.20 cm for static mode, while for kinematic mode, the average positioning accuracy in E, N and U directions can reach 5.17, 3.29 and 9.65 cm, respectively. For dual system (GPS+BDS-3) case, the corresponding three components are 2.04, 1.26 and 3.97 cm for static mode and 3.79, 3.00 and 8.56 cm for kinematic mode. The convergence time of static and kinematic positioning for dual systems with threshold value of 0.1 m is 19.92 min and 29.08 min, respectively. For BDS-3, the convergence time of static and kinematic positioning threshold value of 0.1 m is 64.45 min and 101.33 min, respectively.

Key words BDS-3; PPP-B2b; real-time PPP; positioning performance

Category: Symposium 4: Positioning and applications => 4.3: Techniques and Applications in High Precision GNSS

719

S4-145

High order ionospheric delay characteristics and its influence on uncombined PPP

Xiangyu Tian 、 Hongzhou Chai、 xiao yin
Information engineering university

Regard to the problem of high active ionosphere period, low latitude area with high ionosphere TEC, high ionospheric delay of signal of satellite, serious influencing the PPP position by high order ionosphere delay (HOI). Firstly, Synthetically analysis the solar active period and ionosphere active period, to define the low latitude area and high ionosphere active period. Use the pseudorange smoothed by phase method to calculate the Slant Total Electron Content(STEC), introduce IGRF-13 to calculate high order ionosphere delay. Then implement undifference and uncombined precise point positioning (UC PPP). After work out the solution of the position, analysis the pseudorange and phase residual and time serious of position result of multiple station with long term, and research the influences of the high order ionosphere delay on convergence time and position accuracy on active ionosphere period, low latitude area. The result shows that, the HOI correction is at millimeter level, the influence of it on UC PPP is at sub-millimeter. Thus, the HOI correction is needed to be taken account into the position of millimeter level. It almost can be neglected on other aspects. The research provides the theory reference for the usage of the HOI correction and improvement of the PPP model.

Key words ionosphere active period; HOI; undifference and uncombined; PPP

Category: Symposium 4: Positioning and applications => 4.3: Techniques and Applications in High Precision GNSS

721

S4-146

Refinement of BeiDou Satellite Antenna Phase Center Correction Model and Its Impact on Precision Orbit Determination and Positioning

Xingyuan Yan^{1,2}, Qin Zhang², Guanwen Huang², Shichao Xie², Yu Cao²

1. Sun yat-sen university

2. Chang'an university

Aiming at the lack of high accurate antenna phase correction (PCC) model for the BDS-2 IGSO and MEO satellites, in the BDS-2 and BDS-3 satellites joint precision orbit determination (POD) and precise point positioning (PPP), in this paper, an improved method for estimating PCV and z-offset parameters is used to refine the B1I/B3I ionosphere-free linear combination PCC model for the BDS-2 IGSO and MEO satellites. Compared with the results obtained using the ground-calibrated PCO model published by BeiDou official, the STD of SLR residuals obtained by the POD using the refined PCC model is reduced by 0.6-2.4 cm, and the improvement percentage is about 8.6%-33.3%. The floating PPP solution results, based on the refined BDS-2 satellite PCC model in this paper and the existing BDS-3 PCC model, have been significantly improved by 9.5mm (37.2%) in the elevation direction.

Key words BDS-2; BDS-3; satellite antenna phase center correction model; joint precise orbit determination; precise point position

Category: Symposium 4: Positioning and applications => 4.3: Techniques and Applications in High Precision GNSS

744

S4-147

CAS Real-time SSR Corrections in support of High Accuracy GNSS Applications

Yunbin Yuan¹、Zishen Li²、Wenwu Ding¹、Ningbo Wang²、Bingfeng Tan¹

1. Innovation Academy for Precision Measurement Science and Technology (APM),
Chinese Academy of Sciences (CAS)

2. Aerospace Information Research Institute, Chinese Academy of Sciences
(AIR/CAS)

The accuracy of Global Navigation Satellite System (GNSS) can be largely improved by using GNSS correction services. Such services can enhance GNSS performance and enable positioning accuracies down to the centimeter level by transmitting real-time data streams containing correction information on GNSS signal errors. Benefiting from the Real-Time Services (RTS) of the International GNSS Service (IGS), the Chinese Academy of Sciences (CAS) started the routine generation of State Space Representation (SSR) corrections of the key GNSS errors, including orbits, clocks, biases and global ionosphere, using the open data of the IGS since mid-2019. CAS SSR corrections are transmitted in both RTCM-SSR (SSRA00CAS0, SSRC00CAS0) and IGS-SSR (SSRA00CAS1, SSRC00CAS1) standards supporting GPS, GLONASS, Galileo and BeiDou constellations. GNSS users can freely access CAS SSR streams via IGS (products.igs-ip.net:2101) and CAS (cas-ip.gipp.org.cn:2101) casters. This contribution summarizes the strategies on the generation of CAS real-time orbit, clock, bias and ionosphere corrections, the validation of those SSR corrections as well as their applications in real-time Precise Point Positioning (PPP) applications. In the next step, we will continue the maintenance of CAS real-time services and focus on the generation of regional ionospheric and tropospheric corrections in support PPP-RTK service.

Key words Real-time GNSS, High Accuracy Service (HAS), State Space Representation (SSR), Precise Point positioning (PPP), International GNSS Service (IGS)

Category: Symposium 4: Positioning and applications => 4.3: Techniques and Applications in High Precision GNSS

749

S4-148

Rupture process variations analysis of the 2020 Mw7.4 La Crucecita, Oaxaca, Mexico Earthquake using high-rate GPS, InSAR and Teleseismic data

Guisen Wen¹, Xingxing Li¹, Yingwen Zhao¹, Guangyu Xu²

1. School of Geodesy and Geomatics, Wuhan University

2. Faculty of Geomatics, East China University of Technology

A stable earthquake source rupture model is vital for earthquake emergency responses and understanding the seismogenic tectonics. By taking the 2020 Mw7.4 La Crucecita, Oaxaca, Mexico earthquake as an example, we analyse the variations of the rupture model by using the different datasets, hypocenters, local velocity crust models and focal mechanisms. The moment tensor derived by teleseismic data reveals a low dip thrust event, which is similar to the existing studies. The preliminary rupture process model obtained by the joint data inversion shows that the main rupture area around the hypocenter, the peak slip is about 4.3 m, and the whole rupture process last about 20 s. The checkboard tests show that we can retrieve the slip model well, especially the spatial information of coseismic slip when the InSAR data were added. We also test the resolutions of the waveform and static data inversion, we find that waveform inversion result needs bigger spatial smoothing factor than the static data inversion, since the high-rate GPS data are sparse which have strong spatial constrain on coseismic slip. Besides, we should increase the relative weight of the InSAR data because its high resolutions of spatial constrain when the near-field waveform data are sparse. The variance reduction of teleseismic data (the average is greater 80 %) from the variations analysis is smaller than the other dataset (the average is greater 90 %), which are consistent with the real earthquake analysis because of its energy attenuation property of P wave. The variation analysis shows that the main rupture processes are well consistent and the rupture details are dissimilar. The slip area can be resolved well if we have enough near-field waveform or static data since we can obtain absolute information with respect to the hypocenter. The preliminary result shows that we should consider the uncertainty of the focal mechanism which is more sensitive to the finite-fault inversion model than the others.

Key words Moment tensor inversion, Joint data inversion, Checkboard test, Spatial constrain, Variation analysis

Category: Symposium 4: Positioning and applications => 4.3: Techniques and Applications in High Precision GNSS

753

S4-149

A Comparative Study of BDS Triple-frequency Ambiguity Fixation Algorithm for RTK Positioning

Yangyang Lu、Huizhong Zhu
Liaoning Technical University (LNTU)

In principle, there are three different realizations for the triple-frequency ambiguity resolution. The first one is to fix all the ambiguities of the original frequencies together. However, it is also believed that fixing the combined integer ambiguities with longer wavelength, such as extra-wide-lane (EWL), wide-lane (WL), should be advantageous. Also, it is demonstrated that fixing sequentially EWL, WL and one type of original ambiguities provides better results, as the previously fixed ambiguities increase parameters' precision for later fixings. In this paper, we undertake a comparative study of the three fixing approaches by means of experimental validation. In order to realize the three fixing approaches from the same information in terms of adjustment, we developed a processing strategy to provide fully consistent normal equations. We first generate the normal equation with the original undifferentiated carrier phase ambiguities, then map it into that with the combined and double-differenced ambiguities required by the individual approach for fixing. Four baselines of 258 m, 22 km, 47 km and 53 km are selected and processed in both static and kinematic mode using the three ambiguity-fixing approaches. Indicators including time of first fixed solution (TFFS), the correct fixing rate, positioning accuracy and *RATIO* are used to evaluate and investigate results. We also made a preliminary theoretical explanation of the results by looking into the decorrelation procedure of the ambiguity searching algorithm and the intermediate results. As conclusions, integrated searching of original ambiguities or combined ambiguities has almost the same fixing performance, whereas the sequential fixing of EWL, WL and B1 ambiguities overperforms the integrated searching. By the way, the third-frequency data can shorten the TFFS significantly but can hardly improve the positioning.

Key words BDS; long range RTK; triple-frequency observations; carrier phase ambiguity; LAMBDA; integer ambiguity resolution

Category: Symposium 4: Positioning and applications => 4.3: Techniques and Applications in High Precision GNSS

762

S4-150

The RINEX Ina-CORS Data Download System Enhancement for One Map Policy Implementation Convenient in Indonesia

Isnaini Annuriah Mundakir, Ossy Maulita Budiawati, Wilma Fitri, Akhmad Yulianto
Basuki

Badan Informasi Geospasial (Geospatial Information Authority of Indonesia)

Many efforts have been done by the government to ensure the enactment of One Map Policy in Indonesia. All geospatial data and information gathered in various mapping projects throughout the country must refer to the same national reference system, namely SRGI2013. Ina-CORS network is one of the most efficient and effective tools to be used as reference stations to ensure the single reference system application in Indonesia's area. The RINEX Ina-CORS data have been distributed to users by request via email since 2012 and have just being upgraded to the more advance system as a self-service automatic download via website in 2021. Users can now acquire their desired data automatically via RINEX Ina-CORS data download application embedded on <https://srgi.big.go.id/> website. Since its first public appearance on February 2021, this application has received a positive response from users, indicated by a quite drastic increase in the use of RINEX data during the first 3 months period of operation from an average of 153 users with 4027 data requested and distributed every month during the last 3 months of 2020 to an average of 254 users with 28453 data downloaded through this new established service every month.

Key words RINEX, Ina-CORS, CORS, data download, One Map Policy

Category: Symposium 4: Positioning and applications => 4.3: Techniques and Applications in High Precision GNSS

763

S4-151

Smart-PPP: Towards Real-Time GNSS Precise Point Positioning for Low-cost Smart Devices

Liang Wang¹, Zishen Li¹, Ningbo Wang¹, Zhiyu Wang²

1. Aerospace Information Research Institute (AIR), Chinese Academy of Sciences (CAS)

2. University of Chinese Academy of Sciences

The availability of Global Navigation Satellite System (GNSS) raw measurements from Android smart devices opens up the possibilities of deriving more accurate positioning with advanced techniques. To promote the applying of real-time precise point positioning (PPP) in smart devices, we propose an approach named as Smart-PPP (real-time PPP for smart devices) which can support smart devices to derive positioning results in sub-meter-level accuracy. In the Smart-PPP approach, the uncombined observation model with independent receiver clock parameters for code and carrier-phase measurements is proposed for smart devices. A stochastic model by considering the strong correlation between the measurement errors and the signal strengths is employed for weighting the code and carrier-phase measurements. The real-time State Space Representation (SSR) formatted precise orbit and clock corrections and ionospheric vertical total electron content (VTEC) products are both introduced into smart devices to perform real-time PPP. Some strategies for processing real-time PPP are also proposed in Smart-PPP to handle the observation data of smart devices. For realizing Smart-PPP in smart devices, an application software is developed based on Android platform. The positioning performance of Smart-PPP is validated in static and kinematic cases, respectively. The numerical results show that the Smart-PPP solutions can achieve positioning results with an accuracy of about 0.2–0.5 m in static mode after convergence and about 1.0-meter-level accuracy in kinematic mode. The Smart-PPP results show that the mass-market smart devices have the promising potential to be used in those real-time applications with submeter-level to meter-level accuracy demands.

Key words GNSS; Raw measurements; Smart devices; Precise point positioning (PPP); Smart-PPP

Category: Symposium 4: Positioning and applications => 4.3: Techniques and Applications in High Precision GNSS

766

S4-152

Characteristic analysis of the GNSS satellite clock error

Haojun Li, Jinxing Xiao

College of Surveying and Geo-Informatics, Tongji University

The daily Global Navigation Satellite Systems (GNSS) satellite clock errors for four systems are analyzed using Fast Fourier Transform (FFT). Based on the analyzed period results, the satellite clock error is modeled with mixed-function, which consist of a harmonic function and a polynomial function. The modeling results indicate that GLONASS clock has the largest RMS and is at the same level as the Cs clock of GPS, the RMS of BDS-2 is close to that of the Rb clock carried in GPS satellites, and Galileo has the smallest RMS. The harmonic coefficients for the modeling function show that the amplitudes and initial phases of the Rb clocks carried on Block IIRM and Block IIF for GPS satellites have obvious periodic characteristics with 12 h and 8 h over the year, while those of the Cs clocks have no regularity. The amplitudes of BDS-2 IGSO satellites have obvious periodic characteristics in 12 h, 8 h, and 6 h, and the initial phases of 12 h and 8 h of IGSO satellites also have obvious periodic characteristics. Especially, the amplitudes of Galileo satellites have periodic characteristics of 12 h and 8 h in the full constellation. The correlation of modeling coefficients is used to analyze the stability of four GNSS systems and the results show that 2th coefficients of Galileo satellite show better and more stable than other systems. Additionally, GNSS satellite clock error is predicted with 2 h, 6 h, and 12 h compared with Broadcast Ephemeris (BRDM), Ultra-Rapid (ISU), and IGS final clock product. The results of prediction show that the RMS of 8-period mixed-function is slightly lower than 4-period mixed-function for most satellites of four GNSS systems and modeled clock of most GNSS satellites have preferable accuracy than those of the BRDM and ISU clock products.

Key words GNSS satellite clock; Satellite clock modeling; Precise Point Positioning (PPP)

Category: Symposium 4: Positioning and applications => 4.3: Techniques and Applications in High Precision GNSS

775

S4-153

An enhanced foot-mounted PDR method with adaptive ZUPT and multi-sensors fusion for seamless pedestrian navigation

Xianlu Tao、Xianlu Tao、Feng Zhu、Xiaohong Zhang
Wuhan University

The rapid development of mass-market sensors built in portable devices has inspired a variety of ubiquitous pedestrian navigation applications. However, seamless positioning of consumer applications is still a challenge, especially in GNSS-denied environments and complex pedestrian dynamics. In order to achieve continuous indoor and outdoor positioning for pedestrians, this paper presents an enhanced foot-mounted pedestrian dead-reckoning (PDR) method through multi-source information of zero velocity update (ZUPT), magnetometer, barometer and smartphone GNSS. The improvement of PDR includes three aspects. First, an adaptive zero-velocity detection method is given, which flexibly adapts to different pedestrian dynamics. Secondly, more accurate magnetic heading changes and pressure-based altitude changes are extracted, which effectively reduce the update information noise derived from MEMS magnetometer and barometer. The heuristic drift reduction (HDR) models are also applied to constraint the cumulative errors of heading and altitude during stable pedestrian motions. Finally, the smartphone GNSS positions are integrated with PDR to provide absolute coordinates, and to correct PDR system errors. All of the multi-source information from the MEMS sensors and the constructed virtual constraints are fused by an extended Kalman filter. The field test results demonstrate that the adaptive zero-velocity detector performs well under different pedestrian speeds and motions, the enhanced PDR method has little drift in heading and height, and its cumulative distance error accuracy reaches 0.23%. After integrating with smartphone GNSS, the multi-source information enhanced foot-mounted PDR has the capability to continuously positioning in open sky, building occlusion and indoor scenes under complex pedestrian dynamics.

Key words Foot-mounted pedestrian dead-reckoning (PDR); Android smartphone GNSS; Adaptive zero-velocity detection; Extended Kalman filter; Integrated navigation

Category: Symposium 4: Positioning and applications => 4.3: Techniques and Applications in High Precision GNSS

777

S4-154

Stochastic Model Real-Time Adjustment of Ionospheric Delay in Long-Range RTK Positioning

Jun Li, Huizhong Zhu, Yangyang Lu
Liaoning Technical University

Although ionosphere-free (IF) combination is usually employed to eliminate ionosphere delays and the IF observations are used in precise positioning. Ionospheric delay is a key factor in GNSS positioning. The observation's information of each frequency cannot be treated as an independent observation signal by the traditional IF combination model. Meanwhile, the IF combination model enlarges the observation noise and cannot impose constraints on the ionospheric delay, it can degrade the strength of the float solution and makes the instantaneous ambiguity resolution very difficult especially for the long-range, therefore, the influence of the ionosphere must be taken into account. In this paper, we propose a stochastic model real-time adjustment method of ionospheric delay (RTI), which does not adopt the stochastic model by empirical model or set the empirical value of ionospheric delay (EMI), but consider the ionospheric real-time characteristics in the original observations, and then determines the stochastic model of RTI. Three Baselines of 103 km, 175 km, 200 km are selected and processed in both static and kinematic mode using stochastic model of the RTI and the EMI. Compare the time series of the float ambiguity, and the estimated ionospheric delay, first ambiguity fixed time (FAFT) and the positioning results under different model. The results show that float ambiguity and ionospheric delay are quite different under different stochastic model. At least 8% can be increased by using RTI compared with EMI for FAFT, and at least 6% for positioning results. Finally, the positioning performance of BDS three-frequency observations is analyzed. The average FAFT in static and kinematic modes is 226s and 270s, and the positioning accuracy after convergence is centimeter level, which can meet the requirements of high-precision static and kinematic positioning.

Key words Ionospheric delay; Long-range; stochastic model; Real-time; Virtual observation;

Category: Symposium 4: Positioning and applications => 4.3: Techniques and Applications in High Precision GNSS

795

S4-155

An evaluation of solar radiation pressure models during eclipse seasons for GPS satellite

Longjiang Tang^{1,2}, Aigong Xu¹, Huizhong Zhu¹, Maorong Ge²

1. School of Geomatics, Liaoning Technical University, Fuxin, Liaoning 123000, China

2. GFZ German Research Centre for Geosciences, Potsdam, Germany

The processing strategies of GPS precise orbit determination (POD) has been optimized for more than 20 years and most individual Analysis Centers (ACs). Currently, Non-gravitational disturbance especially solar radiation pressure (SRP) has become one of the most important error sources in current orbit determination. SRP modeling methods for GNSS satellites not identical between individual ACs and performance of each model are also different. Hence, it is hard to conclude which SRP model is better until now and still needs more consideration due to its complicated effect on satellites. For now, the hybrid strategy of combining both specific terms of empirical and physical models have been proved to be beneficial for the orbit quality by many researches. We first deduce the rigorous relationship between ECOM and Box-wing (BW) model and demonstrate that the other unmodeled forces of no-SRP nature can hardly be all absorbed by current ECOM or BW model. Then we evaluate the way of keeping ECOM parameters in Y and B direction active. Solutions of single GPS POD are performed from 2017 to 2019 based on different combination of ECOM1 (5-parameters) or ECOM2 (9-parameters) and BW model (prior values or estimated values by Duan (2021)). The results of SRP coefficients and day boundary discontinuities (DBDs) demonstrate that there are possibly some unmodeled forces and it will affect orbit accuracy especially during eclipse seasons. ECOM1 plus the estimated coefficients of BW performs best for all GPS satellites, where 3-dimensional orbit accuracy of BLOCK IIR and IIF is 4.0 cm during non-eclipse seasons, 4.9 cm, and 5.3 cm during eclipse seasons. An effort of adjusting coefficients to be estimated in ECOM is also. Keeping ECOM parameters in Y and B direction active will make DBDs of BLOCK IIR out of eclipse seasons admirably coincide with those in eclipse seasons.

Key words GPS; Solar radiation pressure; Eclipse season; ECOM1; ECOM2; Box-wing

Category: Symposium 4: Positioning and applications => 4.3: Techniques and Applications in High Precision GNSS

802

S4-156

An experimental combination of IGS repro3 campaign's orbit and clock products using a variance component estimation strategy

Pierre Sakic¹, Benjamin Männel¹, Gustavo Mansur^{1,2}, Andreas Brack¹, Harald Schuh^{1,2}

1. GFZ Deutsches GeoForschungsZentrum

2. Technische Universität Berlin, Institute for Geodesy and Geoinformation Technology

Over the past years, the International GNSS Service (IGS) has put efforts into reprocessing campaigns reanalyzing the full data collected by the IGS network since 1994. The goal is to provide a consistent set of orbits, station coordinates, and earth rotation parameters using state-of-the-art models. Different from the previous campaigns – namely: repro1 and repro2 – the repro3 includes not only GPS and GLONASS but also the Galileo constellation. The main repro3 objective is the contribution to the next realization of the International Terrestrial Reference Frame (ITRF2020). To achieve this goal several Analysis Centers (AC) submitted their specific products, which are combined to provide the final solutions for each product type. In this contribution, we focus on the combination of orbit and clock products.

We will present a consistent orbit and clock solution based on a newly developed combination strategy where the weights are determined by a least-squares variance component estimation (LSVCE). The orbits are combined in iterative processing, first aligning all the products via a Helmert Transformation, second defining which satellites will be used in the LSVCE, and finally normalizing the inverse of the variance as weights that are used to compute a weighted mean. As for the orbits, the clock combination follows similar steps, aligning all the clocks to a common reference, then computing the LSVCE, and determining the weighted mean. It is important to note that for the variance component estimation, individual system models were derived for orbits and clocks. Moreover, we will discuss the weights factor and their stability in the time evolution for each AC depending on the constellations. In addition, an external validation using a Satellite Laser Ranging (SLR) procedure will be shown for the combined solution.

Key words GNSS, IGS, Repro3, Variance Components Estimation, Orbit & clock combination

Category: Symposium 4: Positioning and applications => 4.3: Techniques and Applications in High Precision GNSS

803

S4-157

Rapid earthquake rupture process inversion with real-time high-rate GPS displacements

Jianfei Zang¹、Caijun Xu^{1,2,3}

1. School of Geodesy and Geomatics, Wuhan University
2. Key Laboratory of Geospace Environment and Geodesy, Ministry of Education, Wuhan University
3. Key Laboratory of Geophysical Geodesy, Ministry of Natural Resources, Wuhan University

Unlike seismometers, real-time Global Positioning System (GPS) can record ground motion reliably without saturation in the near field for large earthquakes. These GPS data enable rapid estimation of fault rupture process. A rapidly reliable fault model can improve the accuracy of earthquake early warning and tsunami early warning and is also helpful for the emergency response. The absolute GPS displacements can be achieved by Precise Point Positioning (PPP) or Real-time Precise Point Positioning (RT-PPP). As precisely final ephemeris for PPP has long latency and real-time ephemeris broadcasted by internet for RT-PPP might suffer from interruption, we use variometric approach to retrieve GPS displacements. This method calculates station velocities by differencing continuous phase observations and integrates velocities to obtain displacements. The method can realize real-time positioning with readily available broadcast ephemeris and avoids the estimation of phase ambiguity. To decrease the influence of residual errors especially ephemeris error, we use a local spatial filter to improve the accuracy of variometric displacements. We invert for the 2019 Mw 7.1 Ridgecrest earthquake rupture process and 2016 Mw 7.8 Kaikoura earthquake rupture process using both variometric displacements and PPP displacements. Our results demonstrate that variometric-based inversions are comparable with PPP-based inversions. This study shows the great potential of variometric approach with only broadcast ephemeris for the rapid rupture process inversion of the earthquake.

Key words real-time high-rate GPS; earthquake rupture process inversion; variometric method

Category: Symposium 4: Positioning and applications => 4.3: Techniques and Applications in High Precision GNSS

811

S4-158

An analysis of inter-system biases in BDS/GPS combination kinematic precise point positioning

Nannan Yang¹、Zongqiu Xu¹、Yantian Xu^{2,3}、Longjiang Tang^{1,4}、Aigong Xu¹、Bo Cheng¹

1. Liaoning Technical University

2. The Chinese Academy of Surveying and Mapping Science

3. Key Laboratory of Surveying and Mapping Science and Geospatial Information Technology of Ministry Resources of Natural Resources

4. GFZ German Research Centre for Geosciences

As newly completed Global satellite navigation system, BeiDou Navigation Satellite System (BDS) plays an important role in various navigation applications. In the BDS/GPS tracking data fusion model, the effect of inter-system biases (ISB), consisting of time offset, hardware delay biases and signal distortion delay needs careful consideration. Hence, a detailed analysis of ISB characteristics in BDS/GPS PPP is performed. We propose two ways of estimating ISB, constant estimation (CE) and random walk (RW) and real data from 35 multi-GNSS experimental (MGEX) stations are processed, while 259 MEGX stations are evenly selected for uncalibrated phase delay (UPD) estimation. For ambiguity-float PPP results, the convergence time of CE is 29.5 min, and positioning accuracy are 3.2 cm, 2.1 cm, and 5.5 cm, in east, north and up directions, while convergence time of RW is decreased by 10.5% and positioning accuracy in E, N and U directions is improved by 48.2%, 35.7% and 42.6%, respectively. A similar conclusion can also be deduced from ambiguity-fixed PPP results. Compared with PPP AR results of CE, convergence time of RW is decreased by 11.4% and its positioning accuracy are improved by 52.4%, 38.1% and 44.3%, respectively in three direction. In addition, the average time to first fix (TTFF) of CE is 32.1 min and fixed rate is 42.9%, while it is 29.7 min and 54.3% for RW. From the analysis of convergence time, positioning accuracy, TTFF and the fixed proportion of ambiguity resolution, we can conclude that BDS/GPS combined kinematic PPP performs best when the ISB is estimated as a Random Walk parameter.

Key words inter-system bias, BDS/GPS Combination, Kinematic PPP, Random Walk, convergence time, positioning accuracy.

Category: Symposium 4: Positioning and applications => 4.3: Techniques and Applications in High Precision GNSS

819

S4-159

Estimation of the ionospheric VTEC and satellite DCB from BDS single-frequency PPP with multi-layer mapping function

Ke Su, Shuanggen Jin

Shanghai Astronomical Observatory, Chinese Academy of Sciences

The ionospheric observables and satellite differential code biases (DCBs) act as the significant error sources in the global navigation satellite system (GNSS) positioning, navigation and timing (PNT) services and are challenging to estimate correctly. In this contribution, a refining single-frequency precise point positioning (SFPPP) method is applied to estimate the ionospheric vertical total electron content (VTEC) and satellite DCBs based on the multi-layer ionosphere mapping function (MF). The dual-frequency methods are conducted as well for comparisons, including the dual-frequency carrier-to-code leveling (CCL) and dual-frequency PPP (DFPPP). The methods isolate the ionospheric VTEC values from the slant ionospheric delay with the generalized trigonometric series function (GTSF) and precisely estimate the satellite DCB with the zero-mean condition. The SFPPP-derived VTEC estimates are validated and evaluated by comparing with the International GNSS Service (IGS) products and using ionosphere-corrected (IC) SFPPP in both static and kinematic scenarios, respectively. Using the 74 multi-GNSS experiment (MGEX) network stations for three months, the results indicate that the precision of the estimated VTEC by applying the multi-layer MF is improved for the SFPPP approach. The static and kinematic positioning performances of the BDS IC SFPPP with the ionospheric correction derived from the multi-layer MF SFPPP are better comparing to the single-layer MF. The estimated BDS DCB with the single-frequency solution is stable and of high accuracy. The SFPPP approach with multi-layer MF is demonstrated as a promising and reliable method to retrieve the VTEC and satellite DCB with the low-cost property for the GNSS users.

Key words BeiDou Navigation Satellite System (BDS) · Vertical total electron content (VTEC) · Single-frequency · Precise point positioning (PPP) · Differential code bias (DCB)

Category: Symposium 4: Positioning and applications => 4.3: Techniques and Applications in High Precision GNSS

823

S4-160

A combined GNSS and UWB locating algorithm for indoor and outdoor mixed scenario

Siyuan Wang

Beijing University of Civil Engineering and Architecture

Aiming at the continuous acceleration of urbanization and the increasing demand for ubiquitous positioning in cities, a solution to the unreliability and low positioning accuracy of a single positioning system in a complex environment is proposed. In order to make up for the loss of blind zone in scenario change, we proposed a cooperative positioning system based on GNSSUWB, which can achieve the seamless positioning between buildings in the hybrid scene. Utilizing the advantages of GNSS positioning in an open urban environment, UWB's indoor high-speed short-distance wireless communication and high-precision ranging value characteristics, the original positioning data and ranging information are combined through adaptive extended Kalman filtering to perform combined positioning. The optimal positioning information in different positioning environments will be output after independent judgment in order to achieve a high-precision seamless positioning process. Experiments show that: GNSS, UWB, GNSS/UWB combined positioning experiments are carried out separately, which shows that the GNSS/UWB tight combined fusion positioning system can effectively solve the positioning defects and positioning blind spots in a single system in a complex environment, and it is easy to deploy in practical applications.

Key words Global positioning system; Ultra-wideband; Cooperative positioning; Adaptive extended Kalman filter;

Category: Symposium 4: Positioning and applications => 4.3: Techniques and Applications in High Precision GNSS

833

S4-161

Performance Analysis of GNSS Augmented by LEO Constellation

Xing Su, Hanlin Chen, Qiang Li, Zhimin Liu
Shandong University of Science and Technology

Global Navigation Satellite System (GNSS) is a system that uses radio signals emitted by navigation satellites to perform precise time and range measurement, and provides three-dimensional, all-weather, all-weather positioning, navigation and timing services (PNT) for users around the world. GNSS basic services can only provide meter-level navigation and positioning accuracy. For purpose of users requirements for accuracy, integrity, continuity, availability, and anti-interference, each GNSS system has not only upgraded satellites and improved signal systems, but also established ground-based augmentation system (GBAS) and satellite-based augmentation system (SBAS). Multi-GNSS Fusion Precision Point Positioning (PPP) can shorten the convergence time to a certain extent due to the increase in the number of visible satellites, but because the satellite geometry changes little in a short time, the improvement effect is very limited. In order to solve the problem that GNSS is difficult to achieve rapid convergence for precise point positioning (PPP). Low Earth Orbit (LEO) satellites that broadcast navigation signals are presented for augmentation of GNSS navigation performance, especially for PPP ambiguity convergence. This paper will simulate the GNSS (GPS/GLONASS/Galileo/BDS) constellation and different LEO constellations. The effects of LEO navigation satellites on satellite visibility, position dilution of precision (PDOP), PPP convergence speed and accuracy will be analyzed. The initial analysis results show that with the addition of LEO navigation satellites, the global averaged number of visible satellite is in-creased by about 6, with the improvement of about 22%; the averaged PDOP value is reduced to 1.16, with the reduction of about 25%; the PPP convergence time is reduced from about 30 min to 1-2 min, and PPP accuracy is improved to 2 cm in 3D.

Key words GNSS; LEO Constellation; Satellite Visibility; PDOP; PPP

Category: Symposium 4: Positioning and applications => 4.3: Techniques and Applications in High Precision GNSS

844

S4-162

Study on the stability of GNSS ISB

Shuli Song、 Hanyu Wang、 Weili Zhou、 Guoqiang Jiao、 Zhitao Wang
Shanghai Astronomical Observatory, Chinese Academy of Sciences

With the development of multi-GNSS, it is very favourable to process and apply multiple GNSS jointly for obtaining more stable and reliable positioning, timing and other services. However, the inter-system bias(ISB) between GNSS have to be considered for getting better performance. Especially for the hourly ultra-rapid and real-time multi-GNSS processing in GNSS data analysis center (AC), the feasible and effective processing strategy of ISB is very necessary for getting the satellite orbit and clock products with the consistent reference efficiently. In this article, with two years' ISB series of BDS, Galileo and GLONASS relative to GPS at about 100 global stations, the re-align methodology of ISB datum is studied. The stability, spatio-temporal characteristics and device correlation of all the ISB from more than 10 types of GNSS receivers and antennas are analyzed. Using the mean filter with the sliding windows from 1 to 30 days, the high-frequency variation and predictability of ISB are inspected. The validation in precise orbit determination and point positioning show that, to some extent, the processing efficiency can be improved with fixed ISB predicted within 7 days.

Key words Multi-GNSS, inter-system bias(ISB), PPP, POD

Category: Symposium 4: Positioning and applications => 4.3: Techniques and Applications in High Precision GNSS

845

S4-163

Non-isotropy of the troposphere and its effect on the long-rang RTK

LEI LI、YING XU、XIN CHEN、GUOLIN LIU
Shandong University of Science and Technology

Real-time estimation of high-precision tropospheric delay is the premise of achieving GNSS long-distance network RTK technology. The Slant Total Delay(STD) is different in different azimuth when the elevation of them is the same. Most studies simply consider that the troposphere is isotropic or anisotropic. However, this paper proves that the non-isotropy of the troposphere and accesses its effect on the long-range RTK. The STD of 100 station evenly distributed in the world are estimated using ray tracing method based on the numerical weather prediction (NWP) pressure stratification and surface meteorological parameters (spatial resolution: $1^{\circ}\times 1^{\circ}$, time resolution: 1 h). Comparing these STD with the STD calculated by multiplying Zenith Tropospheric Delay (ZTD) by the VMF mapping function, the non-isotropy of the troposphere is proved. To evaluate impact of the non-isotropy of the troposphere on long-distance network RTK, 24-hour GPS dual frequency observation data of three baselines with the length of 125km, 168km and 233km are collected respectively. Two STD estimation strategies are used in the RTK data processing. One is using the NWP data to inverse the ZTD, then estimating the STD with VMF mapping function and horizontal gradient term. The other one is estimating the STD with ray tracing method. The tropospheric delay residual, ionospheric delay, unknown position and ambiguity are solved together in the observation equation for both strategies .The results show that the average time of ambiguity resolution using VMF + horizontal gradient is 3.5 min, 5.7 min and 8.3 min longer than using ray tracing method.

Key words Tropospheric delay; Non-isotropy; Long-range RTK; NWP

Category: Symposium 4: Positioning and applications => 4.3: Techniques and Applications in High Precision GNSS

854

S4-164

Kinematic positioning through multi-GNSS android pseudoranges: Preliminary tests and results

Amarildo Haxhi, Harris Perakis, Vangelis Zacharis, George Piniotis, Vassilis Gikas

National Technical University of Athens

Notwithstanding, all contemporary smartphone devices offer a versatile platform for personal mobility and ITS-related applications, still the positioning accuracy they achieve does not meet the localization requirements for many applications. Very recent studies on Single Point Positioning (SPP) processing of raw GNSS data in smartphones coupled with appropriate filtering and smoothing techniques demonstrated clearly promising results. More specifically, these studies assume static and pedestrian motion under open-sky conditions test scenarios. Analysis of the results of published research indicate the effect of C/No values, multipath indicators as well as phase observables on the positioning solution quality. This study aims at investigating the potential of the aforementioned processing strategy using raw smartphone multi-GNSS observations for vehicle kinematic positioning. In effect, in this work we adapt and elaborate a similar strategy to those used in static conditions for open-source data collected under a light urban environment. A multitude of GNSS processing strategies were implemented and tested including: (i) single-constellation, (ii) multi-constellation, (iii) pseudorange phase smoothing, (iv) C/No-based filtering, and (v) multipath-based solution rejection scenarios. The validation of the results obtained relies on comparisons against a high-fidelity ground reference trajectory established using geodetic-grade equipment. Preliminary results indicate that single- and multi-GNSS appropriately tuned processing strategies may provide increased availability of solutions with horizontal accuracy under 5 m. The main conclusions drawn from the analysis today indicate that while high-accuracy performance is still limited by low-cost hardware capabilities, non-safety critical applications (e.g., smart mobility with requirements of the order of 3-5 m) can already rely on COTS (Commercial-Off-The-Shelf) devices paired with appropriate processing strategies.

Key words Android GNSS, Single Point Positioning, pseudorange smoothing, kinematic positioning, ITS

**Symposium 5: Global Geodetic
Observing System (GGOS): the
metrological basis for the
monitoring of the System Earth**

**S5.1: Geodetic infrastructure for Earth
System Monitoring**

Category: Symposium 5: Global Geodetic Observing System (GGOS): the metrological basis for the monitoring of the System Earth => 5.1: Geodetic infrastructure for Earth System Monitoring

153

S5-001

New Daily Coordinates of GNSS CORS in Japan Based on the GEONET 5th Analysis Strategy

Naofumi Takamatsu、 Hiroki Muramatsu、 Naohiro Tada、 Keitaro Ohno、 Satoshi Abe、 Satoshi Kawamoto
Geospatial Information Authority of Japan

1. Overview of GEONET and its analysis strategy

Geospatial Information Authority of Japan has operated a dense GNSS observation network system named GEONET since 1996, which consists of more than 1,300 CORS covering most region of Japan. The daily coordinates of all sites are calculated with a consistent analysis strategy and are provided on our website. Nowadays, our products support activities in various fields including crustal deformation monitoring, location based service, and research of earth and planetary science.

In order to handle the update of ITRF and the launch of GPS Block III satellites, we developed a new analysis strategy called “F5”, as a successor of the previous one called “F3”. The official operation of F5 started on April 1st, 2021. The coordinates of all GEONET sites from 1996 are now available on the website (<https://terras.gsi.go.jp>) and have been appended the recent results once per week.

In our presentation, we will show the major improvement points of F5: introduction of global network analysis and update of troposphere modelling.

2. Major improvement of F5

2.1. Introduction of global network analysis

In F3, time series of daily coordinates sometimes suffers from undesired jumps because the time series is based on daily positions of a reference station estimated from only a small number of fiducial sites located in the East Asia. In order to generate the stable time series aligned to ITRF2014, we form a baseline network with around 100 CORS covering the whole earth.

2.2. Update of troposphere modelling

The use of conventional mapping function used in F3 may cause spurious annual height variations up to 3mm (Munekane et al., 2008). We introduce the mapping function based on numerical weather models and change the timestep of troposphere parameter estimation. As a result, we successfully suppressed the spurious annual variation

and found the shorter timestep is better in terms of RMS of baseline vector.

Key words GEONET, F5, daily coordinates, global network analysis, troposphere modelling

Category: Symposium 5: Global Geodetic Observing System (GGOS): the metrological basis for the monitoring of the System Earth => 5.1: Geodetic infrastructure for Earth System Monitoring

163

S5-002

Accuracy evaluation of gravity continuous observation at key comparison site of absolute gravimeter

LiShuang MOU¹、JinYang FENG²、 ShuQing WU²

1. National Institute of Metrology

2. NIM

When the superconducting gravimeter outputs the continuous gravity change value of the gravity comparison reference point, the original output signal is the voltage value. In the process of converting the gravity change value into the acceleration signal of gravity and removing the drift, this process will introduce uncertainty to the continuous observation results. In this paper, the uncertainty of continuous observation results of superconducting gravimeter at the comparison point is analyzed. The calibration factor of superconducting gravimeter is $-928.00 \text{ nm/s}^2/\text{V}$, and the uncertainty is $0.222 \text{ nm/s}^2/\text{V}$. The uncertainty of continuous observation results of superconducting gravimeter introduced by the calibration factor is 0.88 nm/s^2 . After 5.5 years' observation at the same site of superconducting gravimeter and absolute gravimeter, the drift rate of superconducting gravimeter is $-14.66 \text{ nm} / \text{s}^2 / \text{year}$, and the uncertainty is $2.1 \text{ nm} / \text{s}^2 / \text{year}$. The uncertainty of continuous observation results of superconducting gravimeter introduced by the drift is 6.30 nm/s^2 , and the uncertainty introduced by the two variables to the continuous gravity observation results is 6.37 nm/s^2 . In general, it can be considered that the accuracy of continuous observation of the comparison point can meet the requirements of the reference point. In the later stage, the accuracy of gravity continuous observation can be improved by participating in the comparison regularly.

Key words uncertainty; comparison site of absolute gravimeter; superconducting gravimeter; continuous observation of comparison site

Category: Symposium 5: Global Geodetic Observing System (GGOS): the metrological basis for the monitoring of the System Earth => 5.1: Geodetic infrastructure for Earth System Monitoring

164

S5-003

Coordinating global geodesy in Japan: GGOS Japan

Toshimichi Otsubo¹、Basara Miyahara²、Shinobu Kurihara²、Yusuke Yokota³、Yu Takagi²、Shun-ichi Watanabe⁴、Hiroshi Takiguchi⁵、Yuichi Aoyama⁶、Koji Matsuo²

1. Hitotsubashi University

2. Geospatial Information Authority of Japan

3. University of Tokyo

4. Japan Coast Guard

5. Japan Aerospace Exploration Agency

6. National Institute of Polar Research

GGOS Japan, initially called as GGOS Working Group of Japan, was established 8 years ago, in 2013. It is a unique situation that six institutes in Japan have operated geodetic facilities with VLBI and/or SLR and we realized that we needed an entity to coordinate Japan's geodetic plans. Its core members consist of a chair, a secretary, a lead of the outreach working group, a lead of the DOI working group and representatives of five core techniques: VLBI, SLR, GNSS, DORIS and gravity. It is largely supported by tens of people in Japan and also by its parent entity, IAG subcommittee in Japan. It has helped strengthen the collaboration among the space-geodesy agencies in Japan. GGOS Japan has been positioned in GGOS as the first GGOS Affiliate since 2017 and we strived to get connected to international organizations. Our achievements cover a broad range of science and operation: assembling our site list, hosting various domestic/international meetings, planning a special issue in a domestic journal, producing its leaflet and website. GGOS Japan also provides online and offline forums for timely issues, such as assigning Data DOI to geodetic dataset, reviewing operational status of each institute/station, promoting local tie campaigns for ITRF2020.

Key words Space geodesy, GGOS Japan, GGOS

Category: Symposium 5: Global Geodetic Observing System (GGOS): the metrological basis for the monitoring of the System Earth => 5.1: Geodetic infrastructure for Earth System Monitoring

173

S5-004

Four Achievable Control Schemes for Inertial Reference System in Space

Chunyu Xiao, Yun Ma, Hongyin Li, Zebing Zhou

MOE Key Laboratory of Fundamental Physical Quantities Measurement, Hubei Key Laboratory of Gravitation and Quantum Physics, PGMF, School of Physics, Huazhong University of Science and Technology

Inertial Reference System (IRS) is the foundation to realize ultra-low microgravity spacecraft, which can monitor the relative motion of the spacecraft with reference to local geodesic. With this technology, non-gravitational disturbances on the spacecraft can be measured and then compensated, so that the spacecraft can be applied in the fields of satellite gravity recovery, space-borne gravitational experiments and so on. In this paper, four achievable control schemes are proposed to realize the IRS for space missions. Their control strategies, properties, applications, relationships and differences are systematically discussed in detail.

Key words Inertial Reference, Drag-Free, Control Scheme

Category: Symposium 5: Global Geodetic Observing System (GGOS): the metrological basis for the monitoring of the System Earth =» 5.1: Geodetic infrastructure for Earth System Monitoring

192

S5-005

GGOS Bureau of Networks and Observations: Network Status and Related Activities

Michael Pearlman¹、 Dirk Behrend³、 Allison Craddock⁵、 Erricos Pavlis⁷、 Jérôme Saunier⁹、 Elizabeth Bradshaw¹¹、 Riccardo Barzaghi¹³、 Daniela Thaller¹⁴、 Benjamin Maennel²、 Ryan Hippenstiel⁴、 Roland Pail⁶、 C.K. Shum⁸、 Nicholas Brown¹⁰、 Claudia Carabajal¹²

1. Center for Astrophysics
2. GFZ German Research Center for Geosciences, Frankfurt, Germany
3. NVI, Inc./NASA Goddard Space Flight Center, Greenbelt MD, United States
4. National Geodetic Survey, Silver Spring, MD, United States
5. Jet Propulsion Laboratory/California Institute of Technology, Pasadena, CA, United States
6. Technische Universität München, Munich, Germany
7. University of Maryland, Baltimore MD, United States
8. The Ohio State University, Columbus, OH, United States
9. Institut Géographique National, St. Mande, France
10. Geoscience Australia, Canberra, Australia
11. National Oceanography Centre, Liverpool, United Kingdom
12. SSAI, Inc@/NASA Goddard Space Flight Center, Greenbelt MD, United States
13. Politecnico di Milano, Milan, Italy
14. Bundesamt für Kartographie und Geodäsie, Frankfurt, Germany

The GGOS Bureau of Networks and Observations works with the IAG Services (IVS, ILRS, IGS, IDS, IGFS, IERS, and PSMSL) to advocate for the expansion and modernization of space geodetic networks for the maintenance and improvement of the reference frame and other applications, as well as for the integration of the techniques. Of particular interest is the integration of gravimetric and tide gauge networks in view of the forthcoming establishment of a new absolute gravity reference frame. New sites are being established following the GGOS concept of “core” and co-location sites, and new technologies are being implemented to enhance performance in data yield as well as accuracy.

The IAG Committees and Joint Working Groups play an essential role in the Bureau activity. The Standing Committee on Performance Simulations and Architectural Trade-offs (PLATO) uses simulation and analysis techniques to project future network capability and to examine trade-off options. The Committee on Data and Information is working on a strategy for a GGOS metadata system for data products and a more comprehensive long-term plan for an all-inclusive system. The Committee on Satellite Missions is working to enhance communication

with the space missions, to advocate for missions that support GGOS goals and to enhance ground systems support. The IERS Working Group on Site Survey and Co-location (also participating in the Bureau) is working to enhance standardization in procedures, outreach and to encourage new survey groups to participate and improve procedures to determine systems' reference points, a crucial aid in the detection of technique-specific systematic errors.

We will give a brief update on the status and projection of the network infrastructure for the next several years, and the progress and plans of the Committees/Working Groups in their critical role in enhancing data product quality and accessibility to the users, scientists and the general community.

Key words Space Geodesy Networks, IAG Services, SLR, VLBI, DORIS, GNSS, IGFS, PSMSL, IERS, Global Geodetic Reference Systems, International Height Reference System

Category: Symposium 5: Global Geodetic Observing System (GGOS): the metrological basis for the monitoring of the System Earth => 5.1: Geodetic infrastructure for Earth System Monitoring

227

S5-006

VLBI-GNSS co-location at the Ishioka Geodetic Observing Station

Saho Matsumoto、Haruka Ueshiba、Tomokazu Nakakuki、Yu Takagi、Kyonosuke Hayashi、Katsuhiko Mori、Toru Yutsudo、Tomokazu Kobayashi、Yudai Sato
Geospatial Information Authority of Japan

International Terrestrial Reference Frame (ITRF) is constructed by combining observations of four space geodetic techniques, VLBI, SLR, GNSS and DORIS. In order to combine the geodetic reference frames given by these techniques into a single frame, such as ITRF, it is essential to determine local-ties, that is, relative position vectors between instruments of different space geodetic observations. Co-location is surveying and computation to determine the local ties. We, Geospatial Information Authority of Japan has operated two geodetic techniques, VLBI and GNSS, at the Ishioka Geodetic Observing Station (hereafter Ishioka) since 2016 and conducted local-tie surveys every one to three years to determine the local tie-vector between those two antennas.

The reference point of VLBI antenna is defined as the intersection of antenna elevation and azimuth axes and called invariant point of the antenna (IVP). The IVP commonly cannot be measured directly and thus needs to be estimated. There are some choices to estimate the IVP. The one is 'outside method' by which we estimate the IVP from the center of trajectory of a target attached on the outer edge of the antenna. An alternative called 'inside method' is to measure targets attached on the inner wall of the azimuth cabin. By this method, both the target and the survey instrument are installed in the cabin constructed to include the intersection of the axes. Therefore, this method can be applied only to the specific antenna with an observation pillar constructed in it, but was expected to be effective to improve the efficiency of local-tie survey. We conducted local-tie surveys with both methods in 2018 and confirmed higher efficiency of the inside method.

In this presentation, we will report the details of local-tie survey at Ishioka and compare performance of the two methods based on the results obtained from the survey in 2018. We will also discuss the result of the latest local-tie survey at Ishioka.

Key words co-location, local-tie, VLBI, GNSS, invariant point, ITRF2020, Ishioka

Category: Symposium 5: Global Geodetic Observing System (GGOS): the metrological basis for the monitoring of the System Earth => 5.1: Geodetic infrastructure for Earth System Monitoring

239

S5-007

The SUT Method for Precision Estimation of Mixed Additive and Multiplicative Random Error Model in Geodetic Measurement

Chen Tao、Wang Leyang

East China University of Technology, Nanchang, 330013, China

With the rapid development of modern surveying and mapping technology, the measurement random errors represented by electromagnetic wave show as mixed additive and multiplicative random error, and the traditional additive random error model adjustment theories cannot satisfy the need of solving the new model. Although the existing parameter estimation method of mixed additive and multiplicative random error model can achieve second-order unbiased, the precision estimation method can only achieve first-order precision. If the approximate function method is used to obtain the second-order precision information of parameter estimations, it will inevitably require complicated derivation operation due to the complex nonlinear relationship between parameter estimations and observations in the mixed additive and multiplicative random error model. Aiming at this problem, this paper uses the scaled unscented transformation method, which does not require derivative operation and understand the composition of nonlinear function, to obtain the second-order precision information of parameter estimations. Finally, the proposed method is applied to GPS elevation fitting model and digital terrain model, and is compared with existing methods. The results of experiments show that using the proposed method to solve the mixed additive and multiplicative random error model can effectively avoid complicated derivation operation, obtain second-order unbiased parameter estimations and its second-order precision information, which verifies the feasibility and advantages of the proposed method.

Key words Mixed additive and multiplicative random error model; Weighted least squares; Nonlinear iteration; SUT method; Precision estimation

Category: Symposium 5: Global Geodetic Observing System (GGOS): the metrological basis for the monitoring of the System Earth => 5.1: Geodetic infrastructure for Earth System Monitoring

257

S5-008

RAEGE: a Spanish-Portuguese infrastructure of geodetic stations

Jose A. Lopez-Perez
Instituto Geografico Nacional

This presentation shows the current status of the Red Atlantica de Estaciones Geodinamicas y Espaciales (RAEGE), a joint Spanish-Portuguese infrastructure of geodetic stations. It will be composed of four VGOS radio-telescopes, two in Spain (Yebes and Gran Canaria) and two in Portugal (Santa Maria and Flores islands, Azores archipelago). The Yebes VGOS radio-telescope is fully operational and integrated in the VGOS core network since 2016. The Santa Maria VGOS radio-telescope has undergone major maintenance operations and will join regular IVS observations with its tri-band S/X/Ka receiver soon, until it becomes a VGOS station by mid 2022. Additionally, each station will include GNSS receivers, gravimeters and a local-tie network. In particular, the RAEGE-Yebes station will have a Satellite Laser Ranging system, which is under construction. It can be said that RAEGE is the Spanish-Portuguese response to UN resolution 69/266 and GGOS. The current status of all the four RAEGE stations will be presented.

Key words VLBI, VGOS, RAEGE

Category: Symposium 5: Global Geodetic Observing System (GGOS): the metrological basis for the monitoring of the System Earth => 5.1: Geodetic infrastructure for Earth System Monitoring

273

S5-009

Absolute Positioning of Active Radar Transponders from Sentinel-1 Observations — Experiences and Results

Marius Schlaak¹, Christoph Gisinger², Thomas Gruber¹

1. Chair of Astronomical and Physical Geodesy, Technical University of Munich (TUM)

2. Remote Sensing Technology Institute, German Aerospace Center (DLR)

Geodetic monitoring using SAR, requires long term stable and accurate measurements. As an alternative to large passive corner reflectors, smaller active radar transponders have become commercially available off-the shelf. We report results using these Electronic Corner Reflectors (ECRs) for geodetic measurements with Sentinel-1 C-band Synthetic Aperture Radar (SAR) data, after collecting observations for one year from 12 different stations.

In the frame of the ESA project SAR-HSU, 10 ECRs surrounding the Baltic Sea in Sweden, Finland, Poland and Estonia, as well as two ECRs located at the campus of German Aerospace Center (DLR) in Oberpfaffenhofen, Germany have been installed. 3D absolute positioning for each of the 12 ECRs has been conducted following the procedure described in Gisinger et al. 2015 and Gruber et al. 2020. To achieve refined absolute positioning with SAR, precise orbit solutions of Sentinel-1 are used and corrections for atmospheric path delays, solid Earth tidal deformation, and Sentinel-1 specific system corrections are applied. Additionally, the processing accounts for ECR specific corrections biases per incidence angle, the phase center difference between ascending and descending geometries as well as electronic delays within the transponders. The results are analyzed in terms of ECRs' characteristics and performances. Moreover, the accuracies of the geodetic positions are evaluated by comparing them with reference coordinates in terms of their internal and absolute accuracies using confidence ellipsoids as described by Gisinger et al. 2017.

In the paper detailed results for the geolocation and accuracies of ECR positioning using Sentinel-1 observations are provided as well as experiences with the off-the shelf transponders are summarized.

Key words Active Radar Transponder, Electronic Corner Reflector, Absolute Positioning, Synthetic Aperture Radar, SAR

Category: Symposium 5: Global Geodetic Observing System (GGOS): the metrological basis for the monitoring of the System Earth => 5.1: Geodetic infrastructure for Earth System Monitoring

353

S5-010

Probing a southern hemisphere VLBI intensive baseline configuration for dUT1 determination

Sigrid Böhm¹、 Jakob Gruber¹、 Lisa Kern¹、 Jamie McCallum²、 Lucia McCallum²、
Jonathan Quick³、 Matthias Schartner^{4,1}

1. TU Wien

2. University of Tasmania

3. Hartebeesthoek Radio Astronomy Observatory

4. ETH Zürich

The difference of universal time to atomic time UT1-UTC (dUT1) is a key parameter for precise positioning and navigation using space geodetic techniques. Measurements of dUT1 can only be provided by the geodetic Very Long Baseline Interferometry (VLBI). The parameter is routinely estimated twice per week from VLBI 24-hour sessions and with a lower latency from so-called intensive sessions. Routine intensives are observed daily for one hour, on one or sometimes two baselines. All of the current IVS (International VLBI Service for Geodesy and Astrometry) intensive sessions are operated on baselines involving northern hemisphere telescopes only. In 2019 we started the Southern Hemisphere Intensive observing program (SI) as a joint initiative of TU Wien, the University of Tasmania and the Hartebeesthoek Radio Astronomy Observatory. The SI sessions are observed with three VLBI stations located south of the equator: HART15M (South Africa), HOBART12 (Tasmania) and YARRA12M (Western Australia). Observations including HOBART12 are observed in mixed-mode configuration, using the VGOS receiver in Hobart and the legacy systems at the other stations. For the year 2020, we scheduled 38 SI sessions recorded with a high data rate of 1 Gbps to compensate for the reduced sensitivity of the smaller antennas. Starting from April the program is continued with 36 sessions scheduled for 2021. In this contribution, we will primarily focus on the dUT1 results of the sessions from the year 2020, which could be successfully observed, correlated and analyzed.

Key words VLBI, UT1-UTC

Category: Symposium 5: Global Geodetic Observing System (GGOS): the metrological basis for the monitoring of the System Earth => 5.1: Geodetic infrastructure for Earth System Monitoring

426

S5-011

Determination of the Earth's mantle structure based on a joint analysis of gravimetric and seismometric earthquake recordings at the Borowa Gora Geodetic-Geophysical Observatory

Kamila Karkowska^{1,3}, Monika Wilde-Piórko¹, Przemysław Dykowski¹, Tomasz Olszak³, Marcin Sękowski¹, Marcin Polkowski²

1. Institute of Geodesy and Cartography

2. Accenture, Applied Intelligence

3. Warsaw University of Technology

The wide range of frequencies, which are recorded by the contemporary relative gravimeters, allow to use them not only to analyze tidal periods but also for very short-term phenomena e.g. the analysis of recordings of earthquakes. Superconducting gravimeters are capable to detect surface waves of periods even up to 500-600 s, while a typical broad-band seismic sensor, due to its mechanical limitation, can detect them only up to the periods of 200-300 s.

Since late April 2016 at the Borowa Gora Geodetic-Geophysical Observatory of the Institute of Geodesy and Cartography (Warsaw, Poland), which participating in GGOS-PL, the iGrav-027 superconducting gravimeter has been fully operational. A few months later (December 2016), the 151B-120 broadband seismometer has been installed in cooperation with the Department of Lithospheric Physics of the University of Warsaw. Besides these two instruments, the Observatory, since February 2020, temporally has been hosted a spring gravimeter, LaCoste&Romberg ET26 (owned by the Department of Geodesy and Cartography of the Warsaw University of Technology).

This study presents a joint analysis of the gravimetric and seismometric data in the determination of group-velocity dispersion curves of fundamental-mode Rayleigh surface waves. The recordings of earthquakes from the Observatory were collected in a database. Following, the group-velocity dispersion curves were calculated by applying the multiple filter technique. Simultaneous seismometric and gravimetric recordings allow the study of a wider response for incoming seismic waves. In this way, one joint group-velocity dispersion curve of Rayleigh surface waves for a wider range of periods has been estimated, which was then inverted by a linear inversion method to calculate a distribution of shear-wave seismic velocity with depth in the Earth's mantle.

This work was done within the research project No. 2017/27/B/ST10/01600 financed from the funds of the Polish National Science Centre.

Key words relative gravimeter, seismometer, Rayleigh surface waves

Category: Symposium 5: Global Geodetic Observing System (GGOS): the metrological basis for the monitoring of the System Earth =» 5.1: Geodetic infrastructure for Earth System Monitoring

469

S5-012

ILRS: Recent Progress and Plans

Ulrich Schreiber¹、 Michael Pearlman²、 Erricos Pavlis³、 Claudia Carabai⁴、 Jean-Marie Torre⁵、 Toshimichi Obsubo⁶、 Michael Steindorfer⁷

1. Technical University of Munich

2. Center for Astrophysics, Cambridge MA, USA

3. University of Maryland, Baltimore MD, USA

4. SSAI, Inc. @ NASA Goddard Space Flight Center, Code 61A, Greenbelt MD, USA

5. Observatoire de la Côte d'Azur, Nice, France

6. Hitotsubashi University, Tokyo, Japan

7. Space Research Institute, Austrian Academy of Sciences, Graz, Austria

The International Laser Ranging Service (ILRS) continues to improve its services through network expansion and upgrade, improved diagnostic procedures, and upgrades of its modeling and analysis approaches. The challenges of the COVID-19 pandemic and problems with hardware importation and budget issues have delayed the schedule, but progress continues and several new stations are slated to be operational by the end of 2021. Some of these systems will be co-located with VLBI. Top priority tracking continues to be the reference frame development and low orbiting Earth Sensing Satellites, but in coordination with the IGS and the International Committee on GNSS (ICG), coverage on GNSS continues to expand. Some stations are being adapted to accommodate ground and space-time synchronization; a few continue with lunar laser ranging activities, while several others have begun developing new lunar ranging capability. About a dozen stations are active in space-debris tracking for studies of orbital dynamics and reentry predictions. New tools and procedures have been implemented to improve the quality of SLR data and derived products, and to expedite the resolution of performance issues. The ILRS has submitted its contribution to the ITRF2020; some interesting results from the years' analysis activities will be presented. This paper will give an overview of activities underway within the Service, paths forward and presently envisioned, and current issues and challenges.

Key words International Laser Ranging Service, Satellite Laser Ranging, Lunar Laser Ranging, Debris Tracking

Category: Symposium 5: Global Geodetic Observing System (GGOS): the metrological basis for the monitoring of the System Earth => 5.1: Geodetic infrastructure for Earth System Monitoring

490

S5-013

Systematic errors in SLR observation residuals to Swarm satellites

Dariusz Strugarek¹, Krzysztof Sońnica¹, Daniel Arnold², Adrian Jäggi², Mateusz Drożdżewski¹, Grzegorz Bury¹, Radosław Zajdel¹

1. Wrocław University of Environmental and Life Sciences

2. Astronomical Institute, University of Bern

Numerous low Earth orbiters (LEOs) observe the Earth system, including the three ESA Swarm satellites equipped with GNSS receivers and SLR retroreflectors. GNSS technique onboard LEOs is commonly used to derive precise orbit determination (POD) products, whereas the SLR technique is commonly used to validate the POD products based on GNSS. We investigate the detector-specific errors in SLR residuals, which may corrupt the SLR observations. We focus on the dependency of SLR residuals to Swarm satellites for groups of stations divided by the different detector types employed at stations. We found that SLR stations equipped with the compensated single-photon avalanche diodes (CSPAD) detectors are characterized with the smallest SLR residuals; in contrast, multi-channel plates (MCP) and photomultiplier tube (PMT) detectors show a dependency of SLR data to, e.g., satellite nadir angles. We discuss modeling of systematic errors of SLR residuals to LEOs based on the example of Swarm satellites. We conduct tests considering the estimation of SLR range biases and tropospheric biases to improve SLR validation of Swarm GNSS POD products. Proper modeling of troposphere and range biases reduces systematic errors in SLR residuals, as well as decreases the dependency of residuals to the station azimuth angle, Sun-satellite-Earth orientation, and satellite nadir angle.

Key words SLR, GNSS, low Earth orbiters, orbit validation

Category: Symposium 5: Global Geodetic Observing System (GGOS): the metrological basis for the monitoring of the System Earth => 5.1: Geodetic infrastructure for Earth System Monitoring

497

S5-014

Status of the future GGOS core site Metsähovi, Finland

Jyri Näränen, Hannu Koivula, Markku Poutanen, Arttu Raja-Halli, Joonas Eskelinen, Mirjam Bilker-Koivula, Nataliya Zubko, Ulla Kallio
Finnish Geospatial Research Institute FGI, National Land Survey of Finland

Metsähovi Geodetic Research Station (MGRS) in Southern Finland has been undergoing a major upgrade over the past several years. When completed, MGRS will be one of the northernmost GGOS core stations. The station currently houses several GNSS receivers, including an IGS station, an absolute gravimeter FG5-X, two superconducting gravimeters, and a DORIS beacon. Geodetic VLBI sessions coordinated by IVS have been observed since 2005 in collaboration with close-by Metsähovi Radioastronomical Observatory. A new dedicated VGOS radio telescope system is being commissioned together with a new 2kHz SLR system. Local tie measurements linking the different systems are being done and research is carried out to improve the measurement methods. A high-precision time and frequency link between MGRS and the Finnish metrology institute VTT MIKES responsible for the national time (UTC MIKE) has been realized via commercial White Rabbit technology. Metsähovi currently houses two trihedral triangular corner reflectors for geodetic SAR measurements.

We present the current status of the upgrade of Metsähovi and introduce the instrumentation that already contribute and will contribute in the future to various IAG services.

Key words multi-technique, SLR, VLBI, gravimetry, DORIS, local ties

Category: Symposium 5: Global Geodetic Observing System (GGOS): the metrological basis for the monitoring of the System Earth => 5.1: Geodetic infrastructure for Earth System Monitoring

520

S5-015

Interoperability of the GGOS-PL infrastructure in the framework of EPOS-PL+

Krzysztof Sońnica¹, Jerzy Nawrocki², Jolanta Nastula², Mateusz Drożdżewski¹, Radosław Zajdel¹, Jan Kapłon¹, Dariusz Strugarek¹, Kamil Kaźmierski¹, Piotr Patynowski¹, Marcin Mikoś¹, Przemysław Dykowski³, Jan Kryński³, Witold Rohm¹, Dorota Olszewska⁴, Grzegorz Mutke⁵, Adam Lurka⁵

1. Wrocław University of Environmental and Life Sciences
2. Space Research Centre of Polish Academy of Sciences
3. Institute of Geodesy and Cartography
4. Institute of Geophysics, Polish Academy of Sciences
5. The Central Mining Institute

The project European Plate Observing System for Poland (EPOS-PL+) aims at developing, extending, and enhancing the interdisciplinary infrastructure for observing various processes related to solid Earth sciences using the state-of-the-art observational techniques and data processing methodologies. EPOS-PL+ consolidates and gathers experts representing different scientific disciplines, including geophysics, mining, geodesy, geology, geoinformatics, and planetary scientists. One of the tasks of EPOS-PL+ is the extension and consolidation of the infrastructure of the Global Geodetic Observing System for Poland (GGOS-PL) to provide stable, easily accessible, and highly accurate geodetic reference frames. In the framework of GGOS-PL+, two geodetic observatories in Poland will be supported with the new observing infrastructure to provide reference measurements in terms of geometry, timing, and gravimetry. In Borowiec, the existing geometrical GNSS and Satellite Laser Ranging observations, as well as atomic clock infrastructure (hydrogen masers and a cesium fountain) will be complemented by gravimetric tidal observations. In Wrocław, the existing sets of GNSS receivers with a radiometer will be supported by the time transfer by an optical fiber link connection to the Borowiec Observatory, whereas the tidal gravimetric observatory will be extended by a spring gravimeter. The enhancement of the Wrocław infrastructure will also include a robot for the GNSS antenna calibration for low-cost and professional GNSS receivers, as well as a set of mobile geodetic multi-points equipped with various devices, including GNSS receivers, inclinometers, accelerometers, and active Synthetic Aperture Radar (SAR) reflectors. This contribution will provide an overview of the geodetic infrastructure to be established in the framework of the EPOS-

PL+ project co-financed by the European Union from the European Regional Development Fund, Operational Programme Smart Growth.

Key words EPOS-PL, infrastructure, gravimeters, SLR, GNSS

Category: Symposium 5: Global Geodetic Observing System (GGOS): the metrological basis for the monitoring of the System Earth => 5.1: Geodetic infrastructure for Earth System Monitoring

716

S5-016

Optimizing GNSS RTK Infrastructure from the perspective of tropospheric effects

Zhenhong Li¹, Chen Yu², Nigel Penna²

1. Chang'an University

2. Newcastle University

The Network Real-time Kinematic (Network RTK) Global Navigation Satellite Systems (GNSS) positioning technique delivers cm-level positioning quality, using observations from one or more GNSS such as the Global Positioning System (GPS), and now also GLONASS, Galileo and Beidou. National GNSS networks of CORS stations invariably simply established since the 1990s (by service providers including government agencies) based on even geographical spacing, clustered around urban areas, along highways or around plate boundaries. However, little apparent consideration has been given to whether the established CORS are optimally spaced with regards to the ensuing positional accuracy at the user's location, and there is a dearth of information on the optimal CORS configuration needed and whether dominant error sources such as atmospheric delays can be sufficiently interpolated and mitigated with existing CORS infrastructure.

By considering a remaining dominant GNSS error source of atmospheric water vapour and using its mitigation as a proxy for CORS network design, we show how the optimal CORS station spacing must take account of the topography and climate. We provide both global and local illustrations of the optimal CORS station spacing and how such CORS networks and infrastructure should be configured and/or refined. Importantly, the framework that we develop and present also has the potential to be extended to other applications. These include the generation of precise maps of atmospheric water vapour from GNSS CORS which may be useful in meteorology in the nowcasting of rainfall, and assimilation into numerical weather models for precipitation forecasting. Furthermore, the framework concept may be employed to optimize other monitoring networks, e.g. those for soil moisture, air pollution, and tree species monitoring, although their own dominating error source should be identified and the corresponding spatial and temporal variations should be considered.

Reference:

Yu, C., N. T. Penna, and Z. Li (2020), Optimizing Global Navigation Satellite Systems network real-time kinematic infrastructure for homogeneous positioning performance from the perspective of

tropospheric effects, Proceedings of the Royal Society A: Mathematical, Physical and Engineering Sciences, 476(2242), 20200248, doi:10.1098/rspa.2020.0248.

Key words Global Navigation Satellite Systems, network real-time kinematic, continuously operating GNSS reference stations, station spacing, water vapour, precise positioning

Category: Symposium 5: Global Geodetic Observing System (GGOS): the metrological basis for the monitoring of the System Earth => 5.1: Geodetic infrastructure for Earth System Monitoring

729

S5-017

Development of Wideband Receiver for Novel Ground-based Microwave Radiometer -field experiments of the new 20-60 GHz wide-band receiver and its implications to new development of the wide-band VLBI receiver-

Ryuichi ICHIKAWA¹, Hideki UJIHARA^{3,1}, Shinsuke SATOH¹, Yusaku OHTA⁵, Basara MIYAHARA⁷, Hiroshi MUNEKANE⁷, Tomokazu KOBAYASHI⁷, Takeshi NAGASAKI⁹, Osamu TAJIMA³, Kentaro ARAKI¹⁰, Takuya TAJIRI¹⁰, Takeshi MATSUSHIMA¹¹, Hiroshi TAKIGUCHI¹², Nobuo MATSUSHIMA², Tatsuya MOMOTANI⁴, Kenji UTSUNOMIYA⁴, Mamoru SEKIDO¹, Takaaki JIKE⁶, Tomoaki OYAMA⁶, Hiroshi TAKEUCHI¹², Hiroshi IMAI⁸

1. National Institute of Information and Communications Technology

2. National Institute of Advanced Industrial Science and Technology

3. Kyoto University

4. Japan Weather Association

5. Tohoku University

6. National Astronomical Observatory of JAPAN

7. Geospatial Information Authority of Japan

8. Kagoshima University

9. RIKEN

10. Meteorological Research Institute, Japan Meteorological Agency

11. Kyushu University

12. Japan Aerospace Exploration Agency

We are developing a next-generation microwave radiometer to be used in millimeter-wave spectroscopy for the high-resolution and high-precision monitoring of water vapor behavior. The new radiometer will be suitable for not only space geodetic techniques such as VLBI and GNSS, but also field measurements such as monitoring volcanic activities and cumulonimbus cloud generation. We assembled a room-temperature 20-30 GHz receiver without the cooling system in 2019 and carried out the first measurements of the receiver at Okinawa Electromagnetic Technology Center, National Institute of Information and Communications Technology (NICT) in October 2019. So far we have developed a new front-end module including the orthomode transducer (OMT) and a new wideband feed by early December of 2020. The prototype of the complete receiver system has a wide-bandwidth feed of 16-58 GHz for measuring two frequency bands of 16-28 GHz (H₂O) and 50-58 GHz (O₂). We are now evaluating the performance of the new receiver system and we are going to install the receiver into the 90 cm dish or 1.8 m dish antenna. We will start field measurements using the new receiver system in order to detect various scales of water vapor behaviors. We will compare the results of the field experiments with

those of tropospheric delay measurements using the low-cost multi-GNSS receivers and the GNSS Earth Observation Network (GEONET) System of the Geospatial Information Authority of Japan (GSI). In addition, we have started to develop a new wide bandwidth receiver for VLBI based on the present development. The new VLBI receiver will be available for the multi science fields such as geodesy, radio astronomy, spacecraft navigation, and precise time and frequency transfer. We are going to implement a function of water vapor sensing in the new VLBI receiver. We will also present an outlook of future developments.

This work was supported by JSPS KAKENHI Grant Number JP18H03828 and JP21H04524.

Key words Water vapor, microwave radiometer, Geodesy, GNSS, VLBI

Category: Symposium 5: Global Geodetic Observing System (GGOS): the metrological basis for the monitoring of the System Earth => 5.1: Geodetic infrastructure for Earth System Monitoring

865

S5-018

The importance of geodetic infrastructure and its connection to the UN 2030 Agenda

Martin Lidberg¹, Rudiger Haas²

1. Lantmateriet

2. Chalmers university of technology

The United Nations 2030 Agenda for a sustainable development formulates 17 important and ambitious goals. These goals are part of an international plan for the benefit of human society and our vulnerable planet.

The majority of the 17 UN Agenda 2030 goals are directly or indirectly related to the existence and access to a reliable and accurate global geodetic reference frame (GGRF). The GGRF has already earlier been identified by the UN as being crucial for sustainable development. Establishing and maintaining such a GGRF is only possible by making use of an international network of geodetic infrastructure, so-called geodetic core sites.

Only through a close cooperation of an international network of geodetic core sites it is possible to perform the high-precision space geodetic observations that are necessary to determine the terrestrial and celestial reference frames, as well as the earth orientation parameters. Thus, this international cooperation effort relies on worldwide network of well-established and maintained state-of-the-art geodetic infrastructure.

While working on a renewed funding structure for the geodetic infrastructure at the Onsala space observatory, we have had the privilege to spend some time to develop motivation for the global geodetic infrastructure including the geodetic fundamental stations. As part of this work we have mapped 11 of the 17 UN Agenda 2030 goals to GGFR and Geodetic infrastructure including short motivation and explanation for each of these goals. In our poster presentation, we share this description and uncomplicated motivation that may be useful also for others while working for maintaining, renewing and developing components that is part of the Global geodetic infrastructure

Key words Geodetic infrastructure, geodetic fundamental stations, GGRF, Agenda 2030

Category: Symposium 5: Global Geodetic Observing System (GGOS): the metrological basis for the monitoring of the System Earth => 5.1: Geodetic infrastructure for Earth System Monitoring

880

S5-019

Two-dimensional mining surface deformation monitoring and accuracy analysis of ascending and descending SBAS and MSBAS InSAR

Yu Han¹、Qiuxiang Tao¹、Guolin Liu¹、Anye Hou²、Zaijie Guo¹、Fengyun Wang¹

1. Shandong University of Science and Technology, College of Geomatics

2. Qingdao Geotechnical Investigation and Surveying Institute

SBAS InSAR technique has great prospects in the field of surface deformation monitoring with large areas and long-term mining areas. This paper studies and analyzes the principles of SBAS and MSBAS InSAR techniques, and proposes the specific data processing flow. 13 Sentinel-1A ascending SAR images and 14 Sentinel-1B descending SAR images are processed by SBAS and MSBAS InSAR techniques to obtain the vertical ground subsidence and the east-west surface deformation of Jiyang mining area from October 2018 to April 2019. The characteristics of the subsidence basins monitored by ascending and descending SAR data using SBAS and MSBAS InSAR techniques are compared and analyzed. 6 working faces and 5 groups of leveling data (133 leveling points) are used to qualitatively and quantitatively verify the accuracy of vertical ground subsidence monitored by ascending and descending SBAS and MSBAS InSAR. The results show that the vertical ground subsidence monitored by ascending SBAS InSAR is minimum influenced by the ambiguity of the LOS, which means that the LOS of ascending SAR images is the most consistent with the deformation direction of the mining area and the monitored results are the most accuracy. However, in the center of the subsidence basins with low coherence and serious subsidence, there are still obvious differences between the ascending SBAS InSAR- and leveling-monitored results. The research results will be helpful to improve the accuracy and application capabilities of InSAR technique in monitoring mining surface deformation.

Key words ascending and descending orbit, SBAS InSAR, MSBAS InSAR, two-dimensional deformation

Category: Symposium 5: Global Geodetic Observing System (GGOS): the metrological basis for the monitoring of the System Earth =» 5.1: Geodetic infrastructure for Earth System Monitoring

881

S5-020

The development of spaceborne interferometric synthetic aperture radar missions in China

Junli Chen¹、Yanyang Liu²

1. Shanghai academy of space technology
2. Shanghai Institute of satellite engineering

This paper presents an overview of spaceborne interferometric synthetic aperture radar (InSAR) missions in China, including TianHui-2 and LuTan-1. The primary objective of TianHui-2, a single-pass SAR interferometer employing two twin X-band SAR satellites flying in a close formation, is the generation of a global Digital Elevation Model (DEM) with 1:50000 accuracy. . LuTan-1, which is designed to achieve a high-accuracy deformation measurement using differential InSAR, employs two twin L-band SAR satellites flying in pursuit formation with 180 degree separation. An outlook on future interferometric SAR concepts and developments is provided.

Key words interferometric synthetic aperture radar(InSAR); TianHui-2; Lutan-1

**Symposium 5: Global Geodetic
Observing System (GGOS): the
metrological basis for the
monitoring of the System Earth**

**S5.2: Gravity observations and
networks in the framework of GGOS**

Category: Symposium 5: Global Geodetic Observing System (GGOS): the metrological basis for the monitoring of the System Earth => 5.2: Gravity observations and networks in the framework of GGOS
195

S5-021

Summary of the Absolute Gravity Measurements using FG5-210 at Antarctic Research Stations in Antarctica during 2017-2020 Austral Summer Season

Yoichi Fukuda¹、 Yuichi Aoyama^{1,4}、 Jun'ichi Okuno^{1,4}、 Akihisa Hattori⁴、 Koichiro Doi^{1,4}、 Jun Nishijima²、 Takahito Kazama³

1. National Institute of Polar Research

2. Graduate School of Engineering, Kyushu University

3. Department of Geophysics, Graduate School of Science, Kyoto University

4. The Graduate University for Advanced Studies, SOKENDAI

As a part of JSPS (Japan Society for the Promotion of Science) research project "Giant reservoirs of heat/water/material: Global environmental changes driven by Southern Ocean and Antarctic Ice Sheet" launched in 2017, we have been involved in the studies related to "Interaction of the solid Earth and the Antarctic Ice Sheet". The change of the Antarctic ice sheet is one of the hottest topics because it directly relates to the global climate changes through the sea level rise and ocean circulation. For these studies, one of the largest uncertainties is the effects of GIA (Glacial Isostatic Adjustment) mainly due to the insufficient in-situ data for constraining GIA models. In particular, Absolute Gravity (AG) points in Antarctica are very few and unevenly distributed. On the other hands, the AG measurements in Antarctica are also important and required for providing the reference gravity values, particularly for establishing IAGRF in the GGOS framework. Therefore, we intend to reinforce the AG measurements to enhance the number of AG points and the repeated measurements at those points as well.

From these view points, we have conducted the AG measurements using FG5#210 in total 9 points at 5 stations during the period of 2017-2020 Austral summer season as follows; 1 point at Syowa (Japan) in 2017-2018; 1 point at Troll (Norway) and 1 point at Maitri (India), in 2018-2019; and 2 points at Jangbogo (South Korea) and 2 points at Mario Zucchelli (Italy) in 2019-2020. The measurements were successful and more than 10,000 drops of data at the least were observed at each point with the measurement precisions of better than 1 micro-Gals.

The measured AG values were compared with the previous ones to estimate the trends of the gravity changes, except the 2 points in Jangbogo station that were measured by the FG5 at the first time. The gravity trends at Syowa and Mario Zucchelli showed that the gravity decrease probably due to the GIA effect. The gravity changes at Troll

and Maitri stations also show the gravity decreases, though the amount of decreases could be larger than expected from the GIA models.

In the presentation, we will report the details of the measurements and the obtained gravity values. This study was partially supported by JSPS KAKENHI Grant No. 17H06321..

Key words Absolute Gravimeter, Antarctica, GIA, IAGRF

Category: Symposium 5: Global Geodetic Observing System (GGOS): the metrological basis for the monitoring of the System Earth =» 5.2: Gravity observations and networks in the framework of GGOS
288

S5-022

Evaluation of the gravity reference function at the Borowa Gora Observatory

Przemyslaw Dykowski¹, Jan Krynski¹, Marcin Sekowski¹, Monika Wilde-Piorko¹,
Tomasz Olszak²

1. Institute of Geodesy and Cartography

2. Warsaw University of Technology, Department of Geodesy and Cartography

Repeated monthly absolute gravity measurements are conducted with the A10-020 absolute gravimeter on three stations (two indoor, one outdoor) at the Borowa Gora Geodetic-Geophysical Observatory since 2008. In 2016 next to one of the indoor stations (BG-G2) the iGrav-027 superconducting gravimeter was installed and has been running continuously until now. In addition, between 2016 and 2021, repeated gravity surveys have been done with the FG5-230 absolute gravimeter (owned by the Warsaw University of Technology) at the Borowa Gora Observatory. The A10-020 gravimeter participated in the 2015 (also FG5-230) and 2018 international absolute gravimeter comparison campaigns in Europe.

Combined absolute gravity measurements and superconducting gravimeter records allow to evaluate the initial drift and long term stability of the iGrav-027 instrument and at the same time the performance and stability of the A10 and FG5 gravimeters, especially in between instrumental maintenance. Participation of the A10-020 and FG5-230 gravimeters in international gravity comparisons allowed to link the gravity reference function realized by the iGrav-027 gravimeter to the mean gravity reference level defined within the International Gravity Reference System (IGRS). This has proven to be very useful for a variety of applications with the use of both absolute gravimeters, especially during the Covid-19 pandemic and the inability to perform international absolute gravimeter.

Additionally, seismic records at the Borowa Gora Observatory have been analyzed in order to improve the precision of the iGrav-027 gravimeter residuals for better understanding and comparison of the seismometric and gravimetric data, used for determination of the Earth's mantle structure based on tidal gravimetric recordings of earthquakes. This part of work has been done in the research project No. 2017/27/B/ST10/01600 financed from the funds of the Polish National Science Centre.

Key words absolute gravimeter, superconducting gravimeter, International Gravity Reference System

Category: Symposium 5: Global Geodetic Observing System (GGOS): the metrological basis for the monitoring of the System Earth => 5.2: Gravity observations and networks in the framework of GGOS

354

S5-023

Investigation of systematic effects of FG5/FG5X gravimeters

Vojtech Pálinkáš¹, Petr Křen², Pavel Mašika², Miloš Vaško¹

1. Research Institute of Geodesy, Topography and Cartography

2. Czech Metrology Institute

In order to investigate systematic effects of FG5/FG5X gravimeters, which play important role in the realization of the International Gravity Reference System, the following technological and methodological developments have been recently realized:

1) A new measurement system was developed and it is running in parallel with the original system and consists an independent photodiode, analogue-to-digital converter HS5 to digitize the fringe signal and a new method of fringe signal analysis that is based on FFT swept band-pass filtering. This improvement allowed to determine hidden systematic errors of the original system due to the signal distortion, impedance mismatch and electric dispersion that is dependent on the cable length.

2) A position sensitive detector has been used for the measurement of lateral motion of the freely-falling body. The collected data are allowing to determine the Coriolis/Eötvös effect and also the error from the verticality alignment.

3) A method for determination of the diffraction correction was developed, which except its applicability and accuracy, showed on a insufficient optical quality of the original collimator that should be changed for a model with higher quality for better determination of the correction.

4) Low-frequency perturbations (parasitic spatial wave) caused by the dropping mechanism of FG5/X have been detected in residuals. Since the parasitic wave has variable phase, the measurement model of the free fall was improved and the corresponding systematic effect is suppressed by this way.

Except the basic concept of described developments, we will present examples of detected systematic errors.

Key words gravity acceleration, absolute gravimeter, systematic errors

Category: Symposium 5: Global Geodetic Observing System (GGOS): the metrological basis for the monitoring of the System Earth => 5.2: Gravity observations and networks in the framework of GGOS

498

S5-024

Progress of International Gravity Reference System and Frame

Hartmut Wziontek¹、Sylvain Bonvalot²、Reinhard Falk¹、Germinal Gabalda²、
Jaakko Mäkinen³、Vojtech Pálinkáš⁴、Axel Rülke¹、Leonid Vitushkin⁵

1. Federal Agency for Cartography and Geodesy (BKG)
2. Bureau Gravimétrique International (BGI) / Geosciences Environnement Toulouse (GET), France
3. Finnish Geospatial Research Institute (FGI), Finland
4. Research Institute of Geodesy, Topography and Cartography (VÚGTK), Czech Republic
5. D.I.Mendeleev Research Institute for Metrology (VNIIM), Russia

The proposed definition of the International Gravity Reference System (IGRS) is based on the instantaneous acceleration of free-fall, expressed in the International System of Units (SI). This quantity is measured by absolute gravimeters and plays an important role in particular in metrology. By the correction of time depended effects the conventional quantity „acceleration of gravity” is derived. To ensure the invariance of the system over time, the constant components of these corrections are part of the system definition.

A set of conventional models for the correction of temporal gravity changes based on and compatible with International Absolute Gravimeter Base Network (IAGBN) Processing Standards is proposed with the IGRS Conventions 2020.

The International Gravity Reference Frame (IGRF) is realized by measurements with absolute gravimeters (AGs) at the accuracy level of a few- μ Gal. A common reference level and the traceability to the SI of the AGs is ensured by key comparisons at the CIPM level and complemented by repeated regional comparisons. Comparison sites with extended facilities to compare AGs will play an important role to ensure compatibility of AGs in the long-term. Core stations with co-located space geodetic techniques will provide a link to the terrestrial reference frame. Monitoring of temporal gravity variations is therefore recommended for GGOS core sites.

In order to make the gravity system accessible to stakeholders, efforts have been started to build up an infrastructure based on absolute gravity stations. This requires the support of and the cooperation with National agencies, which are encouraged by IAG resolution No. 4 of 2019 to establish compatible first order gravity networks and to provide information about existing absolute gravity observations. Such infrastructure should advantageously replace the previous IGSN71

network. The database AGrav at BGI and BKG will serve as a central archive for observations and all comparison results.

Key words Gravity Reference System and Frame, Absolute Gravimetry, Absolute Gravimeter

Category: Symposium 5: Global Geodetic Observing System (GGOS): the metrological basis for the monitoring of the System Earth => 5.2: Gravity observations and networks in the framework of GGOS
769

S5-025

GGOS Focus Area Unified Height System: achievements and open challenges

Laura Sanchez¹、 Jianliang Huang²、 Riccardo Barzaghi³、 Georgios S. Vergos⁴

1. Deutsches Geodaetisches Forschungsinstitut, Technische Universitaet Muenchen
2. Canadian Geodetic Survey, Surveyor General Branch, Natural Resources Canada
3. Department of Civil and Environmental Engineering, Politecnico di Milano
4. Laboratory of Gravity Field Research and Applications, Department of Geodesy and Surveying, Aristotle University of Thessaloniki

The Global Geodetic Observing System (GGOS) of the International Association of Geodesy (IAG), providing precise geodetic infrastructure and expertise for monitoring the System Earth, promotes the standardization of height systems worldwide. The GGOS Focus Area "Unified Height System" (GGOS-FA-UHS, formerly Theme 1) was established at the 2010 GGOS Planning Meeting (February 1 - 3, Miami, Florida, USA) to lead and coordinate these efforts. During the 2011-2015 term, different discussions focussed on the best possible definition of a global unified vertical reference system resulted in the IAG resolution for the "Definition and realization of an International Height Reference System (IHRS)" that was approved during the 2015 General Assembly of the International Union of Geodesy and Geophysics (IUGG) in Prague, Czech Republic. The immediate objectives of the GGOS-FA-UHS are (1) to outline detailed standards, conventions, and guidelines to make the IAG Resolution applicable, (2) to establish the realization of the IHRS, i.e., the International Height Reference Frame (IHRF), and (3) to create an operational infrastructure that ensures the maintenance and long-term stability of the IHRF. This contribution summarizes the main achievements of the GGOS-FA-UHS and provides a review of the open questions that need to be resolved in the near future.

Key words Global Unified Height System, physical height standardisation

Category: Symposium 5: Global Geodetic Observing System (GGOS): the metrological basis for the monitoring of the System Earth => 5.2: Gravity observations and networks in the framework of GGOS
797
S5-026

The pole tide in terrestrial gravimetry

Jaakko Mäkinen
Finnish Geospatial Research Institute FGI

In the correction for the solid-earth pole tide, terrestrial gravimetry follows conventions that are different from those for 3-D positioning and satellite gravimetry. Since 1988 terrestrial gravimetry follows the IAGBN (International Gravity Basestation Network) Processing Standards. In them the correction for the pole tide refers to the IERS Reference Pole, a fixed quantity. The same principle is now being adopted for the International Gravity Reference System (IGRS) and International Gravity Reference Frame (IGRF). On the other hand, in 3-D positioning the correction for the deformation due to the pole tide refers to a changing position of the pole. This time-dependent reference describes the track of secular or low-frequency polar wander. The reference has changed over the years: from the mean pole linear in time (IERS Conventions 2003) to a piecewise polynomial mean pole (IERS Conventions 2010) and then to the linear secular pole (IERS Conventions update 2019). Each of these references has become or will become embedded in a version ITRFxx of the International Terrestrial Reference Frame. Satellite gravimetry has followed the IERS Conventions. For static gravity values from terrestrial measurements the difference in pole reference does not matter. However, when gravity change rates from absolute-gravity (AG) measurements are compared with vertical velocities from say, GNSS, or with gravity trends from GRACE or GRACE-FO, the difference must be accounted for. The stability of the IAGBN pole tide correction is proving a big advantage as all past AG results in this respect form a homogeneous time series. A simple correction to the AG trend suffices with no need to correct the original AG observations. This would not be the case if the IAGBN Processing Standards had over the years followed the changing IERS mean pole-secular pole conventions. I believe that the IGRS/IGRF pole-tide correction should be maintained as-is.

Key words Absolute gravity, pole tide, IERS Conventions

**Symposium 5: Global Geodetic
Observing System (GGOS): the
metrological basis for the
monitoring of the System Earth**

**S5.3: Standardized geodetic products
for a reliable System Earth observation**

Category: Symposium 5: Global Geodetic Observing System (GGOS): the metrological basis for the monitoring of the System Earth => 5.3: Standardized geodetic products for a reliable System Earth observation

114

S5-027

Geodetic Analyses at the National Geographic Institute of Spain. Current and future projects and prospects

José Carlos Rodríguez¹, Esther Azcue², Víctor Puente², José Antonio López Fernández², José Antonio López-Pérez¹, José Antonio Sánchez Sobrino²,
Marcelino Valdés Pérez², Beatriz Vaquero¹, Pablo De Vicente¹

1. Observatory of Yebes, IGN Spain

2. IGN

The National Geographic Institute of Spain (IGN Spain) develops, operates, and exploits the Spanish national geodetic networks and their associated infrastructure. This includes the permanent networks of reference GNSS stations, legacy and VGOS VLBI telescopes, and a new SLR station that will make of Yebes Observatory a GGOS core site. In order to fully exploit the opportunities offered by the availability of these space geodetic techniques, IGN has been operating GNSS and VLBI Analysis Centres (AC) for a number of years, with an ILRS Associated Analysis Centre added recently.

IGN Spain is a EUREF AC since 2001, contributing with their weekly and daily coordinates solutions to the definition of the European Terrestrial Reference System. Its activities extend far beyond with other projects carried out at the AC that include IBERRED, for geodynamic purposes, and the participation in the European E-GVAP programme for meteorological applications.

Over the last years, IGN Spain has expanded its contribution to geodetic VLBI analysis, starting in 2019 the official submission of Earth Orientation Parameters, station coordinates and source positions to the International VLBI Service for Geodesy and Astrometry. Additionally, a reprocessing activity of the historical VLBI data since 1979 is ongoing, in order to participate in future realizations of the ITRS as part of the IVS contribution.

The latest addition to IGN Spain analysis capabilities is the IGN-Yebes ILRS AAC. Highlights of its activities are the participation in the ITRF2020 reprocessing in collaboration with NSGF AC (UK), and the computation of SLR centre-of-mass corrections for spherical geodetic satellites.

The aspiration at IGN is to further exploit the synergies between these groups and work towards the combined analysis of the data. A description of the IGN Spain geodetic analysis activities, along with its future prospects, is presented.

Key words VLBI, GNSS, SLR, analysis

Category: Symposium 5: Global Geodetic Observing System (GGOS): the metrological basis for the monitoring of the System Earth => 5.3: Standardized geodetic products for a reliable System Earth observation

172

S5-028

New GGOS Website – An Extensive Information Platform about Geodetic Products, Observations and Services

Martin Sehnal¹、 Detlef Angermann²、 Laura Sánchez²、 Kosuke Heki³

1. BEV - Austrian Federal Office of Metrology and Surveying

2. DGFI-TUM, Deutsches Geodätisches Forschungsinstitut, Technical University of Munich

3. Hokkaido University, Japan

The International Association of Geodesy's (IAG) Global Geodetic Observing System (GGOS) is the contribution of Geodesy to the observation of the Earth System. One goal of GGOS is to communicate and advocate the benefits of Geodesy to scientists, user communities, policy makers, funding organizations and society. To reach this goal, it is essential to establish a strong online presence.

In 2020, GGOS refreshed and further developed its website www.ggos.org to optimize usability. The website serves as a source of information about GGOS, geodetic data, products, and services, as well as other non-technical resources for the IAG community. The redesigned GGOS website, which was published in December 2020, now emphasizes more on the "Observing System" than on the "GGOS organization" itself. Therefore, the website was enhanced to provide an extensive information platform to bring the IAG observations, products and services in the focus and to attract users from other disciplines. Visually attractive graphics navigate users to easy understandable introductions about geodetic products or observation techniques. Observation and product descriptions are complemented with a huge selection of web links containing scientific descriptions and data repositories provided by the IAG Services and additional data sources.

In the last half year, the GGOS Coordinating Office, as the main responsible organization unit for the GGOS website, worked intensively together with the members of the GGOS Bureau of Products and Standards (BPS), the GGOS Science Panel and other important persons of the geodetic scientific community, to establish and launch this information platform. Furthermore, the contributions of the IAG Services and other providers of geodetic products are gratefully acknowledged. The new GGOS website contributes to make geodesy more visible and to promote IAG and GGOS at global and multidisciplinary levels.

Key words GGOS website products observations services

Category: Symposium 5: Global Geodetic Observing System (GGOS): the metrological basis for the monitoring of the System Earth =» 5.3: Standardized geodetic products for a reliable System Earth observation

200

S5-029

Understanding the causes of coastal sea level change from geodetic measurements

Dapeng Mu
Shandong University

We made an attempt to determine the causes for coastal mean sea level (CMSL) change, using geodetic measurements, including satellite altimetry and satellite gravimetry (i.e., the Gravity Recovery and Climate Experiment (GRACE) satellite mission). It was demonstrated that geodetic measurements were able to explain the seasonal cycles of CMSL.

Our results suggest that seasonal budget is closed along global coastal zone (a 300 km band, which is consistent with GRACE resolution) for the period 2003-2015. A 1.09 mm/yr rate discrepancy (~28%) is determined for CMSL trend budget. Over the coastal zone, satellite altimetry shows a 3.96 ± 0.38 mm/yr rate, larger than GMSL rise; steric component has a rate of 1.38 ± 0.28 mm/yr, larger than global mean steric rate; GRACE produces a mass rate of 1.46 ± 0.42 mm/yr, substantially smaller than global mean mass rate. GRACE mass rate heavily depends on glacial isostatic adjustment (GIA) correction, implying the crucial role of GIA in closing trend budget, especially for regional scales. We also find that low-degree corrections affect GRACE coastal ocean mass variation, e.g., a different correction strategy may reduce the discrepancy to ~0.9 mm/yr. Although we have been not able to close trend budget for CMSL, our results provide a first insight into CMSL change, and have immediate implications for contemporary coastal sea level rise and climate change. For the first time, we delivered a quantification of CMSL trend budget, whose discrepancy was estimated to be ~1 mm/yr, indicating non-closure of CMSL trend budget. In the meanwhile, the GIA effect was identified as the dominant contribution to CMSL rise. In future, we suggest that efforts should be made to develop advanced methods for robustly selecting proper GIA models, or incorporating local observations, if community intends to make further endeavor to explore CMSL change.

Key words coastal sea level change; GRACE; time-variable gravity; satellite altimetry

Category: Symposium 5: Global Geodetic Observing System (GGOS): the metrological basis for the monitoring of the System Earth => 5.3: Standardized geodetic products for a reliable System Earth observation

284

S5-030

Machine learning prediction for filling the interruptions of tide gauge data using a least square estimation method from nearest stations

Vahidreza Jahanmard¹, Nicole Delpeche-Ellmann², Artu Ellmann¹

1. Department of Civil Engineering and Architecture, Tallinn University of Technology, Ehitajate tee 5, 19086 Tallinn, Estonia

2. Department of Cybernetics, School of Science, Tallinn University of Technology, Akadeemia tee 21, 12618 Tallinn, Estonia

Tide gauge (TG) measurements are one of the most reliable sources of sea level data and are a very important component in understanding changes in the climate. It is common knowledge however that the TG data are negatively interrupted by temporal gaps, along with random interruptions/offsets that occur (due to natural and anthropogenic). Since these data failures can disturb or decrease the quality of each analysis especially for sea level trend analysis, it is necessary to identify and fill the gaps in these time series. In this study we show that realistic sea level heights can be predicted by utilizing machine learning algorithms in connection with neighbouring TG stations. Provided that all the TGs refer to a common vertical datum, such as the geoid model (i.e., an equipotential surface of the Earth's gravity field). In this study a case study is shown in the Baltic Sea where the hourly dynamic topography (DT) records of a network of 74 stations along the Baltic Sea coastline are obtained for the period 2017–2020 that are referred to the new Baltic Sea Chart datum BSCD2000.

To evaluate the quality of DT_{TG} in each target station, a procedure is presented to yield an approximation of sea level from nearby TG stations. This method entails using the records of 'k' neighbouring stations to transfer to the target TG by using a linear least square regression method, and then the estimated DT will be obtained by applying the adjustment by elements method over these 'k' records. The results have provided the estimated DT with an uncertainty of 3.5 cm on average for all stations in the study area. Therefore, one can perform TG data screening with this estimate and identify the residuals greater than 3 standard deviations of outliers. Further, this estimate is used to reconstruct the tide gauge series and to deal with the missing data. Such a method contributes to more accurate analysis in sea level data especially for climate change and marine engineering applications.

Key words sea level, dynamic topography, tide gauge, geoid, hydrogeodesy, Baltic Sea

Category: Symposium 5: Global Geodetic Observing System (GGOS): the metrological basis for the monitoring of the System Earth => 5.3: Standardized geodetic products for a reliable System Earth observation

351

S5-031

The role and activities of the GGOS Bureau of Products and Standards

Detlef Angermann¹, Thomas Gruber¹, Michael Gerstl¹, Robert Heinkelmann², Urs Hugentobler¹, Laura Sanchez¹, Peter Steigenberger³

1. Technical University Munich (TUM)

2. Helmholtz Centre Potsdam, German Research Centre for Geosciences (GFZ)

3. Deutsches Zentrum für Luft- und Raumfahrt (DLR)

The GGOS Bureau of Products and Standards (BPS) supports IAG's Global Geodetic Observing System (GGOS) in its goal to provide consistent geodetic products needed to monitor, map and understand changes in the Earth's shape, rotation and mass distribution. In its present structure, the two Committees "Earth System Modeling" and "Essential Geodetic Variables" as well as the Working Group "Towards a consistent set of parameters for the definition of a new GRS" are associated with the BPS. The BPS contributes to the updating of the IERS Conventions and interacts with external stakeholders regarding standards and conventions, such as ISO, IAU, BIPM, CODATA and the UN GGIM Subcommittee on Geodesy, including its Working Group "Data Sharing and Development of Geodetic Standards". A key objective of the BPS is to keep track and to foster homogenization of adopted geodetic standards and conventions across all IAG components as a fundamental basis for the generation of consistent geometric and gravimetric products. Towards this aim, an updated 2nd version of the BPS inventory of standards and conventions used for the generation of IAG products has been published in the Geodesist's Handbook 2020. In the framework of the renewing of the GGOS website, the BPS supports the GGOS Coordinating Office regarding the representation of geodetic products. In cooperation with the IAG Services, other data providers and the GGOS Science Panel, user-friendly product descriptions have been generated. The updated GGOS website should be an "entrance door" to geodetic products and it should make geodesy more visible to other disciplines and to society.

Key words GGOS Bureau of Products and Standards, BPS inventory, geodetic products, standards

Category: Symposium 5: Global Geodetic Observing System (GGOS): the metrological basis for the monitoring of the System Earth => 5.3: Standardized geodetic products for a reliable System Earth observation

368

S5-032

Evaluating of sea surface heights from multi-mission satellite altimetry by utilizing hydrodynamic and geoid models

Majid Mostafavi¹, Nicole Delpeche-Ellmann², Artu Ellmann¹

1. Department of Civil Engineering and Architecture, Tallinn University of Technology, Tallinn, Estonia

2. Department of Cybernetics, Tallinn University of Technology, Tallinn, Estonia

Satellite altimetry (SA) provides a unique sea surface height (SSH) dataset with an almost global coverage in the coast and offshore areas. In coastal areas (especially in the region less than 10 km from coastline), obtaining accurate SSH tends to be challenging, due to errors of the waveform and the applied corrections in data processing (e.g., range and geophysical corrections). Thus the development of several retracking methods dedicated to the improvements of SA data in coastal zones. In this study we explore the performance of recently developed retrackers (ALES+ SAR for S3 and ALES+ for JA3, from Baltic+SEAL project) that are specifically adapted for coastal and sea ice conditions in the Baltic Sea. The intention is by utilization of two high-resolution geoid models (NKG2015 and EST-GEOID2017) a comparison can be made with tide gauges (TG) and hydrodynamical models (HDM).

The methodology involves comparing SA derived SSH with using two HDM which provide reasonable estimate of sea level data in the study area at reasonable resolution. The HDM however are limited by an undisclosed vertical datum and errors. To overcome this limitation a solution that derives the difference between the TG records and HDM at similar locations provide more reliable estimates of HDM. Utilizing geoid models the HDM results can be referred to SSH. A comparison can be made both with the SSH derived from SA and HDM.

A statistical analysis is performed for three SA missions (Jason-3, Sentinel-3A and Sentinel-3B) that is compared with the two HDM models for the period 2017–2018. The results show that the best agreement of SA derived SSH occurred by using EST-GOEID2017 geoid model along with a preferred HDM model by Sentinel-3A data. Also, highest errors occurred in January–March and December cycles.

Key words Satellite Altimetry, Sea Surface Height, Hydrodynamic Model, Tide gauge, ALES+ retrackers, Hydrogeodesy, Baltic Sea, Geoid

Category: Symposium 5: Global Geodetic Observing System (GGOS): the metrological basis for the monitoring of the System Earth =» 5.3: Standardized geodetic products for a reliable System Earth observation

455

S5-033

Defining Essential Geodetic Variables

Richard Gross
Jet Propulsion Laboratory

The Global Geodetic Observing System (GGOS) of the International Association of Geodesy (IAG) provides the basis on which future advances in geosciences can be built. By considering the Earth system as a whole (including the geosphere, hydrosphere, cryosphere, atmosphere and biosphere), monitoring Earth system components and their interactions by geodetic techniques and studying them from the geodetic point of view, the geodetic community provides the global geosciences community with a powerful tool consisting mainly of high-quality services, standards and references, and theoretical and observational innovations. A new initiative within GGOS is to define Essential Geodetic Variables. Essential Geodetic Variables (EGVs) are observed variables that are crucial (essential) to characterizing the geodetic properties of the Earth and that are key to sustainable geodetic observations. Examples of EGVs might be the positions of reference objects (ground stations, radio sources), Earth orientation parameters, ground- and space-based gravity measurements, etc. Once a list of EGVs has been determined, requirements can be assigned to them. Examples of requirements might be accuracy, spatial and temporal resolution, latency, etc. These requirements on the EGVs can then be used to assign requirements to EGV-dependent products like the terrestrial reference frame. The EGV requirements can also be used to derive requirements on the systems that are used to observe the EGVs, helping to lead to a more sustainable geodetic observing system for reference frame determination and numerous other scientific and societal applications.

Key words Essential Geodetic Variables

Category: Symposium 5: Global Geodetic Observing System (GGOS): the metrological basis for the monitoring of the System Earth => 5.3: Standardized geodetic products for a reliable System Earth observation

533

S5-034

ICGEM's Current Activities and Future Plans

E. Sinem Ince, Sven Reissland

Helmholtz Centre Potsdam, GFZ German Research Centre for Geosciences

International Centre for Global Earth Models (ICGEM) is a service of International Association of Geodesy (IAG). It is worldwide accessible and provides a unique platform to collect, archive and access to a comprehensive list of DOI # assigned citable global gravity field models that are of static, temporal and topographic kind. It continues to update its content with new models and additional features over the years. Beside the calculation and visualization services, educational tools, complementary documentations about the models and methodologies are made available.

The development and use of state-of-the-art global gravity field models now are more crucial than ever for monitoring system Earth and for an improved understanding of the interactions between its sub-components. The gravity products are not only relevant for geodesy, but also for other geosciences including geophysics, glaciology, hydrology, oceanography and climatology. Within the GGOS activities, global gravity field models together with ground gravity measurements are important in the unification of the existing height systems. Moreover, datasets archived in the ICGEM database and gravity field functionals computed via the Calculations Service are directly related to the essential geodetic and gravimetric variables that are currently being developed.

In this contribution, we'll present the current activities of ICGEM and future plans in the direction of creating sustainable research data infrastructure for future new generation very high-resolution global gravity field models and products that contribute to ongoing IAG-GGOS activities.

Key words ICGEM, global gravity field, GGMs, height unification, GGOS

Category: Symposium 5: Global Geodetic Observing System (GGOS): the metrological basis for the monitoring of the System Earth =» 5.3: Standardized geodetic products for a reliable System Earth observation

558

S5-035

Metrological support of astronomical-geodesic and gyroscopic azimuth measuring instruments

Maksim Khanzadian, Andrey Mazurkevich
FSUE VNIIFTRI

To ensure the uniformity of measurements for determining the azimuths of the initial directions, storing these directions, as well as for transmitting the unit of astronomical azimuth from the initial directions to the azimuth measuring instruments, a stationary complex of metrological support for azimuth measuring instruments (KSMO SIA), developed by FSUE "VNIIFTRI", is used.

As the main measuring tool, an optoelectronic astrovisor is used, consisting of a mirror-prism unit, a lens and a television camera. The principle of operation is to determine the azimuth of the normal to the face of the optical guardian of azimuth directions (OHAN) from multiple observations of a set of stars culminating near the meridian on the matrix of the photodetector device of the television camera, as well as to identify the position of the stars according to the astronomical catalogues with reference to the UTC (SU) time scale.

An optical azimuthal direction keeper is a four-sided mirror prism with certified values of the angles between the faces, mounted on the same optical axis with an astrovisor, designed to store the original directions and transmit the azimuths of these directions to gyroscopic, astronomical, and navigational azimuth measuring instruments.

For astronomical and navigational azimuth measuring instruments, a specialized azimuth minipolygon is used, consisting of three foundations fixed at a distance of 300-400 m. One of the points of the azimuthal minipolygon is located in the immediate vicinity of the astropavillon on the same optical axis with the OHAN prism, for transmitting the azimuths of the directions to the points of the azimuthal minipolygon.

Thus, KSMO SIA allows you to fully ensure the unity of all azimuthal measuring instruments with an accuracy that meets all modern requirements.

Key words Metrological support, astronomical azimuth, stationary complex of means of metrological support of azimuth, azimuthal minipolygon, optical-electronic astrovisir.

Category: Symposium 5: Global Geodetic Observing System (GGOS): the metrological basis for the monitoring of the System Earth =» 5.3: Standardized geodetic products for a reliable System Earth observation

628

S5-036

Using WGM2012 to Compute Gravity Anomaly Correction of Levelled Height Differences

Yanhui CAI、Li Zhang、Xu Ma

National Quality Inspecting and Testing Center of Surveying and Mapping

Gravity Anomaly Correction (GAC) of levelled height difference is an important kind of correction in precise leveling, especially for applications of regional height datum establishing, building-deformation monitoring, etc. In order to compute GAC, Bouguer anomaly values at the two points of level line are needed. In most cases, it is very difficult for field surveyor, because Bouguer anomaly value is calculated with a serial of gravity data and corrections. However, WGM2012 released by BGI, is a novel product of high resolution grids and maps of the Earth's gravity anomalies (Bouguer, isostatic and surface free-air), which can be directly applied in GAC calculating. In this paper, a brief introduction of WGM2012 is presented and a bilinear interpolation method to obtain Bouguer anomaly value at any position is suggested, simulated results show WGM2012 has a ground resolution of $1' \times 1'$ and the accuracy of WGM2012 completely meets GAC computing in precise leveling surveying.

Key words Gravity Anomaly, Precise Leveling, WGM2012, Bilinear Interpolation;

Category: Symposium 5: Global Geodetic Observing System (GGOS): the metrological basis for the monitoring of the System Earth => 5.3: Standardized geodetic products for a reliable System Earth observation

759

S5-037

On the Earth dynamical ellipticity

Alberto Escapa¹, Tomas Baenas², Jose Manuel Ferrandiz³

1. University Leon/Alicante, Spain

2. University Centre of Defense, Murcia, Spain

3. University of Alicante, Spain

The Earth dynamical ellipticity H is a key parameter to derive important Earth's properties like its normalized polar moment of inertia or its principal moments of inertia. Its value is determined with high precision from astronomical observations and models of the Earth's precession and nutation. When adding it to a set of fundamental parameters, it is necessary to specify in what tidal system —mean, zero, or free— its value is given. Regrettably, this point has not been commonly addressed in the literature.

In this communication, we revise the status of such question in previous reports on Fundamental Constants of the International Association of Geodesy and in IERS Conventions, providing different recommendations to ensure consistency with other fundamental parameters. We also provide a numerical quantification of the so-called indirect effect of H , based on the researches developed by the authors on the non-rigid Earth precession.

Key words Earth dynamical ellipticity; fundamental constants; Earth rotation

Category: Symposium 5: Global Geodetic Observing System (GGOS): the metrological basis for the monitoring of the System Earth => 5.3: Standardized geodetic products for a reliable System Earth observation

839

S5-038

Assigning Digital Object Identifiers to Geoid Models in the ISG Repository

Mirko Reguzzoni¹, Kirsten Elger², Lorenzo Rossi¹, Daniela Carrion¹

1. Politecnico di Milano

2. GFZ German Research Centre for Geosciences

One of the aims of the International Service for the Geoid (ISG) is to provide scientific users and technicians with an open access to local and regional geoid and quasi-geoid models. Currently, more than two hundred models are stored in the ISG repository and most of them have a public policy rule, e.g., under the Creative Commons Attribution 4.0 International License (CC BY 4.0). Before dissemination, the geoid models are validated and standardized by converting them into a unique ASCII file format. In order to further improve interoperability and reusability of these models, it is crucial to univocally identify the data files (also by stable links), to assign metadata, to grant proper credits to research authors, and to allow for data citation. In these respects, and in cooperation with GFZ Data Services, ISG has extended its services by offering the assignment of Digital Object Identifiers (DOIs) to geoid models archived in the ISG geoid repository. This option was devised in the framework of a GGOS working group and has been operational since summer 2020.

In this work the implemented procedure for the DOI assignment is presented, from the file format conversion, including the metadata collection, till the DOI landing page generation and publication. The connection between the ISG repository and GFZ Data Services is discussed as well. Examples of models labelled with DOIs are shown, commenting the provided information and the ways to access the data.

Key words Geoid, DOI, Interoperability, Data access, Data format, Metadata

**Symposium 5: Global Geodetic
Observing System (GGOS): the
metrological basis for the
monitoring of the System Earth**

S5.4: Geodetic space weather research

Category: Symposium 5: Global Geodetic Observing System (GGOS): the metrological basis for the monitoring of the System Earth => 5.4: Geodetic space weather research

117

S5-039

Ionospheric TEC analysis and modeling using Empirical Mode Decomposition (EMD)

Hamid Moghadaspour¹、 Siavash Iran Pour²、 Alireza Amiri-Simkooei^{3,6}、 Nico Sneeuw⁴、 Saniya Behzadpour^{5,7}、 Torsten Mayer-Gürr⁵

1. Department of Aerospace Engineering, Faculty of Engineering, University of Isfahan, Iran
2. Research Institute of Environmental Studies, University of Isfahan, Iran
3. Department of Control and Operations, Technical University of Delft, The Netherlands
4. Institute of Geodesy, Faculty of Aerospace Engineering and Geodesy, University of Stuttgart, Germany
5. Graz University of Technology, Institute of Geodesy, Graz, Austria
6. Faculty of Civil Engineering and Transportation, University of Isfahan, Iran
7. Leibniz University Hanover, Institute of Geodesy, Hanover, Germany

Ionospheric total electron content (TEC) has an important role in trans-ionospheric delay error in satellite communication, earth observation, space-based navigation, timing applications as well as space weather forecasting services. Affected by several phenomena and transient events, TEC has non-linear and non-stationary behavior. Empirical Mode Decomposition (EMD) in conjunction with Hilbert spectral transform, is ideally suited to extract regular ionospheric variations and deterministic anomalies. The method is fully adaptive and generates the basic functions, called Intrinsic Mode Functions (IMFs), representing nonstationary signals as the sum of zero-mean amplitude and frequency modulation components. In this research work, using EMD method, the TEC time series is decomposed to 27 IMFs which signifies regular and modulated dominant frequencies of the periodic patterns. We then compare the results with the outcomes of the Least Squares Harmonic Estimation (LS-HE) approach. Both methods extract two significant periodic patterns, diurnal periods of $24/n$ hours and annual signals with $365.25/n$ days ($n = 1, 2, \dots$). In addition, EMD shows its capability to detect the effect of solar storms as transient events in the time series. The results of this work emphasize the competency of the EMD technique for TEC analysis and forecasting over specific regions, while it also proves its advantages in computational performance and being independent of the initial assumptions and search regions required in LS-HE.

Key words Ionospheric Total Electron Content, Empirical Mode Decomposition, Least-Squares Harmonic Estimation

Category: Symposium 5: Global Geodetic Observing System (GGOS): the metrological basis for the monitoring of the System Earth => 5.4: Geodetic space weather research

119

S5-040

Use of Empirical Mode Decomposition (EMD) method to investigate the solar storms impact on GRACE range-rate residuals

Hamid Moghadaspour¹、 Siavash Iran Pour²、 Saniya Behzadpour^{3,6}、 Torsten Mayer-Gürr³、 Nico Sneeuw⁴、 Alireza Amiri-Simkooei^{5,7}

1. Department of Aerospace Engineering, Faculty of Engineering, University of Isfahan, Iran
2. Research Institute of Environmental Studies, University of Isfahan, Iran
3. Graz University of Technology, Institute of Geodesy, Graz, Austria
4. Institute of Geodesy, Faculty of Aerospace Engineering and Geodesy, University of Stuttgart, Germany
5. Department of Control and Operations, Technical University of Delft, The Netherlands
6. Leibniz University Hanover, Institute of Geodesy, Hanover, Germany
7. Department of Geomatics Engineering, Faculty of Civil Engineering and Transportation, University of Isfahan, Iran

Detection and extraction of the underlying errors or signals in the GRACE level-1 range-rate residuals is a key for further improvement of the Earth's gravity field models.

In this research work, we investigate the ability of nonlinear and non-stationary "Empirical Mode Decomposition" (EMD) method to decompose GRACE range-rate residuals where the "Intrinsic Mode Functions" (IMF) are employed for identifying the temporal sudden features in the data. In particular, the impact of emitted and radiated large quantities of moving electrons and protons and UV and X-ray radiations through the solar flares on the GRACE range-rate residuals is investigated. Through analyzing the "Total Electron Content" (TEC) of the Earth's ionosphere, the GRACE L1 range-rate residuals from ITSG-2018 dataset and the "Sudden Ionospheric Disturbance" (SID) as a solar activity index, we discuss our findings, where interesting temporal patterns in different datasets are observed.

We show that the EMD algorithm has proven to be a practical tool to decompose time series and detect the correlations between different datasets. The method clearly shows relevance between different effects where the classical analysis is hardly able to represent. We particularly show common temporal signatures in TEC and the drag force on the satellite body caused by the solar flare emissions.

Key words GRACE, Range-rate measurements, Solar flares, Empirical Mode Decomposition

Category: Symposium 5: Global Geodetic Observing System (GGOS): the metrological basis for the monitoring of the System Earth => 5.4: Geodetic space weather research

186

S5-041

3D model to explore the ionosphere and plasmasphere exclusively using satellite-based GNSS data

Fabricio Prol, Mainul Hoque
German Aerospace Center (DLR)

To explore the total capabilities of the total electron content (TEC) observations obtained by satellite-based GNSS (Global Navigation Satellite System) instruments, a 3D ionospheric model was developed combining Radio-Occultation (RO) and POD (Precise Orbit Determination) data. Electron density derived from RO measurements was used to characterize the ionospheric profiles from the peak height up to the low-Earth orbit. The electron density profile was further extrapolated to the plasmasphere in order to create a global background. A tomography technique based on POD data was later used to update the background. It is relevant to notice that, usually, GNSS tomography is highly dependent on external ionospheric/plasmaspheric model to create a background. With the developed model, no external data is necessary to create the background. The results indicate improvement in comparison to NeQuick when evaluated against external topside TEC data as well as to in-situ observations of the Defense Meteorological Satellite Program's mission and Van Allen Probes.

Reference

Prol, F.S.; Hoque, M.M. Topside Ionosphere and Plasmasphere Modelling Using GNSS Radio Occultation and POD Data. *Remote Sens.* 2021, 13, 1559.

Key words Radio-Occultation, COSMIC, TEC, Electron Density, Tomography, GNSS

Category: Symposium 5: Global Geodetic Observing System (GGOS): the metrological basis for the monitoring of the System Earth => 5.4: Geodetic space weather research

312

S5-042

An enhanced mapping function for spaceborne TEC conversion based on the plasmaspheric scale height

Mengjie Wu、 Peng Guo、 Xiaogong Hu

Shanghai Astronomical Observatory, Chinese Academy of Sciences, Shanghai

The mapping function is crucial for the conversion of slant total electron content (TEC) to vertical TEC for low earth orbit (LEO) satellite-based observations. Instead of collapsing the ionosphere into one single shell in commonly used mapping models, we defined a new mapping function assuming the vertical ionospheric distribution as an exponential profiler with one simple parameter, the plasmaspheric scale height in the zenith direction of LEO satellites. The scale height obtained by an empirical model introduces spatial and temporal variances into the mapping function. Furthermore, the majority errors remaining in the TEC conversion associated with the horizontal inhomogeneous distribution of ionosphere are described with a model involving the azimuth angle variation of signal ray paths. The performance of the new method is compared with the mapping function F&K (Foelsche & Kirchengast, 2002) by simulating experiments based on Global Core Plasma Model (GCPM), and discussed along with the latitude, season and local time. The assessment indicates the new mapping function has comparable or better performance than the F&K mapping model with fixed ionospheric effective height. The azimuthal varied pattern is well modeled by the scale height-based obliquity factor and trigonometric function with constant parameters.

Key words radio occultation, TEC, mapping function, plasmaspheric scale height, GCPM

Category: Symposium 5: Global Geodetic Observing System (GGOS): the metrological basis for the monitoring of the System Earth => 5.4: Geodetic space weather research

356

S5-043

Ensemble Machine Learning for Geodetic Space Weather Forecasting

Randa Natras¹, Michael Schmidt²

1. Technical University of Munich

2. Deutsches Geodätisches Forschungsinstitut der Technischen Universität München (DGFI-TUM)

The accuracy and reliability of Global Navigation Satellite System (GNSS) applications can be severely affected by the perturbations in the Earth's ionosphere as a manifestation of space weather. Corrections for these effects could be obtained from a model that considers the complex chain of physical dynamical processes between the Sun, the interplanetary magnetic field, the Earth's magnetic field and the ionosphere, and includes a forecast component to provide an early warning system.

In this study, the vertical total electron content (VTEC) of the ionosphere is forecasted by considering physical processes and utilizing machine learning (ML) techniques based on ensemble learning to approximate non-linear relationships from the data. The data of solar activity, solar wind, interplanetary and geomagnetic field and other information connected to the VTEC variability are used as input to predict VTEC during both quiet and disturbed ionosphere. Ensemble learning combines the multiple ML models with the aim to produce a model with better prediction performance. The most common ensemble methods Bagging (Random Forest) and Boosting (Adaptive Boosting and Gradient Boosting) use combinations of multiple regression trees. The results show that their overall performance, as measured by the root mean square error, does not differ significantly from one another, but they show individual advantages over certain time periods. To develop the optimal VTEC forecast approach, bagging and boosting models are combined into a single model through two approaches of ensemble meta-estimators: voting regressor and stacked generalization. In the first approach, the individual predictions of different models are averaged to form a final model. On the other hand, stacking generalization combines the predictions from the models so that their predicted outputs are used as input for a final meta-model. The final ensemble meta-models show to exceed the prediction performance of each individual models.

Key words Machine Learning, Ensemble Learning, Ionosphere, VTEC, Space Weather

Category: Symposium 5: Global Geodetic Observing System (GGOS): the metrological basis for the monitoring of the System Earth => 5.4: Geodetic space weather research

410

S5-044

Impact of 09-15 November 2012 magnetic cloud storm on vTEC along west Euro-African GPS Chain

Amira Shimeis
NRIAG

This paper presents the monitoring of the latitude variation of the vTEC along west Euro-African GPS Chain (18 ground stations) passing the magnetic equator . During 09-15 November 2012- magnetic cloud storm, We combine the vTEC GPS ground - based measurements to define and understand the Traveling Ionospheric Disturbance (TID). We study fluctuation and so more scintillations at high latitude. The effect of Prompt Penetration Electric (PPE) field at low latitude are observed.

Key words vTEC GPS,TID,PPE

Category: Symposium 5: Global Geodetic Observing System (GGOS): the metrological basis for the monitoring of the System Earth => 5.4: Geodetic space weather research

468

S5-045

Ground and spaced based GNSS for Space Weather Monitoring at GFZ: Overview and Recent Results

Jens Wickert^{1,2}, Christina Arras¹, Andreas Brack¹, Galina Dick¹, Ankur Kepkar^{1,2}, Benjamin Männel¹, Chinh Nguyen Thai¹, Temitope Oluwadare¹, Torsten Schmidt¹, Florian Zus¹, Harald Schuh^{1,2}

1. German Research Centre for Geosciences GFZ, Potsdam, Germany

2. Technische Universität Berlin, Germany

Global Navigation Satellite Systems (GNSS) are significantly affected by propagation effects, induced by the Earth's neutral atmosphere and ionosphere. Both media interact day-to-day with constituents of the interplanetary space and therefore reflect Space Weather related phenomena. GNSS are one of the most important, but also highly sensitive technical infrastructures to the impact of catastrophic Space Weather events. In addition, they are excellent observation tools for operational Space Weather monitoring on a broad range of spatiotemporal scales. Operational GNSS can be exploited especially for ionosphere monitoring and the investigation of vertical atmospheric/ionospheric coupling processes.

We review recent GNSS based Space Weather related research activities at GFZ. Backbone is the operational analysis of regional and global GNSS ground networks to derive information on the general ionospheric state and on the occurrence and intensity of ionospheric disturbances. We also apply the space based GNSS Radio Occultation (RO) method with data from several satellite missions. The RO data provide unique information on vertical atmospheric/ionospheric coupling processes and ionospheric irregularities on a global scale and also allow to demonstrate solar impact to the Earth's ionosphere.

Key words ionospheric disturbances, vertical atmospheric ionospheric coupling, solar cycle, radio occultation, GNSS

Category: Symposium 5: Global Geodetic Observing System (GGOS): the metrological basis for the monitoring of the System Earth => 5.4: Geodetic space weather research

540

S5-046

SWEETS – forecast of satellite orbit decay using L1 interplanetary magnetic field measurements and thermospheric density estimates.

Sandro Krauss¹, Sofia Kroisz², Lukas Drescher², Manuela Temmer², Barbara Suesser Rechberger¹, Saniya Behzadpour¹, Torsten Mayer-Guerr¹

1. Graz University of Technology

2. University of Graz

In the ongoing project SWEETS, we will develop a forecasting model, to predict the expected impact of solar events, like coronal mass ejections, on satellites at different altitudes between 300-800 km. The realization is based on an advanced statistical investigation and evaluation of solar wind plasma and magnetic field data, combined with thermospheric neutral density estimates from various satellites (e.g., GRACE, SWARM, TerraSAR-X, TanDEM-X). We investigate the statistical relation between the different scientific datasets and present preliminary results from the combined evaluation. The findings are further used for the development of a short-term forecasting model called SODA (Satellite Orbit DecAy). Based on several case studies, a validation of the performance of preliminary SODA predictions is done through a comparison between post-processed density estimates and results from the forecasting model. **Key words** Space weather, thermospheric density, orbit decay, prediction, CME

Category: Symposium 5: Global Geodetic Observing System (GGOS): the metrological basis for the monitoring of the System Earth => 5.4: Geodetic space weather research

592

S5-047

Forecasting Global Thermospheric Neutral Density through Calibration and Data Assimilation of GRACE Measurements into the NRLMSISE-00 model

Mona Kosary¹, Ehsan Forootan², Saeed Farzaneh¹, Kristin Vielberg³, Timothy Kodikara⁴, Maike Schumacher²

1. University of Tehran

2. Geodesy and Earth Observation Group, Department of Planning, Aalborg University Rendsburggade 14, 9000 Aalborg, Denmark

3. Institute of Geodesy and Geoinformation, University of Bonn, Nussallee 17, 53115 Bonn, Germany

4. Institute of Solar-Terrestrial Physics, German Aerospace Center (DLR), Kalkhorstweg 53, 17235 Neustrelitz, Germany

The uncertainty in thermospheric neutral density (TND) estimates is one of the largest and persistent sources of uncertainty in orbit determination and prediction (OD/OP) of low Earth orbit space objects. The TNDs required for these applications are typically obtained from corresponding models. However, the simulation and forecasting skills of these models are limited due to the model structures and the calibration period of the model parameters. Here, we present an Ensemble Kalman Filter (EnKF)-based Calibration and Data Assimilation (C/DA) approach that provides the opportunity to update the model's states and simultaneously calibrates the model's most sensitive parameters, such as those related to solar radiation and geomagnetic activity as well as those controlling the calculation of exospheric temperature. The advantage of this approach is that the calibrated parameters can be applied to simulate the global map of global TNDs and forecasting them in future.

In this study, we investigate the improvement of the NRLMSISE-00 model after implementing the C/DA scheme using TNDs derived from the accelerometer measurements of the Gravity Recovery and Climate Experiment mission (GRACE) during February 2015 with a wide range of solar activity. We demonstrate the forecasting skills of C/DA covering the altitude of 300-600 km, though the GRACE measurements were introduced at the altitude of 410 km during the C/DA period. The calibrated model are validated along the Swarm-A, -B, and -C with mean altitude of 480, 480 and 528 km, respectively. The results indicate that our TND forecasts agree well with the POD-derived densities. After implementing the C/DA, the root-mean-squares of error (RMSE) of TND forecasts has been reduced compared to the original NRLMSISE-00 densities, i.e., 51, 57 and 54% along the Swarm-A, -B and -C, respectively. The numerical assessment is useful to demonstrate the

capability of the C/DA technique in reducing the modelling errors and their value for forecasting TNDs for applications such as collision analysis.

Key words Thermospheric Neutral Density (TND), Low-Earth-Orbit (LEO), Calibration and Data Assimilation (C/DA), Accelerometer Measurements, GRACE, Swarm, NRLMSISE-00

Category: Symposium 5: Global Geodetic Observing System (GGOS): the metrological basis for the monitoring of the System Earth => 5.4: Geodetic space weather research

614

S5-048

A latitude-dependent ionospheric variogram model

Tong Liu¹、Yiping Jiang²、Li Liu¹、Mengfei Sun¹、Guochang Xu¹、Zhibin Yu¹

1. Harbin Institute of Technology at Shenzhen

2. The Hong Kong Polytechnic University

The impact of the ionosphere on GNSS has been widely reported. To mitigate the impact of the ionosphere on user accuracy and safety, analysis of ionospheric spatial differences is necessary.

Variogram is a statistic model that describes the spatial correlation between random field and process. It has been used to characterize the ionosphere spatial variability and applied to Wide Area Augmentation System. However, this model is based on the isotropic assumption, i.e., the covariance is only to the Euclidean distance of ionospheric pierce points (IPPs), independent of the direction. However, recent studies show that the ionosphere spatial difference is not isotropic. Both the magnitude of TEC and its perturbation are significantly correlated with latitude. Here, an improved variogram model is proposed to analyze the ionospheric latitude variation. The method consists of 3 parts: 1, divide the study area into 50km-intervals strips in the north direction; 2, calculate the variogram between all the IPPs on each strip; 3, determine range and sill by counting the variation of ionospheric difference with distance. The same procedure is applied to the east direction and the results are regarded as 'nugget effect'.

The theoretical basis of this approach is that, in variogram model, the 'nugget effect' is mainly caused by ionospheric differences in the east direction, and also, the range and sill are mainly determined by the latitude-dependent geomagnetic field. This hypothesis is verified by the results of GNSS-TEC data under different geomagnetically active conditions. Among them, the results on June 24, 2015, a moderate geomagnetic perturbation day, shows that the variogram in the north-south direction ranges from 0 to 2.5m when the IPPs' distance increases from 0km to 2500km, while the variogram in the east-west direction always remains below 0.4m. This analytical model can be applied to Satellite-Based Augmentation System or as a geodetic data product.

Key words satellite navigation; ionosphere; variogram; latitude

Category: Symposium 5: Global Geodetic Observing System (GGOS): the metrological basis for the monitoring of the System Earth => 5.4: Geodetic space weather research

625

S5-049

Deep Learning for Global Ionospheric TEC Forecasting: Different Approaches and Validation

Xiaodong Ren, Pengxin Yang, Jun Chen, Xiaohong Zhang
School of Geodesy and Geomatics

The Total Electron Content (TEC) is a key parameter to describe the variation of ionosphere. The construction of accurate Vertical TEC (VTEC) prediction model has been a challenge and an important task. Deep learning is a learning algorithm for training deep neural networks, which can be used to deal with multiple non-linear data. Regarding the dynamic nonlinear variations of VTEC, we present a deep learning model based on Long Short-Term Memory (LSTM) for prediction. For the model, the input layer contains the forecast parameters, solar activity index, geomagnetic activity index, and daily cycle indexes. The hidden layer is composed of a two-layer LSTM network and a dense layer. The output layer outputs the prediction results for the next 24 hours. The data from 2018 to 2020 provided by the Center for Orbit Determination in Europe (CODE) were used for training and evaluation. Meanwhile, the ten-fold cross-validation method was used for training, which can reduce overfitting. We assessed the performance of the single-station forecasting method by using Global Ionosphere Maps (GIM) and global forecasting method by using spherical harmonic coefficients. The results showed that the bias and RMS of the single-station forecasting method are around 0.05 TECU and 1.15 TECU, while that of the global forecasting method are around 0.01 TECU and 1.30 TECU. Meanwhile, when the single-station forecasting method is employed to forecast the TEC values over a small area, the prediction result is better than that of the global forecasting method. Finally, the accuracy of one day prediction by using single-station forecasting method is better than the forecast product provided by CODE.

Key words Ionosphere; Total Electron Content (TEC); Deep Learning; Forecasting; Model

Category: Symposium 5: Global Geodetic Observing System (GGOS): the metrological basis for the monitoring of the System Earth => 5.4: Geodetic space weather research

732

S5-050

Detection of ionospheric disturbances by modelling the electron density as three-dimensional B-spline expansions: a simulation study

Andreas Goss¹, Michael Schmidt¹, Eren Erdogan¹, Denise Dettmering¹, Florian Seitz¹, Jennifer Müller², Ernst Lexen², Barbara Görres³, Wilhelm F. Kersten³

1. Deutsches Geodätisches Forschungsinstitut der Technischen Universität München (DGFI-TUM)

2. German Space Situational Awareness Center (GSSAC)

3. Bundeswehr GeoInformation Centre (BGIC)

The project OPTIMAP is at the current stage a joint initiative of BGIC, GSSAC and DGFI-TUM. The development of an operational tool for ionospheric mapping and prediction is the main goal of the project.

The ionosphere is characterized by a variety of space- and time-dependent structures. These include Travelling Ionospheric Disturbances (TIDs), as well as plasma bubbles. TIDs propagate in waves at a constant velocity and are distinguished on the basis of their spatial extend and their propagation velocity. The so-called large-scale TIDs (LSTIDs) can reach a wavelength of about 1000 km and a velocity of 300-1000 m/s, medium-scale TIDs (MSTIDs) reach 300 km extend and a speed of max. 300 m/s, while small-scale TIDs (SSTIDs) are defined with an extend smaller than 50 km and a max. velocity of 100 m/s.

Since these structures influence and affect the propagation of electromagnetic signals used for e.g. positioning applications, it is advisable to detect them and, if necessary, to correct their influence. This requires high-resolution electron density models that can represent comparable signal structures.

In OPTIMAP, a 3-D B-spline model was developed for this purpose. The B-spline model can be optimally adapted to the electron density structures, i.e. the model resolution can be selected in such a way that those signal structures can be represented, which correspond to the wavelength of MTIDs and LSTIDs.

Within this contribution, we represent a simulation study for MSTIDs and apply the developed 3-D B-spline approach in order to model and detect the simulated structures.

Key words Ionosphere, TID, Electron density

Category: Symposium 5: Global Geodetic Observing System (GGOS): the metrological basis for the monitoring of the System Earth => 5.4: Geodetic space weather research

848

S5-051

Towards a better understanding of space weather events and their impact on geodetic measurements

Alberto Garcia-Rigo^{1,11*}、Benedikt S. Soja⁴、Anna Belehaki⁶、Jens Berdermann⁷、
Consuelo Cid⁸、Denise Dettmering⁹、Jinsil Lee¹⁰、Anthony J. Mannucci²、Enric
Monte-Moreno⁴、Xiaoqing Pi²、Rami Qahwaji³、Pietro Zucca⁵

1. UPC-IonSAT, Spain
2. JPL, USA
3. UoB, UK
4. UPC-TALP, Spain
5. ASTRON, The Netherlands
6. NOA, Greece
7. DLR, Germany
8. UAH, Spain
9. DGFI-TUM, Germany
10. KAIST, Republic of Korea
11. IEEC, Spain

In the frame of IAG's GGOS (International Association of Geodesy; Global Geodetic Observing System) joint with IAG's Sub-Commission 4.3, there is the Joint Working Group 3 on "Improved understanding of space weather events and their monitoring by satellite missions". This group is part of GGOS' Focus Area on Geodetic Space Weather Research – Observation Techniques and Modeling Approaches and will run until 2023.

In this context, we aim at gaining a better understanding of space weather events and their effect on Near-Earth Environment. In particular, we are analyzing representative storm events in 2013, 2015, 2017 and 2018 using data from certain space geodetic techniques (GNSS, VLBI, DORIS, RO, satellite altimetry) combined with space weather data from different sources (including observations from spacecraft and radio telescopes). Complementary nowcasting and forecasting models and products within the team being used are linked to: Total Electron Content Global Ionospheric Maps (TEC GIMs), ionospheric electron density, geomagnetic disturbances from the Sun to Earth, DORIS ionospheric products, Travelling Ionospheric Disturbances (TIDs) and scintillations, solar flares detection/prediction, Coronal Mass Ejections and Solar Energetic Particle events (CMEs and SEPs), solar corona electron density, dimmings and coronal holes, solar wind, among others.

In this work, we will present an analysis of the correlation between a variety of such measurements/products and the perturbed ionospheric

electron density/TEC conditions induced during the above-mentioned events.

Key words GGOS, space weather, space geodetic techniques

**Symposium 5: Global Geodetic
Observing System (GGOS): the
metrological basis for the
monitoring of the System Earth**

**S5.5: Assimilation of geodetic
observations in the modelling of the
Atmosphere, Cryosphere and
Hydrosphere**

Category: Symposium 5: Global Geodetic Observing System (GGOS): the metrological basis for the monitoring of the System Earth =» 5.5: Assimilation of geodetic observations in the modelling of the Atmosphere, Cryosphere and Hydrosphere

130

S5-052

Crustal response to heavy rains in Japan 2017-2020

Kosuke Heki¹、Wei Zhan^{1,2}、Syachrul Arief^{1,3}

1. Hokkaido University

2. The First Monitoring and Application Center, China Earthquake Administration,
Tianjin, China

3. BIG, Bogor, Indonesia

Weather fronts stagnant above the southwestern (SW) Japan often bring disastrous heavy rains in early summer. Tropical cyclones also cause heavy rains in Japan. Here we study heavy rain episodes in 2017-2020 summer including those by the super typhoon Hagibis in 2019 October, and investigate transient lithospheric subsidence caused by rainwater loads using the daily coordinates of the dense network of continuous GNSS stations. After applying a network filter to remove common mode errors, we isolated subsidence signals up to 1-2 centimeters in flooded regions. Such subsidence recovered in a day as rainwater drained rapidly to nearby ocean promoted by large topographic slopes. Spatiotemporal correlation between subsidence and precipitation is not so high due to rapid post-precipitation redistribution of rainwater. However, correlation is high between volumetric subsidence and total rain over the entire region, i.e. subsidence of $\sim 0.075 \text{ km}^3/\text{Gt}$ occurs on a day with precipitation up to $\sim 10 \text{ Gt}$. This linearity breaks down for rains exceeding $\sim 10 \text{ Gt/day}$ as flood wash out river embankments at many places expanding rainwater drain. We also found it difficult to estimate the total amount of rain from crustal subsidence because of topographic amplification of crustal subsidence signals due to concave terrains around GNSS stations in Japan.

Key words GNSS, heavy rain, crustal subsidence, hydrological model, Japan, typhoon

Category: Symposium 5: Global Geodetic Observing System (GGOS): the metrological basis for the monitoring of the System Earth =» 5.5: Assimilation of geodetic observations in the modelling of the Atmosphere, Cryosphere and Hydrosphere

283

S5-053

Development of synergized method to determine accurate sea level using satellite altimetry and high-resolution geoid model

Vahidreza Jahanmard¹, Nicole Delpeche-Ellmann², Artu Ellmann¹

1. Department of Civil Engineering and Architecture, Tallinn University of Technology, Ehitajate tee 5, 19086 Tallinn, Estonia

2. Department of Cybernetics, School of Science, Tallinn University of Technology, Akadeemia tee 21, 12618 Tallinn, Estonia

This study presents a method that determines accurate sea level by combining different data sources (satellite altimetry (SA), hydrodynamic models (HDM), tide gauges (TG)) to a consistent vertical reference datum. The geoid is a key component linking the vertical datum between the different data sets. Exploring the inconsistencies between the data sources (spatially and temporally) allows useful hints on possible improvements that can be made in the HDM, SA and geoid models. The HDM yields a mathematical model of sea surface dynamics and due to their high temporal and spatial resolutions are one of the best sea level sources in the coast and offshore areas and thus a valuable tool for many engineering and applications. One of the main limitations of HDM is that the vertical reference is not always specified.

The case study is that of the Baltic Sea (northern Europe) where a high-resolution geoid model (NKG2015) and a dense network of geoid-referential TG exist. These TGs were used to reduce the zero mark of the HDM to a stable vertical reference datum that coincides with the geoid. The HDM's sea level variation with respect to the geoid allows us to derive dynamic topography (DT), which gives better quantification of more realistic sea level trends. The SA data (Sentinel-3A) was also corrected to DT using the geoid model and also used to assess the HDM. The comparison between the profiles of DT_{HDM} and DT_{SA} for the period 2017–2019 demonstrates the residual standard deviation of 1.9 cm on average, which is reasonable agreement. However, the spatial distribution of discrepancies in certain areas seems to indicate that improvement is needed for HDM, geoid models and SA data in this region. This is to our knowledge the first time such a study is performed in the Baltic Sea. The results are very necessary for this highly active sea area surrounded by many countries in terms of marine engineering, navigation, and oceanographic studies.

Key words sea level, geoid, satellite altimetry, tide gauge, dynamic topography, vertical reference datum, hydrogeodesy, Baltic Sea

Category: Symposium 5: Global Geodetic Observing System (GGOS): the metrological basis for the monitoring of the System Earth =» 5.5: Assimilation of geodetic observations in the modelling of the Atmosphere, Cryosphere and Hydrosphere

308

S5-054

Long-period Accuracy Evaluation and Spatial-temporal characterization Analysis of Global GNSS-derived Precipitable Water Vapor

Junsheng Ding^{1,2}、Junping Chen^{1,2,3}

1. Shanghai Astronomical Observatory Chinese Academy of Sciences
2. School of Astronomy and Space Science, University of Chinese Academy of Sciences
3. Shanghai Key Laboratory of Space Navigation and Positioning Techniques, Shanghai 200030, China

The ground-based GNSS technology provides high accuracy combined with high spatial and temporal resolution Precipitable Water Vapor (PWV), which with all-weather operation and near real-time access, becoming one of the most important methods of PWV acquisition and monitoring. Comprehensively investigated of GNSS-derived PWV accuracy is valuable for global water vapor synthesis, while previous studies on GNSS PWV are often conducted only regionally at only a few to a few dozen stations and the duration of the experiments is not very long, usually between a few days and a few years, and lack of discussion and analysis of the distribution of accuracy. This study utilized PWV from over 2,000 radiosonde stations from IGRA2 (Integrated Global Radiosonde Archive Version 2) to comprehensively assess the accuracy of globally GNSS-derived PWV from over 14,000 stations from 1994 to 2020, and analyzed the spatial-temporal characterization of accuracy. Experimental results show that, on a global scale, the average bias between GNSS PWV and radiosonde PWV is less than 1mm, and the average RMS is less than 3mm. From a distance scale, the RMS error that distance brings to PWV greatly varies between regions, with a 1 mm for 40 km on a tropical island, while it takes 200 km in a desert region. Moreover, the results indicate that the error in PWV accuracy due to height difference is latitude-dependent and can be up to 10 mm/km at 20-30 latitudes region.

Key words Precipitable Water Vapor, GNSS, Radiosonde, Evaluation, Accuracy Variability

Category: Symposium 5: Global Geodetic Observing System (GGOS): the metrological basis for the monitoring of the System Earth => 5.5: Assimilation of geodetic observations in the modelling of the Atmosphere, Cryosphere and Hydrosphere

443

S5-055

Temporal error covariances of satellite gravimetry-derived ice mass change products

Andreas Groh, Eric Buchta, Martin Horwath, Matthias O. Willen, Thorben Döhne, Benjamin D. Gutknecht, Maria T. Kappelsberger
Technische Universität Dresden

Ice mass changes derived from satellite-observed time-variable gravity field solutions allow to study the temporal evolution of the cryosphere under changing climatic conditions. These products can be used to assess alternative mass change products, e.g. from satellite altimetry or the input-output method, and can be assimilated in geophysical models. For these purposes comprehensive uncertainty measures, accounting for temporal error correlations, are crucial. So far, available mass change products derived from GRACE/GRACE-FO monthly solutions are mostly provided with monthly uncertainties accounting for the temporal uncorrelated noise only. In some instances an uncertainty measure for the linear trend, considering e.g. errors of the glacial isostatic adjustment (GIA) correction and leakage errors, is provided.

In this study, we set up a full error covariance matrix for a GRACE/GRACE-FO-derived mass change time series for the Antarctic Ice Sheet. The error covariance matrix is established independent of the time series' reference value and can thus be conveniently applied to individual use cases. In addition to the monthly uncorrelated noise, we consider uncertainties: (1) of the GIA correction, (2) of the added degree one time series, (3) related to the C20 replacement, (4) of the monthly gravity field solutions, and (5) caused by signal leakage. An individual error covariance matrix is derived for each error component. In this step, we distinguish between long-term, seasonal and residual errors. For the residual errors we derive the error covariance matrix based on the most suitable noise model, identified by testing several noise models (e.g. white, power law, flicker noise, random walk) using a maximum likelihood estimation. Uncertainties of the monthly solutions are inferred from the individual error covariance matrices as well as the combined matrix.

Key words ice mass changes, error covariances, trend uncertainties, Antarctic Ice Sheet

Category: Symposium 5: Global Geodetic Observing System (GGOS): the metrological basis for the monitoring of the System Earth => 5.5: Assimilation of geodetic observations in the modelling of the Atmosphere, Cryosphere and Hydrosphere

444

S5-056

Investigation of the influence factors on ionospheric scintillation monitoring with conventional geodetic receiver and performance evaluation

Wei Li^{1,2}, Shuli Song¹

1. Shanghai Astronomical Observatory, Chinese Academy of Sciences
2. University of Chinese Academy of Sciences

Ionospheric scintillation has an adverse effect on observation of trans-ionospheric signals and will further degrade the performance of satellite navigation and positioning. Therefore, it is of significant interest to monitor ionospheric scintillation and provide elusion solutions for related applications. Benefiting from its widely distribution around the world, conventional geodetic receivers is often used to monitor ionospheric scintillation of a large region. But no study has ever investigated the limiting factors of geodetic receiver for ionospheric scintillation monitoring and has ever evaluated its monitoring ability.

Based on GPS observation data obtained from geodetic receiver and ionospheric scintillation monitoring (ISM) receiver at HISY, GDSZ and HKTK station in year 2015, this work investigated the influence factors that lead to the different performance between geodetic receiver and ISM receiver and evaluated the performance of geodetic receiver in monitoring ionospheric scintillation. The result indicates that low sampling rate, which leads to the difference of S_4 and 30s-5min ROTI in monitoring area and cause misjudgment of cycle slip for 30s-5min ROTI, a limiting factor for ionospheric scintillation monitoring. The other factors that affect performance of geodetic receiver monitoring ability are difference of scale-length of ionospheric irregularities monitored by S_4 and ROTI as well as the non-quantitative relationship between the critical value for scintillation of ROTI and S_4 . Under the influence of frequent cycle slip, the availability of 30s-5min ROTI is close to 70% and the 1s-1min ROTI is above 90% during ionospheric scintillation. The rate of accurate report of ionospheric scintillation by 30s-5min ROTI is around 70% and rate of accurate report of ionospheric scintillation by 1s-1min ROTI is around 80%; the correlation between S_4 and 30s-5min ROTI reaches 0.7 and the correlation between S_4 and 1s-1min ROTI reaches 0.8.

Key words Ionospheric scintillation monitoring, ROTI, S_4 , sampling rate, cycle slip

Category: Symposium 5: Global Geodetic Observing System (GGOS): the metrological basis for the monitoring of the System Earth => 5.5: Assimilation of geodetic observations in the modelling of the Atmosphere, Cryosphere and Hydrosphere

456

S5-057

A Tropospheric Delay Model of Multi-source Data Considering System Deviation Correction

Yongchao Ma¹、Bing Zhang¹、Guochang Xu¹、Zhiping LV^{2,1}

1. Harbin Institute of Technology (Shenzhen)

2. Information Engineering University

Tropospheric delay is an important source of error in space geodesy, and it is also an important data for space scientific research. In order to solve the problem of data simplification in the construction of tropospheric delay model, this paper uses sliding window algorithm to divide the world into regular windows of the same size, and uses the tropospheric delay calculated by ERA-5 meteorological data and the product of discrete IGS tracking stations in 2011-2019 to construct a multi-source data tropospheric delay model considering system deviation correction (*MGTD_CS*). Both the zenith tropospheric delay (ZTD) calculated by ERA-5 data that did not participate in the modeling in 2020 and the precise ZTD products from globally distributed IGS stations in 2020 are treated as reference values to assess the performance of *MGTD_CS* model, the accuracy of the model is 2.05cm and 3.32cm, respectively. The results show that the *MGTD_CS* model has the best accuracy and stability in the world relative GPT2w model, and has strong regional applicability in the region, which greatly improves the effect of regional tropospheric delay correction.

Key words Tropospheric Delay, Multi-source Model, System Deviation Correction

Category: Symposium 5: Global Geodetic Observing System (GGOS): the metrological basis for the monitoring of the System Earth => 5.5: Assimilation of geodetic observations in the modelling of the Atmosphere, Cryosphere and Hydrosphere

461

S5-058

Evaluation of Precipitable Water Vapor from COSMIC-2 Radio Occultation using Radiosonde and GNSS Data

Shuaimin Wang, Tianhe Xu
Institute of Space Science, Shandong University

The change of water vapor plays an important role in weather monitoring and climate change. The Constellation Observing System for Meteorology, Ionosphere and Climate (COSMIC)-2, which is a joint Taiwan-United States satellite mission was successfully launched into the 24° inclination orbit with an initial altitude of about 720km on June 25, 2019. With the increased SNR from advanced receivers and digital beam steering antennas of COSMIC-2, COSMIC-2 improves the penetration ability of soundings and can produce more available data from 46°S to 46°N relative to COSMIC. The PWV values obtained from COSMIC-2 are compared with those from ground-GNSS and radiosonde covering the period from October 1, 2019 to February 2, 2020. The correlation coefficients between COSMIC-2 PWV values and GNSS and radiosonde PWV values are 0.97 and 0.98, respectively, which shows that COSMIC-2 PWV values have a high correlation with the GNSS and radiosonde PWV values. The RMS values of PWV differences between COSMIC-2 and GNSS, and radiosonde are 3.40 mm and 3.93 mm, respectively. The results show that the COSMIC-2 PWV values agree better with the GNSS compared with radiosonde PWV values. The bigger RMS value between COSMIC-2 and radiosonde may be due to the effect of the horizontal drift for tens of kilometers and the humidity sensor precision of radiosonde. In addition, comparison between COSMIC and GNSS as well as radiosonde illustrates that COSMIC PWV agrees well with GNSS PWV as well as radiosonde PWV from 46°S to 46°N. The COSMIC-2 spatial coverage ranges from 46°S to 46°N, mainly including the tropical and subtropical regions. We compare COSMIC-2 PWV values with GNSS and radiosonde PWV values in both these regions. The comparison indicates that COSMIC-2 PWV values in the subtropics have better agreement with GNSS and radiosonde PWV values than those in the tropics. The accuracy difference of COSMIC-2 PWV in the tropical and subtropical regions is mainly due to the effect of super refraction in the tropical regions. The performances of COSMIC-2 PWV in the north and south hemispheres are also verified with the GNSS measurement. The results show that the performances of COSMIC-2 PWV are similar in

the northern and southern hemispheres; they also show that the differences in both hemispheres are not significant.

Key words COSMIC-2; Precipitable Water Vapor; GNSS; Radiosonde

Category: Symposium 5: Global Geodetic Observing System (GGOS): the metrological basis for the monitoring of the System Earth => 5.5: Assimilation of geodetic observations in the modelling of the Atmosphere, Cryosphere and Hydrosphere

624

S5-059

Penetration Depth Inversion in Hyper-Arid Desert from L-band InSAR Data Based on a Coherence Scattering Model

GuanXin Liu, HaiQiang Fu, JianJun Zhu, ChangCheng Wang, QingHua Xie
Central South University

The potential of interferometric synthetic aperture radar (InSAR) for subsurface height estimation has long been recognized; however, this method is greatly limited by the data sources and the various errors encountered in a highly dynamic environment such as a desert. In this paper, a coherence scattering model based on the volume coherence and imaging geometry of the InSAR acquisitions is proposed to retrieve the penetration depth of the synthetic aperture radar (SAR) signal in a hyper-arid desert area. The proposed method includes two main parts: 1) the dielectric constant of the study area is first derived by employing an empirical model with the L-band SAR data, and then the results are used to calibrate the vertical effective wavenumber after the refraction process; and 2) together with the extracted volume coherence from the SAR data, the scattering model is employed to retrieve the penetration depth. The application scope of the vertical effective wavenumber in the volume and temporal decorrelation effect of the model is also discussed in this paper. The method was tested with ALOS-1 PALSAR data from a desert area in southeast Libya. The results show that the average penetration depth of the L-band SAR in the study area is 2.98 m, and the standard deviation is 1.06 m.

Key words InSAR, desert, coherence scattering model, dielectric constant, penetration depth

Category: Symposium 5: Global Geodetic Observing System (GGOS): the metrological basis for the monitoring of the System Earth =» 5.5: Assimilation of geodetic observations in the modelling of the Atmosphere, Cryosphere and Hydrosphere

662

S5-060

On the assessment of ERA5 and GPS-based WRFDA for InSAR Atmospheric Correction

Zhenyi Zhang¹、 Weixing Zhang¹、 Yidong Lou¹、 Hua Wang²、 Yaozong Zhou¹、
Jingna Bai¹

1. Wuhan university

2. The Department of Surveying Engineering, Guangdong University of Technology

The accuracy and applications of synthetic aperture radar interferometry (InSAR) are severely suppressed by the tropospheric error. Numerical Weather Model (NWM) and GPS derived tropospheric delays are commonly used to correct the tropospheric error with considering their complete spatial coverage or high accuracy. However, few researches focus on the fusion of both NWM and GPS for the tropospheric error correction. In this study, we use the Weather Research and Forecasting (WRF) and Data Assimilation (DA) system to assimilate the GPS ZTD into ERA5 (0.25° and 1 hour), and generate the merged NWM products with spatial-temporal resolution of 3 km and 20 s. Thereafter, the tropospheric correction effectiveness from the merged NWM products are evaluated in Pearl River Delta of China. The results show that the estimation and correction of the InSAR tropospheric error may not improve with the increasing spatial-temporal resolution. However, the STD of the interferogram decreased further over 20% by the merged NWM products, indicating the significant effectiveness of GPS ZTD assimilation.

Key words InSAR; tropospheric error; ERA5; GPS; WRFDA

Category: Symposium 5: Global Geodetic Observing System (GGOS): the metrological basis for the monitoring of the System Earth => 5.5: Assimilation of geodetic observations in the modelling of the Atmosphere, Cryosphere and Hydrosphere

888

S5-061

A Metrological Assessment of the Zenith Total Delays from GPS Data Processing in Tropical Areas: The Tahiti

Fangzhao Zhang¹、Jean-Pierre Barriot²、Peng Feng³、Guochang Xu⁴

1. Shandong University of Science and Technology

2. University of French Polynesia

3. Wuhan University

4. Harbin Institute of Technology

The weighted mean temperature of the atmosphere with respect to its water vapor contents is a key parameter in meteorology studies. It is routinely derived by modeling the ratio between the precipitable water vapor (PWV) contents of the atmospheric column from balloon radiosonde (RS) and the zenith wet delays (ZWD) from GNSS propagation of radio signals in the neutral atmosphere. In this paper, we question the accuracy of such a modeling in the case of a remote subtropical humid location in the South Pacific Ocean, the Tahiti Island. Our main conclusion is that the accuracy of the zenith total delays (ZTD) from GNSS processing, for the Tahiti case, is poorer by one order of magnitude than the global claimed accuracy of ZTD delays from worldwide databases. The possible causes of these discrepancies are discussed.

Key words Precipitable Water Vapor; GNSS; Zenith Wet Delays; Zenith Total Delays; Weighted Mean Temperature; Radiosonde

**Symposium 5: Global Geodetic
Observing System (GGOS): the
metrological basis for the
monitoring of the System Earth**

**S5.6: Geodesy contributions to address
societal challenges**

Category: Symposium 5: Global Geodetic Observing System (GGOS): the metrological basis for the monitoring of the System Earth => 5.6: Geodesy contributions to address societal challenges

244

S5-062

The Global Geodetic Observing System (GGOS) - fundamental infrastructure for science and society -

Basara Miyahara¹, Laura Sánchez², Martin Sehnal³, Allison Cradock⁴

1. Geospatial Information Authority of Japan
2. Deutsches Geodätisches Forschungsinstitut, Technical University of Munich
3. BEV, Austrian Federal Office of Metrology and Surveying
4. NASA Jet Propulsion Laboratory

The Global Geodetic Observing System (GGOS) is the contribution of Geodesy to the observation and monitoring of the Earth System. Geodesy is the science of determining the shape of the Earth, its gravity field and its rotation as functions of time. A core element to reach this goal are stable and consistent geodetic reference frames, which provide the fundamental layer for the determination of time-dependent coordinates of points or objects, and for describing the motion of the Earth in space. With modern instrumentation and analytical techniques, Geodesy is nowadays capable of detecting time variations ranging from large and secular scales to very small and transient deformations with increasing spatial and temporal resolution, high accuracy, and decreasing latency. The main objectives of GGOS are a) to provide the observations needed to monitor, map, and understand changes in the Earth's shape, rotation, and mass distribution, b) to provide the global geodetic frame of reference as the fundamental backbone for measuring and consistently interpreting global change processes, c) to benefit science and society by providing the foundation upon which advances in Earth and planetary system science and applications are built. GGOS works tighter with components of the International Association of Geodesy (IAG), more specifically, IAG Services, IAG Commissions and IAG Inter-Commission Committees. The IAG Services provide the infrastructure and products on which all contributions of GGOS are based, and the IAG Commissions and IAG Inter-Commission Committees provide expertise and support to address key scientific issues within GGOS. GGOS is working closely with the Sub-Committee on Geodesy of the UN Committee of Experts on Global Geospatial Information Management (UN-GGIM) and contribute to the implementation of the United Nations' Resolution on the Global Geodetic Reference Frame (UN-GGRF) for Sustainable Development.

Key words Geodesy, GGOS, Global Geodetic Reference Frame, UN-GGIM

Category: Symposium 5: Global Geodetic Observing System (GGOS): the metrological basis for the monitoring of the System Earth => 5.6: Geodesy contributions to address societal challenges

248

S5-063

The status and development of the Asia Pacific Reference Frame (APREF) and its applications

Guorong Hu、 John Dawson、 Ryan Ruddick、 Minghai Jia、 Simon McClusky
Geoscience Australia

In the Asia and Pacific region there has been an increase in the number of GNSS CORS networks over the past decades. This provides an opportunity to improve the definition, realization and maintenance of the regional geodetic reference frame, i.e. the so-called Asia Pacific Reference Frame (APREF) in this region. The APREF project is a collaboration of the Geodetic Reference Framework Working Group of the United Nations Global Geospatial Information Management for Asia and the Pacific (UN-GGIM-AP), and the Reference Frame Sub-Commission 1.3e (SC1.3e) of the International Association of Geodesy (IAG). The project is supporting both scientific and regional geospatial activities by densifying and providing access to the International Reference Frame (ITRF). This presentation overviews the status and development of APREF, including the data flow of the APREF GNSS network, routine analysis as well as quality control of the products. An accuracy assessment of the output and products, including the estimated position and velocity field is presented. Some APREF application examples are also presented, such as monitoring the performance of GNSS stations, and how Australia's national datum was realized using the products of the APREF project.

Key words APREF, ITRF, GNSS

Category: Symposium 5: Global Geodetic Observing System (GGOS): the metrological basis for the monitoring of the System Earth => 5.6: Geodesy contributions to address societal challenges

249

S5-064

The UN Global Geodetic Centre of Excellence (GGCE)

Johannes Bouman

Federal Agency for Cartography and Geodesy (BKG)

The United Nations (UN) has called for enhanced cooperation on global geodesy. In February 2015 the UN General Assembly adopted the resolution “a Global Geodetic Reference Frame for Sustainable Development” recognizing that the Global Geodetic Reference Frame (GGRF) is the foundation of every aspect of the collection and management of national geospatial information and global monitoring of the Earth. In August 2020, the UN Committee of Experts on Global Geospatial Information Management (UN-GGIM) welcomed and supported the proposal from Germany to host a Global Geodetic Centre of Excellence (GGCE), and Germany invites all member states to contribute. The Centre will provide coordination, counselling and assistance to Member States that works to sustain, enhance, access and utilize the Global Geodetic Reference Frame. Further, it will support the objectives of UN-GGIM and its Subcommittee on Geodesy. This presentation will give an overview of the UN Global Geodetic Centre of Excellence, the modalities, its current status and on the road towards developing the work plan.

Key words Global Geodetic Reference Frame (GGRF), Global Geodetic Centre of Excellence (GGCE)

Category: Symposium 5: Global Geodetic Observing System (GGOS): the metrological basis for the monitoring of the System Earth => 5.6: Geodesy contributions to address societal challenges

475

S5-065

GGOS D-A-CH – A new regional affiliate of the Global Geodetic Observing System

Hansjoerg Kutterer¹、 Johannes Boehm²、 Johannes Bouman³、 Roland Pail⁴、
Markus Rothacher⁵、 Harald Schuh⁶

1. Karlsruhe Institute of Technology

2. TU Vienna

3. Federal Agency for Cartography and Geodesy

4. TU Munich

5. ETH Zurich

6. GFZ Potsdam

The Global Geodetic Observing System (GGOS) is a component of the International Association of Geodesy (IAG). GGOS acts as central interface to the scientific community and to society. It works together with the other IAG Components for monitoring the Earth system and for global change research. The structure of GGOS comprises various components. With respect to geodetic activities in countries and regions, GGOS Affiliates represent a structural component that provides a forum for discussions on multi-technique geodetic Earth observation. They work to improve the quality of observation techniques and they encourage collaboration of the respective agencies and institutions in the region.

For joining the efforts in GGOS-related activities in Germany, Austria and Switzerland (D-A-CH region) and better exploiting the potential of GGOS in terms of science and infrastructure, the respective national geodetic commissions established GGOS D-A-CH to act as GGOS Affiliate in the region. A comprehensive white paper named “Geodesy 2030” with contributions of all relevant stakeholders in the D-A-CH region was published (Müller and Pail, 2019; in German). It addresses geodetic focus areas for the next decade with GGOS as key element and backbone, and thus provides a basis for the topical work of GGOS D-A-CH. Recently, a working group was installed to institutionalize, operationalize and promote GGOS D-A-CH as regional GGOS Affiliate. In this contribution, the ideas, the present status and the next steps of GGOS D-A-CH are presented and discussed.

References:

Müller, J.; Pail, R. (2019): Erdmessung 2030. zfv. DOI: 10.12902/zfv-0243-2018.

Key words GGOS, D-A-CH, GGOS Affiliate, Observing System, Earth observation

Category: Symposium 5: Global Geodetic Observing System (GGOS): the metrological basis for the monitoring of the System Earth => 5.6: Geodesy contributions to address societal challenges

559

S5-066

Investigation of a method for reducing the measurement error of time delays between optical signals in phase rangefinders

Anna Deikun
FSUE VNIIFTRI

Measurements of delays between harmonic signals coming through two channels are necessary in optical phase rangefinders - to calculate the phase difference between the reference and measuring signal. The accuracy of such measurements is limited by noise on the signal propagation path and noise in the receiving paths of the equipment.

Distortions of the pulse shape during its propagation through the fiber lead to a systematic error, and the instability of the time position of the pulse front caused by noise leads to a random error. The systematic error can be reduced by selecting the shape of the optical pulses and the spectral characteristics of the lasers used based on data on the properties of the optical fiber. Random error can be reduced by averaging multiple measurements, but the maximum number of measurements that can be performed during a second cycle of operation of systems using individual pulses is limited by the technical capabilities of the equipment.

Calculations of the time shift between signals can be carried out using a method based on fixing in the recorded data the moments of time when the signals reach the specified threshold values. This method is relatively simple to implement, but its disadvantage is a higher random error due to the influence of noise. To overcome these limitations and improve the accuracy of determining the moments of reception of optical signals by the equipment of time scale comparison systems, a method is proposed based on the use of modulation of the amplitude of an optical pulse of a long duration by a harmonic signal or short pulses and reception of optical signals using a reference signal generator.

As a result of the conducted experiments, it was found that the proposed method can significantly reduce the measurement error of the time shift, as well as that it can be used in the development of optical phase rangefinders.

Key words method, phase difference, measurement, experiment, harmonic signals

Category: Symposium 5: Global Geodetic Observing System (GGOS): the metrological basis for the monitoring of the System Earth => 5.6: Geodesy contributions to address societal challenges

678

S5-067

Status and Future Development of GNSS enhancement of Tsunami Early Warning Systems (GTEWS)

John LaBrecque^{1,5}, Allison Allison Craddock^{2,6}, Brendan Crowell³, John Rundle⁴

1. Allison Craddock

2. Jet Propulsion Laboratory

3. University of Washington

4. University of California, Davis

5. University of Texas at Austin ,Center for Space Research

6. Director Central Bureau, International GNSS Service

The GTEWS initiative has demonstrated the utility and cost effectiveness of real time GNSS analysis for the enhancement of tsunami early warning systems as proposed by Resolution #4 of the 2015 IUGG General Assembly. The GTEWS technique measures the land deformation in response to an earthquake to model the potential generation of a tsunami. The GTEWS technique also measures the ionospheric disturbance induced by the tsunami to verify and track tsunami development and propagation. The GTEWS 2017 workshop reviewed the maturity and utility of GTEWS and provided recommendations for its development in reports published by the Global Assessment Report for 2019 of the UN Office for Disaster Risk Reduction and by the Association of Pacific Rim Universities. These reports validate that GTEWS is effective and affordable providing tsunami risk reduction and broad economic benefits to both developing and developed nations. The GTEWS initiative is supported by the 17 institutions of 12 nations that comprise the GATEW working group of the GGOS Focus Area for Geohazards. The Group on Earth Observation has offered the use of the Geodesy4Sendai community activity as a forum for the assembly of the GATEW working group and other principal organizations for implementation of the GTEWS 2017 report. The GGOS and the IUGG Commission of Geophysical Risk and Sustainability have agreed to collaborate in support of the Geodesy4Sendai GTEWS initiative. The IUGG has pledged a grant to support the planning of the GTEWS 2017 implementation meeting within the Geodesy4Sendai activity. The ITU Focus Group on AI for Natural Disaster Management has identified a topic group to advance the application of Artificial Intelligence to GTEWS. Though delayed by COVID 19 pandemic, we expect the GTEWS initiative to accelerate in the coming year as the world recovers from another severe natural disaster.

Key words GNSS, Tsunami, Early Warning, Earthquake, TEC, Real Time GNSS

Category: Symposium 5: Global Geodetic Observing System (GGOS): the metrological basis for the monitoring of the System Earth => 5.6: Geodesy contributions to address societal challenges

691

S5-068

Identifying tools to connect Global Geodetic Reference Frame (GGRF) Capacity Development within the United Nations GGIM Integrated Geospatial Information Framework (IGIF)

Allison Craddock¹、 Graeme Blick²、 Ryan Keenan³、 Mikael Lilje⁴、 Rob Sarib⁵

1. International GNSS Service
2. Land Information New Zealand
3. Positioning Insights
4. Lantmäteriet
5. Department of Infrastructure Planning and Logistics

Effective and sustainable modernization of a nation's geodetic framework relies on the ability of the relevant organizations and other stakeholders to communicate, integrate, and align both their strategic objectives and operational planning with the United Nations Committee of Experts on Global Geospatial Information Management (UN GGIM) Sub-Committee on Geodesy's (SCoG) roadmap for a Global Geodetic Reference Frame (GGRF) for Sustainable Development. In addition, to implement geodetic modernization initiatives through multiple government agencies, a holistic country action plan (CAP) for geospatial information management must incorporate pertinent geodetic outcomes and outputs. Presently, the CAP framework and principles used by nations is the UN GGIM - World Bank Integrated Geospatial Information Framework (IGIF).

From engagement with geospatial and survey communities across emerging nations in the Asia Pacific region, it is evident more assistance and coordination is necessary to articulate integrate and connect geodetic organizational strategies with the requirements of the GGRF roadmap; the strategic pathways of the IGIF; and resourcing for a meaningful and relevant multi-faceted CAP. One of the supporting mechanisms for such planning or preparation, which representatives of the International Federation of Surveyors (FIG) Asia Pacific Capacity Development Network (AP CDN) and the UN SCoG Education, Training and Capacity Building (ETCB) working group are considering, is a policy framework and guide for a "Geodetic and Positioning Thematic Layer" (GPTL). Essentially, this "thematic layer" aims to provide a comprehensive and ever-growing capacity development toolbox in support of the GGRF. This resource will act as a companion guide to the IGIF, providing geodesy-specific guidance and resources that are immediately translatable to broader geospatial needs and efforts.

Consequently, this discussion paper will provide the foundation for discussion about a GPTL dedicated to recognizing, and aligning the geodetic capacity development needs with broader geospatial information management issues and applications; as well as outlining a rigorous, participatory, and inclusive consultation process for the design and development of a thematic layer. Furthermore, this will contribute to a future “white paper” that will concisely describe the issues of a GPTL and initiatives for an appropriate guide and/or policy framework, this paper will seek feedback on: the potential scientific, social, environmental and political benefits of modernizing geodetic infrastructure and systems; the challenges associated with the GGRF roadmap; leveraging the elements of each IGIF strategic pathway; the importance of collaborative efforts; and the capacity development needs and resources in relation to governance, technology and people.

Key words UN, GGIM, GGRF, capacity development, IGIF

Category: Symposium 5: Global Geodetic Observing System (GGOS): the metrological basis for the monitoring of the System Earth => 5.6: Geodesy contributions to address societal challenges

700

S5-069

Embracing challenges through national, regional & international partnership in the Pacific

Andrick Lal
Pacific Community

Partnerships are critical to the successful implementation of the Pacific Geospatial and Surveying Council Strategy 2017-2027. The responsibilities of regional surveyors and geospatial managers frequently correspond to broader initiatives, which all contribute toward achievement of United Nations sustainable development goals. The Pacific Geospatial and Surveying Council (PGSC) relies upon these relationships and is an important contributor towards the global efforts to improve positioning and geospatial information management.

In addition, PGSC aims to collaborate with regional and international organisations, associations, educational institutions and technical groups to support progress on national, regional and global development objectives for sustainable development in the Pacific enabled by world-class geospatial information and surveying services.

Geospatial information underpins the majority of economic and sustainable development activities in the world today. The services provided by Pacific Island geospatial scientists and surveyors contribute to the security and well-being of Pacific people, supporting numerous industries and sectors. These include natural resource management, engineering, climate change adaptation, disaster risk reduction, transport, land ownership, health, and agriculture to name a few.

In November 2014, a group of Pacific regional surveying and geospatial experts met in the margins of the annual Pacific Geospatial Information Systems and Remote Sensing (GIS/RS) User Conference in Suva, Fiji. It was at this meeting that the Pacific Geospatial and Surveying Council (PGSC) was first envisaged and a charter governing its mission and objectives was developed.

The Pacific Community (SPC) established the Pacific Geospatial and Surveying Partnership Desk (<https://pgsc.gem.spc.int/>) to provide secretariat services and support PGSC in achieving its goals and objectives. SPC is the principal scientific and technical organisation in the Pacific region, proudly supporting development since 1947.

In August 2020, the 5th Pacific Geospatial and Surveying Council (PGSC) met virtually, the Council members made the following statements, which is well aligned to the UN Resolution on the adoption of the Global Geodetic Reference Frame: -

- Recognises the critical importance of the United Nations Committee of Experts on Global Geospatial Information Management (UN-GGIM) Integrated Geospatial Information Framework (IGIF) and support the Council members in the operationalisation of the IGIF.

- Encourages members to access the resources and tools of the UN-GGIM Secretariat for the IGIF and agree for the Council to establish a sub-regional collective modality for the IGIF to support the design, development and operationalisation of country action plans for the members.

At the outset of the meeting, the importance of geospatial information as a fundamental economic driver was emphasised.

“One of the key challenges in the region is the lack of a modern reference frame. Eleven out of 14 Pacific island countries are still on local geodetic grids,” said Dr Stuart Minchin, SPC’s Director General.

“A local datum cannot support the new precise positioning technologies that are becoming available with applications for transport, agriculture, and city planning,” Dr Minchin noted. “There are huge opportunities in this region but only if we work together to update our basic datum, and provide the systems, the tools, and the people that can support geospatial information.”

Key words Geodetic, Geospatial, Partnerships

Category: Symposium 5: Global Geodetic Observing System (GGOS): the metrological basis for the monitoring of the System Earth => 5.6: Geodesy contributions to address societal challenges

748

S5-070

Absolute 3D positioning of corner reflectors with Sentinel-1 SAR images for deformation monitoring of Shanghai Yangtze River Bridge

Ruiqing Song、 Jicang Wu、 Xinyou Song、 Yuting Li、 Guowei Tan
College of Surveying and Geo-Informatics, Tongji University, Shanghai 200092,
China

Shanghai Yangtze river bridge is a cross-sea bridge with a total length of 16.6 km. Since it was built in 2009, deformation monitoring is crucial to the operation safety of the Bridge. Traditional point-based surveying methods (e.g. precise leveling, global positioning system) are very sparse in space and time-consuming with high costs, which may lead to deformation phenomenon being not fully explored. Space-borne synthetic aperture radar, with the ability of high spatial resolution, high precision, and all-weather observations, has shown its outstanding capability for a variety of ground mapping applications. With well-controlled orbits of the new generation SAR satellites, the concept of SAR imaging geodesy is emerged, which observes location and deformation of ground point target by utilizing multiple SAR images. The basic idea of SAR imaging geodesy is geometrical intersection based on Range-Doppler equations by using the slant ranges and precise satellite orbit information. By using Sentinel-1 SAR images, the absolute 3D positioning is carried out to the corner reflectors installed at the Bridge. After carefully compensating for the known error sources, such as atmospheric delays, solid earth tide, plate motion and also SAR processing effects, the positioning accuracy of corner reflectors with decimeter-level can be achieved. It offers a new space positioning technology for long term deformation motoring of huge bridges.

Key words Bridge deformation monitoring, Synthetic aperture radar, Corner reflector, Absolute 3D positioning, Sentinel-1

Category: Symposium 5: Global Geodetic Observing System (GGOS): the metrological basis for the monitoring of the System Earth => 5.6: Geodesy contributions to address societal challenges

757

S5-071

Coseismic and early postseismic deformations due to the 2019 earthquake sequence in Ridgecrest, California

Kefeng He, Caijun Xu, Yangmao Wen
Wuhan university

The 2019 Ridgecrest earthquake sequence in the Mojave Desert that ruptured a complex orthogonal conjugate fault system offers a rare opportunity to probe the mechanics of the intraplate lithosphere of the central eastern California shear zone (ECSZ). We used space geodetic data to investigate the coseismic and postseismic deformations attributable to this earthquake sequence. A triangular dislocation inversion scheme was employed to derive the coseismic and postseismic slip distributions on five nonplanar faults in a homogeneous elastic crust. A wide range of viscoelastic relaxation models with varying upper mantle viscosities were also tested to constrain the rheological structure. The inferred coseismic slip exhibited a pronounced (approximately 60%) shallow slip deficit (SSD), only a small proportion of which was recovered by early aseismic afterslip. Inversions of GPS and InSAR data suggest that the near-field postseismic transient was dominated by afterslip at depths of 3~8 km. Viscosity modeling yielded a robust lower bound of approximately 8.0×10^{17} Pa s on the viscosity of the upper mantle. Both the GPS observations and the modeled viscosity at each individual station showed an asymmetric relaxation process on both sides of the faults. The effective viscosity of the mantle asthenosphere to the northeast was inferred to be approximately 2 times lower than that to the southwest, which is consistent with the pattern expected for regional heat flow. A comparison among the static coseismically induced Coulomb stress changes, the cumulative distribution of aftershocks and the afterslip distribution suggests that aftershocks and shallow afterslip could be responses to coseismically induced stresses, but the aftershock and afterslip distribution are poorly correlated. We argue that the pronounced SSD and lack of shallow afterslip during the Ridgecrest earthquake sequence are indicative of an immature fault. Furthermore, we suggest similar rheological structures for the southern and central ECSZ and infer a relatively low effective viscosity for the mantle to the northeast because of its high heat flow. We also propose that the afterslip may illuminate the rate-strengthening regions that mostly slip aseismically, but the aftershocks may illuminate fluid-saturated areas near ruptures.

Key words GPS; InSAR; Coseismic and postseismic modeling; Afterslip; Viscoelastic relaxation

Category: Symposium 5: Global Geodetic Observing System (GGOS): the metrological basis for the monitoring of the System Earth => 5.6: Geodesy contributions to address societal challenges

786

S5-072

GGOS Service and Application Under the PNT Mode

Yamin Dang、Shuqiang Xue、Tao Jiang、Qiang Yang、Wei Wang
Chinese Academy of Surveying and Mapping

The primary mission of GGOS (Global Geodetic Observing System) is to integrate a variety of geodetic infrastructure, observations and models to establish and maintain high-precision geodetic datum, and carry out the research on Earth system monitoring and global change. In the past decade, the applications of Positioning, Navigation and Timing (PNT) in difficult areas such as indoor, underground and underwater environment have posed new challenges to the GGOS. Constructing the geodetic datum under the PNT mode using the GGOS can pave the way for addressing the above application requirements. In addition, multi-source observation data of GGOS can remedy the deficiency of single technique like GNSS (Global Navigation Satellite System). In the past years, China has been developing the PNT mode based geodetic datum system by means of multi-source geodetic observations and techniques. The main achievements include: (1) Realizing the geodetic datum unification between land and sea and seamless navigation in water and underwater. (2) Realizing the International Height Reference System (IHR) in the region of Mount Qomolangma (Everest). (3) Integrating the Continuously Operating Reference Station (CORS), geological, hydrological and meteorological observations for the acquisition of geological disaster precursor.

Key words GGOS, PNT, underwater positioning, IHR, geohazard monitoring

Category: Symposium 5: Global Geodetic Observing System (GGOS): the metrological basis for the monitoring of the System Earth => 5.6: Geodesy contributions to address societal challenges

796

S5-073

News from the GGOS DOI Working Group

Kirsten Elger¹, GGOS DOI Working Group²

1. GFZ German Research Centre for Geosciences
2. Global Geodetic Observing System GGOS

Since late 2018, the “GGOS Working Group on Digital Object Identifiers (DOIs) for Geodetic Data Sets” is meeting regularly to develop best practices, recommendations and advocate for improved global coordination for using DOI to geodetic data and products. The group was established by the International Association of Geodesy’s (IAG) Global Geodetic Observing System (GGOS) and includes international representatives of IAG Services and geodetic data centres and associated members.

Data publications with digital object identifiers (DOI) are best practice for FAIR sharing data. They are fully citable in scholarly literature and many journals require the data underlying a publication to be available. Initial metrics for data citation allows data providers to demonstrate the value of the data collected by institutes and individual scientists. This possibility to get credit for providing data products and running data services has been identified in the group as key requirement for the motivation to implement DOIs to geodetic data.

Our group activities include the collection of data products and already existing and planned DOI activities for IAG services and geodetic data centres, support with the development of new DOI Services along the new recommendations (e.g. for the International Service for the Geoid ISG), and the development of a concept for assigning DOI to hierarchical products that is already implemented for COST-G. Beyond this, we are actively exploring DOI minting and citation practices from other communities in geodesy and geophysics for their potential adoption for geodetic data (e.g. DOI for networks, persistent identifier (PID) for instruments). Our latest discussions focused on geodetic metadata and the possibility to include existing PID’s (like ORCID for researchers, ROR for institutions, PID for instruments) in the geodetic metadata (for stations and data). This presentation provides an update on the group’s activities, results and future ideas.

Key words DOI, IAG Services, data citation, metadata

Category: Symposium 5: Global Geodetic Observing System (GGOS): the metrological basis for the monitoring of the System Earth => 5.6: Geodesy contributions to address societal challenges

815

S5-074

Thinking for the Integration of Satellite Communication, Navigation and Remote-sensing based on the network information SoS

Zuoya Zheng
CAEIT

Under the guidance of the idea of network information SoS, the integration of communication, navigation and remote-sensing (SCNR) has gradually become the mainstream of the development of space-based information network SoS. The development status of integration of SCNR and an integration framework of three networks is discussed in this paper. The development and application prospect of the integration network under the military-civilian integration system are prospected according to national conditions. It will be a valuable reference for the development of SCNR network integration under the idea of network information SoS.

Key words Network Information System of Systems (SoS), Integration of Satellite Communication, Navigation and Remote-sensing (SCNR), Space-based information network

Category: Symposium 5: Global Geodetic Observing System (GGOS): the metrological basis for the monitoring of the System Earth => 5.6: Geodesy contributions to address societal challenges

825

S5-075

SIRGAS and GRFA WG UN-GGIM: Americas interactions for sustainable geodesy

Sonia Costa¹、 Diego Piñón²、 José Antonio Tarrío Mosquera³、 Demián Gomez⁴、
Gabriel Guimarães⁵

1. IBGE

2. Instituto Geografico Nacional

3. Universidad Santiago de Chile

4. Ohio State University

5. Universidade Federal de Uberlândia

The United Nations General Assembly Resolution “Global Geodetic Reference Frame for Sustainable Development”, 26 February 2015 (A / RES / 69 / 266) is a milestone for geodesy, besides satellite space techniques, recognizes the importance of science and strategic decision-makers working together, to make evidence-based decisions concerning global change in the Earth’s crust, sea level, atmosphere and society living. Our society is becoming more dependent on GNSS, the most popular satellite space technique, provides precision, accuracy, and geospatial data interoperability.

With 28 years of geodetic activities in the American continent, Geodetic Reference System for the Americas (SIRGAS) is a voluntary country collaboration to obtain a global geodetic infrastructure following and applying International Association of Geodesy (IAG) standards, recommendations, products, and services. Currently, with more than 400 permanent GNSS stations, SIRGAS-CON network is the most precise geodetic frame in the continent, due to the contribution and collaboration of most American countries, providing GNSS data and weekly coordinates for reference frame monitoring. Although this effort, the American continent is heterogeneous in terms of geodetic knowledge and infrastructure, indicating the need in capacity building and investments.

In 2020 the Regional Committee of United Nations on Global Geospatial Information Management (UN-GGIM: Americas) established the Geodetic Reference Frame for the Americas (GRFA) Working Group to promote and provide mechanisms for capacity development and knowledge transfer in the field of geodesy among the Nations of the Americas. The GRFA was established under recommendations from the UN-GGIM Subcommittee on Geodesy and the scientific guidelines issued by the IAG and SIRGAS. The present work addresses the future

important steps in order to advocate and implement the Global Geodetic Reference Frame (GGRF) in the Americas for sustainable development.

Key words SIRGAS, GRFA, society

Category: Symposium 5: Global Geodetic Observing System (GGOS): the metrological basis for the monitoring of the System Earth => 5.6: Geodesy contributions to address societal challenges

866

S5-076

Group on Earth Observations (GEO) Disaster Risk Reduction (DRR) WG

David Borges
NASA

This presentation will provide latest updates and status of activities across the GEO Disaster Risk Reduction WG.

The GEO DRR WG was established to develop and implement a coherent and crosscutting approach within GEO to advance the use of Earth observations (EO) in support of national disaster risk reduction and resilience strategies, policies, and programs. The guiding global agreements supported by the UN are the Sendai Framework for Disaster Risk Reduction 2015-2030, the Agenda 2030 for sustainable development (SDGs) and the Paris Agreement. The GEO DRR WG will support the translation of the Canberra Declaration and the GEO Strategic Plan into concrete actions within the GEO Work Programme. The WG will coordinate DRR-related activities across the GEO Work Programme in coordination with the GEO Secretariat, and work to improve the GEO community's ability to reduce existing risk and avoid the creation of new risk, ultimately supporting countries to embark on risk and climate resilient development pathways.

Key words Earth observations, disaster risk reduction, resilience, geospatial

Category: Symposium 5: Global Geodetic Observing System (GGOS): the metrological basis for the monitoring of the System Earth => 5.6: Geodesy contributions to address societal challenges

875

S5-077

Towards Indian Forest Sustainability: Satellite-Based Ecological and Nature Hazards Monitoring

C K Shum ^{1,2*}, Soumitri Das ³, Junyi Guo ¹, Yuanyuan Jia ¹, Samuel Malloy ⁴, John Horack ⁴, Vibhor Agarwal ⁵, Orhan Akyilmaz ⁶, Xiaobin Cai ⁷, Tom Darrah ¹, Ehsan Forootan ⁸, Steve Lee ⁹, Peter Luk ¹, Joseph Mascaro ¹⁰, Rongjun Qin ¹¹, Hassan Syed ¹², Metechan Uz ¹, Yu Zhang ¹

1. School of Earth Sciences, The Ohio State University, Columbus, Ohio, USA
2. Innovation Academy for Precision Measurement Science and Technology, Chinese Academy of Sciences, Wuhan, China
3. United States Agency for International Development, Chanakyapuri, New Delhi, India
4. Mechanical and Aerospace Engineering, The Ohio State University
5. Dept. of Geology and Environmental Geosciences, University of Dayton, Ohio, USA
6. Dept. of Geomatics, Istanbul Technical University, Istanbul, Turkey
7. Innovation Academy for Precision Measurement Science and Technology, Chinese Academy of Sciences, Wuhan, China
8. Geodesy and Earth Observation Group, Dept of Planning, Aalborg University, Denmark
9. Stevenson AstroSat, Ltd, Musselburgh, East Lothian, Scotland, United Kingdom
10. Planet, Inc., San Francisco, California, USA
11. Dept. of Civil, Environmental, and Geodetic Engineering, Ohio State University, Columbus, Ohio, USA
12. Dept. of Earth Sciences, Indian Institute of Technology, Kanpur Uttar Pradesh, India

India's forests, which covers over 70 million hectares, support the livelihoods of over 300 million inhabitants. Phenomenal and rapid economic growth in recent decades has adversely impacted pan-Indian forest ecological sustainability, depleted clean water resources and reduced its management efficiency. Climate change is thought to have exacerbated natural hazards with more frequent and intense episodes of flooding and droughts, leading to devastating forest fires, severe insect and pathogen infestations of forests, decreased agricultural productivities; degraded forest ecosystems, watershed quality, human health, and adversely impacted socio-economy of the forest communities. The ultimate objective of this project is to improve forest sustainability in India, focusing on regions in the states of Madhya Pradesh, Himachal Pradesh, Maharashtra, Tamil Nadu, Uttarakhand, and mangrove forests in coastal West Bengal. The physical science component of our research includes the development of a multi-satellite geodetic and other sensor-based Earth observational system, to holistically and timely quantifying physical

and ecological processes impacting pan-India forestry and to monitor natural hazards, water resources, and ecological changes, for improved forest management. Here, we present preliminary results of Pan-India forest and natural hazards monitoring using a suite of example satellite geodetic sensors, including multi-mission radar/laser altimeters, lidar, synthetic aperture radar, GNSS-reflectometry, and satellite gravimetry, as well as using high spatio-temporal resolution optical/multispectral imageries acquired by Planet, Inc cubesat constellations, and others.

Acknowledgements. This research is supported by the United States Agency for International Development under Cooperative Agreement No. 720386CA00002.

Key words Indian forest sustainability, satellite geodesy, remote sensing, GRACE/GRACE-FO, altimetry, SAR, PlanetScope images

**Symposium 5: Global Geodetic
Observing System (GGOS): the
metrological basis for the
monitoring of the System Earth**

**S5.7: Advances in Geodesy for
Geohazard Monitoring and Disaster
Risk Reduction**

Category: Symposium 5: Global Geodetic Observing System (GGOS): the metrological basis for the monitoring of the System Earth =» 5.7 : Advances in Geodesy for Geohazard Monitoring and Disaster Risk Reduction

165

S5-078

Time series InSAR for stability analysis of Ankang airport with expansive soil before operation

Jinzhao SI¹、Shuangcheng ZHANG¹、Yufen NIU²

1 Chang'an University

2. Hebei University of Engineering

The deformation and slope stability of the expansive soil high fill area are key issues in the research of expansive soil disasters. Aiming at the lack of real-time terrain data and the potential ground deformation problems caused by the high degree of filling of the Ankang Airport and the large distribution range of the expansive soil, this paper adopts the Interferometric Synthetic Aperture Radar (InSAR) technology based on elevation correction. And analyze the surface deformation on the eve of Ankang Airport's operation. Deformation results show that: Ankang Airport flight area, terminal area, and expansive soil slope stability affected area three types of typical regional deformation time series results show that Ankang Airport is basically stable on the eve of operation, the cumulative settlement is small, the largest regional deformation is -13.6mm , The maximum deformation inside the airport is -9.7mm , which is far lower than the requirements of civil airport geotechnical engineering design standards. Based on the analysis of the deformation time series and regional precipitation data, it is inferred that the existing small surface deformation time series are characterized by the combined effect of the post-construction settlement of the expansive soil fill area and the expansion and contraction deformation of the expansive soil.

Key words Ankang Airport; Expansive soil; Timing InSAR; DEM correction; Stability

Category: Symposium 5: Global Geodetic Observing System (GGOS): the metrological basis for the monitoring of the System Earth => 5.7 : Advances in Geodesy for Geohazard Monitoring and Disaster Risk Reduction

270

S5-079

Improved multi-baseline maximum likelihood estimation algorithm for InSAR phase unwrapping

Shenke Xiao

China University Of Geosciences ,Beijing

Synthetic aperture Interferometric Radar (InSAR) technology is an important means to obtain surface elevation information and monitor surface deformation. Phase unwrapping directly affects the accuracy of surface elevation. Single baseline InSAR phase unwrapping algorithm has the problems of phase undersampling and phase continuity assumption. Multi baseline algorithm can effectively solve these problems, but the existing multi baseline algorithm has the problems of poor noise robustness or long running time. In this paper, an improved multi baseline maximum likelihood estimation unwrapping algorithm is proposed by combining the maximum likelihood estimation method with unscented Kalman filter. The maximum likelihood estimation method is used for the initial estimation, and then the unscented Kalman filter is used for the reconstruction of the error region to improve the final accuracy. In this paper, simulated data and measured data are used for experimental processing, and compared with single baseline branch cutting method, single baseline minimum norm method and multi baseline maximum likelihood estimation method. The experimental results show that compared with the common phase unwrapping algorithm, the accuracy and operation speed of this method are improved.

Key words phase unwrapping; InSAR; Multi baselin ;maximum likelihood estimation; unscented Kalman filter

Category: Symposium 5: Global Geodetic Observing System (GGOS): the metrological basis for the monitoring of the System Earth => 5.7 : Advances in Geodesy for Geohazard Monitoring and Disaster Risk Reduction

321

S5-080

An Improved Adaptive Method on Mitigating Differential Tropospheric Delays in Time-series InSAR

Mengyao Shi、Junhuan Peng、Honglei Yang、Yuhan Su
China University of Geosciences

Tropospheric delays (TDs) in differential phase of Interferometric Synthetic Aperture Radar (InSAR) causes spatial errors in deformation results derived by InSAR. Although many improvements of the mitigation and correction of the TDs are proposed, such as the measurement by atmospheric application (e.g., MODIS/MERIS, GNSS), InSAR data itself (e.g., PS-InSAR, SBAS-InSAR, StaMPS,) and other atmospheric models (e.g., GACOS, NCVE), the complicated topography conditions, limited and independent measurements lead to uncertainties in the corrected interferograms to some extent. In this paper, we propose an integral method with some cases to correct the TDs adaptively. The research zone is divided into small blocks according to the gradient of elevation. Considering the randomness of elevation and differential phase, spatial heterogeneity in the atmospheric refractive index and the presence of confounding signals, the partial EIV model with different variables and the kriging interpolation with different regression models are applied in different blocks for time-series InSAR (TS-InSAR) applications. We then apply the proposed method with both simulated and real data sets. In the meantime, we discuss and analyze the effects of the proposed method. The results show that the proposed method is superior to the existing method in the detection of deformation inverted from TS-InSAR.

Key words Atmospheric phase correction, EIV model, InSAR, Kriging interpolation method

Category: Symposium 5: Global Geodetic Observing System (GGOS): the metrological basis for the monitoring of the System Earth => 5.7 : Advances in Geodesy for Geohazard Monitoring and Disaster Risk Reduction

350

S5-081

Real-time multi-GNSS solutions for earthquake monitoring in Spain

Víctor Puente

National Geographic Institute of Spain

In the last decades, the data provided by the Global Navigation Satellite Systems have been widely used in seismology to study coseismic displacements and to complement the modelling of the fault slip. Concerning real-time applications, Colosimo et al. (2011) proposed a variometric approach to estimate the delta position triggered by an earthquake using single-differences between consecutive observation epochs of the carrier phase observations registered at a single receiver.

In this contribution, this method is applied to the largest earthquakes that have occurred in Spain and for which there was a GNSS station close to the seismic source. Multi-GNSS data results are presented in the cases they were available and the usage of broadcast versus ultra-rapid products of orbits and clocks is also discussed.

Key words Real-time GNSS, seismology, variometric approach

Category: Symposium 5: Global Geodetic Observing System (GGOS): the metrological basis for the monitoring of the System Earth => 5.7 : Advances in Geodesy for Geohazard Monitoring and Disaster Risk Reduction

395

S5-082

Adjustment of Measurements With Multiplicative Random Errors and Trends

YUN SHI^{1,3}, Peliang Xu²

1. Xi'an University of Science and Technology

2. the Disaster Prevention Research Institute, Kyoto University

3. the Key Laboratory of Coal Resources Exploration and Comprehensive Utilization, Ministry of Natural Resources

Measurements in remote sensing geodesy have been well known to be of speckle noise nature. Although a number of despeckling algorithms have been proposed mainly based on the local weighted statistics in the engineering literature, there are relatively few studies on the statistical adjustment methods for processing the measurements contaminated with the speckle or multiplicative errors. We develop the least squares (LS)-based adjustment methods for the remote sensing measurements with multiplicative errors and trends, evaluate the accuracy of the parameter estimates, and derive the corresponding formulas to estimate the variance of the unit weight. Simulation examples are used to illustrate the developed theory and methods.

InSAR measurements have found a variety of applications in environment and earth sciences. The measurements of remote sensing geodesy have been reported to be of speckle noise nature. Although local statistics and its variants by choosing different weighting schemes have been successfully used for the despeckling of the SAR-type measurements in the engineering literature, the statistical adjustment methods for rigorously processing the measurements contaminated with speckle noise or multiplicative errors can also play an important role to extract precise information from the remote sensing images. We have extended the multiplicative error models to accommodate the deterministic trends, applied the LS-based adjustment methods to estimate the parameters in the extended multiplicative error models, and derived the firstorder approximation of accuracy to evaluate the uncertainty of the parameter estimates. The extension of the models with deterministic trends is of theoretical interest by itself and would be fundamental, for example, to detect the outliers in the measurements with multiplicative errors under the frame of the outlier shift models. Simulation examples have shown that the bias-corrected weighted LS method performs better than the ordinary LS method, even though the latter is theoretically unbiased.

Key words Bias correction, least squares (LS), multiplicative errors, speckle noise

Category: Symposium 5: Global Geodetic Observing System (GGOS): the metrological basis for the monitoring of the System Earth =» 5.7 : Advances in Geodesy for Geohazard Monitoring and Disaster Risk Reduction

412

S5-083

Lessons Learned from the 2020 Uzbekistan Sardoba Dam Failure: An Imaging Geodesy Perspective

Ruya Xiao¹、Mi Jiang²、Zhenhong Li^{3,4,5}、Xiufeng He¹

1. School of Earth Sciences and Engineering, Hohai University

2. School of Geospatial Engineering and Science, Sun Yat-sen University

3. College of Geological Engineering and Geomatics, Chang'an University

4. Key Laboratory of Western China's Mineral Resource and Geological Engineering, Ministry of Education

5. Big Data Center for Geosciences and Satellites (BDCGS)

On 1 May 2020, the Uzbekistan Sardoba Reservoir dam breached. It caused a serious disaster, killing six deaths and forcing more than 100,000 people away from home. The investigation of the tragedy is still ongoing. Here, we investigate the dam failure event from an imaging geodesy perspective: altimetry products from ICESat-2 satellite are used to understanding the topographic environment features in the reservoir surrounding areas; both vertical and horizontal movements of the embankment dam before the collapse are retrieved using multi-temporal InSAR with Sentinel-1 archive data; optical remote sensing images, along with the Global Precipitation Measurement (GPM) products are utilized to exploring the water level and the volume in the reservoir. We conclude that the accident is a result of interactions of both physical and human factors: the physical factor contributing to the failure is internal erosion through the embankment, and the human factor of ignorance leads to the possible opportunities to prevent the event missed. The differential settlement revealed by InSAR at the failure section before the event reaches ~60 mm in two and a half years, which should be a sign of internal erosion. However, the unusual deformation pattern was possibly undetectable due to the resolution limit of current dam monitoring methods. InSAR captures the pre-failure deformation signals well, which suggest it is possible to warn the risk in advance, and the Sardoba dam failure could be possibly avoided with proper intervention. We recommend InSAR deformation monitoring to be listed in the safety programs in the future, to provide detailed deformation and reduce risks of ignorance.

Key words dam failure; InSAR; imaging geodesy; internal erosion

Category: Symposium 5: Global Geodetic Observing System (GGOS): the metrological basis for the monitoring of the System Earth => 5.7 : Advances in Geodesy for Geohazard Monitoring and Disaster Risk Reduction

427

S5-084

Metrological support of laser coordinate measuring systems

ANDREY MAZURKEVICH

FSUE VNIIFTRI (Federal State Unitary Enterprise All - Russian Scientific Research Institute for Physical-engineering and Radiotechnical Metrology)

Currently, specialized reference stands are used for calibration of the spatial characteristics of laser coordinate measuring systems such as laser tracker and laser scanner. This metrological equipment is expensive to operate and requires significant capital expenditures during development and creation. But here it is necessary to take into account that the errors of modern laser coordinate measuring systems are very close to the value of 10 microns. And to ensure the necessary stock of metrological accuracy, it is necessary to use expensive high-tech equipment and highly qualified personnel. In the world, there are now no more than ten such stands, which are mainly located on the territory of manufacturers of measuring equipment and metrological national institutes of a number of countries. At the same time, it is necessary to take into account that the fleet of these measuring instruments has more than doubled in recent years and this trend will continue in the future. Accordingly, there is a problem of evaluating the accuracy characteristics and calibration of laser trackers and scanners in the field of their operation using the existing reference base. To solve this problem, it is possible to use existing reference optical length comparators that operate in the measurement range up to 100 meters and provide the necessary margin of accuracy. Our specialists have developed a method for evaluating the metrological characteristics of laser trackers and scanners, based on converting the coordinates of the measured points into a set of line lengths. The error of determination, which can be estimated from the results of length measurements by the reference comparator. In this case, the device under study is placed perpendicular to the line of sight of the reference comparator, which allows us to evaluate its linear and angular measurement channels in the entire operating range during the measurement process. Testing the technique on the basis of a 60-meter optical comparator from the State Primary Special Standard of the Unit of Length GET 199-2018 confirmed the possibility of evaluating the metrological characteristics of trackers with a measurement error of 8 microns.

Key words Metrological support, laser coordinate measuring systems, error, accuracy, measurement methods

Category: Symposium 5: Global Geodetic Observing System (GGOS): the metrological basis for the monitoring of the System Earth => 5.7 : Advances in Geodesy for Geohazard Monitoring and Disaster Risk Reduction

460

S5-085

Spatio-temporal variations of afterslip and viscoelastic relaxation following the Mw 7.8 Gorkha (Nepal) earthquake

Zhen Tian¹、 Jeffrey Freymueller²、 Zhiqiang Yang³

1. Chang'an University

2. Michigan State University

3. Chang'an University

We use 4 years of 3D GPS data from Nepal and southern Tibet to investigate the postseismic deformation caused by the 2015 Mw 7.8 Gorkha (Nepal) earthquake. We first model afterslip and viscoelastic relaxation separately, but find that this approach results in an overestimate of the total postseismic deformation. We then use an integrated model to simultaneously extract the contributions from afterslip and viscoelastic relaxation by assessing the misfit between observed and simulated displacements during different periods. The results show that the near-field postseismic displacements are dominated by downdip afterslip during the first 2 years, and then viscoelastic relaxation plays the leading role in the following years. In the far-field, however, the observed deformation is mainly controlled by viscoelastic mechanism throughout the postseismic period. The best model supports a laterally heterogeneous rheology: the Tibetan lower crust is viscoelastic with a transient viscosity 5×10^{17} Pa s, steady-state with a high viscosity upper mantle (10^{20} Pa s), and that the same mantle viscosity applies beneath viscosity 5×10^{18} Pa s; we assume in our model that India has an elastic lithosphere 50 km thick and the possible untapped strain inherited from historical events, the regions to the west and south of and the displacements caused by afterslip for ~6 years. Given the afterslip following the earthquake Tibet. We further predict that viscoelastic deformation will be observed in the near-field for ~12 years Kathmandu have the potential to suffer a large earthquake rupture in the future.

Key words GPS postseismic deformation, Gorkha earthquake, afterslip, viscoelastic relaxation

Category: Symposium 5: Global Geodetic Observing System (GGOS): the metrological basis for the monitoring of the System Earth => 5.7 : Advances in Geodesy for Geohazard Monitoring and Disaster Risk Reduction

480

S5-086

The landslide susceptibility mapping based on machine learning methods and InSAR-derived deformation: a case study on the upper reaches of the Jinsha River

Zhuo Jiang、 Chaoying Zhao、 Xiaojie Liu
Chang 'an University

Landslides are generally referred to the downslope movement of soil and rock under the effect of gravity and external triggering factors, which play an essential role in the evolution of landforms, and threatening both human life and economics. Landslide susceptibility is the likelihood of a landslide occurring in an area on the basis of local conditions. Landslide susceptibility mapping (LSM) serves the first and the most important role for decision makers and planners to reduce the loss of people's lives and property from catastrophic disasters. With advances in the computing ability and the emergence of massive multisource data, machine learning methods have been widely used in LSM due to its superior prediction performance and robustness. Landslide inventory map is the foundation of landslide susceptibility mapping, as the modeling process begins with the acquisition of sample data. However, in some cases, there exist no archived landslide inventory map due to the complex geological conditions and remote distance. In recent decades, small baseline subset interferometric synthetic aperture radar (SBAS-InSAR) has become an unprecedented tool to generate landslide inventory map with its high deformation precision and large coverage. The LSM consists of the following five steps: (1) the generation of landslide inventory map based on InSAR-derived deformation maps; (2) the preparation of the conditioning factors and preprocessing; (3) the training of the machine learning models; (4) validation and comparison; and (5) landslide susceptibility mapping and post-processing. Firstly, after identifying the landslide samples, non-landslide samples are randomly selected by setting appropriate thresholds of the slope angle and elevation. Then the potential landslide and non-landslide samples is randomly divided into a training dataset (70%) for generating the machine leaning models and a testing dataset (30%) for validation of the models. Secondly, in this study, we select twelve conditioning factors according to the specific situation of the study area. Discretization, correlation analysis and selection of conditioning factors are conducted using decision tree, Spearman's coefficient and information value technology, respectively. Thirdly, we select three machine learning methods i.e. logistic regression (LR),

random forest (RF) and adaptive boosting (AdaBoost) approaches to train the input data. Fourthly, the results of the models are compared using the receiver operating characteristic (ROC) curve and some classical statistical indices acquired by confusion matrix. Finally, we conduct the post-processing for landslide susceptibility maps to obtain more targeted concerned zones. Results indicate that the Ada model has a highest accuracy of 92.74%, followed by RF (91.3%), and LR (89.16%), and the models have high consistence with kappa index of Ada (0.85), RF (0.83) and LR (0.78). The post-processed susceptibility maps produced by LR and RF model are more consistent with the distribution of the landslide. Therefore, we conclude that RF model is more suitable for landslide susceptibility mapping. Our research has a significant implication for the combination of InSAR landslide identification and landslide susceptibility mapping, especially in areas without archived landslide inventory map, which can provide valuable information for disaster prevention, mitigation, and management.

Key words landslide susceptibility mapping, machine learning methods, SBAS-InSAR technology

Category: Symposium 5: Global Geodetic Observing System (GGOS): the metrological basis for the monitoring of the System Earth => 5.7 : Advances in Geodesy for Geohazard Monitoring and Disaster Risk Reduction

483

S5-087

An approach based on coherence matrix decomposition to improve small baseline processing for land subsidence monitoring

Qian He

China University of Mining and Technology

Time-series InSAR combining permanent scatterers (PS) and distributed scatterers (DS), has been strongly developed in recent years. Since the introduction of SqueeSAR, the research of distributed scatterers (DS) has gradually become a hot topic in the field of time-series InSAR. Unlike PS, DS corresponding to natural targets are affected by temporal and geometrical decorrelation. DS phase optimization is needed due to lower signal-to-noise ratio for the interferometric phase. It is known that the Component extrAction and sElection SAR (CAESAR) is a recently presented technique, which improves the SqueeSAR algorithm by allowing the selection and filtering of scattering mechanisms. The key to CAESAR is the covariance matrix decomposition, which aims to identify the principal components of the measured data. However, this algorithm has several shortcomings: (1) The estimation of covariance matrix is biased when the pixels in boxcar window do not belong to the same feature. (2) Research on covariance matrix is easily affected by backscattered power unbalances among all the SAR images. (3) Temporal coherence is an important parameter for DS pixels selection. It is calculated by all possible combined interferometric pairs, which ignores the adverse effect of low-quality interferometric phase. Therefore, this paper has made improvements to the above points. An approach based on coherence matrix decomposition is proposed to improve small baseline processing. Phase optimization is performed by eigenvalue decomposition and principal component analysis of the coherence matrix constructed based on the identified homogeneous pixels. Moreover, temporal coherence is estimated by the selected interferometric phase with low noise and clear fringes. The results show that the proposed strategy can provide the high spatial density of deformation measurements with accuracy ensured, which proves to be a useful tool for land subsidence monitoring.

Key words coherence matrix decomposition, principal component analysis (PCA), SAR interferometry, distributed scatterers (DS), land Subsidence

Category: Symposium 5: Global Geodetic Observing System (GGOS): the metrological basis for the monitoring of the System Earth => 5.7 : Advances in Geodesy for Geohazard Monitoring and Disaster Risk Reduction

530

S5-088

Different gradient deformation monitoring of the landslide based on Intermittent SBAS (ISBAS) InSAR and SAR offset-tracking methods

Liquan Chen, Chaoying Zhao, Ya Kang, Xiaojie Liu

School of Geological Engineering and Geomatics, Chang'an University

The landslides are widely distributed in mountain area of China, which threaten the safety of residents' life and property. The Synthetic Aperture Radar (SAR) techniques including SAR interferometry and SAR offset-tracking provide effective tools to the identification and monitoring of the potential landslides. However, the different landslides types, failure mechanisms, triggering factors always show the different spatiotemporal deformation characteristics, such as small-gradient and periodic deformation induced by rainfall, large-gradient deformation induced by underground mining. Therefore, phase-based InSAR and amplitude-based SAR offset-tracking methods are involved for different landslide deformation monitoring. However, both techniques have their own limitation due to the decorrelation caused by dense vegetation or large surface displacement, which significantly hinder the deformation time series retrieve due to the sparse coherent targets over all SAR images. To solve this problem, we apply Intermittent Small Baseline Subset (ISBAS) to InSAR and SAR offset-tracking, respectively, which can select optimal composition from all of the interferometric pairs or offset-tracking pairs automatically to calculate the deformation time series pixel by pixel.

The different gradient deformation of the Pingdi landslide and Jianshanying landslide in Guizhou province, China are retrieved successfully by our methods based on 19 ALOS/PALSAR-2 images.

As for Pingdi landslide located in Pingdi Village, Jichang Town, Shuicheng County, Guizhou province, ISBAS InSAR method is applied, where the interferometric pairs to each pixel are selected automatically according to the coherence value. Besides, we also take coherence as the weight to estimate the deformation rates between each two adjacent SAR acquisition dates by least-square or singular value decomposition (SVD) method. Finally, the accumulative deformation time series is trivially obtained by integrating each deformation between two adjacent dates. The results show that the point density of ISBAS InSAR is five times of the conventional SBAS with 5.1316×10^4 points/km² and 1.3078×10^4 points/km², respectively over the landslide area, which significantly increase the landslide deformation results. As for

Jianshanying landslide in Faer Town, Shuicheng County with very large gradient deformation, ISBAS SAR offset-tracking is experienced, where the signal noise ratio (SNR) is used to select the high-quality SAR pairs and determine its weight. Finally, two-dimensional deformation time series are obtained with the similar procedure to ISBAS InSAR. The result of ISBAS SAR offset-tracking is better than that of conventional SAR offset-tracking method, and the maximum cumulative deformation reached 37 m in three years.

In this study, the ISBAS InSAR and ISBAS SAR offset-tracking are applied effectively in the different gradient landslide deformation monitoring. It is validated that two new methods can get much more effective monitoring target than the conventional ones. Therefore, it can be applied to landslide deformation monitoring and failure mode analysis.

Key words ISBAS; InSAR; offset-tracking; landslide monitoring

Category: Symposium 5: Global Geodetic Observing System (GGOS): the metrological basis for the monitoring of the System Earth => 5.7 : Advances in Geodesy for Geohazard Monitoring and Disaster Risk Reduction

539

S5-089

Landslide detection, monitoring and failure mechanism research in Guizhou Province, China with multi-sensor SAR datasets

Chaoying Zhao、Liquan Chen、 Hengyi Chen
Chang'an University

The catastrophic landslide disasters occur frequently in Karst mountainous regions, Yunnan-Guizhou Plateau, China. These disasters are mostly due to vulnerable geological environment and frequent anthropogenic activities, which have caused huge economic loss and casualties. Therefore, the identification of potential landslides and the deformation monitoring of unstable slopes are critical to the research on the failure mechanism and early warning. For this purpose, we firstly take Guizhou Province, with 176,000 km² in area as research region, detect the potential landslides and generate inventory map by using synthetic aperture radar (SAR) interferometry technique, where Radarsat-2, ALOS/PALSAR-2 and Sentinel-1 SAR imagery datasets are involved. Then, we focus on two typical mining-induced landslides but with different surface deformation characteristics, obtain the multi-dimensional historical deformation based on multi-source remote sensing data. Finally, the triggering factors and failure modes of two landslides are revealed.

For the first case, the Pusa landslide, a mining-induced and with small-gradient deformation landslide, is studied, which occurred on 28 August 2017, caused 26 deaths with 9 missing. We recover the pre-event deformation with multi-sensor SAR imagery firstly, and delineate the boundary and source area of this landslide based on the coherence and SAR intensity maps before and after the event. Then, we retrieve the deformation before the Pusa landslide with ALOS/PALSAR-2 and Sentinel-1A/B SAR imagery data. Results show a clear mining-induced deformation pattern before this event. We also detect the line-of-sight (LOS) deformation rate and time series by ascending and descending Sentinel-1A/B SAR imagery data, where we find that the onset of the deformation was four months before landslide event. Finally, we reveal the triggering factors and conceptualize the failure mechanism of the Pusa landslide as the joint effects of rainfall and mining activity.

For the second case, the Jianshanying landslide, a mining-induced and with large-gradient deformation landslide, is studied. To retrieve the historical evolutionary regulation, the surface deformation time series from 2017 to 2020 is firstly estimated by combining multi-temporal SAR

interferometry and improved offset-tracking methods. The maximum cumulative deformation in azimuth and LOS direction reached 37.5 m and 35.7 m, respectively. Then, the spatiotemporal characteristics of Jianshanying landslide is analyzed in terms of LOS deformation with stacking InSAR method and two-dimensional (2D) deformation with improved SAR offset-tracking method. And the different deformation features between sliding body and surrounding areas are uncovered. We point out the “three-section” surface deformation model, that is, the subsidence at the back of the landslide body, the landslide deformation with a steep terrain and the subsidence at the toe of the slope. We further analyze the deformation time series by considering the joint effects of rainfall and underground mining. Finally, we conceptualize the landslide failure mode for the Jianshanying landslide.

Two cases can be extended to the similar landslides monitoring and failure mode research in karst mountainous areas of southwestern, China, which have been identified by SAR interferometry and archived from historical inventory maps.

Key words SAR interferometry; SAR offset tracking; Landslide detection; Deformation monitoring; Failure mechanism

Category: Symposium 5: Global Geodetic Observing System (GGOS): the metrological basis for the monitoring of the System Earth => 5.7 : Advances in Geodesy for Geohazard Monitoring and Disaster Risk Reduction

546

S5-090

A Strain-Model Based InSAR Time Series Method for Geohazards Deformation Monitoring

Jihong Liu¹、 Jun Hu¹、 Roland Burgmann²、 Zhiwei Li¹、 Qian Sun³、 Zhangfeng Ma⁴

1. Central South University

2. University of California, Berkeley

3. Hunan Normal University

4. Hohai University

The ground surface deformation is one of the most intuitive manifestations of geohazards. Accurate deformations monitoring of geohazards can benefit the mechanism interpretation and even the disaster risk reduction. In this work, we propose a new time series InSAR (interferometric synthetic aperture radar) method based on a strain model. Traditionally, the interferometric phases are generally optimized based only on a constant set of statistically homogeneous point throughout the observing period, resulting in the fact that the decorrelated phase cannot be well recovered and possible incoherent (or coherent) phases are (or not) used to optimize the target phase. In the proposed method, the SM, representing the geophysical relationship of spatially adjacent points' deformations, is employed to optimize the interferometric phases interferogram-by-interferogram. The unwrapped phase time series can be estimated from the wrapped interferograms based on the linear iterative weighted least squares method, which is simple and can effectively suppress the decorrelations. Both simulation and the real experiment of the Geysers geothermal field, California are conducted, validating that the proposed method can reduce the decorrelations and simultaneously preserve the deformation signals.

Key words InSAR; Geohazards deformation monitoring; Strain model; The Geysers geothermal field

Category: Symposium 5: Global Geodetic Observing System (GGOS): the metrological basis for the monitoring of the System Earth => 5.7 : Advances in Geodesy for Geohazard Monitoring and Disaster Risk Reduction

548

S5-091

Retrieving complete 3-D ice velocities from multi-baseline and multi-aperture InSAR measurements

Wanji Zheng, Jun Hu
Central South University

As one of the most sensitive area to the climate change, the ice velocity in Antarctic is a fundamental parameter for accessing the global warming process. Over the past decades, with the advantages of having a high precision and large coverage, Interferometric Synthetic Aperture Radar (InSAR) has played a key role in deriving ice velocity in the Antarctic. However, the imaging geometries and digital elevation model (DEM)-induced errors greatly limits the mapping of complete three-dimensional (3-D) ice velocities. In this study, we integrate multi-baseline and multi-aperture InSAR measurements from the ENVISAT ASAR datasets to derive complete 3-D ice velocities in the Grove Mountains area of the Antarctic. The results show that the estimated complete 3-D ice velocities are in good agreement with MEaSURES and GPS observations. As common methods, ignoring the vertical velocity and constrain by Surface Parallel Flow (SPF) also can derive the multiple dimensional deformation. Compared with the conventional 2-D and quasi 3-D ice velocities, the complete 3-D ice velocities can effectively eliminate the effects of DEM errors and elevation changes and are also capable of retrieving the thickness change of the ice, which provides important information on the origin of mass transition.

Key words 3-D; ice velocity; InSAR; MAI; Antarctic; ice thickness

Category: Symposium 5: Global Geodetic Observing System (GGOS): the metrological basis for the monitoring of the System Earth => 5.7 : Advances in Geodesy for Geohazard Monitoring and Disaster Risk Reduction

588

S5-092

Quantifying glacier displacement and glacial lake outburst floods with SAR and optical images: A case study in Jinweng Co Lake, Tibet, China

Liye Yang¹, Zhong Lu², Chaoying Zhao¹, Chengsheng Yang¹

1. Chang'an University

2. Southern Methodist University

On 25 June 2020, the Jinweng Co lake in Yiga village in the Tanggula Mountains experienced an outburst flood, catastrophically damaging farmland and roads. The complex causal factors and potential risk factors for glacial lake outburst flooding (GLOF) are not fully understood. In this paper, we provide a systematic analysis of the contributing factors leading to the GLOF disaster, in terms of hydrometeorological triggering, glacier activity, and abrupt ice accumulation. Multi-source remote sensing approaches and climatic observations have been integrated to analyze the motion of glaciers and glacial lakes. Pixel offset tracking small baseline subsets (PO-SBAS) of Sentinel-1 images, change detection of SAR intensity images, and optical interpretation of Sentinel-2 images were conducted to retrieve the long-term two-dimensional (2D) time series displacement from 2017 to 2020 as well as changes to the lake between pre-event and post-event. Results show the distinct periodic features of increased rate of movement in upstream glaciers during winters. Comparisons between displacement and daily/monthly precipitation reveal that the glacier motion is predominantly controlled by seasonal rainfall. Importantly, the outburst process of the Jinweng Co lake based on Sentinel-2 images was constructed to reveal that the area of the lake decreased by 55.4% and the glacier area decreased by 53.6%. The complicated GLOF is tied to the erosion of the upstream glacier, rainfall drainage systems, and ice blocks or accumulations. In addition, this study discovered the hidden dangers of two nearby lakes, Talong Co lake and Ranzere lake, located upstream from Yiga village; both exhibit a similar periodic characteristic with the collapsed lake. Our research can provide a reference for identification and mitigation of glacial lake outburst disasters in the southeastern of Qinghai-Tibetan Plateau.

Key words Glacial lake outburst flood (GLOF); Glacier time series displacement; Outburst mechanism; Multi-source remote sensing; The Jinweng Co lake.

Category: Symposium 5: Global Geodetic Observing System (GGOS): the metrological basis for the monitoring of the System Earth => 5.7 : Advances in Geodesy for Geohazard Monitoring and Disaster Risk Reduction

590

S5-093

Monitoring and analysis of geological hazards based on loading impact change

Wei Wang, Yamin Dang, Chuanyin Zhang, Qiang Yang
Chinese Academy of Surveying and Mapping

Monitoring is essential to the prevention and control of geological hazards, yet conventional monitoring is often conducted for local geological hazards, and the relation between monitored results and geological hazards remains poorly understood. In this study, regional load deformation field model was constructed based on data from Continuously Operating Reference Stations (CORS). The relation between load-induced changes and geological hazards, as the Regular Characteristics (RCS), are obtained by comparing the geological hazards with the impact of the total load change in the whole region. Geological hazards are more prone to occurring when there are one or more RCS, especially abnormal dynamic environment appear at the same time, such as solid high tide, heavy rainfall, and so on. The RCS included the ground geodesy height change rate increasing, the ground gravity change rate decreasing, the ground vertical deviation diverging, the ground geodesy height gradient growing larger, and the ground gravity gradient growing larger. It was found that the comprehensive observations of CORS and gravity stations can effectively monitor the RCS of the load-induced changes. The results of this study provide more insights associated with the geological hazards monitoring and analysis methods as well as effective support for geological hazard forecasting.

Key words geological hazards monitoring, CORS network, loading change, deformation monitoring

Category: Symposium 5: Global Geodetic Observing System (GGOS): the metrological basis for the monitoring of the System Earth => 5.7 : Advances in Geodesy for Geohazard Monitoring and Disaster Risk Reduction

595

S5-094

Differential Interferometric Synthetic Aperture Radar data for more accurate earthquake catalogs

Chuanhua Zhu^{1,3}、Chisheng Wang¹、Bochen Zhang^{2,4}、Xiaoqiong Qin^{1,4}、Xinjian Shan³

1. Guangdong Key Laboratory of Urban Informatics and Guangdong Laboratory of Artificial Intelligence and Digital Economy (SZ), School of Architecture & Urban Planning, Shenzhen University
2. Guangdong Key Laboratory of Urban Informatics, Shenzhen University
3. State Key Laboratory of Earthquake Dynamics, Institute of Geology, China Earthquake Administration
4. Shenzhen Key Laboratory of Spatial Smart Sensing and Services, Shenzhen University

The accuracy of earthquake catalogs limits the reliability of earthquake hazard assessment and the comprehensive understanding of earthquake mechanisms. Current seismic catalogs are based on the inversion of seismic wave data. The accuracy of their source parameters, reflecting the quantity and layout of seismic stations, and the crustal velocity model used, are often highly uncertain. The open-source and popularization of Interferometric Synthetic Aperture Radar (InSAR) deformation data offer the potential to provide more accurate source parameters for earthquake catalogs. In this study, we used same-source InSAR data and a consistent processing approach (i.e., the same sampling, inversion algorithm, and processing flow) to obtain the fault slip models and source parameters of 26 earthquakes; these were then used them to form a unified InSAR earthquake catalog (U-InSAR). We then compiled a second InSAR earthquake catalog (C-InSAR) based on the source parameters of an additional 77 earthquakes inverted using InSAR deformation data from various sources by previous studies. The C-InSAR catalog was used to evaluate the impact of data sources and processing approach on the consistency of InSAR catalogs; we found no significant differences between the U- and C-InSAR catalogs. Secondly, the combined U- and C-InSAR catalogs were compared with seismological catalogs, and showed significantly improved seismic source locations, depths, fault strikes, and fault dips. Our results confirm the rationality and feasibility of constructing earthquake catalogs using source parameters from a variety of InSAR data sources and inversion algorithms. We emphasize that InSAR catalogs can provide an important supplement, improvement, and/or correction to seismological catalogs, and can provide important basic data for more refined and reliable

research on earthquake mechanisms and hazard assessments. Finally, we set up a preliminary sharing and distribution system for InSAR-based catalogs.

Key words InSAR earthquake catalog, source parameter comparison, unified catalog, sharing system

Category: Symposium 5: Global Geodetic Observing System (GGOS): the metrological basis for the monitoring of the System Earth => 5.7 : Advances in Geodesy for Geohazard Monitoring and Disaster Risk Reduction

598

S5-095

Multi-scale Crustal Deformation around the Southeastern Margin of the Tibetan Plateau from GNSS Observations

Keke Xu

Henan Polytechnic University

We present a multi-scale decomposition model for analyzing the widespread deformation and complex dynamics mechanism of the southeastern margin of the Tibetan Plateau. We firstly carry out simulations to test the performance of the model by synthetic Global Navigation Satellite System(GNSS) data for a network, whose geometry distribution is same with actual Crust Movement Observation Network of China(CMONC) in the southeast edge of the Tibetan Plateau. We then estimate the multi-scale velocity field and strain rate field using observed data with 240 stations between 1999 and 2007. Results show that the deformation field at the different spatial scale corresponds to the different tectonic driving force and strain accumulation coverage. Tectonic background of the Tibetan Plateau, extrusion of the Sichuan-Yunnan rhombic block, rigid block motion, interior deformation of the block and segmented motion of fault zones are separately displayed in the corresponding scale, which provides a strong support keys to the understanding of the controversial deformation models for the tectonic evolution and uplift mechanisms of the Tibetan Plateau. Our results also show that scale 7 with the coverage of about 50 km can better reflect the seismogenic background of mid-strong earthquakes(>Ms5.0) of the region. The convergence area of high compression and inflation strain or the high value area of maximum shear strain at scale 7 is obviously correlated with seismic activities, including 2008 Wenchuan Ms8.0 earthquake, no significant pre-seismic deformation across fault in other scales. Our research provides a new insight into the nature of tectonic deformation and the seismic risk assessment of the southeastern margin of the Tibetan Plateau.

Key words Satellite geodesy; Asia; Wavelet transform; Earthquake interaction, forecasting, and prediction; Mechanics, theory, and modelling

Category: Symposium 5: Global Geodetic Observing System (GGOS): the metrological basis for the monitoring of the System Earth => 5.7 : Advances in Geodesy for Geohazard Monitoring and Disaster Risk Reduction

603

S5-096

An Improved Two-tier Network for Robust PSI Parameter Estimation and Its Application on Deformation Monitoring of Urban Area

Wenqing Wu、 Jun Hu
Central South University

Persistent scatterer interferometry (PSI) has the ability to achieve submeter-scale digital elevation model (DEM) and millimeter-scale deformation. However, it's difficult to maintain good performance under long baseline and large phase gradient. In this paper, an improved two-tier network PSI method is proposed. Such a method can increase parameter estimation robustness and spatial continuity in single-prime mode and urban build environments. Firstly, an optimized first-tier network is constructed by outlier detection and subsets network construction. On this basis, we utilize the ridge estimator as a substitute for the WLS estimator to improve the estimation accuracy in network adjustment. In the second-tier network, the remaining PSs are detected by constructing local star networks, thus increasing the density of the measurements in the first-tier network. The effectiveness of the proposed method for stress deformation monitoring of the buildings is demonstrated on Shenzhen CITIC Building and Shenzhen Convention and Exhibition Center.

Key words Persistent scatterer interferometry (PSI), two-tier network, Shenzhen

Category: Symposium 5: Global Geodetic Observing System (GGOS): the metrological basis for the monitoring of the System Earth => 5.7 : Advances in Geodesy for Geohazard Monitoring and Disaster Risk Reduction

608

S5-097

Structural dynamic displacements detecting through robust integrated model using GNSS and accelerometers

Xu Liu^{1,2}、Jian Wang^{1,2}、Houzeng Han¹

1. Beijing University of Civil Engineering and Architecture

2. Research Center for Urban BIG Data Applications, Beijing University of Civil Engineering and Architecture, Beijing, China

GNSS has been widely used to measure dynamic displacement responses for large civil engineering structures. However, it has the limitation of relatively low frequency of data compared with alternative measurement techniques. Moreover, the accuracy of GNSS data degradation in harsh environment due to the blockage of signals from satellites and Multipath Effect. In this study, an integrated algorithm that includes GNSS and high-rate accelerometer data is proposed to improve the sampling rate and accuracy of dynamic displacements continuously. Based on the dynamics model and observation model, a robust Kalman filter model is constructed using the accelerometer data as the control vector of dynamics model and GNSS as the measurement vector of observation model. The performance of the proposed algorithm is validated by a series of simulation and field tests. The results show that the proposed algorithm can make the dynamic displacements smoother due to the high sampling rate, and the accuracy of the dynamic displacements is effectively improved even with the abnormal GNSS data.

Key words GNSS; accelerometers; dynamic displacements; robust Kalman filter; data fusion

Category: Symposium 5: Global Geodetic Observing System (GGOS): the metrological basis for the monitoring of the System Earth => 5.7 : Advances in Geodesy for Geohazard Monitoring and Disaster Risk Reduction

610

S5-098

Monitoring phosphate mining induced landslides in karst mountainous area using multi-temporal InSAR

Hengyi Chen、Chaoying Zhao、Baohang Wang、Liquan Chen
College of Geological Engineering and Geomatics, Chang'an University

Kaiyang County in China has suffered serious landslides due to its fragile karst topography and the exploitation of phosphate rock for years, which make it is urgent to conduct the landslides investigation and monitoring. SAR Interferometry (InSAR) technology has become one of the mature tools to monitor surface deformation. However, affected by karst geomorphology including dense vegetation, humid climate, and intensive underground mining, the traditional InSAR technology usually faces the challenges of temporal and spatial decorrelation. Therefore, both Stacking and distributed scatterers (DS) InSAR methods are conducted in this paper to identify the unstable slopes and derive the deformation time series with 18 L-band ALOS/PALSAR-2 images. Firstly, we denoise the interferograms based on the statistically homogeneous pixels (SHPS) and eigenvalue decomposition. Then, we investigate the unstable slopes in a wide range of Kaiyang County through the Stacking method. The landslides that heavily affected by large deformation magnitude are taken as the main objects for high-precision deformation time series monitoring subsequently. To this end, we select the high-precision DS point targets according to the temporal coherence and unwrap the denoised interferograms in 3D domain. Finally, we analyze the disaster causal factors by combining the relevant stratum structure, rainfall data, phosphate mining activities and surface deformation time series. The results show that the landslides in the study area are greatly affected by underground mining activities, compared with rainfall and weathering effects. Since most of the phosphate rock is stored in the stratum with weak lithology, the mining activities would accelerate the slope movement. The technical routes in this study could be used to investigate and monitor the unstable slopes in the karst mountainous areas, which would provide valuable insights into mining-induced landslide mitigation and hazard prevention.

Key words InSAR; mining-induced landslide; distributed scatterers; disaster mitigation

Category: Symposium 5: Global Geodetic Observing System (GGOS): the metrological basis for the monitoring of the System Earth => 5.7 : Advances in Geodesy for Geohazard Monitoring and Disaster Risk Reduction

611

S5-099

Attention guided U-Net model for landslide detection

Xuerong Chen¹、Chaoying Zhao^{1,3}、Zhong Lu²

1. School of Geological Engineering and Geomatics, Chang'an University, Xi'an, Shaanxi 710054, China;
2. Department of Earth Sciences, Southern Methodist University, Dallas, TX, 75275
3. Key Laboratory of Western China's Mineral Resources and Geological Engineering, Ministry of Education, Xi'an 710054, Shaanxi, China

Landslide detection is an important basis for susceptibility evaluation and disaster mitigation, which can save residents' lives and reduce property losses. The aim of landslide detection is to record its location, size and extent in a given scale map. Several methods are successfully to detect the landslides, where machine learning algorithms such as Support Vector Machine (SVM), Random Forest (RF), have been gradually applied to remote sensing images for landslide detection in last decades. However, the accuracy of traditional machine learning algorithms is still low and it can hardly be applied in large areas. In recent years, some deep learning algorithms are proposed for landslide detection. One of the effective models is U-Net, which is a classic semantic segmentation algorithm. We point out an attention U-Net (AU-Net) algorithm in this study to combine the attention mechanism and the U-Net model. The accuracy of the AU-Net model in detecting landslides is verified through the landslide datasets in Bijie County, China. We take Recall, F1-Score and IoU are as verification indicators of prediction accuracy. Then we apply the trained AU-Net model to extract unknown landslides in Shuicheng County, close to Bijie County. We divide the 770 landslide samples in the dataset into training set, validation set and test set. In the experiment, images was normalized and augmented. To avoid over-fitting, the Batch Normalization strategy and the Dropout (0.5) strategy are used in the network. The model training results show that AU-Net improves the model accuracy by 0.6% compared to U-Net. The prediction accuracy of Recall, F1-Score and IoU is increased by 0.018, 0.018 and 0.024, respectively. Therefore, AU-Net model can be used in the detection of unknown landslides if it is well trained in the similar landslide-prone region.

Key words landslide detection; remote sensing; Semantic Segmentation

Category: Symposium 5: Global Geodetic Observing System (GGOS): the metrological basis for the monitoring of the System Earth => 5.7 : Advances in Geodesy for Geohazard Monitoring and Disaster Risk Reduction

644

S5-100

Evaluating the performance of global atmospheric models in correcting InSAR tropospheric delay over the Kanto Plain using statistical metrics

Guangqi Jiao^{1,2,3}, Yu Sun^{1,2,3}

1. Key Lab of Spatial Data Mining and Information Sharing of Ministry of Education, Fuzhou 350108, China
2. National & Local Joint Engineering Research Center of Satellite Geospatial Information Technology, Fuzhou 350108, China
3. Academy of Digital (Fujian), Fuzhou 350108, China

Tropospheric delay significantly degrades the reliability and accuracy of InSAR measurements. Such effects can larger correct by applying proper global atmosphere models (GAMs). However, various GAMs are now available in the community to provide different tropospheric delay corrections, which result in significantly different surface deformation maps to lead to erroneous interpretation. Therefore, performance metrics used to quantify the effectiveness of GAMs are necessary to choose the proper GAM.

In this study, we use 66 SAR images from the Sentinel 1A to investigate an area of the Kanto Plain. We adopt three GAMs, including GACOS, MERRA2, and ERA5, to correct the tropospheric delay over the Kanto Plain. We use two methods to form performance metrics of GAMs: 1) We randomly select 100 windows with varied radius from 1 to 100 km. For each window size, we calculate the STDs of all data points within the window before and after applying the correction based on the selected GAMs. Then we calculate the average STD from 100 windows of the same size; 2) We randomly selected a thousand data points in the study region. Then a type of spatial structure function called semi-variogram is used to evaluate the performance of the GAMs. The semi-variogram allows us to calculate the semivariance of different length scales (starting from 0 km to the maximum distance with a step of 1 km). An advantage of the abovementioned methods is that they have taken the spatial scale into account.

Our results indicate significant tropospheric delay over the Kanto Plain region, with varying performance after applying the GAMs. On average, the results after correction show insignificant improvement at spatial scales less than 25 km. We find that correction based on the ERA5 model performs the best in the study area. Finally, we use the ERA5 model to obtain surface deformation, and the results show subsidence of

up to 14 mm/yr along the Sagami-Bay area and uplift of up to 10 mm/yr around Tokyo.

Key words InSAR; tropospheric delay; ERA5; the Kanto Plain

Category: Symposium 5: Global Geodetic Observing System (GGOS): the metrological basis for the monitoring of the System Earth => 5.7 : Advances in Geodesy for Geohazard Monitoring and Disaster Risk Reduction

726

S5-101

Landslide susceptibility assessment using Conv-LSTM model along the Sichuan-Tibet railway

Wubiao Huang、Mingtao Ding、Zhenhong Li、Jianqi Zhuang
Chang'an University

The Sichuan-Tibet railway crosses the most complicated region in the world in terms of landscape, topography and geology. Landslides are one of the most critical natural hazards in this area. Landslide susceptibility mapping is a useful tool for understanding the probability of the spatial distribution of future landslides. The aim of this study is to investigate a deep learning framework, namely convolutional long short-term memory network (Conv-LSTM), for landslide susceptibility mapping along the Sichuan-Tibet railway. Conv-LSTM performs convolution operations on each predisposing factor channel, and delivers the extracted features to a long short-term memory network (LSTM) architecture. The model not only extracts spatial features like convolutional neural network (CNN), but also explores the correlations between these features to prevent overfitting training data . The proposed Conv-LSTM outperforms three state-of-the-art landslide susceptibility mapping methods in terms of accuracy, F-measure and AUC values. Specifically, The AUC values of the proposed Conv-LSTM along the Sichuan-Tibet railway are greater than 0.86, indicating the Conv-LSTM is practical for landslide prevention and management.

Key words Landslide susceptibility mapping, Sichuan-Tibet railway, Convolutional long short-term memory network, Deep learning framework

Category: Symposium 5: Global Geodetic Observing System (GGOS): the metrological basis for the monitoring of the System Earth => 5.7 : Advances in Geodesy for Geohazard Monitoring and Disaster Risk Reduction

727

S5-102

Active geohazards along the Jinsha River Corridor revealed by Sentinel-1 SAR pixel offsets and InSAR observations

Chenglong Zhang^{1,2}, Zhenhong Li^{1,2}, Bo Chen¹, Jing Yang¹, Zhenjiang Liu¹

1. Chang'an University

2. Key Laboratory of Western China's Mineral Resources and Geological Engineering, Ministry of Education, Xi'an, China

Abstract: Geohazards including landslides and debris flows occur frequently in the Jinsha River corridor because of its complex geological settings, steep topography, and humid climate. They not only cause extensive damage to infrastructure including roads and bridges, but also pose serious threats to the property and lives of local residents; for instance, the two recent Baige landslides on October 11 and November 3 2018 formed barrier lakes, blocked the Jinsha River, and seriously threatened the safety of local residents and infrastructure on both sides of the Jinsha River. Hence, it is critical to detect active geohazards along the Jinsha River corridor. InSAR has been proven to be a powerful tool to map active geohazards. It should be noted that the strong topographic variations, dense vegetation and humid climate brings great challenges to the use of InSAR for geohazard detection. In addition, InSAR is incapable to detect large surface displacements with high spatial gradients, and the gradient of the surface displacements caused by geohazards can easily go beyond the maximum detectable deformation gradient of InSAR. In this study, we combined GACOS-assisted InSAR stacking with SAR Pixel Offset technique to detect active geohazards with a broad range of deformation gradients, and a total of 629 active geohazards were found in the Jinsha River corridor. Our analyses show that the active geohazards are mainly located at elevations of 2500-4000 m with slopes between and facing southwest and northwest. A high correlation between precipitation and surface displacement time series can be observed for a large number of active landslides and debris flows, suggesting that precipitation should be one critical driving factor. Spatial correlation analyses indicate that earthquakes and faults should be the controlling factors of the distribution of active geohazards in this region. It is believed that the research findings of this study should directly benefit to hazard mitigation and prevention in the Jinsha River corridor.

Key words Jinsha River; Sentinel-1; Geohazards; GACOS-assisted InSAR stacking; SAR Pixel Offset

Category: Symposium 5: Global Geodetic Observing System (GGOS): the metrological basis for the monitoring of the System Earth => 5.7 : Advances in Geodesy for Geohazard Monitoring and Disaster Risk Reduction

764

S5-103

Scientific infrastructure for monitoring of safety pillars in underground coal mines - Polish study case within EPOS-PL+ project

Jan Kapłon, Maya Ilieva, Krzysztof Sośnica, Grzegorz Jóźków, Kamila Pawłuszek-Filipiak, Kamil Kaźmierski, Przemysław Tymków, Paweł Bogusławski, Jan Sierny, Adrian Kaczmarek, Natalia Wielgocka, Krzysztof Stasch, Grzegorz Marut, Marcin Mikoś, Piotr Patynowski, Adam Pałęcki, Mateusz Drożdżewski
Wrocław University of Environmental and Life Sciences

The main goal of the European Plate Observing System (EPOS) is to bring together a variety of geoscience expertise and techniques aiming at a better understanding of geo-hazards and providing a higher focus on sustainable social prevention of crucial geodynamic phenomena. Within the boundary of these phenomena, the geo-hazard provoked by human mining activity takes his attention too. Poland is a relatively stable, from a geodynamic point of view, territory but is influenced by regional terrain changes and susceptible to ground deformations due to extensive underground mine excavations. On the other hand, the extraction of these resources substantially affect social welfare and the national economy. The Polish national EPOS-PL+ project targets building a multidisciplinary infrastructure over one of the most extensive coal deposits in Europe – the area of Silesia in Poland, whose aim is to monitor the advancement of the human-made geo-hazards and the consequences over the surface changes and social and mining infrastructures. The study case for this research is the Marcel Mine, located within the Upper Silesian Coal Basin (USCB), where the annual subsidence due to coal extraction may exceed 1.5m. USCB is also one of the most densely populated regions in Poland.

The project comprises measurements performed by different geo-techniques, terrestrial, aerial, and space-based, such as GNSS, InSAR, LiDAR, photogrammetry, gravimetry, leveling, and others. Our goal is to develop a concept and methodology for creating integrated products and sustainable solutions for the areas under risk, taking into account the advantages and disadvantages of each of the monitoring techniques. Moreover, based on a large amount of collected data and our expertise, we will propose an optimized methodology for surface deformation predictions using machine learning tools. The final products would support the local, regional and national economic decision-making programs.

Key words geo-hazards monitoring, Polish coal mines, GNSS, InSAR, LiDAR, photogrammetry, gravimetry

Category: Symposium 5: Global Geodetic Observing System (GGOS): the metrological basis for the monitoring of the System Earth => 5.7 : Advances in Geodesy for Geohazard Monitoring and Disaster Risk Reduction

779

S5-104

The new pilot system for Earthquake and Tsunami Risk Estimation by ionospheric sounding (ETREbis) at the IGP Caribbean observatories

Michela Ravanelli¹, Fabio Manta², Giovanni Occhipinti², Mattia Crespi¹

1. Sapienza University of Rome

2. Université de Paris, Institut de Physique du Globe de Paris

The aim of the ETREbis project is to contribute to the fully understanding of the physics and detectability of tsunami genesis by GNSS ionospheric monitoring and to support tsunami warning systems.

ETREbis leverages the Total Variometric Approach (TVA) methodology [1]. TVA is based on the joint application of VADASE (Variometric Approach for Displacements Analysis Standalone Engine) and VARION (Variometric Approach for Real-time Ionosphere Observation). Starting from the same variometric principle, the two algorithms allow for the simultaneous estimation of ground shaking, coseismic displacements and ionospheric total electron content (TEC) disturbances, using the same real-time GNSS data stream. Its feasibility was proven in the real-time scenario of the 2015 Illapel earthquake and tsunami. In particular, the high spatial resolution of the GNSS-TEC observations enables to map the earthquake source extent in real time, that represents the key point of tsunami genesis estimation.

Furthermore, TVA will be coupled with methodology presented in [2]: the ionospheric measurements of the acoustic-gravity wave at the epicenter (AGWepi, following [3]) by GNSS-TEC are able to discriminate, at 8 min, the tsunamigenic nature of tsunami events and to estimate the maximum volume of the displaced water.

The successful results are in the process of being applied at the IGP Observatoire Volcanologique et Sismologique de Guadeloupe in the Caribbean to create the first ETREbis pilot system using 36 real-time GNSS stations.

References

[1] Ravanelli et al., GNSS Total Variometric Approach: First Demonstration of a Tool for Real-Time Tsunami Genesis Estimation. Scientific reports, 11, 2021

[2] Manta et al., Rapid identification of tsunamigenic earthquakes using GNSS ionospheric sounding. Sci Rep 10, 2020

[3] Occhipinti et al., From Sumatra 2004 to Tohoku-Oki 2011: The systematic GPS detection of the ionospheric signature induced by tsunamigenic earthquakes, J. Geophys. Res. SpacePhysics, 2013

Key words GNSS, tsunami early warning systems, GNSS ionospheric sounding, tsunami genesis estimation

Category: Symposium 5: Global Geodetic Observing System (GGOS): the metrological basis for the monitoring of the System Earth => 5.7 : Advances in Geodesy for Geohazard Monitoring and Disaster Risk Reduction

782

S5-105

Analysis of the crustal deformation characteristics of Mount Everest and Tibetan region in the past 20 years

Yamin Dang¹、Chuanlu Cheng²、Guangwei Jiang²、Qiang Yang¹、Yangyang Sun²

1. Chinese Academy of Surveying and Mapping

2. Geodetic Data Processing Center of Ministry of Natural Resources

The Nepal earthquake (also known as the Gorkha earthquake) occurred on 25 April 2015, with a magnitude 8.1Ms, a major aftershock occurred on 12 May 2015 with a moment magnitude (Mw) of 7.3. The impact of these earthquakes on the elevation of Mount Everest has attracted the attention of many scholars. From 2019 to 2020, China and Nepal carried out joint surveys on Mount Everest and determined that the latest snow elevation of Mount Everest based on IHRS is 8848.886 meters. At the same time, China's Mount Everest survey team also carried out GNSS crustal deformation monitoring surveys over this area in 2020. More than 300 GNSS repetitive points data have been collected in this region since 1999, and all these data were reprocessed. Preliminary results show that, unlike Nepal Earthquakes in 1934, the 2015 Nepal earthquake did not have a significant impact on the elevation of Mount Everest. In addition, a comprehensive analysis of the crustal deformation of the Mount Everest and Tibetan areas in the past 20 years has been carried out.

Key words GNSS, earthquake, Mount Everest, crustal deformation

Category: Symposium 5: Global Geodetic Observing System (GGOS): the metrological basis for the monitoring of the System Earth => 5.7 : Advances in Geodesy for Geohazard Monitoring and Disaster Risk Reduction

793

S5-106

CyCLOPS: A National Integrated GNSS/InSAR Strategic Research Infrastructure for Monitoring Geohazards and Forming the Next Generation Datum of the Republic of Cyprus

Chris Danezis^{1,5}, Dimitris Kakoullis^{1,5}, Kyriaki Fotiou^{1,5}, Marina Pekri^{1,5}, Miltiadis Chatzinikos^{1,5}, Christopher Kotsakis², Ramon Brcic³, Michael Eineder³, George Melillos^{1,5}, Marios Nikolaidis^{1,5}, Georgios Ioannou^{1,5}, Andreas Christofe^{1,5}, Nicholas Kyriakides^{1,5}, Marios Tzouvaras^{1,5}, Sylvana Pilidou⁴, Kyriacos Themistocleous^{1,5}, Diofantos Hadjimitsis^{1,5}

1. Cyprus University of Technology
2. Aristotle University of Thessaloniki
3. German Aerospace Center
4. Geological Survey Department
5. ERATOSTHENES Centre of Excellence

The objective of this paper is to introduce CyCLOPS, a novel strategic research infrastructure unit, and present its current progress of implementation, and integration in the National geodetic, geophysical and geotechnical infrastructure of the government-controlled areas of the Republic of Cyprus. CyCLOPS is co-funded by the European Regional Development Fund and the Republic of Cyprus through the Research and Innovation Foundation under the grant agreement RIF/INFRASTRUCTURES/1216/0050. CyCLOPS is developed via the collaboration of the Cyprus University of Technology and the German Aerospace Center (DLR), and supported by the Cyprus Geological Survey Department and the Department of Lands and Surveys. The main objective of CyCLOPS is to establish an integrated infrastructure for space-based monitoring of geohazards using the most prominent earth observation technologies (EO), such as GNSS and InSAR. Furthermore, the infrastructure will densify and form the backbone for the definition of the next generation national datum of the Republic of Cyprus. Eleven Tier-1/2 state-of-the-art GNSS CORS, precise weather stations, tiltmeters and specifically designed InSAR triangular trihedral corner reflectors will be deployed, in a collocated fashion, at selected locations throughout the government-controlled areas of Cyprus. The collocated configuration will be established and installed to be compliant with the most stringent CORS monumentation specifications, support all current GNSS constellations and SAR missions. Finally, one of CyCLOPS' fundamental aims is to actively contribute to the on-going efforts and growing demand for more precise positioning services and high-quality modern reference frames, in conformity with the recommendations of the

UN-GGIM (and its Subcommittee of Geodesy) to establish and enhance national geodetic infrastructures to support the sustainable management of geospatial information on the changing Earth.

Key words GNSS, InSAR, Deformation Monitoring, Reference Frame, CORS, Corner Reflectors, Infrastructure, Cyprus

Category: Symposium 5: Global Geodetic Observing System (GGOS): the metrological basis for the monitoring of the System Earth => 5.7 : Advances in Geodesy for Geohazard Monitoring and Disaster Risk Reduction

800

S5-107

Identification of Potential Landslide in Ya'an-Linzhi Section of Sichuan-Tibet Railway Based on InSAR Technology

Jinmin Zhang, Wu Zhu
Chang'an University

The Ya'an-Linzhi section of Sichuan-Tibet Railway with a total length of 998.64 km is located in the eastern of the Qinghai-Tibet Plateau. Due to the complex geological conditions, the geological disasters including landslide, debris flow, collapse occurred frequently, which posed a huge challenge to the planning and construction of the Sichuan-Tibet Railway. Therefore, the early identification, monitoring, and research of the triggering factors and distribution of geological disasters in this area are of great significance to the construction of the Sichuan-Tibet Railway. Now, the Interferometric Synthetic Aperture Radar (InSAR) has been widely used in the early detection and monitoring of geological disasters due to its high precision, all weather and all day, but most of researchers are only aimed at typical landslides in sections of the railway for detection and monitoring, there are few studies on the identification and inventory of geological disasters along the whole line, especially using L-band SAR data which have a strong penetration ability of vegetation.

This article takes the Ya'an-Linzhi section of the Sichuan-Tibet Railway as the research area, and collects 164 scenes of ALOS/PALSAR-2 ascending SAR data covering the study area from September 2014 to May 2020, the InSAR and hot spot analysis technology have carried out the automatic identification, inventory, monitoring and distribution research of potential geological disasters. First of all, the errors in large-scale InSAR processing such as atmospheric errors, geometric distortions, unwrapping errors, DEM errors are discussed and corrected by pertinent methods to improve the accuracy of InSAR surface deformation. Then, the hot spot analysis technology is used to automatically and quickly identify deformation areas with spatial clustering properties based on the deformation rate obtained by InSAR, and combine them with optical remote sensing images, terrain and other data to analyze them to screen out potential landslide disasters and finally form the disaster inventory maps. Hot spot analysis can effectively eliminate error areas and extract more accurately out of the surface deformation area. Therefore, the problem of missed-judgment and misjudgment in the identification of disaster points has been solved. By using the method in this paper, a total of 548 potential landslide hazard

points along the Ya'an-Linzhi section of the railway are identified. The distribution law is analyzed by using the spatial analysis and statistical methods, it is found that there are more hidden danger points of landslides in the western than the eastern, and they occur frequently on the alpine, valleys, rivers and near the fault zone.

In this study, based on InSAR and hot spot analysis technology, a set of processing for large-scale rapid geological hazard identification is proposed and applied to large-scale landslide identification in Ya'an-Linzhi section of railway, based on the identification results, the distribution law of the disaster points is explored, which provides a reference for large-scale rapid and accurate landslide identification, and provides an important technical support for the planning and construction of the Sichuan-Tibet Railway.

Key words InSAR;Sichuan-Tibet Railway;hot spot analysis;landslide

Category: Symposium 5: Global Geodetic Observing System (GGOS): the metrological basis for the monitoring of the System Earth =» 5.7 : Advances in Geodesy for Geohazard Monitoring and Disaster Risk Reduction

813

S5-108

Monitoring Ground Deformation of Subway Area Using PS-InSAR in Suzhou

Lina Zhang¹、Jicang Wu²、Ruiqing Song²、Ming Yuan¹、Jinwei Qiu¹

1. Suzhou University of science and technology

2. Tongji University

As the artery of city, subway is one of the main transportation for urban residents. Therefore, the safe operation of the subway lines is very important. Because the regional subsidence can affect the safe operation of the subway, it is very important to monitor the surface and underground settlement of the area along the subway lines with high precision regularly. In order to analyze the ground subsidence of subway area in Suzhou, PS-InSAR method is used to extract the ground settlement information of subway area in Suzhou using 48 Sentinel images between 2016 and 2000, and obtain the subsidence rate map and spatial distribution of Line 1, 2, 3, 4, 5 and 6 in Suzhou. The settlement results extracted by InSAR show that the area is relatively stable, and the settlement rate is less than 5mm per year in most region in Suzhou. However, there are some small settlements near Fuyuan Road Station of Line 2 and Tongyuan Road South Station of Line 3. The ground settlement information is analyzed with the period of subway construction and the changes of new buildings on the ground. The results show that spatial distribution of the ground settlement along the subway lines is closely related to the subway construction period and the construction of new ground buildings.

Key words Ground deformation, PS-InSAR, Subway area, Suzhou

Category: Symposium 5: Global Geodetic Observing System (GGOS): the metrological basis for the monitoring of the System Earth => 5.7 : Advances in Geodesy for Geohazard Monitoring and Disaster Risk Reduction

835

S5-109

Numerical Simulation of Storm Surge in the Sea Near Long Island, New York Based on MIKE21

Chengcai Ren¹、Fanlin Yang^{2,3}、Zejie Tu²、Ruijie Shen²、Dianpeng Su²

1. College of Geodesy and Geomatics, Shandong University of Science and Technology

2. Shandong University of Science and Technology, School of Surveying, Mapping and Spatial Information

3. Key Laboratory of Ocean Geomatics, Ministry of Natural Resources of China

The hurricane landfall in coastal regions can cause abnormal fluctuation of the sea level, resulting in storm surge disaster. This paper have utilized the hurricane parameters provided by the IBTrACS(International Best Track Archive for Climate Stewardship) datasets and the MIKE 21Flow Model (FM) to simulate the water level changes caused by the hurricane "SANDY" when it hit Long Island. In addition, to better study the impact of different hurricane paths and levels, two sets of simulation experiments were designed. The former simulated the water level changes under four conditions by adjusting the movement path of the "SANDY" hurricane; The latter simulated the situation when the "KATRINA" (the largest hurricane in American history, level 5), directly landed on Long Island. The experimental results have shown that: (1) Among the four hurricane paths, the maximum increase in water level can reach 2.8 m, and the increase in water level caused by the hurricane that landed on the west side of Long Island was significantly higher than that landed on the east side. (2) When the "KATRINA" hurricane passed through the test area, the maximum increase in water level can reach 5.17 m. There is a certain water reduction process within a period time after the water level increase, and the maximum water level reduction was 1.48 m. The simulation experiments can provide scientific reference for storm surge floodplain research and making adaptation strategies for future extreme storm surges in Long Island.

Key words hurricane; Storm surge; MIKE 21 FM; numerical simulation

Category: Symposium 5: Global Geodetic Observing System (GGOS): the metrological basis for the monitoring of the System Earth => 5.7 : Advances in Geodesy for Geohazard Monitoring and Disaster Risk Reduction

842

S5-110

Multi-sensor geodetic approach to deformation monitoring

Ashutosh Tiwari, Avadh Bihari Narayan, Onkar Dikshit
Indian Institute of Technology Kanpur

Analysis of geodetic observations play an essential role in localization, quantification and monitoring of earth surface deformation, helping in better rescue, security and planning. For these observations, there are differences in surveying techniques, sensors and platforms, processing methodologies, parameters and associated uncertainty. The diversity brings challenges for comparison of deformation estimates derived from different sensors, but at the same time encourages synergistic application to deformation events which cannot be monitored using a single technique. The current study proposes a multi-sensor geodetic approach for deformation detection and monitoring, involving the use of terrestrial laser scanner (TLS), global navigation satellite systems (GNSS), multi-temporal interferometric synthetic aperture radar (MT-InSAR), total station (TS) and unmanned aerial vehicle (UAV). TLS, GNSS and TS are proposed for terrestrial geodetic surveys, while UAV and MT-InSAR can be used for aerial and space-based deformation monitoring respectively. The approach is demonstrated on a site affected by landslides, situated in Kaliyasaur, Uttarakhand, India. Future suggestions for the synergistic use of multiple geodetic sensors are also discussed.

Key words Deformation monitoring, multi-sensor approach, Geodetic surveying

Category: Symposium 5: Global Geodetic Observing System (GGOS): the metrological basis for the monitoring of the System Earth => 5.7 : Advances in Geodesy for Geohazard Monitoring and Disaster Risk Reduction

873

S5-111

Estimating 3D Mining Displacements from Multi-Track InSAR by Incorporating with a Prior Deformation Model

Zefa Yang、Jianjun Zhu、Zhiwei Li、Lixin Wu
Central South University

It is a common method to resolve three-dimensional (3D) deformation components associated with underground mining by incorporating Single-track interferometric synthetic aperture radar (InSAR) with a prior deformation model termed linear proportional model (LPM) (hereinafter referred to as Sin-LPM). Nevertheless, the Sin-LPM method relies on three model parameters that are needed to be in situ collected and neglects their dynamic changes during the period of underground extraction, narrowing the practical applications of the Sin-LPM method and degrading the accuracy of the estimated 3D displacements. In this paper we propose a new method to resolve 3D mining displacements from multi-track InSAR observations by incorporating with the LPM. In which, the model parameters of the LPM are firstly considered as dynamic and further adaptively estimated from the multi-track InSAR observations using a robust solver. Following that, 3D mining displacements are resolved from the multi-track InSAR using the conjugate gradient method. The proposed method were tested in Datong coalfield, China. The results suggest that the proposed method can well estimate 3D mining displacements with a mean error of about 1.8 cm. Compared with the previous Sin-LPM, the proposed method can effectively improve the accuracy of the estimated 3D displacements (e.g., 69% in this study), and can work well even over a large mining area where the model parameters are unknown. The proposed method offers a new insight to improve the InSAR-based retrieval of 3D displacements induced by other anthropologic or geophysical activities.

Key words InSAR; mining deformation; prior model; geohazards

Category: Symposium 5: Global Geodetic Observing System (GGOS): the metrological basis for the monitoring of the System Earth => 5.7 : Advances in Geodesy for Geohazard Monitoring and Disaster Risk Reduction

885

S5-112

Comparing Natural Hazards Assessment using Satellite Imagery Data and Geodetic Earth Observation Data

Thomas Chen

Academy for Mathematics, Science, and Engineering

Natural disasters ravage the world's cities, valleys, and shores on a monthly basis. Having precise and efficient mechanisms for assessing infrastructure damage is essential to channel resources and minimize the loss of life. Using a dataset that includes labeled pre- and post-disaster satellite imagery, the xBD dataset, we train multiple convolutional neural networks to assess building damage on a per-building basis. In order to investigate how to best classify building damage, we present a highly interpretable deep-learning methodology that seeks to explicitly convey the most useful information required to train an accurate classification model. We also delve into which loss functions best optimize these models. Our findings include that ordinal-cross entropy loss is the most optimal loss function to use and that including the type of disaster that caused the damage in combination with a pre- and post-disaster image best predicts the level of damage caused. The highest accuracy percentage on the testing set that we achieve is 74.6%; the non-optimal nature of this is largely attributed to the limited discernibility between the major and minor damage categories. We also make progress in the realm of qualitative representations of which parts of the images that the model is using to predict damage levels, through gradient class-activation maps. Furthermore, we harness geodetic data to monitor surface deformations. We compare the results, based on accuracy of prediction, of these two methodologies, and find that the deep learning-informed satellite imagery-based approach achieves better results. Our research seeks to computationally contribute to aiding in this ongoing and growing humanitarian crisis, heightened by climate change. Specifically, it advances more interpretable machine learning models, which were lacking in previous literature.

Key words earth observation, machine learning, deep learning, computer vision, intercomparison

Symposium 6: ICC symposium

S6.1: ICCT Geodetic Theory

Category: Symposium 6: ICC symposium => 6.1: ICCT Geodetic Theory

61

S6-001

A CFD-based gravitational field modeling method and its potential applications in deep space exploration

Zhi Yin¹, Nico Sneeuw²

1. Jiangsu Ocean University

2. Institute of Geodesy, University of Stuttgart

Existing gravitational field determination methods such as the spherical harmonic inversion method can accurately solve the gravitational fields generated by sphere-like mass bodies. However, the gravitational field solution of a complex-shaped mass body developed slowly in the past half century, encountering the divergence problem when solving the Complex-Boundary Value Problems (CBVPs), which is considered as a challenging open problem in geodesy.

Computational Fluid Dynamics (CFD) is the analysis of systems involving fluid flow, heat transfer and associated phenomena by means of computer-based simulation. With specific constraints, a general flow can be simplified into various flows, among which the potential flow is an idealized one with a Laplacian (i.e., source-free and curl-free) velocity field. Therefore, the potential flow velocity field and the gravitational vector field are equivalent in the sense that both are Laplacian vector fields. With this equivalence, we proposed a new method to solve the CBVPs with the potential flow theory as well as CFD techniques.

We apply the CFD-based approach to determining the gravitational field of Comet 67P/Churyumov-Gerasimenko which has an irregular shape like a “rubber duck”. The gravitational field solution is derived with the commercial CFD software ANSYS/FLUENT, and the result is visualized with a vector field and a plumb line distribution, respectively. The method is validated in a closed loop simulation by comparing the CFD solution with the Newton integration. It shows a good consistency between them, with a relative magnitude discrepancy at percentage level and with a small directional difference root-mean-square (RMS) value of 0.78° . Due to the satisfying performance of the CFD-based approach on solving the CBVPs, we have a good outlook on its potential applications in deep space exploration, such as designing a probe’s orbits, determining an asteroid height system and modeling a gravitational field of multi-bodies.

Key words Geodetic Boundary Value Problem; Gravitational field; Irregular shape; Comet 67P/Churyumov-Gerasimenko; CFD

Category: Symposium 6: ICC symposium => 6.1: ICCT Geodetic Theory

171

S6-002

The general rule of potential field parameters especially for Laplace's equation

Xiao-Le Deng¹、Wen-Bin Shen^{2,4}、Meng Yang³、Jiangjun Ran^{1,5}

1. Department of Earth and Space Sciences, Southern University of Science and Technology, Shenzhen, 518055, China (ranjj@sustech.edu.cn; dengxl@sustech.edu.cn)
2. School of Geodesy and Geomatics, Wuhan University, Wuhan, 430079, China (wbshen@sgg.whu.edu.cn)
3. School of Geospatial Engineering and Science, Sun Yat-Sen University, Zhuhai, 519082, China (yangmeng5@mail.sysu.edu.cn)
4. State Key Laboratory of Information Engineering in Surveying, Mapping and Remote Sensing, Wuhan University, Wuhan, 430079, China
5. Shenzhen Key Laboratory of Deep Offshore Oil and Gas Exploration Technology, Southern University of Science and Technology, Shenzhen, 518055, China

Laplace's equation, being a second-order partial differential equation, means that the sum of second-order partial derivatives of a function with respect to the three directions of the chosen coordinate system equals zero. It forms the basis for the theory of harmonic functions and potential theory widely used in geosciences, i.e., gravitational, electrostatic, and magnetic fields. In this contribution, the general rule of the potential field parameters including the number of defining components and Laplace's equation is provided when the potential field parameters are expanded from the potential up to its m -order tensor ($m \geq 0$). It is interesting that the number of Laplace's equation follows the rule known in combinatorics as a triangular number sequence, which is also observed for the number of defining gradients. Moreover, Laplace's equation of the 5th-order tensor is provided in detail. This contribution can serve as a general reference for properties of the potential field parameters in any scientific or engineering area where potential fields are applied.

Key words Laplace's equation, Potential field, Gravitational field

Category: Symposium 6: ICC symposium =» 6.1: ICCT Geodetic Theory

179

S6-003

An quality assessment of the official GOCE Level 2 GRD SPW 2 products over Norway, Czechia, and Slovakia

Martin Pitonak¹、 Michal Sprlak¹、 Vegard Ophaug²、 Ove C. D. Omang³、 Pavel Novak¹

1. NTIS – New Technologies for the Information Society, Faculty of Applied Sciences, University of West Bohemia

2. Faculty of Science and Technology (RealTek), Norwegian University of Life Sciences

3. Norwegian Mapping Authority

The launch of gravity field dedicated satellite missions at the beginning of the new millennium led to improvement of global gravity field models accuracy. One of this mission was the Gravity field and steady-state Ocean Circulation Explorer (GOCE) which was launched more than ten years ago. As the first Explorer, the satellite carried a novel instrument, gradiometer, which allowed to measure the second-order directional derivatives of the gravitational potential (or gravitational gradients) with uniform quality and a near-global coverage. The mission goal was to determine the static Earth gravity field with ambitious precision of 1-2 cm in terms of geoid heights and 1 mGal in terms of gravity anomalies for the spatial resolutions of 100 km. More than three years of the outstanding measurements resulted in two levels of data products (Level 1b and Level 2), six releases of global gravitational models (GGMs), and several grids of gravitational gradients (see, e.g., ESA-funded GOCE+ GeoExplore project or Space-wise GOCE products). The grids of gravitational gradients represent a step between gravitational gradients measured directly along the GOCE orbit and data directly from GGMs. The last named product found its usage mainly in geophysical applications.

In this contribution, we are going to validate the official Level 2 product GRD_SPW_2 by terrestrial gravity disturbances over two test areas located in Europe, namely in Norway and former Czechoslovakia (now Czechia and Slovakia). GRD_SPW_2 product contains all six gravity gradients at satellite altitude from the space-wise approach computed only from GOCE data for the available time spans correspond to release 2, 4, 5 and 6, and are provided on a 0.2 degree grid. A mathematical model based on the least-squares spectral weighting will be employed and the corresponding spectral weights will be presented for the validation of gravitational gradients grids. This method allows as to continue downward gravitational gradients grids to an irregular topographic surface (not to a mean sphere) and transform them to

gravity disturbances in one step. Prior the comparison, we removed systematic effects such as a tide system conversion or an ellipsoidal correction. Further, we estimated the high-frequency part of gravitational signal called as the omission error and subtracted it from terrestrial data because in gravitational gradients measured at GOCE satellite altitude is attenuated. To do so we employ EGM2008 up to d/o 2160 and the omission error has been a) synthesised from dV_ELL_Earth2014_5480_plusGRS80, b) interpolated from ERTM2160 gravity model, c) calculated from a residual topographic model by forward modelling in the space domain.

Key words Downward continuation, GOCE, GRD_SPW_2 validation, spectral combination method

Category: Symposium 6: ICC symposium => 6.1: ICCT Geodetic Theory

263

S6-004

Inclusion of data uncertainty in machine learning and its application in geodetic data science

Mostafa Kiani Shahvandi, Benedikt Soja
Institute of Geodesy and Photogrammetry, ETH Zurich

Data uncertainty plays an important role in the field of geodesy. We propose to include the uncertainty of data in deep neural network architectures to achieve better generalization, even in small data sets. Inspired by weighted and total least squares, we formulate the problem for both input and target uncertainties, and combine it with the Bayesian learning method. This results in a new form of the loss function in machine learning. Additionally, we consider the error propagation by using data uncertainty as features. As benchmark, we use models without the consideration of data uncertainty. The choice of the model is arbitrary. However, in this study the benchmark model is a single-layer LSTM neural network, which can represent and predict sequential data. We use input uncertainties either as auxiliary features or in a total least squares manner, and output uncertainties as weights in the L2 classical loss function.

To show the efficacy of the proposed method, we use real data of Earth Orientation Parameters (EOP) and various GNSS station position time series across the globe. Prediction of EOP is important for many applications such as spacecraft navigation. For the two polar motion components, dUT1, and GNSS station position time series, we demonstrate that the least-squares-inspired method can outperform both the benchmark (by 45%, 52%, 1%, and 8%, respectively) and the feature-inspired method (65%, 55%, 77%, and 6%). In the case of the LOD time series, the feature-inspired method shows a better performance by 10% and 39% with regard to the benchmark and the least-squares-inspired method, respectively.

Key words Data uncertainty, machine learning, geodetic data science, EOP and GNSS time series

Category: Symposium 6: ICC symposium => 6.1: ICCT Geodetic Theory

275

S6-005

Adaptive Quasi-Monte Carlo Algorithm for Covariance Propagation of GNSS Baseline Vector

Xinlei Luo、Leyang Wang
East China University of Technology

The combined adjustment of GNSS baseline vector network and ground control network has the wide applications in practice. In order to facilitate the subsequent combined adjustment in the two-dimensional network, the stochastic information of the GNSS baselines are usually transferred to the Gaussian plane coordinate system. However, there is a complex nonlinear relationship between the three-dimensional Cartesian coordinate and the Gaussian plane coordinate. The Taylor series expansion based on derivative calculation loses the accuracy of higher-order terms when obtaining stochastic information, and cannot meet the requirements for the adjustment with higher accuracy. The Monte Carlo method based on approximate probability distribution has high simulated burden and low convergence effectiveness. To overcome these disadvantages, we introduce the Quasi-Monte Carlo (QMC) method, and design the implementation procedure of the QMC method for covariance propagation with independent and correlated observations. Considering that the simulation number of QMC method generally is chosen subjectively and its result also cannot be controlled directly, a new QMC algorithm to adaptive determination of simulated number is proposed, namely, Adaptive Quasi-Monte Carlo (AQMC). This approach not only achieves the same estimation accuracy as the QMC method, but also improves the computational efficiency by about 97%. The proposed approach has practical value for the accuracy evaluation of other nonlinear models in GNSS data processing.

Key words GNSS baseline vector; Nonlinear function; Adaptive Quasi-Monte Carlo; Covariance propagation

Category: Symposium 6: ICC symposium => 6.1: ICCT Geodetic Theory

276

S6-006

Crustal density and forward global gravitational field model on the Moon determined from GRAIL and LOLA satellite data

Michal Šprlák¹、Shin-Chan Han²、Will Featherstone³

1. NTIS - New Technologies for the Information Society, Faculty of Applied Sciences, University of West Bohemia, Technická 8, 306 14 Plzeň, Czech Republic
2. School of Engineering, Faculty of Engineering and Built Environment, University of Newcastle, University Drive, Callaghan, NSW 2308, Australia
3. School of Earth and Planetary Sciences, Curtin University of Technology, GPO Box U1987, Perth, WA 6845, Australia

We employ Newton's integral in the spectral domain to solve two geodetic/geophysical tasks for the Moon. Firstly, we determine 3D bulk density distribution within the lunar crust (inverse problem). For this purpose, we develop a linear mathematical model that parameterises the laterally variable density component by surface spherical harmonics. We exploit GL1500E GRAIL gravitational field model and LOLA topography model to determine bulk density estimates for three different cases: 1) constant, 2) laterally variable, and 3) 3D spatially variable (assuming a linear change in the radial direction). Secondly, we calculate lunar gravitational field models inferred by these three crustal compositions (forward problem) up to spherical harmonic degree 2519 corresponding to a spatial resolution of approximately 2.2 km at the lunar equator. Efficacy of these models is assessed with respect to the GRAIL Level 2 gravitational field models. Our spatially variable crustal model represents the best fit globally and also locally in highland areas. We also test the performance of GRAIL models, recent and independent forward models, and our new models against Level 1B GRAIL satellite-to-satellite tracking data focusing on evaluation beyond Level 2 data (i.e., spherical harmonic degrees greater than 650). These medium- and high-frequency signals from our models correlate with the Level 1B observations the best among all global gravitational field models tested. Our high resolution geopotential model with the optimized 3D crustal density variation should be an asset to future lunar lander navigation and geophysical exploration.

Key words Newton's integral, Forward modelling, LOLA, GRAIL

Category: Symposium 6: ICC symposium => 6.1: ICCT Geodetic Theory

314

S6-007

A new robust estimation algorithm for the superstrong breakdown point based on Quasi-Accurate Detection

Hailu Chen¹、Wei Qu^{1,2}、Qin Zhang¹、Yuan Gao¹、Shichuan Liang¹

1. College of Geology Engineering and Geomatics, Chang'an University

2. State Key Laboratory of Geohazard Prevention and Geoenvironment Protection, Chengdu University of Technology

Because of the environmental interference, local crustal activities, or strong seismic activities, Global Navigation Satellite System (GNSS) velocity fields generally contain outliers, which can affect the parameter estimation of the crustal deformation model significantly. The robust M estimation can be used to improve the accuracy of the parameter estimation while retaining as much GNSS observation as possible. The breakdown point of parameter estimation the robust estimation is less than 50% due to use the least-squares residuals as the initial values of the equivalent weight function. First, a new automatic selection strategy is proposed for quasi-accurate observations using quasi-accurate detection (QUAD), and the outliers are roughly identified. Second, the variance of the unit weight of the real error of quasi-accurate errors is used as the initial variance factor and the real error of quasi-accurate errors is used as the initial value for calculation of the robust M estimation to identify and detect large, medium, and small outliers accurately. We evaluate the rigorousness of the least-squares estimation, conventional robust estimation, median method, and new algorithm from four perspectives using simulated GNSS velocity fields, i.e., model parameter estimation, variance factor, distribution of the observation weights, and accuracy of forward deformation fields. The new algorithm eliminates outliers and estimates the model parameters effectively. The robustness of the new algorithm is better than that of the other three when outliers are below 50%. When the proportion of outliers is higher than 50% (60%, 70%, and 80%), the other three algorithms break down, while the new algorithm yields better parameter estimates with a superstrong breakdown point.

Key words Robust M estimation; breakdown point; QUAD; Variance; 2-norm; GNSS crustal deformation model

Category: Symposium 6: ICC symposium => 6.1: ICCT Geodetic Theory

346

S6-008

On determination of the geoid from measured gradients of the Earth's gravity field potential

Pavel Novak, Michal Šprlák, Martin Pitoňák
University of West Bohemia

The geoid is an equipotential surface of the static Earth's gravity field which plays a fundamental role in definition of physical heights related to the mean sea level (orthometric heights) in geodesy and represents a reference surface in many geoscientific studies. Its determination with the cm-level accuracy or better, in particular over dry land, belongs to major tasks of modern geodesy. Traditional data and underlined theory have significantly be affected in recent years by advances in observation techniques. This study reviews new data types represented by gradients of the disturbing gravity potential, both currently available and foreseen, and systematically discusses mathematical models for geoid determination based on the gradient data which are considered data measurable, e.g., by differential accelerometry. Particular mathematical models are based on solutions to boundary-value problems of the potential theory and include both integral transforms and integral equations.

Key words Boundary-value problems; Earth's gravity field; geoid; gravity gradients

Category: Symposium 6: ICC symposium => 6.1: ICCT Geodetic Theory

348

S6-009

Tensor calculus and functional analysis in the iteration solution of the geodetic boundary value problem

Petr Holota¹, Otakar Nesvadba²

1. Research Institute of Geodesy, Topography and Cartography

2. Land Survey Office

An alternative between the boundary complexity and the complexity of the coefficients of the partial differential equation governing the solution is discussed in treating the geodetic boundary value problem. The Laplace operator has a relatively simple structure in terms of spherical or ellipsoidal coordinates frequently used in geodesy. However, the physical surface of the Earth substantially differs from a sphere or an oblate ellipsoid of revolution, even if optimally fitted. The same holds true for the solution domain and the exterior of a sphere or of an oblate ellipsoid of revolution. The situation is more convenient in a system of general curvilinear coordinates such that the physical surface of the Earth (smoothed to a certain degree) is imbedded in the family of coordinate surfaces. Therefore, a transformation of coordinates is applied in treating the geodetic boundary value problem. The idea is generally close to concepts followed also in other branches of engineering and mathematical physics. In our case tensor calculus is used and the Laplace operator is expressed in the new coordinates. Clearly, its structure is more complicated now. In a sense it represents the topography of the physical surface of the Earth. For this reason the Green's function method is used together with the method of successive approximations in the solution of the geodetic boundary value problem expressed in terms of the new coordinates. The structure of iteration steps is analyzed and if possible, it is modified by means of integration by parts. Subsequently, the iteration steps and their convergence are discussed and interpreted, numerically as well as in terms of functional analysis.

Key words Boundary value problems, partial differential operators, Laplace's operator, solution domain, transformation of spatial coordinates, Green's function method, successive approximations

Category: Symposium 6: ICC symposium => 6.1: ICCT Geodetic Theory

387

S6-010

Bayesian modelling of discontinuities and piecewise trends (trend changes) improves coastal vertical land motion estimates

Julius Oelsmann, Marcello Passaro, Laura Sanchez, Denise Dettmering,
Christian Schwatke, Florian Seitz
Deutsches Geodätisches Forschungsinstitut; Technische Universität München
(DGFI-TUM)

One of the major error sources affecting vertical land motion (VLM) estimations are nonlinearities, such as discontinuities or changing velocities over differing periods. Here, we present a novel Bayesian approach to automatically and simultaneously detect such events, together with the commonly estimated motion signatures in coastal Global Navigation Satellite System (GNSS) data. Next to GNSS observations, for the first time, we directly estimate discontinuities and piecewise VLM derived from altimetry and tide-gauge differences (SATTG). We show that, compared to estimating a single linear trend, accounting for time series discontinuities and trend changes significantly increases the agreement of SATTG with GNSS estimates by 0.44 mm/year at 387 globally distributed station pairs.

The Bayesian change point detection is applied to 606 SATTG and 457 GNSS time series. Observed VLM, which is identified as linear (i.e. is not affected by discontinuities), has a substantially higher consistency with large scale VLM effects of Glacial Isostatic Adjustment (GIA) and contemporary mass redistribution (CMR). The standard deviation of SATTG (and GNSS) trend differences with respect to GIA+CMR trends is by 38% (and 51%) lower for VLM which is categorized as linear compared to VLM, in which discontinuities or trend changes are detected. Given that in more than a third of the SATTG time series nonlinearities are detected, the results underpin the importance to account for such features, in particular to avoid extrapolation biases of coastal VLM and its influence on relative sea level change. The Bayesian approach uncovers the potential for a better characterization of SATTG VLM changes on much longer periods than for GNSS observations and is widely applicable to geophysical time series.

Key words Bayesian modelling, discontinuity detection, GNSS time series, vertical land motion, satellite altimetry, tide gauges, trend changes

Category: Symposium 6: ICC symposium => 6.1: ICCT Geodetic Theory

517

S6-011

Sensitivity of GNSS orbits to General Relativistic effects

Krzysztof Sośnica¹, Grzegorz Bury¹, Radosław Zajdel¹, Javier Ventura-Traveset²,
Luis Mendes³

1. Wrocław University of Environmental and Life Sciences

2. European Space Agency, Galileo Navigation Science Office

3. European Space Agency, RHEA Group, Galileo Navigation Science Office, ESAC

Three main orbital effects emerging from general relativity are considered in the International Earth Rotation and Reference Systems Service (IERS) Conventions 2010: the Schwarzschild effect, Lense-Thirring effect, and De Sitter effect, also known as geodetic precession. In this contribution, we study the sensitivity of GNSS orbits to the general relativistic effects, focusing on those effects which can be detected using the current accuracy of GNSS precise orbit determination techniques. We derive theoretic effects using the Gaussian first-order perturbation equations and celestial mechanics for Keplerian elements of GPS, GLONASS, and Galileo satellites. We compare the theoretical effects with the effects derived from the processing of GNSS observations collected by a global network of multi-GNSS stations. Finally, we derive the post-Newtonian parameters characterizing the degree of spacetime curvature and non-linearity of the gravitational field using GNSS orbit perturbations separately for GPS, GLONASS, Galileo, and Galileo satellites in eccentric orbits, as well as for the combined multi-GNSS constellation.

Key words GNSS, Galileo, Schwarzschild, Lense-Thirring, De Sitter, geodetic precession, orbit perturbations

Category: Symposium 6: ICC symposium => 6.1: ICCT Geodetic Theory

704

S6-012

Impact of accelerometers calibration and empirical forces modelling on GRACE precise orbit determination

Thomas Papanikolaou¹, Dimitrios Tsoulis²

1. Aalborg University

2. Aristotle University of Thessaloniki

Precise orbit determination is a major objective in satellite geodesy and data analysis of several geoscientific satellite missions. In the case of satellite gravity missions such as the Gravity Recovery And Climate Experiment (GRACE) mission, the orbit precision requirement is very high (cm level) in order to capture the gravity field modelling of static and time-variable components. GRACE satellites are equipped with on-board accelerometers that form a key observation instrument for the measurement of non-gravitational perturbations at orbital altitude. The accelerometers calibration through a data processing scheme is essential for GRACE applications such as precise orbit determination, gravity field mapping and non-gravitational forces modelling e.g. atmospheric drag and thermosphere models. In the present study, we focus on the estimation of the GRACE accelerometers calibration parameters within an orbit determination approach. We apply an adapted dynamic orbit determination algorithm with extended variational equations. The orbit parameter estimation considers a few deterministic parameters referring to the overall orbit arc length. Such a pure dynamic orbit estimation aims at avoiding absorbing part of the gravity signal within the orbit modelling. In particular, we examine the estimation of accelerometry calibration parameters such as bias and scale factors in combination with empirical forces of cycle-per-revolution (CPR) terms. Empirical accelerations of CPR perturbations aim at capturing periodic mismodelling effects. The applied approach leads to orbital residuals varying within a few cm in the orbital frame while the inter-satellite KBR range-rate data residuals vary within a few $\mu\text{m}/\text{sec}$.

Key words Precise Orbit Determination; Satellite Geodesy; GRACE; Accelerometer calibration; KBR

Symposium 6: ICC symposium

S6.2: ICCG Geodesy for Climate Research

Category: Symposium 6: ICC symposium => 6.2: ICCG Geodesy for Climate Research

68

S6-013

Determination of the velocity field of the African plate from GNSS

Saturday Ehisemhen Usifoh^{1,3,5}, Benjamin Männel³, Pierre Sakic³, Joseph Dodo⁵, Harald Schuh^{2,4}

1. Technical University of Berlin
2. Technical University of Berlin, Germany
3. German Research Center for Geosciences GFZ, Potsdam
4. German Research Center for Geosciences GFZ, Potsdam, Germany
5. Centre for Geodesy and Geodynamics, Toro, Bauchi State, Nigeria

The African Plate is considered as one of the large tectonic plates that make up of sizeable parts of the Earth's crust. It includes not only the Africa continent, but also vast portion of the Atlantic and Indian Oceans. The African Plate includes the Nubia and the Somali plates. The Somalia Plate begins rifting from the African Plate along the East African Rift. The Eastern rift systems of Africa terminate in the north where it meets the Red Sea and Gulf of Aden at the Afar Triple junction. The East African Rift system reaching from the Afar in the northern Ethiopia to Mozambique in the south shows spreading rates of up to 5 mm/yr. This study investigates and provides continent-wide positioning and velocity solution for Africa using continuous GNSS measurements. Twenty years of GNSS data (2000-2020) were analyzed in Precise point processing (PPP) mode with a minimum of three years of continuous observations, using GFZ's EPOS.P8 software. The resulting velocities field of the horizontal and vertical motion at nearly 130 GNSS stations describes the linear velocities and seasonal signals. It thereby provides information consistent with the GNSS velocities that will be used to assess the level of rigidity of stability and estimate the angular rotation vectors that will describe the motion of a stable Nubia, Somalia and its micro-plates, most especially the East African Rifting system.

Key words African plate, Velocity field, GNSS, Precise point processing

Category: Symposium 6: ICC symposium => 6.2: ICCG Geodesy for Climate Research

274

S6-014

Recovering Climate-Related Mass Transport Signals by current and next-generation gravity missions

Marius Schlaak¹、Roland Pail¹、Henryk Dobslaw²、Annette Eicker³、Laura Jensen³

1. Chair of Astronomical and Physical Geodesy, Technical University of Munich (TUM)

2. German Research Centre for Geosciences (GFZ), Potsdam, Germany

3. HafenCity University Hamburg, Hamburg, Germany

Gravity field missions are a unique geodetic measuring system to directly observe mass transport processes in the Earth system. Past and current gravity missions such as CHAMP, GRACE, GOCE and GRACE-FO have improved our understanding of large-scale mass changes, such as the global water cycle, melting of continental ice sheets and mountain glaciers, changes in ocean mass that are closely related to the mass-related component of sea level rise, which are subtle indicators of climate change, on global to regional scale. Therefore, mass transport observations are also very valuable for long-term climate applications. Next Generation Gravity Missions (NGGMs) expected to be launched in the midterm future have set high anticipations for an enhanced monitoring of mass transport in the Earth system with significantly improved spatial and temporal resolution and accuracy. According to the Global Climate Observing System (GCOS), time series of minimum 30 years are needed to decouple natural and anthropogenic forcing mechanisms. This contribution will present results from numerical satellite mission performance simulations designed to evaluate the usefulness of gravity field missions operating over several decades for climate-related applications.

The study is based on modelled mass transport time series obtained from future climate projections until the year 2100 following the representative emission pathway RCP8.5. Numerical closed-loop long-term simulations will assess the recoverability of mass variability signals by means of different NGGM concepts, e.g. GRACE-type in-line single-pair missions, and Bender double-pair mission, assuming realistic noise levels for the key payload. In the evaluation and interpretation of the results, special emphasis shall be given to the identification of (natural or anthropogenic) climate change signals in dependence of the length of the measurement time series, and the quantification of robustness of derived trends and systematic changes.

Key words Mass Transport, Numerical Simulation, Total Water Storage, Next Generation Gravity Mission, NGGM, Climate Projections

Category: Symposium 6: ICC symposium => 6.2: ICCG Geodesy for Climate Research

302

S6-015

The initial process of post-fire ground deformation in Northeastern Siberian permafrost areas detected by L-band and C-band InSAR

Kazuki Yanagiya¹、Masato Furuya²、Go Iwahana^{3,5}、Petr Danilov⁴

1. Hokkaido University

2. Faculty of Science, Hokkaido University

3. Arctic Research Center, Hokkaido University

4. Institute of Northern Applied Ecology, North-Eastern Federal University in Yakutsk

5. International Arctic Research Center, University of Alaska Fairbanks

Wildfire is one of the causes to accelerate permafrost thawing. Once the vegetation layer, which acts as a heat insulator, burned away, the maximum seasonal thaw depth increases, and segregated ice lenses in the transient layer start to melt. Subsequent permafrost thawing causes ground deformation such as thermokarst and slope failure called active layer detachment slide. ECMWF reported the fire intensity and area increased in 2019-20 in North-Eastern Siberia. We focused on the recent fire areas around the Batagay village and analyzed ground deformation by InSAR using two types of SAR data: C-band Sentinel-1 and L-band ALOS2.

The stacked Sentinel-1 InSAR images revealed the initiation process of post-fire ground deformation. In the study area, the winter InSAR pairs are highly coherent. This is because the snow is probably dry, and the microwave could easily penetrate the snow layer. In the first winter after the fire, InSAR images detected the seasonal uplift signals up to 6cm, and the signals finished by early November. Following the fire year, the uplift signals had continued until early December, and the amplitude became a little larger than the first winter. We discussed temporal changes in ground deformation from the first winter to two years later with one-year ALOS2 SM3 InSAR images and thaw depth data. Notably, ALOS2 winter pairs, including even fire periods, were relatively coherent, which has never been reported previously.

High-resolution ALOS2 SM1 InSAR image revealed spatial patterns of the seasonal uplift signal. InSAR image detected uplift signals up to 9cm in the 2020 winter, and the spatial pattern of the signals correlated with gullies that flows to the northeast. The broad range uplift signal was detected between the gullies. Along the gullies, the nearly zero uplift signal was detected on the flank, but the spiky uplift was detected at the bottom. Relatively high soil moisture in the bottom of the valley attributes to this deformation pattern.

Key words InSAR, Permafrost, Wildfire, Sentienl-1, ALOS2, Thermokarst, Frost heave

Category: Symposium 6: ICC symposium => 6.2: ICC Geodesy for Climate Research

330

S6-016

Quantifying barystatic sea-level change from satellite altimetry, GRACE and Argo observations

Hadi Amin¹, Mohammad Bagherbandi^{1,2}, Lars Sjöberg^{2,1}

1. University of Gävle

2. KTH Royal Institute of Technology

Time-varying spherical harmonic coefficients determined from the Gravity Recovery and Climate Experiment (GRACE) data provide a valuable source of information about the water mass exchange that is the main contributor to the Earth's gravity field changes within a period of less than several hundred years. Moreover, by measuring seawater temperature and salinity at different layers of ocean depth, Argo floats help to measure the steric component of global mean sea level (GMSL). In this study, we quantify the rate of barystatic sea-level change using GRACE monthly gravity field models and compare the results with estimates achieved from a GMSL budget closure approach. Our satellite altimetry-based results show a trend of $3.90 \pm 0.14 \text{ mm yr}^{-1}$ for the GMSL rise. About 35% or $1.29 \pm 0.07 \text{ mm yr}^{-1}$ of this rate is caused by the thermosteric contribution, while the remainder is mainly due to the barystatic contribution. Our results confirm that the choice of decorrelation filters does not play a significant role in quantifying the global barystatic sea-level change, and spatial filtering may not be needed. GRACE RL06 solutions result in the barystatic sea-level change trends of $2.25 \pm 0.16 \text{ mm yr}^{-1}$. Accordingly, the residual trend, defined as the difference between the altimetry-derived GMSL and the sum of the steric and barystatic components, amounts to $0.45 \pm 0.44 \text{ mm yr}^{-1}$. The exclusion of the halosteric component results in a lower residual trend of about $0.36 \pm 0.46 \text{ mm yr}^{-1}$ over the same period, which suggests a sea-level budget closed within the uncertainty. This could be a confirmation of a high level of salinity bias particularly after about 2015. Moreover, considering the assumption that the GRACE-based barystatic component includes all mass change signals, the rather large residual trend could be attributed to an additional contribution from the deep ocean, where salinity and temperature cannot be monitored by the current observing systems. The errors from various sources, including the model-based Glacial Isostatic Adjustment signal, independent estimation of geocenter motion that is not quantified in the GRACE solutions, as well as the uncertainty of the second degree of zonal spherical harmonic coefficients, are other possible contributors to the residual trend.

Key words Climate change; Sea-level budget; Decorrelation; Barystatic sea-level change; Steric sea-level change

Category: Symposium 6: ICC symposium => 6.2: ICC Geodesy for Climate Research

366

S6-017

Assessments of integrated water vapor from atmospheric reanalyses against ground-based GPS over Europe

Peng Yuan¹、Roeland Van Malderen²、Xungang Yin³、Hannes Vogelmann⁴、
Joseph Awange⁵、Hansjörg Kutterer⁶

1. Karlsruhe Institute of Technology, Geodetic Institute, Karlsruhe, Germany

2. Royal Meteorological Institute of Belgium, Brussels, Belgium

3. Riverside Technology Inc, Asheville, North Carolina, USA

4. Karlsruhe Institute of Technology, IMK-IFU, Garmisch-Partenkirchen, Germany

5. Curtin University, School of Earth and Planetary Sciences, Perth, Australia

6. Karlsruhe Institute of Technology (KIT)

Water vapor is a crucial component in the Earth's atmosphere. As the medium of moisture and latent heat, the seasonal variation of water vapor is an important process in water cycle. The abnormal spatial-temporal variations of water vapor can trigger extreme weather (e.g., cyclones) and climate (e.g., droughts) events. Moreover, water vapor plays a key role in climate change as it is the most abundant greenhouse gas and characterized with the well-known positive feedback effect. Therefore, quantification of water vapor is important for meteorological and climatic research. Nowadays, various atmospheric reanalyses have been utilized for the estimation of integrated water vapor. However, comprehensive assessments of their integrated water vapor (IWV) products are still quite few. Ground-based GNSS technique is a unique tool for IWV monitoring and its IWV estimation has been adopted as a reference for the assessments of reanalyses. Moreover, GNSS observations have been accumulated for more than two decades and they are reaching the "maturity age" of 30 years for climate research. In this study, we assessed the IWV products derived from six atmospheric reanalyses, including the latest fifth generation global reanalysis ERA5 and its predecessor ERA-interim from ECMWF, MERRA2 provided by NASA's Global Modeling and Assimilation Office (GAMO), the CFSR from NOAA's National Centers for Environmental Prediction (NCEP), the NCEP-DOE Reanalysis 2 from the NCEP and the Department of Energy (DOE), and the JRA55 from Japan Meteorological Agency (JMA). The reanalyses' IWV estimates were compared with more than 100 GPS stations over Europe during 1994-2018 with the longest period of 25 years. Their agreements in daily time series, diurnal cycle and diurnal variability, annual climatology and inter-annual variability, and trends were assessed.

Key words Water Vapor, GNSS, Reanalysis, ERA5, Model assessment

Category: Symposium 6: ICC symposium => 6.2: ICCG Geodesy for Climate Research

367

S6-018

Preliminary results of the third IGS TIGA Reprocessing at GFZ

Benjamin Männel¹, Tilo Schöne¹, Markus Bradke¹, Harald Schuh^{1,2}

1. GFZ German Research Centre for Geosciences, Potsdam, Germany

2. Technische Universität Berlin, Germany

The IGS Tide Gauge Benchmark Monitoring - Working Group (TIGA-WG) is providing highly consistent coordinate time series for GNSS stations directly at or near tide gauges to separate potential vertical land motion from sea level variation. The station position and vertical velocity results are needed in various geodetic and geophysical applications, such as global and regional sea level change, calibration of satellite altimeters, and the unification of global height systems. In the IGS repro3 campaign framework, the TIGA Analysis Center at GFZ German Research Centre for Geosciences performed a dedicated TIGA reprocessing involving 344 stations (including 102 dedicated TIGA stations) for the period 1994 until 2020. A classical network approach was used by introducing and fixing the GFZ repro3 satellite orbits, clock corrections, and Earth rotation parameters. The datum is realized by applying no-net-translation and no-net-rotation conditions to the 66 stations of the simplified IGS core station network.

In this presentation, we will show preliminary results of this dedicated TIGA reprocessing. After summarizing the processing details, we will first focus on a stability assessment of the TIGA stations. The second part will discuss the derived station coordinate time series and the associated velocity field. In the third part we will present an initial comparison against sea level measurements provided by the tide gauges and altimetry. Overall, the GFZ TIGA results contribute to the combined TIGA solution and will be publicly available for further investigations.

Key words GNSS; tide gauges; TIGA

Category: Symposium 6: ICC symposium => 6.2: ICC Geodesy for Climate Research

381

S6-019

Evaluating hydrological angular momentum determined from CMIP6 historical simulations

Jolanta Nastula¹, Justyna Śliwińska¹, Małgorzata Wińska², Tomasz Kur¹,
Aleksander Partyka¹

1. Space Research Centre, Polish Academy of Sciences, Warsaw, Poland

2. Faculty of Civil Engineering, Warsaw University of Technology, Warsaw, Poland

In the frame of the Coupled Model Intercomparison Project phase 6 (CMIP6), a number of climate models developed by multiple modeling groups are made available to the public in a standardized format. Such models deliver physical, chemical and biological properties of the atmosphere, oceans and continental hydrosphere both in the past and in the future, providing important information to understand past and future climate changes. The CMIP6 models are useful in many scientific applications regarding evolution of processes occurring in the atmosphere, ocean and hydrosphere.

In this presentation, we use soil moisture and snow water equivalent variables obtained from historical simulations of CMIP6 to assess the role of continental hydrosphere in polar motion (PM) excitation. PM is an essential parameter needed to transform the coordinates from the celestial to the terrestrial reference frame and vice versa, playing a crucial role in precise positioning and navigation. To achieve our goals, we compute the hydrological angular momentum (HAM) series and analyse their variability in a wide variety of oscillations. An important part of this study is validation of HAM estimates performed by comparing them with the hydrological signal in geodetically observed PM excitation. The goal is to find the CMIP6 simulations which are most appropriate for interpretation of PM variations.

Overall, the correspondence between the hydrological signal in observed PM excitation and HAM received from CMIP6 is lower than the previously obtained consistency with GRACE (Gravity Recovery and Climate Experiment) results, and the level of agreement depends on oscillation considered and model used. However, our results shows that it is possible to find a CMIP6 model that provides HAM series more compatible with the hydrological signal in observed PM excitation than HAM from GRACE, especially for annual oscillations.

Key words CMIP6, GRACE, polar motion excitation, hydrology, climate model evaluation

Category: Symposium 6: ICC symposium => 6.2: ICCG Geodesy for Climate Research

495

S6-020

Innovative methodology for downscaling GRACE observations for the purpose of groundwater storage determination

Monika Birylo¹、Zofia Rzepecka¹、Justyna Śliwińska²、Jolanta Nastula²

1. University of Warmia and Mazury in Olsztyn, Olsztyn, Poland

2. Space Research Centre, Polish Academy of Sciences, Warsaw, Poland

The aim of this study is to present a methodology for elaboration an innovative high-resolution groundwater storage (GWS) variations model based on many sources of observations, like GRACE/GRACE-FO (Gravity Recovery and Climate Experiment/Gravity Recovery and Climate Experiment Follow On) products, groundwater wells data, soil types data, meteorological and hydrological data from GLDAS (Global Land Assimilation Model).

Elaboration and determination of groundwater storage will be carried out using a high-resolution groundwater model determined with a machine learning methods: artificial neural networks (ANN) and boosted regression trees (BRT). This will let us to calculate accurate enough model for understanding, observing, and analysing all phenomena occurring in the hydrosphere, especially when considering local groundwater changes. In order to quantify GWS variations at the local scale, low-resolution global GRACE/GRACE-FO data are used together with higher resolution datasets that are related to single locations such as hydrological, meteorological, geodetic, and geological data.

Key words groundwater, GRACE, GLDAS, downscaling, ANN, BRT

Category: Symposium 6: ICC symposium => 6.2: ICC Geodesy for Climate Research

500

S6-021

GNSS for the Global Climate Observing System: Precipitable Water Vapor Processing Centre at GFZ

Galina Dick¹、 Florian Zus¹、 Jens Wickert^{1,2}、 Benjamin Männel¹、 Markus Bradke¹、
Markus Ramatschi¹、 Kyriakos Balidakis¹、 Karina Wilgan^{1,2}、 Harald Schuh^{1,2}

1. GFZ German Research Centre for Geosciences, Potsdam, Germany

2. Technische Universität Berlin, Germany

The Global Climate Observing System (GCOS), supported by a number of international partners and the World Meteorological Organization (WMO), is establishing a reference climate observation network, the GCOS Reference Upper Air Network (GRUAN), which currently comprises 30 globally distributed observing sites. The final network is envisaged to consist of around 40 stations, designed to detect long-term trends of key climate variables such as temperature and humidity in the upper atmosphere, thus providing a cornerstone to more reliable monitoring of signals of global and regional climate change. GRUAN observations are required to be of reference quality, with known biases removed and with an associated uncertainty value, based on careful characterization of all sources of measurement. Due to the inherent high accuracy and long-term stability, GNSS-derived precipitable water (GNSS-PW) measurement has been included as a priority one measurement of the essential climate variable water vapor.

GFZ contributes to GRUAN by running the GNSS Data Central Processing Centre for PW products according to defined requirements and maintains GNSS sites. Currently 18 of the GRUAN sites are equipped with GNSS receivers, half of them are running by GFZ. At the beginning of 2021 the data processing of GNSS-PW and its associated documentation has been GRUAN certified. We overview GRUAN and its GNSS component, show the current status and future developments. The operational determination strategy of GNSS-PW data products including uncertainty estimation will be presented. Recent results of validation studies, such as comparisons with measurements of radiosondes and a water vapor radiometer as well as comparisons with other geodetic techniques (VLBI), indicate a very high agreement of better than 1 mm for the GNSS-PW data products derived for GRUAN sites.

Key words GNSS-based Precipitable Water Vapor, GCOS Reference Upper Air Network GRUAN

Category: Symposium 6: ICC symposium => 6.2: ICC Geodesy for Climate Research

526

S6-022

What can long-term trend estimates from satellite gravimetry contribute to climate research?

Andreas Kvas¹, Eva Boergens², Henryk Dobslaw², Andreas Guentner²

1. Graz University of Technology

2. GFZ German Research Centre for Geosciences

The satellite missions GRACE and GRACE Follow-On (GRACE-FO) have substantially improved our understanding of the Earth system by providing monthly snapshots of surface mass change. With a growing data record currently spanning almost 20 years, this data set is well suited to investigate long-term changes in, for example, water storage, ice- and ocean mass. In contrast to other remote sensing techniques, satellite gravimetry is based on geophysical inversion rather than direct imaging. This process introduces high-frequency spatial noise caused by the downward continuation from satellite altitude to Earth's surface. To reduce the impact of this noise, derived mass change grids are typically constrained in the inversion process, or low-pass filtered in post-processing. Accumulating satellite observations over longer time spans reduces the magnitude of the high-frequency noise and thus requires weaker implicit or explicit filtering. Consequently, the smaller spatial leakage allows to investigate smaller spatial scales at the cost of temporal resolution.

We focus on the extreme case of a single linear trend estimated over the whole GRACE/GRACE-FO observation time span and provide a rigorous uncertainty and leakage analysis in comparison with trend estimates from ITSG and GFZ RL06 monthly solutions. First, we discuss the differences of the two trend estimates on a global scale and then apply the findings to selected regions and aquifers. This enables us to gauge to which degree drying and wetting trends can be resolved and localized and to quantify the different uncertainty levels for specific processes like aquifer depletion.

Key words GRACE/GRACE-FO; long-term trends; localized signals; aquifer depletion

Category: Symposium 6: ICC symposium => 6.2: ICC Geodesy for Climate Research

527

S6-023

Investigating the relationship between Length of Day and El-Nino using wavelet coherence method

Shrishail Raut^{1,4}, Sadegh Modiri², Robert Heinkelmann¹, Kyriakos Balidakis¹,
Santiago Belda³, Chaipayorn Kitpracha¹, Harald Schuh^{1,4}

1. GFZ German Research Centre for Geosciences

2. BKG, Frankfurt

3. UAVAC, University of Alicante, Alicante, Spain

4. Technical University of Berlin

The relationship between the length of day (LOD) and El-Nino Southern Oscillation (ENSO) is well studied since the 1980s. LOD is the negative time-derivative of UT1-UTC which is a part of the Earth Orientation Parameters (EOP). EOP can be determined using space geodetic techniques such as Very Long Baseline Interferometry (VLBI), Global Navigation Satellite System (GNSS), etc. ENSO is a climate phenomenon occurring over the tropical eastern Pacific Ocean that mainly affects the tropics and the subtropics. Extreme ENSO events can cause extreme weather like flooding and droughts in many parts of the world.

In this work, we investigated the effect of ENSO on the LOD from 1979 to the present using the wavelet coherence method. This method computes the correlation between the two non-stationary time-series in the time-frequency plane and uses the analytical Morlet wavelet. In this work, we used Multivariate ENSO index version 2 (MEI v.2) and Southern Oscillation Index (SOI) as climate index for the ENSO and LOD time-series from IERS (EOP 14 C04 (IAU2000A)). The initial results show strong coherence of 0.7 to 0.9 at major ENSO events for the periods around 50 -100 days and 2-7 years

Key words Length of day, El-Nino, Climate, Geodesy

Category: Symposium 6: ICC symposium => 6.2: ICC Geodesy for Climate Research

645

S6-024

Meteorological and Tidal Effects on GNSS Reflected Signal in Mediterranean Coasts of Turkey

Cansu Beşel, Emine Tanır Kayıkçı

Karadeniz Technical University, Faculty of Engineering, Department of Geomatics Engineering, Trabzon, Turkey

Sea level is a key component of climate change and plays an important role in the hydrological cycle. Rising sea levels have significant impacts such as environmental, social, and economic along with coastal areas. Global Navigation Satellite System Interferometric Reflectometry (GNSS-IR) enables to retrieve sea level heights using the reflected signal. Moreover, GNSS-IR is considered a promising alternative to conventional tide gauges. This study focuses on the determination of meteorological and tidal effects on GNSS reflected signals from the sea surface. We used Signal-to-Noise Ratio (SNR) data from the MERS IGS (International GNSS Service) network station located on the Mediterranean coast of Turkey. Time series of SNR data were analyzed to determine sea level variations. The various meteorological parameters such as temperature, air pressure, and wind speed, which were acquired from the nearby Erdemli tide gauge operated by the Turkish National Sea Level Monitoring System (TUDES), were utilized. Furthermore, tidal harmonic analysis was applied to both MERS station and Erdemli tide gauge to calculate tidal constituents which are an important parameter for the investigation of sea level variations. For this stage, tidal constituents were used including annual constituent, semi-annual term, long-term constituents, diurnal tides, semi-diurnal tides, third-diurnal tides, sixth-diurnal tides, quarter-diurnal tides, and third-diurnal tide. We compared the tidal constituents estimated from GNSS-IR and tide gauge observations. On the other hand, SNR amplitudes were compared to meteorological and tide parameters to investigate the effect on GNSS reflected signal from the sea surface. The results of meteorological parameters have shown that as temperature increases the SNR amplitudes decrease in the Mediterranean coasts of Turkey. In tidal harmonic analysis, the annual constituent (SA) is the largest tidal constituent with an amplitude higher than 11 cm.

Key words Sea Level, GNSS Interferometric Reflectometry, Meteorological Parameters, Tidal Harmonic Analysis

Category: Symposium 6: ICC symposium => 6.2: ICCG Geodesy for Climate Research

722

S6-025

Spatial-temporal variations in ice velocity of the Northeast Greenland Ice Stream and their control factors related with climate warming

Xi Lu

University of Chinese Academy of Sciences

The Northeast Greenland Ice Stream (NEGIS), which drains the largest basin in the Greenland ice sheet, has been experiencing rapid retreat and continuous mass loss since the 21st century, but numerical model predictions suggest no significant mass loss for this sector, leading to an under-estimation of future global sea-level rise. To better understand these rapid dynamic changes in recent years and control processes, we characterized spatial-temporal variations in the annual ice velocity of the three significant glaciers in NEGIS over the last 33 years (1985-2018). Further, to investigate possible forcing mechanisms capable of triggering dynamic changes, we then compared spatial characteristics of ice velocity and the topography of each glacier. We also evaluated the dynamic response between air temperature, runoff, surface elevation change, and temporal evolution of ice velocity to investigate their relationship and understand the potential effects of the dynamic changes of glaciers in this region.

Our preliminary results suggest that the velocities of the three glaciers show distinct spatial characteristics, which vary with the bed slope direction. In addition, there was a substantially significant and widespread fluctuation in 2000. A time lag of 6 years was found between the inception of air temperature rise and the onset of glaciers acceleration in 2000, suggesting that increased air temperature acted slowly but have triggered the dynamic acceleration of the glaciers in 2000. The increases of runoff and surface elevation change show a temporal consistency around 2000 with the changes of ice velocity, suggesting that the response between them is very sensitive and an inevitable response mechanism that needs to be further determined. This monotonous trend increases since the 21st century proved that NEGIS had made a positive and sensitive response to the temperature rise and highlighted the necessity of observing and further studying the internal mechanism of dynamic changes.

Key words NEGIS, ice velocity, climate warming, control factors

Category: Symposium 6: ICC symposium => 6.2: ICC Geodesy for Climate Research

776

S6-026

Contribution of glacier mass loss to river runoff in the source region of the Yangtze River during 2000-2018

Lin Liu¹、Liming Jiang²、 Hansheng Wang²

1. Huazhong University of Science and Technology

2. Innovation Academy for Precision Measurement Science and Technology,
Chinese Academy of Sciences

With rapid climatic warming, glaciers in the source region of the Yangtze River (SRYR) generally experienced apparent terminus retreats over the past several decades. However, the influence of glacier melting in the river runoff of the SRYR remains poorly known due to lack of glacier mass balance measurements. In this study, we derived the glacier mass changes of the SRYR in 2000-2018 by comparing the digital elevation models (DEMs) produced from ZiYuan-3 tri-stereo scenes with the SRTM DEM. Glacier mass balances were spatially heterogeneous (range from -0.55 ± 0.12 to -0.14 ± 0.05 m w.e. yr^{-1}) in the SRYR, which may be mainly attributed to the spatial difference in snowfall variation. Overall, the glacier mass loss of -0.343 ± 0.055 Gt yr^{-1} was estimated for the entire SRYR. By using the hydrological data recorded by the Zhimenda station, we calculated the annual runoff of 17.84 Gt yr^{-1} between 2000 and 2018. Therefore, the contribution of glacier mass loss to the river runoff of the SRYR was only $1.9 \pm 0.3\%$ in 2000-2018. Our results reveal that glacier melting was not the major water resource in the SRYR during recent decades.

Acknowledgments: This study was jointly supported by the National Key Research and Development Program (2017YFA0603103 and 2018YFC1406102) and the National Natural Science Foundation of China (41431070, 41704023 and 41590854).

Key words Glacier mass loss, the source region of the Yangtze River, runoff

Category: Symposium 6: ICC symposium => 6.2: ICCG Geodesy for Climate Research

810

S6-027

Land Water Storage Variabilities in GRACE and Climate Models – How do they compare and which future changes can we expect?

Laura Jensen¹、Annette Eicker¹、Henryk Dobslaw²、Roland Pail³

1. HafenCity University Hamburg

2. Helmholtz Centre Potsdam, German Research Centre for Geosciences (GFZ),
Potsdam, Germany

3. Technische Universität München, Institute of Astronomical and Physical Geodesy

Climate change will affect terrestrial water storage (TWS) during the next decades by impacting the seasonal cycle, interannual variations, and long-term linear trends. But how exactly will the variability change in the future? Reliable projections are needed not only for sensible water management but also as input for long-term performance studies of possible Next Generation Gravity Missions (NGGMs).

In this contribution, an ensemble of climate model projections provided by the Coupled Model Intercomparison Project Phase 6 (CMIP6) covering the years 2002 – 2100 is utilized to assess possible changes in TWS variability. To demonstrate performance and identify shortcomings of the models we first compare modeled TWS to globally observed TWS from the Gravity Recovery and Climate Experiment (GRACE) and its follow-on mission (GRACE-FO) in the time span 2002 – 2020. We then analyze changes in the variability of TWS from model projections until the end of the century and the consensus on such changes within the model ensemble.

Based on these projections, we find that present-day GRACE accuracies are sufficient to detect amplitude and phase changes in the seasonal cycle in one third of the land surface after 30 years of observation, whereas a five times more accurate NGGM mission could resolve such changes almost everywhere outside the most arid landscapes of our planet. We also select one individual model experiment out of the CMIP6 ensemble that closely matches both GRACE observations and the multi-model median of all CMIP6 realizations. This model run might serve as basis for multi-decadal satellite mission performance studies to demonstrate the suitability of NGGM satellite missions to monitor long-term climate variations in the terrestrial water cycle.

Key words GRACE, climate models, water storage, NGGM

Category: Symposium 6: ICC symposium => 6.2: ICCG Geodesy for Climate Research
816
S6-028

Using satellite geodesy for carbon cycle research

Alexandra Klemme¹, Thorsten Warneke¹, Heinrich Bovensmann¹, Matthias Weigelt², Jürgen Müller², Justus Notholt¹, Claus Lämmerzahl³

1. Institute of Environmental Physics, University of Bremen

2. Institute of Geodesy (IfE), Leibniz Universität Hannover

3. Centre of Applied Space Technology and Microgravity (ZARM), University of Bremen

Research in the global carbon cycle system is important to understand human induced impacts on global warming and to assess realistic climate change mitigation strategies. Carbon dioxide (CO₂) and methane (CH₄) are the two most important anthropogenic greenhouse gases and therefore in the focus of global climate research. Their atmospheric concentrations are determined by anthropogenic emissions as well as exchange with oceans and the terrestrial biosphere. For the prediction of future atmospheric concentrations of CO₂ and CH₄ it is important to understand how the natural exchange fluxes respond to a changing climate. One important research topic is a change in the hydrological cycle, which has a direct impact on exchange fluxes of CO₂ and CH₄ between the biosphere and the atmosphere. In this project, we aim to combine information about the hydrological cycle from geodetic satellites (e.g. GRACE & GRACE-FO) with carbon cycle observations from other available satellites. Specifically, we plan to investigate the impact of a changing water level in soils on CH₄ emissions from wetlands and on the photosynthetic activity of plants.

Key words carbon cycle, hydrological cycle, greenhouse gas emissions, CO₂, CH₄, GRACE, GRACE-FO

Category: Symposium 6: ICC symposium => 6.2: ICCG Geodesy for Climate Research

826

S6-029

River discharge estimation from high-resolution altimetry

Luciana Fenoglio¹, Elena Zakharova², Quang Duong³, Salvatore Dinardo⁴,
Jürgen Kusche¹, Matthias Gärtner¹, Hakan Ahmet¹, Jerome Benveniste⁵,
Bahtiyor Zohidov¹

1. University of Bonn

2. Maynooth University, Ireland

3. Bundesanstalt für Gewässerkunde, Koblenz, Germany

4. CLS (Collect Localisation Satellites), Toulouse, France

5. ESA

River discharge is a key variable to quantify the water cycle and its flux. The study focuses on the river Rhine, evaluating river discharge from water level and slope measured by existing and future satellites. Various methods are used, including the empirical rating curve method, the semi-empirical Bjerklie method and the physically-based method based on hydraulic equations. Water level estimated by the dedicated SAMOSA+ GPOD/ESA Sentinel-3 products are shown to be more accurate than the standard Copernicus data. The water level time-series at the Virtual Gauge (VG) and at the nearest in-situ stations have root-mean-square differences between 0.10 m and 0.30 m at half of the 17 VGs. The altimeter-derived water height and slope is used to derive the discharge. The normalized RMSE of discharge is 3-7% from the empirical rating curve method and 20% from the semi-empirical Bjerklie method. Physically-based algorithms are applied to in-situ data and to simulated measurements of river slope, height and width from the future SWOT mission. This last will provide innovatively derived river discharge up to 4 times in the 21-day repeat science phase and once per day in the calibration phase. Daily synthetic water surface slopes and elevations are generated from in-situ and model data. The accuracy of the water discharge is investigated for various choices of reach lengths, number of time-series and time-sampling. Similarly, the effect of the priori information on the accuracy of the flow water discharge is investigated. The high-resolution and innovative estimation of river discharge allows an improved monitoring of discharge on short time-scales and, combined with modelling, an evaluation of impacts of water and land use, modification of watershed and river network on long time-scales. This is of primary importance for a sustainable management of the water resource especially in ungauged rivers.

Key words river discharge, SWOT mission, SAR altimetry, climate change

Category: Symposium 6: ICC symposium =» 6.2: ICC Geodesy for Climate Research

859

S6-030

Closure of global sea-level and ocean-mass budgets: progress and prospects with a focus on uncertainty characterisation

Martin Horwath¹, Benjamin D. Gutknecht¹, Anny Cazenave^{4,15}, Hindumathi Kulaiappan Palanisamy^{4,17}, Florence Marti⁹, Ben Marzeion¹⁰, Frank Paul¹², Raymond Le Bris¹², Anna E. Hogg¹³, Inès Otosaka², Andrew Shepherd², Petra Döll^{5,16}, Denise Cáceres⁵, Hannes Müller Schmied^{5,16}, Johnny A. Johannessen⁸, Jan Even Øie Nilsen^{8,18}, Roshin P. Raj⁸, René Forsberg¹¹, Louise Sandberg Sørensen¹¹, Valentina R. Barletta¹¹, Sebastian B. Simonsen¹¹, Per Knudsen¹¹, Ole Baltazar Andersen¹¹, Heidi Randall¹¹, Stine K. Rose^{11,19}, Christopher J. Merchant¹⁴, Claire R. Macintosh¹⁴, Karina von Schuckmann³, Kristin Novotny¹, Andreas Groh¹, Marco Restano⁶, Jérôme Benveniste⁷

1. Technische Universität Dresden
2. Centre for Polar Observation and Modelling, University of Leeds, UK
3. Mercator Ocean International, Toulouse, France
4. LEGOS Toulouse, France
5. Institute of Physical Geography, Goethe University Frankfurt, Frankfurt am Main, Germany
6. Serco/ESRIN, Italy
7. ESA ESRIN, Italy
8. Nansen Environmental and Remote Sensing Center, Bergen, Norway
9. LEGOS, Toulouse, France
10. Institut of Geography and MARUM - Center for Marine Environmental Sciences, University of Bremen, Germany
11. Technical University of Denmark, Denmark
12. University of Zurich, Switzerland
13. University of Leeds, UK
14. University of Reading and National Centre for Earth Observation, UK
15. International Space Science Institute, Bern, Switzerland
16. Senckenberg Leibniz Biodiversity and Climate Research Centre (SBIK-F), Frankfurt am Main, Germany
17. Centre for Climate Research Singapore, Meteorological Service Singapore, Singapore
18. Institute of Marine Research, Bergen, Norway
- 19.

Studies of the global sea-level budget and ocean-mass budget are essential to assess the reliability of our knowledge of sea-level change and its contributors. Here we present and discuss results from the Sea-Level Budget Closure (SLBC_cci) project conducted in the framework of ESA's Climate Change Initiative (CCI). Focussing on the periods 1993-2016 (P1, the altimetry era) and 2003-2016 (P2, the GRACE and Argo era), we have developed and advanced datasets on global mean sea level (from satellite altimetry), the steric component (from Argo and sea-surface temperature data), the mass component (from GRACE) and the

individual mass contributions from glaciers, ice sheets, and land water storage change from satellite data and modeling approaches. The sea-level budget is closed for P1 and P2. The ocean-mass budget, only evaluated for P2, is also closed. Budget closure applies to the mean linear trends as well as to monthly anomalies of sea level and its components. Budget closure means that the observed total effect agrees to the sum of independently assessed components within the combined uncertainties of the budget elements. Hence, budget assessments and their interpretation depend on a consistent uncertainty characterisation across all budget elements, including error correlations. We discuss the progress made in uncertainty characterisation, current limitations and challenges and prospects on future work.

Key words sea-level budget, ocean-mass change, steric sea-level change, ice-sheet mass balance, glacier mass balance, land water storage change, GRACE, satellite altimetry, global mean sea level

Category: Symposium 6: ICC symposium =» 6.2: ICCG Geodesy for Climate Research

879

S6-031

Solid Earth Deformation Sensing Using Multi-Decadal Satellite Altimetry

C K Shum ^{1,2*}, Ting-Yi Yang ³, Chungyen Kuo ⁴, Vibhor Agarwal ⁵, Orhan Akyilmaz ⁶, Lifeng Bao ², Chunxi Guo ⁷, Yuanyuan Jia ¹, Jianliang Nie ⁷, Metehan Uz ⁶, Xuechen Yang ¹, Yuchan Yi ¹

1. School of Earth Sciences, The Ohio State University, Columbus, Ohio, USA
2. Innovation Academy for Precision Measurement Science and Technology, Chinese Academy of Sciences, Wuhan, China
3. Polaris Geospatial Services, Columbus, Ohio, USA
4. Department of Geomatics, National Cheng Kung University, Tainan, Taiwan
5. Dept. of Geology and Environmental Geosciences, University of Dayton, Ohio, USA
6. Dept. of Geomatics, Istanbul Technical University, Istanbul, Turkey
7. Centre for Geodetic Data Processing, National Administration of Surveying, Mapping and Geoinformation, X'ian, China

It is estimated that by 2025, five billion people worldwide will live in water-stressed regions. These worldwide water stresses are exacerbated by more frequent and more severe droughts resulting from an increasingly warmer climate. Severe spatially and temporally land subsidence is highly correlated with excessive anthropogenic groundwater pumping, leading to depleted and under-recharged aquifers, and with sediment compaction/loading, and anthropogenic mineral extractions in the coastal deltaic regions. Our scientific objective is to study solid Earth deformation processes in the world's large aquifers and deltaic regions. Here, we present preliminary results using a novel methodology to monitor 2-D solid Earth deformation in selected study regions at adequately dense spatio-temporal resolutions and accuracies, by exploiting multi-decade satellite radar altimetry over solid Earth, which is not originally designed for this purpose. We estimate satellite altimetry derived subsidence over the low gradient croplands in the San Joaquin Valley, California, USA, which is associated with excessive groundwater extractions for agricultural irrigations; and in Laizhou Bay and Tengzhou, Shandong, northeast China, which are associated with anthropogenic gold mining excavation, and groundwater withdrawal/sediment load, respectively. The multi-mission altimetry-derived land deformation results are compared using various waveform retracked retrievals. The altimetry-derived land deformation evolutions are compared with available GPS and InSAR derived vertical velocities, and others. Finally, plausible correlations of the multi-altimetry land deformation evolutions, 2002–2020, with drought and flood episodes in the San Joaquin Valley are presented.

Acknowledgements. This research is supported by National Aeronautics and Space Administration Earth Surface and Interior Program Grant No. 80NSSC20K0494.

Key words Satellite altimetry, Waveform retracking, Land subsidence, GPS, InSAR, Aquifers

Symposium 6: ICC symposium

S6.3: ICCM Seafloor geodesy, marine positioning and undersea navigation

Category: Symposium 6: ICC symposium => 6.3: ICCM Seafloor geodesy, marine positioning and undersea navigation

106

S6-032

Geoscientific contributions of the GNSS-A Seafloor Geodetic Observation array (SGO-A) in the subduction zones around Japan, operated by the Japan Coast Guard

Yusuke Yokota¹, Tadashi Ishikawa², Shun-ichi Watanabe², Yuto Nakamura²

1. University of Tokyo

2. Hydrographic and Oceanographic Department, Japan Coast Guard

The Japan Coast Guard (JCG) has been deploying the GNSS–Acoustic ranging combination technique (GNSS-A) Seafloor Geodetic Observation array SGO-A for the precise seafloor positioning in the global geodetic reference frame for more than 20 years. This system has made it possible to discuss the subduction process of plate boundaries, associated earthquakes, and postseismic deformations on the cm order. The 2011 Tohoku earthquake and its postseismic deformations, the coupling condition in the Nankai Trough in the southern part of the Japan Islands, and the detection of shallow slow slip event are important geodetic measurement results in two decades and give important suggestions in seismology and earthquake disaster prevention. In recent years, the observation accuracy and frequency have reached 1.5 cm (1σ) and 4 – 6 times/year, respectively. So, this observation system is expected to contribute to the detection of a slow slip event and time evolution of postseismic deformation and coupling condition. Because the determination of an ocean plate motion related to global geodesy relies on GNSS observations at the islands, the GNSS-A may contribute to global geodesy by monitoring on the ocean plate in the future.

Key words GNSS-A; seafloor geodesy

Category: Symposium 6: ICC symposium => 6.3: ICCM Seafloor geodesy, marine positioning and undersea navigation

121

S6-033

Overview of the GNSS-A Seafloor Geodetic Observation Array (SGO-A) in the subduction zones around Japan, operated by the Japan Coast Guard

Shun-ichi Watanabe¹, Tadashi Ishikawa¹, Yuto Nakamura¹, Yusuke Yokota²

1. Japan Coast Guard

2. University of Tokyo

The Japan Coast Guard (JCG) has been developing the GNSS–Acoustic ranging combination technique (GNSS-A) for the precise seafloor positioning in the global geodetic reference frame for more than 20 years. By tying the hydroacoustic trilateration survey to the GNSS-based global reference frame via a sea-surface platform, GNSS-A realizes the “global” positioning of the seafloor. Each GNSS-A site consists of multiple acoustic mirror transponders to enhance the positioning robustness and the system redundancy. Introducing the analysis process for the estimation of underwater sound speed field, we now obtain the seafloor positions with a precision of several centimeters. As of 2021, the JCG has 27 of the GNSS-A sites in the subduction zone around Japan, to construct the “Seafloor Geodetic Observation Array (SGO-A)”. In this presentation, we introduce the overview of the SGO-A concept, analysis procedures and products. Our GNSS-A data are partly available in public via the internet. We also developed an open source analysis software named “GARPOS” for our GNSS-A data, to spread the seafloor geodetic community.

Key words GNSS-A; Seafloor Geodetic Observation Array; seafloor positioning; GARPOS

Category: Symposium 6: ICC symposium => 6.3: ICCM Seafloor geodesy, marine positioning and undersea navigation

242

S6-034

Robust adaptive Kalman filter for underwater acoustic navigation with systematic error model correction

Junting Wang^{1,2}, Tianhe Xu¹, Yangfan Liu¹, Dapeng Mu¹

1. Institute of Space Science, Shandong University, Weihai, China

2. State Key Laboratory of Geo-Information Engineering, Xian, China

Underwater acoustic navigation using seafloor datum points has become the most efficient approach for ocean navigation. The key issue is how to model and correct the systematic error for the acoustic navigation in the seawater. We therefore propose a robust adaptive Kalman filter (KF) for underwater acoustic navigation with systematic error correction. Based on the systematic error estimated by seafloor datum point data, the proposed algorithm first uses wavelet transform to eliminate the noise of systematic error, whose period and amplitude are estimated by fast Fourier transform. Then the systematic error correction model can be constructed by using the polynomial fitting. After that, an improved observation equation combined the systematic error correction model and the slant distance correction of target velocity estimation is constructed. Finally, a robust adaptive KF based on the forecast residual innovation with the systematic error correction is developed for underwater acoustic navigation. The proposed algorithm is verified by a real experiment for underwater acoustic navigation in the South China Sea. The results demonstrate that the proposed algorithm can efficiently correct the systematic error of acoustic navigation without adding redundant estimated parameters. Compared with the standard KF, the navigation accuracy of the proposed algorithm can be significantly improved.

Key words Underwater high-precision acoustic navigation; Systematic error model; Polynomial model; Adaptive robust KF

Category: Symposium 6: ICC symposium => 6.3: ICCM Seafloor geodesy, marine positioning and undersea navigation

267

S6-035

Multi-beam underwater topography distortion correction based on SVP inversion

Yangfan Liu, Tianhe Xu, Junting Wang, Dapeng Mu
Institute of Space Science, Shandong University, Weihai, China

High-precision Multi-beam sounding requires real-time and accurate sound velocity profile (SVP). The commonly used SVP has a representative error, which can cause the underwater topography distortion of multi-beam edge beam. We analyze the influence of the representative error on the multi-beam sounding, and propose a method of correcting underwater topography distortion based on SVP inversion. This method firstly decomposes the SVP using empirical orthogonal function (EOF), which converts the SVP inversion process into the time coefficient optimization process. The time coefficient is then optimized by simulated annealing algorithm (SA) based on a cost function, which is constructed by the sounding consistency of the corresponding beams in the overlapped area of adjacent swaths. Finally, the inverted SVP is calculated by the optimal time coefficient, and then the distortion of underwater topography is corrected by the inverted SVP. The proposed algorithm is verified by three types of experiments based on measured SVPs. The results show that the error of inverted SVP is smaller than that of the commonly used SVP, and the root mean square errors of sounding are reduced for flat, inclined, and undulating topographies by the proposed method, compared to those of the method based on reconstructed SVP. Those results suggest that the proposed method can significantly improve the precision of multi-beam sounding, and efficiently correct the distortion of the various underwater topographies.

Key words Multi-beam bathymetric system; Underwater topography correction; SVP inversion; EOF; SA; Cost function

Category: Symposium 6: ICC symposium => 6.3: ICCM Seafloor geodesy, marine positioning and undersea navigation

438

S6-036

High Precision Positioning in Coastal Areas via GNSS/INS Equipped Buoys: A Case Study from the Bass Strait Altimeter Validation Site

Boye Zhou¹, Christopher Watson², Matt King², Jack Beardsley², Benoit Legresy³

1. University of Tasmania, Surveying and Spatial Sciences, School of Technology, Environments and Design, Hobart, TAS, Australia,

2. University of Tasmania

3. The Commonwealth Scientific and Industrial Research Organisation, Oceans and Atmosphere, Hobart, TAS, Australia

High precision positioning in the marine domain is required for a range of applications including altimeter validation, ocean tide modelling and ocean hazard warning. Several approaches of processing are available yet assessing precision and accuracy in the dynamic environment is challenging. In this study, we evaluated positioning quality using the historical archive of GPS buoy deployments at our altimeter validation facility. Using high-rate GPS data from recent deployments in comparison with data from in-situ oceanographic moorings, we assessed the solution precision of two processing approaches: differential GPS and PPP. Over ~30 km baselines the phase differencing approach does not always yield the best precision highlighting the value of the PPP approach in the open ocean. Both solutions revealed systematic differences with the mooring datasets, prompting us to address two previously ignored issues in water level determination by buoys: changes to buoyancy as a function of external forcing, and biases induced by the platform dynamics. From the mooring data and a regional numerical model, our study shows a strong correlation between surface currents, wind stress and buoy-against-mooring residuals. An empirical model correction reduces the residual energy by 50% over low frequency bands. Positional effects associated with platform orientation derived from the GNSS/INS buoy are up to 2 cm which is expected to be higher under rougher sea states. Our results indicate a comparable level of precision achieved by differential GPS and PPP, which holds important implications for extension further into the open ocean for high precision positioning. Regardless of the strategy, our results highlight the benefits of considering platform orientation in the solution. To determine the water level (e.g. for altimeter validation), the effect of tether tension is also vital. Failure to consider these will introduce systematic bias at frequencies where tidal currents dominate.

Key words Altimeter validation; GNSS Buoy; INS; buoyancy displacement; platform orientation

Category: Symposium 6: ICC symposium => 6.3: ICCM Seafloor geodesy, marine positioning and undersea navigation

450

S6-037

A Nonlinear Gauss-Helmert Model and Its Robust Solution for Seafloor Control Point Positioning

Yingcai Kuang¹、Zhiping Lu^{1,2}、Fangchao Wang¹

1. Information Engineering University

2. Harbin Institute of Technology (Shenzhen)

Using GNSS-acoustic (GNSS-A) technology to establish the seafloor geodetic datum is both feasible and flexible, and has become an important way to obtain the absolute position information of seafloor control points. In marine survey, the systematic errors and gross errors caused by GNSS dynamic positioning, inaccurate sound velocity profile measurement and ocean ambient noise are inevitable, and their interference will be directly reflected in the positioning results. To realize the accurate calculation of the seafloor point coordinates, this paper firstly points out that the general method based on the error propagation law (the EPL model) has defects in essence. A more rigorous way is to incorporate the transducer position errors into the coefficient matrix of the underwater observation equation, and the time-varying part of the sound velocity profile measurement errors should be taken into account. Therefore, the Gauss-Helmert (GH) model for seafloor control point positioning is proposed. Then, considering the dual nonlinearity of the model, the Lagrange objective function is constructed to derive the solution method of the new model. On this basis, giving consideration to the gross error pollution of the observation information, the robust estimation principle is introduced, and the robust solution steps of the new model are given. Finally, the simulation experiment and the testing experiment in the sea area near Jiaozhou Bay are used to verify the performance of the new model. The results show that the function relationship and stochastic model of the nonlinear GH model for seafloor point positioning are reasonably described. Under the ideal situation of no gross errors with different water depths or different transducer position errors, the accuracy and stability of the new method are both higher than those of the EPL model. When the observation information is polluted by gross errors, the robust algorithm of the new model can identify the abnormal information accurately. By improving the robustness of the observation space and structure space, the positioning precision of the 3D point deviation results can be optimized, and the solution performance of the new method is superior to that of the general method.

Key words GNSS-A technology; transducer position error; sound velocity profile measurement; nonlinear GH model; robust estimation

Category: Symposium 6: ICC symposium => 6.3: ICCM Seafloor geodesy, marine positioning and undersea navigation

454

S6-038

BATHYMETRIC DATA FITTING BASED ON LINEAR-COMPLEMENTARY FOURIER SERIES OF B-SPLINE FUNCTION

Ruichen Zhang¹、Shaofeng Bian²、Bing Ji²

1. China University of Petroleum

2. Naval University of Engineering

In the paper, the bathymetric data fitting model based on Fourier series is analyzed, and the paper introduces two expanded Fourier series methods, the expansion model of Fourier series based on linear complementarity and the expansion model of Fourier series based on B-spline function.

Firstly, the principle of bathymetric data gridding and parametric inversion process are introduced. As for gridding principle, the weight of the central-beam bathymetric data should be increased, and the weight of the edge-beam bathymetric data should be decreased; for the grid nodes near the edge beam, bathymetric data selection should be enlarged as much as possible in order to contain more bathymetric data as input data in the process of gridding. And parametric inversion process of bathymetric data fitting method based on the two-dimensional Discrete Fourier series model is systematically carried out in the paper. It can be seen that the series of trigonometric functions in the Fourier series model are orthogonal and independent of each other. Therefore, the sine and cosine functions with large coefficients in Fourier series model has the control power.

In data preprocessing, according to the periodicity of Fourier series function, the expansion model of Discrete Fourier series based on Linear-complementarity is proposed. After comparing and analyzing three different complementary methods (None complementarity, Constant complementarity and Linear complementarity), the results show that the Linear-complementary Fourier series expansion model can effectively improve the convergence speed of modeling.

Thirdly, after analyzing the relationship between Continuous Fourier series fitting model and B-spline function, the expansion model of Continuous Fourier series method based on B-spline function is proposed. And the parametric inversion of B-spline fitting method based on the two-dimensional Continuous Fourier series model is systematically deduced in the paper.

Finally, combining these two expansion methods, the paper introduced the Linear-complementary Fourier series fitting method based on B-spline function. Compared with the traditional Fourier series model, the

results show that the convergence speed, accuracy and stability of the Linear-complementary Fourier series fitting method based on B-spline function have been improved, which shows its feasibility and extensibility in the field of bathymetric data processing.

Key words Fourier series; B-spline; linear-complementarity; bathymetric data processing; fitting

Category: Symposium 6: ICC symposium => 6.3: ICCM Seafloor geodesy, marine positioning and undersea navigation

560

S6-039

Further evaluation of the impact of Earth's curvature on coastal sea level altimetry with ground-based GNSS Reflectometry

Vitor Hugo Almeida Junior, Felipe Geremia-Nievinski
Federal University of Rio Grande do Sul (UFRGS)

The global mean sea level is rising at an increasing rate. Ground-based GNSS Reflectometry (GNSS-R) is a promising alternative for coastal sea level measurements. GNSS-R works as a bistatic radar, based on radio waves continuously emitted by GNSS satellites that are reflected on the Earth's surface. The interferometric delay between reflected and direct waves can be used to perform sea level altimetry. The geometrical modeling of delay normally involves a planar and horizontal reflector surface. However, this assumption is not necessarily valid for reflection points far away from the antenna. An osculating sphere is thus more appropriate for representing the reflector surface. In the present work, we quantify the effect of Earth's curvature on ground-based GNSS-R altimetry. Firstly, we modeled the interferometric delay for each plane and sphere and then we calculated the differences between the two, simulating scenarios for varying satellite elevation (from zenith down to the spherical horizon) and varying antenna height (from 10 m to 500 m). Then, we developed an altimetry correction based on half of the rate of change of the delay difference with respect to the sine of elevation angle. Considering a 1-cm altimetry threshold for sea-level measurements, we observed that the altimetry correction is needed above 200 m, for any elevation angle. Furthermore, the correction is also needed at 5°, 10°, 20°, and 30° satellite elevation, for an antenna altitude of 30 m, 60 m, 120 m, and 160 m, respectively.

Key words GNSS-R, Remote sensing, Altimetry correction

Category: Symposium 6: ICC symposium => 6.3: ICCM Seafloor geodesy, marine positioning and undersea navigation

583

S6-040

Outlier Detection Based on Epoch-differential for Seafloor Geodetic Positioning

Shuqiang XUE

Chinese Academy of Surveying and Mapping

The GNSS-acoustic (GNSS-A) observations for seafloor geodetic positioning are seriously affected by the sound speed field (SSF) spatial-temporal error as well as the spatial-temporal error in GNSS positioning. Those spatial-temporal errors are hardly modelled and cause a thorny model error to the positioning model such that the observation residuals are generally large-valued to affect the gross error detection. Besides, the arm-length vector error and the initial positional error can also cause large-valued residuals. This work discusses the error sources in the acoustic positioning and the influence of these errors on the seafloor geodetic positioning, and then we propose an outlier detection method based on the epoch-differential which is used to reduce the spatial-temporal errors and common errors. A cross validation algorithm for the outlier detection based on the differential observations is proposed. The proposed results are verified in a deep-sea seafloor geodetic positioning, and it shows that the differential observations are very sensitive to both large and small outliers that can be perfectly detected before performing the positioning procedure.

Key words Outlier detection; differential; seafloor positioning; algorithm

Category: Symposium 6: ICC symposium => 6.3: ICCM Seafloor geodesy, marine positioning and undersea navigation

663

S6-041

Comparative analysis of construction methods of regional marine three-dimensional sound velocity field

Chaoyi Wu¹、Fanlin Yang^{1,2}、Mingzhen Xin¹、Jinjin Wei¹、Xiaofei Zhang¹

1. College of Geodesy and Geomatics, Shandong University of Science and Technology

2. Key Laboratory of Ocean Geomatics, Ministry of Natural Resources of China

The spatial-temporal changes of the sound velocity in seawater make the propagation path of sound waves is not straight, which is called the refraction effect. It is necessary to use the measured sound velocity profiles (SVP) to correct the continuous curved sound ray into straight in underwater acoustic positioning to eliminate the positioning error caused by the refraction effect. Although the measurement accuracy of SVP can reach 0.02m/s, the acquisition of real-time continuous profiles is almost impossible in practical operations. Several sound velocity stations are usually placed based on the range and shape of the survey area, and the SVP are collected to reflect the spatial-temporal changes of the sound velocity.

The regional marine three-dimensional sound velocity field is a mathematical model that describes the spatial-temporal changes of the sound velocity based on the sufficient SVP over a period. This paper mainly discusses the methods and comparative analyses of constructing regional marine three-dimensional sound velocity field by using three models of Empirical Orthogonal Function (EOF), Back Propagation Neural Network (BPNN) and General Regression Neural Network (GRNN). In a certain experimental sea area, 26 SVP data were obtained for analysis. The research results show that:(1) When EOF is used to construct the regional marine three-dimensional sound velocity field, the positioning error caused by sound velocity is less than 0.5m; (2) When BPNN is used, the positioning error caused by sound velocity is less than 0.2m; (3) The accuracy of the SVP reconstructed by GRNN is better than that of BPNN, but the prediction accuracy is lower, indicating that GRNN is more dependent on the samples. The research proves that these three models are feasible in constructing the marine three-dimensional sound velocity field, which has the certain value for researches and applications of underwater acoustic positioning.

Key words underwater acoustic positioning; sound velocity field; Empirical Orthogonal Function; Back Propagation Neural Network; General Regression Neural Network

Category: Symposium 6: ICC symposium => 6.3: ICCM Seafloor geodesy, marine positioning and undersea navigation

665

S6-042

Analysis of Interactive Multiple Model Kalman Filter Algorithm for Ultra Short Baseline Tracking Autonomous Underwater Vehicle

Xiaofei Zhang¹、Mingzhen Xin¹、Fanlin Yang^{1,2}、Jinjin Wei¹、Chaoyi Wu¹

1. College of Geodesy and Geomatics, Shandong University of Science and Technology

2. Key Laboratory of Ocean Geomatics, Ministry of Natural Resources of China

Under the influence of complex marine environment changes, the tracking of autonomous underwater vehicles (AUV) using ultra short baseline (USBL) may be affected by various errors. The Kalman Filter (KF) is usually used to reduce the effects of dynamic positioning errors. The KF needs to construct a motion model that matches the actual motion state. However, AUV has the characteristics of strong maneuverability, so it is difficult to determine a priori single motion model to achieve the matching of all motion states. To solve this problem, the interactive multiple model Kalman Filter (IMMKF) method is used to process the USBL tracking AUV data.

An AUV tracking experiment is designed to compare the filtering performance of KF and IMMKF based on different motion model sets. Single-model KF adopts Constant Velocity (CV) model, Constant Acceleration (CA) model, Singer model, Current Statistical (CS) model, and IMMKF adopts CV/CA/Singer、CV/CA/CS、CV/Singer/CS、CA/Singer/CS, and multi-sensor integrated navigation (USBL/INS/DVL) tracking results are used as reference values. The experiment results show that: (1) For the single-model KF, the KF (CS) model has the highest filtering accuracy. (2) For the IMMKF, the filtering accuracy of the IMMKF (CA/CS/Singer) model is the highest. (3) Comparing KF and IMMKF, the filtering accuracy of IMMKF (CA/CS/Singer) and IMMKF (CV/CS/Singer) is higher than that of single-model KF. However, the filtering accuracy of IMMKF (CV/CS/Singer) and IMMKF (CV/CA/Singer) models is worse than that of the single model KF (CS). In conclusion, the motion state of AUV has the characteristics of low speed and high maneuverability, and it is difficult to determine a priori motion state that matches all the actual motion. Therefore, when multiple model sets are constructed reasonably, the IMMKF algorithm has better state adaptability than the single-model KF algorithm.

Key words ultra short baseline; autonomous underwater vehicles; interactive multiple model; Kalman Filter; motion model

Category: Symposium 6: ICC symposium => 6.3: ICCM Seafloor geodesy, marine positioning and undersea navigation

739

S6-043

Research on the Method of Establishing Calibration System for Marine Sonar Equipment Based on Prototype Tank

Yunyue Chen^{1,2}、Anmin Zhang²、Yufen Cao¹、Yicheng Liu¹、Minming Zhang¹

1. Tianjin Research Institute for Water Transport Engineering, Ministry of Transport

2. Tianjin University

Abstract: The development of marine sonar equipment has greatly promoted the development of marine geodesy. However, without scientific calibration methods, high quality developments in marine geodesy will not be guaranteed. The objectives of this study are carried out a series of calibration methods for marine sonar equipment, such as multibeam echosounder, ADCP(acoustic doppler current profile meter).

This paper shows that:(1) One calibration method for multibeam echosounder based on prototype tank and 6-dof (degrees of freedom) control mechanism can realize the calibration of the full band sounding accuracy of multibeam echosounder within the measuring range of 180 m. Expanded uncertainty of bathymetry is 60 mm. (2) Non-contact synchronous video velocity calibration method based on unmanned ship can be used to the calibration of velocity and flow direction for ADCP. Expanded uncertainty of velocity is 0.01 m/s, expanded uncertainty of flow direction is 1.2 angel. (3) Ultrasonic wave gauge calibration equipment is carried out to do full range calibration of wave height and wave period based on the tank of 75 m in length. Expanded uncertainty of wave height is 0.03 m.

Key words marine geodesy, calibration, multibeam echosounder, ADCP,wave gauge,prototype tank

Category: Symposium 6: ICC symposium => 6.3: ICCM Seafloor geodesy, marine positioning and undersea navigation

858

S6-044

Seafloor single point positioning using GNSS-Acoustic technique with horizontal sound speed gradient estimation

Yang Liu、Yanxiong Liu、Guanxu Chen、Menghao Li
First Institute of Oceanography, Ministry of Natural Resources

We propose using Global Navigation Satellite System–Acoustic (GNSS-A) technique with sound speed gradient estimation for seafloor single point positioning, which can achieve centimeter-level accuracy. In our experiment, the single seafloor station in 3000-meter depth could be precisely positioned to 3 cm in horizontal and 5 cm in vertical direction. The positioning accuracy was evaluated by comparison between solutions from different independent ship tracks. The vertical component was compared with the pressure gauge derived depth. The estimated horizontal sound speed gradient was validated by multiple SVP/CTD measurements and ocean currents measurements, which was also manifested in the observed moored array movements.

Key words Global Navigation Satellite System–Acoustic; sound speed gradient; seafloor single point positioning

Symposium 6: ICC symposium

S6.4: QuGe Novel Sensors and Quantum Technology for Geodesy

Category: Symposium 6: ICC symposium => 6.4: QuGe Novel Sensors and Quantum Technology for Geodesy

126

S6-045

Improved evaluation of the transportable strontium lattice clock at PTB for chronometric leveling

Ingo Nosske, Chetan Vishwakarma, Sofia Herbers, Roman Schwarz, Sören Dörscher, Christian Lisdat
Physikalisch-Technische Bundesanstalt

After laboratory optical atomic clocks have reached fractional frequency uncertainties in the 10^{-18} regime, it is an ongoing task to miniaturize these complex devices and to make them transportable, without affecting their reliability or accuracy. This effort is in part motivated by promising prospects in geodesy. Together with accurate frequency transfer via fiber links, due to the gravitational redshift such accurate clocks can measure gravitational potential differences in the $0.1 \text{ m}^2 \text{ s}^{-2}$ regime (corresponding to cm height differences on Earth's surface) with high spatial and temporal resolution, and could such be used to establish an accurate height reference system.

At PTB, we have been operating a transportable strontium lattice clock in an air-conditioned car trailer, which has been successfully employed in international measurement campaigns, e.g. in the Alps. Here we present a recent improved uncertainty evaluation of the clock, bringing its total uncertainty into the very low 10^{-17} range. Furthermore, we report on results of a clock comparison with our new stationary strontium clock in 2021. These show an agreement of the two clocks within their current combined uncertainties of about 2×10^{-17} . In addition, we present our plans on a new physics package by which we aim to enter the 10^{-18} uncertainty and cm height resolution regime.

This work receives funding from DFG within CRC 1464 (TerraQ, project A04) and under Germany's Excellence Strategy—EXC-2123 QuantumFrontiers—390837967. It is supported by the Max Planck–RIKEN–PTB Center for Time, Constants and Fundamental Symmetries.

Key words Chronometric Leveling, Clock Comparisons, Transportable Optical Clocks

Category: Symposium 6: ICC symposium => 6.4: QuGe Novel Sensors and Quantum Technology for Geodesy

193

S6-046

Characteristics of Novel Differential Lunar Laser Ranging Compared to Classical Lunar Laser Ranging

Mingyue Zhang^{1,2,4}、Jürgen Müller¹、Liliane Biskupek¹、Vishwa Vijay Singh^{1,3}

1. Institute of Geodesy (IfE), Leibniz University Hannover

2. State Key Laboratory of Geodesy and Earth's Dynamics, Institute of Geodesy and Geophysics, APM, Chinese Academy of Sciences, Wuhan 430077, China

3. Institute for Satellite Geodesy and Inertial Sensing, German Aerospace Center (DLR), Callinstraße 36, 30167 Hannover, Germany

4. University of Chinese Academy of Sciences, Beijing 100049, China

A new lunar laser ranging (LLR) station of JPL at the Table Mountain Observatory can allow a novel way of lunar tracking: differential lunar laser ranging (DLLR). There, fast switching between two or more lunar reflectors would be possible in future to get DLLR observations by differencing two consecutive ranges. This new kind of observable will largely decrease the atmospheric and station-related errors, resulting in a very high accuracy of about 30 μm . Using such accurate data will give us the opportunity to obtain better knowledge of the interior and the rotation of the Moon. Additionally, DLLR is expected to improve other parameters of the Earth-Moon dynamics, including those relevant for relativity tests, for example, test of the equivalence principle and a possible time-variation of the gravitational constant G . Presently, our group works on the simulation of DLLR data and investigates its characteristics, like the sensitivity and the impact of different switching intervals by comparing with LLR. DLLR keeps the same sensitivities as LLR for some parameters (group A), for example, the lunar rotation parameters, while it becomes less sensitive to other parameters (group B), such as station positions and velocities, resulting from its cancelling effect on the station part. However, thanks to its excellent measurement accuracy, DLLR can still keep the estimated accuracies for group B at the same level as LLR and significantly enhance the estimation of group A. The correlation between stations and reflectors is increased by DLLR. Nevertheless, larger switching intervals (e.g., 15 min) will be helpful for their decorrelation. In future, we will combine DLLR with classical LLR data to benefit from both observations. In this presentation, we will show first simulation results on the specific characteristics and the benefit of DLLR.

Key words Differential Lunar Laser Ranging, Lunar Laser Ranging, Novel geodetic technology

Category: Symposium 6: ICC symposium => 6.4: QuGe Novel Sensors and Quantum Technology for Geodesy

245

S6-047

Towards high-precision International Height Reference System Using Two-Way Space Laser Time Transfer Link

Abdelrahim Ruby^{1,4,5}, Wen-Bin Shen^{1,4}, Ahmed Shaker⁵, Shen Ziyu², Pengfei Zhang¹, Chenghui Cai¹, Wei Xu¹, Mostafa Ashry³, An Ning¹, Lei Wang¹, Lihong Li¹

1. Time and Frequency Geodesy Center, School of Geodesy and Geomatics, Wuhan University, Wuhan 430079, China.
2. School of Resource, Environmental Science and Engineering, Hubei University of Science and Technology, Xianning 437100, China
3. Civil Engineering Department, Faculty of Engineering, Minia University, Minia 61111, Egypt
4. State Key Laboratory of Information Engineering in Surveying, Mapping and Remote Sensing, Wuhan University, Wuhan 430079, China.
5. Department of Surveying Engineering, Faculty of Engineering at Shoubra, Benha University, Cairo 11629, Egypt.

The Establishment of a high-precision International Height Reference System (IHRIS) is one of the most important goals in geodetic community. One of the conventions for the definition of IHRIS is for the vertical differences between the potential of reference stations and the geoidal potential (geopotential number). Therefore, the challenge is to achieve high precision and global uniformity in the geopotential numbers for the reference stations. Currently, relativistic geodesy provides a novel method for determining geopotential or height differences between distant stations by using Einstein's general relativity theory, which concludes that a precise atomic clock runs quicker at a position with higher potential. Now, there are several methods for converting the running rates of atomic clocks at arbitrary two stations to geopotential or height differences between them, most of them are based on microwave signals from satellites. Future optical space links, which will gather several ultra-stable clocks, as Laser Time Transfer (LTT) on China Space Station (CSS) and European Laser Timing (ELT) on Atomic Clock Ensemble in Space (ACES) are a promising approach to compare time or frequency of atomic clocks at reference stations, where the atmospheric delays in optical domain are less affected compared to the microwave approaches. Consequently, we propose the Two-way Laser Time Transfer Link (TWLTTL) for the realization of a global height unification system based on the worldwide distribution of laser stations. This study is supported by the National Natural Science Foundations of China (NSFC) under Grants 42030105, 41721003, 41804012, 41631072,

41874023, Space Station Project (2020)228, and the Natural Science Foundation of Hubei Province of China under Grant 2019CFB611.

Key words Relativistic geodesy, geopotential, Height system unification, IHRS, Laser Time Transfer

Category: Symposium 6: ICC symposium => 6.4: QuGe Novel Sensors and Quantum Technology for Geodesy

278

S6-048

The Benefit of Accelerometers based on Cold Atom Interferometry for Future Satellite Gravity Missions

Annike Knabe¹, Manuel Schilling², Hu Wu¹, Alireza HosseiniArani^{1,2}, Jürgen Müller^{1,2}, Franck Pereira dos Santos³, Quentin Beaufiles³

1. Institute of Geodesy, Leibniz University Hannover

2. DLR-Institute for Satellite Geodesy and Inertial Sensing, c/o Leibniz University Hannover

3. LNE-SYRTE, Observatoire de Paris, PSL Research University, CNRS, Sorbonne University Paris

Satellite gravity missions, like GRACE and GRACE Follow-On, successfully map the Earth's gravity field and its change in time. With the addition of the laser ranging interferometer to GRACE-FO, a significant improvement over GRACE concerning inter-satellite ranging was achieved. Now, one of the major limiting factors is the accelerometer for measuring the non-gravitational forces acting on the satellite. The classical electrostatic accelerometers are affected by a drift in low frequencies. This drawback can be counterbalanced by an accelerometer based on cold atom interferometry (CAI) due to its high long-term stability. The CAI concept has already been successfully demonstrated in ground experiments and is expected to show an even higher sensitivity in space.

In order to investigate the potential of the CAI concept for future satellite gravity missions, a closed-loop simulation is performed. The sensitivity of the CAI accelerometer is estimated based on state-of-the-art ground sensors and published space scenarios. The sensor performance is tested for different scenarios and the recovered gravity field results are evaluated. It is shown that a classical accelerometer aided by CAI technology improves the results of the gravity field recovery. The non-gravitational accelerations are modelled using a detailed surface model of a GRACE-like satellite body. This is needed for a realistic determination of the variations of the non-gravitational accelerations during one interferometer cycle. It is demonstrated that the corresponding error contribution to the CAI accelerometer is significant. We consider different orbit altitudes and also analyze the influence of drag compensation.

We acknowledge the support by the Deutsche Forschungsgemeinschaft (DFG) via EXC 2123 "QuantumFrontiers, Project-ID 390837967" and the CRC 1464 "TerraQ, Project-ID 434617780", and that by DLR-Institute for Satellite Geodesy and Inertial Sensing and its initial funding by the

Ministry of Science and Culture of the German State of Lower Saxony
from “Niedersächsisches Vorab”.

Key words cold atom interferometer accelerometry; future satellite gravity missions; gravity field recovery, closed-loop simulation

Category: Symposium 6: ICC symposium => 6.4: QuGe Novel Sensors and Quantum Technology for Geodesy

363

S6-049

A geodetic determination of the gravitational potential difference toward a 100-km-scale clock frequency comparison in a plate subduction zone

Yoshiyuki Tanaka¹, Yosuke Aoki²

1. Department of Earth and Planetary Science, University of Tokyo

2. Earthquake Research Institute, University of Tokyo

Time runs faster where the gravitational potential energy is higher. Based on this nature (gravitational red shift), the potential difference between two fiber-linked optical clocks on the Earth's surface can be estimated by measuring their frequency difference. Fractional uncertainties of such measurements are basically regardless of fiber lengths and have achieved the order of 10^{-18} for an averaging time of several hours. The potential difference can be converted into a height difference, with the difference of 1×10^{-18} in frequency corresponding to approximately 1 cm. This efficient technique to measure height changes (chronometric leveling) is expected to replace a classical method based on geodetic leveling and gravity survey. Recently, an experiment to confirm gravitational red shift using transportable optical lattice clocks was performed in Japan, with a 450-meter vertical link connecting the ground and the observatory of the Tokyo Skytree. The chronometric potential difference was verified with geodetic methods and the results by both methods agreed with each other within the order of 1 cm. As the next step, it is planned to test the validity of these clocks for a 100-km-scale fiber network around Tokyo. In this study, we determine the static gravitational potential difference between the clock sites for this fiber network with a classical geodetic approach. When a measurement uncertainty reaches 1 cm in height, the effects of temporal variations in the gravitational potential on the measurement need to be considered, due to geophysical phenomena such as tides. Our result shows that major uncertainties come from the uncertainties in the height measurement by geodetic leveling and that tidal potential changes during the height measurement can cause a few-mm systematic errors. Other effects due to variations in the non-tidal ocean bottom pressure, atmospheric pressure and groundwater are much smaller in this spatial scale.

Key words optical lattice clock, chronometric leveling, relativistic geodesy, GNSS, gravitational potential, crustal deformation

Category: Symposium 6: ICC symposium => 6.4: QuGe Novel Sensors and Quantum Technology for Geodesy

429

S6-050

Towards a transportable aluminum ion quantum logic optical clock for relativistic geodesy

Stephan Hannig¹, Benjamin Kraus¹, Constantin Nauk¹, Johannes Kramer¹,
Fabian Dawel¹, Lennart Pelzer¹, Nicolas Spethmann¹, Piet Schmidt^{1,2}

1. PTB

2. Leibniz Universität Hannover, 30167 Hannover, Germany

After a brief introduction into relativistic geodesy, single ion clocks, and quantum logic spectroscopy, we present PTB's efforts to build a transportable aluminum ion clock. Compared to other species, the aluminum clock transition is very insensitive to blackbody radiation. The linear and quadratic Zeeman shifts are small and the electric quadrupole shift is negligible. Therefore, aluminum is a promising candidate for highly accurate optical clocks. However, a co-trapped calcium ion is required for sympathetic cooling and state readout via quantum logic spectroscopy.

The transportable clock setup benefits from our experience gained during development of a similar but stationary clock apparatus with an estimated preliminary apparatus-related systematic fractional frequency uncertainty of $1.9 \cdot 10^{-18}$ [1]. Other key-components are a segmented multi-layer trap made of AlN substrates [2] and a transportable reference cavity for the clock laser.

We present the concepts, setups and characterization results of robust optical components developed for transportable experiments. Firstly, a mechanically robust fourth-harmonic generation unit consisting of two consecutive single-pass second-harmonic generation stages is shown. By comparison to a second FHG setup, we find that UV light with a fractional frequency instability of below $1 \cdot 10^{-16}$ at 1 s can be generated. Moreover, we show a prototype of a fiberized single-pass acousto-optical modulator unit for 267 nm clock light and robust optical breadboarding for UV applications employing Zerodur components [3].

[1] S. Hannig et al. (2019), Towards a transportable aluminium ion quantum logic optical clock, Rev. Sci. Instrum. 90, 053204

[2] Burgermeister, T. (2019). Development and characterization of a linear ion trap for an improved optical clock performance. Phd thesis, Leibniz Universität Hannover.

[3] M. Mihm et al. (2019), ZERODUR based optical systems for quantum gas experiments in space, Acta Astronautica, Vol. 159, pp. 166-169

Key words Optical clocks, relativistic geodesy, chronometric levelling

Category: Symposium 6: ICC symposium => 6.4: QuGe Novel Sensors and Quantum Technology for Geodesy

462

S6-051

A Simplified Comparison Between Two Proposed Designs for a Future Earth Gravity Mission With and Without Strongly Reduced Non-Gravitational Acceleration Noise Level Requirements

Peter Bender
University of Colorado

Several types of candidates have been proposed for a Next Generation Gravity Mission to follow after GRACE Follow-On. One candidate would have similar accelerometers to those on GRACE F-O and nearly the same acceleration noise level requirement. However, it would have laser interferometry between the two satellites and fly at a considerably lower altitude. Another option would be a similar mission but with a strongly reduced acceleration noise level requirement. This could be achieved by replacing the accelerometers with highly simplified versions of the Gravitational Reference Sensors demonstrated very successfully on the LISA Pathfinder mission. To compare the expected scientific results from these options, a preliminary evaluation has been made of the expected geopotential height variation uncertainty for different orbital frequencies expected from the two missions. For the orbit, a satellite altitude of 362 km was chosen, giving 172 revolutions in 11 days. The results for one revolution arcs were obtained at frequencies of 20, 40, 60, 80, 100, and 120 cycles per revolution. The results were as follows:

Case 1: [383, 80.6, 33.3, 18.0, 11.3, 7.7] $\times 10^{-9}$ m/(cycles/rev)^{0.5};

Case 2: [4.0, 2.1, 1.6, 1.4, 1.2, 1.1] $\times 10^{-9}$ m/(cycles/rev)^{0.5}.

For global mean solutions over periods of more than a few days, the improvements in signal-to-noise ratio at the lower to medium frequencies would be limited by temporal aliasing. However, for high latitude regions where the ground tracks are closer together, the separation between tracks would be less than about 250 km over periods of 1.5 days, so that temporal aliasing would be limited. But the main advantages would be from the ability to make strong tests of potentially improved methods for understanding mass distribution changes based on other geophysical data and from the improved accuracy at the higher frequencies.

Key words Next generation earth gravity mission; Simplified gravitational reference sensors; Accuracy for geopotential height variations

Category: Symposium 6: ICC symposium => 6.4: QuGe Novel Sensors and Quantum Technology for Geodesy

479

S6-052

ESA Activities and Perspectives on Quantum Space Gravimetry

Olivier Carraz¹, Luca Massotti¹, Ilias Daras², Roger Haagmans², Pierluigi Silvestrin²

1. RHEA for ESA

2. ESA

In the past decade, it has been shown that atom quantum sensors are an emerging technology that can be used for measuring the Earth's gravity field. Whereas classical accelerometers, based e.g. on capacitive sensing and electrostatic actuation, are limited by relatively high noise at low frequencies, Cold Atom Interferometers (CAI) have the potential of very low noise over the entire frequency range combined with a very low systematic error, which also has the benefit that they do not need any calibration phase. Several studies related to these new sensor concepts were initiated at ESA, mainly focusing on technology development for different instrument configurations (gravity gradiometers and satellite-to-satellite ranging systems) and including validation activities, e.g. two successful airborne surveys with a CAI gravimeter. We will present the conclusions of these different mission and instrument studies:

- The first airborne gravity survey during the ESA Cryovex/KAREN 2017 campaign using this technology was conducted by DTU and ONERA. The measurements did not show any drift and the accuracy was found to be less than 4 mGal at 11 km resolution. A second campaign has been conducted by ONERA and CNES in 2019 reaching classical airborne survey state-of-the-art performance.
- A first space quantum gravity mission concept based on a gravity gradiometer that delivers a very high common mode rejection, so relaxing the drag-compensation requirements.
- A second concept based on CAI accelerometers for correcting low frequency errors of electrostatic accelerometers used in a low-low satellite-to-satellite ranging concept in order to measure non-gravitational accelerations.

A technology roadmap will be outlined for potential implementation of a Quantum Space Gravimetry Pathfinder mission before the end of this decade, aimed at improving state of the art accelerometers in the low frequency band and pave the way to developing a full quantum gravity mission after 2030.

Key words Quantum Space Gravimetry Pathfinder, Cold Atom Interferometer, Gravity gradiometer

Category: Symposium 6: ICC symposium => 6.4: QuGe Novel Sensors and Quantum Technology for Geodesy

481

S6-053

The Application Sagnac Interferometry in the Geosciences

Ulrich Schreiber¹, Jan Kodet², Alexander Velikoseltsev³, Thomas Kluegel⁴

1. Technical University of Munich, Geodetic Observatory Wettzell, Germany

2. Technical University of Munich

3. St. Petersburg State Electrotechnical University LETI, Department of Laser Measurement and Navigation Systems, Russia

4. Federal Agency of Cartography and Geodesy, Geodetic Observatory Wettzell, Germany

Absolute inertial rotation sensing at high resolution and high long-term stability, permanently available, is still a dream in space geodesy. However, the large single component active Sagnac interferometer G at the Geodetic Observatory Wettzell is already getting very close in the demonstration of the necessary sensor resolution as well as the required measurement stability of the entire interferometer. Some of the requirements for the sensor layout to provide the necessary sensitivity and stability are generating contradicting demands on the hardware design and the operational parameters. Larger sensors, for example, are more sensitive, while stability is much easier to obtain from smaller devices. Over the last two years, we have carefully optimized the operations of the G ring laser such that we have sufficient sensitivity to measure the variable part of the Earth rotation signal in the frequency range just under 1 micro-Hz, corresponding to a period of the Length-of-Day signal of 14 days. However, in the presence of 1/f-noise, generated by non-reciprocal behavior of the laser cavity, this tiny signal is currently just outside the window of detection. This paper explains where we are and how to improve the current situation.

Key words ring laser, Sagnac Interferometry, quantum devices

Category: Symposium 6: ICC symposium => 6.4: QuGe Novel Sensors and Quantum Technology for Geodesy

499

S6-054

Kalman-filter Based Hybridization of Classic and Cold Atom Interferometry Accelerometers for Future Satellite Gravity Missions

Alireza HosseiniArani^{1,3}, Benjamin Tennstedt², Manuel Schilling³, Annike Knabe²,
Hu Wu², Jürgen Müller^{2,3}, Steffen Schön²

1. Institute of Geodesy, Leibniz University Hannover, Germany

2. Institute of Geodesy, Leibniz University Hannover

3. DLR-Institute for Satellite Geodesy and Inertial Sensing, c/o Leibniz University Hannover, Germany

Proof-of-principle demonstrations have been made for cold atom interferometer (CAI) sensors. Using CAI-based accelerometers in the next generation of satellite gravimetry missions can provide long-term stability and precise measurements of the non-gravitational forces acting on the satellites. This would allow a better understanding of relevant climate change processes (e.g. ice-mass loss in Greenland or global sea level rise) and several geophysical phenomena (e.g. post-glacial rebound) which requires long-term monitoring of mass variations with sufficient spatial and temporal resolution.

The proposed accuracy and long-term stability of CAI-based accelerometers appear promising, while there are some major drawbacks in the long dead times and the comparatively small dynamic range of the sensor. One promising way to handle the drawbacks of atom interferometry is to use it in hybrid combination together with conventional navigation sensors. This study discusses a specific possible solution to employ the measurements of a CAI accelerometer together with a classical accelerometer resp. IMU in a GRACE-like satellite gravimetry mission by applying a Kalman filter framework.

A hybrid navigation solution of these two sensors for applications on ground has already been demonstrated in simulations. It allows an improved accuracy of the navigation solution with respect to the reference trajectory in comparison to a standard strapdown solution with conventional inertial sensors. Here, we adapt this method to a space-based GRACE-like gravimetry mission. A closed-loop simulation is performed, where the modeling of the non-gravitational forces is based on a detailed surface model of the satellite body. The sensitivity of the CAI accelerometer is estimated based on state-of-the-art ground sensors and further published space scenarios. We will discuss the challenges, potential solutions, and possible performance limits of the proposed hybrid accelerometry scenario.

We acknowledge the support by the Deutsche Forschungsgemeinschaft (DFG) via EXC 2123 “QuantumFrontiers, Project-ID 390837967“ and the CRC 1464 "TerraQ, Project-ID 434617780", and that by DLR-Institute for Satellite Geodesy and Inertial Sensing and its initial funding by the Ministry of Science and Culture of the German State of Lower Saxony from “Niedersächsisches Vorab”.

Key words Future Satellite Gravity Missions, satellite gravimetry, Cold Atom Interferometry, CAI, Hybrid accelerometer, Kalman filter

Category: Symposium 6: ICC symposium => 6.4: QuGe Novel Sensors and Quantum Technology for Geodesy
556
S6-055

Geopotential difference determination by TWSTFT

Peng Cheng¹、Wenbin Shen²

1. Wuhan University

2. State Key Laboratory of Information Engineering in Surveying, Mapping and Remote Sensing

The quick development of the two-way satellite time and frequency transfer (TWSTFT) technique provides a good opportunity to determine the geopotential difference based on the general relativity theory (GRT). In this study, we use the TWSTFT technique to directly compute clock offsets between two clocks at two stations for the purpose of determining the geopotential difference, referred to as TWSTFT geopotential determination (TGD). To validate the TGD approach, we carried out the clock transfer experiment between JiuGong mountain (Xianning, China) and Wuhan University (Wuhan, China). By transferring time signals between the two sites by TWSTFT technique, we calculated the time difference and determined the geopotential difference between the two sites. The results show that the approach could be applied to determining the geopotential difference. This study was supported by the National Natural Science Foundations of China (Grant Nos. 42030105, 41721003, 41804012, 41631072, 41874023, 41574007), and Space Station Project (Grant No. 2020-228).

Key words TWSTFT; geopotential difference; GRT

Category: Symposium 6: ICC symposium => 6.4: QuGe Novel Sensors and Quantum Technology for Geodesy

576

S6-056

Unifying the world height system based on gravity frequency shift equation via optic fibers

Anh The Hoang^{1,3}, Wen-Bin Shen^{2,4}

1. Time and Frequency Geodesy Center, Department of Geophysics, School of Geodesy and Geomatics, Wuhan University, Wuhan 430079, China.
(wbshen@sgg.whu.edu.cn)
2. Time and Frequency Geodesy Center, Department of Geophysics, School of Geodesy and Geomatics, Wuhan University, Wuhan 430079, China.
(wbshen@sgg.whu.edu.cn)
3. School of Agriculture and Natural Resource, Vinh University, Vinh City- 460000, Vietnam
4. State Key Laboratory of Information Engineering in Surveying, Mapping and Remote Sensing, Wuhan University, Wuhan 430079, China

Orthometric height datum system plays key role in geodetic community. However, each nation or region holds its own height system. These height systems are predominantly determined by classical spirit leveling and are inhomogeneous due to the mean sea level being not an equipotential surface. Hence, unifying world height system is an open problem at present. Gravity frequency shift equation provides potential approach to unify the world height system by comparing the frequencies of the two remote clocks via optic fibers. Here we formulate a model to unify the world height system based on optical fiber frequency transfer (OFFT) method, which holds the highest accuracy level based on gravity frequency shift at present. The basic idea is that we set several intermediate stations between two remote stations located at two continents separated by an ocean. We transfer the frequency signals from one station to another intermediate station, and obtain the gravity frequency shift information between the two remote stations, realizing the height propagation from one station to another. Quick developments of optical clocks and frequency comparison technique provide good opportunity to realize the unification of world height system. This study is supported by National Natural Science Foundation of China (NSFC) (grant Nos. 41721003, 42030105, 41631072, 41874023, 41804012), and Space Station Project (2020)228.

Key words world height system, optical clocks, gravity frequency shift, frequency signal transfer, geopotential

Category: Symposium 6: ICC symposium => 6.4: QuGe Novel Sensors and Quantum Technology for Geodesy

622

S6-057

The MOCAS^T+ study: proposal of a quantum gravimetry mission integrating atomic clocks and cold atom gradiometers

Federica Migliaccio¹、Carla Braitenberg²、Sergio Mottini³、Gabriele Rosi^{4,7}、Mirko Reguzzoni¹、Fiodor Sorrentino^{5,7}、Guglielmo Maria Tino^{6,7}、Khulan Batsukh¹、Öykü Koç¹、Alberto Pastorutti²、Tommaso Pivetta²、Lorenzo Rossi¹

1. Politecnico di Milano

2. University of Trieste

3. Thales Alenia Space Italia

4. Istituto Nazionale di Fisica Nucleare Firenze

5. Istituto Nazionale di Fisica Nucleare Genova

6. University of Florence

7. AtomSensors

MOCAS^T+ (MONitoring mass variations by Cold Atom Sensors and Time measures) is a study of a quantum technology mission for the improvement of the monitoring of mass transport and mass variations above and below the Earth surface. The study is jointly carried out by several Italian research groups and is funded by the Italian Space Agency (ASI).

In the MOCAS^T+ study the proposed payload is based on an innovative concept: the integration of two different technologies, based on atomic interferometry gravity sensors and on the measurement of time/frequency with optical clocks. This integration requires an evolution in the methodology for the measurement of gravity, in which the atomic interferometer is based on strontium atoms instead of rubidium. A strategy based on the use of three clocks in combination with an optical link in heterodyne has been identified to better mitigate baseline fluctuations. Observations of differences of the gravitational potential (which will contribute to the estimate of the low frequencies of the Earth gravity field model) and of second derivatives of the gravitational potential along one or more orthogonal directions have been simulated at positions along the satellites' orbits. A first set of simulations has taken into account different mission configurations and has led to a mission profile based on a "Bender" constellation (two satellite pairs flying in an in-line formation, one in a polar orbit and the other in an orbit with an inclination of about 67°).

The idea is that the addition of clock measurements to gradiometric observations would result in the possibility of improving the estimation of time-variable gravity models even at low harmonic degrees, with consequent advantages in the modelling of mass transport and its global variations: this is fundamental information, for example in the study of

variations in the hydrological cycle and of the relative mass exchange between the atmosphere, oceans, cryosphere and solid earth.

Key words Quantum gravimetry, atomic clocks, mass transport, hydrology cycle

Category: Symposium 6: ICC symposium => 6.4: QuGe Novel Sensors and Quantum Technology for Geodesy

636

S6-058

Determination of the geopotential difference and orthometric height difference based on the two-way satellite time transfer observations

An Ning¹、Wen-Bin Shen¹、Ziyu Shen²、Chenghui Cai¹、Wei Xu¹、Lihong Li¹

1. Wuhan University

2. School of Resources, Environmental Science and Engineering, Hubei University of Science and Technology

Based on general relativity theory, an atomic clock's running rate will change with gravity potential (geopotential). Then we may precisely determine the geopotential difference between two stations equipped with precise atomic clocks. There are different ways to compare the time elapse between remote two atomic clocks, one of which is the two-way satellite time and frequency transfer (TWSTFT). Here we provide experimental results use the TWSTFT observations covering the period from December 7, 2016 to January 3, 2017 at China Aerospace Science & Industry Corporation (CASIC), Beijing. After synchronizing two hydrogen clocks at positions at the same height, the clocks were separated with a height difference of 22.2 m and compared for a period based on the TWSTFT technique. Using the EEMD method to filter out the noises, we obtained the time elapse between the two clocks. Results show that the height difference determined based on the clock comparison is comparable with the given height 22.2 m, coinciding with the stability of the hydrogen clocks used in our experiments.

Key words Two-Way Satellite time and frequency transfer, Atomic clock, General relativity theory

Category: Symposium 6: ICC symposium => 6.4: QuGe Novel Sensors and Quantum Technology for Geodesy

673

S6-059

Status of gravimetric measurements and modelling along a 10m atom interferometer

Manuel Schilling¹, Étienne Wodey², Ludger Timmen³, Dorothee Tell², Klaus H. Zipfel², Dennis Schlippert², Christian Schubert¹, Ernst M. Rasel², Jürgen Müller³

1. German Aerospace Center Institute for Satellite Geodesy and Inertial Sensing

2. Leibniz University Hannover Institute of Quantum Optics

3. Leibniz University Hannover Institute of Geodesy

Transportable quantum sensors become more common especially in gravimetry and measurements on longer timescales or field campaigns are carried out. Large scale atom interferometers are much rarer and mostly used for experiments in fundamental physics but can also be operated as gravimeter. The extended free fall time of atoms compared to transportable devices paves the way towards a new measurement standard in absolute gravimetry with a potential stability of better than 1 nm/s² at 1 second integration time. In contrast, the reference values at gravimetric key comparisons, which provide the highest accuracy today, achieve an accuracy of 10 nm/s².

At the Leibniz University Hannover, we are currently building a very long baseline atom interferometer (VLBAI) with a 10 m vertical free fall zone. The impact of the instrument on the local gravity field and vice versa was determined by gravimetric measurements during the construction. A 3D model of the VLBAI and its environment was created to calculate the gravitational effect of the masses on experiments of the atom interferometer. The model is then compared to episodic gravimetric measurements. The knowledge of local gravity and its gradient is required to establish the instrument's uncertainty budget and enable the transfer of gravimetric measurements to nearby devices for comparison. We report on the progress of the gravimetric measurements and modelling in parallel to the construction of the VLBAI.

Supported by the Deutsche Forschungsgemeinschaft (DFG, German Research Foundation) through: major research equipment (VLBAI), CRC 1464 "TerraQ" – 239994235, CRC 1227 "DQ-mat" – 274200144, Germany's Excellence Strategy EXC-2123 "QuantumFrontiers" – 390837967. Supported by "Niedersächsisches Vorab" through the "Quantum- and Nano-Metrology (QUANOMET)" initiative (Project QT3) and initial funding of the DLR-SI institute, and the German Federal Ministry of Education and Research through the Photonics Research Germany program.

Key words atom interferometer, gravimetry, 3d modelling

Category: Symposium 6: ICC symposium => 6.4: QuGe Novel Sensors and Quantum Technology for Geodesy

674

S6-060

High-Performance Clock Networks and Their Application in Geodesy

Hu Wu¹, Dennis Philipp², Eva Hackmann², Jürgen Müller¹, Claus Lämmerzahl²

1. Institute of Geodesy (IfE), Leibniz University Hannover, Germany

2. Center of Applied Space Technology and Microgravity (ZARM), University of Bremen, Germany

The advancement of quantum technology brings new opportunities in precision measurements, which yields novel sensors for accelerometry, gradiometry, chronometry and so on. For chronometry, high-performance clock networks, i.e., optical clocks connected by dedicated frequency transfer techniques, are capable to observe the gravitational redshift effect. This can be applied to infer the point-wise gravity potential (or physical height) difference between long-distance sites. This concept is termed as relativistic geodesy with clocks, or chronometric geodesy. It opens a new door to obtain geodetic measurements.

In this study, we address the potential of high-performance clock networks for a few typical geodetic applications. Since clock networks with a fractional frequency uncertainty of 1.0×10^{-18} can determine the physical height differences between distant points with the target accuracy level of 1.0 cm, we study their potential for the realization of a homogeneous and accurate global physical height reference frame. We will show simulation results to demonstrate that clocks are powerful to unify the practically-used local height systems. Clocks are also considered to be operated at locations of interest, e.g., in Greenland and Amazon, where they can continuously track changes w.r.t. reference clock stations. The resulting time-series of gravity potential values can probably reveal the time-variable gravity signals at these locations. Moreover, clocks are assumed on-board a pair of co-orbiting satellites to collect relative gravity potential values with a global coverage. In this scenario, we will run closed-loop simulations to evaluate the potential of clocks for detecting time-variable gravity signals from space.

We gratefully acknowledge the financial support by the Deutsche Forschungsgemeinschaft (DFG, German Research Foundation) under Germany's Excellence Strategy EXC-2123 "QuantumFrontiers" (Project-ID: 390837967). The study is also funded by the Deutsche Forschungsgemeinschaft (DFG, German Research Foundation) under

the research program SFB 1464 “TerraQ - Relativistic and Quantum-based Geodesy” (Project-ID 434617780).

Key words Optical clock networks, Relativistic geodesy, Height system, Gravity field

Category: Symposium 6: ICC symposium => 6.4: QuGe Novel Sensors and Quantum Technology for Geodesy

681

S6-061

Gravimetry by nanoscale parametric amplifiers driven by radiation-induced dispersion force modulation

Fabrizio Pinto
Izmir University of Economics

We present simulations of nano-electromechanical oscillators being designed for gravimetry and accelerometry applications. At parametric resonance, highly scalable parametric oscillators driven by variable Casimir forces are expected to deliver an extremely competitive performance over traditional sensors [1]. By adopting archetypal plane-plane and plane-sphere geometries [2], we replace excitation mechanisms based on undesirable external mechanical boundary actuation [1] by illumination-induced interboundary dispersion force modulation [3] - a remarkable phenomenon first shown in semiconductors in ground-breaking experiments carried out in Germany several decades ago [4]. The application of such an approach, already shown to be promising in gravitational wave detection with nanodevices [5], suggests a new class of gravimetry products based on dispersion force engineering as an emerging enabling general purpose technology [6].

References

- [1] M. Imboden et al., Design of a Casimir-driven parametric amplifier. 10.1063/1.4896732
- [2] F. Pinto, Casimir forces: Fundamental theory, computation, and nanodevices applications. 10.1007/978-94-024-1544-5_8
- [3] F. Pinto, Engine cycle of an optically controlled vacuum energy transducer. 10.1103/PhysRevB.60.14740
- [4] W. Arnold, S. Hunklinger, and K. Dransfeld, Influence of optical absorption on the Van der Waals interaction between solids. 10.1103/PhysRevB.21.1713
- [5] F. Pinto, Gravitational-wave response of parametric amplifiers driven by radiation-induced dispersion force modulation. 10.1142/9789813226609_0405
- [6] F. Pinto, The future of van der Waals force enabled technology-transfer into the aerospace marketplace. 10.1016/B978-0-12-812667-7.00029-X

Key words Casimir-force parametric amplifiers, dispersion force engineering, dispersion force manipulation, nanoscale gravimeters

Category: Symposium 6: ICC symposium => 6.4: QuGe Novel Sensors and Quantum Technology for Geodesy
698
S6-062

Defining a unified height system for Egypt using the ACES microwave links

Mostafa Ashry^{1,2,3}, WenBin Shen^{2,1}, Abdelreheem Ruby^{1,2,4}, Hussein Abd-Elmotaal³

1. Wuhan University
2. Time and Frequency Geodesy Center, School of Geodesy and Geomatics, Wuhan University, Wuhan 430079, China.
3. Civil Engineering Department, Faculty of Engineering, Minia University, Minia 61111, Egypt.
4. Department of Surveying Engineering, Faculty of Engineering at Shoubra, Benha University, Cairo 11629, Egypt.

According to general relativity theory, a precise clock runs at different rates at positions with different geopotential. Atomic Clock Ensemble in Space (ACES) is a mission using high-performance clocks and links to test fundamental laws of physics in space. The ACES microwave link (MWL) will make the ACES clock signal available to ground laboratories equipped with atomic clocks. The ACES-MWL will allow space-to-ground and ground-to-ground comparisons of atomic frequency standards. In this study, we try to create a datum file at the orbit of the ACES using the orbit information and using the available global geopotential models to get the geopotential at the orbit level. After that, using the MWL between ACES and ground stations to determine the geopotential differences between ACES and these stations at a specific time. Finally using the datum file, the geopotential at the ground stations are calculated. The TFC (tri frequency combination) uses the uplink of carrier frequency 13.475 GHz (Ku band) and downlinks of carrier frequencies 14.70333 GHz (Ku band) and 2248 MHz (S-band) to transfer time and frequency. This study is supported by the National Natural Science Foundations of China (NSFC) under Grants 42030105, 41721003, 41804012, 41631072, 41874023, Space Station Project (2020)228, and the Natural Science Foundation of Hubei Province of China under Grant 2019CFB611.

Key words ACES, EIGEN-6C4, microwave link, unified height system for Egypt.

Category: Symposium 6: ICC symposium => 6.4: QuGe Novel Sensors and Quantum Technology for Geodesy

731

S6-063

Higher order ionospheric effects on microwave frequency transfer between spacecraft and ground station

Pengfei Zhang¹、Wen-Bin Shen^{1,3}、Chenxiang Wang¹、Ziyu Shen²、Rui Xu¹、
Chenghui Cai¹、Wei Xu¹、Abdelrahim Ruby^{1,3,4}、Mostafa Ashry^{1,3,5}

1. School of Geodesy and Geomatics, Wuhan University, Wuhan 430079, China.
2. School of Resource, Environmental Science and Engineering, Hubei University of Science and Technology, Xianning, Hubei, China.
3. State Key Laboratory of Information Engineering in Surveying, Mapping and Remote Sensing, Wuhan University, Wuhan 430079, China.
4. Department of Surveying Engineering, Faculty of Engineering at Shoubra, Benha University, Cairo 11629, Egypt.
5. Civil Engineering Department, Faculty of Engineering, Minia University, Minia Minia 61111, Egypt.

Microwave frequency transfer between spacecraft and a ground station plays key role in testing gravitational redshift. During its propagation in space with medium, a microwave signal will experience ionospheric refraction and path bending, giving rise to its time delay and frequency change. Due to the limitation of the accuracy and stability of atomic clocks, previous studies usually only considered the impact of the first order term of the ionospheric frequency shift. With the implementation of the Atomic Clock Ensemble in Space (ACES) on board the International Space Station (ISS) as well as the high-precise time and frequency system on board the Chinese Space Station (CSS), the spacecraft will payload the atomic clocks and optic clocks with stabilities of 10^{-16} and 10^{-18} , respectively. To improve the accuracy level of testing gravitational redshift, it is necessary to consider higher-order ionospheric frequency shifts. In this study, we investigated higher-order ionospheric frequency shifts in different cases. Investigations show that, for the ACES signals with frequencies about 2.5 GHz and 14 GHz, the second-order ionospheric frequency shifts are about 10^{-15} and 10^{-17} , respectively. And for the CSS signals with frequencies about 21 GHz and 30 GHz, the second-order ionospheric frequency shifts are about 10^{-17} and 10^{-18} , respectively. The third-order ionospheric frequency shift is about 10^{-17} level for 2.5GHz and less than 10^{-18} level for all signals with frequencies spanning from 10 GHz to 30 GHz. Hence, to measure the gravitational potential with decimeter or centimeter accuracy level, it is necessary to consider the second-order ionospheric frequency shift. This study is supported by the National -Natural Science Foundations of China (NSFC) under Grants 42030105, 41721003, 41804012, 41631072, 41874023,

Space Station Project (2020)228, and the Natural Science Foundation of Hubei Province of China under Grant 2019CFB611.

Key words higher order ionosphere frequency shift Chinese Space Station Atomic Clock

Category: Symposium 6: ICC symposium => 6.4: QuGe Novel Sensors and Quantum Technology for Geodesy

736

S6-064

Novel Sensors and Quantum Technology for Geodesy (QuGe)

Jürgen Müller¹, Marcelo Santos²

1. Leibniz University Hannover

2. University of New Brunswick

Current developments in quantum physics and the application of general relativity opens up enhanced prospects for satellite geodesy, gravimetric Earth observation and reference systems. These novel concepts include the application of atom interferometry for realizing quantum gravimetry/radiometry in space and on ground, the enhanced use of laser interferometry for inter-satellite tracking and accelerometry at future gravity field missions, and relativistic geodesy with clocks for the determination of gravity potential differences via gravitational redshift measurements. In close collaboration between physics and geodesy, the new IAG project “Novel Sensors and Quantum Technology for Geodesy (QuGe)” exploits the high potential of quantum technology and novel measurement concepts for various innovative applications in geodesy.

We present the basic idea and general structure of QuGe with its 3 active working groups. We also briefly illustrate those novel techniques and the beneficial application of the new methods for gravimetric Earth observation on ground and in space.

Key words Quantum gravimetry on ground and in space, Relativistic geodesy with clocks

Category: Symposium 6: ICC symposium => 6.4: QuGe Novel Sensors and Quantum Technology for Geodesy

771

S6-065

Gravity data acquisition with the transportable absolute Quantum Gravimeter QG-1

Nina Heine¹、Marat Musakaev¹、Sven Abend¹、Ludger Timmen²、Waldemar Herr³、
Jürgen Müller²、Ernst M. Rasel¹

1. Institute of Quantum Optics, Leibniz University Hannover

2. Institut für Erdmessung, Leibniz University Hannover

3. Institut für Satellitengeodäsie und Inertialsensorik, Deutsches Zentrum für Luft- und Raumfahrt (DLR)

The determination of the local gravity value with an uncertainty $< 3 \text{ nm/s}^2$ is the objective of the transportable Quantum Gravimeter QG-1. It derives the local gravity value from the interferometric signal of magnetically collimated Bose-Einstein condensates (BECs) released into free-fall and detected by absorption imaging. The reduced projected uncertainty in contrast to cold atom gravimeters is facilitated by the minimised initial velocity and expansion rate of the BEC.

In this contribution we describe the sensor head unit, the implementation of the measurement concept and the resulting projected uncertainty contributions. We present a preliminary evaluation of gravity data recorded with the Quantum Gravimeter, showing the operability of the device and the validity of the concept. We indicate the immediate next steps to increase the instrument's sensitivity and to verify the measurement's level of uncertainty.

We acknowledge financial support from "Niedersächsisches Vorab" through "Förderung von Wissenschaft und Technik in Forschung und Lehre" for the initial funding of research in the DLR-SI Institute. Funded by the Deutsche Forschungsgemeinschaft (DFG, German Research Foundation) under Germany's Excellence Strategy – EXC-2123 QuantumFrontiers – 390837967 and under Project-ID 434617780 – SFB 1464 TerraQ - Relativistic and Quantum-based Geodesy.

Key words quantum gravimetry, quantum sensor, atom interferometer

IAG 2021

Beijing • June 28-July 2, 2021

